

Copyrighted Material

FUNDAMENTALS OF FINITE ELEMENT ANALYSIS

DAVID V. HUTTON

Copyrighted Material



Higher Education

FUNDAMENTALS OF FINITE ELEMENT ANALYSIS

Published by McGraw-Hill, a business unit of The McGraw-Hill Companies, Inc., 1221 Avenue of the Americas, New York, NY 10020. Copyright © 2004 by The McGraw-Hill Companies, Inc. All rights reserved. No part of this publication may be reproduced or distributed in any form or by any means, or stored in a database or retrieval system, without the prior written consent of The McGraw-Hill Companies, Inc., including, but not limited to, in any network or other electronic storage or transmission, or broadcast for distance learning.

Some ancillaries, including electronic and print components, may not be available to customers outside the United States.

This book is printed on acid-free paper.

International 1 2 3 4 5 6 7 8 9 0 QPF/QPF 0 9 8 7 6 5 4 3

Domestic 1 2 3 4 5 6 7 8 9 0 QPF/QPF 0 9 8 7 6 5 4 3

ISBN 0-07-239536-2

ISBN 0-07-112231-1 (ISE)

Publisher: *Elizabeth A. Jones*

Sponsoring editor: *Jonathan Plant*

Developmental editor: *Lisa Kalner Williams*

Marketing manager: *Sarah Martin*

Senior project manager: *Kay J. Brimeyer*

Production supervisor: *Kara Kudronowicz*

Media project manager: *Jodi K. Banowetz*

Senior media technology producer: *Phillip Meek*

Designer: *K. Wayne Harms*

Cover designer: *Scan Communication Group Inc.*

Senior photo research coordinator: *Lori Hancock*

Compositor: *Interactive Composition Corporation*

Typeface: *10.5/12 Times Roman*

Printer: *Quebecor World Fairfield, PA*

Library of Congress Cataloging-in-Publication Data

Hutton, David V.

Fundamentals of finite element analysis / David V. Hutton. — 1st ed.

p. cm.

ISBN 0-07-239536-2

1. Finite element method. I. Title.

TA347.F5H88 2004

620'.001'51535—dc21

2003048735

CIP

INTERNATIONAL EDITION ISBN 0-07-112231-1

Copyright © 2004. Exclusive rights by The McGraw-Hill Companies, Inc., for manufacture and export. This book cannot be re-exported from the country to which it is sold by McGraw-Hill.

The International Edition is not available in North America.

BRIEF TABLE OF CONTENTS

Preface xi

- 1 Basic Concepts of the Finite Element Method 1**
- 2 Stiffness Matrices, Spring and Bar Elements 19**
- 3 Truss Structures: The Direct Stiffness Method 51**
- 4 Flexure Elements 91**
- 5 Method of Weighted Residuals 131**
- 6 Interpolation Functions for General Element Formulation 163**
- 7 Applications in Heat Transfer 222**
- 8 Applications in Fluid Mechanics 293**
- 9 Applications in Solid Mechanics 327**
- 10 Structural Dynamics 387**

Appendix A Matrix Mathematics 447

Appendix B Equations of Elasticity 455

Appendix C Solution Techniques for Linear Algebraic Equations 463

Appendix D The Finite Element Personal Computer Program 473

Appendix E Problems for Computer Solution 476

Index 488

EXPANDED TABLE OF CONTENTS

Preface xi

Chapter 1

Basic Concepts of the Finite Element Method 1

- 1.1 Introduction 1
- 1.2 How does the Finite Element Method Work? 1
 - 1.2.1 *Comparison of Finite Element and Exact Solutions 4*
 - 1.2.2 *Comparison of Finite Element and Finite Difference Methods 7*
- 1.3 A General Procedure for Finite Element Analysis 10
 - 1.3.1 *Preprocessing 10*
 - 1.3.2 *Solution 10*
 - 1.3.3 *Postprocessing 11*
- 1.4 Brief History of the Finite Element Method 11
- 1.5 Examples of Finite Element Analysis 12
- 1.6 Objectives of the Text 16

Chapter 2

Stiffness Matrices, Spring and Bar Elements 19

- 2.1 Introduction 19
- 2.2 Linear Spring as a Finite Element 20
 - 2.2.1 *System Assembly in Global Coordinates 23*
- 2.3 Elastic Bar, Spar/Link/Truss Element 31
- 2.4 Strain Energy, Castigliano's First Theorem 38
- 2.5 Minimum Potential Energy 44
- 2.6 Summary 47

Chapter 3

Truss Structures: The Direct Stiffness Method 51

- 3.1 Introduction 51
- 3.2 Nodal Equilibrium Equations 53
- 3.3 Element Transformation 58
 - 3.3.1 *Direction Cosines 61*
- 3.4 Direct Assembly of Global Stiffness Matrix 61
- 3.5 Boundary Conditions, Constraint Forces 67
- 3.6 Element Strain and Stress 68
- 3.7 Comprehensive Example 72
- 3.8 Three-Dimensional Trusses 79
- 3.9 Summary 83

Chapter 4

Flexure Elements 91

- 4.1 Introduction 91
- 4.2 Elementary Beam Theory 91
- 4.3 Flexure Element 94
- 4.4 Flexure Element Stiffness Matrix 98
- 4.5 Element Load Vector 102
- 4.6 Work Equivalence for Distributed Loads 106
- 4.7 Flexure Element with Axial Loading 114
- 4.8 A General Three-Dimensional Beam Element 120
- 4.9 Closing Remarks 124

Chapter 5

Method of Weighted Residuals 131

- 5.1 Introduction 131
- 5.2 Method of Weighted Residuals 131

- 5.3 The Galerkin Finite Element Method** 140
 - 5.3.1 Element Formulation* 142
- 5.4 Application of Galerkin's Method to Structural Elements** 148
 - 5.4.1 Spar Element* 148
 - 5.4.2 Beam Element* 149
- 5.5 One-Dimensional Heat Conduction** 152
- 5.6 Closing Remarks** 158

Chapter 6

Interpolation Functions for General Element Formulation 163

- 6.1 Introduction** 163
- 6.2 Compatibility and Completeness Requirements** 164
 - 6.2.1 Compatibility* 165
 - 6.2.2 Completeness* 166
- 6.3 Polynomial Forms: One-Dimensional Elements** 166
 - 6.3.1 Higher-Order One-Dimensional Elements* 170
- 6.4 Polynomial Forms: Geometric Isotropy** 174
- 6.5 Triangular Elements** 176
 - 6.5.1 Area Coordinates* 179
 - 6.5.2 Six-Node Triangular Element* 181
 - 6.5.3 Integration in Area Coordinates* 182
- 6.6 Rectangular Elements** 184
- 6.7 Three-Dimensional Elements** 187
 - 6.7.1 Four-Node Tetrahedral Element* 188
 - 6.7.2 Eight-Node Brick Element* 191
- 6.8 Isoparametric Formulation** 193
- 6.9 Axisymmetric Elements** 202
- 6.10 Numerical Integration: Gaussian Quadrature** 206
- 6.11 Closing Remarks** 214

Chapter 7

Applications in Heat Transfer 222

- 7.1 Introduction** 222
- 7.2 One-Dimensional Conduction: Quadratic Element** 222
- 7.3 One-Dimensional Conduction with Convection** 227
 - 7.3.1 Finite Element Formulation* 228
 - 7.3.2 Boundary Conditions* 231
- 7.4 Heat Transfer in Two Dimensions** 235
 - 7.4.1 Finite Element Formulation* 236
 - 7.4.2 Boundary Conditions* 240
 - 7.4.3 Symmetry Conditions* 253
 - 7.4.4 Element Resultants* 254
 - 7.4.5 Internal Heat Generation* 259
- 7.5 Heat Transfer with Mass Transport** 261
- 7.6 Heat Transfer in Three Dimensions** 267
 - 7.6.1 System Assembly and Boundary Conditions* 269
- 7.7 Axisymmetric Heat Transfer** 271
 - 7.7.1 Finite Element Formulation* 273
- 7.8 Time-Dependent Heat Transfer** 277
 - 7.8.1 Finite Difference Methods for the Transient Response: Initial Conditions* 279
 - 7.8.2 Central Difference and Backward Difference Methods* 283
- 7.9 Closing Remarks** 285

Chapter 8

Applications in Fluid Mechanics 293

- 8.1 Introduction** 293
- 8.2 Governing Equations for Incompressible Flow** 295
 - 8.2.1 Rotational and Irrotational Flow* 296
- 8.3 The Stream Function in Two-Dimensional Flow** 298
 - 8.3.1 Finite Element Formulation* 299
 - 8.3.2 Boundary Conditions* 300

- 8.4 The Velocity Potential Function in Two-Dimensional Flow 304
 - 8.4.1 *Flow around Multiple Bodies* 312
- 8.5 Incompressible Viscous Flow 314
 - 8.5.1 *Stokes Flow* 315
 - 8.5.2 *Viscous Flow with Inertia* 321
- 8.6 Summary 323

Chapter 9

Applications in Solid Mechanics 327

- 9.1 Introduction 327
- 9.2 Plane Stress 328
 - 9.2.1 *Finite Element Formulation: Constant Strain Triangle* 330
 - 9.2.2 *Stiffness Matrix Evaluation* 333
 - 9.2.3 *Distributed Loads and Body Force* 335
- 9.3 Plane Strain: Rectangular Element 342
- 9.4 Isoparametric Formulation of the Plane Quadrilateral Element 347
- 9.5 Axisymmetric Stress Analysis 356
 - 9.5.1 *Finite Element Formulation* 359
 - 9.5.2 *Element Loads* 360
- 9.6 General Three-Dimensional Stress Elements 364
 - 9.6.1 *Finite Element Formulation* 365
- 9.7 Strain and Stress Computation 368
- 9.8 Practical Considerations 372
- 9.9 Torsion 375
 - 9.9.1 *Boundary Condition* 377
 - 9.9.2 *Torque* 377
 - 9.9.3 *Finite Element Formulation* 378
- 9.10 Summary 382

Chapter 10

Structural Dynamics 387

- 10.1 Introduction 387
- 10.2 The Simple Harmonic Oscillator 387
 - 10.2.1 *Forced Vibration* 392

- 10.3 Multiple Degrees-of-Freedom Systems 394
 - 10.3.1 *Many Degrees-of-Freedom Systems* 398
- 10.4 Bar Elements: Consistent Mass Matrix 402
- 10.5 Beam Elements 407
- 10.6 Mass Matrix for a General Element: Equations of Motion 412
- 10.7 Orthogonality of the Principal Modes 418
- 10.8 Harmonic Response Using Mode Superposition 422
- 10.9 Energy Dissipation: Structural Damping 424
 - 10.9.1 *General Structural Damping* 427
- 10.10 Transient Dynamic Response 432
- 10.11 Bar Element Mass Matrix in Two-Dimensional Truss Structures 434
- 10.12 Practical Considerations 442
- 10.13 Summary 443

Appendix A

Matrix Mathematics 447

- A.1 Definitions 447
- A.2 Algebraic Operations 449
- A.3 Determinants 450
- A.4 Matrix Inversion 451
- A.5 Matrix Partitioning 454

Appendix B

Equations of Elasticity 455

- B.1 Strain-Displacement Relations 455
- B.2 Stress-Strain Relations 458
- B.3 Equilibrium Equations 460
- B.4 Compatibility Equations 461

Appendix C**Solution Techniques for Linear Algebraic Equations 463**

- C.1 Cramer's Method 463
- C.2 Gauss Elimination 465
- C.3 *LU* Decomposition 467
- C.4 Frontal Solution 470

Appendix D**The Finite Element Personal Computer Program 473**

- D.1 Preprocessing 473
- D.2 Solution 474
- D.3 Postprocessing 474

Appendix E**Problems for Computer Solution 476**

- E.1 Chapter 3 476
- E.2 Chapter 4 479
- E.3 Chapter 7 481
- E.4 Chapter 9 484
- E.5 Chapter 10 487

Index 488

PREFACE

Fundamentals of Finite Element Analysis is intended to be the text for a senior-level finite element course in engineering programs. The most appropriate major programs are civil engineering, engineering mechanics, and mechanical engineering. The finite element method is such a widely used analysis-and-design technique that it is essential that undergraduate engineering students have a basic knowledge of the theory and applications of the technique. Toward that objective, I developed and taught an undergraduate “special topics” course on the finite element method at Washington State University in the summer of 1992. The course was composed of approximately two-thirds theory and one-third use of commercial software in solving finite element problems. Since that time, the course has become a regularly offered technical elective in the mechanical engineering program and is generally in high demand. During the developmental process for the course, I was never satisfied with any text that was used, and we tried many. I found the available texts to be at one extreme or the other; namely, essentially no theory and all software application, or all theory and no software application. The former approach, in my opinion, represents training in using computer programs, while the latter represents graduate-level study. I have written this text to seek a middle ground.

Pedagogically, I believe that training undergraduate engineering students to use a particular software package without providing knowledge of the underlying theory is a disservice to the student and can be dangerous for their future employers. While I am acutely aware that most engineering programs have a specific finite element software package available for student use, I do not believe that the text the students use should be tied only to that software. Therefore, I have written this text to be software-independent. I emphasize the basic theory of the finite element method, in a context that can be understood by undergraduate engineering students, and leave the software-specific portions to the instructor.

As the text is intended for an undergraduate course, the prerequisites required are statics, dynamics, mechanics of materials, and calculus through ordinary differential equations. Of necessity, partial differential equations are introduced but in a manner that should be understood based on the stated prerequisites. Applications of the finite element method to heat transfer and fluid mechanics are included, but the necessary derivations are such that previous coursework in those topics is not required. Many students will have taken heat transfer and fluid mechanics courses, and the instructor can expand the topics based on the students’ background.

Chapter 1 is a general introduction to the finite element method and includes a description of the basic concept of dividing a domain into finite-size subdomains. The finite difference method is introduced for comparison to the

finite element method. A general procedure in the sequence of model definition, solution, and interpretation of results is discussed and related to the generally accepted terms of preprocessing, solution, and postprocessing. A brief history of the finite element method is included, as are a few examples illustrating application of the method.

Chapter 2 introduces the concept of a finite element stiffness matrix and associated displacement equation, in terms of interpolation functions, using the linear spring as a finite element. The linear spring is known to most undergraduate students so the mechanics should not be new. However, representation of the spring as a finite element *is* new but provides a simple, concise example of the finite element method. The premise of spring element formulation is extended to the bar element, and energy methods are introduced. The first theorem of Castigliano is applied, as is the principle of minimum potential energy. Castigliano's theorem is a simple method to introduce the undergraduate student to minimum principles without use of variational calculus.

Chapter 3 uses the bar element of Chapter 2 to illustrate assembly of global equilibrium equations for a structure composed of many finite elements. Transformation from element coordinates to global coordinates is developed and illustrated with both two- and three-dimensional examples. The direct stiffness method is utilized and two methods for global matrix assembly are presented. Application of boundary conditions and solution of the resultant constraint equations is discussed. Use of the basic displacement solution to obtain element strain and stress is shown as a postprocessing operation.

Chapter 4 introduces the beam/flexure element as a bridge to continuity requirements for higher-order elements. Slope continuity is introduced and this requires an adjustment to the assumed interpolation functions to insure continuity. Nodal load vectors are discussed in the context of discrete and distributed loads, using the method of work equivalence.

Chapters 2, 3, and 4 introduce the basic procedures of finite-element modeling in the context of simple structural elements that should be well-known to the student from the prerequisite mechanics of materials course. Thus the emphasis in the early part of the course in which the text is used can be on the finite element method without introduction of new physical concepts. The bar and beam elements can be used to give the student practical truss and frame problems for solution using available finite element software. If the instructor is so inclined, the bar and beam elements (in the two-dimensional context) also provide a relatively simple framework for student development of finite element software using basic programming languages.

Chapter 5 is the springboard to more advanced concepts of finite element analysis. The method of weighted residuals is introduced as the fundamental technique used in the remainder of the text. The Galerkin method is utilized exclusively since I have found this method is both understandable for undergraduate students and is amenable to a wide range of engineering problems. The material in this chapter repeats the bar and beam developments and extends the finite element concept to one-dimensional heat transfer. Application to the bar

and beam elements illustrates that the method is in agreement with the basic mechanics approach of Chapters 2–4. Introduction of heat transfer exposes the student to additional applications of the finite element method that are, most likely, new to the student.

Chapter 6 is a stand-alone description of the requirements of interpolation functions used in developing finite element models for *any* physical problem. Continuity and completeness requirements are delineated. Natural (serendipity) coordinates, triangular coordinates, and volume coordinates are defined and used to develop interpolation functions for several element types in two- and three-dimensions. The concept of isoparametric mapping is introduced in the context of the plane quadrilateral element. As a precursor to following chapters, numerical integration using Gaussian quadrature is covered and several examples included. The use of two-dimensional elements to model three-dimensional axisymmetric problems is included.

Chapter 7 uses Galerkin's finite element method to develop the finite element equations for several commonly encountered situations in heat transfer. One-, two- and three-dimensional formulations are discussed for conduction and convection. Radiation is not included, as that phenomenon introduces a nonlinearity that undergraduate students are not prepared to deal with at the intended level of the text. Heat transfer with mass transport is included. The finite difference method in conjunction with the finite element method is utilized to present methods of solving time-dependent heat transfer problems.

Chapter 8 introduces finite element applications to fluid mechanics. The general equations governing fluid flow are so complex and nonlinear that the topic is introduced via ideal flow. The stream function and velocity potential function are illustrated and the applicable restrictions noted. Example problems are included that note the analogy with heat transfer and use heat transfer finite element solutions to solve ideal flow problems. A brief discussion of viscous flow shows the nonlinearities that arise when nonideal flows are considered.

Chapter 9 applies the finite element method to problems in solid mechanics with the proviso that the material response is linearly elastic and small deflection. Both plane stress and plane strain are defined and the finite element formulations developed for each case. General three-dimensional states of stress and axisymmetric stress are included. A model for torsion of noncircular sections is developed using the Prandtl stress function. The purpose of the torsion section is to make the student aware that all torsionally loaded objects are not circular and the analysis methods must be adjusted to suit geometry.

Chapter 10 introduces the concept of dynamic motion of structures. It is not presumed that the student has taken a course in mechanical vibrations; as a result, this chapter includes a primer on basic vibration theory. Most of this material is drawn from my previously published text *Applied Mechanical Vibrations*. The concept of the mass or inertia matrix is developed by examples of simple spring-mass systems and then extended to continuous bodies. Both lumped and consistent mass matrices are defined and used in examples. Modal analysis is the basic method espoused for dynamic response; hence, a considerable amount of

text material is devoted to determination of natural modes, orthogonality, and modal superposition. Combination of finite difference and finite element methods for solving transient dynamic structural problems is included.

The appendices are included in order to provide the student with material that might be new or may be “rusty” in the student’s mind.

Appendix A is a review of matrix algebra and should be known to the student from a course in linear algebra.

Appendix B states the general three-dimensional constitutive relations for a homogeneous, isotropic, elastic material. I have found over the years that undergraduate engineering students do not have a firm grasp of these relations. In general, the student has been exposed to so many special cases that the three-dimensional equations are not truly understood.

Appendix C covers three methods for solving linear algebraic equations. Some students may use this material as an outline for programming solution methods. I include the appendix only so the reader is aware of the algorithms underlying the software he/she will use in solving finite element problems.

Appendix D describes the basic computational capabilities of the FEPC software. The FEPC (FEPfinite element program for the PCpersonal computer) was developed by the late Dr. Charles Knight of Virginia Polytechnic Institute and State University and is used in conjunction with this text with permission of his estate. Dr. Knight’s programs allow analysis of two-dimensional programs using bar, beam, and plane stress elements. The appendix describes in general terms the capabilities and limitations of the software. The FEPC program is available to the student at www.mhhe.com/hutton.

Appendix E includes problems for several chapters of the text that should be solved via commercial finite element software. Whether the instructor has available ANSYS, ALGOR, COSMOS, etc., these problems are oriented to systems having many degrees of freedom and not amenable to hand calculation. Additional problems of this sort will be added to the website on a continuing basis.

The textbook features a Web site (www.mhhe.com/hutton) with finite element analysis links and the FEPC program. At this site, instructors will have access to PowerPoint images and an Instructors’ Solutions Manual. Instructors can access these tools by contacting their local McGraw-Hill sales representative for password information.

I thank Raghu Agarwal, Rong Y. Chen, Nels Madsen, Robert L. Rankin, Joseph J. Rencis, Stephen R. Swanson, and Lonny L. Thompson, who reviewed some or all of the manuscript and provided constructive suggestions and criticisms that have helped improve the book.

I am grateful to all the staff at McGraw-Hill who have labored to make this project a reality. I especially acknowledge the patient encouragement and professionalism of Jonathan Plant, Senior Editor, Lisa Kalner Williams, Developmental Editor, and Kay Brimeyer, Senior Project Manager.

David V. Hutton
Pullman, WA

CHAPTER

1

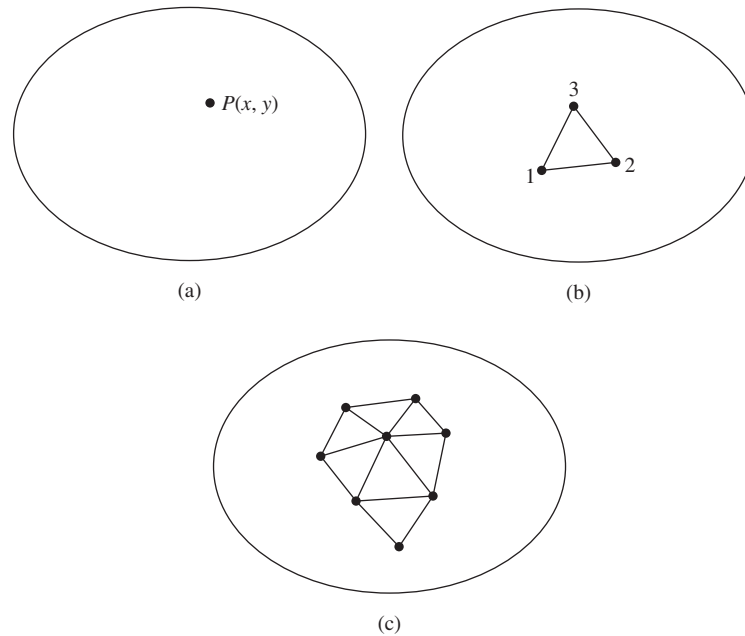
Basic Concepts of the Finite Element Method

1.1 INTRODUCTION

The finite element method (FEM), sometimes referred to as *finite element analysis* (FEA), is a computational technique used to obtain approximate solutions of boundary value problems in engineering. Simply stated, a boundary value problem is a mathematical problem in which one or more dependent variables must satisfy a differential equation everywhere within a known domain of independent variables and satisfy specific conditions on the boundary of the domain. Boundary value problems are also sometimes called *field* problems. The field is the domain of interest and most often represents a physical structure. The *field variables* are the dependent variables of interest governed by the differential equation. The *boundary conditions* are the specified values of the field variables (or related variables such as derivatives) on the boundaries of the field. Depending on the type of physical problem being analyzed, the field variables may include physical displacement, temperature, heat flux, and fluid velocity to name only a few.

1.2 HOW DOES THE FINITE ELEMENT METHOD WORK?

The general techniques and terminology of finite element analysis will be introduced with reference to Figure 1.1. The figure depicts a volume of some material or materials having known physical properties. The volume represents the domain of a boundary value problem to be solved. For simplicity, at this point, we assume a two-dimensional case with a single field variable $\phi(x, y)$ to be determined at every point $P(x, y)$ such that a known governing equation (or equations) is satisfied exactly at every such point. Note that this implies an exact

**Figure 1.1**

(a) A general two-dimensional domain of field variable $\phi(x, y)$.
(b) A three-node finite element defined in the domain. (c) Additional elements showing a partial finite element mesh of the domain.

mathematical solution is obtained; that is, the solution is a closed-form algebraic expression of the independent variables. In practical problems, the domain may be geometrically complex as is, often, the governing equation and the likelihood of obtaining an exact closed-form solution is very low. Therefore, approximate solutions based on numerical techniques and digital computation are most often obtained in engineering analyses of complex problems. Finite element analysis is a powerful technique for obtaining such approximate solutions with good accuracy.

A small triangular element that encloses a finite-sized subdomain of the area of interest is shown in Figure 1.1b. That this element is *not* a differential element of size $dx \times dy$ makes this a *finite element*. As we treat this example as a two-dimensional problem, it is assumed that the thickness in the z direction is constant and z dependency is not indicated in the differential equation. The vertices of the triangular element are numbered to indicate that these points are nodes. A *node* is a specific point in the finite element at which the value of the field variable is to be explicitly calculated. *Exterior* nodes are located on the boundaries of the finite element and may be used to connect an element to adjacent finite elements. Nodes that do not lie on element boundaries are *interior* nodes and cannot be connected to any other element. The triangular element of Figure 1.1b has only exterior nodes.

If the values of the field variable are computed only at nodes, how are values obtained at other points within a finite element? The answer contains the crux of the finite element method: The values of the field variable computed at the nodes are used to approximate the values at nonnodal points (that is, in the element interior) by *interpolation* of the nodal values. For the three-node triangle example, the nodes are all exterior and, at any other point within the element, the field variable is described by the approximate relation

$$\phi(x, y) = N_1(x, y)\phi_1 + N_2(x, y)\phi_2 + N_3(x, y)\phi_3 \quad (1.1)$$

where ϕ_1 , ϕ_2 , and ϕ_3 are the values of the field variable at the nodes, and N_1 , N_2 , and N_3 are the *interpolation functions*, also known as *shape functions* or *blending functions*. In the finite element approach, the nodal values of the field variable are treated as unknown *constants* that are to be determined. The interpolation functions are most often polynomial forms of the independent variables, derived to satisfy certain required conditions at the nodes. These conditions are discussed in detail in subsequent chapters. The major point to be made here is that the interpolation functions are predetermined, *known* functions of the independent variables; and these functions describe the variation of the field variable within the finite element.

The triangular element described by Equation 1.1 is said to have 3 *degrees of freedom*, as three nodal values of the field variable are required to describe the field variable everywhere in the element. This would be the case if the field variable represents a scalar field, such as temperature in a heat transfer problem (Chapter 7). If the domain of Figure 1.1 represents a thin, solid body subjected to plane stress (Chapter 9), the field variable becomes the displacement vector and the values of two components must be computed at each node. In the latter case, the three-node triangular element has 6 degrees of freedom. In general, the number of degrees of freedom associated with a finite element is equal to the product of the number of nodes and the number of values of the field variable (and possibly its derivatives) that must be computed at each node.

How does this element-based approach work over the entire domain of interest? As depicted in Figure 1.1c, every element is connected *at its exterior nodes* to other elements. The finite element equations are formulated such that, at the nodal connections, the value of the field variable at any connection is the same for each element connected to the node. Thus, continuity of the field variable at the nodes is ensured. In fact, finite element formulations are such that continuity of the field variable across interelement boundaries is also ensured. This feature avoids the physically unacceptable possibility of gaps or voids occurring in the domain. In structural problems, such gaps would represent physical separation of the material. In heat transfer, a “gap” would manifest itself in the form of different temperatures at the same physical point.

Although continuity of the field variable from element to element is inherent to the finite element formulation, interelement continuity of gradients (i.e., derivatives) of the field variable does not generally exist. This is a critical observation. In most cases, such derivatives are of more interest than are field variable values. For example, in structural problems, the field variable is displacement but

the true interest is more often in strain and stress. As *strain* is defined in terms of first derivatives of displacement components, strain is not continuous across element boundaries. However, the magnitudes of discontinuities of derivatives can be used to assess solution accuracy and convergence as the number of elements is increased, as is illustrated by the following example.

1.2.1 Comparison of Finite Element and Exact Solutions

The process of representing a physical domain with finite elements is referred to as *meshing*, and the resulting set of elements is known as the finite element *mesh*. As most of the commonly used element geometries have straight sides, it is generally impossible to include the entire physical domain in the element mesh if the domain includes curved boundaries. Such a situation is shown in Figure 1.2a, where a curved-boundary domain is meshed (quite coarsely) using square elements. A refined mesh for the same domain is shown in Figure 1.2b, using smaller, more numerous elements of the same type. Note that the refined mesh includes significantly more of the physical domain in the finite element representation and the curved boundaries are more closely approximated. (Triangular elements could approximate the boundaries even better.)

If the interpolation functions satisfy certain mathematical requirements (Chapter 6), a finite element solution for a particular problem converges to the exact solution of the problem. That is, as the number of elements is increased and the physical dimensions of the elements are decreased, the finite element solution changes incrementally. The incremental changes decrease with the mesh refinement process and approach the exact solution asymptotically. To illustrate convergence, we consider a relatively simple problem that has a known solution. Figure 1.3a depicts a tapered, solid cylinder fixed at one end and subjected to a tensile load at the other end. Assuming the displacement at the point of load application to be of interest, a first approximation is obtained by considering the cylinder to be uniform, having a cross-sectional area equal to the average area

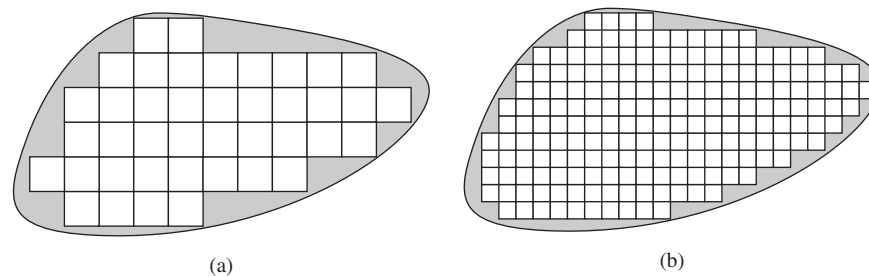


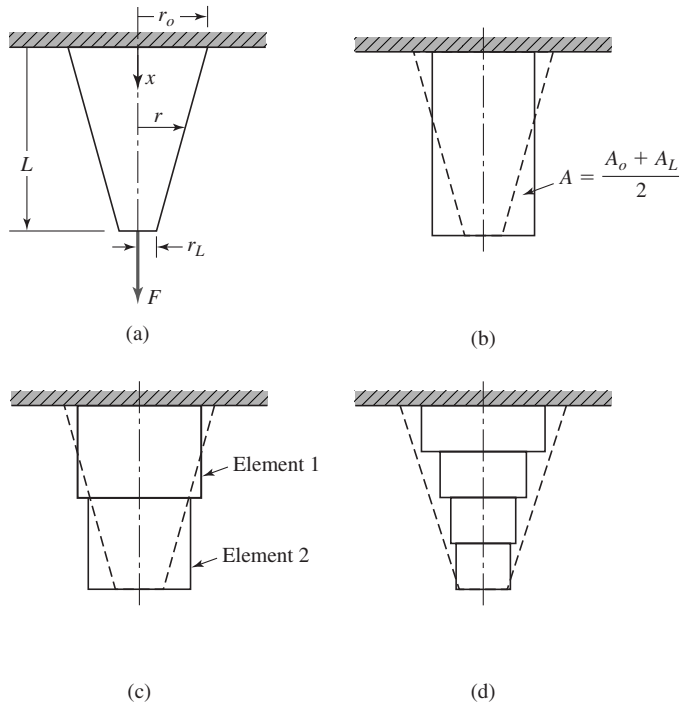
Figure 1.2

(a) Arbitrary curved-boundary domain modeled using square elements. Stippled areas are not included in the model. A total of 41 elements is shown. (b) Refined finite element mesh showing reduction of the area not included in the model. A total of 192 elements is shown.

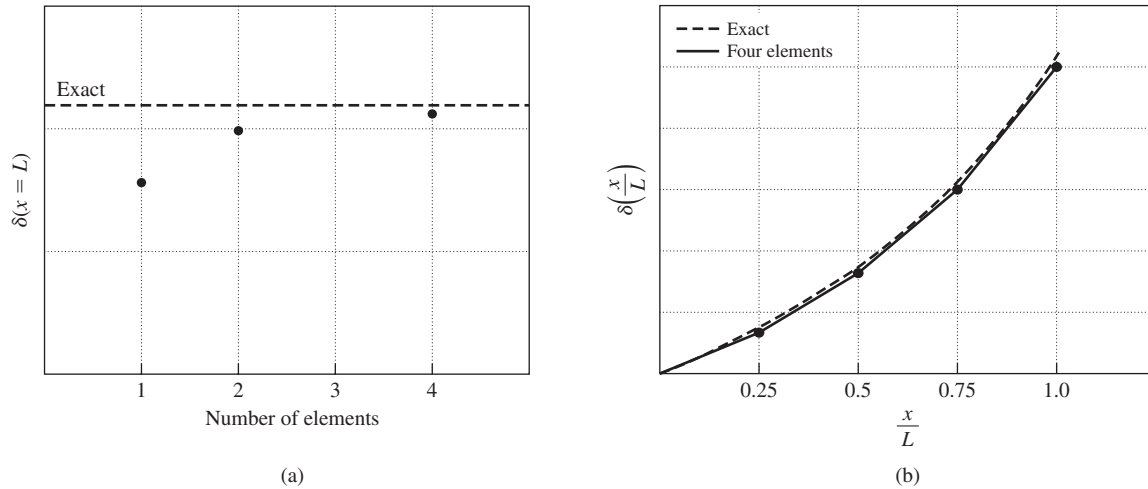
1.2 How Does the Finite Element Method Work?

5

of the cylinder (Figure 1.3b). The uniform bar is a *link* or *bar* finite element (Chapter 2), so our first approximation is a one-element, finite element model. The solution is obtained using the strength of materials theory. Next, we model the tapered cylinder as two uniform bars in series, as in Figure 1.3c. In the two-element model, each element is of length equal to half the total length of the cylinder and has a cross-sectional area equal to the average area of the corresponding half-length of the cylinder. The mesh refinement is continued using a four-element model, as in Figure 1.3d, and so on. For this simple problem, the displacement of the end of the cylinder for each of the finite element models is as shown in Figure 1.4a, where the dashed line represents the known solution. Convergence of the finite element solutions to the exact solution is clearly indicated.

**Figure 1.3**

(a) Tapered circular cylinder subjected to tensile loading: $r(x) = r_0 - (x/L)(r_0 - r_L)$. (b) Tapered cylinder as a single axial (bar) element using an average area. Actual tapered cylinder is shown as dashed lines. (c) Tapered cylinder modeled as two, equal-length, finite elements. The area of each element is average over the respective tapered cylinder length. (d) Tapered circular cylinder modeled as four, equal-length finite elements. The areas are average over the respective length of cylinder (element length = $L/4$).

**Figure 1.4**

(a) Displacement at $x = L$ for tapered cylinder in tension of Figure 1.3. (b) Comparison of the exact solution and the four-element solution for a tapered cylinder in tension.

On the other hand, if we plot displacement as a function of position along the length of the cylinder, we can observe convergence as well as the approximate nature of the finite element solutions. Figure 1.4b depicts the exact strength of materials solution and the displacement solution for the four-element models. We note that the displacement variation in each element is a linear approximation to the true nonlinear solution. The linear variation is directly attributable to the fact that the interpolation functions for a bar element are linear. Second, we note that, as the mesh is refined, the displacement solution converges to the nonlinear solution at *every point* in the solution domain.

The previous paragraph discussed convergence of the displacement of the tapered cylinder. As will be seen in Chapter 2, displacement is the primary field variable in structural problems. In most structural problems, however, we are interested primarily in stresses induced by specified loadings. The stresses must be computed via the appropriate stress-strain relations, and the strain components are derived from the displacement field solution. Hence, strains and stresses are referred to as *derived* variables. For example, if we plot the element stresses for the tapered cylinder example just cited for the exact solution as well as the finite element solutions for two- and four-element models as depicted in Figure 1.5, we observe that the stresses are constant in each element and represent a *discontinuous* solution of the problem in terms of stresses and strains. We also note that, as the number of elements increases, the jump discontinuities in stress decrease in magnitude. This phenomenon is characteristic of the finite element method. The formulation of the finite element method for a given problem is such that the primary field variable is continuous from element to element but

1.2 How Does the Finite Element Method Work?

7

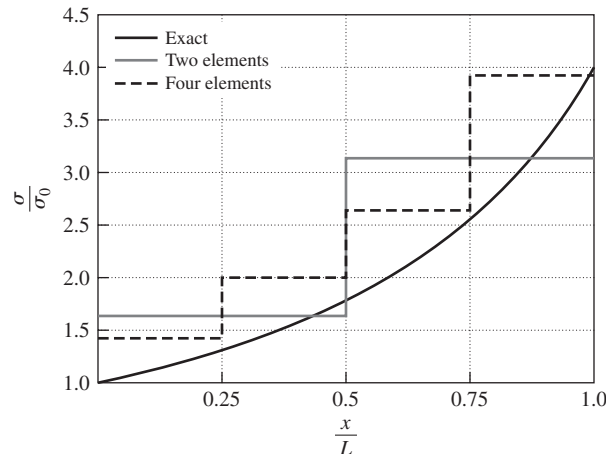


Figure 1.5
Comparison of the computed axial stress value in a tapered cylinder: $\sigma_0 = F/A_0$.

the derived variables are not necessarily continuous. In the limiting process of mesh refinement, the derived variables become closer and closer to continuity.

Our example shows how the finite element solution converges to a *known* exact solution (the exactness of the solution in this case is that of strength of materials theory). If we know the exact solution, we would not be applying the finite element method! So how do we assess the accuracy of a finite element solution for a problem with an unknown solution? The answer to this question is not simple. If we did not have the dashed line in Figure 1.3 representing the exact solution, we could still discern convergence to *a* solution. Convergence of a numerical method (such as the finite element method) is by no means assurance that the convergence is to the correct solution. A person using the finite element analysis technique must examine the solution analytically in terms of (1) numerical convergence, (2) reasonableness (does the result make sense?), (3) whether the physical laws of the problem are satisfied (is the structure in equilibrium? Does the heat output balance with the heat input?), and (4) whether the discontinuities in value of derived variables across element boundaries are reasonable. Many such questions must be posed and examined prior to accepting the results of a finite element analysis as representative of a correct solution useful for design purposes.

1.2.2 Comparison of Finite Element and Finite Difference Methods

The *finite difference* method is another numerical technique frequently used to obtain approximate solutions of problems governed by differential equations. Details of the technique are discussed in Chapter 7 in the context of transient heat

transfer. The method is also illustrated in Chapter 10 for transient dynamic analysis of structures. Here, we present the basic concepts of the finite difference method for purposes of comparison.

The finite difference method is based on the definition of the derivative of a function $f(x)$ that is

$$\frac{df(x)}{dx} = \lim_{\Delta x \rightarrow 0} \frac{f(x + \Delta x) - f(x)}{\Delta x} \quad (1.2)$$

where x is the independent variable. In the finite difference method, as implied by its name, derivatives are calculated via Equation 1.2 using small, but finite, values of Δx to obtain

$$\frac{df(x)}{dx} \approx \frac{f(x + \Delta x) - f(x)}{\Delta x} \quad (1.3)$$

A differential equation such as

$$\frac{df}{dx} + x = 0 \quad 0 \leq x \leq 1 \quad (1.4)$$

is expressed as

$$\frac{f(x + \Delta x) - f(x)}{\Delta x} + x = 0 \quad (1.5)$$

in the finite difference method. Equation 1.5 can be rewritten as

$$f(x + \Delta x) = f(x) - x(\Delta x) \quad (1.6)$$

where we note that the equality must be taken as “approximately equals.” From differential equation theory, we know that the solution of a first-order differential equation contains one constant of integration. The constant of integration must be determined such that one given condition (a boundary condition or initial condition) is satisfied. In the current example, we assume that the specified condition is $x(0) = A = \text{constant}$. If we choose an *integration step* Δx to be a small, constant value (the integration step is not *required* to be constant), then we can write

$$x_{i+1} = x_i + \Delta x \quad i = 0, N \quad (1.7)$$

where N is the total number of steps required to cover the domain. Equation 1.6 is then

$$f_{i+1} = f_i - x_i(\Delta x) \quad f_0 = A \quad i = 0, N \quad (1.8)$$

Equation 1.8 is known as a *recurrence relation* and provides an approximation to the value of the unknown function $f(x)$ at a number of discrete points in the domain of the problem.

To illustrate, Figure 1.6a shows the exact solution $f(x) = 1 - x^2/2$ and a finite difference solution obtained with $\Delta x = 0.1$. The finite difference solution is shown at the discrete points of function evaluation only. The manner of variation

1.2 How Does the Finite Element Method Work?

9

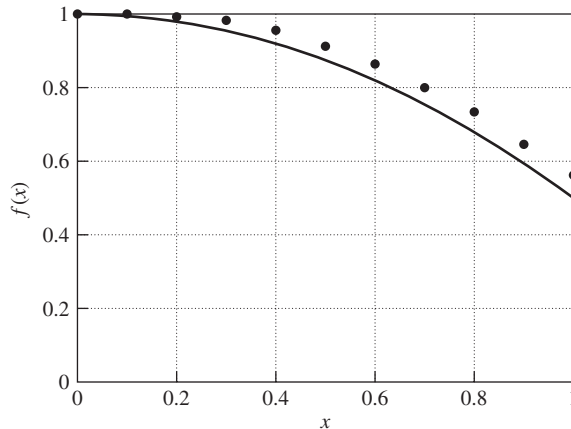


Figure 1.6
Comparison of the exact and finite difference
solutions of Equation 1.4 with $f_0 = A = 1$.

of the function between the calculated points is not known in the finite difference method. One can, of course, linearly interpolate the values to produce an approximation to the curve of the exact solution but the manner of interpolation is not an a priori determination in the finite difference method.

To contrast the finite difference method with the finite element method, we note that, in the finite element method, the variation of the field variable in the physical domain is an integral part of the procedure. That is, based on the selected interpolation functions, the variation of the field variable throughout a finite element is specified as an integral part of the problem formulation. In the finite difference method, this is not the case: The field variable is computed at specified points only. The major ramification of this contrast is that derivatives (to a certain level) can be computed in the finite element approach, whereas the finite difference method provides data only on the variable itself. In a structural problem, for example, both methods provide displacement solutions, but the finite element solution can be used to directly compute strain components (first derivatives). To obtain strain data in the finite difference method requires additional considerations not inherent to the mathematical model.

There are also certain similarities between the two methods. The integration points in the finite difference method are analogous to the nodes in a finite element model. The variable of interest is explicitly evaluated at such points. Also, as the integration step (step size) in the finite difference method is reduced, the solution is expected to converge to the exact solution. This is similar to the expected convergence of a finite element solution as the mesh of elements is refined. In both cases, the refinement represents reduction of the mathematical model from finite to infinitesimal. And in both cases, differential equations are reduced to algebraic equations.

Probably the most descriptive way to contrast the two methods is to note that the finite difference method models the differential equation(s) of the problem and uses numerical integration to obtain the solution at discrete points. The finite element method models the entire domain of the problem and uses known physical principles to develop algebraic equations describing the approximate solutions. Thus, the finite difference method models differential equations while the finite element method can be said to more closely model the physical problem at hand. As will be observed in the remainder of this text, there are cases in which a combination of finite element and finite difference methods is very useful and efficient in obtaining solutions to engineering problems, particularly where dynamic (transient) effects are important.

1.3 A GENERAL PROCEDURE FOR FINITE ELEMENT ANALYSIS

Certain steps in formulating a finite element analysis of a physical problem are common to all such analyses, whether structural, heat transfer, fluid flow, or some other problem. These steps are embodied in commercial finite element software packages (some are mentioned in the following paragraphs) and are implicitly incorporated in this text, although we do not necessarily refer to the steps explicitly in the following chapters. The steps are described as follows.

1.3.1 Preprocessing

The preprocessing step is, quite generally, described as defining the model and includes

- Define the geometric domain of the problem.
- Define the element type(s) to be used (Chapter 6).
- Define the material properties of the elements.
- Define the geometric properties of the elements (length, area, and the like).
- Define the element connectivities (mesh the model).
- Define the physical constraints (boundary conditions).
- Define the loadings.

The preprocessing (model definition) step is critical. In no case is there a better example of the computer-related axiom “garbage in, garbage out.” A perfectly computed finite element solution is of absolutely no value if it corresponds to the wrong problem.

1.3.2 Solution

During the solution phase, finite element software assembles the governing algebraic equations in matrix form and computes the unknown values of the primary field variable(s). The computed values are then used by back substitution to

compute additional, derived variables, such as reaction forces, element stresses, and heat flow.

As it is not uncommon for a finite element model to be represented by tens of thousands of equations, special solution techniques are used to reduce data storage requirements and computation time. For static, linear problems, a *wave front solver*, based on Gauss elimination (Appendix C), is commonly used. While a complete discussion of the various algorithms is beyond the scope of this text, the interested reader will find a thorough discussion in the Bathe book [1].

1.3.3 Postprocessing

Analysis and evaluation of the solution results is referred to as *postprocessing*. Postprocessor software contains sophisticated routines used for sorting, printing, and plotting selected results from a finite element solution. Examples of operations that can be accomplished include

- Sort element stresses in order of magnitude.
- Check equilibrium.
- Calculate factors of safety.
- Plot deformed structural shape.
- Animate dynamic model behavior.
- Produce color-coded temperature plots.

While solution data can be manipulated many ways in postprocessing, the most important objective is to apply sound engineering judgment in determining whether the solution results are physically reasonable.

1.4 BRIEF HISTORY OF THE FINITE ELEMENT METHOD

The mathematical roots of the finite element method dates back at least a half century. Approximate methods for solving differential equations using trial solutions are even older in origin. Lord Rayleigh [2] and Ritz [3] used trial functions (in our context, interpolation functions) to approximate solutions of differential equations. Galerkin [4] used the same concept for solution. The drawback in the earlier approaches, compared to the modern finite element method, is that the trial functions must apply over the *entire* domain of the problem of concern. While the Galerkin method provides a very strong basis for the finite element method (Chapter 5), not until the 1940s, when Courant [5] introduced the concept of piecewise-continuous functions in a subdomain, did the finite element method have its real start.

In the late 1940s, aircraft engineers were dealing with the invention of the jet engine and the needs for more sophisticated analysis of airframe structures to withstand larger loads associated with higher speeds. These engineers, without the benefit of modern computers, developed matrix methods of force analysis,

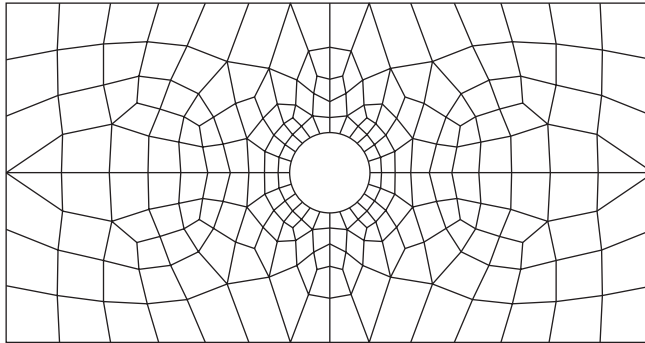
collectively known as the *flexibility method*, in which the unknowns are the forces and the knowns are displacements. The finite element method, in its most often-used form, corresponds to the *displacement method*, in which the unknowns are system displacements in response to applied force systems. In this text, we adhere exclusively to the displacement method. As will be seen as we proceed, the term *displacement* is quite general in the finite element method and can represent physical displacement, temperature, or fluid velocity, for example. The term *finite element* was first used by Clough [6] in 1960 in the context of plane stress analysis and has been in common usage since that time.

During the decades of the 1960s and 1970s, the finite element method was extended to applications in plate bending, shell bending, pressure vessels, and general three-dimensional problems in elastic structural analysis [7–11] as well as to fluid flow and heat transfer [12, 13]. Further extension of the method to large deflections and dynamic analysis also occurred during this time period [14, 15]. An excellent history of the finite element method and detailed bibliography is given by Noor [16].

The finite element method is computationally intensive, owing to the required operations on very large matrices. In the early years, applications were performed using mainframe computers, which, at the time, were considered to be very powerful, high-speed tools for use in engineering analysis. During the 1960s, the finite element software code NASTRAN [17] was developed in conjunction with the space exploration program of the United States. NASTRAN was the first major finite element software code. It was, and still is, capable of hundreds of thousands of degrees of freedom (nodal field variable computations). In the years since the development of NASTRAN, many commercial software packages have been introduced for finite element analysis. Among these are ANSYS [18], ALGOR [19], and COSMOS/M [20]. In today's computational environment, most of these packages can be used on desktop computers and engineering workstations to obtain solutions to large problems in static and dynamic structural analysis, heat transfer, fluid flow, electromagnetics, and seismic response. In this text, we do not utilize or champion a particular code. Rather, we develop the fundamentals for understanding of finite element analysis to enable the reader to use such software packages with an educated understanding.

1.5 EXAMPLES OF FINITE ELEMENT ANALYSIS

We now present, briefly, a few examples of the types of problems that can be analyzed via the finite element method. Figure 1.7 depicts a rectangular region with a central hole. The area has been “meshed” with a finite element grid of two-dimensional elements assumed to have a constant thickness in the z direction. Note that the mesh of elements is irregular: The element shapes (triangles and quadrilaterals) and sizes vary. In particular, note that around the geometric discontinuity of the hole, the elements are of smaller size. This represents not only

**Figure 1.7**

A mesh of finite elements over a rectangular region having a central hole.

an improvement in geometric accuracy in the vicinity of the discontinuity but also solution accuracy, as is discussed in subsequent chapters.

The geometry depicted in Figure 1.7 could represent the finite element model of several physical problems. For plane stress analysis, the geometry would represent a thin plate with a central hole subjected to edge loading in the plane depicted. In this case, the finite element solution would be used to examine stress concentration effects in the vicinity of the hole. The element mesh shown could also represent the case of fluid flow around a circular cylinder. In yet another application, the model shown could depict a heat transfer fin attached to a pipe (the hole) from which heat is transferred to the fin for dissipation to the surroundings. In each case, the formulation of the equations governing physical behavior of the elements in response to external influences is quite different.

Figure 1.8a shows a truss module that was at one time considered a building-block element for space station construction [21]. Designed to fold in accordion fashion into a small volume for transport into orbit, the module, when deployed, extends to overall dimensions $1.4 \text{ m} \times 1.4 \text{ m} \times 2.8 \text{ m}$. By attaching such modules end-to-end, a truss of essentially any length could be obtained. The structure was analyzed via the finite element method to determine the vibration characteristics as the number of modules, thus overall length, was varied. As the connections between the various structural members are pin or ball-and-socket joints, a simple axial tension-compression element (Chapter 2) was used in the model. The finite element model of one module was composed of 33 elements. A sample vibration shape of a five-module truss is shown in Figure 1.8b.

The truss example just described involves a rather large structure modeled by a small number of relatively large finite elements. In contrast, Figure 1.9 shows the finite element model of a very thin tube designed for use in heat

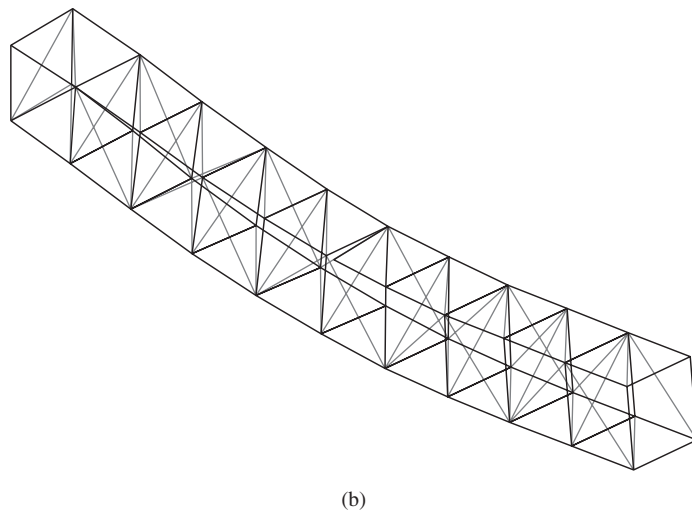
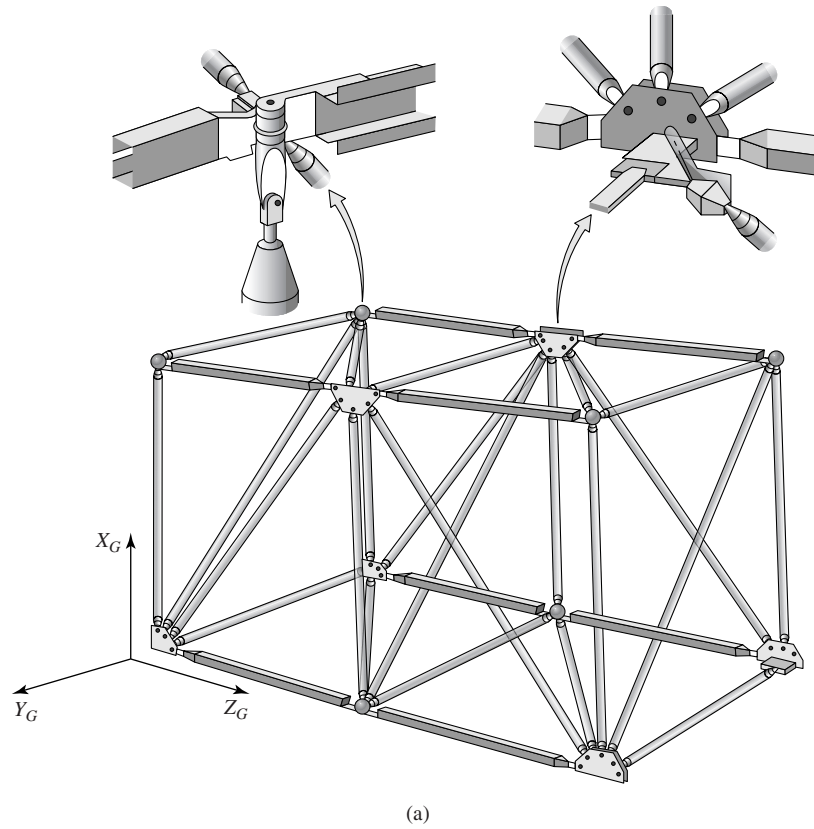


Figure 1.8

(a) Deployable truss module showing details of folding joints.

(b) A sample vibration-mode shape of a five-module truss as obtained via finite element analysis. (Courtesy: AIAA)

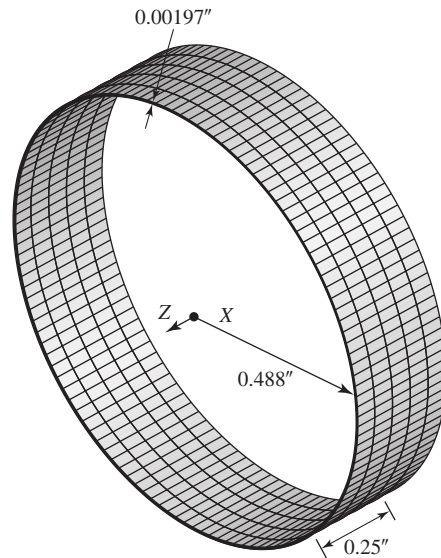
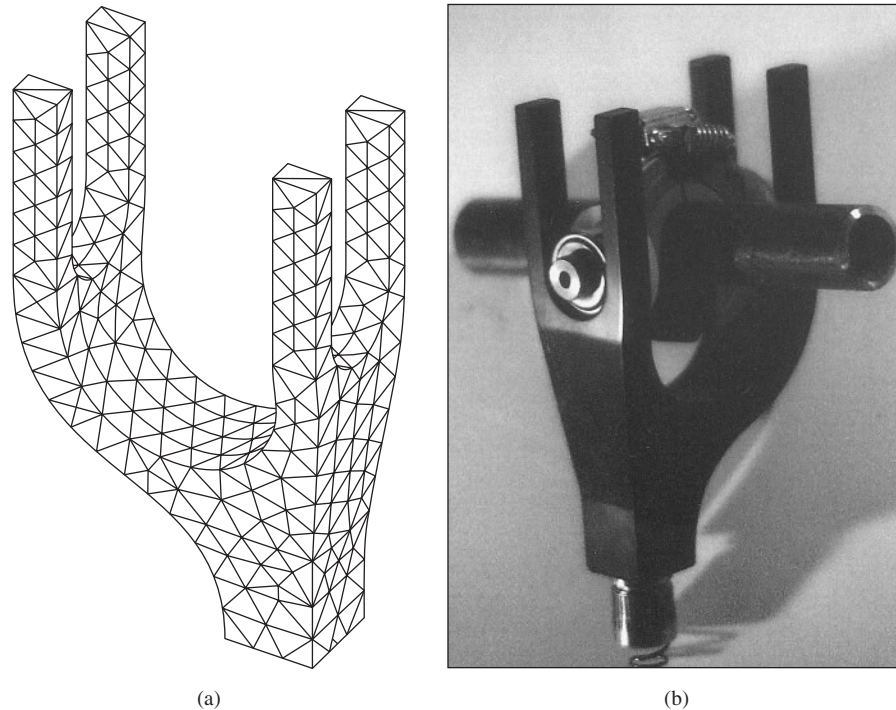


Figure 1.9
Finite element model of a thin-walled
heat exchanger tube.

transfer in a spacecraft application. The tube has inside diameter of 0.976 in. and wall thickness 0.00197 in. and overall length 36 in. Materials considered for construction of the tube were copper and titanium alloys. Owing to the wall thickness, prototype tubes were found to be very fragile and difficult to handle without damage. The objectives of the finite element analysis were to examine the bending, torsional, and buckling loads allowable. The figure shows the finite element mesh used to model a section of the tube only 0.25 in. in length. This model contains 1920 three-dimensional solid elements, each having eight nodes with 3 degrees of freedom at each node. Such a large number of elements was required for a small structure in consideration of computational accuracy. The concern here was the so-called *aspect ratio* of the elements, as is defined and discussed in subsequent chapters.

As a final example, Figure 1.10a represents the finite element model of the main load-carrying component of a prosthetic device. The device is intended to be a hand attachment to an artificial arm. In use, the hand would allow a lower arm amputee to engage in weight lifting as part of a physical fitness program. The finite element model was used to determine the stress distribution in the component in terms of the range of weight loading anticipated, so as to properly size the component and select the material. Figure 1.10b shows a prototype of the completed hand design.

**Figure 1.10**

(a) A finite element model of a prosthetic hand for weightlifting. (b) Completed prototype of a prosthetic hand, attached to a bar.
(Courtesy of Payam Sadat. All rights reserved.)

1.6 OBJECTIVES OF THE TEXT

I wrote *Fundamentals of Finite Element Analysis* for use in senior-level finite element courses in engineering programs. The majority of available textbooks on the finite element method are written for graduate-level courses. These texts are heavy on the theory of finite element analysis and rely on mathematical techniques (notably, *variational calculus*) that are not usually in the repertoire of undergraduate engineering students. Knowledge of advanced mathematical techniques is not required for successful use of this text. The prerequisite study is based on the undergraduate coursework common to most engineering programs: linear algebra, calculus through differential equations, and the usual series of statics, dynamics, and mechanics of materials. Although not required, prior study of fluid mechanics and heat transfer is helpful. Given this assumed background, the finite element method is developed on the basis of physical laws (equilibrium, conservation of mass, and the like), the principle of minimum potential energy (Chapter 2), and Galerkin's finite element method (introduced and developed in Chapter 5).

As the reader progresses through the text, he or she will discern that we cover a significant amount of finite element theory in addition to application examples. Given the availability of many powerful and sophisticated finite element software packages, why study the theory? The finite element method is a tool, and like any other tool, using it without proper instruction can be quite dangerous. My premise is that the proper instruction in this context includes understanding the basic theory underlying formulation of finite element models of physical problems. As stated previously, critical analysis of the results of a finite element model computation is essential, since those results may eventually become the basis for design. Knowledge of the theory is necessary for both proper modeling and evaluation of computational results.

REFERENCES

1. Bathe, K.-J. *Finite Element Procedures*. Englewood Cliffs, NJ: Prentice-Hall, 1996.
2. Lord Rayleigh. "On the Theory of Resonance." *Transactions of the Royal Society (London)* A161 (1870).
3. Ritz, W. "Über eine neue Methode zur Lösung gewissen Variations-Probleme der mathematischen Physik." *J. Reine Angew. Math.* 135 (1909).
4. Galerkin, B. G. "Series Solution of Some Problems of Elastic Equilibrium of Rods and Plates" [in Russian]. *Vestn. Inzh. Tekh.* 19 (1915).
5. Courant, R. "Variational Methods for the Solution of Problems of Equilibrium and Vibrations." *Bulletin of the American Mathematical Society* 49 (1943).
6. Clough, R. W. "The Finite Element Method in Plane Stress Analysis." *Proceedings, American Society of Civil Engineers, Second Conference on Electronic Computation*, Pittsburgh, 1960.
7. Melosh, R. J. "A Stiffness Method for the Analysis of Thin Plates in Bending." *Journal of Aerospace Sciences* 28, no. 1 (1961).
8. Grafton, P. E., and D. R. Strome. "Analysis of Axisymmetric Shells by the Direct Stiffness Method." *Journal of the American Institute of Aeronautics and Astronautics* 1, no. 10 (1963).
9. Gallagher, R. H. "Analysis of Plate and Shell Structures." *Proceedings, Symposium on the Application of Finite Element Methods in Civil Engineering*, Vanderbilt University, Nashville, 1969.
10. Wilson, E. L. "Structural Analysis of Axisymmetric Solids." *Journal of the American Institute of Aeronautics and Astronautics* 3, (1965).
11. Melosh, R. J. "Structural Analysis of Solids." *Journal of the Structural Division, Proceedings of the American Society of Civil Engineers*, August 1963.
12. Martin, H. C. "Finite Element Analysis of Fluid Flows." *Proceedings of the Second Conference on Matrix Methods in Structural Mechanics*, Wright-Patterson Air Force Base, Kilborn, Ohio, October 1968.
13. Wilson, E. L., and R. E. Nickell. "Application of the Finite Element Method to Heat Conduction Analysis." *Nuclear Engineering Design* 4 (1966).

14. Turner, M. J., E. H. Dill, H. C. Martin, and R. J. Melosh. "Large Deflections of Structures Subjected to Heating and External Loads." *Journal of Aeronautical Sciences* 27 (1960).
15. Archer, J. S. "Consistent Mass Matrix Formulations for Structural Analysis Using Finite Element Techniques." *Journal of the American Institute of Aeronautics and Astronautics* 3, no. 10 (1965).
16. Noor, A. K. "Bibliography of Books and Monographs on Finite Element Technology." *Applied Mechanics Reviews* 44, no. 6 (1991).
17. MSC/NASTRAN. Lowell, MA: MacNeal-Schwindler Corp.
18. ANSYS. Houston, PA: Swanson Analysis Systems Inc.
19. ALGOR. Pittsburgh: Algor Interactive Systems.
20. COSMOS/M. Los Angeles: Structural Research and Analysis Corp.
21. Hutton, D. V. "Modal Analysis of a Deployable Truss Using the Finite Element Method." *Journal of Spacecraft and Rockets* 21, no. 5 (1984).

CHAPTER 2

Stiffness Matrices, Spring and Bar Elements

2.1 INTRODUCTION

The primary characteristics of a finite element are embodied in the element *stiffness matrix*. For a structural finite element, the stiffness matrix contains the geometric and material behavior information that indicates the resistance of the element to deformation when subjected to loading. Such deformation may include axial, bending, shear, and torsional effects. For finite elements used in nonstructural analyses, such as fluid flow and heat transfer, the term *stiffness matrix* is also used, since the matrix represents the resistance of the element to change when subjected to external influences.

This chapter develops the finite element characteristics of two relatively simple, one-dimensional structural elements, a linearly elastic spring and an elastic tension-compression member. These are selected as introductory elements because the behavior of each is relatively well-known from the commonly studied engineering subjects of statics and strength of materials. Thus, the “bridge” to the finite element method is not obscured by theories new to the engineering student. Rather, we build on known engineering principles to introduce finite element concepts. The linear spring and the tension-compression member (hereafter referred to as a *bar* element and also known in the finite element literature as a *spar*, *link*, or *truss* element) are also used to introduce the concept of *interpolation functions*. As mentioned briefly in Chapter 1, the basic premise of the finite element method is to describe the continuous variation of the field variable (in this chapter, physical displacement) in terms of discrete values at the finite element nodes. In the interior of a finite element, as well as along the boundaries (applicable to two- and three-dimensional problems), the field variable is described via interpolation functions (Chapter 6) that must satisfy prescribed conditions.

Finite element analysis is based, dependent on the type of problem, on several mathematic/physical principles. In the present introduction to the method,

we present several such principles applicable to finite element analysis. First, and foremost, for spring and bar systems, we utilize the principle of static equilibrium but—and this is essential—we include *deformation* in the development; that is, we are not dealing with rigid body mechanics. For extension of the finite element method to more complicated elastic structural systems, we also state and apply the first theorem of Castigliano [1] and the more widely used principle of minimum potential energy [2]. Castigliano's first theorem, in the form presented, may be new to the reader. The first theorem is the counterpart of Castigliano's second theorem, which is more often encountered in the study of elementary strength of materials [3]. Both theorems relate displacements and applied forces to the equilibrium conditions of a mechanical system in terms of mechanical energy. The use here of Castigliano's first theorem is for the distinct purpose of introducing the concept of minimum potential energy without resort to the higher mathematic principles of the calculus of variations, which is beyond the mathematical level intended for this text.

2.2 LINEAR SPRING AS A FINITE ELEMENT

A linear elastic spring is a mechanical device capable of supporting axial loading only and constructed such that, over a reasonable operating range (meaning extension or compression beyond undeformed length), the elongation or contraction of the spring is directly proportional to the applied axial load. The constant of proportionality between deformation and load is referred to as the *spring constant*, *spring rate*, or *spring stiffness* [4], generally denoted as k , and has units of force per unit length. Formulation of the linear spring as a finite element is accomplished with reference to Figure 2.1a. As an elastic spring supports axial loading only, we select an *element coordinate system* (also known as a *local coordinate system*) as an x axis oriented along the length of the spring, as shown. The element coordinate system is embedded in the element and chosen, by geometric convenience, for simplicity in describing element behavior. The element

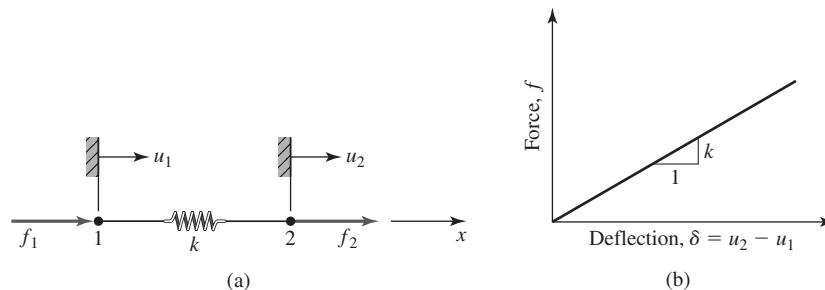


Figure 2.1

(a) Linear spring element with nodes, nodal displacements, and nodal forces.
(b) Load-deflection curve.

or local coordinate system is contrasted with the *global* coordinate system. The global coordinate system is that system in which the behavior of a complete structure is to be described. By *complete structure* is meant the assembly of many finite elements (at this point, several springs) for which we desire to compute response to loading conditions. In this chapter, we deal with cases in which the local and global coordinate systems are essentially the same except for translation of origin. In two- and three-dimensional cases, however, the distinctions are quite different and require mathematical rectification of element coordinate systems to a common basis. The common basis is the global coordinate system.

Returning attention to Figure 2.1a, the ends of the spring are the *nodes* and the nodal displacements are denoted by u_1 and u_2 and are shown in the positive sense. If these nodal displacements are known, the total elongation or contraction of the spring is known as is the *net force* in the spring. At this point in our development, we require that forces be applied to the element only at the nodes (distributed forces are accommodated for other element types later), and these are denoted as f_1 and f_2 and are also shown in the positive sense.

Assuming that both the nodal displacements are zero when the spring is undeformed, the net spring deformation is given by

$$\delta = u_2 - u_1 \quad (2.1)$$

and the resultant axial force in the spring is

$$f = k\delta = k(u_2 - u_1) \quad (2.2)$$

as is depicted in Figure 2.1b.

For equilibrium, $f_1 + f_2 = 0$ or $f_1 = -f_2$, and we can rewrite Equation 2.2 in terms of the applied nodal forces as

$$f_1 = -k(u_2 - u_1) \quad (2.3a)$$

$$f_2 = k(u_2 - u_1) \quad (2.3b)$$

which can be expressed in matrix form (see Appendix A for a review of matrix algebra) as

$$\begin{bmatrix} k & -k \\ -k & k \end{bmatrix} \begin{Bmatrix} u_1 \\ u_2 \end{Bmatrix} = \begin{Bmatrix} f_1 \\ f_2 \end{Bmatrix} \quad (2.4)$$

or

$$[k_e]\{u\} = \{f\} \quad (2.5)$$

where

$$[k_e] = \begin{bmatrix} k & -k \\ -k & k \end{bmatrix} \quad (2.6)$$

is defined as the element stiffness matrix in the element coordinate system (or local system), $\{u\}$ is the column matrix (vector) of nodal displacements, and $\{f\}$ is the column matrix (vector) of element nodal forces. (In subsequent chapters,

the matrix notation is used extensively. A general matrix is designated by brackets [] and a column matrix (vector) by braces { }.)

Equation 2.6 shows that the element stiffness matrix for the linear spring element is a 2×2 matrix. This corresponds to the fact that the element exhibits two nodal displacements (or degrees of freedom) and that the two displacements are not independent (that is, the body is continuous and elastic). Furthermore, the matrix is symmetric. A symmetric matrix has off-diagonal terms such that $k_{ij} = k_{ji}$. Symmetry of the stiffness matrix is indicative of the fact that the body is linearly elastic and each displacement is related to the other by the same physical phenomenon. For example, if a force F (positive, tensile) is applied at node 2 with node 1 held fixed, the *relative* displacement of the two nodes is the same as if the force is applied *symmetrically* (negative, tensile) at node 1 with node 2 fixed. (Counterexamples to symmetry are seen in heat transfer and fluid flow analyses in Chapters 7 and 8.) As will be seen as more complicated structural elements are developed, this is a general result: An element exhibiting N degrees of freedom has a corresponding $N \times N$, symmetric stiffness matrix.

Next consider solution of the system of equations represented by Equation 2.4. In general, the nodal forces are prescribed and the objective is to solve for the unknown nodal displacements. Formally, the solution is represented by

$$\begin{Bmatrix} u_1 \\ u_2 \end{Bmatrix} = [k_e]^{-1} \begin{Bmatrix} f_1 \\ f_2 \end{Bmatrix} \quad (2.7)$$

where $[k_e]^{-1}$ is the inverse of the element stiffness matrix. However, this inverse matrix does not exist, since the determinant of the element stiffness matrix is identically zero. Therefore, the element stiffness matrix is *singular*, and this also proves to be a general result in most cases. The physical significance of the singular nature of the element stiffness matrix is found by reexamination of Figure 2.1a, which shows that no displacement constraint whatever has been imposed on motion of the spring element; that is, the spring is not connected to any physical object that would prevent or limit motion of either node. With no constraint, it is not possible to solve for the nodal displacements individually. Instead, only the *difference* in nodal displacements can be determined, as this difference represents the elongation or contraction of the spring element owing to elastic effects. As discussed in more detail in the general formulation of interpolation functions (Chapter 6) and structural dynamics (Chapter 10), a properly formulated finite element must allow for constant value of the field variable. In the example at hand, this means rigid body motion. We can see the rigid body motion capability in terms of a single spring (element) and in the context of several connected elements. For a single, unconstrained element, if arbitrary forces are applied at each node, the spring not only deforms axially but also undergoes acceleration according to Newton's second law. Hence, there exists not only deformation but overall motion. If, in a connected system of spring elements, the overall system response is such that nodes 1 and 2 of a particular element displace the same amount, there is no elastic deformation of the spring and therefore

no elastic force in the spring. This physical situation must be included in the element formulation. The capability is indicated mathematically by singularity of the element stiffness matrix. As the stiffness matrix is formulated on the basis of *deformation* of the element, we cannot expect to compute nodal displacements if there is no deformation of the element.

Equation 2.7 indicates the mathematical operation of inverting the stiffness matrix to obtain solutions. In the context of an individual element, the singular nature of an element stiffness matrix precludes this operation, as the inverse of a singular matrix does not exist. As is illustrated profusely in the remainder of the text, the general solution of a finite element problem, in a global, as opposed to element, context, involves the solution of equations of the form of Equation 2.5. For realistic finite element models, which are of huge dimension in terms of the matrix order ($N \times N$) involved, computing the inverse of the stiffness matrix is a very inefficient, time-consuming operation, which should not be undertaken except for the very simplest of systems. Other, more-efficient solution techniques are available, and these are discussed subsequently. (Many of the end-of-chapter problems included in this text are of small order and can be efficiently solved via matrix inversion using “spreadsheet” software functions or software such as MATLAB.)

2.2.1 System Assembly in Global Coordinates

Derivation of the element stiffness matrix for a spring element was based on equilibrium conditions. The same procedure can be applied to a connected system of spring elements by writing the equilibrium equation for each node. However, rather than drawing free-body diagrams of each node and formally writing the equilibrium equations, the nodal equilibrium equations can be obtained more efficiently by considering the effect of each element separately and adding the element force contribution to each nodal equation. The process is described as “assembly,” as we take individual stiffness components and “put them together” to obtain the system equations. To illustrate, via a simple example, the assembly of element characteristics into *global* (or *system*) equations, we next consider the system of two linear spring elements connected as shown in Figure 2.2.

For generality, it is assumed that the springs have different spring constants k_1 and k_2 . The nodes are numbered 1, 2, and 3 as shown, with the springs sharing node 2 as the physical connection. Note that these are *global* node numbers. The *global* nodal displacements are identified as U_1 , U_2 , and U_3 , where the upper case is used to indicate that the quantities represented are *global* or *system* displacements as opposed to individual element displacements. Similarly, applied nodal

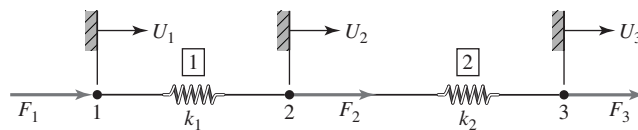


Figure 2.2 System of two springs with node numbers, element numbers, nodal displacements, and nodal forces.

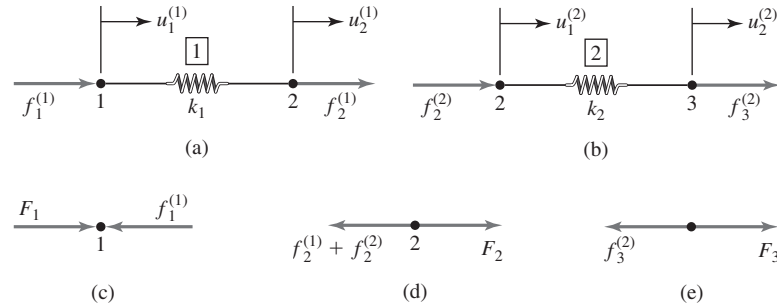


Figure 2.3 Free-body diagrams of elements and nodes for the two-element system of Figure 2.2.

forces are F_1 , F_2 , and F_3 . Assuming the system of two spring elements to be in equilibrium, we examine free-body diagrams of the springs individually (Figure 2.3a and 2.3b) and express the equilibrium conditions for each spring, using Equation 2.4, as

$$\begin{bmatrix} k_1 & -k_1 \\ -k_1 & k_1 \end{bmatrix} \begin{Bmatrix} u_1^{(1)} \\ u_2^{(1)} \end{Bmatrix} = \begin{Bmatrix} f_1^{(1)} \\ f_2^{(1)} \end{Bmatrix} \quad (2.8a)$$

$$\begin{bmatrix} k_2 & -k_2 \\ -k_2 & k_2 \end{bmatrix} \begin{Bmatrix} u_1^{(2)} \\ u_2^{(2)} \end{Bmatrix} = \begin{Bmatrix} f_2^{(2)} \\ f_3^{(2)} \end{Bmatrix} \quad (2.8b)$$

where the superscript is element number.

To begin “assembling” the equilibrium equations describing the behavior of the system of two springs, the displacement *compatibility conditions*, which relate element displacements to system displacements, are written as

$$u_1^{(1)} = U_1 \quad u_2^{(1)} = U_2 \quad u_1^{(2)} = U_2 \quad u_2^{(2)} = U_3 \quad (2.9)$$

The compatibility conditions state the physical fact that the springs are connected at node 2, remain connected at node 2 after deformation, and hence, must have the same nodal displacement at node 2. Thus, element-to-element displacement continuity is enforced at nodal connections. Substituting Equations 2.9 into Equations 2.8, we obtain

$$\begin{bmatrix} k_1 & -k_1 \\ -k_1 & k_1 \end{bmatrix} \begin{Bmatrix} U_1 \\ U_2 \end{Bmatrix} = \begin{Bmatrix} f_1^{(1)} \\ f_2^{(1)} \end{Bmatrix} \quad (2.10a)$$

and

$$\begin{bmatrix} k_2 & -k_2 \\ -k_2 & k_2 \end{bmatrix} \begin{Bmatrix} U_2 \\ U_3 \end{Bmatrix} = \begin{Bmatrix} f_2^{(2)} \\ f_3^{(2)} \end{Bmatrix} \quad (2.10b)$$

Here, we use the notation $f_i^{(j)}$ to represent the force exerted on element j at node i .

Equation 2.10 is the equilibrium equations for each spring element expressed in terms of the specified global displacements. In this form, the equations clearly show that the elements are physically connected at node 2 and have the same displacement U_2 at that node. These equations are not yet amenable to direct combination, as the displacement vectors are not the same. We expand both matrix equations to 3×3 as follows (while formally expressing the facts that element 1 is not connected to node 3 and element 2 is not connected to node 1):

$$\begin{bmatrix} k_1 & -k_1 & 0 \\ -k_1 & k_1 & 0 \\ 0 & 0 & 0 \end{bmatrix} \begin{Bmatrix} U_1 \\ U_2 \\ 0 \end{Bmatrix} = \begin{Bmatrix} f_1^{(1)} \\ f_2^{(1)} \\ 0 \end{Bmatrix} \quad (2.11)$$

$$\begin{bmatrix} 0 & 0 & 0 \\ 0 & k_2 & -k_2 \\ 0 & -k_2 & k_2 \end{bmatrix} \begin{Bmatrix} 0 \\ U_2 \\ U_3 \end{Bmatrix} = \begin{Bmatrix} 0 \\ f_2^{(2)} \\ f_3^{(2)} \end{Bmatrix} \quad (2.12)$$

The addition of Equations 2.11 and 2.12 yields

$$\begin{bmatrix} k_1 & -k_1 & 0 \\ -k_1 & k_1 + k_2 & -k_2 \\ 0 & -k_2 & k_2 \end{bmatrix} \begin{Bmatrix} U_1 \\ U_2 \\ U_3 \end{Bmatrix} = \begin{Bmatrix} f_1^{(1)} \\ f_2^{(1)} + f_2^{(2)} \\ f_3^{(2)} \end{Bmatrix} \quad (2.13)$$

Next, we refer to the free-body diagrams of each of the three nodes depicted in Figure 2.3c, 2.3d, and 2.3e. The equilibrium conditions for nodes 1, 2, and 3 show that

$$f_1^{(1)} = F_1 \quad f_2^{(1)} + f_2^{(2)} = F_2 \quad f_3^{(2)} = F_3 \quad (2.14)$$

respectively. Substituting into Equation 2.13, we obtain the final result:

$$\begin{bmatrix} k_1 & -k_1 & 0 \\ -k_1 & k_1 + k_2 & -k_2 \\ 0 & -k_2 & k_2 \end{bmatrix} \begin{Bmatrix} U_1 \\ U_2 \\ U_3 \end{Bmatrix} = \begin{Bmatrix} F_1 \\ F_2 \\ F_3 \end{Bmatrix} \quad (2.15)$$

which is of the form $[K]\{U\} = \{F\}$, similar to Equation 2.5. However, Equation 2.15 represents the equations governing the *system* composed of two connected spring elements. By direct consideration of the equilibrium conditions, we obtain the system stiffness matrix $[K]$ (note use of upper case) as

$$[K] = \begin{bmatrix} k_1 & -k_1 & 0 \\ -k_1 & k_1 + k_2 & -k_2 \\ 0 & -k_2 & k_2 \end{bmatrix} \quad (2.16)$$

Note that the system stiffness matrix is (1) symmetric, as is the case with all linear systems referred to orthogonal coordinate systems; (2) singular, since no constraints are applied to prevent rigid body motion of the system; and (3) the system matrix is simply a superposition of the individual element stiffness matrices with proper assignment of element nodal displacements and associated stiffness coefficients to system nodal displacements. The superposition procedure is formalized in the context of frame structures in the following paragraphs.

EXAMPLE 2.1

Consider the two element system depicted in Figure 2.2 given that

Node 1 is attached to a fixed support, yielding the displacement constraint $U_1 = 0$.
 $k_1 = 50 \text{ lb./in.}$, $k_2 = 75 \text{ lb./in.}$, $F_2 = F_3 = 75 \text{ lb.}$

for these conditions determine nodal displacements U_2 and U_3 .

■ Solution

Substituting the specified values into Equation 2.15 yields

$$\begin{bmatrix} 50 & -50 & 0 \\ -50 & 125 & -75 \\ 0 & -75 & 75 \end{bmatrix} \begin{Bmatrix} 0 \\ U_2 \\ U_3 \end{Bmatrix} = \begin{Bmatrix} F_1 \\ 75 \\ 75 \end{Bmatrix}$$

and we note that, owing to the constraint of zero displacement at node 1, nodal force F_1 becomes an unknown reaction force. Formally, the first algebraic equation represented in this matrix equation becomes

$$-50U_2 = F_1$$

and this is known as a *constraint equation*, as it represents the equilibrium condition of a node at which the displacement is constrained. The second and third equations become

$$\begin{bmatrix} 125 & -75 \\ -75 & 75 \end{bmatrix} \begin{Bmatrix} U_2 \\ U_3 \end{Bmatrix} = \begin{Bmatrix} 75 \\ 75 \end{Bmatrix}$$

which can be solved to obtain $U_2 = 3 \text{ in.}$ and $U_3 = 4 \text{ in.}$ Note that the matrix equations governing the unknown displacements are obtained by simply striking out the first row and column of the 3×3 matrix system, since the constrained displacement is zero. Hence, the constraint does not affect the values of the *active* displacements (we use the term *active* to refer to displacements that are unknown and must be computed). Substitution of the calculated values of U_2 and U_3 into the constraint equation yields the value $F_1 = -150 \text{ lb.}$, which value is clearly in equilibrium with the applied nodal forces of 75 lb. each. We also illustrate element equilibrium by writing the equations for each element as

$$\begin{bmatrix} 50 & -50 \\ -50 & 50 \end{bmatrix} \begin{Bmatrix} 0 \\ 3 \end{Bmatrix} = \begin{Bmatrix} f_1^{(1)} \\ f_2^{(1)} \end{Bmatrix} = \begin{Bmatrix} -150 \\ 150 \end{Bmatrix} \text{ lb.} \quad \text{for element 1}$$

$$\begin{bmatrix} 75 & -75 \\ -75 & 75 \end{bmatrix} \begin{Bmatrix} 3 \\ 4 \end{Bmatrix} = \begin{Bmatrix} f_2^{(2)} \\ f_3^{(2)} \end{Bmatrix} = \begin{Bmatrix} -75 \\ 75 \end{Bmatrix} \text{ lb.} \quad \text{for element 2}$$

Example 2.1 illustrates the general procedure for solution of finite element models: Formulate the system equilibrium equations, apply the specified constraint conditions, solve the reduced set of equations for the “active” displacements, and substitute the computed displacements into the constraint equations to obtain the unknown reactions. While not directly applicable for the spring element, for

more general finite element formulations, the computed displacements are also substituted into the strain relations to obtain element strains, and the strains are, in turn, substituted into the applicable stress-strain equations to obtain element stress values.

EXAMPLE 2.2

Figure 2.4a depicts a system of three linearly elastic springs supporting three equal weights W suspended in a vertical plane. Treating the springs as finite elements, determine the vertical displacement of each weight.

■ Solution

To treat this as a finite element problem, we assign node and element numbers as shown in Figure 2.4b and ignore, for the moment, that displacement U_1 is known to be zero by the fixed support constraint. Per Equation 2.6, the stiffness matrix of each element is (preprocessing)

$$[k^{(1)}] = \begin{bmatrix} 3k & -3k \\ -3k & 3k \end{bmatrix}$$

$$[k^{(2)}] = \begin{bmatrix} 2k & -2k \\ -2k & 2k \end{bmatrix}$$

$$[k^{(3)}] = \begin{bmatrix} k & -k \\ -k & k \end{bmatrix}$$

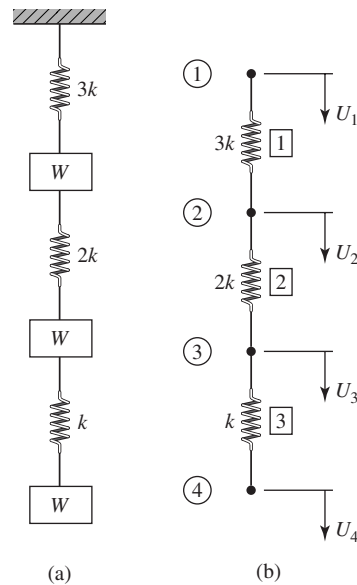


Figure 2.4 Example 2.2: elastic spring supporting weights.

The element-to-global displacement relations are

$$u_1^{(1)} = U_1 \quad u_2^{(1)} = u_1^{(2)} = U_2 \quad u_2^{(2)} = u_1^{(3)} = U_3 \quad u_2^{(3)} = U_4$$

Proceeding as in the previous example, we then write the individual element equations as

$$\begin{bmatrix} 3k & -3k & 0 & 0 \\ -3k & 3k & 0 & 0 \\ 0 & 0 & 0 & 0 \\ 0 & 0 & 0 & 0 \end{bmatrix} \begin{Bmatrix} U_1 \\ U_2 \\ U_3 \\ U_4 \end{Bmatrix} = \begin{Bmatrix} f_1^{(1)} \\ f_2^{(1)} \\ 0 \\ 0 \end{Bmatrix} \quad (1)$$

$$\begin{bmatrix} 0 & 0 & 0 & 0 \\ 0 & 2k & -2k & 0 \\ 0 & -2k & 2k & 0 \\ 0 & 0 & 0 & 0 \end{bmatrix} \begin{Bmatrix} U_1 \\ U_2 \\ U_3 \\ U_4 \end{Bmatrix} = \begin{Bmatrix} 0 \\ f_1^{(2)} \\ f_2^{(2)} \\ 0 \end{Bmatrix} \quad (2)$$

$$\begin{bmatrix} 0 & 0 & 0 & 0 \\ 0 & 0 & 0 & 0 \\ 0 & 0 & k & -k \\ 0 & 0 & -k & k \end{bmatrix} \begin{Bmatrix} U_1 \\ U_2 \\ U_3 \\ U_4 \end{Bmatrix} = \begin{Bmatrix} 0 \\ 0 \\ f_1^{(3)} \\ f_2^{(3)} \end{Bmatrix} \quad (3)$$

Adding Equations 1–3, we obtain

$$k \begin{bmatrix} 3 & -3 & 0 & 0 \\ -3 & 5 & -2 & 0 \\ 0 & -2 & 3 & -1 \\ 0 & 0 & -1 & 1 \end{bmatrix} \begin{Bmatrix} U_1 \\ U_2 \\ U_3 \\ U_4 \end{Bmatrix} = \begin{Bmatrix} F_1 \\ W \\ W \\ W \end{Bmatrix} \quad (4)$$

where we utilize the fact that the sum of the element forces at each node must equal the applied force at that node and, at node 1, the force is an unknown reaction.

Applying the displacement constraint $U_1 = 0$ (*this is also preprocessing*), we obtain

$$-3kU_2 = F_1 \quad (5)$$

as the constraint equation and the matrix equation

$$k \begin{bmatrix} 5 & -2 & 0 \\ -2 & 3 & -1 \\ 0 & -1 & 1 \end{bmatrix} \begin{Bmatrix} U_2 \\ U_3 \\ U_4 \end{Bmatrix} = \begin{Bmatrix} W \\ W \\ W \end{Bmatrix} \quad (6)$$

for the active displacements. Again note that Equation 6 is obtained by eliminating the constraint equation from 4 corresponding to the prescribed zero displacement.

Simultaneous solution (*the solution step*) of the algebraic equations represented by Equation 6 yields the displacements as

$$U_2 = \frac{W}{k} \quad U_3 = \frac{2W}{k} \quad U_4 = \frac{3W}{k}$$

and Equation 5 gives the reaction force as

$$F_1 = -3W$$

(This is *postprocessing*.)

Note that the solution is exactly that which would be obtained by the usual statics equations. Also note the general procedure as follows:

- Formulate the individual element stiffness matrices.
- Write the element to global displacement relations.
- Assemble the global equilibrium equation in matrix form.
- Reduce the matrix equations according to specified constraints.
- Solve the system of equations for the unknown nodal displacements (primary variables).
- Solve for the reaction forces (secondary variable) by back-substitution.

EXAMPLE 2.3

Figure 2.5 depicts a system of three linear spring elements connected as shown. The node and element numbers are as indicated. Node 1 is fixed to prevent motion, and node 3 is given a specified displacement δ as shown. Forces $F_2 = -F$ and $F_4 = 2F$ are applied at nodes 2 and 4. Determine the displacement of each node and the force required at node 3 for the specified conditions.

■ Solution

This example includes a *nonhomogeneous* boundary condition. In previous examples, the boundary conditions were represented by zero displacements. In this example, we have both a zero (homogeneous) and a specified nonzero (nonhomogeneous) displacement condition. The algebraic treatment must be different as follows. The system equilibrium equations are expressed in matrix form (Problem 2.6) as

$$\begin{bmatrix} k & -k & 0 & 0 \\ -k & 4k & -3k & 0 \\ 0 & -3k & 5k & -2k \\ 0 & 0 & -2k & 2k \end{bmatrix} \begin{Bmatrix} U_1 \\ U_2 \\ U_3 \\ U_4 \end{Bmatrix} = \begin{Bmatrix} F_1 \\ F_2 \\ F_3 \\ F_4 \end{Bmatrix} = \begin{Bmatrix} F_1 \\ -F \\ F_3 \\ 2F \end{Bmatrix}$$

Substituting the specified conditions $U_1 = 0$ and $U_3 = \delta$ results in the system of equations

$$\begin{bmatrix} k & -k & 0 & 0 \\ -k & 4k & -3k & 0 \\ 0 & -3k & 5k & -2k \\ 0 & 0 & -2k & 2k \end{bmatrix} \begin{Bmatrix} 0 \\ U_2 \\ \delta \\ U_4 \end{Bmatrix} = \begin{Bmatrix} F_1 \\ -F \\ F_3 \\ 2F \end{Bmatrix}$$

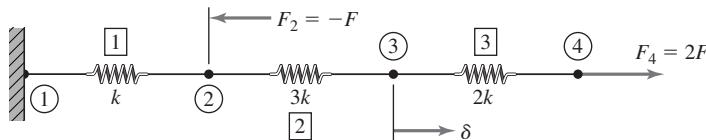


Figure 2.5 Example 2.3: Three-element system with specified nonzero displacement at node 3.

Since $U_1 = 0$, we remove the first row and column to obtain

$$\begin{bmatrix} 4k & -3k & 0 \\ -3k & 5k & -2k \\ 0 & -2k & 2k \end{bmatrix} \begin{Bmatrix} U_2 \\ \delta \\ U_4 \end{Bmatrix} = \begin{Bmatrix} -F \\ F_3 \\ 2F \end{Bmatrix}$$

as the system of equations governing displacements U_2 and U_4 and the unknown nodal force F_3 . This last set of equations clearly shows that we cannot simply strike out the row and column corresponding to the *nonzero* specified displacement δ because it appears in the equations governing the active displacements. To illustrate a general procedure, we rewrite the last matrix equation as

$$\begin{bmatrix} 5k & -3k & -2k \\ -3k & 4k & 0 \\ -2k & 0 & 2k \end{bmatrix} \begin{Bmatrix} \delta \\ U_2 \\ U_4 \end{Bmatrix} = \begin{Bmatrix} F_3 \\ -F \\ 2F \end{Bmatrix}$$

Next, we formally partition the stiffness matrix and write

$$\begin{bmatrix} 5k & -3k & -2k \\ -3k & 4k & 0 \\ -2k & 0 & 2k \end{bmatrix} \begin{Bmatrix} \delta \\ U_2 \\ U_4 \end{Bmatrix} = \begin{bmatrix} [K_{\delta\delta}] & [K_{\delta U}] \\ [K_{U\delta}] & [K_{UU}] \end{bmatrix} \begin{Bmatrix} \{\delta\} \\ \{U\} \end{Bmatrix} = \begin{Bmatrix} \{F_\delta\} \\ \{F_U\} \end{Bmatrix}$$

with

$$\begin{aligned} [K_{\delta\delta}] &= [5k] \\ [K_{\delta U}] &= [-3k \quad -2k] \\ [K_{U\delta}] &= [K_{\delta U}]^T = \begin{bmatrix} -3k \\ -2k \end{bmatrix} \\ [K_{UU}] &= \begin{bmatrix} 4k & 0 \\ 0 & 2k \end{bmatrix} \\ \{\delta\} &= \{\delta\} \\ \{U\} &= \begin{Bmatrix} U_2 \\ U_4 \end{Bmatrix} \\ \{F_\delta\} &= \{F_3\} \\ \{F_U\} &= \begin{Bmatrix} -F \\ 2F \end{Bmatrix} \end{aligned}$$

From the second “row” of the partitioned matrix equations, we have

$$[K_{U\delta}]\{\delta\} + [K_{UU}]\{U\} = \{F_U\}$$

and this can be solved for the unknown displacements to obtain

$$\{U\} = [K_{UU}]^{-1}(\{F\} - [K_{U\delta}]\{\delta\})$$

provided that $[K_{UU}]^{-1}$ exists. Since the constraints have been applied correctly, this inverse does exist and is given by

$$[K_{UU}]^{-1} = \begin{bmatrix} \frac{1}{4k} & 0 \\ 0 & \frac{1}{2k} \end{bmatrix}$$

2.3 Elastic Bar, Spar/Link/Truss Element

31

Substituting, we obtain the unknown displacements as

$$\{U\} = \begin{Bmatrix} U_2 \\ U_4 \end{Bmatrix} = \begin{bmatrix} \frac{1}{4k} & 0 \\ 0 & \frac{1}{2k} \end{bmatrix} \begin{Bmatrix} -F + 3k\delta \\ 2F + 2k\delta \end{Bmatrix} = \begin{Bmatrix} -\frac{F}{4k} + \frac{3\delta}{4} \\ \frac{F}{k} + \delta \end{Bmatrix}$$

The required force at node 3 is obtained by substitution of the displacement into the upper partition to obtain

$$F_3 = -\frac{5}{4}F + \frac{3}{4}k\delta$$

Finally, the reaction force at node 1 is

$$F_1 = -kU_2 = \frac{F}{4} - \frac{3}{4}k\delta$$

As a check on the results, we substitute the computed and prescribed displacements into the individual element equations to insure that equilibrium is satisfied.

Element 1

$$\begin{bmatrix} k & -k \\ -k & k \end{bmatrix} \begin{Bmatrix} 0 \\ U_2 \end{Bmatrix} = \begin{Bmatrix} -kU_2 \\ kU_2 \end{Bmatrix} = \begin{Bmatrix} f_1^{(1)} \\ f_2^{(1)} \end{Bmatrix}$$

which shows that the nodal forces on element 1 are equal and opposite as required for equilibrium.

Element 2

$$\begin{bmatrix} 3k & -3k \\ -3k & 3k \end{bmatrix} \begin{Bmatrix} U_2 \\ U_3 \end{Bmatrix} = \begin{bmatrix} 3k & -3k \\ -3k & 3k \end{bmatrix} \begin{Bmatrix} -\frac{F}{4k} + \frac{3}{4}\delta \\ \delta \end{Bmatrix} \\ = \begin{Bmatrix} -\frac{3F}{4k} - \frac{3}{4}k\delta \\ \frac{3F}{4k} + \frac{3}{4}k\delta \end{Bmatrix} = \begin{Bmatrix} f_2^{(2)} \\ f_3^{(2)} \end{Bmatrix}$$

which also verifies equilibrium.

Element 3

$$\begin{bmatrix} 2k & -2k \\ -2k & 2k \end{bmatrix} \begin{Bmatrix} U_3 \\ U_4 \end{Bmatrix} = \begin{bmatrix} 2k & -2k \\ -2k & 2k \end{bmatrix} \begin{Bmatrix} \delta \\ \frac{F}{k} + \delta \end{Bmatrix} = \begin{Bmatrix} -2F \\ 2F \end{Bmatrix} = \begin{Bmatrix} f_3^{(3)} \\ f_4^{(3)} \end{Bmatrix}$$

Therefore element 3 is in equilibrium as well.

2.3 ELASTIC BAR, SPAR/LINK/TRUSS ELEMENT

While the linear elastic spring serves to introduce the concept of the stiffness matrix, the usefulness of such an element in finite element analysis is rather limited. Certainly, springs are used in machinery in many cases and the availability of a finite element representation of a linear spring is quite useful in such cases. The

spring element is also often used to represent the elastic nature of supports for more complicated systems. A more generally applicable, yet similar, element is an elastic bar subjected to axial forces only. This element, which we simply call a *bar element*, is particularly useful in the analysis of both two- and three-dimensional frame or truss structures. Formulation of the finite element characteristics of an elastic bar element is based on the following assumptions:

1. The bar is geometrically straight.
2. The material obeys Hooke's law.
3. Forces are applied only at the ends of the bar.
4. The bar supports axial loading only; bending, torsion, and shear are not transmitted to the element via the nature of its connections to other elements.

The last assumption, while quite restrictive, is not impractical; this condition is satisfied if the bar is connected to other structural members via pins (2-D) or ball-and-socket joints (3-D). Assumptions 1 and 4, in combination, show that this is inherently a one-dimensional element, meaning that the elastic displacement of any point along the bar can be expressed in terms of a single independent variable. As will be seen, however, the bar element can be used in modeling both two- and three-dimensional structures. The reader will recognize this element as the familiar two-force member of elementary statics, meaning, for equilibrium, the forces exerted on the ends of the element must be colinear, equal in magnitude, and opposite in sense.

Figure 2.6 depicts an elastic bar of length L to which is affixed a uniaxial coordinate system x with its origin arbitrarily placed at the left end. This is the *element* coordinate system or reference frame. Denoting axial displacement at any position along the length of the bar as $u(x)$, we define nodes 1 and 2 at each end as shown and introduce the nodal displacements $u_1 = u(x = 0)$ and $u_2 = u(x = L)$. Thus, we have the continuous field variable $u(x)$, which is to be expressed (approximately) in terms of two nodal variables u_1 and u_2 . To accomplish this discretization, we assume the existence of *interpolation* functions $N_1(x)$ and $N_2(x)$ (also known as *shape* or *blending* functions) such that

$$u(x) = N_1(x)u_1 + N_2(x)u_2 \quad (2.17)$$

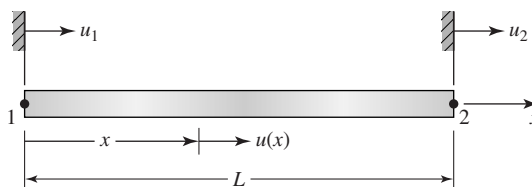


Figure 2.6 A bar (or truss) element with element coordinate system and nodal displacement notation.

(It must be emphasized that, although an equality is indicated by Equation 2.17, the relation, for finite elements in general, is an approximation. For the bar element, the relation, in fact, is exact.) To determine the interpolation functions, we require that the boundary values of $u(x)$ (the nodal displacements) be identically satisfied by the discretization such that

$$u(x = 0) = u_1 \quad u(x = L) = u_2 \quad (2.18)$$

Equations 2.17 and 2.18 lead to the following boundary (nodal) conditions:

$$N_1(0) = 1 \quad N_2(0) = 0 \quad (2.19)$$

$$N_1(L) = 0 \quad N_2(L) = 1 \quad (2.20)$$

which must be satisfied by the interpolation functions. It is required that the displacement expression, Equation 2.17, satisfy the end (nodal) conditions identically, since the nodes will be the connection points between elements and the displacement continuity conditions are enforced at those connections. As we have two conditions that must be satisfied by each of two one-dimensional functions, the simplest forms for the interpolation functions are polynomial forms:

$$N_1(x) = a_0 + a_1x \quad (2.21)$$

$$N_2(x) = b_0 + b_1x \quad (2.22)$$

where the polynomial coefficients are to be determined via satisfaction of the boundary (nodal) conditions. We note here that any number of mathematical forms of the interpolation functions could be assumed while satisfying the required conditions. The reasons for the linear form is explained in detail in Chapter 6.

Application of conditions represented by Equation 2.19 yields $a_0 = 1$, $b_0 = 0$ while Equation 2.20 results in $a_1 = -(1/L)$ and $b_1 = x/L$. Therefore, the interpolation functions are

$$N_1(x) = 1 - x/L \quad (2.23)$$

$$N_2(x) = x/L \quad (2.24)$$

and the continuous displacement function is represented by the discretization

$$u(x) = (1 - x/L)u_1 + (x/L)u_2 \quad (2.25)$$

As will be found most convenient subsequently, Equation 2.25 can be expressed in matrix form as

$$u(x) = [N_1(x) \quad N_2(x)] \begin{Bmatrix} u_1 \\ u_2 \end{Bmatrix} = [N] \{u\} \quad (2.26)$$

where $[N]$ is the row matrix of interpolation functions and $\{u\}$ is the column matrix (vector) of nodal displacements.

Having expressed the displacement field in terms of the nodal variables, the task remains to determine the relation between the nodal displacements and applied forces to obtain the stiffness matrix for the bar element. Recall from

elementary strength of materials that the deflection δ of an elastic bar of length L and uniform cross-sectional area A when subjected to axial load P is given by

$$\delta = \frac{PL}{AE} \quad (2.27)$$

where E is the modulus of elasticity of the material. Using Equation 2.27, we obtain the equivalent spring constant of an elastic bar as

$$k = \frac{P}{\delta} = \frac{AE}{L} \quad (2.28)$$

and could, by analogy with the linear elastic spring, immediately write the stiffness matrix as Equation 2.6. While the result is exactly correct, we take a more general approach to illustrate the procedures to be used with more complicated element formulations.

Ultimately, we wish to compute the nodal displacements given some loading condition on the element. To obtain the necessary equilibrium equations relating the displacements to applied forces, we proceed from displacement to strain, strain to stress, and stress to loading, as follows. In uniaxial loading, as in the bar element, we need consider only the normal strain component, defined as

$$\varepsilon_x = \frac{du}{dx} \quad (2.29)$$

which, when applied to Equation 2.25, gives

$$\varepsilon_x = \frac{u_2 - u_1}{L} \quad (2.30)$$

which shows that the spar element is a constant strain element. This is in accord with strength of materials theory: The element has constant cross-sectional area and is subjected to constant forces at the end points, so the strain does not vary along the length. The axial stress, by Hooke's law, is then

$$\sigma_x = E\varepsilon_x = E \frac{u_2 - u_1}{L} \quad (2.31)$$

and the associated axial force is

$$P = \sigma_x A = \frac{AE}{L}(u_2 - u_1) \quad (2.32)$$

Taking care to observe the correct algebraic sign convention, Equation 2.32 is now used to relate the applied nodal forces f_1 and f_2 to the nodal displacements u_1 and u_2 . Observing that, if Equation 2.32 has a positive sign, the element is in tension and nodal force f_2 must be in the positive coordinate direction while nodal force f_1 must be equal and opposite for equilibrium; therefore,

$$f_1 = -\frac{AE}{L}(u_2 - u_1) \quad (2.33)$$

$$f_2 = \frac{AE}{L}(u_2 - u_1) \quad (2.34)$$

2.3 Elastic Bar, Spar/Link/Truss Element

35

Equations 2.33 and 2.34 are expressed in matrix form as

$$\frac{AE}{L} \begin{bmatrix} 1 & -1 \\ -1 & 1 \end{bmatrix} \begin{Bmatrix} u_1 \\ u_2 \end{Bmatrix} = \begin{Bmatrix} f_1 \\ f_2 \end{Bmatrix} \quad (2.35)$$

Comparison of Equation 2.35 to Equation 2.4 shows that the stiffness matrix for the bar element is given by

$$[k_e] = \frac{AE}{L} \begin{bmatrix} 1 & -1 \\ -1 & 1 \end{bmatrix} \quad (2.36)$$

As is the case with the linear spring, we observe that the element stiffness matrix for the bar element is symmetric, singular, and of order 2×2 in correspondence with two nodal displacements or *degrees of freedom*. It must be emphasized that the stiffness matrix given by Equation 2.36 is expressed in the *element coordinate system*, which in this case is one-dimensional. Application of this element formulation to analysis of two- and three-dimensional structures is considered in the next chapter.

EXAMPLE 2.4

Figure 2.7a depicts a tapered elastic bar subjected to an applied tensile load P at one end and attached to a fixed support at the other end. The cross-sectional area varies linearly from A_0 at the fixed support at $x = 0$ to $A_0/2$ at $x = L$. Calculate the displacement of the end of the bar (a) by modeling the bar as a single element having cross-sectional area equal to the area of the actual bar at its midpoint along the length, (b) using two bar elements of equal length and similarly evaluating the area at the midpoint of each, and (c) using integration to obtain the exact solution.

■ **Solution**

- (a) For a single element, the cross-sectional area is $3A_0/4$ and the element “spring constant” is

$$k = \frac{AE}{L} = \frac{3A_0E}{4L}$$

and the element equations are

$$\frac{3A_0E}{4L} \begin{bmatrix} 1 & -1 \\ -1 & -1 \end{bmatrix} \begin{Bmatrix} U_1 \\ U_2 \end{Bmatrix} = \begin{Bmatrix} F_1 \\ P \end{Bmatrix}$$

The element and nodal displacements are as shown in Figure 2.7b. Applying the constraint condition $U_1 = 0$, we find

$$U_2 = \frac{4PL}{3A_0E} = 1.333 \frac{PL}{A_0E}$$

as the displacement at $x = L$.

- (b) Two elements of equal length $L/2$ with associated nodal displacements are depicted in Figure 2.7c. For element 1, $A_1 = 7A_0/8$ so

$$k_1 = \frac{A_1E}{L_1} = \frac{7A_0E}{8(L/2)} = \frac{7A_0E}{4L}$$

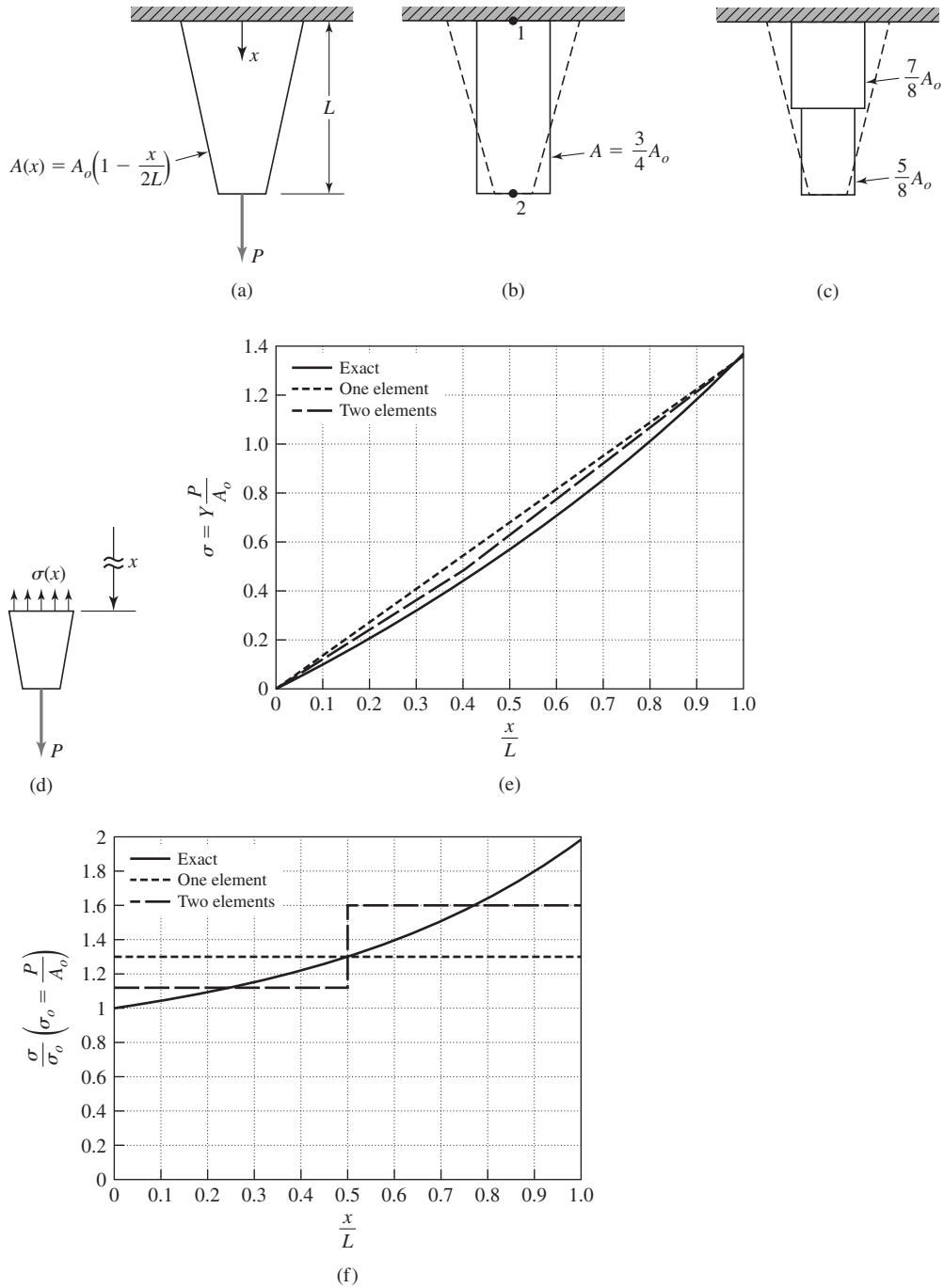


Figure 2.7
 (a) Tapered axial bar, (b) one-element model, (c) two-element model, (d) free-body diagram for an exact solution, (e) displacement solutions, (f) stress solutions.

2.3 Elastic Bar, Spar/Link/Truss Element

37

while for element 2, we have

$$A_1 = \frac{5A_0}{8} \quad \text{and} \quad k_2 = \frac{A_2 E}{L_2} = \frac{5A_0 E}{8(L/2)} = \frac{5A_0 E}{4L}$$

Since no load is applied at the center of the bar, the equilibrium equations for the system of two elements is

$$\begin{bmatrix} k_1 & -k_1 & 0 \\ -k_1 & k_1 + k_2 & -k_2 \\ 0 & -k_2 & k_2 \end{bmatrix} \begin{Bmatrix} U_1 \\ U_2 \\ U_3 \end{Bmatrix} = \begin{Bmatrix} F_1 \\ 0 \\ P \end{Bmatrix}$$

Applying the constraint condition $U_1 = 0$ results in

$$\begin{bmatrix} k_1 + k_2 & -k_2 \\ -k_2 & k_2 \end{bmatrix} \begin{Bmatrix} U_2 \\ U_3 \end{Bmatrix} = \begin{Bmatrix} 0 \\ P \end{Bmatrix}$$

Adding the two equations gives

$$U_2 = \frac{P}{k_1} = \frac{4PL}{7A_0 E}$$

and substituting this result into the first equation results in

$$U_3 = \frac{k_1 + k_2}{k_2} = \frac{48PL}{35A_0 E} = 1.371 \frac{PL}{A_0 E}$$

- (c) To obtain the exact solution, we refer to Figure 2.7d, which is a free-body diagram of a section of the bar between an arbitrary position x and the end $x = L$. For equilibrium,

$$\sigma_x A = P \quad \text{and since} \quad A = A(x) = A_0 \left(1 - \frac{x}{2L}\right)$$

the axial stress variation along the length of the bar is described by

$$\sigma_x = \frac{P}{A_0 \left(1 - \frac{x}{2L}\right)}$$

Therefore, the axial strain is

$$\epsilon_x = \frac{\sigma_x}{E} = \frac{P}{EA_0 \left(1 - \frac{x}{2L}\right)}$$

Since the bar is fixed at $x = 0$, the displacement at $x = L$ is given by

$$\begin{aligned} \delta &= \int_0^L \epsilon_x \, dx = \frac{P}{EA_0} \int_0^L \frac{dx}{\left(1 - \frac{x}{2L}\right)} \\ &= \frac{2PL}{EA_0} [-\ln(2L - x)]_0^L = \frac{2PL}{EA_0} [\ln(2L) - \ln L] = \frac{2PL}{EA_0} \ln 2 = 1.386 \frac{PL}{A_0 E} \end{aligned}$$

Comparison of the results of parts b and c reveals that the two element solution exhibits an error of only about 1 percent in comparison to the exact solution from strength of materials theory. Figure 2.7e shows the displacement variation along the length for the three solutions. It is extremely important to note, however, that the computed axial stress for the finite element solutions varies significantly from that of the exact solution. The axial stress for the two-element solution is shown in Figure 2.7f, along with the calculated stress from the exact solution. Note particularly the discontinuity of calculated stress values for the two elements at the connecting node. This is typical of the derived, or secondary, variables, such as stress and strain, as computed in the finite element method. As more and more smaller elements are used in the model, the values of such discontinuities decrease, indicating solution convergence. In structural analyses, the finite element user is most often more interested in stresses than displacements, hence it is essential that convergence of the secondary variables be monitored.

2.4 STRAIN ENERGY, CASTIGLIANO'S FIRST THEOREM

When external forces are applied to a body, the mechanical work done by those forces is converted, in general, into a combination of kinetic and potential energies. In the case of an elastic body constrained to prevent motion, all the work is stored in the body as elastic potential energy, which is also commonly referred to as *strain energy*. Here, strain energy is denoted U_e and mechanical work W . From elementary statics, the mechanical work performed by a force \vec{F} as its point of application moves along a path from position 1 to position 2 is defined as

$$W = \int_1^2 \vec{F} \cdot d\vec{r} \quad (2.37)$$

where

$$d\vec{r} = dx\vec{i} + dy\vec{j} + dz\vec{k} \quad (2.38)$$

is a differential vector along the path of motion. In Cartesian coordinates, work is given by

$$W = \int_{x_1}^{x_2} F_x dx + \int_{y_1}^{y_2} F_y dy + \int_{z_1}^{z_2} F_z dz \quad (2.39)$$

where F_x , F_y , and F_z are the Cartesian components of the force vector.

For linearly elastic deformations, deflection is directly proportional to applied force as, for example, depicted in Figure 2.8 for a linear spring. The slope of the force-deflection line is the spring constant such that $F = k\delta$. Therefore, the work required to deform such a spring by an arbitrary amount δ_0 from its

2.4 Strain Energy, Castigliano's First Theorem

39

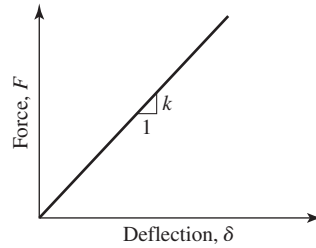


Figure 2.8 Force-deflection relation for a linear elastic spring.

free length is

$$W = \int_0^{\delta_0} F \, d\delta = \int_0^{\delta_0} k\delta \, d\delta = \frac{1}{2}k\delta_0^2 = U_e \quad (2.40)$$

and we observe that the work and resulting elastic potential energy are quadratic functions of displacement and have the units of force-length. This is a general result for linearly elastic systems, as will be seen in many examples throughout this text.

Utilizing Equation 2.28, the strain energy for an axially loaded elastic bar fixed at one end can immediately be written as

$$U_e = \frac{1}{2}k\delta^2 = \frac{1}{2} \frac{AE}{L} \delta^2 \quad (2.41)$$

However, for a more general purpose, this result is converted to a different form (applicable to a bar element only) as follows:

$$U_e = \frac{1}{2}k\delta^2 = \frac{1}{2} \frac{AE}{L} \left(\frac{PL}{AE} \right)^2 = \frac{1}{2} \left(\frac{P}{A} \right) \left(\frac{P}{AE} \right) AL = \frac{1}{2} \sigma \epsilon V \quad (2.42)$$

where V is the total volume of deformed material and the quantity $\frac{1}{2}\sigma\epsilon$ is *strain energy per unit volume*, also known as *strain energy density*. In Equation 2.42, stress and strain values are those corresponding to the *final* value of applied force. The factor $\frac{1}{2}$ arises from the linear relation between stress and strain as the load is applied from zero to the final value P . In general, for uniaxial loading, the strain energy per unit volume u_e is defined by

$$u_e = \int_0^{\epsilon} \sigma \, d\epsilon \quad (2.43)$$

which is extended to more general states of stress in subsequent chapters. We note that Equation 2.43 represents the area under the elastic stress-strain diagram.

Presently, we will use the work-strain energy relation to obtain the governing equations for the bar element using the following theorem.

Castigliano's First Theorem [1]

For an elastic system in equilibrium, the partial derivative of total strain energy with respect to deflection at a point is equal to the applied force in the direction of the deflection at that point.

Consider an elastic body subjected to N forces F_j for which the total strain energy is expressed as

$$U_e = W = \sum_{j=1}^N \int_0^{\delta_j} F_j d\delta_j \quad (2.44)$$

where δ_j is the deflection at the point of application of force F_j in the direction of the line of action of the force. If all points of load application are fixed except one, say, i , and that point is made to deflect an infinitesimal amount $\Delta\delta_i$ by an incremental infinitesimal force ΔF_i , the change in strain energy is

$$\Delta U_e = \Delta W = F_i \Delta\delta_i + \int_0^{\Delta\delta_i} \Delta F_i d\delta_i \quad (2.45)$$

where it is assumed that the original force F_i is constant during the infinitesimal change. The integral term in Equation 2.45 involves the product of infinitesimal quantities and can be neglected to obtain

$$\frac{\Delta U_e}{\Delta\delta_i} = F_i \quad (2.46)$$

which in the limit as $\Delta\delta_i$ approaches zero becomes

$$\frac{\partial U}{\partial\delta_i} = F_i \quad (2.47)$$

The first theorem of Castigliano is a powerful tool for finite element formulation, as is now illustrated for the bar element. Combining Equations 2.30, 2.31, and 2.43, total strain energy for the bar element is given by

$$U_e = \frac{1}{2} \sigma_x \epsilon_x V = \frac{1}{2} E \left(\frac{u_2 - u_1}{L} \right)^2 AL \quad (2.48)$$

Applying Castigliano's theorem with respect to each displacement yields

$$\frac{\partial U_e}{\partial u_1} = \frac{AE}{L} (u_1 - u_2) = f_1 \quad (2.49)$$

$$\frac{\partial U_e}{\partial u_2} = \frac{AE}{L} (u_2 - u_1) = f_2 \quad (2.50)$$

which are observed to be identical to Equations 2.33 and 2.34.

The first theorem of Castigliano is also applicable to rotational displacements. In the case of rotation, the partial derivative of strain energy with respect to a rotational displacement is equal to the moment/torque applied at the point of concern in the sense of the rotation. The following example illustrates the application in terms of a simple torsional member.

EXAMPLE 2.5

A solid circular shaft of radius R and length L is subjected to constant torque T . The shaft is fixed at one end, as shown in Figure 2.9. Formulate the elastic strain energy in terms of the angle of twist θ at $x = L$ and show that Castigliano's first theorem gives the correct expression for the applied torque.

■ Solution

From strength of materials theory, the shear stress at any cross section along the length of the member is given by

$$\tau = \frac{Tr}{J}$$

where r is radial distance from the axis of the member and J is polar moment of inertia of the cross section. For elastic behavior, we have

$$\gamma = \frac{\tau}{G} = \frac{Tr}{JG}$$

where G is the shear modulus of the material, and the strain energy is then

$$\begin{aligned} U_e &= \frac{1}{2} \int_V \tau \gamma \, dV = \frac{1}{2} \int_0^L \left[\int_A \left(\frac{Tr}{J} \right) \left(\frac{Tr}{JG} \right) dA \right] dx \\ &= \frac{T^2}{2J^2G} \int_0^L \int_A r^2 \, dA \, dx = \frac{T^2 L}{2JG} \end{aligned}$$

where we have used the definition of the polar moment of inertia

$$J = \int_A r^2 \, dA$$

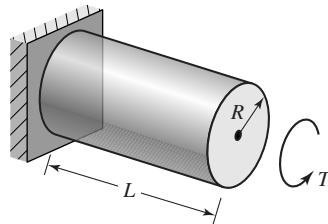


Figure 2.9 Example 2.5:
Circular cylinder subjected to
torsion.

Again invoking the strength of materials results, the angle of twist at the end of the member is known to be

$$\theta = \frac{TL}{JG}$$

so the strain energy can be written as

$$U_e = \frac{1}{2} \frac{L}{JG} \left(\frac{JG\theta}{L} \right)^2 = \frac{JG}{2L} \theta^2$$

Per Castigliano's first theorem,

$$\frac{\partial U_e}{\partial \theta} = T = \frac{JG\theta}{L}$$

which is exactly the relation shown by strength of materials theory. The reader may think that we used circular reasoning in this example, since we utilized many previously known results. However, the formulation of strain energy must be based on known stress and strain relationships, and the application of Castigliano's theorem is, indeed, a different concept.

For linearly elastic systems, formulation of the strain energy function in terms of displacements is relatively straightforward. As stated previously, the strain energy for an elastic system is a quadratic function of displacements. The quadratic nature is simplistically explained by the facts that, in elastic deformation, stress is proportional to force (or moment or torque), stress is proportional to strain, and strain is proportional to displacement (or rotation). And, since the elastic strain energy is equal to the mechanical work expended, a quadratic function results. Therefore, application of Castigliano's first theorem results in linear algebraic equations that relate displacements to applied forces. This statement follows from the fact that a derivative of a quadratic term is linear. The coefficients of the displacements in the resulting equations are the components of the stiffness matrix of the system for which the strain energy function is written. Such an energy-based approach is the simplest, most-straightforward method for establishing the stiffness matrix of many structural finite elements.

EXAMPLE 2.6

- Apply Castigliano's first theorem to the system of four spring elements depicted in Figure 2.10 to obtain the system stiffness matrix. The vertical members at nodes 2 and 3 are to be considered rigid.
- Solve for the displacements and the reaction force at node 1 if

$$k_1 = 4 \text{ N/mm} \quad k_2 = 6 \text{ N/mm} \quad k_3 = 3 \text{ N/mm}$$

$$F_2 = -30 \text{ N} \quad F_3 = 0 \quad F_4 = 50 \text{ N}$$

2.4 Strain Energy, Castigliano's First Theorem

43

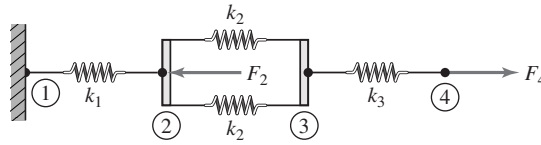


Figure 2.10 Example 2.6: Four spring elements.

■ Solution

- (a) The total strain energy of the system of four springs is expressed in terms of the nodal displacements and spring constants as

$$U_e = \frac{1}{2}k_1(U_2 - U_1)^2 + 2 \left[\frac{1}{2}k_2(U_3 - U_2)^2 \right] + \frac{1}{2}k_3(U_4 - U_3)^2$$

Applying Castigliano's theorem, using each nodal displacement in turn,

$$\frac{\partial U_e}{\partial U_1} = F_1 = k_1(U_2 - U_1)(-1) = k_1(U_1 - U_2)$$

$$\frac{\partial U_e}{\partial U_2} = F_2 = k_1(U_2 - U_1) + 2k_2(U_3 - U_2)(-1) = -k_1U_1 + (k_1 + 2k_2)U_2 - 2k_2U_3$$

$$\frac{\partial U_e}{\partial U_3} = F_3 = 2k_2(U_3 - U_2) + k_3(U_4 - U_3)(-1) = -2k_2U_2 + (2k_2 + k_3)U_3 - k_3U_4$$

$$\frac{\partial U_e}{\partial U_4} = F_4 = k_3(U_4 - U_3) = -k_3U_3 + k_3U_4$$

which can be written in matrix form as

$$\begin{bmatrix} k_1 & -k_1 & 0 & 0 \\ -k_1 & k_1 + 2k_2 & -2k_2 & 0 \\ 0 & -2k_2 & 2k_2 + k_3 & -k_3 \\ 0 & 0 & -k_3 & k_3 \end{bmatrix} \begin{Bmatrix} U_1 \\ U_2 \\ U_3 \\ U_4 \end{Bmatrix} = \begin{Bmatrix} F_1 \\ F_2 \\ F_3 \\ F_4 \end{Bmatrix}$$

and the system stiffness matrix is thus obtained via Castigliano's theorem.

- (b) Substituting the specified numerical values, the system equations become

$$\begin{bmatrix} 4 & -4 & 0 & 0 \\ -4 & 16 & -12 & 0 \\ 0 & -12 & 15 & -3 \\ 0 & 0 & -3 & 3 \end{bmatrix} \begin{Bmatrix} 0 \\ U_2 \\ U_3 \\ U_4 \end{Bmatrix} = \begin{Bmatrix} F_1 \\ -30 \\ 0 \\ 50 \end{Bmatrix}$$

Eliminating the constraint equation, the active displacements are governed by

$$\begin{bmatrix} 16 & -12 & 0 \\ -12 & 15 & -3 \\ 0 & -3 & 3 \end{bmatrix} \begin{Bmatrix} U_2 \\ U_3 \\ U_4 \end{Bmatrix} = \begin{Bmatrix} -30 \\ 0 \\ 50 \end{Bmatrix}$$

which we solve by manipulating the equations to convert the coefficient matrix (the

stiffness matrix) to upper-triangular form; that is, all terms below the main diagonal become zero.

Step 1. Multiply the first equation (row) by 12, multiply the second equation (row) by 16, add the two and replace the second equation with the resulting equation to obtain

$$\begin{bmatrix} 16 & -12 & 0 \\ 0 & 96 & -48 \\ 0 & -3 & 3 \end{bmatrix} \begin{Bmatrix} U_2 \\ U_3 \\ U_4 \end{Bmatrix} = \begin{Bmatrix} -30 \\ -360 \\ 50 \end{Bmatrix}$$

Step 2. Multiply the third equation by 32, add it to the second equation, and replace the third equation with the result. This gives the triangularized form desired:

$$\begin{bmatrix} 16 & -12 & 0 \\ 0 & 96 & -48 \\ 0 & 0 & 48 \end{bmatrix} \begin{Bmatrix} U_2 \\ U_3 \\ U_4 \end{Bmatrix} = \begin{Bmatrix} -30 \\ -360 \\ 1240 \end{Bmatrix}$$

In this form, the equations can now be solved from the “bottom to the top,” and it will be found that, at each step, there is only one unknown. In this case, the sequence is

$$U_4 = \frac{1240}{48} = 25.83 \text{ mm}$$

$$U_3 = \frac{1}{96}[-360 + 48(25.83)] = 9.17 \text{ mm}$$

$$U_2 = \frac{1}{16}[-30 + 12(9.17)] = 5.0 \text{ mm}$$

The reaction force at node 1 is obtained from the constraint equation

$$F_1 = -4U_2 = -4(5.0) = -20 \text{ N}$$

and we observe system equilibrium since the external forces sum to zero as required.

2.5 MINIMUM POTENTIAL ENERGY

The first theorem of Castigliano is but a forerunner to the general principle of *minimum potential energy*. There are many ways to state this principle, and it has been proven rigorously [2]. Here, we state the principle without proof but expect the reader to compare the results with the first theorem of Castigliano. The principle of minimum potential energy is stated as follows:

Of all displacement states of a body or structure, subjected to external loading, that satisfy the geometric boundary conditions (imposed displacements), the displacement state that also satisfies the equilibrium equations is such that the total potential energy is a minimum for stable equilibrium.

We emphasize that the *total* potential energy must be considered in application of this principle. The total potential energy includes the stored elastic potential energy (the strain energy) as well as the potential energy of applied loads. As is customary, we use the symbol Π for total potential energy and divide the total potential energy into two parts, that portion associated with strain energy U_e and the portion associated with external forces U_F . The total potential energy is

$$\Pi = U_e + U_F \quad (2.51)$$

where it is to be noted that the term external *forces* also includes moments and torques.

In this text, we will deal only with elastic systems subjected to *conservative* forces. A *conservative force* is defined as one that does mechanical work independent of the path of motion and such that the work is reversible or recoverable. The most common example of a *nonconservative* force is the force of sliding friction. As the friction force always acts to oppose motion, the work done by friction forces is always negative and results in energy loss. This loss shows itself physically as generated heat. On the other hand, the mechanical work done by a conservative force, Equation 2.37, is reversed, and therefore recovered, if the force is released. Therefore, the mechanical work of a conservative force is considered to be a loss in potential energy; that is,

$$U_F = -W \quad (2.52)$$

where W is the mechanical work defined by the scalar product integral of Equation 2.37. The total potential energy is then given by

$$\Pi = U_e - W \quad (2.53)$$

As we show in the following examples and applications to solid mechanics in Chapter 9, the strain energy term U_e is a quadratic function of system displacements and the work term W is a linear function of displacements. Rigorously, the minimization of total potential energy is a problem in the *calculus of variations* [5]. We do not suppose that the intended audience of this text is familiar with the calculus of variations. Rather, we simply impose the minimization principle of calculus of multiple variable functions. If we have a total potential energy expression that is a function of, say, N displacements $U_i, i = 1, \dots, N$; that is,

$$\Pi = \Pi(U_1, U_2, \dots, U_N) \quad (2.54)$$

then the total potential energy will be minimized if

$$\frac{\partial \Pi}{\partial U_i} = 0 \quad i = 1, \dots, N \quad (2.55)$$

Equation 2.55 will be shown to represent N algebraic equations, which form the finite element approximation to the solution of the differential equation(s) governing the response of a structural system.

EXAMPLE 2.7

Repeat the solution to Example 2.6 using the principle of minimum potential energy.

■ Solution

Per the previous example solution, the elastic strain energy is

$$U_e = \frac{1}{2}k_1(U_2 - U_1)^2 + 2\left[\frac{1}{2}k_2(U_3 - U_2)^2\right] + \frac{1}{2}k_3(U_4 - U_3)^2$$

and the potential energy of applied forces is

$$U_F = -W = -F_1U_1 - F_2U_2 - F_3U_3 - F_4U_4$$

Hence, the total potential energy is expressed as

$$\begin{aligned}\Pi &= \frac{1}{2}k_1(U_2 - U_1)^2 + 2\left[\frac{1}{2}k_2(U_3 - U_2)^2\right] \\ &\quad + \frac{1}{2}k_3(U_4 - U_3)^2 - F_1U_1 - F_2U_2 - F_3U_3 - F_4U_4\end{aligned}$$

In this example, the principle of minimum potential energy requires that

$$\frac{\partial \Pi}{\partial U_i} = 0 \quad i = 1, 4$$

giving in sequence $i = 1, 4$, the algebraic equations

$$\frac{\partial \Pi}{\partial U_1} = k_1(U_2 - U_1)(-1) - F_1 = k_1(U_1 - U_2) - F_1 = 0$$

$$\begin{aligned}\frac{\partial \Pi}{\partial U_2} &= k_1(U_2 - U_1) + 2k_2(U_3 - U_2)(-1) - F_2 \\ &= -k_1U_1 + (k_1 + 2k_2)U_2 - 2k_2U_3 - F_2 = 0\end{aligned}$$

$$\begin{aligned}\frac{\partial \Pi}{\partial U_3} &= 2k_2(U_3 - U_2) + k_3(U_4 - U_3)(-1) - F_3 \\ &= -2k_2U_2 + (2k_2 + k_3)U_3 - k_3U_4 - F_3 = 0\end{aligned}$$

$$\frac{\partial \Pi}{\partial U_4} = k_3(U_4 - U_3) - F_4 = -k_3U_3 + k_3U_4 - F_4 = 0$$

which, when written in matrix form, are

$$\begin{bmatrix} k_1 & -k_1 & 0 & 0 \\ -k_1 & k_1 + 2k_2 & -2k_2 & 0 \\ 0 & -2k_2 & 2k_2 + k_3 & -k_3 \\ 0 & 0 & -k_3 & k_3 \end{bmatrix} \begin{Bmatrix} U_1 \\ U_2 \\ U_3 \\ U_4 \end{Bmatrix} = \begin{Bmatrix} F_1 \\ F_2 \\ F_3 \\ F_4 \end{Bmatrix}$$

and can be seen to be identical to the previous result. Consequently, we do not resolve the system numerically, as the results are known.

We now reexamine the energy equation of the Example 2.7 to develop a more-general form, which will be of significant value in more complicated systems to be discussed in later chapters. The system or global displacement vector is

$$\{U\} = \begin{Bmatrix} U_1 \\ U_2 \\ U_3 \\ U_4 \end{Bmatrix} \quad (2.56)$$

and, as derived, the global stiffness matrix is

$$[K] = \begin{bmatrix} k_1 & -k_1 & 0 & 0 \\ -k_1 & k_1 + 2k_2 & -2k_2 & 0 \\ 0 & -2k_2 & 2k_2 + k_3 & -k_3 \\ 0 & 0 & -k_3 & k_3 \end{bmatrix} \quad (2.57)$$

If we form the matrix triple product

$$\begin{aligned} \frac{1}{2}\{U\}^T [K] \{U\} &= \frac{1}{2} [U_1 \quad U_2 \quad U_3 \quad U_4] \\ &\times \begin{bmatrix} k_1 & -k_1 & 0 & 0 \\ -k_1 & k_1 + 2k_2 & -2k_2 & 0 \\ 0 & -2k_2 & 2k_2 + k_3 & -k_3 \\ 0 & 0 & -k_3 & k_3 \end{bmatrix} \begin{Bmatrix} U_1 \\ U_2 \\ U_3 \\ U_4 \end{Bmatrix} \end{aligned} \quad (2.58)$$

and carry out the matrix operations, we find that the expression is identical to the strain energy of the system. As will be shown, the matrix triple product of Equation 2.58 represents the strain energy of any elastic system. If the strain energy can be expressed in the form of this triple product, the stiffness matrix will have been obtained, since the displacements are readily identifiable.

2.6 SUMMARY

Two linear mechanical elements, the idealized elastic spring and an elastic tension-compression member (bar) have been used to introduce the basic concepts involved in formulating the equations governing a finite element. The element equations are obtained by both a straightforward equilibrium approach and a strain energy method using the first theorem of Castigliano. The principle of minimum potential also is introduced. The next chapter shows how the one-dimensional bar element can be used to demonstrate the finite element model assembly procedures in the context of some simple two- and three-dimensional structures.

REFERENCES

1. Budynas, R. *Advanced Strength and Applied Stress Analysis*. 2d ed. New York: McGraw-Hill, 1998.
2. Love, A. E. H. *A Treatise on the Mathematical Theory of Elasticity*. New York: Dover Publications, 1944.

3. Beer, F. P., E. R. Johnston, and J. T. DeWolf. *Mechanics of Materials*. 3d ed. New York: McGraw-Hill, 2002.
4. Shigley, J., and R. Mischke. *Mechanical Engineering Design*. New York: McGraw-Hill, 2001.
5. Forray, M. J. *Variational Calculus in Science and Engineering*. New York: McGraw-Hill, 1968.

PROBLEMS

2.1–2.3 For each assembly of springs shown in the accompanying figures (Figures P2.1–P2.3), determine the global stiffness matrix using the system assembly procedure of Section 2.2.

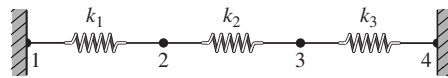


Figure P2.1

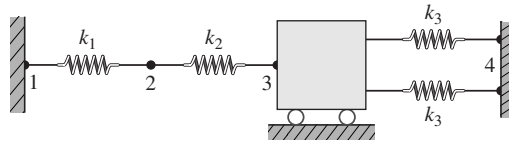


Figure P2.2

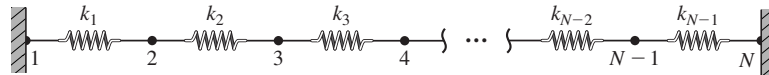


Figure P2.3

2.4 For the spring assembly of Figure P2.4, determine force F_3 required to displace node 2 an amount $\delta = 0.75$ in. to the right. Also compute displacement of node 3. Given

$$k_1 = 50 \text{ lb./in.} \quad \text{and} \quad k_2 = 25 \text{ lb./in.}$$

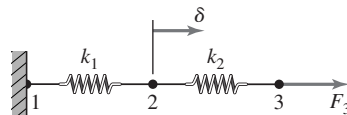


Figure P2.4

2.5 In the spring assembly of Figure P2.5, forces F_2 and F_4 are to be applied such that the resultant force in element 2 is zero and node 4 displaces an amount

$\delta = 1$ in. Determine (a) the required values of forces F_2 and F_4 , (b) displacement of node 2, and (c) the reaction force at node 1.

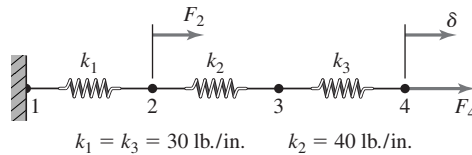


Figure P2.5

- 2.6 Verify the global stiffness matrix of Example 2.3 using (a) direct assembly and (b) Castigliano's first theorem.
- 2.7 Two trolleys are connected by the arrangement of springs shown in Figure P2.7. (a) Determine the complete set of equilibrium equations for the system in the form $[K]\{U\} = \{F\}$. (b) If $k = 50 \text{ lb./in.}$, $F_1 = 20 \text{ lb.}$, and $F_2 = 15 \text{ lb.}$, compute the displacement of each trolley and the force in each spring.

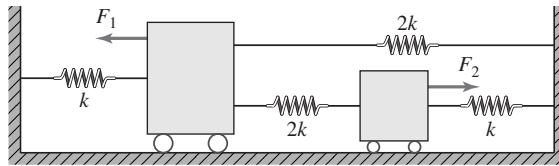


Figure P2.7

- 2.8 Use Castigliano's first theorem to obtain the matrix equilibrium equations for the system of springs shown in Figure P2.8.

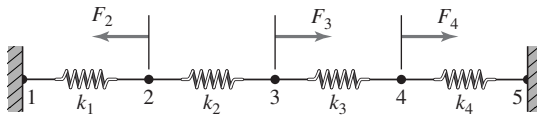


Figure P2.8

- 2.9 In Problem 2.8, let $k_1 = k_2 = k_3 = k_4 = 10 \text{ N/mm}$, $F_2 = 20 \text{ N}$, $F_3 = 25 \text{ N}$, $F_4 = 40 \text{ N}$ and solve for (a) the nodal displacements, (b) the reaction forces at nodes 1 and 5, and (c) the force in each spring.
- 2.10 A steel rod subjected to compression is modeled by two bar elements, as shown in Figure P2.10. Determine the nodal displacements and the axial stress in each element. What other concerns should be examined?

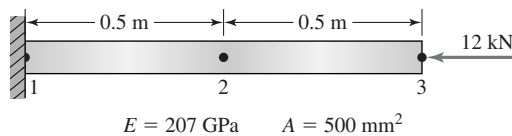


Figure P2.10

2.11 Figure P2.11 depicts an assembly of two bar elements made of different materials. Determine the nodal displacements, element stresses, and the reaction force.

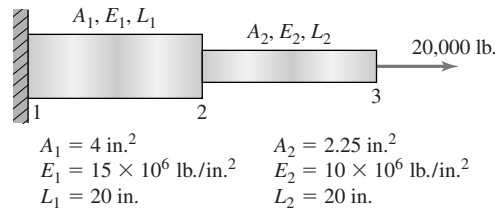


Figure P2.11

2.12 Obtain a four-element solution for the tapered bar of Example 2.4. Plot element stresses versus the exact solution. Use the following numerical values:

$$E = 10 \times 10^6 \text{ lb./in.}^2 \quad A_0 = 4 \text{ in.}^2 \quad L = 20 \text{ in.} \quad P = 4000 \text{ lb.}$$

2.13 A weight W is suspended in a vertical plane by a linear spring having spring constant k . Show that the equilibrium position corresponds to minimum total potential energy.

2.14 For a bar element, it is proposed to discretize the displacement function as

$$u(x) = N_1(x)u_1 + N_2(x)u_2$$

with interpolation functions

$$N_1(x) = \cos \frac{\pi x}{2L}$$

$$N_2(x) = \sin \frac{\pi x}{2L}$$

Are these valid interpolation functions? (Hint: Consider strain and stress variations.)

2.15 The torsional element shown in Figure P2.15 has a solid circular cross section and behaves elastically. The nodal displacements are rotations θ_1 and θ_2 and the associated nodal loads are applied torques T_1 and T_2 . Use the potential energy principle to derive the element equations in matrix form.

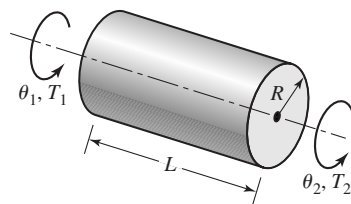


Figure P2.15

CHAPTER 3

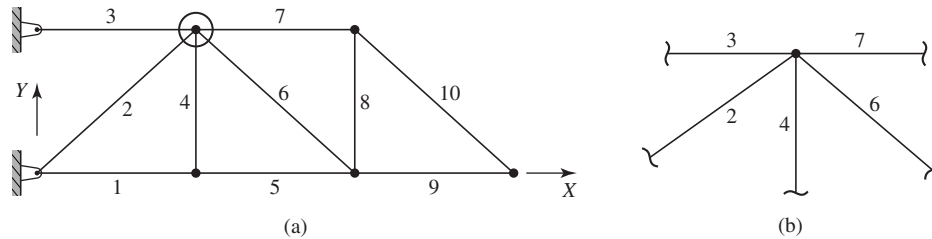
Truss Structures: The Direct Stiffness Method

3.1 INTRODUCTION

The simple line elements discussed in Chapter 2 introduced the concepts of nodes, nodal displacements, and element stiffness matrices. In this chapter, creation of a finite element model of a mechanical system composed of any number of elements is considered. The discussion is limited to *truss structures*, which we define as structures composed of straight elastic members subjected to axial forces only. Satisfaction of this restriction requires that all members of the truss be bar elements and that the elements be connected by pin joints such that each element is free to rotate about the joint. Although the bar element is inherently one dimensional, it is quite effectively used in analyzing both two- and three-dimensional trusses, as is shown.

The *global* coordinate system is the reference frame in which displacements of the structure are expressed and usually chosen by convenience in consideration of overall geometry. Considering the simple cantilever truss shown in Figure 3.1a, it is logical to select the global *XY* axes as parallel to the predominant geometric “axes” of the truss as shown. If we examine the circled joint, for example, redrawn in Figure 3.1b, we observe that five *element nodes* are physically connected at one *global node* and the *element x* axes do not coincide with the *global X* axis. The physical connection and varying geometric orientation of the elements lead to the following premises inherent to the finite element method:

1. The element nodal displacement of each connected element must be the same as the displacement of the connection node in the global coordinate system; the mathematical formulation, as will be seen, enforces this requirement (displacement compatibility).

**Figure 3.1**

(a) Two-dimensional truss composed of ten elements. (b) Truss joint connecting five elements.

2. The physical characteristics (in this case, the stiffness matrix and element force) of each element must be transformed, mathematically, to the global coordinate system to represent the structural properties in the global system in a consistent mathematical frame of reference.
3. The individual element parameters of concern (for the bar element, axial stress) are determined after solution of the problem in the global coordinate system by transformation of results back to the element reference frame (postprocessing).

Why are we basing the formulation on displacements? Generally, a design engineer is more interested in the stress to which each truss member is subjected, to compare the stress value to a known material property, such as the yield strength of the material. Comparison of computed stress values to material properties may lead to changes in material or geometric properties of individual elements (in the case of the bar element, the cross-sectional area). The answer to the question lies in the nature of physical problems. It is much easier to predict the loading (forces and moments) to which a structure is subjected than the deflections of such a structure. If the external loads are specified, the relations between loads and displacements are formulated in terms of the stiffness matrix and we solve for displacements. Back-substitution of displacements into individual element equations then gives us the strains and stresses in each element as desired. This is the *stiffness* method and is used exclusively in this text. In the alternate procedure, known as the *flexibility* method [1], displacements are taken as the known quantities and the problem is formulated such that the forces (more generally, the stress components) are the unknown variables. Similar discussion applies to nonstructural problems. In a heat transfer situation, the engineer is most often interested in the rate of heat flow into, or out of, a particular device. While temperature is certainly of concern, temperature is not the primary variable of interest. Nevertheless, heat transfer problems are generally formulated such that temperature is the primary dependent variable and heat flow is a secondary, computed variable in analogy with strain and stress in structural problems.

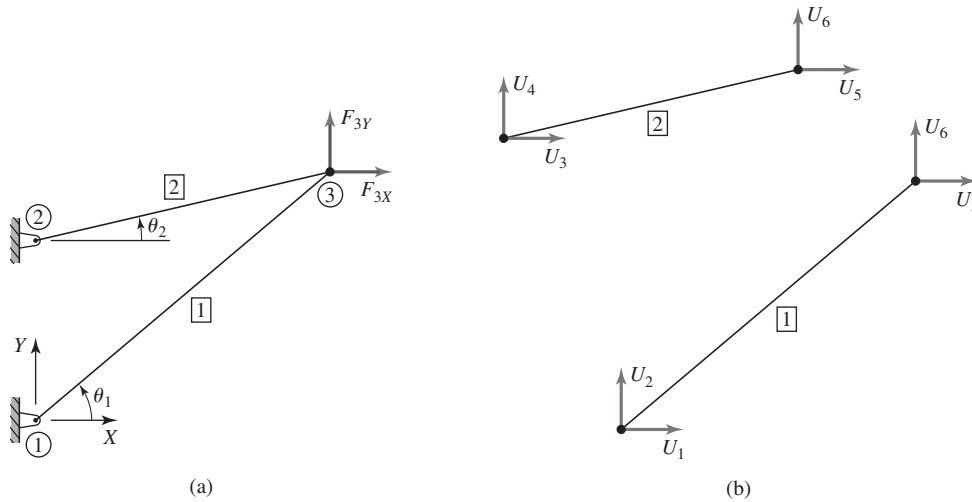
Returning to consideration of Figure 3.1b, where multiple elements are connected at a global node, the geometry of the connection determines the relations

between element displacements and global displacements as well as the contributions of individual elements to overall structural stiffness. In the *direct stiffness* method, the stiffness matrix of each element is transformed from the element coordinate system to the global coordinate system. The individual terms of each transformed element stiffness matrix are then added directly to the global stiffness matrix as determined by element connectivity (as noted, the connectivity relations ensure compatibility of displacements at joints and nodes where elements are connected). For example and simply by intuition at this point, elements 3 and 7 in Figure 3.1b should contribute stiffness only in the global X direction; elements 2 and 6 should contribute stiffness in both X and Y global directions; element 4 should contribute stiffness only in the global Y direction. The element transformation and stiffness matrix assembly procedures to be developed in this chapter indeed verify the intuitive arguments just made.

The direct stiffness assembly procedure, subsequently described, results in exactly the same system of equations as would be obtained by a formal equilibrium approach. By a *formal equilibrium approach*, we mean that the equilibrium equations for each joint (node) in the structure are explicitly expressed, including deformation effects. This should *not* be confused with the method of joints [2], which results in computation of forces only and does not take displacement into account. Certainly, if the force in each member is known, the physical properties of the member can be used to compute displacement. However, enforcing compatibility of displacements at connections (global nodes) is algebraically tedious. Hence, we have another argument for the stiffness method: Displacement compatibility is assured via the formulation procedure. Granted that we have to “backtrack” to obtain the information of true interest (strain, stress), but the backtracking is algebraic and straightforward, as will be illustrated.

3.2 NODAL EQUILIBRIUM EQUATIONS

To illustrate the required conversion of element properties to a global coordinate system, we consider the one-dimensional bar element as a structural member of a two-dimensional truss. Via this relatively simple example, the *assembly* procedure of essentially any finite element problem formulation is illustrated. We choose the element type (in this case we have only one selection, the bar element); specify the geometry of the problem (element connectivity); formulate the algebraic equations governing the problem (in this case, static equilibrium); specify the boundary conditions (known displacements and applied external forces); solve the system of equations for the global displacements; and back-substitute displacement values to obtain *secondary* variables, including strain, stress, and reaction forces at constrained locations (boundary conditions). The reader is advised to note that we use the term *secondary* variable only in the mathematical sense; strain and stress are secondary only in the sense that the values are computed after the general solution for displacements. The strain and stress values are of *primary importance* in design.

**Figure 3.2**

(a) A two-element truss with node and element numbers. (b) Global displacement notation.

Conversion of element equations from element coordinates to global coordinates and assembly of the global equilibrium equations are described first in the two-dimensional case with reference to Figure 3.2a. The figure depicts a simple two-dimensional truss composed of two structural members joined by pin connections and subjected to applied external forces. The pin connections are taken as the nodes of two bar elements as shown; node and element numbers, as well as the selected global coordinate system are also shown. The corresponding global displacements are shown in Figure 3.2b. The convention used here for global displacements is that U_{2i-1} is displacement in the global X direction of node i and U_{2i} is displacement of node i in the global Y direction. The convention is by no means restrictive; the convention is selected such that displacements in the direction of the global X axis are odd numbered and displacements in the direction of the global Y axis are even numbered. (In using FEM software, the reader will find that displacements are denoted in various fashions, U_X , U_Y , U_Z , etc.) Orientation angle θ for each element is measured as positive from the global X axis to the element x axis, as shown. Node numbers are circled while element numbers are in boxes. Element numbers are superscripted in the notation.

To obtain the equilibrium conditions, free-body diagrams of the three connecting nodes and the two elements are drawn in Figure 3.3. Note that the external forces are numbered via the same convention as the global displacements. For node 1, (Figure 3.3a), we have the following equilibrium equations in the global X and Y directions, respectively:

$$F_1 - f_1^{(1)} \cos \theta_1 = 0 \quad (3.1a)$$

$$F_2 - f_1^{(1)} \sin \theta_1 = 0 \quad (3.1b)$$

3.2 Nodal Equilibrium Equations

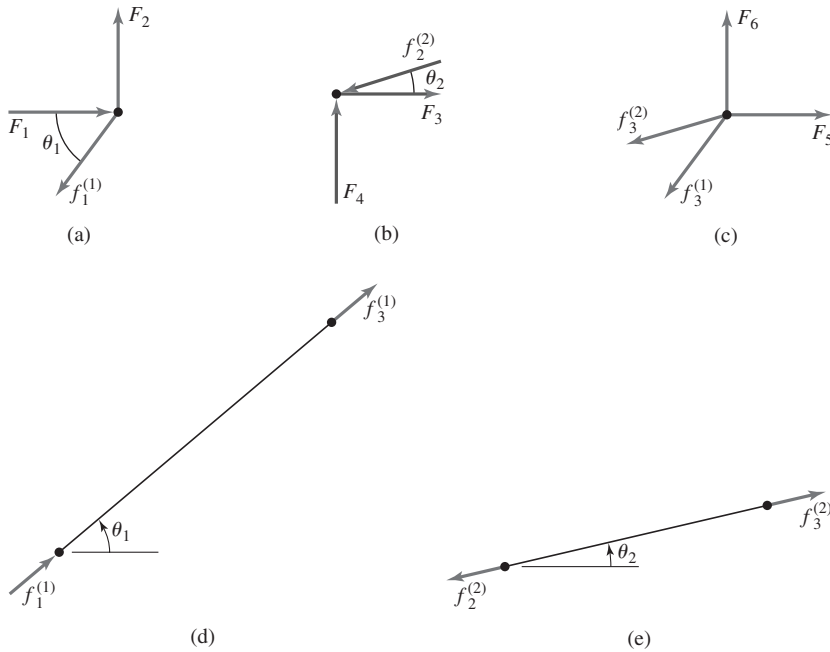


Figure 3.3

(a)–(c) Nodal free-body diagrams. (d) and (e) Element free-body diagrams.

and for node 2,

$$F_3 - f_2^{(2)} \cos \theta_2 = 0 \tag{3.2a}$$

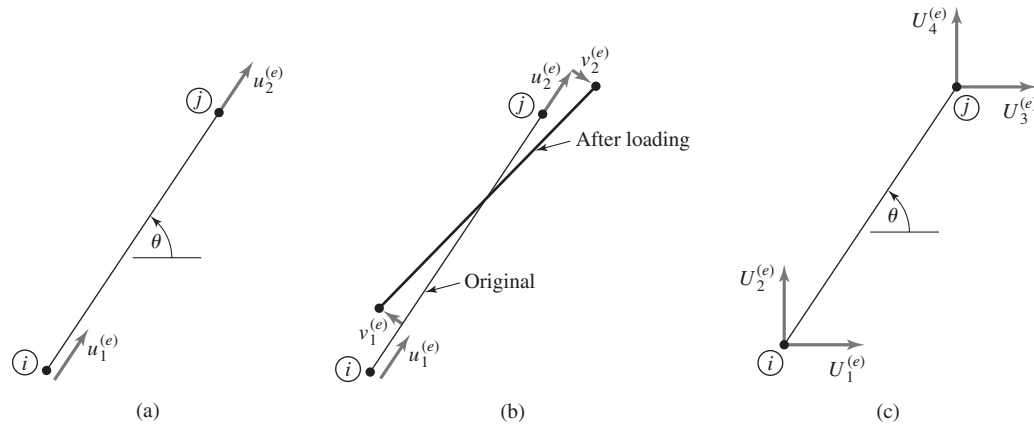
$$F_4 - f_2^{(2)} \sin \theta_2 = 0 \tag{3.2b}$$

while for node 3,

$$F_5 - f_3^{(1)} \cos \theta_1 - f_3^{(2)} \cos \theta_2 = 0 \tag{3.3a}$$

$$F_6 - f_3^{(1)} \sin \theta_1 - f_3^{(2)} \sin \theta_2 = 0 \tag{3.3b}$$

Equations 3.1–3.3 simply represent the conditions of static equilibrium from a rigid body mechanics standpoint. Assuming external loads F_5 and F_6 are known, these six nodal equilibrium equations formally contain eight unknowns (forces). Since the example truss is statically determinate, we can invoke the additional equilibrium conditions applicable to the truss as a whole as well as those for the individual elements (Figures 3.3d and 3.3e) and eventually solve for all of the forces. However, a more systematic procedure is obtained if the formulation is transformed so that the unknowns are nodal displacements. Once the transformation is accomplished, we find that the number of unknowns is exactly the same as the number of nodal equilibrium equations. In addition, static *indeterminacy* is automatically accommodated. As the reader may recall from study of mechanics of materials, the solution of statically indeterminate systems requires

**Figure 3.4**

(a) Bar element at orientation θ . (b) General displacements of a bar element. (c) Bar element global displacements.

specification of one or more displacement relations; hence, the displacement formulation of the finite element method includes such situations.

To illustrate the transformation to displacements, Figure 3.4a depicts a bar element connected at nodes i and j in a general position in a two-dimensional (2-D) truss structure. As a result of external loading on the truss, we assume that nodes i and j undergo 2-D displacement, as shown in Figure 3.4b. Since the element must remain connected at the structural joints, the connected element nodes must undergo the same 2-D displacements. This means that the element is subjected not only to axial motion but rotation as well. To account for the rotation, we added displacements v_1 and v_2 at element nodes 1 and 2, respectively, in the direction perpendicular to the element x axis. Owing to the assumption of smooth pin joint connections, the perpendicular displacements are not associated with element stiffness; nevertheless, these displacements must exist so that the element remains connected to the structural joint so that the element displacements are compatible with (i.e., the same as) joint displacements. Although the element undergoes a rotation in general, for computation purposes, orientation angle θ is assumed to be the same as in the undeformed structure. This is a result of the assumption of small, elastic deformations and is used throughout the text.

To now relate element nodal displacements referred to the element coordinates to element displacements in global coordinates, Figure 3.4c shows element nodal displacements in the global system using the notation

$$U_1^{(e)} = \text{element node 1 displacement in the global } X \text{ direction}$$

$$U_2^{(e)} = \text{element node 1 displacement in the global } Y \text{ direction}$$

$$U_3^{(e)} = \text{element node 2 displacement in the global } X \text{ direction}$$

$$U_4^{(e)} = \text{element node 2 displacement in the global } Y \text{ direction}$$

Again, note the use of capital letters for global quantities and the superscript notation to refer to an individual element. As the nodal displacements must be the same in both coordinate systems, we can equate vector components of global displacements to element system displacements to obtain the relations

$$\begin{aligned} u_1^{(e)} &= U_1^{(e)} \cos \theta + U_2^{(e)} \sin \theta \\ v_1^{(e)} &= -U_1^{(e)} \sin \theta + U_2^{(e)} \cos \theta \end{aligned} \quad (3.4a)$$

$$\begin{aligned} u_2^{(e)} &= U_3^{(e)} \cos \theta + U_4^{(e)} \sin \theta \\ v_2^{(e)} &= -U_3^{(e)} \sin \theta + U_4^{(e)} \cos \theta \end{aligned} \quad (3.4b)$$

As noted, the v displacement components are not associated with element stiffness, hence not associated with element forces, so we can express the axial deformation of the element as

$$\delta^{(e)} = u_2^{(e)} - u_1^{(e)} = (U_3^{(e)} - U_1^{(e)}) \cos \theta + (U_4^{(e)} - U_2^{(e)}) \sin \theta \quad (3.5)$$

The net axial force acting on the element is then

$$f^{(e)} = k^{(e)} \delta^{(e)} = k^{(e)} \{ (U_3^{(e)} - U_1^{(e)}) \cos \theta + (U_4^{(e)} - U_2^{(e)}) \sin \theta \} \quad (3.6)$$

Utilizing Equation 3.6 for element 1 (Figure 3.3d) while noting that the displacements of element 1 are related to the specified global displacements as $U_1^{(1)} = U_1$, $U_2^{(1)} = U_2$, $U_3^{(1)} = U_5$, $U_4^{(1)} = U_6$, we have the force in element 1 as

$$f_3^{(1)} = -f_1^{(1)} = k^{(1)} [(U_5 - U_1) \cos \theta_1 + (U_6 - U_2) \sin \theta_1] \quad (3.7)$$

and similarly for element 2 (Figure 3.3e):

$$f_3^{(2)} = -f_2^{(2)} = k^{(2)} [(U_5 - U_3) \cos \theta_2 + (U_6 - U_4) \sin \theta_2] \quad (3.8)$$

Note that, in writing Equations 3.7 and 3.8, we invoke the condition that the displacements of node 3 (U_5 and U_6) are the same for each element. To reiterate, this assumption is actually a requirement, since on a physical basis, the structure must remain connected at the joints after deformation. Displacement compatibility at the nodes is a fundamental requirement of the finite element method.

Substituting Equations 3.7 and 3.8 into the nodal equilibrium conditions (Equations 3.1–3.3) yields

$$-k^{(1)} [(U_5 - U_1) \cos \theta_1 + (U_6 - U_2) \sin \theta_1] \cos \theta_1 = F_1 \quad (3.9)$$

$$-k^{(1)} [(U_5 - U_1) \cos \theta_1 + (U_6 - U_2) \sin \theta_1] \sin \theta_1 = F_2 \quad (3.10)$$

$$-k^{(2)} [(U_5 - U_3) \cos \theta_2 + (U_6 - U_4) \sin \theta_2] \cos \theta_2 = F_3 \quad (3.11)$$

$$-k^{(2)} [(U_5 - U_3) \cos \theta_2 + (U_6 - U_4) \sin \theta_2] \sin \theta_2 = F_4 \quad (3.12)$$

$$\begin{aligned} &k^{(2)} [(U_5 - U_3) \cos \theta_2 + (U_6 - U_4) \sin \theta_2] \cos \theta_2 \\ &+ k^{(1)} [(U_5 - U_3) \cos \theta_1 + (U_6 - U_4) \sin \theta_1] \cos \theta_1 = F_5 \end{aligned} \quad (3.13)$$

$$\begin{aligned} &k^{(2)} [(U_5 - U_3) \cos \theta_2 + (U_6 - U_4) \sin \theta_2] \sin \theta_2 \\ &+ k^{(1)} [(U_5 - U_1) \cos \theta_1 + (U_6 - U_2) \sin \theta_1] \sin \theta_1 = F_6 \end{aligned} \quad (3.14)$$

Equations 3.9 through 3.14 are equivalent to the matrix form

$$\begin{bmatrix} k^{(1)}c^2\theta_1 & k^{(1)}s\theta_1c\theta_1 & 0 & 0 & -k^{(1)}c^2\theta_1 & -k^{(1)}s\theta_1c\theta_1 \\ k^{(1)}s\theta_1c\theta_1 & k^{(1)}s^2\theta_1 & 0 & 0 & -k^{(1)}s\theta_1c\theta_1 & -k^{(1)}s^2\theta_1 \\ 0 & 0 & k^{(2)}c^2\theta_2 & k^{(2)}s\theta_2c\theta_2 & -k^{(2)}c^2\theta_2 & -k^{(2)}s\theta_2c\theta_2 \\ 0 & 0 & k^{(2)}s\theta_2c\theta_2 & k^{(2)}s^2\theta_2 & -k^{(2)}s\theta_2c\theta_2 & -k^{(2)}s^2\theta_2 \\ -k^{(1)}c^2\theta_{12} & -k_1s\theta_1c\theta_1 & -k^{(2)}c^2\theta_2 & -k^{(2)}s\theta_2c\theta_2 & k^{(1)}c^2\theta_1 + k^{(2)}c^2\theta_2 & k^{(1)}s\theta_1c\theta_1 + k^{(2)}s\theta_2c\theta_2 \\ -k_1s\theta_1c\theta_1 & -k^{(1)}s^2\theta_1 & -k^{(2)}s\theta_2c\theta_2 & -k^{(2)}s^2\theta_2 & k^{(1)}s\theta_1c\theta_1 + k^{(2)}s\theta_2c\theta_2 & k^{(1)}s^2\theta_1 + k^{(2)}s^2\theta_2 \end{bmatrix} \begin{Bmatrix} U_1 \\ U_2 \\ U_3 \\ U_4 \\ U_5 \\ U_6 \end{Bmatrix} = \begin{Bmatrix} F_1 \\ F_2 \\ F_3 \\ F_4 \\ F_5 \\ F_6 \end{Bmatrix} \quad (3.15)$$

The six algebraic equations represented by matrix Equation 3.15 express the complete set of equilibrium conditions for the two-element truss. Equation 3.15 is of the form

$$[K]\{U\} = \{F\} \quad (3.16)$$

where $[K]$ is the global stiffness matrix, $\{U\}$ is the vector of nodal displacements, and $\{F\}$ is the vector of applied nodal forces. We observe that the global stiffness matrix is a 6×6 symmetric matrix corresponding to six possible global displacements. Application of boundary conditions and solution of the equations are deferred at this time, pending further discussion.

3.3 ELEMENT TRANSFORMATION

Formulation of global finite element equations by direct application of equilibrium conditions, as in the previous section, proves to be quite cumbersome except for the very simplest of models. By writing the nodal equilibrium equations in the global coordinate system and introducing the displacement formulation, the procedure of the previous section implicitly transformed the individual element characteristics (the stiffness matrix) to the global system. A direct method for transforming the stiffness characteristics on an element-by-element basis is now developed in preparation for use in the direct assembly procedure of the following section.

Recalling the bar element equations expressed in the element frame as

$$\frac{AE}{L} \begin{bmatrix} 1 & -1 \\ -1 & 1 \end{bmatrix} \begin{Bmatrix} u_1^{(e)} \\ u_2^{(e)} \end{Bmatrix} = \begin{bmatrix} k_e & -k_e \\ -k_e & k_e \end{bmatrix} \begin{Bmatrix} u_1^{(e)} \\ u_2^{(e)} \end{Bmatrix} = \begin{Bmatrix} f_1^{(e)} \\ f_2^{(e)} \end{Bmatrix} \quad (3.17)$$

the present objective is to transform these equilibrium equations into the global coordinate system in the form

$$[K^{(e)}] \begin{Bmatrix} U_1^{(e)} \\ U_2^{(e)} \\ U_3^{(e)} \\ U_4^{(e)} \end{Bmatrix} = \begin{Bmatrix} F_1^{(e)} \\ F_2^{(e)} \\ F_3^{(e)} \\ F_4^{(e)} \end{Bmatrix} \quad (3.18)$$

In Equation 3.18, $[K^{(e)}]$ represents the element stiffness matrix in the global coordinate system, the vector $\{F^{(e)}\}$ on the right-hand side contains the element nodal force components in the global frame, displacements $U_1^{(e)}$ and $U_3^{(e)}$ are parallel to the global X axis, while $U_2^{(e)}$ and $U_4^{(e)}$ are parallel to the global Y axis. The relation between the element axial displacements in the element coordinate system and the element displacements in global coordinates (Equation 3.4) is

$$u_1^{(e)} = U_1^{(e)} \cos \theta + U_2^{(e)} \sin \theta \quad (3.19)$$

$$u_2^{(e)} = U_3^{(e)} \cos \theta + U_4^{(e)} \sin \theta \quad (3.20)$$

which can be written in matrix form as

$$\begin{Bmatrix} u_1^{(e)} \\ u_2^{(e)} \end{Bmatrix} = \begin{bmatrix} \cos \theta & \sin \theta & 0 & 0 \\ 0 & 0 & \cos \theta & \sin \theta \end{bmatrix} \begin{Bmatrix} U_1^{(e)} \\ U_2^{(e)} \\ U_3^{(e)} \\ U_4^{(e)} \end{Bmatrix} = [R] \begin{Bmatrix} U_1^{(e)} \\ U_2^{(e)} \\ U_3^{(e)} \\ U_4^{(e)} \end{Bmatrix} \quad (3.21)$$

where

$$[R] = \begin{bmatrix} \cos \theta & \sin \theta & 0 & 0 \\ 0 & 0 & \cos \theta & \sin \theta \end{bmatrix} \quad (3.22)$$

is the transformation matrix of element *axial* displacements to global displacements. (Again note that the element nodal displacements in the direction perpendicular to the element axis, v_1 and v_2 , are not considered in the stiffness matrix development; these displacements come into play in dynamic analyses in Chapter 10.) Substituting Equation 3.22 into Equation 3.17 yields

$$\begin{bmatrix} k_e & -k_e \\ -k_e & k_e \end{bmatrix} \begin{bmatrix} \cos \theta & \sin \theta & 0 & 0 \\ 0 & 0 & \cos \theta & \sin \theta \end{bmatrix} \begin{Bmatrix} U_1^{(e)} \\ U_2^{(e)} \\ U_3^{(e)} \\ U_4^{(e)} \end{Bmatrix} = \begin{Bmatrix} f_1^{(e)} \\ f_2^{(e)} \end{Bmatrix} \quad (3.23)$$

or

$$\begin{bmatrix} k_e & -k_e \\ -k_e & k_e \end{bmatrix} [R] \begin{Bmatrix} U_1^{(e)} \\ U_2^{(e)} \\ U_3^{(e)} \\ U_4^{(e)} \end{Bmatrix} = \begin{Bmatrix} f_1^{(e)} \\ f_2^{(e)} \end{Bmatrix} \quad (3.24)$$

While we have transformed the equilibrium equations from element displacements to global displacements as the unknowns, the equations are still expressed in the element coordinate system. The first of Equation 3.23 is the equilibrium condition for element node 1 in the element coordinate system. If we multiply

this equation by $\cos \theta$, we obtain the equilibrium equation for the node in the X direction of the global coordinate system. Similarly, multiplying by $\sin \theta$, the Y direction global equilibrium equation is obtained. Exactly the same procedure with the second equation expresses equilibrium of element node 2 in the global coordinate system. The same desired operations described are obtained if we premultiply both sides of Equation 3.24 by $[R]^T$, the transpose of the transformation matrix; that is,

$$[R]^T \begin{bmatrix} k_e & -k_e \\ -k_e & k_e \end{bmatrix} [R] \begin{Bmatrix} U_1^{(e)} \\ U_2^{(e)} \\ U_3^{(e)} \\ U_4^{(e)} \end{Bmatrix} = \begin{bmatrix} \cos \theta & 0 \\ \sin \theta & 0 \\ 0 & \cos \theta \\ 0 & \sin \theta \end{bmatrix} \begin{Bmatrix} f_1^{(e)} \\ f_2^{(e)} \end{Bmatrix} = \begin{Bmatrix} f_1^{(e)} \cos \theta \\ f_1^{(e)} \sin \theta \\ f_2^{(e)} \cos \theta \\ f_2^{(e)} \sin \theta \end{Bmatrix} \quad (3.25)$$

Clearly, the right-hand side of Equation 3.25 represents the components of the element forces in the global coordinate system, so we now have

$$[R]^T \begin{bmatrix} k_e & -k_e \\ -k_e & k_e \end{bmatrix} [R] \begin{Bmatrix} U_1^{(e)} \\ U_2^{(e)} \\ U_3^{(e)} \\ U_4^{(e)} \end{Bmatrix} = \begin{Bmatrix} F_1^{(e)} \\ F_2^{(e)} \\ F_3^{(e)} \\ F_4^{(e)} \end{Bmatrix} \quad (3.26)$$

Matrix Equation 3.26 represents the equilibrium equations for element nodes 1 and 2, expressed in the global coordinate system. Comparing this result with Equation 3.18, the element stiffness matrix in the global coordinate frame is seen to be given by

$$[K^{(e)}] = [R]^T \begin{bmatrix} k_e & -k_e \\ -k_e & k_e \end{bmatrix} [R] \quad (3.27)$$

Introducing the notation $c = \cos \theta$, $s = \sin \theta$ and performing the matrix multiplications on the right-hand side of Equation 3.27 results in

$$[K^{(e)}] = k_e \begin{bmatrix} c^2 & sc & -c^2 & -sc \\ sc & s^2 & -sc & -s^2 \\ -c^2 & -sc & c^2 & sc \\ -sc & -s^2 & sc & s^2 \end{bmatrix} \quad (3.28)$$

where $k_e = AE/L$ is the characteristic axial stiffness of the element.

Examination of Equation 3.28 shows that the symmetry of the element stiffness matrix is preserved in the transformation to global coordinates. In addition, although not obvious by inspection, it can be shown that the determinant is zero, indicating that, after transformation, the stiffness matrix remains singular. This is to be expected, since as previously discussed, rigid body motion of the element is possible in the absence of specified constraints.

3.3.1 Direction Cosines

In practice, a finite element model is constructed by defining nodes at specified coordinate locations followed by definition of elements by specification of the nodes connected by each element. For the case at hand, nodes i and j are defined in global coordinates by (X_i, Y_i) and (X_j, Y_j) . Using the nodal coordinates, element length is readily computed as

$$L = [(X_j - X_i)^2 + (Y_j - Y_i)^2]^{1/2} \quad (3.29)$$

and the unit vector directed from node i to node j is

$$\boldsymbol{\lambda} = \frac{1}{L}[(X_j - X_i)\mathbf{I} + (Y_j - Y_i)\mathbf{J}] = \cos \theta_X \mathbf{I} + \cos \theta_Y \mathbf{J} \quad (3.30)$$

where \mathbf{I} and \mathbf{J} are unit vectors in global coordinate directions X and Y , respectively. Recalling the definition of the scalar product of two vectors and referring again to Figure 3.4, the trigonometric values required to construct the element transformation matrix are also readily determined from the nodal coordinates as the *direction cosines* in Equation 3.30

$$\cos \theta = \cos \theta_X = \boldsymbol{\lambda} \cdot \mathbf{I} = \frac{X_j - X_i}{L} \quad (3.31)$$

$$\sin \theta = \cos \theta_Y = \boldsymbol{\lambda} \cdot \mathbf{J} = \frac{Y_j - Y_i}{L} \quad (3.32)$$

Thus, the element stiffness matrix of a bar element in global coordinates can be completely determined by specification of the nodal coordinates, the cross-sectional area of the element, and the modulus of elasticity of the element material.

3.4 DIRECT ASSEMBLY OF GLOBAL STIFFNESS MATRIX

Having addressed the procedure of transforming the element characteristics of the one-dimensional bar element into the global coordinate system of a two-dimensional structure, we now address a method of obtaining the global equilibrium equations via an element-by-element assembly procedure. The technique of directly assembling the global stiffness matrix for a finite element model of a truss is discussed in terms of the simple two-element system depicted in Figure 3.2. Assuming the geometry and material properties to be completely specified, the element stiffness matrix in the global frame can be formulated for each element using Equation 3.28 to obtain

$$[K^{(1)}] = \begin{bmatrix} k_{11}^{(1)} & k_{12}^{(1)} & k_{13}^{(1)} & k_{14}^{(1)} \\ k_{21}^{(1)} & k_{22}^{(1)} & k_{23}^{(1)} & k_{24}^{(1)} \\ k_{31}^{(1)} & k_{32}^{(1)} & k_{33}^{(1)} & k_{34}^{(1)} \\ k_{41}^{(1)} & k_{42}^{(1)} & k_{43}^{(1)} & k_{44}^{(1)} \end{bmatrix} \quad (3.33)$$

for element 1 and

$$[K^{(2)}] = \begin{bmatrix} k_{11}^{(2)} & k_{12}^{(2)} & k_{13}^{(2)} & k_{14}^{(2)} \\ k_{21}^{(2)} & k_{22}^{(2)} & k_{23}^{(2)} & k_{24}^{(2)} \\ k_{31}^{(2)} & k_{32}^{(2)} & k_{33}^{(2)} & k_{34}^{(2)} \\ k_{41}^{(2)} & k_{42}^{(2)} & k_{43}^{(2)} & k_{44}^{(2)} \end{bmatrix} \quad (3.34)$$

for element 2. The stiffness matrices given by Equations 3.33 and 3.34 contain 32 terms, which together will form the 6×6 system matrix containing 36 terms. To “assemble” the individual element stiffness matrices into the global stiffness matrix, it is necessary to observe the correspondence of individual element displacements to global displacements and allocate the associated element stiffness terms to the correct location in the global matrix. For element 1 of Figure 3.2, the element displacements correspond to global displacements per

$$\{U^{(1)}\} = \begin{Bmatrix} U_1^{(e)} \\ U_2^{(e)} \\ U_3^{(e)} \\ U_4^{(e)} \end{Bmatrix} \Rightarrow \begin{Bmatrix} U_1 \\ U_2 \\ U_5 \\ U_6 \end{Bmatrix} \quad (3.35)$$

while for element 2

$$\{U^{(2)}\} = \begin{Bmatrix} U_1^{(e)} \\ U_2^{(e)} \\ U_3^{(e)} \\ U_4^{(e)} \end{Bmatrix} \Rightarrow \begin{Bmatrix} U_3 \\ U_4 \\ U_5 \\ U_6 \end{Bmatrix} \quad (3.36)$$

Equations 3.35 and 3.36 are the connectivity relations for the truss and explicitly indicate how each element is connected in the structure. For example, Equation 3.35 clearly shows that element 1 is not associated with global displacements U_3 and U_4 (therefore, not connected to global node 2) and, hence, contributes no stiffness terms affecting those displacements. This means that element 1 has no effect on the third and fourth rows and columns of the global stiffness matrix. Similarly, element 2 contributes nothing to the first and second rows and columns.

Rather than write individual displacement relations, it is convenient to place all the element to global displacement data in a single table as shown in Table 3.1.

Table 3.1 Nodal Displacement Correspondence Table

Global Displacement	Element 1 Displacement	Element 2 Displacement
1	1	0
2	2	0
3	0	1
4	0	2
5	3	3
6	4	4

3.4 Direct Assembly of Global Stiffness Matrix

63

The first column contains the entire set of global displacements in numerical order. Each succeeding column represents an element and contains the number of the element displacement corresponding to the global displacement in each row. A zero entry indicates no connection, therefore no stiffness contribution. The individual terms in the global stiffness matrix are then obtained by allocating the element stiffness terms per the table as follows:

$$K_{11} = k_{11}^{(1)} + 0$$

$$K_{12} = k_{12}^{(1)} + 0$$

$$K_{13} = 0 + 0$$

$$K_{14} = 0 + 0$$

$$K_{15} = k_{13}^{(1)} + 0$$

$$K_{16} = k_{14}^{(1)} + 0$$

$$K_{22} = k_{22}^{(1)} + 0$$

$$K_{23} = 0 + 0$$

$$K_{24} = 0 + 0$$

$$K_{25} = k_{23}^{(1)} + 0$$

$$K_{26} = k_{24}^{(1)} + 0$$

$$K_{33} = 0 + k_{11}^{(2)}$$

$$K_{34} = 0 + k_{12}^{(2)}$$

$$K_{35} = 0 + k_{13}^{(2)}$$

$$K_{36} = 0 + k_{14}^{(2)}$$

$$K_{44} = 0 + k_{22}^{(2)}$$

$$K_{45} = 0 + k_{23}^{(2)}$$

$$K_{46} = 0 + k_{24}^{(2)}$$

$$K_{55} = k_{33}^{(1)} + k_{33}^{(2)}$$

$$K_{56} = k_{34}^{(1)} + k_{34}^{(2)}$$

$$K_{66} = k_{44}^{(1)} + k_{44}^{(2)}$$

where the known symmetry of the stiffness matrix has been implicitly used to avoid repetition. It is readily shown that the resulting global stiffness matrix is identical in every respect to that obtained in Section 3.2 via the equilibrium equations. This is the direct stiffness method; the global stiffness matrix is “assembled” by direct addition of the individual element stiffness terms per the nodal displacement correspondence table that defines element connectivity.

EXAMPLE 3.1

For the truss shown in Figure 3.2, $\theta_1 = \pi/4$, $\theta_2 = 0$, and the element properties are such that $k_1 = A_1 E_1 / L_1$, $k_2 = A_2 E_2 / L_2$. Transform the element stiffness matrix of each element into the global reference frame and assemble the global stiffness matrix.

■ Solution

For element 1, $\cos \theta_1 = \sin \theta_1 = \sqrt{2}/2$ and $c^2 \theta_1 = s^2 \theta_1 = c \theta_1 s \theta_1 = \frac{1}{2}$, so substitution into Equation 3.33 gives

$$[K^{(1)}] = \frac{k_1}{2} \begin{bmatrix} 1 & 1 & -1 & -1 \\ 1 & 1 & -1 & -1 \\ -1 & -1 & 1 & 1 \\ -1 & -1 & 1 & 1 \end{bmatrix}$$

For element 2, $\cos \theta_2 = 1$, $\sin \theta_2 = 0$ which gives the transformed stiffness matrix as

$$[K^{(2)}] = k_2 \begin{bmatrix} 1 & 0 & -1 & 0 \\ 0 & 0 & 0 & 0 \\ -1 & 0 & 1 & 0 \\ 0 & 0 & 0 & 0 \end{bmatrix}$$

Assembling the global stiffness matrix directly using Equations 3.35 and 3.36 gives

$$K_{11} = k_1/2$$

$$K_{12} = k_1/2$$

$$K_{13} = 0$$

$$K_{14} = 0$$

$$K_{15} = -k_1/2$$

$$K_{16} = -k_1/2$$

$$K_{22} = k_1/2$$

$$K_{23} = 0$$

$$K_{24} = 0$$

$$K_{25} = -k_1/2$$

$$K_{26} = -k_1/2$$

$$K_{33} = k_2$$

$$K_{34} = 0$$

$$K_{35} = -k_2$$

$$K_{36} = 0$$

$$K_{44} = 0$$

$$K_{45} = 0$$

$$K_{46} = 0$$

3.4 Direct Assembly of Global Stiffness Matrix

65

$$K_{55} = k_1/2 + k_2$$

$$K_{56} = k_1/2$$

$$K_{66} = k_1/2$$

The complete global stiffness matrix is then

$$[K] = \begin{bmatrix} k_1/2 & k_1/2 & 0 & 0 & -k_1/2 & -k_1/2 \\ k_1/2 & k_1/2 & 0 & 0 & -k_1/2 & -k_1/2 \\ 0 & 0 & k_2 & 0 & -k_2 & 0 \\ 0 & 0 & 0 & 0 & 0 & 0 \\ -k_1/2 & -k_1/2 & -k_2 & 0 & k_1/2 + k_2 & k_1/2 \\ -k_1/2 & -k_1/2 & 0 & 0 & k_1/2 & k_1/2 \end{bmatrix}$$

The previously described embodiment of the direct stiffness method is straightforward but cumbersome and inefficient in practice. The main problem inherent to the method lies in the fact that each term of the global stiffness matrix is computed sequentially and accomplishment of this sequential construction requires that each element be considered at each step. A technique that is much more efficient and well-suited to digital computer operations is now described. In the second method, the element stiffness matrix for each element is considered in sequence, and the element stiffness terms added to the global stiffness matrix per the nodal connectivity table. Thus, all terms of an individual element stiffness matrix are added to the global matrix, after which that element need not be considered further. To illustrate, we rewrite Equations 3.33 and 3.34 as

$$[K^{(1)}] = \begin{array}{cccc} & 1 & 2 & 5 & 6 \\ \begin{bmatrix} k_{11}^{(1)} & k_{12}^{(1)} & k_{13}^{(1)} & k_{14}^{(1)} \\ k_{21}^{(1)} & k_{22}^{(1)} & k_{23}^{(1)} & k_{24}^{(1)} \\ k_{31}^{(1)} & k_{32}^{(1)} & k_{33}^{(1)} & k_{34}^{(1)} \\ k_{41}^{(1)} & k_{42}^{(1)} & k_{43}^{(1)} & k_{44}^{(1)} \end{bmatrix} & 1 \\ & 2 \\ & 5 \\ & 6 \end{array} \quad (3.37)$$

$$[K^{(2)}] = \begin{array}{cccc} & 3 & 4 & 5 & 6 \\ \begin{bmatrix} k_{11}^{(2)} & k_{12}^{(2)} & k_{13}^{(2)} & k_{14}^{(2)} \\ k_{21}^{(2)} & k_{22}^{(2)} & k_{23}^{(2)} & k_{24}^{(2)} \\ k_{31}^{(2)} & k_{32}^{(2)} & k_{33}^{(2)} & k_{34}^{(2)} \\ k_{41}^{(2)} & k_{42}^{(2)} & k_{43}^{(2)} & k_{44}^{(2)} \end{bmatrix} & 3 \\ & 4 \\ & 5 \\ & 6 \end{array} \quad (3.38)$$

In this depiction of the stiffness matrices for the two individual elements, the numbers to the right of each row and above each column indicate the global displacement associated with the corresponding row and column of the element stiffness matrix. Thus, we combine the nodal displacement correspondence table with the individual element stiffness matrices. For the element matrices, each

individual component is now labeled as associated with a specific row-column position of the global stiffness matrix and can be added directly to that location. For example, Equation 3.38 shows that the $k_{24}^{(2)}$ component of element 2 is to be added to global stiffness component K_{46} (and via symmetry K_{64}). Thus, we can take each element in turn and add the individual components of the element stiffness matrix to the proper locations in the global stiffness matrix.

The form of Equations 3.37 and 3.38 is convenient for illustrative purposes only. For actual computations, inclusion of the global displacement numbers within the element stiffness matrix is unwieldy. A streamlined technique suitable for computer application is described next. For a 2-D truss modeled by spar elements, the following conventions are adopted:

1. The global nodes at which each element is connected are denoted by i and j .
2. The origin of the element coordinate system is located at node i and the element x axis has a positive sense in the direction from node i to node j .
3. The global displacements at element nodes are U_{2i-1} , U_{2i} , U_{2j-1} , and U_{2j} as noted in Section 3.2.

Using these conventions, all the information required to define element connectivity and assemble the global stiffness matrix is embodied in an *element-node connectivity* table, which lists element numbers in sequence and shows the global node numbers i and j to which each element is connected. For the two-element truss of Figure 3.2, the required data are as shown in Table 3.2.

Using the nodal data of Table 3.2, we define, for each element, a 1×4 *element displacement location vector* as

$$[L^{(e)}] = [2i - 1 \quad 2i \quad 2j - 1 \quad 2j] \quad (3.39)$$

where each value is the global displacement number corresponding to element stiffness matrix rows and columns 1, 2, 3, 4 respectively. For the truss of Figure 3.2, the element displacement location vectors are

$$[L^{(1)}] = [1 \quad 2 \quad 5 \quad 6] \quad (3.40)$$

$$[L^{(2)}] = [3 \quad 4 \quad 5 \quad 6] \quad (3.41)$$

Before proceeding, let us note the quantity of information that can be obtained from simple-looking Table 3.2. With the geometry of the structure defined, the (X, Y) global coordinates of each node are specified. Using these data, the length of each element and the direction cosines of element orientation

Table 3.2 Element-Node Connectivity Table for Figure 3.2

Element	Node	
	i	j
1	1	3
2	2	3

are computed via Equations 3.29 and 3.30, respectively. Specification of the cross-sectional area A and modulus of elasticity E of each element allows computation of the element stiffness matrix in the global frame using Equation 3.28. Finally, the element stiffness matrix terms are added to the global stiffness matrix using the element displacement location vector.

In the context of the current example, the reader is to imagine a 6×6 array of mailboxes representing the global stiffness matrix, each of which is originally empty (i.e., the stiffness coefficient is zero). We then consider the stiffness matrix of an individual element in the (2-D) global reference frame. Per the location vector (addresses) for the element, the individual values of the element stiffness matrix are placed in the appropriate mailbox. In this fashion, each element is processed in sequence and its stiffness characteristics added to the global matrix. After all elements are processed, the array of mailboxes contains the global stiffness matrix.

3.5 BOUNDARY CONDITIONS, CONSTRAINT FORCES

Having obtained the global stiffness matrix via either the equilibrium equations or direct assembly, the system displacement equations for the example truss of Figure 3.2 are of the form

$$[K] \begin{Bmatrix} U_1 \\ U_2 \\ U_3 \\ U_4 \\ U_5 \\ U_6 \end{Bmatrix} = \begin{Bmatrix} F_1 \\ F_2 \\ F_3 \\ F_4 \\ F_5 \\ F_6 \end{Bmatrix} \quad (3.42)$$

As noted, the global stiffness matrix is a singular matrix; therefore, a unique solution to Equation 3.42 cannot be obtained directly. However, in developing these equations, we have not yet taken into account the constraints imposed on system displacements by the support conditions that must exist to preclude rigid body motion. In this example, we observe the displacement boundary conditions

$$U_1 = U_2 = U_3 = U_4 = 0 \quad (3.43)$$

leaving only U_5 and U_6 to be determined. Substituting the boundary condition values and expanding Equation 3.42 we have, formally,

$$\begin{aligned} K_{15}U_5 + K_{16}U_6 &= F_1 \\ K_{25}U_5 + K_{26}U_6 &= F_2 \\ K_{35}U_5 + K_{36}U_6 &= F_3 \\ K_{45}U_5 + K_{46}U_6 &= F_4 \\ K_{55}U_5 + K_{56}U_6 &= F_5 \\ K_{56}U_5 + K_{66}U_6 &= F_6 \end{aligned} \quad (3.44)$$

as the *reduced* system equations (this is the partitioned set of matrix equations, written explicitly for the active displacements). In this example, F_1 , F_2 , F_3 , and F_4 are the components of the reaction forces at constrained nodes 1 and 2, while F_5 and F_6 are global components of applied external force at node 3. Given the external force components, the last two of Equations 3.44 can be explicitly solved for displacements U_5 and U_6 . The values obtained for these two displacements are then substituted into the constraint equations (the first four of Equations 3.44) and the reaction force components computed.

A more general approach to application of boundary conditions and computation of reactions is as follows. Letting the subscript c denote constrained displacements and subscript a denote unconstrained (active) displacements, the system equations can be partitioned (Appendix A) to obtain

$$\begin{bmatrix} K_{cc} & K_{ca} \\ K_{ac} & K_{aa} \end{bmatrix} \begin{Bmatrix} U_c \\ U_a \end{Bmatrix} = \begin{Bmatrix} F_c \\ F_a \end{Bmatrix} \quad (3.45)$$

where the values of the constrained displacements U_c are known (but not necessarily zero), as are the applied external forces F_a . Thus, the unknown, active displacements are obtained via the lower partition as

$$[K_{ac}]\{U_c\} + [K_{aa}]\{U_a\} = \{F_a\} \quad (3.46a)$$

$$\{U_a\} = [K_{aa}]^{-1}(\{F_a\} - [K_{ac}]\{U_c\}) \quad (3.46b)$$

where we have assumed that the specified displacements $\{U_c\}$ are not necessarily zero, although that is usually the case in a truss structure. (Again, note that, for numerical efficiency, methods other than matrix inversion are applied to obtain the solutions formally represented by Equations 3.46.) Given the displacement solution of Equations 3.46, the reactions are obtained using the upper partition of matrix Equation 3.45 as

$$\{F_c\} = [K_{cc}]\{U_c\} + [K_{ca}]\{U_a\} \quad (3.47)$$

where $[K_{ca}] = [K_{ac}]^T$ by the symmetry property of the stiffness matrix.

3.6 ELEMENT STRAIN AND STRESS

The final computational step in finite element analysis of a truss structure is to utilize the global displacements obtained in the solution step to determine the strain and stress in each element of the truss. For an element connecting nodes i and j , the element nodal displacements *in the element coordinate system* are given by Equations 3.19 and 3.20 as

$$\begin{aligned} u_1^{(e)} &= U_1^{(e)} \cos \theta + U_2^{(e)} \sin \theta \\ u_2^{(e)} &= U_3^{(e)} \cos \theta + U_4^{(e)} \sin \theta \end{aligned} \quad (3.48)$$

and the element axial strain (utilizing Equation 2.29 and the discretization and interpolation functions of Equation 2.25) is then

$$\begin{aligned}\epsilon^{(e)} &= \frac{du^{(e)}(x)}{dx} = \frac{d^{(e)}}{dx} [N_1(x) \quad N_2(x)] \begin{Bmatrix} u_1^{(e)} \\ u_2^{(e)} \end{Bmatrix} \\ &= \begin{bmatrix} -1 & 1 \\ L^{(e)} & L^{(e)} \end{bmatrix} \begin{Bmatrix} u_1^{(e)} \\ u_2^{(e)} \end{Bmatrix} = \frac{u_2^{(e)} - u_1^{(e)}}{L^{(e)}}\end{aligned}\quad (3.49)$$

where $L^{(e)}$ is element length. The element axial stress is then obtained via application of Hooke's law as

$$\sigma^{(e)} = E\epsilon^{(e)} \quad (3.50)$$

Note, however, that the global solution does not give the element axial displacement directly. Rather, the element displacements are obtained from the global displacements via Equations 3.48. Recalling Equations 3.21 and 3.22, the element strain in terms of global system displacements is

$$\epsilon^{(e)} = \frac{du^{(e)}(x)}{dx} = \frac{d}{dx} [N_1(x) \quad N_2(x)] [R] \begin{Bmatrix} U_1^{(e)} \\ U_2^{(e)} \\ U_3^{(e)} \\ U_4^{(e)} \end{Bmatrix} \quad (3.51)$$

where $[R]$ is the element transformation matrix defined by Equation 3.22. The element stresses for the bar element in terms of global displacements are those given by

$$\sigma^{(e)} = E\epsilon^{(e)} = E \frac{du^{(e)}(x)}{dx} = E \frac{d^{(e)}}{dx} [N_1(x) \quad N_2(x)] [R] \begin{Bmatrix} U_1^{(e)} \\ U_2^{(e)} \\ U_3^{(e)} \\ U_4^{(e)} \end{Bmatrix} \quad (3.52)$$

As the bar element is formulated here, a positive axial stress value indicates that the element is in tension and a negative value indicates compression per the usual convention. Note that the stress calculation indicated in Equation 3.52 must be performed on an element-by-element basis. If desired, the element forces can be obtained via Equation 3.23.

EXAMPLE 3.2

The two-element truss in Figure 3.5 is subjected to external loading as shown. Using the same node and element numbering as in Figure 3.2, determine the displacement components of node 3, the reaction force components at nodes 1 and 2, and the element displacements, stresses, and forces. The elements have modulus of elasticity $E_1 = E_2 = 10 \times 10^6 \text{ lb/in.}^2$ and cross-sectional areas $A_1 = A_2 = 1.5 \text{ in.}^2$.

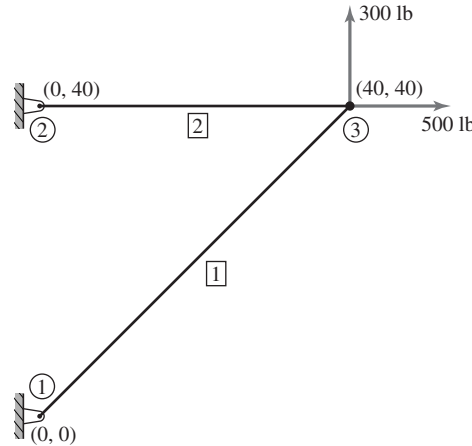


Figure 3.5 Two-element truss with external loading.

■ **Solution**

The nodal coordinates are such that $\theta_1 = \pi/4$ and $\theta_2 = 0$ and the element lengths are $L_1 = \sqrt{40^2 + 40^2} \approx 56.57$ in., $L_2 = 40$ in. The characteristic element stiffnesses are then

$$k_1 = \frac{A_1 E_1}{L_1} = \frac{1.5(10)(10^6)}{56.57} = 2.65(10^5) \text{ lb/in.}$$

$$k_2 = \frac{A_2 E_2}{L_2} = \frac{1.5(10)(10^6)}{40} = 3.75(10^5) \text{ lb/in.}$$

As the element orientation angles and numbering scheme are the same as in Example 3.1, we use the result of that example to write the global stiffness matrix as

$$[K] = \begin{bmatrix} 1.325 & 1.325 & 0 & 0 & -1.325 & -1.325 \\ 1.325 & 1.325 & 0 & 0 & -1.325 & -1.325 \\ 0 & 0 & 3.75 & 0 & -3.75 & 0 \\ 0 & 0 & 0 & 0 & 0 & 0 \\ -1.325 & -1.325 & -3.75 & 0 & 5.075 & 1.325 \\ -1.325 & -1.325 & 0 & 0 & 1.325 & 1.325 \end{bmatrix} 10^5 \text{ lb/in.}$$

Incorporating the displacement constraints $U_1 = U_2 = U_3 = U_4 = 0$, the global equilibrium equations are

$$10^5 \begin{bmatrix} 1.325 & 1.325 & 0 & 0 & -1.325 & -1.325 \\ 1.325 & 1.325 & 0 & 0 & -1.325 & -1.325 \\ 0 & 0 & 3.75 & 0 & -3.75 & 0 \\ 0 & 0 & 0 & 0 & 0 & 0 \\ -1.325 & -1.325 & -3.75 & 0 & 5.075 & 1.325 \\ -1.325 & -1.325 & 0 & 0 & 1.325 & 1.325 \end{bmatrix} \begin{Bmatrix} 0 \\ 0 \\ 0 \\ 0 \\ U_5 \\ U_6 \end{Bmatrix} = \begin{Bmatrix} F_1 \\ F_2 \\ F_3 \\ F_4 \\ 500 \\ 300 \end{Bmatrix}$$

3.6 Element Strain and Stress

71

and the dashed lines indicate the partitioning technique of Equation 3.45. Hence, the active displacements are governed by

$$10^5 \begin{bmatrix} 5.075 & 1.325 \\ 1.325 & 1.325 \end{bmatrix} \begin{Bmatrix} U_5 \\ U_6 \end{Bmatrix} = \begin{Bmatrix} 500 \\ 300 \end{Bmatrix}$$

Simultaneous solution gives the displacements as

$$U_5 = 5.333 \times 10^{-4} \text{ in.} \quad \text{and} \quad U_6 = 1.731 \times 10^{-3} \text{ in.}$$

As all the constrained displacement values are zero, the reaction forces are obtained via Equation 3.47 as

$$\begin{Bmatrix} F_1 \\ F_2 \\ F_3 \\ F_4 \end{Bmatrix} = \{F_c\} = [K_{ca}]\{U_a\} = 10^5 \begin{bmatrix} -1.325 & -1.325 \\ -1.325 & -1.325 \\ -3.75 & 0 \\ 0 & 0 \end{bmatrix} \begin{Bmatrix} 0.5333 \\ 1.731 \end{Bmatrix} 10^{-3} = \begin{Bmatrix} -300 \\ -300 \\ -200 \\ 0 \end{Bmatrix} \text{ lb}$$

and we note that the net force on the structure is zero, as required for equilibrium. A check of moments about any of the three nodes also shows that moment equilibrium is satisfied.

For element 1, the element displacements in the element coordinate system are

$$\begin{Bmatrix} u_1^{(1)} \\ u_2^{(1)} \end{Bmatrix} = [R^{(1)}] \begin{Bmatrix} U_1 \\ U_2 \\ U_5 \\ U_6 \end{Bmatrix} = \frac{\sqrt{2}}{2} \begin{bmatrix} 1 & 1 & 0 & 0 \\ 0 & 0 & 1 & 1 \end{bmatrix} \begin{Bmatrix} 0 \\ 0 \\ 0.5333 \\ 1.731 \end{Bmatrix} 10^{-3} = \begin{Bmatrix} 0 \\ 1.6 \end{Bmatrix} 10^{-3} \text{ in.}$$

Element stress is computed using Equation 3.52:

$$\sigma^{(1)} = E_1 \begin{bmatrix} -\frac{1}{L_1} & \frac{1}{L_1} \end{bmatrix} [R^{(1)}] \begin{Bmatrix} U_1 \\ U_2 \\ U_5 \\ U_6 \end{Bmatrix}$$

Using the element displacements just computed, we have

$$\sigma^{(1)} = 10(10^6) \begin{bmatrix} -\frac{1}{56.57} & \frac{1}{56.57} \end{bmatrix} \begin{Bmatrix} 0 \\ 1.6 \end{Bmatrix} 10^{-3} \approx 283 \text{ lb/in.}^2$$

and the positive results indicate tensile stress.

The element nodal forces via Equation 3.23 are

$$\begin{Bmatrix} f_1^{(1)} \\ f_2^{(1)} \end{Bmatrix} = \begin{bmatrix} k_1 & -k_1 \\ -k_1 & k_1 \end{bmatrix} \begin{Bmatrix} u_1^{(1)} \\ u_2^{(1)} \end{Bmatrix} = 2.65(10^5) \begin{bmatrix} 1 & -1 \\ -1 & 1 \end{bmatrix} \begin{Bmatrix} 0 \\ 1.6 \end{Bmatrix} 10^{-3} \\ = \begin{Bmatrix} -424 \\ 424 \end{Bmatrix} \text{ lb}$$

and the algebraic signs of the element nodal forces also indicate tension.

For element 2, the same procedure in sequence gives

$$\begin{Bmatrix} u_1^{(2)} \\ u_2^{(2)} \end{Bmatrix} = [R^{(2)}] \begin{Bmatrix} U_1 \\ U_2 \\ U_5 \\ U_6 \end{Bmatrix} = \begin{bmatrix} 1 & 0 & 0 & 0 \\ 0 & 0 & 1 & 0 \end{bmatrix} \begin{Bmatrix} 0 \\ 0 \\ 0.5333 \\ 1.731 \end{Bmatrix} 10^{-3} = \begin{Bmatrix} 0 \\ 0.5333 \end{Bmatrix} 10^{-4} \text{ in.}$$

$$\sigma^{(2)} = 10(10^6) \begin{bmatrix} -\frac{1}{40} & \frac{1}{40} \end{bmatrix} \begin{Bmatrix} 0 \\ 0.5333 \end{Bmatrix} 10^{-3} \approx 133 \text{ lb/in.}^2$$

$$\begin{Bmatrix} f_1^{(2)} \\ f_2^{(2)} \end{Bmatrix} = \begin{bmatrix} k_2 & -k_2 \\ -k_2 & k_2 \end{bmatrix} \begin{Bmatrix} u_1^{(2)} \\ u_2^{(2)} \end{Bmatrix} = 3.75(10^5) \begin{bmatrix} 1 & -1 \\ -1 & 1 \end{bmatrix} \begin{Bmatrix} 0 \\ 0.5333 \end{Bmatrix} 10^{-3} = \begin{Bmatrix} -200 \\ 200 \end{Bmatrix} \text{ lb}$$

also indicating tension.

The finite method is intended to be a general purpose procedure for analyzing problems for which the general solution is not known; however, it is informative in the examples of this chapter (since the bar element poses an exact formulation) to check the solutions in terms of axial stress computed simply as F/A for an axially loaded member. The reader is encouraged to compute the axial stress by the simple stress formula for each example to verify that the solutions via the stiffness-based finite element method are correct.

3.7 COMPREHENSIVE EXAMPLE

As a comprehensive example of two-dimensional truss analysis, the structure depicted in Figure 3.6a is analyzed to obtain displacements, reaction forces, strains, and stresses. While we do not include all computational details, the example illustrates the required steps, in sequence, for a finite element analysis.

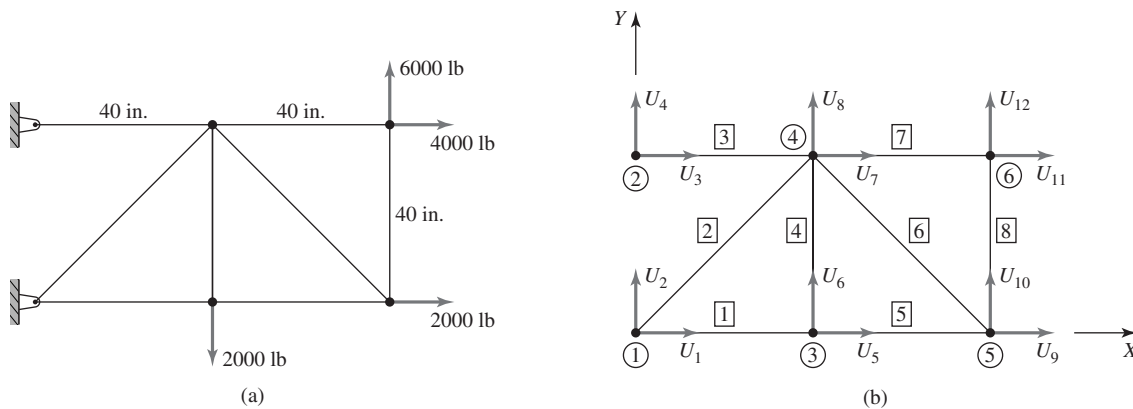


Figure 3.6

(a) For each element, $A = 1.5 \text{ in.}^2$, $E = 10 \times 10^6 \text{ psi}$. (b) Node, element, and global displacement notation.

Step 1. Specify the global coordinate system, assign node numbers, and define element connectivity, as shown in Figure 3.6b.

Step 2. Compute individual element stiffness values:

$$k^{(1)} = k^{(3)} = k^{(4)} = k^{(5)} = k^{(7)} = k^{(8)} = \frac{1.5(10^7)}{40} = 3.75(10^5) \text{ lb/in.}$$

$$k^{(2)} = k^{(6)} = \frac{1.5(10^7)}{40\sqrt{2}} = 2.65(10^5) \text{ lb/in.}$$

Step 3. Transform element stiffness matrices into the global coordinate system. Utilizing Equation 3.28 with

$$\theta_1 = \theta_3 = \theta_5 = \theta_7 = 0 \quad \theta_4 = \theta_8 = \pi/2 \quad \theta_2 = \pi/4 \quad \theta_6 = 3\pi/4$$

we obtain

$$[K^{(1)}] = [K^{(3)}] = [K^{(5)}] = [K^{(7)}] = 3.75(10^5) \begin{bmatrix} 1 & 0 & -1 & 0 \\ 0 & 0 & 0 & 0 \\ -1 & 0 & 1 & 0 \\ 0 & 0 & 0 & 0 \end{bmatrix}$$

$$[K^{(4)}] = [K^{(8)}] = 3.75(10^5) \begin{bmatrix} 0 & 0 & 0 & 0 \\ 0 & 1 & 0 & -1 \\ 0 & 0 & 0 & 0 \\ 0 & -1 & 0 & 1 \end{bmatrix}$$

$$[K^{(2)}] = \frac{2.65(10^5)}{2} \begin{bmatrix} 1 & 1 & -1 & -1 \\ 1 & 1 & -1 & -1 \\ -1 & -1 & 1 & 1 \\ -1 & -1 & 1 & 1 \end{bmatrix}$$

$$[K^{(6)}] = \frac{2.65(10^5)}{2} \begin{bmatrix} 1 & -1 & -1 & 1 \\ -1 & 1 & 1 & -1 \\ -1 & 1 & 1 & -1 \\ 1 & -1 & -1 & 1 \end{bmatrix}$$

Step 4a. Construct the element-to-global displacement correspondence table. With reference to Figure 3.6c, the connectivity and displacement relations are shown in Table 3.3.

Step 4b. Alternatively and more efficiently, form the element-node connectivity table (Table 3.4), and the corresponding element global displacement location vector for each element is

$$L^{(1)} = [1 \quad 2 \quad 5 \quad 6]$$

$$L^{(2)} = [1 \quad 2 \quad 7 \quad 8]$$

$$L^{(3)} = [3 \quad 4 \quad 7 \quad 8]$$

$$L^{(4)} = [5 \quad 6 \quad 7 \quad 8]$$

Table 3.3 Connectivity and Displacement Relations

Global	Elem. 1	Elem. 2	Elem. 3	Elem. 4	Elem. 5	Elem. 6	Elem. 7	Elem. 8
1	1	1	0	0	0	0	0	0
2	2	2	0	0	0	0	0	0
3	0	0	1	0	0	0	0	0
4	0	0	2	0	0	0	0	0
5	3	0	0	1	1	0	0	0
6	4	0	0	2	2	0	0	0
7	0	3	3	3	0	3	1	0
8	0	4	4	4	0	4	2	0
9	0	0	0	0	3	1	0	1
10	0	0	0	0	4	2	0	2
11	0	0	0	0	0	0	3	3
12	0	0	0	0	0	0	4	4

Table 3.4 Element-Node Connectivity

Element	Node	
	<i>i</i>	<i>j</i>
1	1	3
2	1	4
3	2	4
4	3	4
5	3	5
6	5	4
7	4	6
8	5	6

$$L^{(5)} = [5 \quad 6 \quad 9 \quad 10]$$

$$L^{(6)} = [9 \quad 10 \quad 7 \quad 8]$$

$$L^{(7)} = [7 \quad 8 \quad 11 \quad 12]$$

$$L^{(8)} = [9 \quad 10 \quad 11 \quad 12]$$

Step 5. Assemble the global stiffness matrix per either Step 4a or 4b. The resulting components of the global stiffness matrix are

$$K_{11} = k_{11}^{(1)} + k_{11}^{(2)} = (3.75 + 2.65/2)10^5$$

$$K_{12} = k_{12}^{(1)} + k_{12}^{(2)} = (0 + 2.65/2)10^5$$

$$K_{13} = K_{14} = 0$$

$$K_{15} = k_{13}^{(1)} = -3.75(10^5)$$

$$K_{16} = k_{14}^{(1)} = 0$$

$$K_{17} = k_{13}^{(2)} = -(2.65/2)10^5$$

3.7 Comprehensive Example

75

$$K_{18} = k_{14}^{(2)} = -(2.65/2)10^5$$

$$K_{19} = K_{1,10} = K_{1,11} = K_{1,12} = 0$$

$$K_{22} = k_{22}^{(1)} + k_{22}^{(2)} = 0 + (2.65/2)10^5$$

$$K_{23} = K_{24} = 0$$

$$K_{25} = k_{23}^{(1)} = 0$$

$$K_{26} = k_{24}^{(1)} = 0$$

$$K_{27} = k_{23}^{(2)} = -(2.65/2)10^5$$

$$K_{28} = k_{24}^{(2)} = -(2.65/2)10^5$$

$$K_{29} = K_{2,10} = K_{2,11} = K_{2,12} = 0$$

$$K_{33} = k_{11}^{(3)} = 3.75(10^5)$$

$$K_{34} = k_{12}^{(3)} = 0$$

$$K_{35} = K_{36} = 0$$

$$K_{37} = k_{13}^{(3)} = -3.75(10^5)$$

$$K_{38} = k_{14}^{(3)} = 0$$

$$K_{39} = K_{3,10} = K_{3,11} = K_{3,12} = 0$$

$$K_{44} = k_{22}^{(3)} = 0$$

$$K_{45} = K_{46} = 0$$

$$K_{47} = k_{23}^{(3)} = 0$$

$$K_{48} = k_{24}^{(3)} = 0$$

$$K_{49} = K_{4,10} = K_{4,11} = K_{4,12} = 0$$

$$K_{55} = k_{33}^{(1)} + k_{11}^{(4)} + k_{11}^{(5)} = (3.75 + 0 + 3.75)10^5$$

$$K_{56} = k_{34}^{(1)} + k_{12}^{(4)} + k_{12}^{(5)} = 0 + 0 + 0 = 0$$

$$K_{57} = k_{13}^{(4)} = 0$$

$$K_{58} = k_{14}^{(4)} = 0$$

$$K_{59} = k_{13}^{(5)} = -3.75(10^5)$$

$$K_{5,10} = k_{14}^{(5)} = 0$$

$$K_{5,11} = K_{5,12} = 0$$

$$K_{66} = k_{44}^{(2)} + k_{22}^{(4)} + k_{22}^{(5)} = (0 + 3.75 + 0)10^5$$

$$K_{67} = k_{23}^{(4)} = 0$$

$$K_{68} = k_{24}^{(4)} = -3.75(10^5)$$

$$K_{69} = k_{23}^{(5)} = 0$$

$$K_{6,10} = k_{24}^{(5)} = 0$$

$$K_{6,11} = K_{6,12} = 0$$

$$\begin{aligned} K_{77} &= k_{33}^{(2)} + k_{33}^{(3)} + k_{33}^{(4)} + k_{33}^{(6)} + k_{11}^{(7)} \\ &= (2.65/2 + 3.75 + 0 + 2.65/2 + 3.75)10^5 \end{aligned}$$

$$\begin{aligned} K_{78} &= k_{34}^{(2)} + k_{34}^{(3)} + k_{34}^{(4)} + k_{34}^{(6)} + k_{12}^{(7)} \\ &= (2.65/2 + 0 + 0 - 2.65/2 + 0)10^5 = 0 \end{aligned}$$

$$K_{79} = k_{13}^{(6)} = -(2.65/2)10^5$$

$$K_{7,10} = k_{23}^{(6)} = (2.65/2)10^5$$

$$K_{7,11} = k_{13}^{(7)} = -3.75(10^5)$$

$$K_{7,12} = k_{14}^{(7)} = 0$$

$$\begin{aligned} K_{88} &= k_{44}^{(2)} + k_{44}^{(3)} + k_{44}^{(4)} + k_{44}^{(6)} + k_{22}^{(7)} \\ &= (2.65/2 + 0 + 3.75 + 2.65/2 + 0)10^5 \end{aligned}$$

$$K_{89} = k_{14}^{(6)} = (2.65/2)10^5$$

$$K_{8,10} = k_{24}^{(6)} = -(2.65/2)10^5$$

$$K_{8,11} = k_{23}^{(7)} = 0$$

$$K_{8,12} = k_{24}^{(7)} = 0$$

$$K_{99} = k_{33}^{(5)} + k_{11}^{(6)} + k_{11}^{(8)} = (3.75 + 2.65/2 + 0)10^5$$

$$K_{9,10} = k_{34}^{(5)} + k_{12}^{(6)} + k_{12}^{(8)} = (0 - 2.65/2 + 0)10^5$$

$$K_{9,11} = k_{13}^{(8)} = 0$$

$$K_{9,12} = k_{14}^{(8)} = 0$$

$$K_{10,10} = k_{44}^{(5)} + k_{22}^{(6)} + k_{22}^{(8)} = (0 + 2.65/2 + 3.75)10^5$$

$$K_{10,11} = k_{23}^{(8)} = 0$$

$$K_{10,12} = k_{24}^{(8)} = -3.75(10^5)$$

$$K_{11,11} = k_{33}^{(7)} + k_{33}^{(8)} = (3.75 + 0)10^5$$

$$K_{11,12} = k_{34}^{(7)} + k_{34}^{(8)} = 0 + 0$$

$$K_{12,12} = k_{44}^{(7)} + k_{44}^{(8)} = (0 + 3.75)10^5$$

Step 6. Apply the constraints as dictated by the boundary conditions. In this example, nodes 1 and 2 are fixed so the displacement constraints are

$$U_1 = U_2 = U_3 = U_4 = 0$$

Therefore, the first four equations in the 12×12 matrix system

$$[K]\{U\} = \{F\}$$

are constraint equations and can be removed from consideration since the applied displacements are all zero (if not zero, the constraints are considered as in Equation 3.46, in which case the nonzero constraints impose additional forces on the unconstrained displacements). The constraint forces cannot be obtained until the unconstrained displacements are computed. So, we effectively strike out the first four rows and columns of the global equations to obtain

$$[K_{aa}] \begin{Bmatrix} U_5 \\ U_6 \\ U_7 \\ U_8 \\ U_9 \\ U_{10} \\ U_{11} \\ U_{12} \end{Bmatrix} = \begin{Bmatrix} 0 \\ -2000 \\ 0 \\ 0 \\ 2000 \\ 0 \\ 4000 \\ 6000 \end{Bmatrix}$$

as the system of equations governing the “active” displacements.

- Step 7.** Solve the equations corresponding to the unconstrained displacements. For the current example, the equations are solved using a spreadsheet program, inverting the (relatively small) global stiffness matrix to obtain

$$\begin{Bmatrix} U_5 \\ U_6 \\ U_7 \\ U_8 \\ U_9 \\ U_{10} \\ U_{11} \\ U_{12} \end{Bmatrix} = \begin{Bmatrix} 0.02133 \\ 0.04085 \\ -0.01600 \\ 0.04619 \\ 0.04267 \\ 0.15014 \\ -0.00533 \\ 0.16614 \end{Bmatrix} \text{ in.}$$

- Step 8.** Back-substitute the displacement data into the constraint equations to compute reaction forces. Utilizing Equation 3.37, with $\{U_c\} = \{0\}$, we use the four equations previously ignored to compute the force components at nodes 1 and 2. The constraint equations are of the form

$$K_{i5}U_5 + K_{i6}U_6 + \cdots + K_{i,12}U_{12} = F_i \quad i = 1, 4$$

and, on substitution of the computed displacements, yield

$$\begin{Bmatrix} F_1 \\ F_2 \\ F_3 \\ F_4 \end{Bmatrix} = \begin{Bmatrix} -12,000 \\ -4,000 \\ 6,000 \\ 0 \end{Bmatrix} \text{ lb}$$

The reader is urged to utilize these reaction force components and check the equilibrium conditions of the structure.

- Step 9.** Compute strain and stress in each element. The major computational task completed in Step 7 provides the displacement components of each node in the global coordinate system. With this information and the known constrained displacements, the displacements of each element in its element coordinate system can be obtained; hence, the strain and stress in each element can be computed.

For element 2, for example, we have

$$u_1^{(2)} = U_1 \cos \theta_2 + U_2 \sin \theta_2 = 0$$

$$\begin{aligned} u_2^{(2)} &= U_7 \cos \theta_2 + U_8 \sin \theta_2 = (-0.01600 + 0.04618)\sqrt{2}/2 \\ &= 0.02134 \end{aligned}$$

The axial strain in element 2 is then

$$\epsilon^{(2)} = \frac{u_2^{(2)} - u_1^{(2)}}{L^{(2)}} = \frac{0.02133}{40\sqrt{2}} = 3.771(10^{-4})$$

and corresponding axial stress is

$$\sigma^{(2)} = E\epsilon^{(2)} = 3771 \text{ psi}$$

The results for element 2 are presented as an example only. In finite element software, the results for each element are available and can be examined as desired by the user of the software (postprocessing).

Results for each of the eight elements are shown in Table 3.5; and per the usual sign convention, positive values indicate tensile stress while negative values correspond to compressive stress. In obtaining the computed results for this example, we used a spreadsheet program to invert the stiffness matrix, MATLAB to solve via matrix inversion, and a popular finite element software package. The solutions resulting from each procedure are identical.

Table 3.5 Results for the Eight Elements

Element	Strain	Stress, psi
1	$5.33(10^{-4})$	5333
2	$3.77(10^{-4})$	3771
3	$-4.0(10^{-4})$	-4000
4	$1.33(10^{-4})$	1333
5	$5.33(10^{-4})$	5333
6	$-5.67(10^{-4})$	-5657
7	$2.67(10^{-4})$	2667
8	$4.00(10^{-4})$	4000

3.8 THREE-DIMENSIONAL TRUSSES

Three-dimensional (3-D) trusses can also be modeled using the bar element, provided the connections between elements are such that only axial load is transmitted. Strictly, this requires that all connections be ball-and-socket joints. Even when the connection restriction is not precisely satisfied, analysis of a 3-D truss using bar elements is often of value in obtaining preliminary estimates of member stresses, which in context of design, is valuable in determining required structural properties. Referring to Figure 3.7 which depicts a one-dimensional bar element connected to nodes i and j in a 3-D global reference frame, the unit vector along the element axis (i.e., the element reference frame) expressed in the global system is

$$\lambda^{(e)} = \frac{1}{L}[(X_j - X_i)\mathbf{I} + (Y_j - Y_i)\mathbf{J} + (Z_j - Z_i)\mathbf{K}] \quad (3.53)$$

or

$$\lambda^{(e)} = \cos \theta_x \mathbf{I} + \cos \theta_y \mathbf{J} + \cos \theta_z \mathbf{K} \quad (3.54)$$

Thus, the element displacements are expressed in components in the 3-D global system as

$$u_1^{(e)} = U_1^{(e)} \cos \theta_x + U_2^{(e)} \cos \theta_y + U_3^{(e)} \cos \theta_z \quad (3.55)$$

$$u_2^{(e)} = U_4^{(e)} \cos \theta_x + U_5^{(e)} \cos \theta_y + U_6^{(e)} \cos \theta_z \quad (3.56)$$

Here, we use the notation that element displacements 1 and 4 are in the global X direction, displacements 2 and 5 are in the global Y direction, and element displacements 3 and 6 are in the global Z direction.

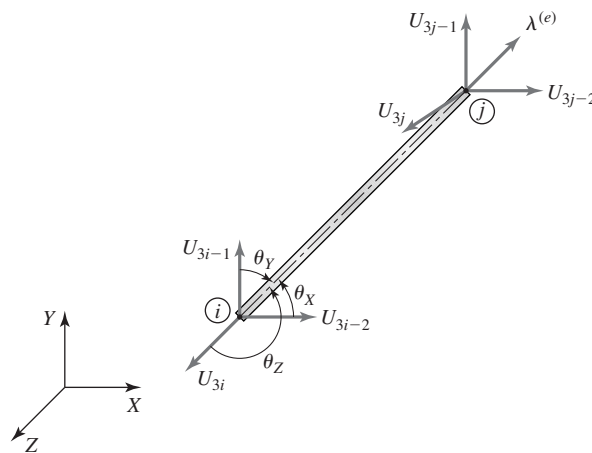


Figure 3.7 Bar element in a 3-D global coordinate system.

Analogous to Equation 3.21, Equations 3.55 and 3.56 can be expressed as

$$\begin{Bmatrix} u_1^{(e)} \\ u_2^{(e)} \end{Bmatrix} = \begin{bmatrix} \cos \theta_x & \cos \theta_y & \cos \theta_z & 0 & 0 & 0 \\ 0 & 0 & 0 & \cos \theta_x & \cos \theta_y & \cos \theta_z \end{bmatrix} \begin{Bmatrix} U_1^{(e)} \\ U_2^{(e)} \\ U_3^{(e)} \\ U_4^{(e)} \\ U_5^{(e)} \\ U_6^{(e)} \end{Bmatrix} = [R]\{U^{(e)}\} \quad (3.57)$$

where $[R]$ is the transformation matrix mapping the one-dimensional element displacements into a three-dimensional global coordinate system. Following the identical procedure used for the 2-D case in Section 3.3, the element stiffness matrix in the element coordinate system is transformed into the 3-D global coordinates via

$$[K^{(e)}] = [R]^T \begin{bmatrix} k_e & -k_e \\ -k_e & k_e \end{bmatrix} [R] \quad (3.58)$$

Substituting for the transformation matrix $[R]$ and performing the multiplication results in

$$[K^{(e)}] = k_e \begin{bmatrix} c_x^2 & c_x c_y & c_x c_z & -c_x^2 & -c_x c_y & -c_x c_z \\ c_x c_y & c_y^2 & c_y c_z & -c_x c_x & -c_y^2 & -c_y c_z \\ c_x c_z & c_y c_z & c_z^2 & -c_x c_z & -c_y c_z & -c_z^2 \\ -c_x^2 & -c_x c_x & -c_x c_z & c_x^2 & c_x c_y & c_x c_z \\ -c_x c_y & -c_y^2 & -c_y c_z & c_x c_y & c_y^2 & c_y c_z \\ -c_x c_z & -c_y c_z & -c_z^2 & c_x c_z & c_y c_z & c_z^2 \end{bmatrix} \quad (3.59)$$

as the 3-D global stiffness matrix for the one-dimensional bar element where

$$\begin{aligned} c_x &= \cos \theta_x \\ c_y &= \cos \theta_y \\ c_z &= \cos \theta_z \end{aligned} \quad (3.60)$$

Assembly of the global stiffness matrix (hence, the equilibrium equations), is identical to the procedure discussed for the two-dimensional case with the obvious exception that three displacements are to be accounted for at each node.

EXAMPLE 3.3

The three-member truss shown in Figure 3.8a is connected by ball-and-socket joints and fixed at nodes 1, 2, and 3. A 5000-lb force is applied at node 4 in the negative Y direction, as shown. Each of the three members is identical and exhibits a characteristic axial stiffness of $3(10^5)$ lb/in. Compute the displacement components of node 4 using a finite element model with bar elements.

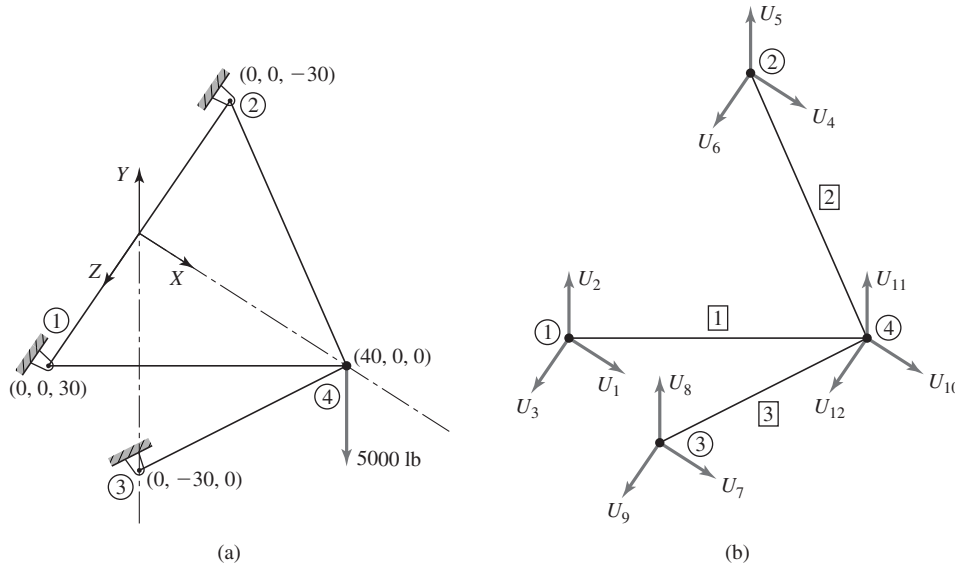


Figure 3.8
(a) A three-element, 3-D truss. (b) Numbering scheme.

■ Solution

First, note that the 3-D truss with four nodes has 12 possible displacements. However, since nodes 1–3 are fixed, nine of the possible displacements are known to be zero. Therefore, we need assemble only a portion of the system stiffness matrix to solve for the three unknown displacements. Utilizing the numbering scheme shown in Figure 3.8b and the element-to-global displacement correspondence table (Table 3.6), we need consider only the equations

$$\begin{bmatrix} K_{10,10} & K_{10,11} & K_{10,12} \\ K_{11,10} & K_{11,11} & K_{11,12} \\ K_{12,10} & K_{12,11} & K_{12,12} \end{bmatrix} \begin{Bmatrix} U_{10} \\ U_{11} \\ U_{12} \end{Bmatrix} = \begin{Bmatrix} 0 \\ -5000 \\ 0 \end{Bmatrix}$$

Prior to assembling the terms required in the system stiffness matrix, the individual element stiffness matrices must be transformed to the global coordinates as follows.

Element 1

$$\lambda^{(1)} = \frac{1}{50}[(40 - 0)\mathbf{I} + (0 - 0)\mathbf{J} + (0 - 30)\mathbf{K}] = 0.8\mathbf{I} - 0.6\mathbf{K}$$

Hence, $c_x = 0.8$, $c_y = 0$, $c_z = -0.6$, and Equation 3.59 gives

$$[K^{(1)}] = 3(10^5) \begin{bmatrix} 0.64 & 0 & -0.48 & -0.64 & 0 & 0.48 \\ 0 & 0 & 0 & 0 & 0 & 0 \\ -0.48 & 0 & 0.36 & 0.48 & 0 & -0.36 \\ -0.64 & 0 & 0.48 & 0.64 & 0 & -0.48 \\ 0 & 0 & 0 & 0 & 0 & 0 \\ 0.48 & -0 & -0.36 & -0.48 & 0 & 0.36 \end{bmatrix} \text{ lb/in.}$$

Table 3.6 Element-to-Global Displacement Correspondence

Global Displacement	Element 1	Element 2	Element 3
1	1	0	0
2	2	0	0
3	3	0	0
4	0	1	0
5	0	2	0
6	0	3	0
7	0	0	1
8	0	0	2
9	0	0	3
10	4	4	4
11	5	5	5
12	6	6	6

Element 2

$$\lambda^{(2)} = \frac{1}{50}[(40 - 0)\mathbf{I} + (0 - 0)\mathbf{J} + (0 - (-30))\mathbf{K}] = 0.8\mathbf{I} + 0.6\mathbf{K}$$

$$[K^{(2)}] = 3(10^5) \begin{bmatrix} 0.64 & 0 & 0.48 & -0.64 & 0 & -0.48 \\ 0 & 0 & 0 & 0 & 0 & 0 \\ 0.48 & 0 & 0.36 & -0.48 & 0 & -0.36 \\ -0.64 & 0 & -0.48 & 0.64 & 0 & 0.48 \\ 0 & 0 & 0 & 0 & 0 & 0 \\ -0.48 & 0 & -0.36 & 0.48 & 0 & 0.36 \end{bmatrix} \text{ lb/in.}$$

Element 3

$$\lambda^{(3)} = \frac{1}{50}[(40 - 0)\mathbf{I} + (0 - (-30))\mathbf{J} + (0 - 0)\mathbf{K}] = 0.8\mathbf{I} + 0.6\mathbf{J}$$

$$[K^{(3)}] = 3(10^5) \begin{bmatrix} 0.64 & 0.48 & 0 & -0.64 & -0.48 & 0 \\ 0.48 & 0.36 & 0 & -0.48 & -0.36 & 0 \\ 0 & 0 & 0 & 0 & 0 & 0 \\ -0.64 & -0.48 & 0 & 0.64 & 0.48 & 0 \\ -0.48 & -0.36 & 0 & 0.48 & 0.36 & 0 \\ 0 & 0 & 0 & 0 & 0 & 0 \end{bmatrix} \text{ lb/in.}$$

Referring to the last three rows of the displacement correspondence table, the required terms of the global stiffness matrix are assembled as follows:

$$K_{10,10} = k_{44}^{(1)} + k_{44}^{(2)} + k_{44}^{(3)} = 3(10^5)(0.64 + 0.64 + 0.64) = 5.76(10^5) \text{ lb/in.}$$

$$K_{10,11} = K_{11,10} = k_{45}^{(1)} + k_{45}^{(2)} + k_{45}^{(3)} = 3(10^5)(0 + 0 + 0.48) = 1.44(10^5) \text{ lb/in.}$$

$$K_{10,12} = K_{12,10} = k_{46}^{(1)} + k_{46}^{(2)} + k_{46}^{(3)} = 3(10^5)(-0.48 + 0.48 + 0) = 0 \text{ lb/in.}$$

$$K_{11,11} = k_{55}^{(1)} + k_{55}^{(2)} + k_{55}^{(3)} = 3(10^5)(0 + 0 + 0.36) = 1.08(10^5) \text{ lb/in.}$$

$$K_{11,12} = K_{12,11} = k_{56}^{(1)} + k_{56}^{(2)} + k_{56}^{(3)} = 3(10^5)(0 + 0 + 0) = 0 \text{ lb/in.}$$

$$K_{12,12} = k_{66}^{(1)} + k_{66}^{(2)} + k_{66}^{(3)} = 3(10^5)(0.36 + 0.36 + 0) = 2.16(10^5) \text{ lb/in.}$$

The system of equations to be solved for the displacements of node 4 are

$$10^5 \begin{bmatrix} 5.76 & 1.44 & 0 \\ 1.44 & 1.08 & 0 \\ 0 & 0 & 2.16 \end{bmatrix} \begin{Bmatrix} U_{10} \\ U_{11} \\ U_{12} \end{Bmatrix} = \begin{Bmatrix} 0 \\ -5000 \\ 0 \end{Bmatrix}$$

and simultaneous solution yields

$$U_{10} = 0.01736 \text{ in.}$$

$$U_{11} = -0.06944 \text{ in.}$$

$$U_{12} = 0$$

While the complete analysis is not conducted in the context of this example, the reaction forces, element strains, and element stresses would be determined by the same procedures followed in Section 3.7 for the two-dimensional case. It must be pointed out that the procedures required to obtain the individual element resultants are quite readily obtained by the matrix operations described here. Once the displacements have been calculated, the remaining (so-called) secondary variables (strain, stress, axial force) are readily computed using the matrices and displacement interpolation functions developed in the formulation of the original displacement problem.

3.9 SUMMARY

This chapter develops the complete procedure for performing a finite element analysis of a structure and illustrates it by several examples. Although only the simple axial element has been used, the procedure described is common to the finite element method for all element and analysis types, as will become clear in subsequent chapters. The direct stiffness method is by far the most straightforward technique for assembling the system matrices required for finite element analysis and is also very amenable to digital computer programming techniques.

REFERENCES

1. DaDeppo, D. *Introduction to Structural Mechanics and Analysis*. Upper Saddle River, NJ: Prentice-Hall, 1999.
2. Beer, F. P., and E. R. Johnston. *Vector Mechanics for Engineers, Statics and Dynamics*, 6th ed. New York: McGraw-Hill, 1997.

PROBLEMS

- 3.1 In the two-member truss shown in Figure 3.2, let $\theta_1 = 45^\circ$, $\theta_2 = 15^\circ$, and $F_5 = 5000 \text{ lb}$, $F_6 = 3000 \text{ lb}$.
 - a. Using only static force equilibrium equations, solve for the force in each member as well as the reaction force components.
 - b. Assuming each member has axial stiffness $k = 52000 \text{ lb/in.}$, compute the axial deflection of each member.
 - c. Using the results of part b, calculate the X and Y displacements of node 3.

- 3.2 Calculate the X and Y displacements of node 3 using the finite element approach and the data given in Problem 3.1. Also calculate the force in each element. How do your solutions compare to the results of Problem 3.1?
- 3.3 Verify Equation 3.28 by direct multiplication of the matrices.
- 3.4 Show that the transformed stiffness matrix for the bar element as given by Equation 3.28 is singular.
- 3.5 Each of the bar elements depicted in Figure P3.5 has a solid circular cross-section with diameter $d = 1.5$ in. The material is a low-carbon steel having modulus of elasticity $E = 30 \times 10^6$ psi. The nodal coordinates are given in a global (X, Y) coordinate system (in inches). Determine the element stiffness matrix of each element in the global system.

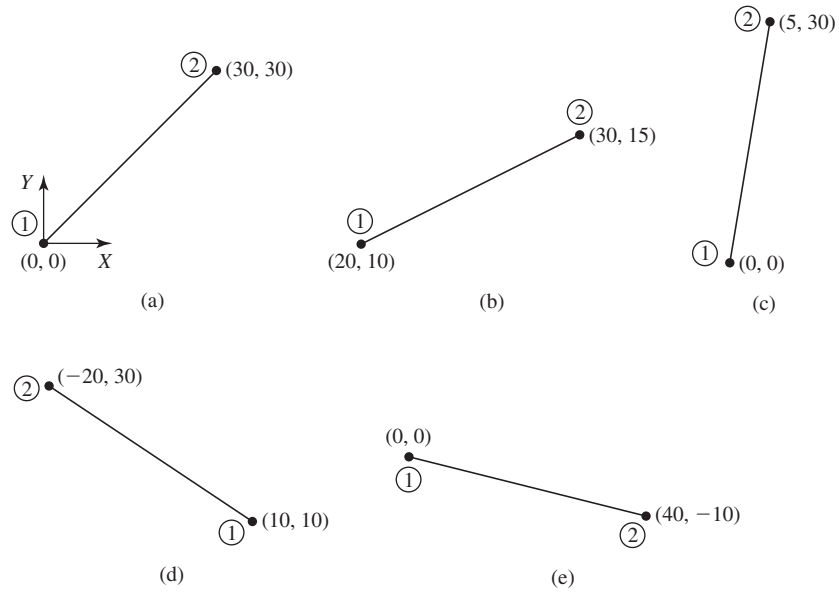


Figure P3.5

- 3.6 Repeat Problem 3.5 for the bar elements in Figure P3.6. For these elements, $d = 40$ mm, $E = 69$ GPa, and the nodal coordinates are in meters.

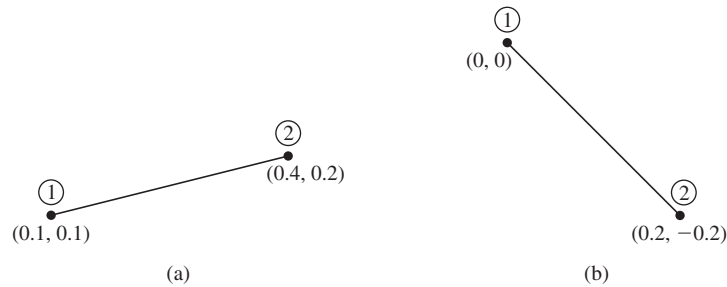


Figure P3.6

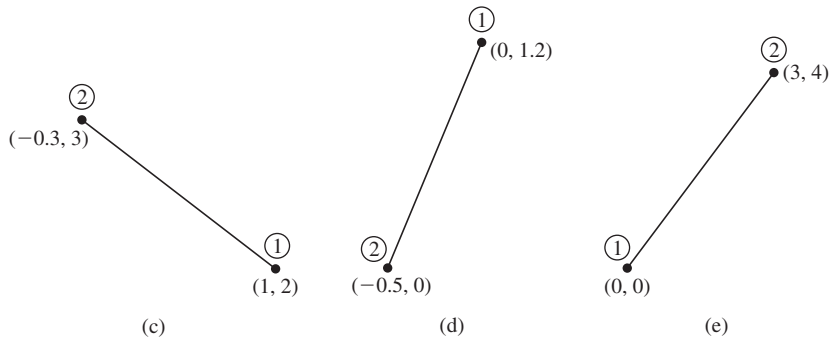


Figure P3.6 (Continued)

3.7 For each of the truss structures shown in Figure P3.7, construct an element-to-global displacement correspondence table in the form of Table 3.1.

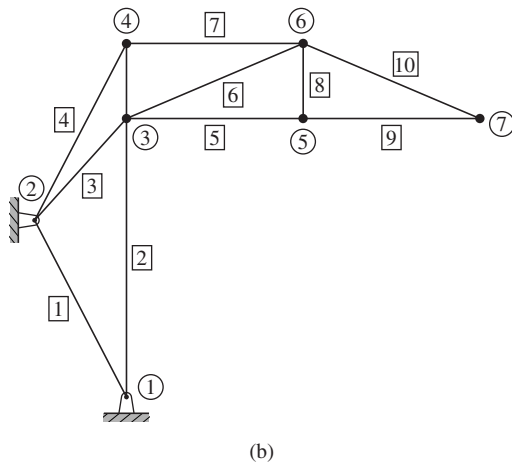
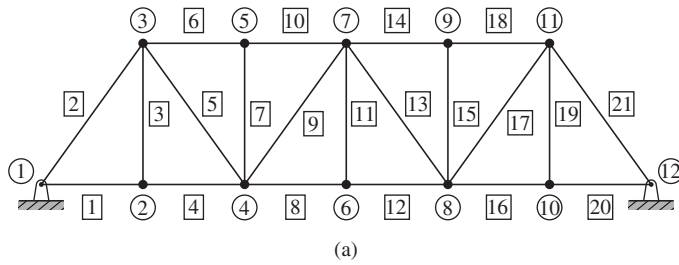


Figure P3.7

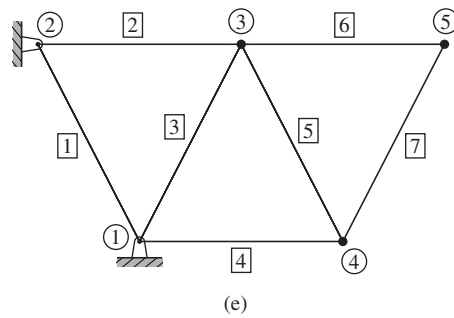
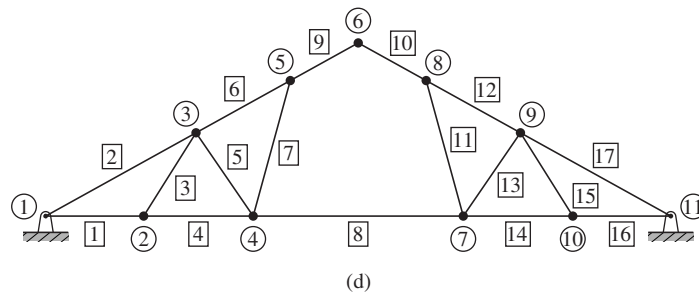
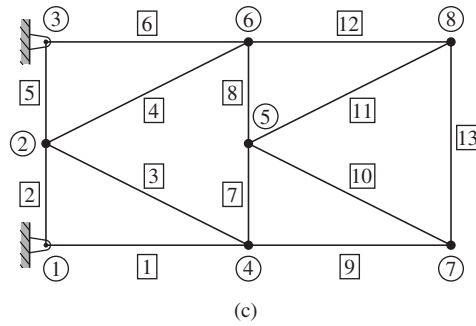


Figure P3.7 (Continued)

- 3.8 For each of the trusses of Figure P3.7, express the connectivity data for each element in the form of Equation 3.39.
- 3.9 For each element shown in Figure P3.9, the global displacements have been calculated as $U_1 = 0.05$ in., $U_2 = 0.02$ in., $U_3 = 0.075$ in., $U_4 = 0.09$ in. Using the finite element equations, calculate
- Element axial displacements at each node.
 - Element strain.
 - Element stress.
 - Element nodal forces.
- Do the calculated stress values agree with $\sigma = F/A$? Let $A = 0.75$ in.², $E = 10 \times 10^6$ psi, $L = 40$ in. for each case.

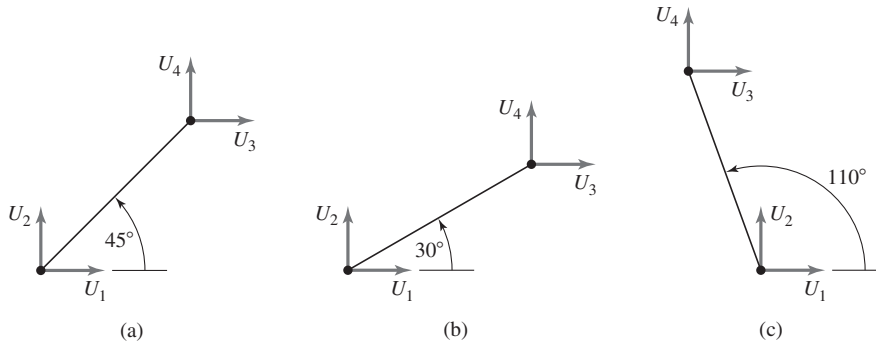


Figure P3.9

- 3.10** The plane truss shown in Figure P3.10 is subjected to a downward vertical load at node 2. Determine via the direct stiffness method the deflection of node 2 in the global coordinate system specified and the axial stress in each element. For both elements, $A = 0.5 \text{ in.}^2$, $E = 30 \times 10^6 \text{ psi}$.

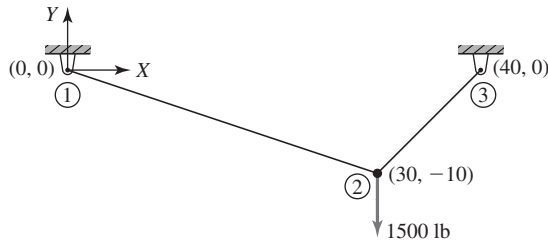


Figure P3.10

- 3.11** The plane truss shown in Figure P3.11 is composed of members having a square $15 \text{ mm} \times 15 \text{ mm}$ cross section and modulus of elasticity $E = 69 \text{ GPa}$.
- Assemble the global stiffness matrix.
 - Compute the nodal displacements in the global coordinate system for the loads shown.
 - Compute the axial stress in each element.

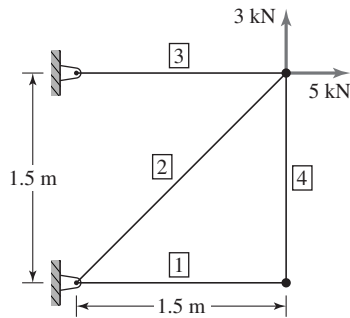


Figure P3.11

- 3.12 Repeat Problem 3.11 assuming elements 1 and 4 are removed.
- 3.13 The cantilever truss in Figure P3.13 was constructed by a builder to support a winch and cable system (not shown) to lift and lower construction materials. The truss members are nominal 2×4 southern yellow pine (actual dimensions 1.75 in. \times 3.5 in.; $E = 2 \times 10^6$ psi). Using the direct stiffness method, calculate
- The global displacement components of all unconstrained nodes.
 - Axial stress in each member.
 - Reaction forces at constrained nodes.
 - Check the equilibrium conditions.

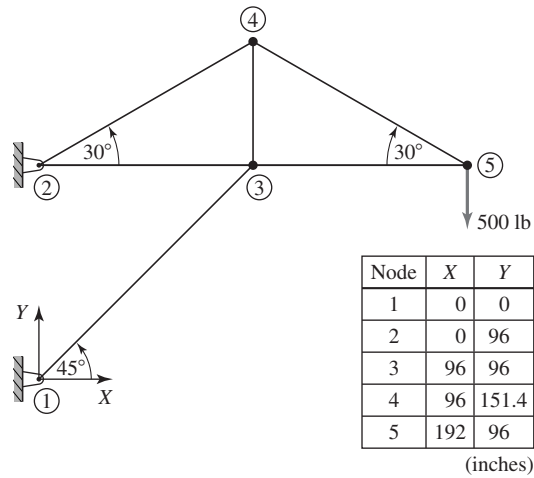


Figure P3.13

- 3.14 Figure P3.14 shows a two-member plane truss supported by a linearly elastic spring. The truss members are of a solid circular cross section having $d = 20$ mm and $E = 80$ GPa. The linear spring has stiffness constant 50 N/mm.
- Assemble the system global stiffness matrix and calculate the global displacements of the unconstrained node.
 - Compute the reaction forces and check the equilibrium conditions.
 - Check the energy balance. Is the strain energy in balance with the mechanical work of the applied force?

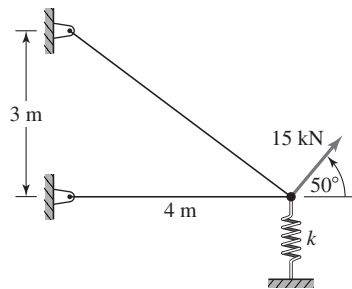


Figure P3.14

- 3.15 Repeat Problem 3.14 if the spring is removed.
- 3.16 Owing to a faulty support connection, node 1 in Problem 3.13 moves 0.5 in. horizontally to the left when the load is applied. Repeat the specified computations for this condition. Does the solution change? Why or why not?
- 3.17 Given the following system of algebraic equations

$$\begin{bmatrix} 10 & -10 & 0 & 0 \\ -10 & 20 & -10 & 0 \\ 0 & -10 & 20 & -10 \\ 0 & 0 & -10 & 10 \end{bmatrix} \begin{Bmatrix} x_1 \\ x_2 \\ x_3 \\ x_4 \end{Bmatrix} = \begin{Bmatrix} F_1 \\ F_2 \\ F_3 \\ F_4 \end{Bmatrix}$$

and the specified conditions

$$x_1 = 0 \quad x_3 = 1.5 \quad F_2 = 20 \quad F_4 = 35$$

calculate x_2 and x_4 . Do this by interchanging rows and columns such that x_1 and x_3 correspond to the first two rows and use the partitioned matrix approach of Equation 3.45.

- 3.18 Given the system

$$\begin{bmatrix} 50 & -50 & 0 & 0 \\ -50 & 100 & -50 & 0 \\ 0 & -50 & 75 & -25 \\ 0 & 0 & -25 & 25 \end{bmatrix} \begin{Bmatrix} U_1 \\ U_2 \\ U_3 \\ U_4 \end{Bmatrix} = \begin{Bmatrix} 30 \\ F_2 \\ 40 \\ 40 \end{Bmatrix}$$

and the specified condition $U_2 = 0.5$, use the approach specified in Problem 3.17 to solve for U_1, U_3, U_4 , and F_2 .

- 3.19 For the truss shown in Figure P3.19, solve for the global displacement components of node 3 and the stress in each element. The elements have cross-sectional area $A = 1.0 \text{ in.}^2$ and modulus of elasticity $15 \times 10^6 \text{ psi}$.

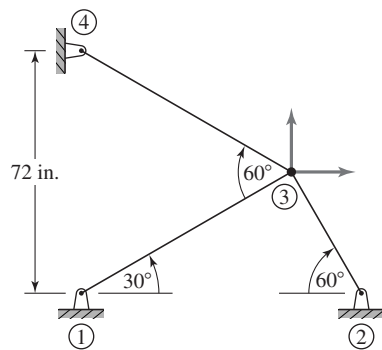


Figure P3.19

- 3.20 Each bar element shown in Figure P3.20 is part of a 3-D truss. The nodal coordinates (in inches) are specified in a global (X, Y, Z) coordinate system. Given $A = 2 \text{ in.}^2$ and $E = 30 \times 10^6 \text{ psi}$, calculate the global stiffness matrix of each element.

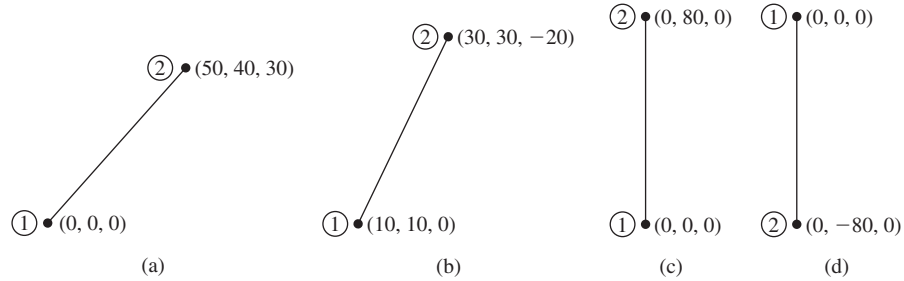


Figure P3.20

- 3.21 Verify Equation 3.59 via direct computation of the matrix product.
- 3.22 Show that the axial stress in a bar element in a 3-D truss is given by

$$\sigma = E\varepsilon = E \begin{bmatrix} \frac{dN_1}{dx} & \frac{dN_2}{dx} \end{bmatrix} \begin{Bmatrix} u_1^{(e)} \\ u_2^{(e)} \end{Bmatrix} = E \begin{bmatrix} -\frac{1}{L} & \frac{1}{L} \end{bmatrix} [R] \{U^{(e)}\}$$

and note that the expression is the same as for the 2-D case.

- 3.23 Determine the axial stress and nodal forces for each bar element shown in Figure P3.20, given that node 1 is fixed and node 2 has global displacements $U_4 = U_5 = U_6 = 0.06$ in.
- 3.24 Use Equations 3.55 and 3.56 to express strain energy of a bar element in terms of the global displacements. Apply Castigliano's first theorem and show that the resulting global stiffness matrix is identical to that given by Equation 3.58.
- 3.25 Repeat Problem 3.24 using the principle of minimum potential energy.
- 3.26 Assemble the global stiffness matrix of the 3-D truss shown in Figure P3.26 and compute the displacement components of node 4. Also, compute the stress in each element.

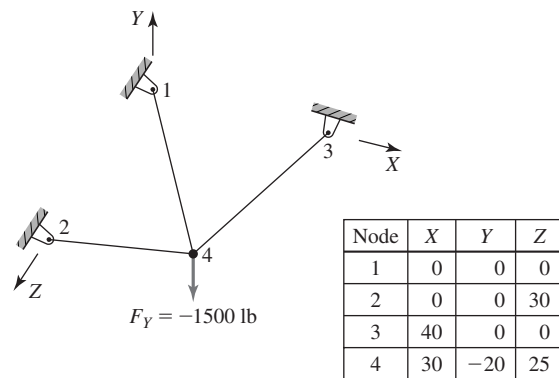


Figure P3.26 Coordinates given in inches. For each element $E = 10 \times 10^6$ psi, $A = 1.5$ in.².

CHAPTER 4

Flexure Elements

4.1 INTRODUCTION

The one-dimensional, axial load-only elements discussed in Chapters 2 and 3 are quite useful in analyzing the response to load of many simple structures. However, the restriction that these elements are not capable of transmitting bending effects precludes their use in modeling more commonly encountered structures that have welded or riveted joints. In this chapter, elementary beam theory is applied to develop a *flexure* (beam) element capable of properly exhibiting transverse bending effects. The element is first presented as a line (one-dimensional) element capable of bending in a plane. In the context of developing the discretized equations for this element, we present a general procedure for determining the interpolation functions using an assumed polynomial form for the field variable. The development is then extended to two-plane bending and the effects of axial loading and torsion are added.

4.2 ELEMENTARY BEAM THEORY

Figure 4.1a depicts a simply supported beam subjected to a general, distributed, transverse load $q(x)$ assumed to be expressed in terms of force per unit length. The coordinate system is as shown with x representing the axial coordinate and y the transverse coordinate. The usual assumptions of elementary beam theory are applicable here:

1. The beam is loaded only in the y direction.
2. Deflections of the beam are small in comparison to the characteristic dimensions of the beam.
3. The material of the beam is linearly elastic, isotropic, and homogeneous.
4. The beam is prismatic and the cross section has an axis of symmetry in the plane of bending.

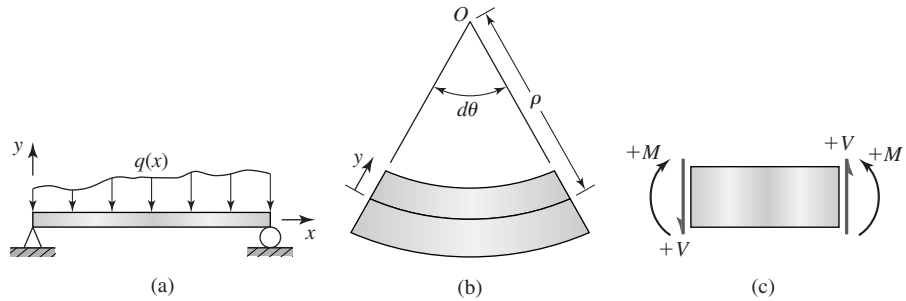


Figure 4.1
 (a) Simply supported beam subjected to arbitrary (negative) distributed load.
 (b) Deflected beam element. (c) Sign convention for shear force and bending moment.

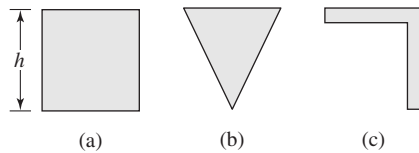


Figure 4.2 Beam cross sections:
 (a) and (b) satisfy symmetry conditions for the simple bending theory, (c) does not satisfy the symmetry requirement.

The ramifications of assumption 4 are illustrated in Figure 4.2, which depicts two cross sections that satisfy the assumption and one cross section that does not. Both the rectangular and triangular cross sections are symmetric about the xy plane and bend only in that plane. On the other hand, the L-shaped section possesses no such symmetry and bends out of the xy plane, even under loading only in that plane. With regard to the figure, assumption 2 can be roughly quantified to mean that the maximum deflection of the beam is much less than dimension h . A generally applicable rule is that the maximum deflection is less than $0.1h$.

Considering a differential length dx of a beam after bending as in Figure 4.1b (with the curvature greatly exaggerated), it is intuitive that the top surface has decreased in length while the bottom surface has increased in length. Hence, there is a “layer” that must be undeformed during bending. Assuming that this layer is located distance ρ from the center of curvature O and choosing this layer (which, recall, is known as the *neutral surface*) to correspond to $y = 0$, the length after bending at any position y is expressed as

$$ds = (\rho - y) d\theta \tag{4.1}$$

and the bending strain is then

$$\varepsilon_x = \frac{ds - dx}{dx} = \frac{(\rho - y) d\theta - \rho d\theta}{\rho d\theta} = -\frac{y}{\rho} \quad (4.2)$$

From basic calculus, the radius of curvature of a planar curve is given by

$$\rho = \frac{\left[1 + \left(\frac{dv}{dx}\right)^2\right]^{3/2}}{\frac{d^2v}{dx^2}} \quad (4.3)$$

where $v = v(x)$ represents the deflection curve of the neutral surface.

In keeping with small deflection theory, slopes are also small, so Equation 4.3 is approximated by

$$\rho = \frac{1}{\frac{d^2v}{dx^2}} \quad (4.4)$$

such that the normal strain in the direction of the longitudinal axis as a result of bending is

$$\varepsilon_x = -y \frac{d^2v}{dx^2} \quad (4.5)$$

and the corresponding normal stress is

$$\sigma_x = E\varepsilon_x = -Ey \frac{d^2v}{dx^2} \quad (4.6)$$

where E is the modulus of elasticity of the beam material. Equation 4.6 shows that, at a given cross section, the normal stress varies linearly with distance from the neutral surface.

As no net axial force is acting on the beam cross section, the resultant force of the stress distribution given by Equation 4.6 must be zero. Therefore, at any axial position x along the length, we have

$$F_x = \int_A \sigma_x dA = - \int_A Ey \frac{d^2v}{dx^2} dA = 0 \quad (4.7)$$

Noting that at an arbitrary cross section the curvature is constant, Equation 4.7 implies

$$\int_A y dA = 0 \quad (4.8)$$

which is satisfied if the xz plane ($y = 0$) passes through the centroid of the area. Thus, we obtain the well-known result that the neutral surface is perpendicular to the plane of bending and passes through the centroid of the cross-sectional area.

Similarly, the internal bending moment at a cross section must be equivalent to the resultant moment of the normal stress distribution, so

$$M(x) = - \int_A y \sigma_x \, dA = E \frac{d^2 v}{dx^2} \int_A y^2 \, dA \quad (4.9)$$

The integral term in Equation 4.9 represents the moment of inertia of the cross-sectional area about the z axis, so the bending moment expression becomes

$$M(x) = EI_z \frac{d^2 v}{dx^2} \quad (4.10)$$

Combining Equations 4.6 and 4.10, we obtain the normal stress equation for beam bending:

$$\sigma_x = - \frac{M(x)y}{I_z} = -yE \frac{d^2 v}{dx^2} \quad (4.11)$$

Note that the negative sign in Equation 4.11 ensures that, when the beam is subjected to positive bending moment per the convention depicted in Figure 4.1c, compressive (negative) and tensile (positive) stress values are obtained correctly depending on the sign of the y location value.

4.3 FLEXURE ELEMENT

Using the elementary beam theory, the 2-D beam or *flexure* element is now developed with the aid of the first theorem of Castigliano. The assumptions and restrictions underlying the development are the same as those of elementary beam theory with the addition of

1. The element is of length L and has two nodes, one at each end.
2. The element is connected to other elements only at the nodes.
3. Element loading occurs only at the nodes.

Recalling that the basic premise of finite element formulation is to express the continuously varying field variable in terms of a finite number of values evaluated at element nodes, we note that, for the flexure element, the field variable of interest is the transverse displacement $v(x)$ of the neutral surface away from its straight, undeflected position. As depicted in Figure 4.3a and 4.3b, transverse deflection of a beam is such that the variation of deflection along the length is not adequately described by displacement of the end points only. The end deflections can be identical, as illustrated, while the deflected shape of the two cases is quite different. Therefore, the flexure element formulation must take into account the slope (rotation) of the beam as well as end-point displacement. In addition to avoiding the potential ambiguity of displacements, inclusion of beam element nodal rotations ensures compatibility of rotations at nodal connections between

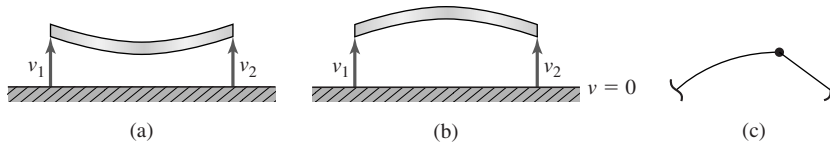


Figure 4.3 (a) and (b) Beam elements with identical end deflections but quite different deflection characteristics. (c) Physically unacceptable discontinuity at the connecting node.

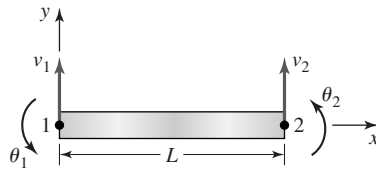


Figure 4.4 Beam element nodal displacements shown in a positive sense.

elements, thus precluding the physically unacceptable discontinuity depicted in Figure 4.3c.

In light of these observations regarding rotations, the nodal variables to be associated with a flexure element are as depicted in Figure 4.4. Element nodes 1 and 2 are located at the ends of the element, and the nodal variables are the transverse displacements v_1 and v_2 at the nodes and the slopes (rotations) θ_1 and θ_2 . The nodal variables as shown are in the positive direction, and it is to be noted that the slopes are to be specified in radians. For convenience, the superscript (e) indicating element properties is not used at this point, as it is understood in context that the current discussion applies to a single element. When multiple elements are involved in examples to follow, the superscript notation is restored.

The displacement function $v(x)$ is to be discretized such that

$$v(x) = f(v_1, v_2, \theta_1, \theta_2, x) \quad (4.12)$$

subject to the boundary conditions

$$v(x = x_1) = v_1 \quad (4.13)$$

$$v(x = x_2) = v_2 \quad (4.14)$$

$$\left. \frac{dv}{dx} \right|_{x=x_1} = \theta_1 \quad (4.15)$$

$$\left. \frac{dv}{dx} \right|_{x=x_2} = \theta_2 \quad (4.16)$$

Before proceeding, we assume that the element coordinate system is chosen such that $x_1 = 0$ and $x_2 = L$ to simplify the presentation algebraically. (This is not at all restrictive, since $L = x_2 - x_1$ in any case.)

Considering the four boundary conditions and the one-dimensional nature of the problem in terms of the independent variable, we assume the displacement function in the form

$$v(x) = a_0 + a_1x + a_2x^2 + a_3x^3 \quad (4.17)$$

The choice of a cubic function to describe the displacement is not arbitrary. While the general requirements of interpolation functions is discussed in Chapter 6, we make a few pertinent observations here. Clearly, with the specification of four boundary conditions, we can determine no more than four constants in the assumed displacement function. Second, in view of Equations 4.10 and 4.17, the second derivative of the assumed displacement function $v(x)$ is linear; hence, the bending moment varies linearly, at most, along the length of the element. This is in accord with the assumption that loads are applied only at the element nodes, as indicated by the bending moment diagram of a loaded beam element shown in Figure 4.5. If a distributed load were applied to the element across its length, the bending moment would vary at least quadratically.

Application of the boundary conditions 4.13–4.16 in succession yields

$$v(x = 0) = v_1 = a_0 \quad (4.18)$$

$$v(x = L) = v_2 = a_0 + a_1L + a_2L^2 + a_3L^3 \quad (4.19)$$

$$\left. \frac{dv}{dx} \right|_{x=0} = \theta_1 = a_1 \quad (4.20)$$

$$\left. \frac{dv}{dx} \right|_{x=L} = \theta_2 = a_1 + 2a_2L + 3a_3L^2 \quad (4.21)$$

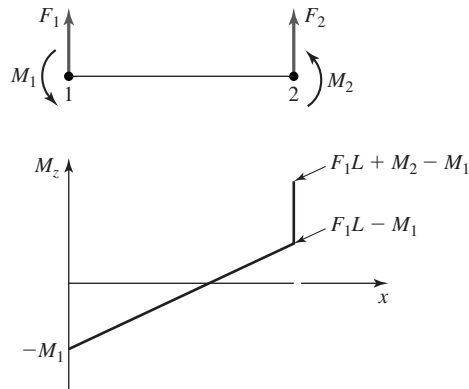


Figure 4.5 Bending moment diagram for a flexure element. Sign convention per the strength of materials theory.

Equations 4.18–4.21 are solved simultaneously to obtain the coefficients in terms of the nodal variables as

$$a_0 = v_1 \quad (4.22)$$

$$a_1 = \theta_1 \quad (4.23)$$

$$a_2 = \frac{3}{L^2}(v_2 - v_1) - \frac{1}{L}(2\theta_1 + \theta_2) \quad (4.24)$$

$$a_3 = \frac{2}{L^3}(v_1 - v_2) + \frac{1}{L^2}(\theta_1 + \theta_2) \quad (4.25)$$

Substituting Equations 4.22–4.25 into Equation 4.17 and collecting the coefficients of the nodal variables results in the expression

$$\begin{aligned} v(x) = & \left(1 - \frac{3x^2}{L^2} + \frac{2x^3}{L^3}\right)v_1 + \left(x - \frac{2x^2}{L} + \frac{x^3}{L^2}\right)\theta_1 \\ & + \left(\frac{3x^2}{L^2} - \frac{2x^3}{L^3}\right)v_2 + \left(\frac{x^3}{L^2} - \frac{x^2}{L}\right)\theta_2 \end{aligned} \quad (4.26)$$

which is of the form

$$v(x) = N_1(x)v_1 + N_2(x)\theta_1 + N_3(x)v_2 + N_4(x)\theta_2 \quad (4.27a)$$

or, in matrix notation,

$$v(x) = [N_1 \quad N_2 \quad N_3 \quad N_4] \begin{Bmatrix} v_1 \\ \theta_1 \\ v_2 \\ \theta_2 \end{Bmatrix} = [N] \{\delta\} \quad (4.27b)$$

where N_1 , N_2 , N_3 , and N_4 are the interpolation functions that describe the distribution of displacement in terms of nodal values in the nodal displacement vector $\{\delta\}$.

For the flexure element, it is convenient to introduce the dimensionless length coordinate

$$\xi = \frac{x}{L} \quad (4.28)$$

so that Equation 4.26 becomes

$$\begin{aligned} v(x) = & (1 - 3\xi^2 + 2\xi^3)v_1 + L(\xi - 2\xi^2 + \xi^3)\theta_1 + (3\xi^2 - 2\xi^3)v_2 \\ & + L\xi^2(\xi - 1)\theta_2 \end{aligned} \quad (4.29)$$

where $0 \leq \xi \leq 1$. This form proves more amenable to the integrations required to complete development of the element equations in the next section.

As discussed in Chapter 3, displacements are important, but the engineer is most often interested in examining the stresses associated with given loading conditions. Using Equation 4.11 in conjunction with Equation 4.27b, the normal

stress distribution on a cross section located at axial position x is given by

$$\sigma_x(x, y) = -yE \frac{d^2[N]}{dx^2} \{\delta\} \quad (4.30)$$

Since the normal stress varies linearly on a cross section, the maximum and minimum values on any cross section occur at the outer surfaces of the element, where distance y from the neutral surface is largest. As is customary, we take the maximum stress to be the largest tensile (positive) value and the minimum to be the largest compressive (negative) value. Hence, we rewrite Equation 4.30 as

$$\sigma_x(x) = y_{\max} E \frac{d^2[N]}{dx^2} \{\delta\} \quad (4.31)$$

and it is to be understood that Equation 4.31 represents the maximum and minimum normal stress values at any cross section defined by axial coordinate x . Also y_{\max} represents the largest distances (one positive, one negative) from the neutral surface to the outside surfaces of the element. Substituting for the interpolation functions and carrying out the differentiations indicated, we obtain

$$\begin{aligned} \sigma_x(x) = y_{\max} E \left[\left(\frac{12x}{L^3} - \frac{6}{L^2} \right) v_1 + \left(\frac{6x}{L^2} - \frac{4}{L} \right) \theta_1 + \left(\frac{6}{L^2} - \frac{12x}{L^3} \right) v_2 \right. \\ \left. + \left(\frac{6x}{L^2} - \frac{2}{L} \right) \theta_2 \right] \end{aligned} \quad (4.32)$$

Observing that Equation 4.32 indicates a linear variation of normal stress along the length of the element and since, once the displacement solution is obtained, the nodal values are known constants, we need calculate only the stress values at the cross sections corresponding to the nodes; that is, at $x = 0$ and $x = L$. The stress values at the nodal sections are given by

$$\sigma_x(x = 0) = y_{\max} E \left[\frac{6}{L^2} (v_2 - v_1) - \frac{2}{L} (2\theta_1 + \theta_2) \right] \quad (4.33)$$

$$\sigma_x(x = L) = y_{\max} E \left[\frac{6}{L^2} (v_1 - v_2) + \frac{2}{L} (2\theta_2 + \theta_1) \right] \quad (4.34)$$

The stress computations are illustrated in following examples.

4.4 FLEXURE ELEMENT STIFFNESS MATRIX

We may now utilize the discretized approximation of the flexure element displacement to examine stress, strain, and strain energy exhibited by the element under load. The total strain energy is expressed as

$$U_e = \frac{1}{2} \int_V \sigma_x \epsilon_x dV \quad (4.35)$$

where V is total volume of the element. Substituting for the stress and strain per Equations 4.5 and 4.6,

$$U_e = \frac{E}{2} \int_V y^2 \left(\frac{d^2 v}{dx^2} \right)^2 dV \quad (4.36)$$

which can be written as

$$U_e = \frac{E}{2} \int_0^L \left(\frac{d^2 v}{dx^2} \right)^2 \left(\int_A y^2 dA \right) dx \quad (4.37)$$

Again recognizing the area integral as the moment of inertia I_z about the centroidal axis perpendicular to the plane of bending, we have

$$U_e = \frac{EI_z}{2} \int_0^L \left(\frac{d^2 v}{dx^2} \right)^2 dx \quad (4.38)$$

Equation 4.38 represents the strain energy of bending for any constant cross-section beam that obeys the assumptions of elementary beam theory. For the strain energy of the finite element being developed, we substitute the discretized displacement relation of Equation 4.27 to obtain

$$U_e = \frac{EI_z}{2} \int_0^L \left(\frac{d^2 N_1}{dx^2} v_1 + \frac{d^2 N_2}{dx^2} \theta_1 + \frac{d^2 N_3}{dx^2} v_2 + \frac{d^2 N_4}{dx^2} \theta_2 \right)^2 dx \quad (4.39)$$

as the approximation to the strain energy. We emphasize that Equation 4.39 is an approximation because the discretized displacement function is not in general an exact solution for the beam flexure problem.

Applying the first theorem of Castigliano to the strain energy function with respect to nodal displacement v_1 gives the transverse force at node 1 as

$$\frac{\partial U_e}{\partial v_1} = F_1 = EI_z \int_0^L \left(\frac{d^2 N_1}{dx^2} v_1 + \frac{d^2 N_2}{dx^2} \theta_1 + \frac{d^2 N_3}{dx^2} v_2 + \frac{d^2 N_4}{dx^2} \theta_2 \right) \frac{d^2 N_1}{dx^2} dx \quad (4.40)$$

while application of the theorem with respect to the rotational displacement gives the moment as

$$\frac{\partial U_e}{\partial \theta_1} = M_1 = EI_z \int_0^L \left(\frac{d^2 N_1}{dx^2} v_1 + \frac{d^2 N_2}{dx^2} \theta_1 + \frac{d^2 N_3}{dx^2} v_2 + \frac{d^2 N_4}{dx^2} \theta_2 \right) \frac{d^2 N_2}{dx^2} dx \quad (4.41)$$

For node 2, the results are

$$\frac{\partial U_e}{\partial v_2} = F_2 = EI_z \int_0^L \left(\frac{d^2 N_1}{dx^2} v_1 + \frac{d^2 N_2}{dx^2} \theta_1 + \frac{d^2 N_3}{dx^2} v_2 + \frac{d^2 N_4}{dx^2} \theta_2 \right) \frac{d^2 N_3}{dx^2} dx \quad (4.42)$$

$$\frac{\partial U_e}{\partial \theta_2} = M_2 = EI_z \int_0^L \left(\frac{d^2 N_1}{dx^2} v_1 + \frac{d^2 N_2}{dx^2} \theta_1 + \frac{d^2 N_3}{dx^2} v_2 + \frac{d^2 N_4}{dx^2} \theta_2 \right) \frac{d^2 N_4}{dx^2} dx \quad (4.43)$$

Equations 4.40–4.43 algebraically relate the four nodal displacement values to the four applied nodal forces (here we use *force* in the general sense to include applied moments) and are of the form

$$\begin{bmatrix} k_{11} & k_{12} & k_{13} & k_{14} \\ k_{21} & k_{22} & k_{23} & k_{24} \\ k_{31} & k_{32} & k_{33} & k_{34} \\ k_{41} & k_{42} & k_{43} & k_{44} \end{bmatrix} \begin{Bmatrix} v_1 \\ \theta_1 \\ v_2 \\ \theta_2 \end{Bmatrix} = \begin{Bmatrix} F_1 \\ M_1 \\ F_2 \\ M_2 \end{Bmatrix} \quad (4.44)$$

where k_{mn} , $m, n = 1, 4$ are the coefficients of the element stiffness matrix. By comparison of Equations 4.40–4.43 with the algebraic equations represented by matrix Equation 4.44, it is seen that

$$k_{mn} = k_{nm} = EI_z \int_0^L \frac{d^2 N_m}{dx^2} \frac{d^2 N_n}{dx^2} dx \quad m, n = 1, 4 \quad (4.45)$$

and the element stiffness matrix is symmetric, as expected for a linearly elastic element.

Prior to computing the stiffness coefficients, it is convenient to convert the integration to the dimensionless length variable $\xi = x/L$ by noting

$$\int_0^L f(x) dx = \int_0^1 f(\xi) L d\xi \quad (4.46)$$

$$\frac{d}{dx} = \frac{1}{L} \frac{d}{d\xi} \quad (4.47)$$

so the integrations of Equation 4.45 become

$$k_{mn} = k_{nm} = EI_z \int_0^L \frac{d^2 N_m}{dx^2} \frac{d^2 N_n}{dx^2} dx = \frac{EI_z}{L^3} \int_0^1 \frac{d^2 N_m}{d\xi^2} \frac{d^2 N_n}{d\xi^2} d\xi \quad m, n = 1, 4 \quad (4.48)$$

The stiffness coefficients are then evaluated as follows:

$$\begin{aligned} k_{11} &= \frac{EI_z}{L^3} \int_0^1 (12\xi - 6)^2 d\xi = \frac{36EI_z}{L^3} \int_0^1 (4\xi^2 - 4\xi + 1) d\xi \\ &= \frac{36EI_z}{L^3} \left(\frac{4}{3} - 2 + 1 \right) = \frac{12EI_z}{L^3} \end{aligned}$$

$$k_{12} = k_{21} = \frac{EI_z}{L^3} \int_0^1 (12\xi - 6)(6\xi - 4)L d\xi = \frac{6EI_z}{L^2}$$

$$k_{13} = k_{31} = \frac{EI_z}{L^3} \int_0^1 (12\xi - 6)(6 - 12\xi) d\xi = -\frac{12EI_z}{L^3}$$

$$k_{14} = k_{41} = \frac{EI_z}{L^3} \int_0^1 (12\xi - 6)(6\xi - 2)L d\xi = \frac{6EI_z}{L^2}$$

Continuing the direct integration gives the remaining stiffness coefficients as

$$\begin{aligned} k_{22} &= \frac{4EI_z}{L} \\ k_{23} = k_{32} &= -\frac{6EI_z}{L^2} \\ k_{24} = k_{42} &= \frac{2EI_z}{L} \\ k_{33} &= \frac{12EI_z}{L^3} \\ k_{34} = k_{43} &= -\frac{6EI_z}{L^3} \\ k_{44} &= \frac{4EI_z}{L} \end{aligned}$$

The complete stiffness matrix for the flexure element is then written as

$$[k_e] = \frac{EI_z}{L^3} \begin{bmatrix} 12 & 6L & -12 & 6L \\ 6L & 4L^2 & -6L & 2L^2 \\ -12 & -6L & 12 & -6L \\ 6L & 2L^2 & -6L & 4L^2 \end{bmatrix} \quad (4.49)$$

Symmetry of the element stiffness matrix is apparent, as previously observed. Again, the element stiffness matrix can be shown to be singular since rigid body motion is possible unless the element is constrained in some manner. The element stiffness matrix as given by Equation 4.49 is valid in any consistent system of units *provided* the rotational degrees of freedom (slopes) are expressed in *radians*.

4.5 ELEMENT LOAD VECTOR

In Equations 4.40–4.43, the element forces and moments were treated as required by the first theorem of Castigliano as being in the direction of the associated displacements. These directions are in keeping with the assumed positive directions of the nodal displacements. However, as depicted in Figures 4.6a and 4.6b, the usual convention for shear force and bending moment in a beam are such that

$$\begin{Bmatrix} F_1 \\ M_1 \\ F_2 \\ M_2 \end{Bmatrix} \Rightarrow \begin{Bmatrix} -V_1 \\ -M_1 \\ V_2 \\ M_2 \end{Bmatrix} \quad (4.50)$$

In Equation 4.50, the column matrix (vector) on the left represents positive nodal forces and moments per the finite element formulations. The right-hand side contains the corresponding signed shear forces and bending moments per the beam theory sign convention.

If two flexure elements are joined at a common node, the internal shear forces are equal and opposite *unless* an external force is applied at that node, in which case the sum of the internal shear forces must equal the applied load. Therefore, when we assemble the finite element model using flexure elements, the force at a node is simply equal to any external force at that node. A similar argument holds for bending moments. At the juncture between two elements (i.e., a node), the internal bending moments are equal and opposite, thus self-equilibrating, *unless* a concentrated bending moment is applied at that node. In this event, the internal moments sum to the applied moment. These observations are illustrated in Figure 4.6c, which shows a simply supported beam subjected to a concentrated force and concentrated moment acting at the midpoint of the

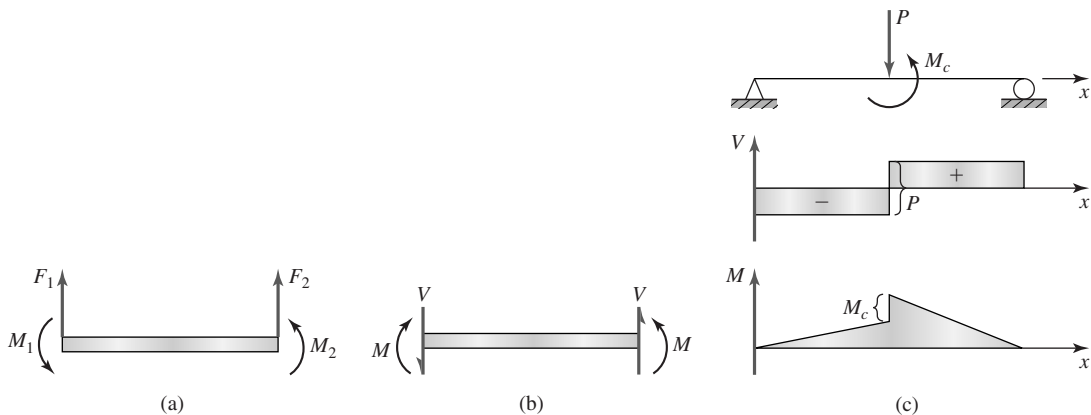


Figure 4.6

(a) Nodal load positive convention. (b) Positive convention from the strength of materials theory. (c) Shear and bending moment diagrams depicting nodal load effects.

beam length. As shown by the shear force diagram, a jump discontinuity exists at the point of application of the concentrated force, and the magnitude of the discontinuity is the magnitude of the applied force. Similarly, the bending moment diagram shows a jump discontinuity in the bending moment equal to the magnitude of the applied bending moment. Therefore, if the beam were to be divided into two finite elements with a connecting node at the midpoint, the net force at the node is the applied external force and the net moment at the node is the applied external moment.

EXAMPLE 4.1

Figure 4.7a depicts a statically indeterminate beam subjected to a transverse load applied at the midspan. Using two flexure elements, obtain a solution for the midspan deflection.

■ Solution

Since the flexure element requires loading only at nodes, the elements are taken to be of length $L/2$, as shown in Figure 4.7b. The individual element stiffness matrices are then

$$\begin{aligned}
 [k^{(1)}] &= [k^{(2)}] = \frac{EI_z}{(L/2)^3} \begin{bmatrix} 12 & 6L/2 & -12 & 6L/2 \\ 6L/2 & 4L^2/4 & -6L/2 & 2L^2/4 \\ -12 & -6L/2 & 12 & -6L/2 \\ 6L/2 & 2L^2/4 & -6L/2 & 4L^2/4 \end{bmatrix} \\
 &= \frac{8EI_z}{L^3} \begin{bmatrix} 12 & 3L & -12 & 3L \\ 3L & L^2 & -3L & L^2/2 \\ -12 & -3L & 12 & -3L \\ 3L & L^2/2 & -3L & L^2 \end{bmatrix}
 \end{aligned}$$

Note particularly that the length of each element is $L/2$. The appropriate boundary conditions are $v_1 = \theta_1 = v_3 = 0$ and the element-to-system displacement correspondence table is Table 4.1.

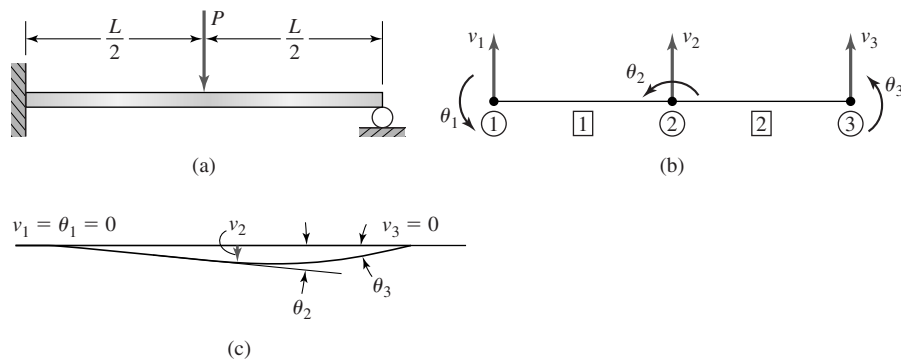


Figure 4.7

(a) Loaded beam of Example 4.1. (b) Element and displacement designations. (c) Displacement solution.

Table 4.1 Element-to-System Displacement Correspondence

Global Displacement	Element 1	Element 2
1	1	0
2	2	0
3	3	1
4	4	2
5	0	3
6	0	4

Assembling the global stiffness matrix per the displacement correspondence table we obtain in order (and using the symmetry property)

$$K_{11} = k_{11}^{(1)} = \frac{96EI_z}{L^3}$$

$$K_{12} = k_{12}^{(1)} = \frac{24EI_z}{L^2}$$

$$K_{13} = k_{13}^{(1)} = \frac{-96EI_z}{L^3}$$

$$K_{14} = k_{14}^{(1)} = \frac{24EI_z}{L^2}$$

$$K_{22} = k_{22}^{(1)} = \frac{8EI_z}{L}$$

$$K_{23} = k_{23}^{(1)} = \frac{-24EI_z}{L^2}$$

$$K_{24} = k_{24}^{(1)} = \frac{4EI_z}{L}$$

$$K_{25} = K_{26} = 0$$

$$K_{33} = k_{33}^{(1)} + k_{11}^{(2)} = \frac{192EI_z}{L^3}$$

$$K_{34} = k_{34}^{(1)} + k_{12}^{(2)} = 0$$

$$K_{35} = k_{13}^{(2)} = \frac{-96EI_z}{L^3}$$

$$K_{36} = k_{14}^{(2)} = \frac{24EI_z}{L^2}$$

$$K_{44} = k_{44}^{(1)} + k_{22}^{(1)} = \frac{16EI_z}{L}$$

$$K_{45} = k_{23}^{(2)} = \frac{-24EI_z}{L^2}$$

$$K_{46} = k_{24}^{(2)} = \frac{4EI_z}{L}$$

$$K_{55} = k_{33}^{(2)} = \frac{96EI_z}{L^3}$$

$$K_{56} = k_{34}^{(2)} = \frac{-24EI_z}{L^2}$$

$$K_{66} = k_{44}^{(2)} = \frac{8EI_z}{L}$$

Using the general form

$$[K]\{U\} = \{F\}$$

we obtain the system equations as

$$\frac{EI_z}{L^3} \begin{bmatrix} 96 & 24L & -96 & 24L & 0 & 0 \\ 24L & 8L^2 & -24L & 4L^2 & 0 & 0 \\ -96 & -24L & 192 & 0 & -96 & 24L \\ 24L & 4L^2 & 0 & 16L^2 & -24L & 4L^2 \\ 0 & 0 & -96 & -24L & 96 & 24L \\ 0 & 0 & 24L & 4L^2 & 24L & 8L^2 \end{bmatrix} \begin{Bmatrix} v_1 \\ \theta_1 \\ v_2 \\ \theta_2 \\ v_3 \\ \theta_3 \end{Bmatrix} = \begin{Bmatrix} F_1 \\ M_1 \\ F_2 \\ M_2 \\ F_3 \\ M_3 \end{Bmatrix}$$

Invoking the boundary conditions $v_1 = \theta_1 = v_3 = 0$, the reduced equations become

$$\frac{EI_z}{L^3} \begin{bmatrix} 192 & 0 & 24L \\ 0 & 16L^2 & 4L^2 \\ 24L & 4L^2 & 8L^2 \end{bmatrix} \begin{Bmatrix} v_2 \\ \theta_2 \\ \theta_3 \end{Bmatrix} = \begin{Bmatrix} -P \\ 0 \\ 0 \end{Bmatrix}$$

Yielding the nodal displacements as

$$v_2 = \frac{-7PL^3}{768EI_z} \quad \theta_2 = \frac{-PL^2}{128EI_z} \quad \theta_3 = \frac{PL^2}{32EI_z}$$

The deformed beam shape is shown in superposition with a plot of the undeformed shape with the displacements noted in Figure 4.7c. Substitution of the nodal displacement values into the constraint equations gives the reactions as

$$F_1 = \frac{EI_z}{L^3}(-96v_2 + 24L\theta_2) = \frac{11P}{16}$$

$$F_3 = \frac{EI_z}{L^3}(-96v_2 - 24L\theta_2 - 24L\theta_3) = \frac{5P}{16}$$

$$M_1 = \frac{EI_z}{L^3}(-24Lv_2 + 4L^2\theta_2) = \frac{3PL}{16}$$

Checking the overall equilibrium conditions for the beam, we find

$$\sum F_y = \frac{11P}{16} - P + \frac{5P}{16} = 0$$

and summing moments about node 1,

$$\sum M = \frac{3PL}{16} - P\frac{L}{2} + \frac{5P}{16}L = 0$$

Thus, the finite element solution satisfies global equilibrium conditions.

The astute reader may wish to compare the results of Example 4.1 with those given in many standard beam deflection tables, in which case it will be found that the results are in exact agreement with elementary beam theory. In general, the finite element method is an approximate method, but in the case of the flexure element, the results are exact in certain cases. In this example, the deflection equation of the neutral surface is a cubic equation and, since the interpolation functions are cubic, the results are exact. When distributed loads exist, however, the results are not necessarily exact, as will be discussed next.

4.6 WORK EQUIVALENCE FOR DISTRIBUTED LOADS

The restriction that loads be applied only at element nodes for the flexure element must be dealt with if a distributed load is present. The usual approach is to replace the distributed load with nodal forces and moments such that the mechanical work done by the nodal load system is equivalent to that done by the distributed load. Referring to Figure 4.1, the mechanical work performed by the distributed load can be expressed as

$$W = \int_0^L q(x)v(x) dx \quad (4.51)$$

The objective here is to determine the equivalent nodal loads so that the work expressed in Equation 4.51 is the same as

$$W = \int_0^L q(x)v(x) dx = F_{1q}v_1 + M_{1q}\theta_1 + F_{2q}v_2 + M_{2q}\theta_2 \quad (4.52)$$

where F_{1q} , F_{2q} are the equivalent forces at nodes 1 and 2, respectively, and M_{1q} and M_{2q} are the equivalent nodal moments. Substituting the discretized displacement function given by Equation 4.27, the work integral becomes

$$W = \int_0^L q(x)[N_1(x)v_1 + N_2(x)\theta_1 + N_3(x)v_2 + N_4(x)\theta_2] dx \quad (4.53)$$

4.6 Work Equivalence for Distributed Loads

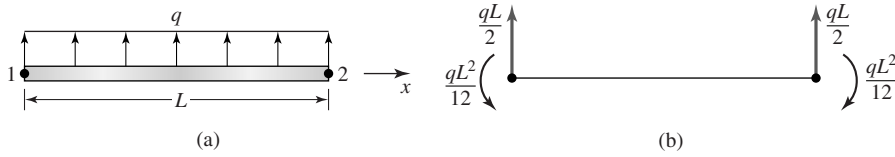


Figure 4.8 Work-equivalent nodal forces and moments for a uniform distributed load.

Comparison of Equations 4.52 and 4.53 shows that

$$F_{1q} = \int_0^L q(x)N_1(x) dx \quad (4.54)$$

$$M_{1q} = \int_0^L q(x)N_2(x) dx \quad (4.55)$$

$$F_{2q} = \int_0^L q(x)N_3(x) dx \quad (4.56)$$

$$M_{2q} = \int_0^L q(x)N_4(x) dx \quad (4.57)$$

Hence, the nodal force vector representing a distributed load on the basis of work equivalence is given by Equations 4.54–4.57. For example, for a uniform load $q(x) = q = \text{constant}$, integration of these equations yields

$$\begin{Bmatrix} F_{1q} \\ M_{1q} \\ F_{2q} \\ M_{2q} \end{Bmatrix} = \begin{Bmatrix} \frac{qL}{2} \\ \frac{qL^2}{12} \\ \frac{qL}{2} \\ -\frac{qL^2}{12} \end{Bmatrix} \quad (4.58)$$

The equivalence of a uniformly distributed load to the corresponding nodal loads on an element is shown in Figure 4.8.

EXAMPLE 4.2

The simply supported beam shown in Figure 4.9a is subjected to a uniform transverse load, as shown. Using two equal-length elements and work-equivalent nodal loads, obtain a finite element solution for the deflection at midspan and compare it to the solution given by elementary beam theory.

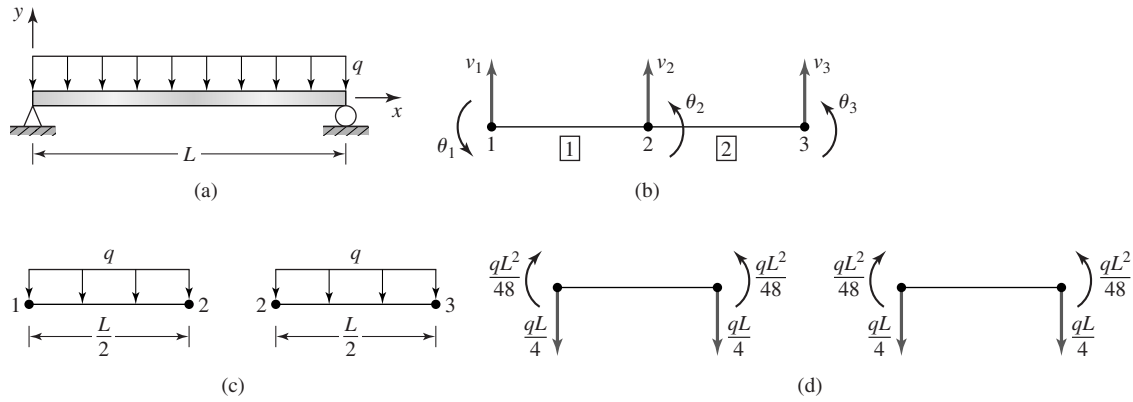


Figure 4.9
 (a) Uniformly loaded beam of Example 4.2. (b) Node, element, and displacement notation. (c) Element loading. (d) Work-equivalent nodal loads.

■ **Solution**

Per Figure 4.9b, we number the nodes and elements as shown and note the boundary conditions $v_1 = v_3 = 0$. We could also note the symmetry condition that $\theta_2 = 0$. However, in this instance, we let that fact occur as a result of the solution process. The element stiffness matrices are identical, given by

$$\begin{aligned}
 [k^{(1)}] &= [k^{(2)}] = \frac{EI_z}{(L/2)^3} \begin{bmatrix} 12 & 6L/2 & -12 & 6L/2 \\ 6L/2 & 4L^2/4 & -6L/2 & 2L^2/4 \\ -12 & -6L/2 & 12 & -6L/2 \\ 6L/2 & 2L^2/4 & -6L/2 & 4L^2/4 \end{bmatrix} \\
 &= \frac{8EI_z}{L^3} \begin{bmatrix} 12 & 3L & -12 & 3L \\ 3L & L^2 & -3L & L^2/2 \\ -12 & -3L & 12 & -3L \\ 3L & L^2/2 & -3L & L^2 \end{bmatrix}
 \end{aligned}$$

(again note that the individual element length $L/2$ is used to compute the stiffness terms), and Table 4.2 is the element connectivity table, so the assembled global stiffness matrix is

$$[K] = \frac{8EI_z}{L^3} \begin{bmatrix} 12 & 3L & -12 & 3L & 0 & 0 \\ 3L & L^2 & -3L & L^2/2 & 0 & 0 \\ -12 & -3L & 24 & 0 & -12 & 3L \\ 3L & L^2/2 & 0 & 2L^2 & -3L & L^2/2 \\ 0 & 0 & -12 & -3L & 12 & -3L \\ 0 & 0 & 3L & L^2/2 & -3L & L^2 \end{bmatrix}$$

The work-equivalent loads for each element are computed with reference to Figure 4.9c and the resulting loads shown in Figure 4.9d. Observing that there are reaction forces at both nodes 1 and 3 in addition to the equivalent forces from the distributed load, the

4.6 Work Equivalence for Distributed Loads

109

Table 4.2 Element Connectivity

Global Displacement	Element 1	Element 2
1	1	0
2	2	0
3	3	1
4	4	2
5	0	3
6	0	4

global equilibrium equations become

$$[K] \begin{Bmatrix} v_1 \\ \theta_1 \\ v_2 \\ \theta_2 \\ v_3 \\ \theta_3 \end{Bmatrix} = \begin{Bmatrix} \frac{-qL}{4} + F_1 \\ \frac{-qL^2}{48} \\ \frac{-qL}{2} \\ 0 \\ \frac{-qL}{4} + F_3 \\ \frac{qL^2}{48} \end{Bmatrix}$$

where the work-equivalent nodal loads have been utilized per Equation 4.58, with each element length = $L/2$ and $q(x) = -q$, as shown in Figure 4.9c. Applying the constraint and symmetry conditions, we obtain the system

$$\frac{8EI_z}{L^3} \begin{bmatrix} L^2 & -3L & L^2/2 & 0 \\ -3L & 24 & 0 & 3L \\ L^2/2 & 0 & 2L^2 & L^2/2 \\ 0 & 3L & L^2/2 & L^2 \end{bmatrix} \begin{Bmatrix} \theta_1 \\ v_2 \\ \theta_2 \\ \theta_3 \end{Bmatrix} = \begin{Bmatrix} \frac{-qL^2}{48} \\ \frac{-qL}{2} \\ 0 \\ \frac{qL^2}{48} \end{Bmatrix}$$

which, on simultaneous solution, gives the displacements as

$$\begin{aligned} \theta_1 &= -\frac{qL^3}{24EI_z} \\ \theta_2 &= 0 \\ v_2 &= -\frac{5qL^4}{384EI_z} \\ \theta_3 &= \frac{qL^3}{24EI_z} \end{aligned}$$

As expected, the slope of the beam at midspan is zero, and since the loading and support conditions are symmetric, the deflection solution is also symmetric, as indicated by

the end slopes. The nodal displacement results from the finite element analysis of this example are exactly the results obtained by a strength of materials approach. This is due to applying the work-equivalent nodal loads. However, the general deflected shape as given by the finite element solution is *not* the same as the strength of materials result. The equation describing the deflection of the neutral surface is a quartic function of x and, since the interpolation functions used in the finite element model are cubic, the deflection curve varies somewhat from the exact solution.

EXAMPLE 4.3

In Figure 4.10a, beam OC is supported by a smooth pin connection at O and supported at B by an elastic rod BD , also through pin connections. A concentrated load $F = 10$ kN is applied at C . Determine the deflection of point C and the axial stress in member BD . The modulus of elasticity of the beam is 207 GPa (steel) and the dimensions of the cross section are 40 mm \times 40 mm. For elastic rod BD , the modulus of elasticity is 69 GPa (aluminum) and the cross-sectional area is 78.54 mm².

■ Solution

This is the first example in which we use multiple element types, as the beam is modeled with flexure elements and the elastic rod as a bar element. Clearly, the horizontal member

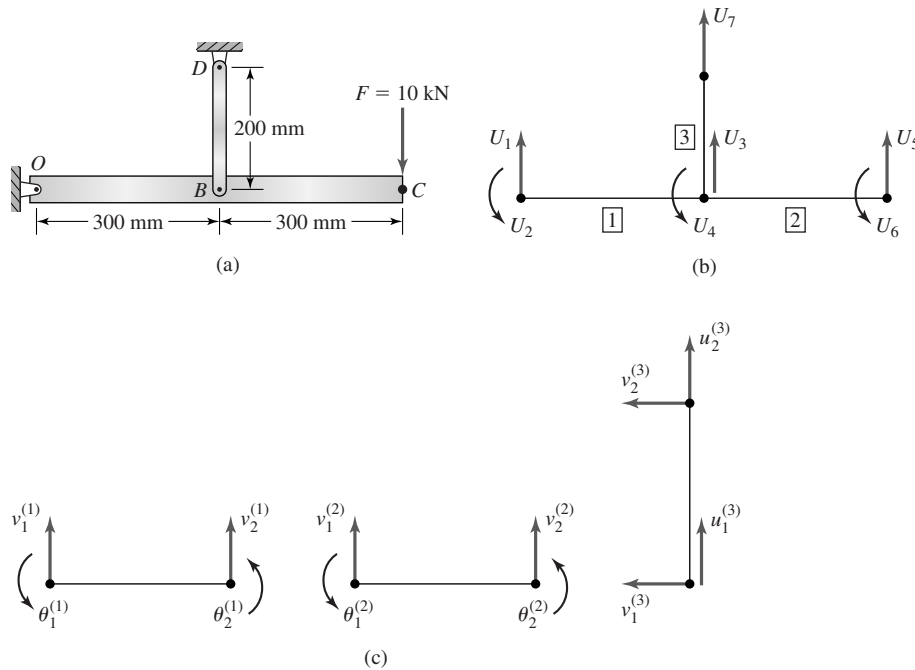


Figure 4.10
(a) Supported beam. (b) Global coordinate system and variables. (c) Individual element displacements.

4.6 Work Equivalence for Distributed Loads

111

Table 4.3 Displacement Scheme

Global	Figure 4.10b	Element 1	Element 2	Element 3
1	U_1	$v_1^{(1)}$	0	0
2	U_2	$\theta_1^{(1)}$	0	0
3	U_3	$v_2^{(1)}$	$v_1^{(2)}$	$u_1^{(3)}$
4	U_4	$\theta_2^{(1)}$	$\theta_1^{(2)}$	0
5	U_5	0	$v_2^{(2)}$	0
6	U_6	0	$\theta_2^{(2)}$	0
7	U_7	0	0	$u_2^{(3)}$

Table 4.4 Element-Displacement Correspondence

Global Displacement	Element 1	Element 2	Element 3
1	1	0	0
2	2	0	0
3	3	1	1
4	4	2	0
5	0	3	0
6	0	4	0
7	0	0	3

is subjected to bending loads, so the assumptions of the bar element do not apply to this member. On the other hand, the vertical support member is subjected to only axial loading, since the pin connections cannot transmit moment. Therefore, we use two different element types to simplify the solution and modeling. The global coordinate system and global variables are shown in Figure 4.10b, where the system is divided into two flexure elements (1 and 2) and one spar element (3). For purposes of numbering in the global stiffness matrix, the displacement scheme in Table 4.3 is used.

While the notation shown in Figure 4.10b may appear to be inconsistent with previous notation, it is simpler in terms of the global equations to number displacements successively. By proper assignment of element displacements to global displacements, the distinction between linear and rotational displacements are clear. The individual element displacements are shown in Figure 4.10c, where we show the bar element in its general 2-D configuration, even though, in this case, we know that $v_1^{(3)} = v_2^{(3)} = 0$ and those displacements are ignored in the solution.

The element displacement correspondence is shown in Table 4.4. For the beam elements, the moment of inertia about the z axis is

$$I_z = \frac{bh^3}{12} = \frac{40(40^3)}{12} = 213333 \text{ mm}^4$$

For elements 1 and 2,

$$\frac{EI_z}{L^3} = \frac{207(10^3)(213333)}{300^3} = 1635.6 \text{ N/mm}$$

Table 4.5 Global Stiffness Matrix

	1	2	3	4	5	6	7
1	19,627.2	2.944×10^6	-19,627.2	2.944×10^6	0	0	0
2	2.944×10^6	5.888×10^8	-2.944×10^6	2.944×10^8	0	0	0
3	-19,627.2	-2.944×10^6	66,350.4	0	-19,627.2	2.944×10^6	-27,096
4	2.944×10^6	2.944×10^8	0	11.78×10^8	-2.944×10^6	2.944×10^8	0
5	0	0	-19,627.2	-2.944×10^6	19,627.2	-2.944×10^6	0
6	0	0	2.944×10^6	2.944×10^8	-2.944×10^6	5.889×10^8	0
7	0	0	-27,096	0	0	0	27,096

so the element stiffness matrices are (per Equation 4.48)

$$[k^{(1)}] = [k^{(2)}] = 1,635.6 \begin{bmatrix} 12 & 1,800 & -12 & 1,800 \\ 1,800 & 360,000 & -1,800 & 180,000 \\ -12 & -1,800 & 12 & -1,800 \\ 1,800 & 180,000 & -1,800 & 360,000 \end{bmatrix}$$

while for element 3,

$$\frac{AE}{L} = \frac{78.54(69)(10^3)}{200} = 27096 \text{ N/mm}$$

so the stiffness matrix for element 3 is

$$[k^{(3)}] = 27,096 \begin{bmatrix} 1 & -1 \\ -1 & 1 \end{bmatrix}$$

Assembling the global stiffness matrix per the displacement correspondence table (noting that we use a “short-cut” for element 3, since the stiffness of the element in the global X direction is meaningless), we obtain the results in Table 4.5. The constraint conditions are $U_1 = U_7 = 0$ and the applied force vector is

$$\begin{Bmatrix} F_1 \\ M_1 \\ F_2 \\ M_2 \\ F_3 \\ M_3 \\ F_4 \end{Bmatrix} = \begin{Bmatrix} R_1 \\ 0 \\ 0 \\ 0 \\ -10,000 \\ 0 \\ R_4 \end{Bmatrix}$$

where we use R to indicate a reaction force. If we apply the constraint conditions and solve the resulting 5×5 system of equations, we obtain the results

$$\begin{aligned} \theta_1 &= 9.3638(10^{-4}) \text{ rad} \\ v_2 &= -0.73811 \text{ mm} \\ \theta_2 &= -0.0092538 \text{ rad} \\ v_3 &= -5.5523 \text{ mm} \\ \theta_3 &= -0.019444 \text{ rad} \end{aligned}$$

4.6 Work Equivalence for Distributed Loads

113

(Note that we intentionally carry more significant decimal digits than necessary to avoid “round-off” inaccuracies in secondary calculations.) To obtain the axial stress in member BD , we utilize Equation 3.52 with $\theta^{(3)} = \pi/2$:

$$\sigma_{BD} = 69(10^3) \begin{bmatrix} -\frac{1}{200} & \frac{1}{200} \end{bmatrix} \begin{bmatrix} 0 & 1 & 0 & 0 \\ 0 & 0 & 0 & 1 \end{bmatrix} \begin{Bmatrix} 0 \\ -0.7381 \\ 0 \\ 0 \end{Bmatrix} = 254.6 \text{ MPa}$$

The positive result indicates tensile stress.

The reaction forces are obtained by substitution of the computed displacements into the first and seventh equations (the constraint equations):

$$\begin{aligned} R_1 &= 2.944(10^6)[9.3638(10^{-4})] - 19,627.2(-0.73811) \\ &\quad + 2.944(10^6)(-0.0092538) \approx -10,000 \text{ N} \\ R_4 &= -27,096(-0.73811) + 27,096(0) = 20,000 \text{ N} \end{aligned}$$

and within the numerical accuracy used in this example, the system is in equilibrium. The reader is urged to check moment equilibrium about the left-hand node and note that, by statics alone, the force in element 3 should be 20,000 N and the axial stress computed by F/A is 254.6 MPa.

The bending stresses at nodes 1 and 2 in the flexure elements are computed via Equations 4.33 and 4.34, respectively, noting that for the square cross section $y_{\max/\min} = 20 \text{ mm}$. For element 1,

$$\begin{aligned} \sigma_x^{(1)}(x=0) &= \pm 20(207)(10^3) \left[\frac{6}{300^2}(-0.738 - 0) - \frac{2}{300}(-2)(0.00093 - 0.0092) \right] \\ &\approx 0 \end{aligned}$$

at node 1. Note that the computed stress at node 1 should be identically zero, since this node is a pin joint and cannot support bending moment.

For node 2 of element 1, we find

$$\begin{aligned} \sigma_x^{(1)}(x=L) &= \pm 20(207)(10^3) \left[\frac{6}{300^2}(0 + 0.738) + \frac{2}{300}(-2)(0.0092 - 0.00093) \right] \\ &\approx \pm 281.3 \text{ MPa} \end{aligned}$$

For element 2, we similarly compute the stresses at each node as

$$\begin{aligned} \sigma_x^{(2)}(x=0) &= \pm 20(207)(10^3) \\ &\quad \times \left[\frac{6}{300^2}(-5.548 + 0.738) - \frac{2}{300}(-2)(0.0092 - 0.0194) \right] \approx \pm 281.3 \text{ MPa} \end{aligned}$$

$$\begin{aligned} \sigma_x^{(2)}(x=L) &= \pm 20(207)(10^3) \\ &\quad \times \left[\frac{6}{300^2}(-0.73811 + 5.5523) + \frac{2}{300}(-2)(0.019444 - 0.009538) \right] \approx 0 \text{ MPa} \end{aligned}$$

and the latter result is also to be expected, as the right end of the beam is free of bending moment. We need to carefully observe here that the bending stress is the same at the

juncture of the two flexure elements; that is, at node 2. This is *not* the usual situation in finite element analysis. The formulation requires displacement and slope continuity but, in general, no continuity of higher-order derivatives. Since the flexure element developed here is based on a cubic displacement function, the element does not often exhibit moment (hence, stress) continuity. The convergence of derivative functions is paramount to examining the accuracy of a finite element solution to a given problem. We must examine the numerical behavior of the derived variables as the finite element “mesh” is refined.

4.7 FLEXURE ELEMENT WITH AXIAL LOADING

The major shortcoming of the flexure element developed so far is that force loading must be transverse to the axis of the element. Effectively, this means that the element can be used only in end-to-end modeling of linear beam structures. If the element is formulated to also support axial loading, the applicability is greatly extended. Such an element is depicted in Figure 4.11, which shows, in addition to the nodal transverse deflections and rotations, axial displacements at the nodes. Thus, the element allows axial as well as transverse loading. It must be pointed out that there are many ramifications to this seemingly simple extension. If the axial load is compressive, the element could buckle. If the axial load is tensile and significantly large, a phenomenon known as *stress stiffening* can occur. The phenomenon of stress stiffening can be likened to tightening of a guitar string. As the tension is increased, the string becomes more resistant to motion perpendicular to the axis of the string.

The same effect occurs in structural members in tension. As shown in Figure 4.12, in a beam subjected to both transverse and axial loading, the effect of the axial load on bending is directly related to deflection, since the deflection at a specific point becomes the moment arm for the axial load. In cases of small elastic deflection, the additional bending moment attributable to the axial loading is negligible. However, in most finite element software packages, buckling and stress stiffening analyses are available as *options* when such an element is used in an analysis. (The reader should be aware that buckling and stress stiffening effects are checked *only if the software user so specifies*.) For the present purpose, we assume the axial loads are such that these secondary effects are not of concern and the axial loading is independent of bending effects.

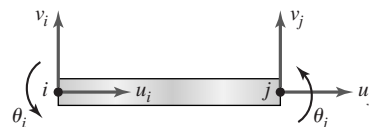


Figure 4.11 Nodal displacements of a beam element with axial stiffness.

4.7 Flexure Element with Axial Loading

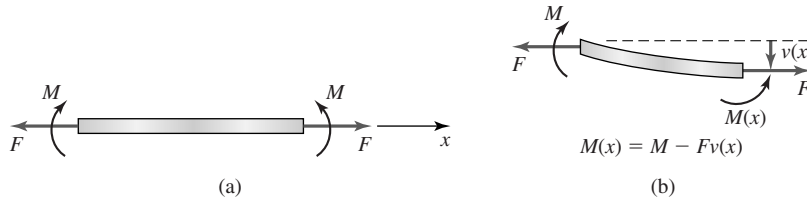


Figure 4.12

(a) Beam with bending moment and axial load. (b) Section of beam, illustrating how tensile load reduces bending moment, hence, “stiffening” the beam.

This being the case, we can simply add the spar element stiffness matrix to the flexure element stiffness matrix to obtain the 6×6 element stiffness matrix for a flexure element with axial loading as

$$[k_e] = \begin{bmatrix} \frac{AE}{L} & -\frac{AE}{L} & 0 & 0 & 0 & 0 \\ -\frac{AE}{L} & \frac{AE}{L} & 0 & 0 & 0 & 0 \\ 0 & 0 & \frac{12EI_z}{L^3} & \frac{6EI_z}{L^2} & -\frac{12EI_z}{L^3} & \frac{6EI_z}{L^2} \\ 0 & 0 & \frac{6EI_z}{L^2} & \frac{4EI_z}{L} & -\frac{6EI_z}{L^2} & \frac{2EI_z}{L} \\ 0 & 0 & -\frac{12EI_z}{L^3} & -\frac{6EI_z}{L^2} & \frac{12EI_z}{L^3} & -\frac{6EI_z}{L^2} \\ 0 & 0 & \frac{6EI_z}{L^2} & \frac{2EI_z}{L} & -\frac{6EI_z}{L^2} & \frac{4EI_z}{L} \end{bmatrix} \quad (4.59)$$

which is seen to be simply

$$[k_e] = \begin{bmatrix} [k_{axial}] & [0] \\ [0] & [k_{flexure}] \end{bmatrix} \quad (4.60)$$

and is a noncoupled superposition of axial and bending stiffnesses.

Adding axial capability to the beam element eliminates the restriction that such elements be aligned linearly and enables use of the element in the analysis of planar frame structures in which the joints have bending resistance. For such applications, orientation of the element in the global coordinate system must be considered, as was the case with the spar element in trusses. Figure 4.13a depicts an element oriented at an arbitrary angle ψ from the X axis of a global reference frame and shows the element nodal displacements. Here, we use ψ to indicate the orientation angle to avoid confusion with the nodal slope, denoted θ . Figure 4.13b shows the assigned global displacements for the element, where again we have adopted a single symbol for displacement with a numerically increasing subscript from node to node. Before proceeding, note that it is convenient here to reorder the element stiffness matrix given by Equation 4.59 so that the element

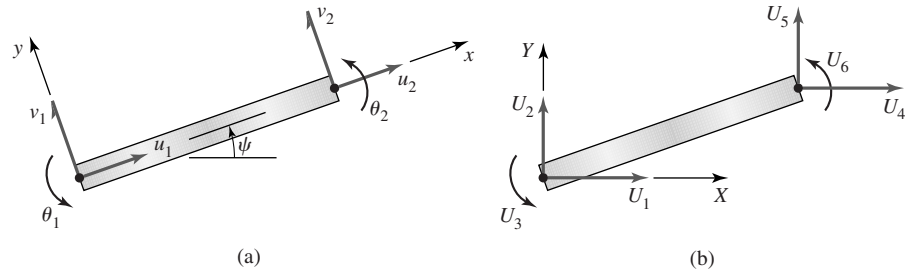


Figure 4.13

(a) Nodal displacements in the element coordinate system. (b) Nodal displacements in the global coordinate system.

displacement vector in the element reference frame is given as

$$\{\delta\} = \begin{Bmatrix} u_1 \\ v_1 \\ \theta_1 \\ u_2 \\ v_2 \\ \theta_2 \end{Bmatrix} \quad (4.61)$$

and the element stiffness matrix becomes

$$[k_e] = \begin{bmatrix} \frac{AE}{L} & 0 & 0 & -\frac{AE}{L} & 0 & 0 \\ 0 & \frac{12EI_z}{L^3} & \frac{6EI_z}{L^2} & 0 & -\frac{12EI_z}{L^3} & \frac{6EI_z}{L^2} \\ 0 & \frac{6EI_z}{L^2} & \frac{4EI_z}{L} & 0 & -\frac{6EI_z}{L^2} & \frac{2EI_z}{L} \\ -\frac{AE}{L} & 0 & 0 & \frac{AE}{L} & 0 & 0 \\ 0 & -\frac{12EI_z}{L^3} & -\frac{6EI_z}{L^2} & 0 & \frac{12EI_z}{L^3} & -\frac{6EI_z}{L^2} \\ 0 & \frac{6EI_z}{L^2} & \frac{2EI_z}{L} & 0 & -\frac{6EI_z}{L^2} & \frac{4EI_z}{L} \end{bmatrix} \quad (4.62)$$

Using Figure 4.13, the element displacements are written in terms of the global displacements as

$$\begin{aligned} u_1 &= U_1 \cos \psi + U_2 \sin \psi \\ v_1 &= -U_1 \sin \psi + U_2 \cos \psi \\ \theta_1 &= U_3 \\ u_2 &= U_4 \cos \psi + U_5 \sin \psi \\ v_2 &= -U_4 \sin \psi + U_5 \cos \psi \\ \theta_2 &= U_6 \end{aligned} \quad (4.63)$$

Equations 4.63 can be written in matrix form as

$$\begin{Bmatrix} u_1 \\ v_1 \\ \theta_1 \\ u_2 \\ v_2 \\ \theta_2 \end{Bmatrix} = \begin{bmatrix} \cos \psi & \sin \psi & 0 & 0 & 0 & 0 \\ -\sin \psi & \cos \psi & 0 & 0 & 0 & 0 \\ 0 & 0 & 1 & 0 & 0 & 0 \\ 0 & 0 & 0 & \cos \psi & \sin \psi & 0 \\ 0 & 0 & 0 & -\sin \psi & \cos \psi & 0 \\ 0 & 0 & 0 & 0 & 0 & 1 \end{bmatrix} \begin{Bmatrix} U_1 \\ U_2 \\ U_3 \\ U_4 \\ U_5 \\ U_6 \end{Bmatrix} = [R]\{U\} \quad (4.64)$$

where $[R]$ is the transformation matrix that relates element displacements to global displacements. In a manner exactly analogous to that of Section 3.3, it is readily shown that the 6×6 element stiffness matrix in the global system is given by

$$[K_e] = [R]^T [k_e] [R] \quad (4.65)$$

Owing to its algebraic complexity, Equation 4.65 is not expanded here to obtain a general result. Rather, the indicated computations are best suited for specific element characteristics and performed by computer program.

Assembly of the system equations for a finite element model using the beam-axial element is accomplished in an identical fashion to the procedures followed for trusses as discussed in Chapter 3. The following simple example illustrates the procedure.

EXAMPLE 4.4

The frame of Figure 4.14a is composed of identical beams having a 1-in. square cross section and a modulus of elasticity of 10×10^6 psi. The supports at O and C are to be considered completely fixed. The horizontal beam is subjected to a uniform load of intensity 10 lb/in., as shown. Use two beam-axial elements to compute the displacements and rotation at B .

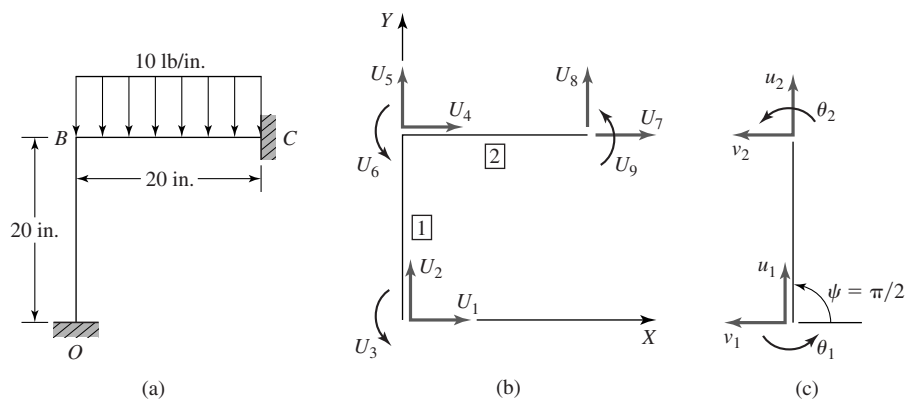


Figure 4.14

(a) Frame of Example 4.4. (b) Global coordinate system and displacement numbering. (c) Transformation of element 1.

■ Solution

Using the specified data, The cross-sectional area is

$$A = 1(1) = 1 \text{ in.}^2$$

And the area moment of inertia about the z axis is

$$I_z = bh^3/12 = 1/12 = 0.083 \text{ in.}^4$$

The characteristic axial stiffness is

$$AE/L = 1(10 \times 10^6)/20 = (5 \times 10^5) \text{ lb/in.}$$

and the characteristic bending stiffness is

$$EI_z/L^3 = 10 \times 10^6(0.083)/20^3 = 104.2 \text{ lb/in.}$$

Denoting member OB as element 1 and member BC as element 2, the stiffness matrices in the element coordinate systems are identical and given by

$$[k^{(1)}] = [k^{(2)}] = \begin{bmatrix} 5(10^5) & 0 & 0 & -5(10^5) & 0 & 0 \\ 0 & 1,250.4 & 12,504 & 0 & -1,250.4 & 12,504 \\ 0 & 12,504 & 166,720 & 0 & -12,504 & 83,360 \\ -5(10^5) & 0 & 0 & 5(10^5) & 0 & 0 \\ 0 & -1,250.4 & -12,504 & 0 & 1,250.4 & -12,504 \\ 0 & 12,504 & 83,360 & 0 & -12,504 & 166,720 \end{bmatrix}$$

Choosing the global coordinate system and displacement numbering as in Figure 4.14b, we observe that element 2 requires no transformation, as its element coordinate system is aligned with the global system. However, as shown in Figure 4.14c, element 1 requires transformation. Using $\psi = \pi/2$, Equations 4.64 and 4.65 are applied to obtain

$$[K^{(1)}] = \begin{bmatrix} 1,250.4 & 0 & -12,504 & 1,250.4 & 0 & -12,504 \\ 0 & 5(10^5) & 0 & 0 & -5(10^5) & 0 \\ -12,504 & 0 & 166,720 & 12,504 & 0 & 83,360 \\ 1,250.4 & 0 & 12,504 & 1,250.4 & 0 & 12,504 \\ 0 & -5(10^5) & 0 & 0 & 5(10^5) & 0 \\ -12,504 & 0 & 83,360 & 12,504 & 0 & 166,720 \end{bmatrix}$$

Note particularly how the stiffness matrix of element 1 changes as a result of the 90° rotation. The values of individual components in the stiffness matrix are unchanged. The positions of the terms in the matrix are changed to reflect, quite simply, the directions of bending and axial displacements of the element when described in the global (system) coordinate system.

The displacement correspondence table is shown in Table 4.6 and the assembled system stiffness matrix, by the direct assembly procedure, is in Table 4.7. Note, as usual, the “overlap” of the element stiffness matrices at the displacements associated with the common node. At these positions in the global stiffness matrix, the stiffness terms from the individual element stiffness matrices are additive.

4.7 Flexure Element with Axial Loading

Table 4.6 Displacement Correspondence

Global	Element 1	Element 2
1	1	0
2	2	0
3	3	0
4	4	1
5	5	2
6	6	3
7	0	4
8	0	5
9	0	6

Table 4.7 System Stiffness Matrix

$$[K] = \begin{bmatrix} 1,250.4 & 0 & -12,504 & 1,250.4 & 0 & -12,504 & 0 & 0 & 0 \\ 0 & 500,000 & 0 & 0 & -500,000 & 0 & 0 & 0 & 0 \\ -12,504 & 0 & 166,720 & 12,504 & 0 & 833,360 & 0 & 0 & 0 \\ 1,250.4 & 0 & 12,504 & 501,250.4 & 0 & 12,504 & -500,000 & 0 & 0 \\ 0 & -500,000 & 0 & 0 & 501,250.4 & 12,504 & 0 & -1,250.4 & 12,504 \\ -12,504 & 0 & 83,360 & 12,504 & 12,504 & 333,440 & 0 & -12,504 & 83,360 \\ 0 & 0 & 0 & -500,000 & 0 & 0 & 500,000 & 0 & 0 \\ 0 & 0 & 0 & 0 & -1,250.4 & -12,504 & 0 & 1,250.4 & -12,504 \\ 0 & 0 & 0 & 0 & 12,504 & 83,360 & 0 & -12,504 & 166,720 \end{bmatrix}$$

Using the system stiffness matrix, the assembled system equations are

$$[K] \begin{Bmatrix} U_1 \\ U_2 \\ U_3 \\ U_4 \\ U_5 \\ U_6 \\ U_7 \\ U_8 \\ U_9 \end{Bmatrix} = \begin{Bmatrix} R_{X1} \\ R_{Y1} \\ M_{R1} \\ 0 \\ -100 \\ -333.3 \\ R_{X3} \\ R_{Y3} - 100 \\ M_{R3} + 333.3 \end{Bmatrix}$$

where we denote the forces at nodes 1 and 3 as reaction components, owing to the displacement constraints $U_1 = U_2 = U_3 = U_7 = U_8 = U_9 = 0$. Taking the constraints into account, the equations to be solved for the active displacements are then

$$\begin{bmatrix} 501,250.4 & 0 & 12,504 \\ 0 & 501,250.4 & 12,504 \\ 12,504 & 12,504 & 333,440 \end{bmatrix} \begin{Bmatrix} U_4 \\ U_5 \\ U_6 \end{Bmatrix} = \begin{Bmatrix} 0 \\ -100 \\ -16.7 \end{Bmatrix}$$

Simultaneous solution gives the displacement values as

$$U_4 = 2.47974(10^{-5}) \text{ in.}$$

$$U_5 = -1.74704(10^{-4}) \text{ in.}$$

$$U_6 = -9.94058(10^{-4}) \text{ rad}$$

As usual, the reaction components can be obtained by substituting the computed displacements into the six constraint equations.

For the beam element with axial capability, the stress computation must take into account the superposition of bending stress and direct axial stress. For element 1, for example, we use Equation 4.63 with $\psi = \pi/2$ to compute the element displacement as

$$\begin{Bmatrix} u_1 \\ v_1 \\ \theta_1 \\ u_2 \\ v_2 \\ \theta_2 \end{Bmatrix} = \begin{bmatrix} 0 & 1 & 0 & 0 & 0 & 0 \\ -1 & 0 & 0 & 0 & 0 & 0 \\ 0 & 0 & 1 & 0 & 0 & 0 \\ 0 & 0 & 0 & 0 & 1 & 0 \\ 0 & 0 & 0 & -1 & 0 & 0 \\ 0 & 0 & 0 & 0 & 0 & 1 \end{bmatrix} \begin{Bmatrix} U_1 \\ U_2 \\ U_3 \\ U_4 \\ U_5 \\ U_6 \end{Bmatrix} = \begin{Bmatrix} 0 \\ 0 \\ 0 \\ -1.74704(10^{-4}) \\ -2.47974(10^{-5}) \\ -9.94058(10^{-4}) \end{Bmatrix}$$

The bending stress is computed at nodes 1 and 2 via Equations 4.33 and 4.34 as

$$\begin{aligned} \sigma_x(x=0) &= \pm 0.5(10)(10^6) \left[\frac{6}{20^2}(-2.47974)(10^{-5}) - \frac{2}{20}(-9.94058)(10^{-4}) \right] \\ &= \pm 495.2 \text{ psi} \end{aligned}$$

$$\begin{aligned} \sigma_x(x=L) &= \pm 0.5(10)(10^6) \left[\frac{6}{20^2}(2.47974)(10^{-5}) + \frac{2}{20}(2)(-9.94058)(10^{-4}) \right] \\ &= \pm 992.2 \text{ psi} \end{aligned}$$

and the axial stress is

$$\sigma_{\text{axial}} = 10(10^6) \frac{-1.74704(10^{-4})}{20} = -87.35 \text{ psi}$$

Therefore, the largest stress magnitude occurs at node 2, at which the compressive axial stress adds to the compressive portion of the bending stress distribution to give

$$\sigma = 1079.6 \text{ psi} \quad (\text{compressive})$$

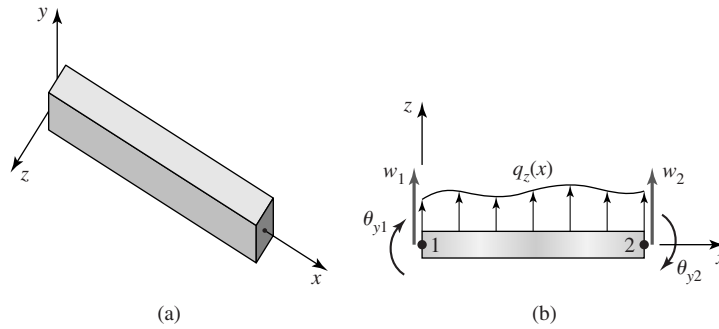
4.8 A GENERAL THREE-DIMENSIONAL BEAM ELEMENT

A general three-dimensional beam element is capable of both axial and torsional deflections as well as two-plane bending. To examine the stiffness characteristics of such an element and obtain the element stiffness matrix, we first extend the beam-axial element of the previous section to include two-plane bending, then add torsional capability.

Figure 4.15a shows a beam element with an attached three-dimensional element coordinate system in which the x axis corresponds to the longitudinal axis

4.8 A General Three-Dimensional Beam Element

121

**Figure 4.15**

(a) Three-dimensional beam element. (b) Nodal displacements in element xz plane.

of the beam and is assumed to pass through the centroid of the beam cross section. The y and z axes are assumed to correspond to the *principal axes for area moments of inertia of the cross section* [1]. If this is not the case, treatment of simultaneous bending in two planes and superposition of the results as in the following element development will *not* produce correct results [2].

For bending about the z axis (i.e., the plane of bending is the xy plane), the element stiffness matrix is given by Equation 4.48. For bending about the y axis, the plane of bending is the xz plane, as in Figure 4.15b, which depicts a beam element defined by nodes 1 and 2 and subjected to a distributed load $q_z(x)$ shown acting in the positive z direction. Nodal displacements in the z direction are denoted w_1 and w_2 , while nodal rotations are θ_{y1} and θ_{y2} . For this case, it is necessary to add the axis subscript to the nodal rotations to specifically identify the axis about which the rotations are measured. In this context, the rotations corresponding to xy plane bending henceforth are denoted θ_{z1} and θ_{z2} . It is also important to note that, in Figure 4.15b, the y axis is perpendicular to the plane of the page with the positive sense *into* the page. Therefore, the rotations shown are positive about the y axis per the right-hand rule. Noting the difference in the positive sense of rotation relative to the linear displacements, a development analogous to that used for the flexure element in Sections 4.3 and 4.4 results in the element stiffness matrix for xz plane bending as

$$[k_e]_{xz} = \frac{EI_y}{L^3} \begin{bmatrix} 12 & -6L & -12 & -6L \\ -6L & 4L^2 & 6L & 2L^2 \\ -12 & 6L & 12 & 6L \\ -6L & 2L^2 & 6L & 4L^2 \end{bmatrix} \quad (4.66)$$

The only differences between the xz plane bending stiffness matrix and that for xy plane bending are seen to be sign changes in the off-diagonal terms and the fact that the characteristic stiffness depends on the area moment of inertia I_y .

Combining the spar element stiffness matrix, the xy plane flexure stiffness matrix, and the xz plane stiffness matrix given by Equation 4.60, the element

equilibrium equations for a two-plane bending element with axial stiffness are written in matrix form as

$$\begin{bmatrix} [k_{axial}] & [0] & [0] \\ [0] & [k_{bending}]_{xy} & [0] \\ [0] & [0] & [k_{bending}]_{xz} \end{bmatrix} \begin{Bmatrix} u_1 \\ u_2 \\ v_1 \\ \theta_{z1} \\ v_2 \\ \theta_{z2} \\ w_1 \\ \theta_{y1} \\ w_2 \\ \theta_{y2} \end{Bmatrix} = \begin{Bmatrix} f_{x1} \\ f_{x2} \\ f_{y1} \\ M_{z1} \\ f_{y2} \\ M_{z2} \\ f_{z1} \\ M_{y1} \\ f_{z2} \\ M_{y2} \end{Bmatrix} \quad (4.67)$$

where the 10×10 element stiffness matrix has been written in the shorthand form

$$[k_e] = \begin{bmatrix} [k_{axial}] & [0] & [0] \\ [0] & [k_{bending}]_{xy} & [0] \\ [0] & [0] & [k_{bending}]_{xz} \end{bmatrix} \quad (4.68)$$

The equivalent nodal loads corresponding to a distributed load are computed on the basis of work equivalence, as in Section 4.6. For a uniform distributed load $q_z(x) = q_z$, the equivalent nodal load vector is found to be

$$\begin{Bmatrix} f_{qz1} \\ M_{qz1} \\ f_{qz2} \\ M_{qz2} \end{Bmatrix} = \begin{Bmatrix} \frac{q_z L}{2} \\ -\frac{q_z L^2}{12} \\ \frac{q_z L}{2} \\ \frac{q_z L^2}{12} \end{Bmatrix} \quad (4.69)$$

The addition of torsion to the general beam element is accomplished with reference to Figure 4.16a, which depicts a circular cylinder subjected to torsion via twisting moments applied at its ends. A corresponding torsional finite element

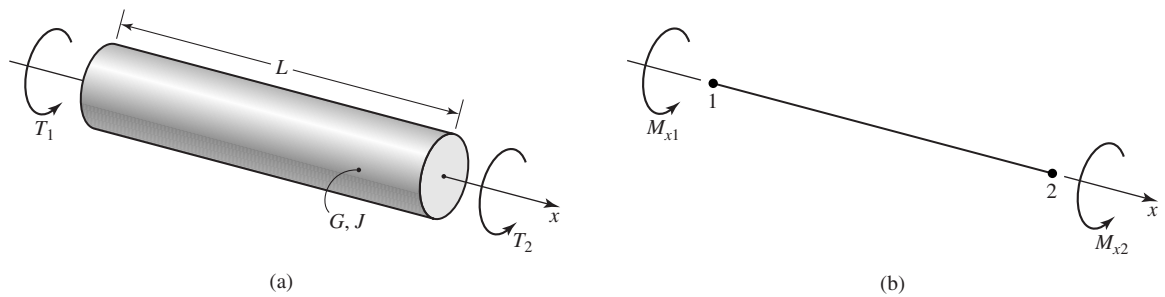


Figure 4.16 (a) Circular cylinder subjected to torsion. (b) Torsional finite element notation.

4.8 A General Three-Dimensional Beam Element

123

is shown in Figure 4.16b, where the nodes are 1 and 2, the axis of the cylinder is the x axis, and twisting moments are positive according to the right-hand rule. From elementary strength of materials, it is well known that the angle of twist per unit length of a uniform, elastic circular cylinder subjected to torque T is given by

$$\phi = \frac{T}{JG} \quad (4.70)$$

where J is polar moment of inertia of the cross-sectional area and G is the shear modulus of the material. As the angle of twist per unit length is constant, the total angle of twist of the element can be expressed in terms of the nodal rotations and twisting moments as

$$\theta_{x2} - \theta_{x1} = \frac{TL}{JG} \quad (4.71)$$

or

$$T = \frac{JG}{L}(\theta_{x2} - \theta_{x1}) = k_T(\theta_{x2} - \theta_{x1}) \quad (4.72)$$

Comparison of Equation 4.72 with Equation 2.2 for a linearly elastic spring and consideration of the equilibrium condition $M_{x1} + M_{x2} = 0$ lead directly to the element equilibrium equations:

$$\frac{JG}{L} \begin{bmatrix} 1 & -1 \\ -1 & 1 \end{bmatrix} \begin{Bmatrix} \theta_{x1} \\ \theta_{x2} \end{Bmatrix} = \begin{Bmatrix} M_{x1} \\ M_{x2} \end{Bmatrix} \quad (4.73)$$

so the torsional stiffness matrix is

$$[k_{\text{torsion}}] = \frac{JG}{L} \begin{bmatrix} 1 & -1 \\ -1 & 1 \end{bmatrix} \quad (4.74)$$

While this development is, strictly speaking, applicable only to a circular cross section, an equivalent torsional stiffness $J_{eq}G/L$ is known for many common structural cross sections and can be obtained from standard structural tables or strength of materials texts.

Adding the torsional characteristics to the general beam element, the element equations become

$$\begin{bmatrix} [k_{\text{axial}}] & [0] & [0] & [0] \\ [0] & [k_{\text{bending}}]_{xy} & [0] & [0] \\ [0] & [0] & [k_{\text{bending}}]_{xz} & [0] \\ [0] & [0] & [0] & [k_{\text{torsion}}] \end{bmatrix} \begin{Bmatrix} u_1 \\ u_2 \\ v_1 \\ \theta_{z1} \\ v_2 \\ \theta_{z2} \\ w_1 \\ \theta_{y1} \\ w_2 \\ \theta_{y2} \\ \theta_{x1} \\ \theta_{x2} \end{Bmatrix} = \begin{Bmatrix} f_{x1} \\ f_{x2} \\ f_{y1} \\ M_{z2} \\ f_{y2} \\ M_{z2} \\ f_{z1} \\ M_{y1} \\ f_{z2} \\ M_{y2} \\ M_{x1} \\ M_{x2} \end{Bmatrix} \quad (4.75)$$

and the final stiffness matrix for a general 3-D beam element is observed to be a 12×12 symmetric matrix composed of the individual stiffness matrices representing axial loading, two-plane bending, and torsion.

The general beam element can be utilized in finite element analyses of three-dimensional frame structures. As with most finite elements, it is often necessary to transform the element matrices from the element coordinate system to the global coordinates. The transformation procedure is quite similar to that discussed for the bar and two-dimensional beam elements, except, of course, for the added algebraic complexity arising from the size of the stiffness matrix and certain orientation details required.

4.9 CLOSING REMARKS

In this chapter, finite elements for beam bending are formulated using elastic flexure theory from elementary strength of materials. The resulting elements are very useful in modeling frame structures in two or three dimensions. A general three-dimensional beam element including axial, bending, and torsional effects is developed by, in effect, superposition of a spar element, two flexure elements, and a torsional element.

In development of the beam elements, stiffening of the elements owing to tensile loading, the possibility of buckling under compressive axial loading, and transverse shear effects have not been included. In most commercial finite element software packages, each of these concerns is an option that can be taken into account at the user's discretion.

REFERENCES

1. Beer, F. P., E. R. Johnston, and J. T. DeWolf. *Mechanics of Materials*, 3rd ed. New York: McGraw-Hill, 2002.
2. Budynas, R. *Advanced Strength and Applied Stress Analysis*, 2nd ed. New York: McGraw-Hill, 1999.

PROBLEMS

- 4.1 Two identical beam elements are connected at a common node as shown in Figure P4.1. Assuming that the nodal displacements v_i , θ_i are known, use Equation 4.32 to show that the normal stress σ_x is, in general, discontinuous at the common element boundary (i.e., at node 2). Under what condition(s) would the stress be continuous?

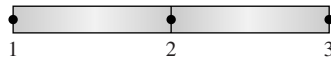


Figure P4.1

- 4.2 For the beam element loaded as shown in Figure P4.2, construct the shear force and bending moment diagrams. What is the significance of these diagrams with respect to Equations 4.10, 4.17, and the relation $V = \frac{dM}{dx}$ from strength of materials theory?

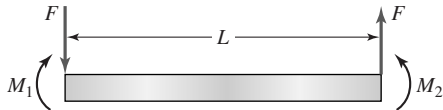


Figure P4.2

- 4.3 For a uniformly loaded beam as shown in Figure P4.3, the strength of materials theory gives the maximum deflection as

$$v_{\max} = -\frac{5qL^4}{384EI_z}$$

at $x = L/2$. Treat this beam as a single finite element and compute the maximum deflection. How do the values compare?

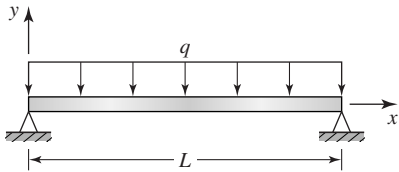


Figure P4.3

- 4.4 The beam element shown in Figure P4.4 is subjected to a linearly varying load of maximum intensity q_o . Using the work-equivalence approach, determine the nodal forces and moments.

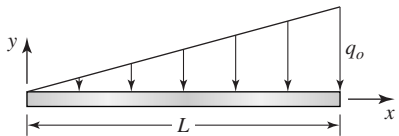


Figure P4.4

- 4.5 Use the results of Problem 4.4 to calculate the deflection at node 2 of the beam shown in Figure P4.5 if the beam is treated as a single finite element.

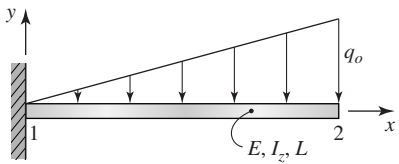


Figure P4.5

- 4.6 For the beam element of Figure P4.5, compute the reaction force and moment at node 1. Compute the maximum bending stress assuming beam height is $2h$. How does the stress value compare to the maximum stress obtained by the strength of materials approach?
- 4.7 Repeat Problem 4.5 using two equal length elements. For this problem, let $E = 30 \times 10^6$ psi, $I_z = 0.1$ in.⁴, $L = 10$ in., $q_o = 10$ lb/in.
- 4.8 Consider the beam shown in Figure P4.8. What is the minimum number of elements that can be used to model this problem? Construct the global nodal load vector corresponding to your answer.

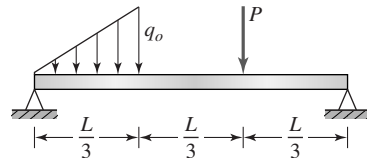


Figure P4.8

- 4.9 What is the justification for writing Equation 4.36 in the form of Equation 4.37?
- 4.10–4.15 For each beam shown in the associated figure, compute the deflection at the element nodes. The modulus of elasticity is $E = 10 \times 10^6$ psi and the cross section is as shown in each figure. Also compute the maximum bending stress. Use the finite element method with the minimum number of elements for each case.

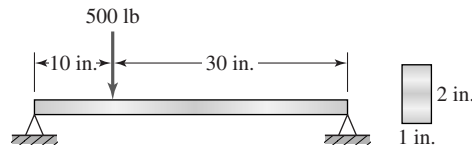


Figure P4.10

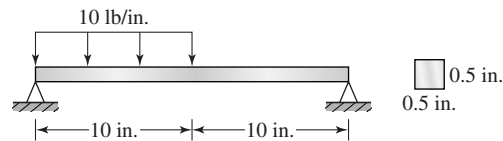


Figure P4.11

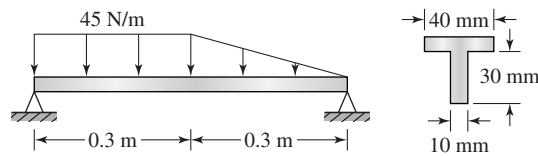


Figure P4.12

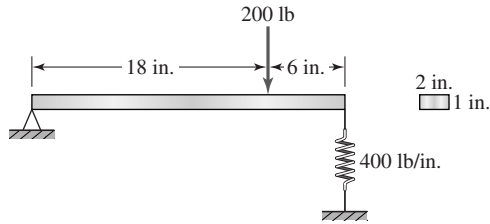


Figure P4.13

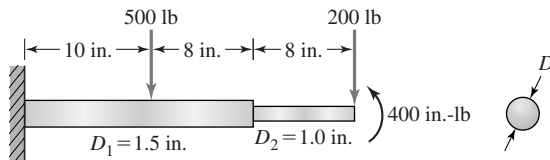


Figure P4.14

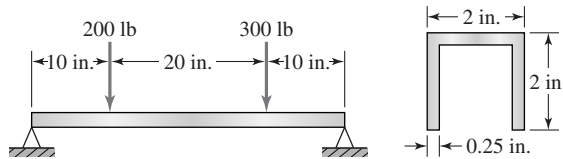


Figure P4.15

- 4.16 The tapered beam element shown in Figure P4.16 has uniform thickness t and varies linearly in height from $2h$ to h . Beginning with Equation 4.37, derive the strain energy expression for the element in a form similar to Equation 4.39.

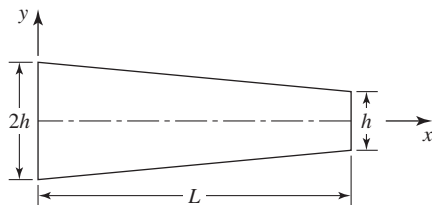


Figure P4.16

- 4.17 Use the result of Problem 4.16 to derive the value of component k_{11} of the element stiffness matrix.
- 4.18 The complete stiffness matrix for the tapered element of Figure P4.16 is given by

$$[k] = \frac{Eth^3}{60L^3} \begin{bmatrix} 243 & 156L & -243 & 87L \\ 156L & 56L^2 & -156L & 42L^2 \\ -243 & -156L & 243 & -87L \\ 87L & 42L^2 & -87L & 45L^2 \end{bmatrix}$$

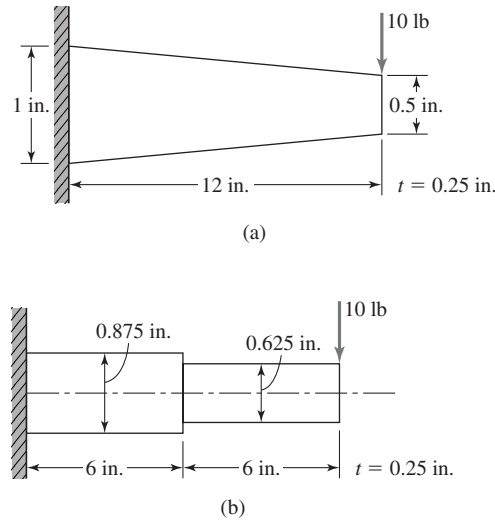


Figure P4.18

- a. Using the given stiffness matrix with $E = 10(10^6)$, compute the deflection of node 2 for the tapered element loaded as shown in Figure P4.18a.
 - b. Approximate the tapered beam using two straight elements, as in Figure P4.18b, and compute the deflection.
 - c. How do the deflection results compare?
 - d. How do the stress computations compare?
- 4.19** The six equilibrium equations for a beam-axial element in the element coordinate system are expressed in matrix form as

$$[k_e] \{\delta\} = \{f_e\}$$

with $\{\delta\}$ as given by Equation 4.61, $[k_e]$ by Equation 4.62, and $\{f_e\}$ as the nodal force vector

$$\{f_e\} = [f_{1x} \quad f_{1y} \quad M_1 \quad f_{2x} \quad f_{2y} \quad M_2]^T$$

For an element oriented at an arbitrary angle ψ relative to the global X axis, convert the equilibrium equations to the global coordinate system and verify Equation 4.65.

- 4.20** Use Equation 4.63 to express the strain energy of a beam-axial element in terms of global displacements. Apply the principle of minimum potential energy to derive the expression for the element equilibrium equations in the global coordinate system. (Warning: This is algebraically tedious.)
- 4.21** The two-dimensional frame structure shown in Figure P4.21 is composed of two 2×4 in. steel members ($E = 10 \times 10^6$ psi), and the 2-in. dimension is perpendicular to the plane of loading. All connections are treated as welded joints. Using two beam-axial elements and the node numbers as shown, determine

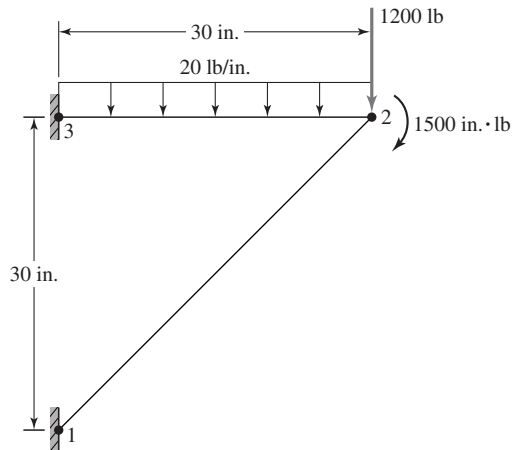


Figure P4.21

- a. The global stiffness matrix.
 - b. The global load vector.
 - c. The displacement components of node 2.
 - d. The reaction forces and moments at nodes 1 and 3.
 - e. Maximum stress in each element.
- 4.22 Repeat Problem 4.21 for the case in which the connection at node 2 is a pin joint.
- 4.23 The frame structure shown in Figure P4.23 is the support structure for a hoist located at the point of application of load W . The supports at A and B are completely fixed. Other connections are welded. Assuming the structure to be modeled using the minimum number of beam-axial elements:

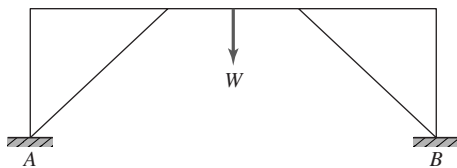


Figure P4.23

- a. How many elements are needed?
- b. What is the size of the assembled global stiffness matrix?
- c. What are the constraint (boundary) conditions?
- d. What is the size of the reduced global stiffness matrix after application of the constraint conditions?
- e. Assuming a finite element solution is obtained for this problem, what steps could be taken to judge the accuracy of the solution?

4.24 Repeat Problem 4.23 for the frame structure shown in Figure P4.24.

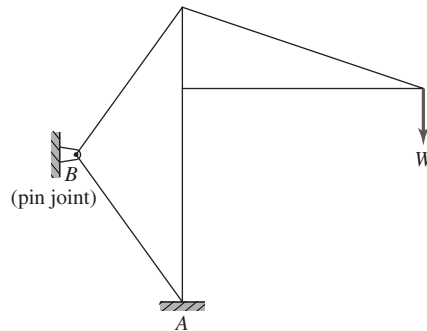


Figure P4.24

4.25 Verify Equation 4.69 by direct calculation.

4.26 The cantilevered beam depicted in Figure P4.26 is subjected to two-plane bending. The loads are applied such that the planes of bending correspond to the principal moments of inertia. Noting that no axial or torsional loadings are present, model the beam as a single element (that is, construct the 8×8 stiffness matrix containing bending terms only) and compute the deflections of the free end, node 2. Determine the exact location and magnitude of the maximum bending stress. (Use $E = 207$ GPa.)

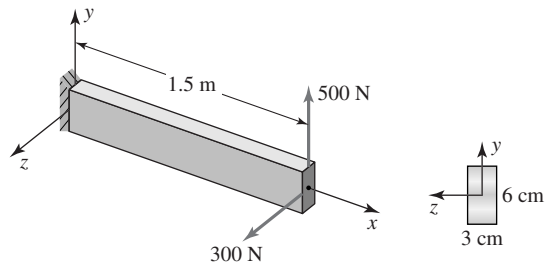


Figure P4.26

4.27 Repeat Problem 4.26 for the case in which the concentrated loads are replaced by uniform distributed loads $q_y = 6$ N/cm and $q_z = 4$ N/cm acting in the positive coordinate directions, respectively.

CHAPTER 5

Method of Weighted Residuals

5.1 INTRODUCTION

Chapters 2, 3, and 4 introduced some of the basic concepts of the finite element method in terms of the so-called line elements. The linear elastic spring, the bar element and the flexure element are line elements because structural properties can be described in terms of a single spatial variable that identifies position along the longitudinal axis of the element. The displacement-force relations for the line elements are straightforward, as these relations are readily described using only the concepts of elementary strength of materials. To extend the method of finite element analysis to more general situations, particularly nonstructural applications, additional mathematical techniques are required. In this chapter, the method of weighted residuals is described in general and Galerkin's method of weighted residuals [1] is emphasized as a tool for finite element formulation for essentially any field problem governed by a differential equation.

5.2 METHOD OF WEIGHTED RESIDUALS

It is a basic fact that most practical problems in engineering are governed by differential equations. Owing to complexities of geometry and loading, rarely are exact solutions to the governing equations possible. Therefore, approximate techniques for solving differential equations are indispensable in engineering analysis. Indeed, the finite element method is such a technique. However, the finite element method is based on several other, more-fundamental, approximate techniques, one of which is discussed in detail in this section and subsequently applied to finite element formulation.

The *method of weighted residuals* (MWR) is an approximate technique for solving boundary value problems that utilizes *trial functions* satisfying the

prescribed boundary conditions and an integral formulation to minimize error, in an average sense, over the problem domain. The general concept is described here in terms of the one-dimensional case but, as is shown in later chapters, extension to two and three dimensions is relatively straightforward. Given a differential equation of the general form

$$D[y(x), x] = 0 \quad a < x < b \quad (5.1)$$

subject to homogeneous boundary conditions

$$y(a) = y(b) = 0 \quad (5.2)$$

the method of weighted residuals seeks an approximate solution in the form

$$y^*(x) = \sum_{i=1}^n c_i N_i(x) \quad (5.3)$$

where y^* is the approximate solution expressed as the product of c_i unknown, constant parameters to be determined and $N_i(x)$ trial functions. The major requirement placed on the trial functions is that they be *admissible functions*; that is, the trial functions are continuous over the domain of interest and satisfy the specified boundary conditions exactly. In addition, the trial functions should be selected to satisfy the “physics” of the problem in a general sense. Given these somewhat lax conditions, it is highly unlikely that the solution represented by Equation 5.3 is exact. Instead, on substitution of the assumed solution into the differential Equation 5.1, a residual error (hereafter simply called *residual*) results such that

$$R(x) = D[y^*(x), x] \neq 0 \quad (5.4)$$

where $R(x)$ is the residual. Note that the residual is also a function of the unknown parameters c_i . The method of weighted residuals requires that the unknown parameters c_i be evaluated such that

$$\int_a^b w_i(x) R(x) dx = 0 \quad i = 1, n \quad (5.5)$$

where $w_i(x)$ represents n arbitrary weighting functions. We observe that, on integration, Equation 5.5 results in n algebraic equations, which can be solved for the n values of c_i . Equation 5.5 expresses that the sum (integral) of the weighted residual error over the domain of the problem is zero. Owing to the requirements placed on the trial functions, the solution is exact at the end points (the boundary conditions must be satisfied) but, in general, at any interior point the residual error is nonzero. As is subsequently discussed, the MWR may capture the exact solution under certain conditions, but this occurrence is the exception rather than the rule.

Several variations of MWR exist and the techniques vary primarily in how the weighting factors are determined or selected. The most common techniques are point collocation, subdomain collocation, least squares, and Galerkin’s

method [1]. As it is quite simple to use and readily adaptable to the finite element method, we discuss only Galerkin's method.

In Galerkin's weighted residual method, the weighting functions are chosen to be identical to the trial functions; that is,

$$w_i(x) = N_i(x) \quad i = 1, n \quad (5.6)$$

Therefore, the unknown parameters are determined via

$$\int_a^b w_i(x) R(x) dx = \int_a^b N_i(x) R(x) dx = 0 \quad i = 1, n \quad (5.7)$$

again resulting in n algebraic equations for evaluation of the unknown parameters. The following examples illustrate details of the procedure.

EXAMPLE 5.1

Use Galerkin's method of weighted residuals to obtain an approximate solution of the differential equation

$$\frac{d^2y}{dx^2} - 10x^2 = 5 \quad 0 \leq x \leq 1$$

with boundary conditions $y(0) = y(1) = 0$.

■ Solution

The presence of the quadratic term in the differential equation suggests that trial functions in polynomial form are suitable. For homogeneous boundary conditions at $x = a$ and $x = b$, the general form

$$N(x) = (x - x_a)^p (x - x_b)^q$$

with p and q being positive integers greater than zero, automatically satisfies the boundary conditions and is continuous in $x_a \leq x \leq x_b$. Using a single trial function, the simplest such form that satisfies the stated boundary conditions is

$$N_1(x) = x(x - 1)$$

Using this trial function, the approximate solution per Equation 5.3 is

$$y^*(x) = c_1 x(x - 1)$$

and the first and second derivatives are

$$\frac{dy^*}{dx} = c_1(2x - 1)$$

$$\frac{d^2y^*}{dx^2} = 2c_1$$

respectively. (We see, at this point, that the selected trial solution does not satisfy the physics of the problem, since we have obtained a constant second derivative. The differential equation is such that the second derivative must be a quadratic function of x . Nevertheless, we continue the example to illustrate the procedure.)

Substitution of the second derivative of $y^*(x)$ into the differential equation yields the residual as

$$R(x; c_1) = 2c_1 - 10x^2 - 5$$

which is clearly nonzero. Substitution into Equation 5.7 gives

$$\int_0^1 x(x-1)(2c_1 - 10x^2 - 5) dx = 0$$

which after integration yields $c_1 = 4$, so the approximate solution is obtained as

$$y^*(x) = 4x(x-1)$$

For this relatively simple example, we can compare the approximate solution result with the exact solution, obtained by integrating the differential equation twice as follows:

$$\frac{dy}{dx} = \int \frac{d^2y}{dx^2} dx = \int (10x^2 + 5) dx = \frac{10x^3}{3} + 5x + C_1$$

$$y(x) = \int \frac{dy}{dx} dx = \int \left(\frac{10x^3}{3} + 5x + C_1 \right) dx = \frac{5x^4}{6} + \frac{5x^2}{2} + C_1x + C_2$$

Applying the boundary condition $y(0) = 0$ gives $C_2 = 0$, while the condition $y(1) = 0$ becomes

$$\frac{5}{6} + \frac{5}{2} + C_1 = 0$$

from which $C_1 = -10/3$. Hence, the exact solution is given by

$$y(x) = \frac{5}{6}x^4 + \frac{5}{2}x^2 - \frac{10}{3}x$$

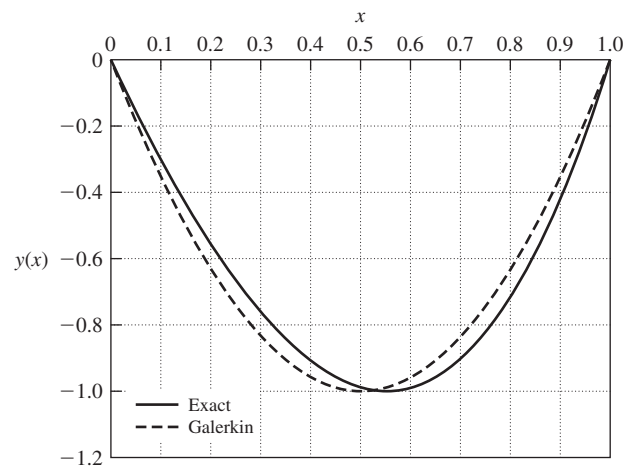


Figure 5.1 Solutions to Example 5.1.

A graphical comparison of the two solutions is depicted in Figure 5.1, which shows that the approximate solution is in reasonable agreement with the exact solution. However, note that the one-term approximate solution is symmetric over the interval of interest. That this is not correct can be seen by examining the differential equation. The prime driving “force” is the quadratic term in x ; therefore, it is unlikely that the solution is symmetric. The following example expands the solution and shows how the method approaches the exact solution.

EXAMPLE 5.2

Obtain a two-term Galerkin solution for the problem of Example 5.1 using the trial functions

$$N_1(x) = x(x - 1) \quad N_2(x) = x^2(x - 1)$$

■ Solution

The two-term approximate solution is

$$y^* = c_1x(x - 1) + c_2x^2(x - 1)$$

and the second derivative is

$$\frac{d^2y^*}{dx^2} = 2c_1 + 2c_2(3x - 1)$$

Substituting into the differential equation, we obtain the residual

$$R(x; c_1, c_2) = 2c_1 + 2c_2(3x - 1) - 10x^2 - 5$$

Using the trial functions as the weighting functions per Galerkin’s method, the residual equations become

$$\int_0^1 x(x - 1)[2c_1 + 2c_2(3x - 1) - 10x^2 - 5] dx = 0$$

$$\int_0^1 x^2(x - 1)[2c_1 + 2c_2(3x - 1) - 10x^2 - 5] dx = 0$$

After integration and simplification, we obtain the algebraic equations

$$-\frac{c_1}{3} - \frac{c_2}{6} + \frac{4}{3} = 0$$

$$-\frac{c_1}{6} - \frac{2c_2}{15} + \frac{3}{4} = 0$$

Simultaneous solution results in

$$c_1 = \frac{19}{6} \quad c_2 = \frac{5}{3}$$

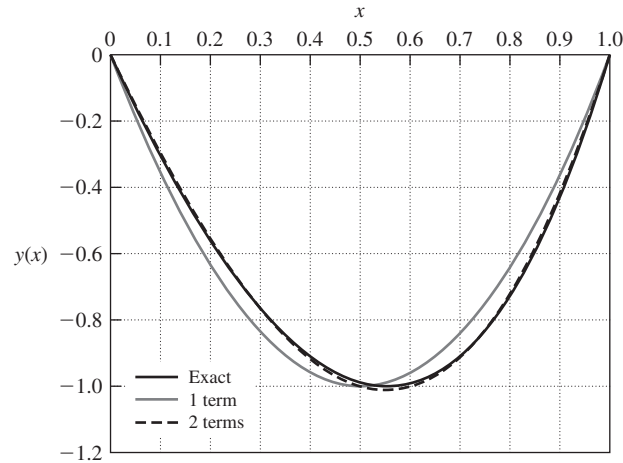


Figure 5.2 Solutions to Example 5.2.

so the two-term approximate solution is

$$y^* = \frac{19}{6}x(x-1) + \frac{5}{3}x^2(x-1) = \frac{5}{3}x^3 + \frac{3}{2}x^2 - \frac{19}{6}x$$

For comparison, the exact, one-term and two-term solutions are plotted in Figure 5.2. The differences in the exact and two-term solutions are barely discernible.

EXAMPLE 5.3

Use Galerkin's method of weighted residuals to obtain a one-term approximation to the solution of the differential equation

$$\frac{d^2y}{dx^2} + y = 4x \quad 0 \leq x \leq 1$$

with boundary conditions $y(0) = 0$, $y(1) = 1$.

■ Solution

Here the boundary conditions are not homogeneous, so a modification is required. Unlike the case of homogeneous boundary conditions, it is not possible to construct a trial solution of the form $c_1 N_1(x)$ that satisfies both stated boundary conditions. Instead, we assume a trial solution as

$$y^* = c_1 N_1(x) + f(x)$$

where $N_1(x)$ satisfies the homogeneous boundary conditions and $f(x)$ is chosen to satisfy the nonhomogeneous condition. (Note that, if both boundary conditions were nonhomogeneous, two such functions would be included.) One such solution is

$$y^* = c_1 x(x-1) + x$$

which satisfies $y(0) = 0$ and $y(1) = 1$ identically.

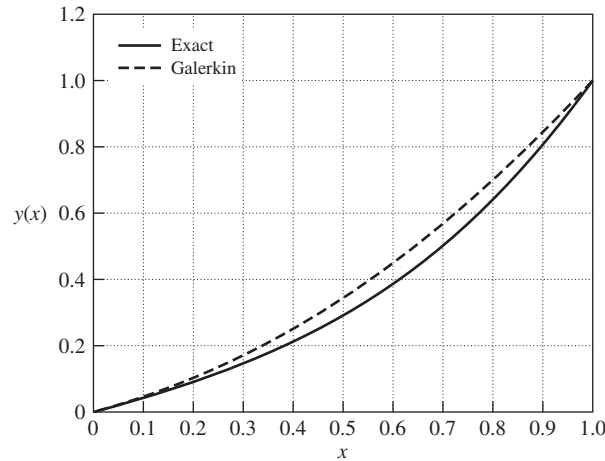


Figure 5.3 Solutions to Example 5.3.

Substitution into the differential equation results in the residual

$$R(x; c_1) = \frac{d^2 y^*}{dx^2} + y^* - 4x = 2c_1 + c_1 x^2 - c_1 x + x - 4x = c_1 x^2 - c_1 x + 2c_1 - 3x$$

and the weighted residual integral becomes

$$\int_0^1 N_1(x) R(x; c_1) dx = \int_0^1 x(x-1)(c_1 x^2 + c_1 x - 2c_1 - 3x) dx = 0$$

While algebraically tedious, the integration is straightforward and yields

$$c_1 = 5/6$$

so the approximate solution is

$$y^*(x) = \frac{5}{6}x(x-1) + x = \frac{5}{6}x^2 + \frac{1}{6}x$$

As in the previous example, we have the luxury of comparing the approximate solution to the exact solution, which is

$$y(x) = 4x - 3.565 \sin x$$

The approximate solution and the exact solution are shown in Figure 5.3 for comparison. Again, the agreement is observed to be reasonable but could be improved by adding a second trial function.

How does one know when the MWR solution is accurate enough? That is, how do we determine whether the solution is close to the exact solution? This question of *convergence* must be addressed in all approximate solution techniques. If we do not know the exact solution, and we seldom do, we must

develop some criterion to determine accuracy. In general, for the method of weighted residuals, the procedure is to continue obtaining solutions while increasing the number of trial functions and note the behavior of the solution. If the solution changes very little as we increase the number of trial functions, we can say that the solution converges. Whether the solution converges to the correct solution is yet another question. While beyond the scope of this book, a large body of theoretical mathematics addresses the questions of convergence and whether the convergence is to the correct solution. In the context of this work, we assume that a converging solution converges to the correct solution. Certain checks, external to the solution procedure, can be made to determine the “reasonableness” of a numerical solution in the case of physical problems. These checks include equilibrium, energy balance, heat and fluid flow balance, and others discussed in following chapters.

In the previous examples, we used trial functions “concocted” to satisfy boundary conditions automatically but not based on a systematic procedure. While absolutely nothing is wrong with this approach, we now present a procedure, based on polynomial trial functions, that gives a method for increasing the number of trial functions systematically and, hence, aids in examining convergence. The procedure is illustrated in the context of the following example.

EXAMPLE 5.4

Solve the problem of Examples 5.1 and 5.2 by assuming a general polynomial form for the solution as

$$y^*(x) = c_0 + c_1x + c_2x^2 + \dots$$

■ Solution

For a first trial, we take only the quadratic form

$$y^*(x) = c_0 + c_1x + c_2x^2$$

and apply the boundary conditions to obtain

$$y^*(0) = 0 = c_0$$

$$y^*(1) = 0 = c_1 + c_2$$

The second boundary condition equations show that c_1 and c_2 are not independent if the homogeneous boundary condition is to be satisfied exactly. Instead, we obtain the *constraint* relation $c_2 = -c_1$. The trial solution becomes

$$y^*(x) = c_1x + c_2x^2 = c_1x - c_1x^2 = c_1x(1 - x)$$

and is the same as the solution obtained in Example 5.1.

Next we add the cubic term and write the trial solution as

$$y^*(x) = c_0 + c_1x + c_2x^2 + c_3x^3$$

Application of the boundary conditions results in

$$y^*(0) = 0 = c_0$$

$$y^*(1) = 0 = c_1 + c_2 + c_3$$

so we have the constraint relation

$$c_1 + c_2 + c_3 = 0$$

Expressing the constraint as $c_3 = -(c_1 + c_2)$, the trial solution becomes

$$y^*(x) = c_1x + c_2x^2 + c_3x^3 = c_1x + c_2x^2 - (c_1 + c_2)x^3 = c_1x(1 - x^2) + c_2x^2(1 - x)$$

and we have obtained two trial functions, each identically satisfying the boundary conditions. Determination of the constants for the two-term solution is left as an end-of-chapter exercise. Instead, we add the quartic term and examine the trial solution

$$y^*(x) = c_0 + c_1x + c_2x^2 + c_3x^3 + c_4x^4$$

and the boundary conditions give

$$c_0 = 0$$

$$c_1 + c_2 + c_3 + c_4 = 0$$

We use the constraint relation to eliminate (arbitrarily) c_4 to obtain

$$\begin{aligned} y^*(x) &= c_1x + c_2x^2 + c_3x^3 - (c_1 + c_2 + c_3)x^4 \\ &= c_1x(1 - x^3) + c_2x^2(1 - x^2) + c_3x^3(1 - x) \end{aligned}$$

Substituting into the differential equation, the residual is found to be

$$R(x; c_1, c_2, c_3) = -12c_1x^2 + c_2(2 - 12x^2) + c_3(6x - 12x^2) - 10x^2 - 5$$

If we set the residual expression equal to zero and equate coefficients of powers of x , we find that the residual is exactly zero if

$$c_1 = -\frac{10}{3}$$

$$c_2 = \frac{5}{2}$$

$$c_3 = 0$$

$$c_4 = \frac{5}{6}$$

so that $y^*(x) = \frac{5}{6}x^4 + \frac{5}{2}x^2 - \frac{10}{3}x$ and we have obtained the exact solution.

The procedure detailed in the previous example represents a systematic procedure for developing polynomial trial functions and is also applicable to the case of nonhomogeneous boundary conditions. Algebraically, the process is straightforward but becomes quite tedious as the number of trial functions is increased (i.e., the order of the polynomial). Having outlined the general technique of Galerkin's method of weighted residuals, we now develop Galerkin's finite element method based on MWR.

5.3 THE GALERKIN FINITE ELEMENT METHOD

The classic method of weighted residuals described in the previous section utilizes trial functions that are global; that is, each trial function must apply over the entire domain of interest and identically satisfy the boundary conditions. Particularly in the more practical cases of two- and three-dimensional problems governed by partial differential equations, “discovery” of appropriate trial functions and determination of the accuracy of the resulting solutions are formidable tasks. However, the concept of minimizing the residual error is readily adapted to the finite element context using the Galerkin approach as follows. For illustrative purposes, we consider the differential equation

$$\frac{d^2y}{dx^2} + f(x) = 0 \quad a \leq x \leq b \tag{5.8}$$

subject to boundary conditions

$$y(a) = y_a \quad y(b) = y_b \tag{5.9}$$

The problem domain is divided into M “elements” (Figure 5.4a) bounded by $M + 1$ values x_i of the independent variable, so that $x_1 = x_a$ and $x_{M+1} = x_b$ to

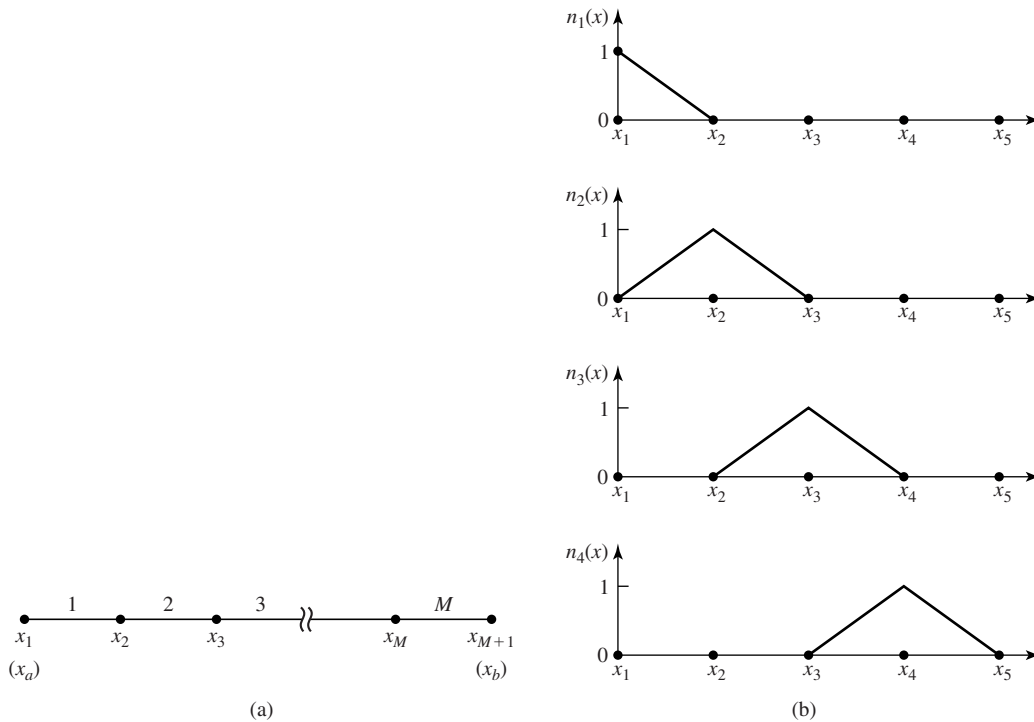


Figure 5.4 (a) Domain $x_a \leq x \leq x_b$ discretized into M elements. (b) First four trial functions. Note the overlap of only two trial functions in each element domain.

ensure inclusion of the global boundaries. An approximate solution is assumed in the form

$$y^*(x) = \sum_{i=1}^{M+1} y_i n_i(x) \quad (5.10)$$

where y_i is the value of the solution function at $x = x_i$ and $n_i(x)$ is a corresponding trial function. Note that, in this approach, the unknown constant parameters c_i of the method of weighted residuals become unknown discrete values of the solution function evaluated at specific points in the domain. There also exists a major difference in the trial functions. As used in Equation 5.10, the trial functions $n_i(x)$ are nonzero over only a small portion of the global problem domain. Specifically, a trial function $n_i(x)$ is nonzero only in the interval $x_{i-1} < x < x_{i+1}$, and for ease of illustration, we use linear functions defined as follows:

$$\begin{aligned} n_i(x) &= \frac{x - x_{i-1}}{x_i - x_{i-1}} & x_{i-1} \leq x \leq x_i \\ n_i(x) &= \frac{x_{i+1} - x}{x_{i+1} - x_i} & x_i \leq x \leq x_{i+1} \\ n_i(x) &= 0 & x < x_{i-1} \quad x > x_{i+1} \end{aligned} \quad (5.11)$$

Clearly, in this case, the trial functions are simply linear interpolation functions such that the value of the solution $y(x)$ in $x_i < x < x_{i+1}$ is a linear combination of adjacent “nodal” values y_i and y_{i+1} . The first four trial functions are as shown in Figure 5.4b, and we observe that, in the interval $x_2 \leq x \leq x_3$, for example, the approximate solution as given by Equation 5.10 is

$$y^*(x) = y_2 n_2(x) + y_3 n_3(x) = y_2 \frac{x_3 - x}{x_3 - x_2} + y_3 \frac{x - x_2}{x_3 - x_2} \quad (5.12)$$

(The trial functions used here are linear but higher-order functions can also be used, as is subsequently demonstrated by application of the technique to a beam element.)

Substitution of the assumed solution (5.10) into the governing Equation 5.8 yields the residual

$$R(x; y_i) = \sum_{i=1}^{M+1} \left[\frac{d^2 y^*}{dx^2} + f(x) \right] = \sum_{i=1}^{M+1} \left[\frac{d^2}{dx^2} \{y_i n_i(x)\} + f(x) \right] \quad (5.13)$$

to which we apply Galerkin’s weighted residual method, using each trial function as a weighting function, to obtain

$$\int_{x_a}^{x_b} n_j(x) R(x; y_i) dx = \int_{x_a}^{x_b} n_j(x) \sum_{i=1}^{M+1} \left[\frac{d^2}{dx^2} \{y_i n_i(x)\} + f(x) \right] dx = 0$$

$$j = 1, M + 1 \quad (5.14)$$

In light of Equation 5.11 and Figure 5.4b, we observe that, in any interval $x_j \leq x \leq x_{j+1}$, only two of the trial functions are nonzero. Taking this observation into account, Equation 5.14 can be expressed as

$$\int_{x_j}^{x_{j+1}} n_j(x) \left[\frac{d^2}{dx^2} (y_j n_j(x) + y_{j+1} n_{j+1}(x)) + f(x) \right] dx = 0 \quad j = 1, M + 1 \quad (5.15)$$

Integration of Equation 5.15 yields $M + 1$ algebraic equations in the $M + 1$ unknown nodal solution values y_j , and these equations can be written in the matrix form

$$[K]\{y\} = \{F\} \quad (5.16)$$

where $[K]$ is the system “stiffness” matrix, $\{y\}$ is the vector of nodal “displacements” and $\{F\}$ is the vector of nodal “forces.” Equation 5.14 is the formal statement of the Galerkin finite element method and includes both element formation and system assembly steps. Written in terms of integration over the full problem domain, this formulation clearly shows the mathematical basis in the method of weighted residuals. However, Equations 5.15 show that integration over only each element is required for each of the equations. We now proceed to examine separate element formulation based on Galerkin’s method.

5.3.1 Element Formulation

If the exact solution for Equation 5.8 is obtained, then that solution satisfies the equation in any subdomain in (a, b) as well. Consider the problem

$$\frac{d^2 y}{dx^2} + f(x) = 0 \quad x_j \leq x \leq x_{j+1} \quad (5.17)$$

where x_j and x_{j+1} are contained in (a, b) and define the nodes of a finite element. The appropriate boundary conditions applicable to Equation 5.17 are

$$y(x_j) = y_j \quad y(x_{j+1}) = y_{j+1} \quad (5.18)$$

and these are the unknown values of the solution at the end points of the subdomain. Next we propose an approximate solution of the form

$$y^{(e)}(x) = y_j N_1(x) + y_{j+1} N_2(x) \quad (5.19)$$

where superscript (e) indicates that the solution is for the finite element and the interpolation functions are now defined as

$$N_1(x) = \frac{x_{j+1} - x}{x_{j+1} - x_j} \quad x_j \leq x \leq x_{j+1} \quad (5.20a)$$

$$N_2(x) = \frac{x - x_j}{x_{j+1} - x_j} \quad x_j \leq x \leq x_{j+1} \quad (5.20b)$$

Note the relation between the interpolation functions defined in Equation 5.20 and the trial functions in Equation 5.11. The interpolation functions correspond to the overlapping portions of the trial functions applicable in a single element domain. Also note that the interpolation functions satisfy the conditions

$$\begin{aligned} N_1(x = x_j) &= 1 & N_1(x = x_{j+1}) &= 0 \\ N_2(x = x_j) &= 0 & N_2(x = x_{j+1}) &= 1 \end{aligned} \quad (5.21)$$

such that the element boundary (nodal) conditions, Equation 5.18, are identically satisfied. Substitution of the assumed solution into Equation 5.19 gives the residual as

$$R^{(e)}(x; y_j, y_{j+1}) = \frac{d^2 y^{(e)}}{dx^2} + f(x) = \frac{d^2}{dx^2} [y_j N_1(x) + y_{j+1} N_2(x)] + f(x) \neq 0 \quad (5.22)$$

where the superscript is again used to indicate that the residual is for the *element*. Applying the Galerkin weighted residual criterion results in

$$\int_{x_j}^{x_{j+1}} N_i(x) R^{(e)}(x; y_j, y_{j+1}) dx = \int_{x_j}^{x_{j+1}} N_i(x) \left[\frac{d^2 y^{(e)}}{dx^2} + f(x) \right] dx = 0 \quad i = 1, 2 \quad (5.23)$$

or

$$\int_{x_j}^{x_{j+1}} N_i(x) \frac{d^2 y^{(e)}}{dx^2} dx + \int_{x_j}^{x_{j+1}} N_i(x) f(x) dx = 0 \quad i = 1, 2 \quad (5.24)$$

as the element residual equations.

Applying integration by parts to the first integral results in

$$N_i(x) \frac{dy^{(e)}}{dx} \Big|_{x_j}^{x_{j+1}} - \int_{x_j}^{x_{j+1}} \frac{dN_i}{dx} \frac{dy^{(e)}}{dx} dx + \int_{x_j}^{x_{j+1}} N_i(x) f(x) dx = 0 \quad i = 1, 2 \quad (5.25)$$

which, after evaluation of the nonintegral term and rearranging is equivalent to the two equations, is

$$\int_{x_j}^{x_{j+1}} \frac{dN_1}{dx} \frac{dy^{(e)}}{dx} dx = \int_{x_j}^{x_{j+1}} N_1(x) f(x) dx + \frac{dy^{(e)}}{dx} \Big|_{x_j} \quad (5.26a)$$

$$\int_{x_j}^{x_{j+1}} \frac{dN_2}{dx} \frac{dy^{(e)}}{dx} dx = \int_{x_j}^{x_{j+1}} N_2(x) f(x) dx - \frac{dy^{(e)}}{dx} \Big|_{x_{j+1}} \quad (5.26b)$$

Note that, in arriving at the form of Equation 5.26, explicit use has been made of Equation 5.21 in evaluation of the interpolation functions at the element nodes.

Integration of Equation 5.24 by parts results in three benefits [2]:

1. The highest order of the derivatives appearing in the element equations has been reduced by one.
2. As will be observed explicitly, the stiffness matrix was made symmetric. If we did not integrate by parts, one of the trial functions in each equation would be differentiated twice and the other trial function not differentiated at all.
3. Integration by parts introduces the gradient boundary conditions at the element nodes. The physical significance of the gradient boundary conditions becomes apparent in subsequent physical applications.

Setting $j = 1$ for notational simplicity and substituting Equation 5.19 into Equation 5.26 yields

$$\int_{x_1}^{x_2} \frac{dN_1}{dx} \left[y_1 \frac{dN_1}{dx} + y_2 \frac{dN_2}{dx} \right] dx = \int_{x_1}^{x_2} N_1(x) f(x) dx + \left. \frac{dy^{(e)}}{dx} \right|_{x_1} \quad (5.27a)$$

$$\int_{x_1}^{x_2} \frac{dN_2}{dx} \left[y_1 \frac{dN_1}{dx} + y_2 \frac{dN_2}{dx} \right] dx = \int_{x_1}^{x_2} N_2(x) f(x) dx - \left. \frac{dy^{(e)}}{dx} \right|_{x_2} \quad (5.27b)$$

which are of the form

$$\begin{bmatrix} k_{11} & k_{12} \\ k_{21} & k_{22} \end{bmatrix} \begin{Bmatrix} y_1 \\ y_2 \end{Bmatrix} = \begin{Bmatrix} F_1 \\ F_2 \end{Bmatrix} \quad (5.28)$$

The terms of the coefficient (element stiffness) matrix are defined by

$$k_{ij} = \int_{x_1}^{x_2} \frac{dN_i}{dx} \frac{dN_j}{dx} dx \quad i, j = 1, 2 \quad (5.29)$$

and the element nodal forces are given by the right-hand sides of Equation 5.27.

If the described Galerkin procedure for element formulation is followed and the system equations are assembled in the usual manner of the direct stiffness method, the resulting system equations are identical in every respect to those obtained by the procedure represented by Equation 5.13. It is important to observe that, during the assembly process, when two elements are joined at a common node as in Figure 5.5, for example, the assembled system equation for the node contains a term on the right-hand side of the form

$$-\left. \frac{dy^{(3)}}{dx} \right|_{x_4} + \left. \frac{dy^{(4)}}{dx} \right|_{x_4} \quad (5.30)$$

If the finite element solution were the exact solution, the first derivatives for each element indicated in expression 5.30 would be equal and the value of the expression would be zero. However, finite element solutions are seldom exact, so these

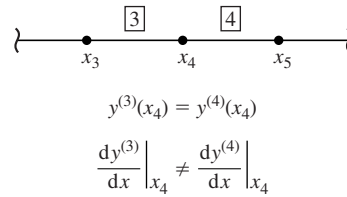


Figure 5.5 Two elements joined at a node.

terms are not, in general, zero. Nevertheless, in the assembly procedure, it is assumed that, at all interior nodes, the gradient terms appear as equal and opposite from the adjacent elements and thus cancel unless an external influence acts at the node. At global boundary nodes however, the gradient terms may be specified boundary conditions or represent “reactions” obtained via the solution phase. In fact, a very powerful technique for assessing accuracy of finite element solutions is to examine the magnitude of gradient discontinuities at nodes or, more generally, interelement boundaries.

EXAMPLE 5.5

Use Galerkin’s method to formulate a linear finite element for solving the differential equation

$$x \frac{d^2 y}{dx^2} + \frac{dy}{dx} - 4x = 0 \quad 1 \leq x \leq 2$$

subject to $y(1) = y(2) = 0$.

■ Solution

First, note that the differential equation is equivalent to

$$\frac{d}{dx} \left(x \frac{dy}{dx} \right) - 4x = 0$$

which, after two direct integrations and application of boundary conditions, has the exact solution

$$y(x) = x^2 - \frac{3}{\ln 2} \ln x - 1$$

For the finite element solution, the simplest approach is to use a two-node element for which the element solution is assumed as

$$y(x) = N_1(x)y_1 + N_2(x)y_2 = \frac{x_2 - x}{x_2 - x_1}y_1 + \frac{x - x_1}{x_2 - x_1}y_2$$

where y_1 and y_2 are the nodal values. The residual equation for the element is

$$\int_{x_1}^{x_2} N_i \left[\frac{d}{dx} \left(x \frac{dy}{dx} \right) - 4x \right] dx = 0 \quad i = 1, 2$$

which becomes, after integration of the first term by parts,

$$N_i x \frac{dy}{dx} \Big|_{x_1}^{x_2} - \int_{x_1}^{x_2} x \frac{dN_i}{dx} \frac{dy}{dx} dx - \int_{x_1}^{x_2} 4x N_i dx = 0 \quad i = 1, 2$$

Substituting the element solution form and rearranging, we have

$$\int_{x_1}^{x_2} x \frac{dN_i}{dx} \left(\frac{dN_1}{dx} y_1 + \frac{dN_2}{dx} y_2 \right) dx = N_i x \frac{dy}{dx} \Big|_{x_1}^{x_2} - \int_{x_1}^{x_2} 4x N_i dx \quad i = 1, 2$$

Expanding the two equations represented by the last result after substitution for the interpolation functions and first derivatives yields

$$\frac{1}{(x_2 - x_1)^2} \int_{x_1}^{x_2} x (y_1 - y_2) dx = -x_1 \frac{dy}{dx} \Big|_{x_1}^{x_2} - 4 \int_{x_1}^{x_2} x \frac{x_2 - x}{x_2 - x_1} dx$$

$$\frac{1}{(x_2 - x_1)^2} \int_{x_1}^{x_2} x (y_2 - y_1) dx = x_2 \frac{dy}{dx} \Big|_{x_2}^{x_1} - 4 \int_{x_1}^{x_2} x \frac{x - x_1}{x_2 - x_1} dx$$

Integration of the terms on the left reveals the element stiffness matrix as

$$[k^{(e)}] = \frac{x_2^2 - x_1^2}{2(x_2 - x_1)^2} \begin{bmatrix} 1 & -1 \\ -1 & 1 \end{bmatrix}$$

while the gradient boundary conditions and nodal forces are evident on the right-hand side of the equations.

To illustrate, a two-element solution is formulated by taking equally spaced nodes at $x = 1, 1.5, 2$ as follows.

Element 1

$$x_1 = 1 \quad x_2 = 1.5 \quad k = 2.5$$

$$F_1^{(1)} = -4 \int_1^{1.5} x \frac{1.5 - x}{1.5 - 1} dx = -1.166666\dots$$

$$F_2^{(1)} = -4 \int_1^{1.5} x \frac{x - 1}{1.5 - 1} dx = -1.33333\dots$$

Element 2

$$x_1 = 1.5 \quad x_2 = 2 \quad k = 3.5$$

$$F_1^{(2)} = -4 \int_{1.5}^2 x \frac{2 - x}{2 - 1.5} dx = -1.66666\dots$$

$$F_2^{(2)} = -4 \int_{1.5}^2 x \frac{x - 1.5}{2 - 1.5} dx = -1.83333\dots$$

5.3 The Galerkin Finite Element Method

147

The element equations are then

$$\begin{bmatrix} 2.5 & -2.5 \\ -2.5 & 2.5 \end{bmatrix} \begin{Bmatrix} y_1^{(1)} \\ y_2^{(1)} \end{Bmatrix} = \begin{Bmatrix} -1.1667 - \frac{dy}{dx}\Big|_{x_1} \\ -1.3333 + 1.5 \frac{dy}{dx}\Big|_{x_2} \end{Bmatrix}$$

$$\begin{bmatrix} 3.5 & -3.5 \\ -3.5 & 3.5 \end{bmatrix} \begin{Bmatrix} y_1^{(2)} \\ y_2^{(2)} \end{Bmatrix} = \begin{Bmatrix} -1.6667 - 1.5 \frac{dy}{dx}\Big|_{x_2} \\ -1.8333 + 2 \frac{dy}{dx}\Big|_{x_3} \end{Bmatrix}$$

Denoting the system nodal values as Y_1, Y_2, Y_3 at $x = 1, 1.5, 2$, respectively, the assembled system equations are

$$\begin{bmatrix} 2.5 & -2.5 & 0 \\ -2.5 & 6 & -3.5 \\ 0 & -3.5 & 3.5 \end{bmatrix} \begin{Bmatrix} Y_1 \\ Y_2 \\ Y_3 \end{Bmatrix} = \begin{Bmatrix} -1.1667 - \frac{dy}{dx}\Big|_{x_1} \\ -3 \\ -1.8333 + 2 \frac{dy}{dx}\Big|_{x_3} \end{Bmatrix}$$

Applying the global boundary conditions $Y_1 = Y_3 = 0$, the second of the indicated equations gives $Y_2 = -0.5$ and substitution of this value into the other two equations yields the values of the gradients at the boundaries as

$$\frac{dy}{dx}\Big|_{x_1} = -2.4167 \quad \frac{dy}{dx}\Big|_{x_3} = 1.7917$$

For comparison, the exact solution gives

$$y(x = 1.5) = Y_2 = -0.5049 \quad \frac{dy}{dx}\Big|_{x_1} = -2.3281 \quad \frac{dy}{dx}\Big|_{x_3} = 1.8360$$

While the details will be left as an end-of-chapter problem, a four-element solution for this example (again, using equally spaced nodes $x_i \Rightarrow (1, 1.25, 1.5, 1.75, 2)$) results in the global equations

$$\begin{bmatrix} 4.5 & -4.5 & 0 & 0 & 0 \\ -4.5 & 10 & -5.5 & 0 & 0 \\ 0 & -5.5 & 12 & -6.5 & 0 \\ 0 & 0 & -6.5 & 14 & -7.5 \\ 0 & 0 & 0 & -7.5 & 7.5 \end{bmatrix} \begin{Bmatrix} Y_1 \\ Y_2 \\ Y_3 \\ Y_4 \\ Y_5 \end{Bmatrix} = \begin{Bmatrix} -0.5417 - \frac{dy}{dx}\Big|_{x_1} \\ -1.25 \\ -1.5 \\ -1.75 \\ -0.9583 + 2 \frac{dy}{dx}\Big|_{x_5} \end{Bmatrix}$$

Applying the boundary conditions $Y_1 = Y_5 = 0$ and solving the remaining 3×3 system gives the results

$$Y_2 = -0.4026$$

$$Y_3 = -0.5047$$

$$Y_4 = -0.3603$$

$$\frac{dy}{dx}\Big|_{x_1} = -2.350$$

$$\frac{dy}{dx}\Big|_{x_5} = 1.831$$

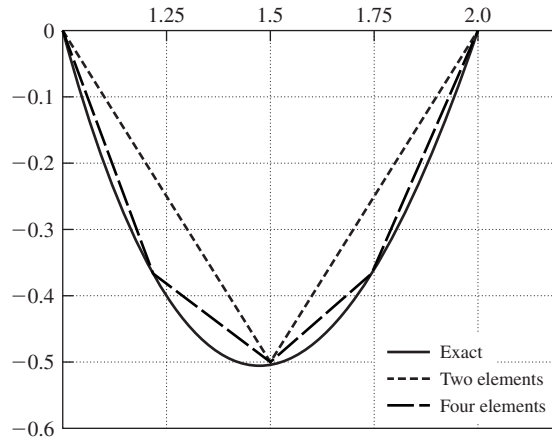


Figure 5.6 Two-element, four-element, and exact solutions to Example 5.5.

For comparison, the exact, two-element, and four-element solutions are shown in Figure 5.6. The two-element solution is seen to be a crude approximation except at the element nodes and derivative discontinuity is significant. The four-element solution has the computed values of $y(x)$ at the nodes being nearly identical to the exact solution. With four elements, the magnitudes of the discontinuities of first derivatives at the nodes are reduced but still readily apparent.

5.4 APPLICATION OF GALERKIN'S METHOD TO STRUCTURAL ELEMENTS

5.4.1 Spar Element

Reconsidering the elastic bar or spar element of Chapter 2 and recalling that the bar is a constant strain (therefore, constant stress) element, the applicable equilibrium equation is obtained using Equations 2.29 and 2.30 as

$$\frac{d\sigma_x}{dx} = \frac{d}{dx}(E\varepsilon_x) = E \frac{d^2u(x)}{dx^2} = 0 \quad (5.31)$$

where we assume constant elastic modulus. Denoting element length by L , the displacement field is discretized by Equation 2.17:

$$u(x) = u_1N_1(x) + u_2N_2(x) = u_1\left(1 - \frac{x}{L}\right) + u_2\frac{x}{L} \quad (5.32)$$

5.4 Application of Galerkin's Method to Structural Elements

149

And, since the domain of interest is the volume of the element, the Galerkin residual equations become

$$\iiint_V N_i(x) \left(E \frac{d^2 u}{dx^2} \right) dV = \int_0^L N_i \left(E \frac{d^2 u}{dx^2} \right) A dx = 0 \quad i = 1, 2 \quad (5.33)$$

where $dV = A dx$ and A is the constant cross-sectional area of the element. Integrating by parts and rearranging, we obtain

$$AE \int_0^L \frac{dN_i}{dx} \frac{du}{dx} dx = \left[N_i AE \frac{du}{dx} \right]_0^L \quad (5.34)$$

which, utilizing Equation 5.32, becomes

$$AE \int_0^L \frac{dN_1}{dx} \frac{d}{dx} (u_1 N_1 + u_2 N_2) dx = -AE \frac{du}{dx} \Big|_{x=0} = -AE \epsilon|_{x=0} = -A\sigma|_{x=0} \quad (5.35a)$$

$$AE \int_0^L \frac{dN_2}{dx} \frac{d}{dx} (u_1 N_1 + u_2 N_2) dx = AE \frac{du}{dx} \Big|_{x=L} = AE \epsilon|_{x=L} = A\sigma_{x=L} \quad (5.35b)$$

From the right sides of Equation 5.35, we observe that, for the bar element, the gradient boundary condition simply represents the applied nodal force since $\sigma A = F$.

Equation 5.35 is readily combined into matrix form as

$$AE \int_0^L \begin{bmatrix} \frac{dN_1}{dx} & \frac{dN_1}{dx} & \frac{dN_1}{dx} & \frac{dN_2}{dx} \\ \frac{dN_1}{dx} & \frac{dN_2}{dx} & \frac{dN_2}{dx} & \frac{dN_2}{dx} \end{bmatrix} dx \begin{Bmatrix} u_1 \\ u_2 \end{Bmatrix} = \begin{Bmatrix} F_1 \\ F_2 \end{Bmatrix} \quad (5.36)$$

where the individual terms of the matrix are integrated independently.

Carrying out the indicated differentiations and integrations, we obtain

$$\frac{AE}{L} \begin{bmatrix} 1 & -1 \\ -1 & 1 \end{bmatrix} \begin{Bmatrix} u_1 \\ u_2 \end{Bmatrix} = \begin{Bmatrix} F_1 \\ F_2 \end{Bmatrix} \quad (5.37)$$

which is the same result as obtained in Chapter 2 for the bar element. This simply illustrates the equivalence of Galerkin's method and the methods of equilibrium and energy (Castigliano) used earlier for the bar element.

5.4.2 Beam Element

Application of the Galerkin method to the beam element begins with consideration of the equilibrium conditions of a differential section taken along the

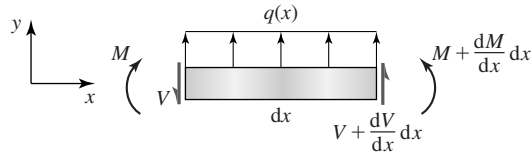


Figure 5.7 Differential section of a loaded beam.

longitudinal axis of a loaded beam as depicted in Figure 5.7 where $q(x)$ represents a distributed load expressed as force per unit length. Whereas q may vary arbitrarily, it is assumed to be constant over a differential length dx . The condition of force equilibrium in the y direction is

$$-V + \left(V + \frac{dV}{dx} dx \right) + q(x) dx = 0 \quad (5.38)$$

from which

$$\frac{dV}{dx} = -q(x) \quad (5.39)$$

Moment equilibrium about a point on the left face is expressed as

$$M + \frac{dM}{dx} dx - M + \left(V + \frac{dV}{dx} dx \right) dx + [q(x) dx] \frac{dx}{2} = 0 \quad (5.40)$$

which (neglecting second-order differentials) gives

$$\frac{dM}{dx} = -V \quad (5.41)$$

Combining Equations 5.39 and 5.41, we obtain

$$\frac{d^2 M}{dx^2} = q(x) \quad (5.42)$$

Recalling, from the elementary strength of materials theory, the *flexure formula* corresponding to the sign conventions of Figure 5.7 is

$$M = EI_z \frac{d^2 v}{dx^2} \quad (5.43)$$

(where in keeping with the notation of Chapter 4, v represents displacement in the y direction), which in combination with Equation 5.42 provides the governing equation for beam flexure as

$$\frac{d^2}{dx^2} \left(EI_z \frac{d^2 v}{dx^2} \right) = q(x) \quad (5.44)$$

5.4 Application of Galerkin's Method to Structural Elements

151

Galerkin's finite element method is applied by taking the displacement solution in the form

$$v(x) = N_1(x)v_1 + N_2(x)\theta_1 + N_3(x)v_2 + N_4(x)\theta_2 = \sum_{i=1}^4 N_i(x)\delta_i \quad (5.45)$$

as in Chapter 4, using the interpolation functions of Equation 4.26. Therefore, the element residual equations are

$$\int_{x_1}^{x_2} N_i(x) \left[\frac{d^2}{dx^2} \left(EI_z \frac{d^2 v}{dx^2} \right) - q(x) \right] dx = 0 \quad i = 1, 4 \quad (5.46)$$

Integrating the derivative term by parts and assuming a constant EI_z , we obtain

$$N_i(x) EI_z \frac{d^3 v}{dx^3} \Big|_{x_1}^{x_2} - EI_z \int_{x_1}^{x_2} \frac{dN_i}{dx} \frac{d^3 v}{dx^3} dx - \int_{x_1}^{x_2} N_i q(x) dx = 0 \quad i = 1, 4 \quad (5.47)$$

and since

$$V = -\frac{dM}{dx} = -\frac{d}{dx} \left(EI_z \frac{d^2 v}{dx^2} \right) = -EI_z \frac{d^3 v}{dx^3} \quad (5.48)$$

we observe that the first term of Equation 5.47 represents the shear force conditions at the element nodes. Integrating again by parts and rearranging gives

$$\begin{aligned} EI_z \int_{x_1}^{x_2} \frac{d^2 N_i}{dx^2} \frac{d^2 v}{dx^2} dx &= \int_{x_1}^{x_2} N_i q(x) dx - N_i EI_z \frac{d^3 v}{dx^3} \Big|_{x_1}^{x_2} \\ &+ \frac{dN_i}{dx} EI_z \frac{d^2 v}{dx^2} \Big|_{x_1}^{x_2} \quad i = 1, 4 \end{aligned} \quad (5.49)$$

and, per Equation 5.43, the last term on the right introduces the moment conditions at the element boundaries. Integration by parts was performed twice in the preceding development for reasons similar to those mentioned in the context of the bar element. By so doing, the order of the two derivative terms appearing in the first integral in Equation 5.49 are the same, and the resulting stiffness matrix is thus symmetric, and the shear forces and bending moments at element nodes now explicitly appear in the element equations.

Equation 5.49 can be written in the matrix form $[k]\{\delta\} = \{F\}$ where the terms of the stiffness matrix are defined by

$$k_{ij} = EI_z \int_{x_1}^{x_2} \frac{d^2 N_i}{dx^2} \frac{d^2 N_j}{dx^2} dx \quad i, j = 1, 4 \quad (5.50)$$

which is identical to results previously obtained by other methods. The terms of the element force vector are defined by

$$F_i = \int_{x_1}^{x_2} N_i q(x) dx - N_i EI_z \left. \frac{d^3 v}{dx^3} \right|_{x_1}^{x_2} + \left. \frac{dN_i}{dx} EI_z \frac{d^2 v}{dx^2} \right|_{x_1}^{x_2} \quad i = 1, 4 \quad (5.51a)$$

or, using Equations 5.43 and 5.48,

$$F_i = \int_{x_1}^{x_2} N_i q(x) dx + N_i V(x) \Big|_{x_1}^{x_2} + \left. \frac{dN_i}{dx} M(x) \right|_{x_1}^{x_2} \quad i = 1, 4 \quad (5.51b)$$

where the integral term represents the equivalent nodal forces and moments produced by the distributed load. If $q(x) = q = \text{constant}$ (positive upward), substitution of the interpolation functions into Equation 5.51 gives the element nodal force vector as

$$\{F\} = \begin{Bmatrix} \frac{qL}{2} - V_1 \\ \frac{qL^2}{12} - M_1 \\ \frac{qL}{2} + V_2 \\ -\frac{qL^2}{12} + M_2 \end{Bmatrix} \quad (5.52)$$

Where two beam elements share a common node, one of two possibilities occurs regarding the shear and moment conditions:

1. If no external force or moment is applied at the node, the shear and moment values of Equation 5.52 for the adjacent elements are equal and opposite, cancelling in the assembly step.
2. If a concentrated force is applied at the node, the sum of the boundary shear forces for the adjacent elements must equal the applied force.

Similarly, if a concentrated moment is applied, the sum of the boundary bending moments must equal the applied moment. Equation 5.52 shows that the effects of a distributed load are allocated to the element nodes. Finite element software packages most often allow the user to specify a “pressure” on the transverse face of the beam. The specified pressure actually represents a distributed load and is converted to the nodal equivalent loads in the software.

5.5 ONE-DIMENSIONAL HEAT CONDUCTION

Application of the Galerkin finite method to the problem of one-dimensional, steady-state heat conduction is developed with reference to Figure 5.8a, which depicts a solid body undergoing heat conduction in the direction of the x axis

5.5 One-Dimensional Heat Conduction

153

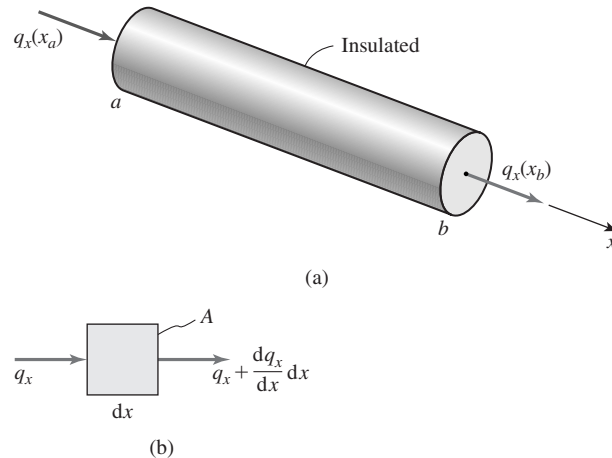


Figure 5.8 Insulated body in one-dimensional heat conduction.

only. Surfaces of the body normal to the x axis are assumed to be perfectly insulated, so that no heat loss occurs through these surfaces. Figure 5.8b shows the control volume of differential length dx of the body, which is assumed to be of constant cross-sectional area and uniform material properties. The principle of conservation of energy is applied to obtain the governing equation as follows:

$$E_{\text{in}} + E_{\text{generated}} = E_{\text{increase}} + E_{\text{out}} \quad (5.53)$$

Equation 5.53 states that the energy entering the control volume plus energy generated internally by any heat source present must equal the increase in internal energy plus the energy leaving the control volume. For the volume of Figure 5.8b, during a time interval dt , Equation 5.53 is expressed as

$$q_x A dt + Q A dx dt = \Delta U + \left(q_x + \frac{\partial q_x}{\partial x} dx \right) A dt \quad (5.54)$$

where

q_x = heat flux across boundary (W/m^2 , $\text{Btu}/\text{hr}\cdot\text{ft}^2$);

Q = internal heat generation rate (W/m^3 , $\text{Btu}/\text{hr}\cdot\text{ft}^3$);

U = internal energy (W , Btu).

The last term on the right side of Equation 5.54 is a two-term Taylor series expansion of $q_x(x, t)$ evaluated at $x + dx$. Note the use of partial differentiation, since for now, we assume that the dependent variables vary with time as well as spatial position.

The heat flux is expressed in terms of the temperature gradient via Fourier's law of heat conduction:

$$q_x = -k_x \frac{\partial T}{\partial x} \quad (5.55)$$

where k_x = material thermal conductivity in the x direction (W/m-°C, Btu/hr-ft-°F) and $T = T(x, t)$ is temperature. The increase in internal energy is

$$\Delta U = \rho c A dx dT \quad (5.56)$$

where

c = material specific heat (J/kg-°C, Btu/slug-°F);

ρ = material density (kg/m³, slug/ft³).

Substituting Equations 5.55 and 5.56 into 5.54 gives

$$Q A dx dt = \rho c A dx dT + \frac{\partial}{\partial x} \left(-k_x \frac{\partial T}{\partial x} \right) A dx dt \quad (5.57)$$

Assuming that the thermal conductivity is constant, Equation 5.57 becomes

$$Q = \rho c \frac{\partial T}{\partial t} - k_x \frac{\partial^2 T}{\partial x^2} \quad (5.58)$$

For now we are interested only in steady-state heat conduction and for the steady state $\partial T/\partial t = 0$, so the governing equation for steady-state, one-dimensional conduction is obtained as

$$k_x \frac{d^2 T}{dx^2} + Q = 0 \quad (5.59)$$

Next, the Galerkin finite element method is applied to Equation 5.59 to obtain the element equations. A two-node element with linear interpolation functions is used and the temperature distribution in an element expressed as

$$T(x) = N_1(x)T_1 + N_2(x)T_2 \quad (5.60)$$

where T_1 and T_2 are the temperatures at nodes 1 and 2, which define the element, and the interpolation functions N_1 and N_2 are given by Equation 5.20. As in previous examples, substitution of the discretized solution (5.60) into the governing differential Equation 5.55 results in the residual integrals:

$$\int_{x_1}^{x_2} \left(k_x \frac{d^2 T}{dx^2} + Q \right) N_i(x) A dx = 0 \quad i = 1, 2 \quad (5.61)$$

where we note that the integration is over the volume of the element, that is, the domain of the problem, with $dV = A dx$.

Integrating the first term by parts (for reasons already discussed) yields

$$k_x A N_i(x) \frac{dT}{dx} \Big|_{x_1}^{x_2} - k_x A \int_{x_1}^{x_2} \frac{dN_i}{dx} \frac{dT}{dx} dx + A \int_{x_1}^{x_2} Q N_i(x) dx = 0 \quad i = 1, 2 \quad (5.62)$$

Evaluating the first term at the limits as indicated, substituting Equation 5.60 into the second term, and rearranging, Equation 5.58 results in the two equations

$$k_x A \int_{x_1}^{x_2} \frac{dN_1}{dx} \left(\frac{dN_1}{dx} T_1 + \frac{dN_2}{dx} T_2 \right) dx = A \int_{x_1}^{x_2} Q N_1 dx - k_x A \left. \frac{dT}{dx} \right|_{x_1} \quad (5.63)$$

$$k_x A \int_{x_1}^{x_2} \frac{dN_2}{dx} \left(\frac{dN_1}{dx} T_1 + \frac{dN_2}{dx} T_2 \right) dx = A \int_{x_1}^{x_2} Q N_2 dx + k_x A \left. \frac{dT}{dx} \right|_{x_2} \quad (5.64)$$

Equations 5.63 and 5.64 are of the form

$$[k]\{T\} = \{f_Q\} + \{f_g\} \quad (5.65)$$

where $[k]$ is the element conductance (“stiffness”) matrix having terms defined by

$$k_{lm} = k_x A \int_{x_1}^{x_2} \frac{dN_l}{dx} \frac{dN_m}{dx} dx \quad l, m = 1, 2 \quad (5.66)$$

The first term on the right-hand side of Equation 5.65 is the nodal “force” vector arising from internal heat generation with values defined by

$$\begin{aligned} f_{Q1} &= A \int_{x_1}^{x_2} Q N_1 dx \\ f_{Q2} &= A \int_{x_1}^{x_2} Q N_2 dx \end{aligned} \quad (5.67)$$

and vector $\{f_g\}$ represents the gradient boundary conditions at the element nodes. Performing the integrations indicated in Equation 5.66 gives the conductance matrix as

$$[k] = \frac{k_x A}{L} \begin{bmatrix} 1 & -1 \\ -1 & 1 \end{bmatrix} \quad (5.68)$$

while for constant internal heat generation Q , Equation 5.67 results in the nodal vector

$$\{f_Q\} = \begin{Bmatrix} \frac{QAL}{2} \\ \frac{QAL}{2} \end{Bmatrix} \quad (5.69)$$

The element gradient boundary conditions, using Equation 5.55, described by

$$\{f_g\} = k_x A \left\{ \begin{array}{c} -\frac{dT}{dx} \Big|_{x_1} \\ \frac{dT}{dx} \Big|_{x_2} \end{array} \right\} = A \left\{ \begin{array}{c} q|_{x_1} \\ -q|_{x_2} \end{array} \right\} \quad (5.70)$$

are such that, at internal nodes where elements are joined, the values for the adjacent elements are equal and opposite, cancelling mathematically. At external nodes, that is, at the ends of the body being analyzed, the gradient values may be specified as known heat flux input and output or computed if the specified boundary condition is a temperature. In the latter case, the gradient computation is analogous to computing reaction forces in a structural model. Also note that the area is a common term in the preceding equations and, since it is assumed to be constant over the element length, could be ignored in each term. However, as will be seen in later chapters when we account for other heat transfer conditions, the area should remain in the equations as defined. These concepts are illustrated in the following example.

EXAMPLE 5.6

The circular rod depicted in Figure 5.9 has an outside diameter of 60 mm, length of 1 m, and is perfectly insulated on its circumference. The left half of the cylinder is aluminum, for which $k_x = 200 \text{ W/m}\cdot^\circ\text{C}$ and the right half is copper having $k_x = 389 \text{ W/m}\cdot^\circ\text{C}$. The extreme right end of the cylinder is maintained at a temperature of 80°C , while the left end is subjected to a heat input rate 4000 W/m^2 . Using four equal-length elements, determine the steady-state temperature distribution in the cylinder.

■ Solution

The elements and nodes are chosen as shown in the bottom of Figure 5.9. For aluminum elements 1 and 2, the conductance matrices are

$$[k_{al}] = \frac{k_x A}{L} \begin{bmatrix} 1 & -1 \\ -1 & 1 \end{bmatrix} = \frac{200(\pi/4)(0.06)^2}{0.25} \begin{bmatrix} 1 & -1 \\ -1 & 1 \end{bmatrix} = 2.26 \begin{bmatrix} 1 & -1 \\ -1 & 1 \end{bmatrix} \text{ W}^\circ\text{C}$$

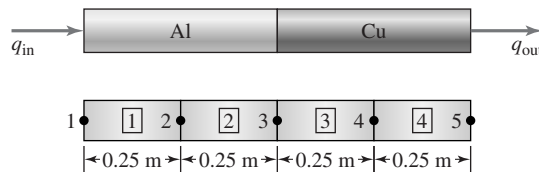


Figure 5.9 Circular rod of Example 5.6.

5.5 One-Dimensional Heat Conduction

157

while, for copper elements 3 and 4,

$$[k_{cu}] = \frac{k_x A}{L} \begin{bmatrix} 1 & -1 \\ -1 & 1 \end{bmatrix} = \frac{389(\pi/4)(0.06)^2}{0.25} \begin{bmatrix} 1 & -1 \\ -1 & 1 \end{bmatrix} = 4.40 \begin{bmatrix} 1 & -1 \\ -1 & 1 \end{bmatrix} \text{ W/}^\circ\text{C}$$

Applying the end conditions $T_5 = 80^\circ\text{C}$ and $q_1 = 4000 \text{ W/m}^2$, the assembled system equations are

$$\begin{bmatrix} 2.26 & -2.26 & 0 & 0 & 0 \\ -2.26 & 4.52 & -2.26 & 0 & 0 \\ 0 & -2.26 & 6.66 & -4.40 & 0 \\ 0 & 0 & -4.40 & 8.80 & -4.40 \\ 0 & 0 & 0 & -4.40 & 4.40 \end{bmatrix} \begin{Bmatrix} T_1 \\ T_2 \\ T_3 \\ T_4 \\ 80 \end{Bmatrix} = \begin{Bmatrix} 4000 \\ 0 \\ 0 \\ 0 \\ -q_5 \end{Bmatrix} \frac{\pi(0.06)^2}{4}$$

$$= \begin{Bmatrix} 11.31 \\ 0 \\ 0 \\ 0 \\ -0.0028q_5 \end{Bmatrix}$$

Accounting for the known temperature at node 5, the first four equations can be written as

$$\begin{bmatrix} 2.26 & -2.26 & 0 & 0 \\ -2.26 & 4.52 & -2.26 & 0 \\ 0 & -2.26 & 6.66 & -4.40 \\ 0 & 0 & -4.40 & 8.80 \end{bmatrix} \begin{Bmatrix} T_1 \\ T_2 \\ T_3 \\ T_4 \end{Bmatrix} = \begin{Bmatrix} 11.31 \\ 0 \\ 0 \\ 352.0 \end{Bmatrix}$$

The system of equations is triangularized (used here simply to illustrate another solution method) by the following steps. Replace the second equation by the sum of the first and second to obtain

$$\begin{bmatrix} 2.26 & -2.26 & 0 & 0 \\ 0 & 2.26 & -2.26 & 0 \\ 0 & -2.26 & 6.66 & -4.40 \\ 0 & 0 & -4.40 & 8.80 \end{bmatrix} \begin{Bmatrix} T_1 \\ T_2 \\ T_3 \\ T_4 \end{Bmatrix} = \begin{Bmatrix} 11.31 \\ 11.31 \\ 0 \\ 352.0 \end{Bmatrix}$$

Next, replace the third equation by the sum of the second and third

$$\begin{bmatrix} 2.26 & -2.26 & 0 & 0 \\ 0 & 2.26 & -2.26 & 0 \\ 0 & 0 & 4.40 & -4.40 \\ 0 & 0 & -4.40 & 8.80 \end{bmatrix} \begin{Bmatrix} T_1 \\ T_2 \\ T_3 \\ T_4 \end{Bmatrix} = \begin{Bmatrix} 11.31 \\ 11.31 \\ 11.31 \\ 352.0 \end{Bmatrix}$$

Finally, replace the fourth with the sum of the third and fourth to obtain

$$\begin{bmatrix} 2.26 & -2.26 & 0 & 0 \\ 0 & 2.26 & -2.26 & 0 \\ 0 & 0 & 4.40 & -4.40 \\ 0 & 0 & 0 & 4.40 \end{bmatrix} \begin{Bmatrix} T_1 \\ T_2 \\ T_3 \\ T_4 \end{Bmatrix} = \begin{Bmatrix} 11.31 \\ 11.31 \\ 11.31 \\ 363.31 \end{Bmatrix}$$

The triangularized system then gives the nodal temperatures in succession as

$$T_4 = 82.57^\circ\text{C}$$

$$T_3 = 85.15^\circ\text{C}$$

$$T_2 = 90.14^\circ\text{C}$$

$$T_1 = 95.15^\circ\text{C}$$

The fifth equation of the system is

$$-4.40T_4 + 4.40(80) = -0.0028q_5$$

which, on substitution of the computed value of T_4 , results in

$$q_5 = 4038.6 \text{ W/m}^2$$

As this is assumed to be a steady-state situation, the heat flow from the right-hand end of the cylinder, node 5, should be exactly equal to the inflow at the left end. The discrepancy in this case is due simply to round-off error in the computations, which were accomplished via a hand calculator for this example. If the values are computed to “machine accuracy” and no intermediate rounding is used, the value of the heat flow at node 5 is found to be exactly 4000 W/m^2 . In fact, it can be shown that, for this example, the finite element solution is exact.

5.6 CLOSING REMARKS

The method of weighted residuals, especially the embodiment of the Galerkin finite element method, is a powerful mathematical tool that provides a technique for formulating a finite element solution approach to practically any problem for which the governing differential equation and boundary conditions can be written. For situations in which a principle such as the first theorem of Castigliano or the principle of minimum potential energy is applicable, the Galerkin method produces exactly the same formulation. In subsequent chapters, the Galerkin method is extended to two- and three-dimensional cases of structural analysis, heat transfer, and fluid flow. Prior to examining specific applications, we examine, in the next chapter, the general requirements of interpolation functions for the formulation of a finite element approach to any type of problem.

REFERENCES

1. Stasa, F. L. *Applied Element Analysis for Engineers*. New York: Holt, Rinehart, and Winston, 1985.
2. Burnett, D. S. *Finite Element Analysis*. Reading, MA: Addison-Wesley, 1987.

PROBLEMS

- 5.1 Verify the integration and subsequent determination of c_1 in Example 5.1.
- 5.2 Using the procedure discussed in Example 5.4, determine three trial functions for the problem of Example 5.1.
- 5.3 It has been stated that the trial functions used in the method of weighted residuals generally satisfy the physics of the problem described by the differential equation to be solved. Why does the trial function assumed in Example 5.3 not satisfy the physics of the problem?
- 5.4 For each of the following differential equations and stated boundary conditions, obtain a one-term solution using Galerkin's method of weighted residuals and the specified trial function. In each case, compare the one-term solution to the exact solution.

a.

$$\frac{d^2y}{dx^2} + y = 2x \quad 0 \leq x \leq 1$$
$$y(0) = 0$$
$$y(1) = 0$$
$$N_1(x) = x(1 - x^2)$$

b.

$$\frac{d^2y}{dx^2} + y = 2 \sin x \quad 0 \leq x \leq 1$$
$$y(0) = 0$$
$$y(1) = 0$$
$$N_1(x) = \sin \pi x$$

c.

$$\frac{dy}{dx} + y^2 = 4x \quad 0 \leq x \leq 1$$
$$y(0) = 0$$
$$y(1) = 0$$
$$N_1(x) = x^2(1 - x)$$

d.

$$\frac{dy}{dx} - y = 2 \quad 0 \leq x \leq 10$$
$$y(0) = 0$$
$$y(10) = 0$$
$$N_1(x) = x^2(10 - x)^2$$

e.

$$\frac{d^2y}{dx^2} - 3 \frac{dy}{dx} + y = x \quad 0 \leq x \leq 1$$
$$y(0) = 0$$
$$y(1) = 0$$
$$N_1(x) = x(x - 1)^2$$

- 5.5(a)–(e)** For each of the differential equations given in Problem 5.4, use the method of Example 5.4 to determine the trial functions for a two-term approximate solution using Galerkin's method of weighted residuals.
- 5.6** For the four-element solution of Example 5.5, verify the correctness of the assembled system equations. Apply the boundary conditions and solve the reduced system of equations. Compute the first derivatives at each node of each element. Are the derivatives continuous across the nodal connections between elements?
- 5.7** Each of the following differential equations represents a physical problem, as indicated. For each case given, formulate the finite element equations (that is, determine the stiffness matrix and load vectors) using Galerkin's finite element method for a two-node element of length L with the interpolation functions

$$N_1(x) = 1 - \frac{x}{L} \quad N_2(x) = \frac{x}{L}$$

- a. One-dimensional heat conduction with linearly varying internal heat generation

$$k_x A \frac{d^2 T}{dx^2} + Q_0 A x = 0$$

where k_x , Q_0 , and A are constants.

- b. One-dimensional heat conduction with surface convection

$$k_x A \frac{d^2 T}{dx^2} - h P T = h P T_a$$

where k_x , Q_0 , A , h , P , and T_a are constants.

- c. Torsion of an elastic circular cylinder

$$JG \frac{d^2 \theta}{dx^2} = 0$$

where J and G are constants.

- 5.8** A two-dimensional beam is subjected to a linearly varying distributed load given by $q(x) = q_0 x$, $0 \leq x \leq L$, where L is total beam length and q_0 is a constant. For a finite element located between nodes at arbitrary positions x_i and x_j so that $x_i < x_j$ and $L_e = x_j - x_i$ is the element length, determine the components of the force vector at the element nodes using Galerkin's finite element method. (Note that this is simply the last term in Equation 5.47 adjusted appropriately for element location.)
- 5.9** Repeat Problem 5.8 for a quadratically distributed load $q(x) = q_0 x^2$.
- 5.10** Considering the results of either Problem 5.8 or 5.9, are the distributed loads allocated to element nodes on the basis of static equilibrium? If your answer is no, why not and how is the distribution made?
- 5.11** A tapered cylinder that is perfectly insulated on its periphery is held at constant temperature 212°F at $x = 0$ and at temperature 80°F at $x = 4$ in. The cylinder diameter varies from 2 in. at $x = 0$ to 1 in. at $x = L = 4$ in. per Figure P5.11. The conductance coefficient is $k_x = 64 \text{ Btu/hr-ft-}^\circ\text{F}$. Formulate a four-element finite element model of this problem and solve for the nodal temperatures and

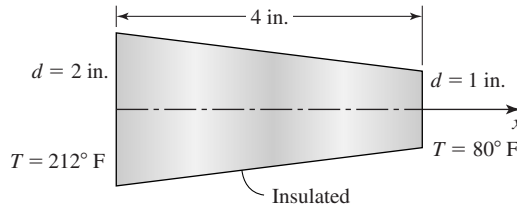


Figure P5.11

the heat flux values at the element boundaries. Use Galerkin's finite element method.

- 5.12** Consider a tapered uniaxial tension-compression member subjected to an axial load as shown in Figure P5.12. The cross-sectional area varies as $A = A_0(1 - x/2L)$, where L is the length of the member and A_0 is the area at $x = 0$. Given the governing equation

$$E \frac{d^2 u}{dx^2} = 0$$

as in Equation 5.31, obtain the Galerkin finite element equations per Equation 5.33.

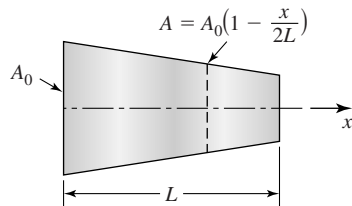
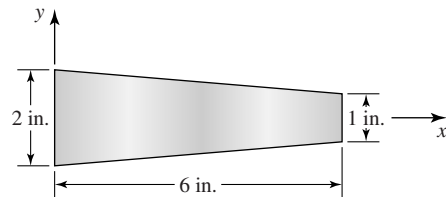


Figure P5.12

- 5.13** Many finite element software systems have provision for a tapered beam element. Beginning with Equation 5.46, while noting that I_z is not constant, develop the finite element equations for a tapered beam element.
- 5.14** Use the results of Problem 5.13 to determine the stiffness matrix for the tapered beam element shown in Figure P5.14.



Uniform thickness $t = 0.75$ in.
 $E = 30 \times 10^6$ lb/in.²

Figure P5.14

5.15 Consider a two-dimensional problem governed by the differential equation

$$\frac{\partial^2 \phi}{\partial x^2} + \frac{\partial^2 \phi}{\partial y^2} = 0$$

(this is Laplace's equation) in a specified two-dimensional domain with specified boundary conditions. How would you apply the Galerkin finite element method to this problem?

5.16 Reconsider Equation 5.24. If we do *not* integrate by parts and simply substitute the discretized solution form, what is the result? Explain.

5.17 Given the differential equation

$$\frac{d^2 y}{dx^2} + 4y = x$$

Assume the solution as a power series

$$y(x) = \sum_{i=0}^n a_i x^i = a_0 + a_1 x + a_2 x^2 + \dots$$

and obtain the relations governing the coefficients of the power series solution. How does this procedure compare to the Galerkin method?

5.18 The differential equation

$$\frac{dy}{dx} + y = 3 \quad 0 \leq x \leq 1$$

has the exact solution

$$y(x) = 3 + C e^{-x}$$

where $C = \text{constant}$. Assume that the domain is $0 \leq x \leq 1$ and the specified boundary condition is $y(0) = 0$. Show that, if the procedure of Example 5.4 is followed, the exact solution is obtained.

CHAPTER

6

Interpolation Functions for General Element Formulation

6.1 INTRODUCTION

The structural elements introduced in the previous chapters were formulated on the basis of known principles from elementary strength of materials theory. We have also shown, by example, how Galerkin's method can be applied to a heat conduction problem. This chapter examines the requirements for interpolation functions in terms of solution accuracy and convergence of a finite element analysis to the exact solution of a general field problem. Interpolation functions for various common element shapes in one, two, and three dimensions are developed, and these functions are used to formulate finite element equations for various types of physical problems in the remainder of the text.

With the exception of the beam element, all the interpolation functions discussed in this chapter are applicable to finite elements used to obtain solutions to problems that are said to be C^0 -continuous. This terminology means that, across element boundaries, only the zeroth-order derivatives of the field variable (i.e., the field variable itself) are continuous. On the other hand, the beam element formulation is such that the element exhibits C^1 -continuity, since the first derivative of the transverse displacement (i.e., slope) is continuous across element boundaries, as discussed previously and repeated later for emphasis. In general, in a problem having C^n -continuity, derivatives of the field variable up to and including n th-order derivatives are continuous across element boundaries.

6.2 COMPATIBILITY AND COMPLETENESS REQUIREMENTS

The line elements (spring, truss, beam) illustrate the general procedures used to formulate and solve a finite element problem and are quite useful in analyzing truss and frame structures. Such structures, however, tend to be well defined in terms of the number and type of elements used. In most engineering problems, the domain of interest is a continuous solid body, often of irregular shape, in which the behavior of one or more field variables is governed by one or more partial differential equations. The objective of the finite element method is to discretize the domain into a number of finite elements for which the governing equations are algebraic equations. Solution of the resulting system of algebraic equations then gives an *approximate* solution to the problem. As with any approximate technique, the question, How accurate is the solution? must be addressed.

In finite element analysis, solution accuracy is judged in terms of convergence as the element “mesh” is refined. There are two major methods of mesh refinement. In the first, known as *h-refinement*, mesh refinement refers to the process of increasing the number of elements used to model a given domain, consequently, reducing individual element size. In the second method, *p-refinement*, element size is unchanged but the order of the polynomials used as interpolation functions is increased. The objective of mesh refinement in either method is to obtain sequential solutions that exhibit asymptotic convergence to values representing the exact solution. While the theory is beyond the scope of this book, mathematical proofs of convergence of finite element solutions to correct solutions are based on a specific, regular mesh refinement procedure defined in [1]. Although the proofs are based on regular meshes of elements, irregular or unstructured meshes (such as in Figure 1.7) can give very good results. In fact, use of unstructured meshes is more often the case, since (1) the geometries being modeled are most often irregular and (2) the automeshing features of most finite element software packages produce irregular meshes.

An example illustrating regular *h-refinement* as well as solution convergence is shown in Figure 6.1a, which depicts a rectangular elastic plate of uniform thickness fixed on one edge and subjected to a concentrated load on one corner.

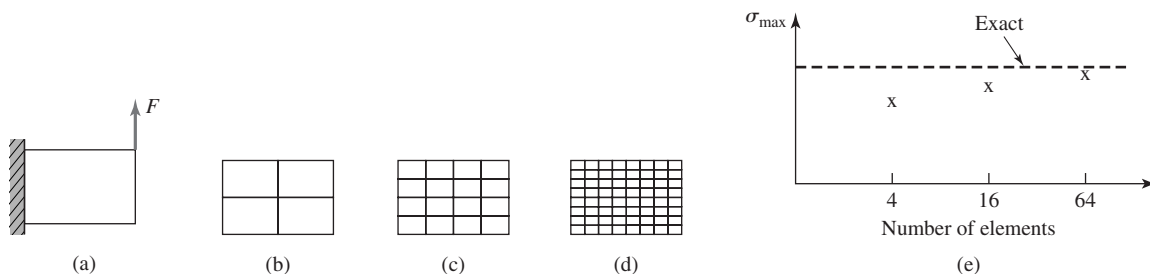


Figure 6.1 Example showing convergence as element mesh is refined.

This problem is modeled using rectangular plane stress elements (Chapter 9) and three meshes used in sequence, as shown (Figure 6.1b–6.1d). Solution convergence is depicted in Figure 6.1e in terms of maximum normal stress in the x direction. For this example, the exact solution is taken to be the maximum bending stress computed using elementary beam theory. The true exact solution is the plane stress solution from the theory of elasticity. However, the maximum normal stress is not appreciably changed in the elasticity solution.

The need for convergence during regular mesh refinement is rather clear. If convergence is not obtained, the engineer using the finite element method has absolutely no indication whether the results are indicative of a meaningful approximation to the correct solution. For a general field problem in which the field variable of interest is expressed on an element basis in the discretized form

$$\phi^{(e)}(x, y, z) = \sum_{i=1}^M N_i(x, y, z) \phi_i \quad (6.1)$$

where M is the number of element degrees of freedom, the interpolation functions must satisfy two primary conditions to ensure convergence during mesh refinement: the *compatibility* and *completeness* requirements, described as follows.

6.2.1 Compatibility

Along element boundaries, the field variable and its partial derivatives up to one order less than the highest-order derivative appearing in the integral formulation of the element equations must be continuous. Given the discretized representation of Equation 6.1, it follows that the interpolation functions must meet this condition, since these functions determine the spatial variation of the field variable.

Recalling the application of Galerkin's method to the formulation of the truss element equations, the first derivative of the displacement appears in Equation 5.34. Therefore, the displacement must be continuous across element boundaries, but none of the displacement derivatives is required to be continuous across such boundaries. Indeed, as observed previously, the truss element is a constant strain element, so the first derivative is, in general, discontinuous at the boundaries. Similarly, the beam element formulation, Equation 5.49, includes the second derivative of displacement, and compatibility requires continuity of both the displacement and the slope (first derivative) at the element boundaries.

In addition to satisfying the criteria for convergence, the compatibility condition can be given a physical meaning as well. In structural problems, the requirement of displacement continuity along element boundaries ensures that no gaps or voids develop in the structure as a result of modeling procedure. Similarly the requirement of slope continuity for the beam element ensures that no "kinks" are developed in the deformed structure. In heat transfer problems, the compatibility requirement prevents the physically unacceptable possibility of jump discontinuities in temperature distribution.

6.2.2 Completeness

In the limit as element size shrinks to zero in mesh refinement, the field variable and its partial derivatives up to, and including, the highest-order derivative appearing in the integral formulation must be capable of assuming constant values. Again, because of the discretization, the completeness requirement is directly applicable to the interpolation functions.

The completeness requirement ensures that a displacement field within a structural element can take on a constant value, representing rigid body motion, for example. Similarly, constant slope of a beam element represents rigid body rotation, while a state of constant temperature in a thermal element corresponds to no heat flux through the element. In addition to the rigid body motion consideration, the completeness requirement also ensures the possibility of constant values of (at least) first derivatives. This feature assures that a finite element is capable of constant strain, constant heat flow, or constant fluid velocity, for example.

The foregoing discussion of convergence and requirements for interpolation functions is by no means rigorous nor greatly detailed. References [1–5] lead the interested reader to an in-depth study of the theoretical details. The purpose here is to present the requirements and demonstrate application of those requirements to development of appropriate interpolation functions to a number of commonly used elements of various shape and complexity.

6.3 POLYNOMIAL FORMS: ONE-DIMENSIONAL ELEMENTS

As illustrated by the methods and examples of Chapter 5, formulation of finite element characteristics requires differentiation and integration of the interpolation functions in various forms. Owing to the simplicity with which polynomial functions can be differentiated and integrated, polynomials are the most commonly used interpolation functions. Recalling the truss element development of Chapter 2, the displacement field is expressed via the first-degree polynomial

$$u(x) = a_0 + a_1x \quad (6.2)$$

In terms of nodal displacement, Equation 6.2 is determined to be equivalent to

$$u(x) = \left(1 - \frac{x}{L}\right)u_1 + \frac{x}{L}u_2 \quad (6.3)$$

The coefficients a_0 and a_1 are obtained by applying the nodal conditions $u(x = 0) = u_1$ and $u(x = L) = u_2$. Then, collecting coefficients of the nodal displacements, the interpolation functions are obtained as

$$N_1 = 1 - \frac{x}{L} \quad N_2 = \frac{x}{L} \quad (6.4)$$

Equation 6.3 shows that, if $u_1 = u_2$, the element displacement field corresponds to rigid body motion and no straining of the element occurs. The first

derivative of Equation 6.3 with respect to x yields a constant value that, as we already know, represents the element axial strain. Hence, the truss element satisfies the completeness requirement, since both displacement and strain can take on constant values regardless of element size. Also note that the truss element satisfies the compatibility requirement automatically, since only displacement is involved, and displacement compatibility is enforced at the nodal connections via the system assembly procedure.

In light of the completeness requirement, we can now see that choice of the linear polynomial representation of the displacement field, Equation 6.2, was not arbitrary. Inclusion of the constant term a_0 ensures the possibility of rigid body motion, while the first-order term provides for a constant first derivative. Further, *only* two terms can be included in the representation, as only two boundary conditions have to be satisfied, corresponding to the two element degrees of freedom. Conversely, if the linear term were to be replaced by a quadratic term a_2x^2 , for example, the coefficients could still be obtained to mathematically satisfy the nodal displacement conditions, but constant first derivative (other than a value of zero) could not be obtained under any circumstances.

Determination of the interpolation functions for the truss element, as just described, is quite simple. Nevertheless, the procedure is typical of that used to determine the interpolation functions for any element in which polynomials are utilized. Prior to examination of more complex elements, we revisit the development of the beam element interpolation functions with specific reference to the compatibility and completeness requirements. Recalling from Chapter 5 that the integral formulation (via Galerkin's method, Equation 5.49 for the two-dimensional beam element includes the second derivative of displacement, the compatibility condition requires that both displacement and the first derivative of displacement (slope) be continuous at the element boundaries. By including the slopes at element nodes as nodal variables in addition to nodal displacements, the compatibility condition is satisfied via the system assembly procedure. As we have seen, the beam element then has 4 degrees of freedom and the displacement field is represented as the cubic polynomial

$$v(x) = a_0 + a_1x + a_2x^2 + a_3x^3 \quad (6.5)$$

which is ultimately to be expressed in terms of interpolation functions and nodal variables as

$$v(x) = N_1v_1 + N_2\theta_1 + N_3v_2 + N_4\theta_2 = [N_1 \quad N_2 \quad N_3 \quad N_4] \begin{Bmatrix} v_1 \\ \theta_1 \\ v_2 \\ \theta_2 \end{Bmatrix} \quad (6.6)$$

Rewriting Equation 6.5 as the matrix product,

$$v(x) = [1 \quad x \quad x^2 \quad x^3] \begin{Bmatrix} a_0 \\ a_1 \\ a_2 \\ a_3 \end{Bmatrix} \quad (6.7)$$

the nodal conditions

$$\begin{aligned} v(x=0) &= v_1 \\ \left. \frac{dv}{dx} \right|_{x=0} &= \theta_1 \\ v(x=L) &= v_2 \\ \left. \frac{dv}{dx} \right|_{x=L} &= \theta_2 \end{aligned} \quad (6.8)$$

are applied to obtain

$$v_1 = [1 \quad 0 \quad 0 \quad 0] \begin{Bmatrix} a_0 \\ a_1 \\ a_2 \\ a_3 \end{Bmatrix} \quad (6.9)$$

$$\theta_1 = [0 \quad 1 \quad 0 \quad 0] \begin{Bmatrix} a_0 \\ a_1 \\ a_2 \\ a_3 \end{Bmatrix} \quad (6.10)$$

$$v_2 = [1 \quad L \quad L^2 \quad L^3] \begin{Bmatrix} a_0 \\ a_1 \\ a_2 \\ a_3 \end{Bmatrix} \quad (6.11)$$

$$\theta_2 = [0 \quad 1 \quad 2L \quad 3L^2] \begin{Bmatrix} a_0 \\ a_1 \\ a_2 \\ a_3 \end{Bmatrix} \quad (6.12)$$

The last four equations are combined into the equivalent matrix form

$$\begin{Bmatrix} v_1 \\ \theta_1 \\ v_2 \\ \theta_2 \end{Bmatrix} = \begin{bmatrix} 1 & 0 & 0 & 0 \\ 0 & 1 & 0 & 0 \\ 1 & L & L^2 & L^3 \\ 0 & 1 & 2L & 3L^2 \end{bmatrix} \begin{Bmatrix} a_0 \\ a_1 \\ a_2 \\ a_3 \end{Bmatrix} \quad (6.13)$$

The system represented by Equation 6.13 can be solved for the polynomial coefficients by inverting the coefficient matrix to obtain

$$\begin{Bmatrix} a_0 \\ a_1 \\ a_2 \\ a_3 \end{Bmatrix} = \begin{bmatrix} 1 & 0 & 0 & 0 \\ 0 & 1 & 0 & 0 \\ -\frac{3}{L^2} & -\frac{2}{L} & \frac{3}{L^2} & -\frac{1}{L} \\ \frac{2}{L^3} & \frac{1}{L^2} & -\frac{2}{L^3} & \frac{1}{L^2} \end{bmatrix} \begin{Bmatrix} v_1 \\ \theta_1 \\ v_2 \\ \theta_2 \end{Bmatrix} \quad (6.14)$$

The interpolation functions can now be obtained by substituting the coefficients given by Equation 6.14 into Equation 6.5 and collecting coefficients of the nodal variables. However, the following approach is more direct and algebraically simpler. Substitute Equation 6.14 into Equation 6.7 and equate to Equation 6.6 to obtain

$$\begin{aligned}
 v(x) &= [1 \quad x \quad x^2 \quad x^3] \begin{bmatrix} 1 & 0 & 0 & 0 \\ 0 & 1 & 0 & 0 \\ -\frac{3}{L^2} & -\frac{2}{L} & \frac{3}{L^2} & -\frac{1}{L} \\ \frac{2}{L^3} & \frac{1}{L^2} & -\frac{2}{L^3} & \frac{1}{L^2} \end{bmatrix} \begin{Bmatrix} v_1 \\ \theta_1 \\ v_2 \\ \theta_2 \end{Bmatrix} \\
 &= [N_1 \quad N_2 \quad N_3 \quad N_4] \begin{Bmatrix} v_1 \\ \theta_1 \\ v_2 \\ \theta_2 \end{Bmatrix} \quad (6.15)
 \end{aligned}$$

The interpolation functions are

$$[N_1 \quad N_2 \quad N_3 \quad N_4] = [1 \quad x \quad x^2 \quad x^3] \begin{bmatrix} 1 & 0 & 0 & 0 \\ 0 & 1 & 0 & 0 \\ -\frac{3}{L^2} & -\frac{2}{L} & \frac{3}{L^2} & -\frac{1}{L} \\ \frac{2}{L^3} & \frac{1}{L^2} & -\frac{2}{L^3} & \frac{1}{L^2} \end{bmatrix} \quad (6.16)$$

and note that the results of Equation 6.16 are identical to those shown in Equation 4.26.

The reader may wonder why we repeat the development of the beam element interpolation functions. The purpose is twofold: (1) to establish a general procedure for use with polynomial representations of the field variable and (2) to revisit the beam element formulation in terms of compatibility and completeness requirements. The general procedure begins with expressing the field variable as a polynomial of order one fewer than the number of degrees of freedom exhibited by the element. Using the examples of the truss and beam elements, it has been shown that a two-node element may have 2 degrees of freedom, as in the truss element where only displacement continuity is required, or 4 degrees of freedom, as in the beam element where slope continuity is required. Next the nodal (boundary) conditions are applied and the coefficients of the polynomial are computed accordingly. Finally, the polynomial coefficients are substituted into the field variable representation in terms of nodal variables to obtain the explicit form of the interpolation functions.

Examination of the completeness condition for the beam element requires a more-detailed thought process. The polynomial representation of the displacement field is such that only the third derivative is *guaranteed* to have a constant

value, since any lower-order derivative involves the spatial variable. However, if we examine the conditions under which the element undergoes rigid body translation, for example, we find that the nodal forces must be of equal magnitude and the same sense and the applied nodal moments must be zero. Also, for rigid body translation, the slopes at the nodes of the element are zero. In such case, the second derivative of deflection, directly proportional to bending moment, is zero and the shear force, directly related to the third derivative of deflection, is constant. (Simply recall the shear force and bending moment relations from the mechanics of materials theory.) Therefore, the field variable representation as a cubic polynomial allows rigid body translation. In the case of the beam element, we must also verify the possibility of rigid body rotation. This consideration, as well as those of constant bending moment and shear force, is left for end-of-chapter problems.

6.3.1 Higher-Order One-Dimensional Elements

In formulating the truss element and the one-dimensional heat conduction element (Chapter 5), only line elements having a single degree of freedom at each of two nodes are considered. While quite appropriate for the problems considered, the linear element is by no means the only one-dimensional element that can be formulated for a given problem type. Figure 6.2 depicts a three-node line element in which node 2 is an *interior* node. As mentioned briefly in Chapter 1, an interior node is *not* connected to any other node in any other element in the model. Inclusion of the interior node is a mathematical tool to increase the order of approximation of the field variable. Assuming that we deal with only 1 degree of freedom at each node, the appropriate polynomial representation of the field variable is

$$\phi(x) = a_0 + a_1x + a_2x^2 \quad (6.17)$$

and the nodal conditions are

$$\begin{aligned} \phi(x = 0) &= \phi_1 \\ \phi\left(x = \frac{L}{2}\right) &= \phi_2 \\ \phi(x = L) &= \phi_3 \end{aligned} \quad (6.18)$$

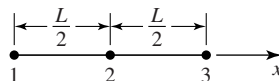


Figure 6.2 A three-node line element. Node 2 is an interior node.

Applying the general procedure outlined previously in the context of the beam element, we apply the nodal (boundary) conditions to obtain

$$\begin{Bmatrix} \phi_1 \\ \phi_2 \\ \phi_3 \end{Bmatrix} = \begin{bmatrix} 1 & 0 & 0 \\ 1 & \frac{L}{2} & \frac{L^2}{4} \\ 1 & L & L^2 \end{bmatrix} \begin{Bmatrix} a_0 \\ a_1 \\ a_2 \end{Bmatrix} \quad (6.19)$$

from which the interpolation functions are obtained via the following sequence

$$\begin{Bmatrix} a_0 \\ a_1 \\ a_2 \end{Bmatrix} = \begin{bmatrix} 1 & 0 & 0 \\ -\frac{3}{L} & \frac{4}{L} & -\frac{1}{L} \\ \frac{2}{L^2} & -\frac{4}{L^2} & \frac{2}{L^2} \end{bmatrix} \begin{Bmatrix} \phi_1 \\ \phi_2 \\ \phi_3 \end{Bmatrix} \quad (6.20a)$$

$$\begin{aligned} \phi(x) &= [1 \quad x \quad x^2] \begin{bmatrix} 1 & 0 & 0 \\ -\frac{3}{L} & \frac{4}{L} & -\frac{1}{L} \\ \frac{2}{L^2} & -\frac{4}{L^2} & \frac{2}{L^2} \end{bmatrix} \begin{Bmatrix} \phi_1 \\ \phi_2 \\ \phi_3 \end{Bmatrix} \\ &= [N_1 \quad N_2 \quad N_3] \begin{Bmatrix} \phi_1 \\ \phi_2 \\ \phi_3 \end{Bmatrix} \end{aligned} \quad (6.20b)$$

$$N_1(x) = 1 - \frac{3}{L}x + \frac{2}{L^2}x^2$$

$$N_2(x) = \frac{4x}{L} \left(1 - \frac{x}{L}\right) \quad (6.20c)$$

$$N_3(x) = \frac{x}{L} \left(\frac{2x}{L} - 1\right)$$

Note that each interpolation function varies quadratically in x and has value of unity at its associated node and value zero at the other two nodes, as illustrated in Figure 6.3. These observations lead to a shortcut method of concocting the interpolation functions for a C^0 line element as products of monomials as follows. Let $s = x/L$ such that $s_1 = 0$, $s_2 = 1/2$, $s_3 = 1$ are the nondimensional coordinates of nodes 1, 2, and 3, respectively. Instead of following the formal procedure used previously, we hypothesize, for example,

$$N_1(s) = C_1(s - s_2)(s - s_3) \quad (6.21)$$

where C_1 is a constant. The first monomial term ensures that N_1 has a value of zero at node 2 and the second monomial term ensures the same at node 3. Therefore, we need to determine only the value of C_1 to provide unity value at node 1.

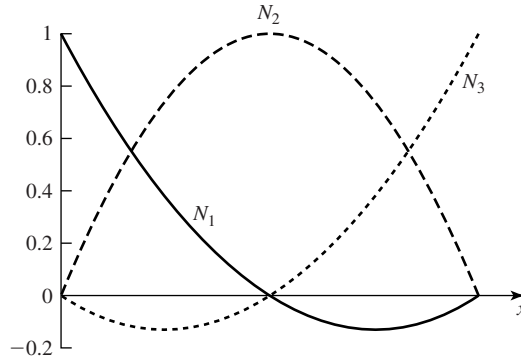


Figure 6.3 Spatial variation of interpolation functions for a three-node line element.

Substituting $s = 0$, we obtain

$$N_1(s = 0) = 1 = C_1 \left(0 - \frac{1}{2}\right)(0 - 1) \tag{6.22}$$

yielding $C_1 = 2$ and

$$N_1(s) = 2 \left(s - \frac{1}{2}\right)(s - 1) \tag{6.23}$$

Following similar logic and procedure shows that

$$N_2(s) = -4s(s - 1) \tag{6.24}$$

$$N_3(s) = 2s \left(s - \frac{1}{2}\right) \tag{6.25}$$

Substituting $s = x/L$ in Equations 6.23–6.25 and expanding shows that the results are identical to those given in Equation 6.20. The monomial-based procedure can be extended to line elements of any order as illustrated by the following example.

EXAMPLE 6.1

Use the monomial method to obtain the interpolation functions for the four-node line element shown in Figure 6.4.

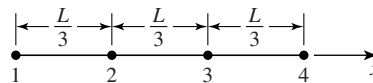


Figure 6.4 Four-node line element of Example 6.1.

■ Solution

Using $s = x/L$, we have $s_1 = 0$, $s_2 = 1/3$, $s_3 = 2/3$, and $s_4 = 1$. The monomial terms of interest are s , $s - 1/3$, $s - 2/3$, and $s - 1$. The monomial products

$$N_1(s) = C_1 \left(s - \frac{1}{3} \right) \left(s - \frac{2}{3} \right) (s - 1)$$

$$N_2(s) = C_2 s \left(s - \frac{2}{3} \right) (s - 1)$$

$$N_3(s) = C_3 s \left(s - \frac{1}{3} \right) (s - 1)$$

$$N_4(s) = C_4 s \left(s - \frac{1}{3} \right) \left(s - \frac{2}{3} \right)$$

automatically satisfy the required zero-value conditions for each interpolation function. Hence, we need evaluate only the constants C_i such that $N_i(s = s_i) = 1$, $i = 1, 4$. Applying each of the four unity-value conditions, we obtain

$$N_1(0) = 1 = C_1 \left(-\frac{1}{3} \right) \left(-\frac{2}{3} \right) (-1)$$

$$N_2\left(\frac{1}{3}\right) = 1 = C_2 \left(\frac{1}{3}\right) \left(-\frac{1}{3}\right) \left(-\frac{2}{3}\right)$$

$$N_3\left(\frac{2}{3}\right) = 1 = C_3 \left(\frac{2}{3}\right) \left(\frac{1}{3}\right) \left(-\frac{1}{3}\right)$$

$$N_4(1) = 1 = C_4(1) \left(\frac{2}{3}\right) \left(\frac{1}{3}\right)$$

from which $C_1 = -\frac{9}{2}$, $C_2 = \frac{27}{2}$, $C_3 = -\frac{27}{2}$, $C_4 = \frac{9}{2}$.

The interpolation functions are then given as

$$N_1(s) = -\frac{9}{2} \left(s - \frac{1}{3} \right) \left(s - \frac{2}{3} \right) (s - 1)$$

$$N_2(s) = \frac{27}{2} s \left(s - \frac{2}{3} \right) (s - 1)$$

$$N_3(s) = -\frac{27}{2} s \left(s - \frac{1}{3} \right) (s - 1)$$

$$N_4(s) = \frac{9}{2} s \left(s - \frac{1}{3} \right) \left(s - \frac{2}{3} \right)$$

6.4 POLYNOMIAL FORMS: GEOMETRIC ISOTROPY

The previous discussion of one-dimensional (line) elements revealed that the polynomial representation of the field variable must contain the same number of terms as the number of nodal degrees of freedom. In addition, to satisfy the completeness requirement, the polynomial representation for an M -degree of freedom element should contain all powers of the independent variable up to and including $M - 1$. Another way of stating the latter requirement is that the polynomial is *complete*. In two and three dimensions, polynomial representations of the field variable, in general, satisfy the compatibility and completeness requirements if the polynomial exhibits the property known as *geometric isotropy* [1]. A mathematical function satisfies geometric isotropy if the functional form does not change under a translation or rotation of coordinates. In two dimensions, a complete polynomial of order M can be expressed as

$$P_M(x, y) = \sum_{k=0}^{N_t^{(2)}} a_k x^i y^j \quad i + j \leq M \tag{6.26}$$

where $N_t^{(2)} = [(M + 1)(M + 2)]/2$ is the total number of terms. A complete polynomial as expressed by Equation 6.26 satisfies the condition of geometric isotropy, since the two variables, x and y , are included in each term in similar powers. Therefore, a translation or rotation of coordinates is not prejudicial to either independent variable.

A graphical method of depicting complete two-dimensional polynomials is the so-called Pascal triangle shown in Figure 6.5. Each horizontal line represents a polynomial of order M . A complete polynomial of order M must contain all terms shown above the horizontal line. For example, a complete quadratic polynomial in two dimensions must contain six terms. Hence, for use in a finite element representation of a field variable, a complete quadratic expression requires six nodal degrees of freedom in the element. We examine this particular case in the context of triangular elements in the next section.

In addition to the complete polynomials, incomplete polynomials also exhibit geometric isotropy if the incomplete polynomial is *symmetric*. In this context, symmetry implies that the independent variables appear as “equal and

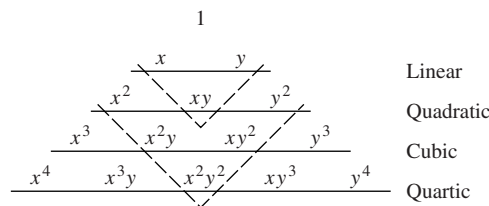


Figure 6.5 Pascal triangle for polynomials in two dimensions.

opposite pairs,” ensuring that each independent variable plays an equal role in the polynomial. For example, the four-term incomplete quadratic polynomial

$$P(x, y) = a_0 + a_1x + a_2y + a_3x^2 \tag{6.27}$$

is not symmetric, as there is a quadratic term in x but the corresponding quadratic term in y does not appear. On the other hand, the incomplete quadratic polynomial

$$P(x, y) = a_0 + a_1x + a_2y + a_3xy \tag{6.28}$$

is symmetric, as the quadratic term gives equal “weight” to both variables.

A very convenient way of visualizing some of the commonly used incomplete but symmetric polynomials of a given order is also afforded by the Pascal triangle. Again referring to Figure 6.5, the dashed lines show the terms that must be included in an incomplete yet symmetric polynomial of a given order. (These are, of course, not the only incomplete, symmetric polynomials that can be constructed.) All terms above the dashed lines must be included in a polynomial representation if the function is to exhibit geometric isotropy. This feature of polynomials is utilized to a significant extent in following the development of various element interpolation functions.

As in the two-dimensional case, to satisfy the geometric isotropy requirements, the polynomial expression of the field variable in three dimensions must be complete or incomplete but symmetric. Completeness and symmetry can also be depicted graphically by the “Pascal pyramid” shown in Figure 6.6. While the three-dimensional case is a bit more difficult to visualize, the basic premise

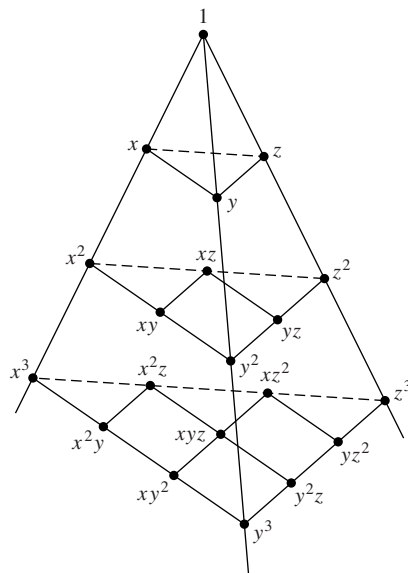


Figure 6.6 Pascal “pyramid” for polynomials in three dimensions.

remains that each independent variable must be of equal “strength” in the polynomial. For example, the 3-D quadratic polynomial

$$P(x, y, z) = a_0 + a_1x + a_2y + a_3z + a_4x^2 + a_5y^2 + a_6z^2 + a_7xy + a_8xz + a_9yz \quad (6.29)$$

is complete and could be applied to an element having 10 nodes. Similarly, an incomplete, symmetric form such as

$$P(x, y, z) = a_0 + a_1x + a_2y + a_3z + a_4x^2 + a_5y^2 + a_6z^2 \quad (6.30)$$

or

$$P(x, y, z) = a_0 + a_1x + a_2y + a_3z + a_4xy + a_5xz + a_6yz \quad (6.31)$$

could be used for elements having seven nodal degrees of freedom (an unlikely case, however).

Geometric isotropy is not an *absolute* requirement for field variable representation [1], hence, interpolation functions. As demonstrated by many researchers, incomplete representations are quite often used and solution convergence attained. However, in terms of *h*-refinement, use of geometrically isotropic representations guarantees satisfaction of the compatibility and completeness requirements. For the *p*-refinement method, the reader is reminded that the interpolation functions in any finite element analysis solution are approximations to the power series expansion of the problem solution. As we increase the number of element nodes, the order of the interpolation functions increases and, in the limit, as the number of nodes approaches infinity, the polynomial expression of the field variable approaches the power series expansion of the solution.

6.5 TRIANGULAR ELEMENTS

The interpolation functions for triangular elements are inherently formulated in two dimensions and a family of such elements exists. Figure 6.7 depicts the first three elements (linear, quadratic, and cubic) of the family. Note that, in the case of the cubic element, an internal node exists. The internal node is required to

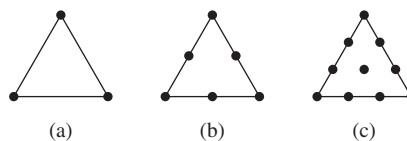


Figure 6.7 Triangular elements:
(a) 3-node linear, (b) 6-node quadratic,
(c) 10-node cubic.

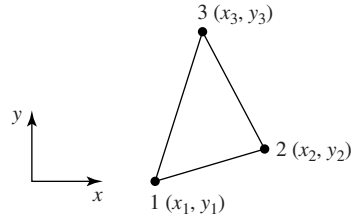


Figure 6.8 A general three-node triangular element referred to global coordinates.

obtain geometric isotropy, as is subsequently discussed. The triangular elements are not limited to two-dimensional problems. In fact, the triangular elements can be used in axisymmetric 3-D cases (discussed later in this chapter) as well as in structural analyses involving out-of-plane bending, as in plate and shell structures. In the latter cases, the nodal degrees of freedom include first derivatives of the field variable as well as the field variable itself. While plate and shell problems are beyond the scope of this book, we allude to those problems again briefly in Chapter 9.

Figure 6.8 depicts a general, three-node triangular element to which we attach an element coordinate system that is, for now, assumed to be the same as the global system. Here, it is assumed that only 1 degree of freedom is associated with each node. We express the field variable in the polynomial form

$$\phi(x, y) = a_0 + a_1x + a_2y \quad (6.32)$$

Applying the nodal conditions

$$\begin{aligned} \phi(x_1, y_1) &= \phi_1 \\ \phi(x_2, y_2) &= \phi_2 \\ \phi(x_3, y_3) &= \phi_3 \end{aligned} \quad (6.33)$$

and following the general procedure previously outlined, we obtain

$$\begin{bmatrix} 1 & x_1 & y_1 \\ 1 & x_2 & y_2 \\ 1 & x_3 & y_3 \end{bmatrix} \begin{Bmatrix} a_0 \\ a_1 \\ a_2 \end{Bmatrix} = \begin{Bmatrix} \phi_1 \\ \phi_2 \\ \phi_3 \end{Bmatrix} \quad (6.34)$$

To solve for the polynomial coefficients, the matrix of coefficients in Equation 6.34 must be inverted. Inversion of the matrix is algebraically tedious but straightforward, and we find

$$a_0 = \frac{1}{2A} [\phi_1(x_2y_3 - x_3y_2) + \phi_2(x_3y_1 - x_1y_3) + \phi_3(x_1y_2 - x_2y_1)]$$

$$a_1 = \frac{1}{2A}[\phi_1(y_2 - y_3) + \phi_2(y_3 - y_1) + \phi_3(y_1 - y_2)]$$

$$a_2 = \frac{1}{2A}[\phi_1(x_3 - x_2) + \phi_2(x_1 - x_3) + \phi_3(x_2 - x_1)]$$
(6.35)

Substituting the values into Equation 6.32 and collecting coefficients of the nodal variables, we obtain

$$\phi(x, y) = \frac{1}{2A} \left\{ \begin{array}{l} [(x_2y_3 - x_3y_2) + (y_2 - y_3)x + (x_3 - x_2)y]\phi_1 \\ + [(x_3y_1 - x_1y_3) + (y_3 - y_1)x + (x_1 - x_3)y]\phi_2 \\ + [(x_1y_2 - x_2y_1) + (y_1 - y_2)x + (x_2 - x_1)y]\phi_3 \end{array} \right\} \quad (6.36)$$

Given the form of Equation 6.36, the interpolation functions are observed to be

$$N_1(x, y) = \frac{1}{2A}[(x_2y_3 - x_3y_2) + (y_2 - y_3)x + (x_3 - x_2)y]$$

$$N_2(x, y) = \frac{1}{2A}[(x_3y_1 - x_1y_3) + (y_3 - y_1)x + (x_1 - x_3)y] \quad (6.37)$$

$$N_3(x, y) = \frac{1}{2A}[(x_1y_2 - x_2y_1) + (y_1 - y_2)x + (x_2 - x_1)y]$$

where A is the area of the triangular element. Given the coordinates of the three vertices of a triangle, it can be shown that the area is given by

$$A = \frac{1}{2} \begin{vmatrix} 1 & x_1 & y_1 \\ 1 & x_2 & y_2 \\ 1 & x_3 & y_3 \end{vmatrix} \quad (6.38)$$

Note that the algebraically complex form of the interpolation functions arises primarily from the choice of the element coordinate system of Figure 6.8. As the linear representation of the field variable exhibits geometric isotropy, location and orientation of the element coordinate axes can be chosen arbitrarily without affecting the interpolation results. If, for example, the element coordinate system shown in Figure 6.9 is utilized, considerable algebraic simplification results. In the coordinate system shown, we have $x_1 = y_1 = y_2 = 0$, $2A = x_2y_3$,

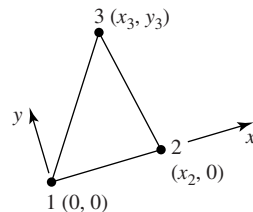


Figure 6.9 Three-node triangle having an element coordinate system attached to the element.

and the interpolation functions become

$$\begin{aligned} N_1(x, y) &= \frac{1}{x_2 y_3} [x_2 y_3 - y_3 x + (x_3 - x_2) y] \\ N_2(x, y) &= \frac{1}{x_2 y_3} [y_3 x - x_3 y] \\ N_3(x, y) &= \frac{y}{y_3} \end{aligned} \quad (6.39)$$

which are clearly of a simpler form than Equation 6.37. The simplification is not without cost, however. If the element coordinate system is directly associated with element orientation, as in Figure 6.9, the element characteristic matrices must be transformed to a common global coordinate system during model assembly. (Recall the transformation of stiffness matrices demonstrated for bar and beam elements earlier.) As finite element models usually employ a large number of elements, the additional computations required for element transformation can be quite time consuming. Consequently, computational efficiency is improved if each element coordinate system is oriented such that the axes are parallel to the global axes. The transformation step is then unnecessary when model assembly takes place. In practice, most commercial finite element software packages provide for use of either type element coordinate as a user option [6].

Returning to Equation 6.32, observe that it is possible for the field variable to take on a constant value, as per the completeness requirement, and that the first partial derivatives with respect to the independent variables x and y are constants. The latter shows that the gradients of the field variable are constant in both coordinate directions. For a planar structural element, this results in constant strain components. In fact, in structural applications, the three-node triangular element is commonly known as a *constant strain triangle* (CST, for short). In the case of heat transfer, the element produces constant temperature gradients, therefore, constant heat flow within an element.

6.5.1 Area Coordinates

When expressed in Cartesian coordinates, the interpolation functions for the triangular element are algebraically complex. Further, the integrations required to obtain element characteristic matrices are cumbersome. Considerable simplification of the interpolation functions as well as the subsequently required integration is obtained via the use of *area coordinates*. Figure 6.10 shows a three-node triangular element divided into three areas defined by the nodes and an arbitrary interior point $P(x, y)$. Note: P is *not* a node. The area coordinates of P are defined as

$$L_1 = \frac{A_1}{A} \quad L_2 = \frac{A_2}{A} \quad L_3 = \frac{A_3}{A} \quad (6.40)$$

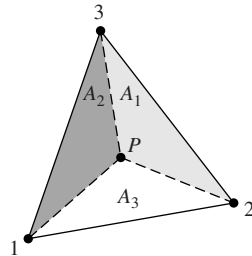


Figure 6.10 Areas used to define area coordinates for a triangular element.

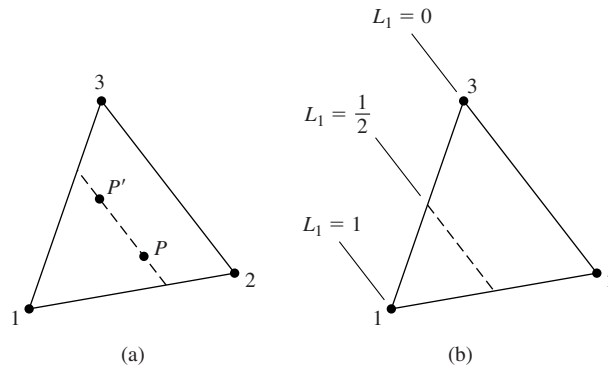


Figure 6.11

- (a) Area A_1 associated with either P or P' is constant.
- (b) Lines of the constant area coordinate L_1 .

where A is the total area of the triangle. Clearly, the area coordinates are not independent, since

$$L_1 + L_2 + L_3 = 1 \tag{6.41}$$

The dependency is to be expected, since Equation 6.40 expresses the location of a point in two-dimensions using three coordinates.

The important properties of area coordinates for application to triangular finite elements are now examined with reference to Figure 6.11. In Figure 6.11a, a dashed line parallel to the side defined by nodes 2 and 3 is indicated. For any two points P and P' on this line, the areas of the triangles formed by nodes 2 and 3 and either P or P' are identical. This is because the base and height of any triangle so formed are constants. Further, as the dashed line is moved closer to node 1, area A_1 increases linearly and has value $A_1 = A$, when evaluated at node 1. Therefore, area coordinate L_1 is constant on any line parallel to the side of the triangle opposite node 1 and varies linearly from a value of unity at node 1 to value of zero along the side defined by nodes 2 and 3, as depicted in Figure 6.11b. Similar arguments can be made for the behavior of L_2 and L_3 . These observations

can be used to write the following conditions satisfied by the area coordinates when evaluated at the nodes:

$$\begin{aligned}
 \text{Node 1: } & L_1 = 1 \quad L_2 = L_3 = 0 \\
 \text{Node 2: } & L_2 = 1 \quad L_1 = L_3 = 0 \\
 \text{Node 3: } & L_3 = 1 \quad L_1 = L_2 = 0
 \end{aligned}
 \tag{6.42}$$

The conditions expressed by Equation 6.42 are exactly the conditions that must be satisfied by interpolation functions at the nodes of the triangular element. So, we express the field variable as

$$\phi(x, y) = L_1\phi_1 + L_2\phi_2 + L_3\phi_3
 \tag{6.43}$$

in terms of area coordinates. Is this different from the field variable representation of Equation 6.36? If the area coordinates are expressed explicitly in terms of the nodal coordinates, the two field variable representations are shown to be identical. The true advantages of area coordinates are seen more readily in developing interpolation functions for higher-order elements and performing integration of various forms of the interpolation functions.

6.5.2 Six-Node Triangular Element

A six-node element is shown in Figure 6.12a. The additional nodes 4, 5, and 6 are located at the midpoints of the sides of the element. As we have six nodes, a complete polynomial representation of the field variable is

$$\phi(x, y) = a_0 + a_1x + a_2y + a_3x^2 + a_4xy + a_5y^2
 \tag{6.44}$$

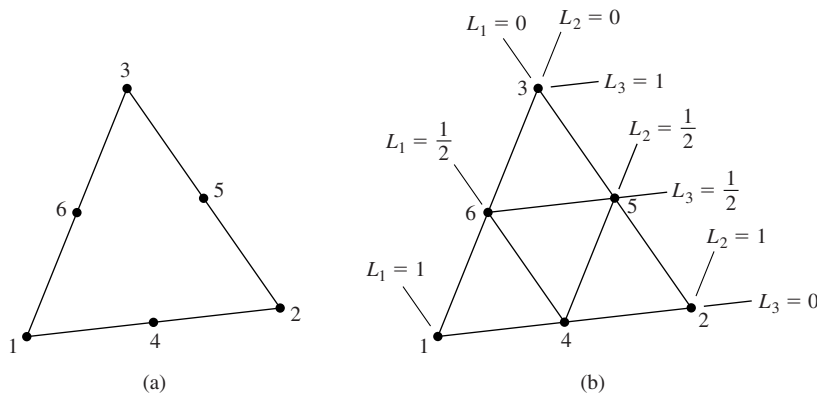


Figure 6.12 Six-node triangular elements: (a) Node numbering convention. (b) Lines of constant values of the area coordinates.

which is ultimately to be expressed in terms of interpolation functions and nodal values as

$$\phi(x, y) = \sum_{i=1}^6 N_i(x, y)\phi_i \quad (6.45)$$

As usual, each interpolation function must be such that its value is unity when evaluated at its associated node and zero when evaluated at any of the other five nodes. Further, each interpolation is a quadratic function, since the field variable representation is quadratic.

Figure 6.12b shows the six-node element with lines of constant values of the area coordinates passing through the nodes. Using this figure and a bit of logic, the interpolation functions are easily “constructed” in area coordinates. For example, interpolation function $N_1(x, y) = N_1(L_1, L_2, L_3)$ must have value of zero at nodes 2, 3, 4, 5, and 6. Noting that $L_1 = 1/2$ at nodes 4 and 6, inclusion of the term $L_1 - 1/2$ ensures a zero value at those two nodes. Similarly, $L_1 = 0$ at nodes 2, 3, 4, so the term L_1 satisfies the conditions at those three nodes. Therefore, we propose

$$N_1 = L_1 \left(L_1 - \frac{1}{2} \right) \quad (6.46)$$

However, evaluation of Equation 6.46 at node 1, where $L_1 = 1$, results in $N_1 = 1/2$. As N_1 must be unity at node 1, Equation 6.46 is modified to

$$N_1 = 2L_1 \left(L_1 - \frac{1}{2} \right) = L_1(2L_1 - 1) \quad (6.47a)$$

which satisfies the required conditions at each of the six nodes and is a quadratic function, since L_1 is a linear function of x and y .

Applying the required nodal conditions to the remaining five interpolation functions in turn, we obtain

$$N_2 = L_2(2L_2 - 1) \quad (6.47b)$$

$$N_3 = L_3(2L_3 - 1) \quad (6.47c)$$

$$N_4 = 4L_1L_2 \quad (6.47d)$$

$$N_5 = 4L_2L_3 \quad (6.47e)$$

$$N_6 = 4L_1L_3 \quad (6.47f)$$

Using a similarly straightforward procedure, interpolation functions for additional higher-order triangular elements can be constructed. The 10-node cubic element is left as an exercise.

6.5.3 Integration in Area Coordinates

As seen in Chapter 5 and encountered again in later chapters, integration of various forms of the interpolation functions over the domain of an element are

required in formulating element characteristic matrices and load vectors. When expressed in area coordinates, integrals of the form

$$\iint_A L_1^a L_2^b L_3^c \, dA \quad (6.48)$$

(where A is the total area of a triangle defined by nodes 1, 2, 3) must often be evaluated. The relation

$$\iint_A L_1^a L_2^b L_3^c \, dA = (2A) \frac{a!b!c!}{(a+b+c+2)!} \quad (6.49)$$

has been shown [7] to be valid for all exponents a, b, c that are positive integers (recall $0! = 1$). Therefore, integration in area coordinates is quite straightforward.

EXAMPLE 6.2

As will be shown in Chapter 7, the convection terms of the stiffness matrix for a 2-D heat transfer element are of the form

$$k_{ij} = \int_A h N_i N_j \, dA$$

where h is the convection coefficient and A is element area. Use the interpolation functions for a six-node triangular element given by Equation 6.47 to compute k_{24} .

■ Solution

Using Equation 6.47b and 6.47d, we have

$$N_2 = L_2(2L_2 - 1)$$

$$N_4 = 4L_1L_2$$

so (assuming h is a constant)

$$k_{24} = h \int_A L_2(2L_2 - 1)4L_1L_2 \, dA = h \int_A (8L_1L_2^3 - 4L_1L_2^2) \, dA$$

Applying Equation 6.49, we have

$$h \int_A 8L_1L_2^3 \, dA = 8h(2A) \frac{(1!)(3!)(0!)}{(1+3+0+2)!} = \frac{96hA}{720} = \frac{2hA}{15}$$

$$h \int_A 4L_1L_2^2 \, dA = 4h(2A) \frac{(1!)(2!)(0!)}{(1+2+0+2)!} = \frac{16hA}{120} = \frac{2hA}{15}$$

Therefore,

$$k_{24} = \frac{2hA}{15} - \frac{2hA}{15} = 0$$

6.6 RECTANGULAR ELEMENTS

Rectangular elements are convenient for use in modeling regular geometries, can be used in conjunction with triangular elements, and form the basis for development of general quadrilateral elements. The simplest of the rectangular family of elements is the four-node rectangle shown in Figure 6.13, where it is assumed that the sides of the rectangular are parallel to the global Cartesian axes. By convention, we number the nodes sequentially in a counterclockwise direction, as shown. As there are four nodes and 4 degrees of freedom, a four-term polynomial expression for the field variable is appropriate. Since there is no complete four-term polynomial in two dimensions, the incomplete, symmetric expression

$$\phi(x, y) = a_0 + a_1x + a_2y + a_3xy \tag{6.50}$$

is used to ensure geometric isotropy. Applying the four nodal conditions and writing in matrix form gives

$$\begin{Bmatrix} \phi_1 \\ \phi_2 \\ \phi_3 \\ \phi_4 \end{Bmatrix} = \begin{bmatrix} 1 & x_1 & y_1 & x_1y_1 \\ 1 & x_2 & y_2 & x_2y_2 \\ 1 & x_3 & y_3 & x_3y_3 \\ 1 & x_4 & y_4 & x_4y_4 \end{bmatrix} \begin{Bmatrix} a_0 \\ a_1 \\ a_2 \\ a_3 \end{Bmatrix} \tag{6.51}$$

which formally gives the polynomial coefficients as

$$\begin{Bmatrix} a_0 \\ a_1 \\ a_2 \\ a_3 \end{Bmatrix} = \begin{bmatrix} 1 & x_1 & y_1 & x_1y_1 \\ 1 & x_2 & y_2 & x_2y_2 \\ 1 & x_3 & y_3 & x_3y_3 \\ 1 & x_4 & y_4 & x_4y_4 \end{bmatrix}^{-1} \begin{Bmatrix} \phi_1 \\ \phi_2 \\ \phi_3 \\ \phi_4 \end{Bmatrix} \tag{6.52}$$

In terms of the nodal values, the field variable is then described by

$$\phi(x, y) = [1 \quad x \quad y \quad xy]\{a\} = [1 \quad x \quad y \quad xy] \begin{bmatrix} 1 & x_1 & y_1 & x_1y_1 \\ 1 & x_2 & y_2 & x_2y_2 \\ 1 & x_3 & y_3 & x_3y_3 \\ 1 & x_4 & y_4 & x_4y_4 \end{bmatrix}^{-1} \begin{Bmatrix} \phi_1 \\ \phi_2 \\ \phi_3 \\ \phi_4 \end{Bmatrix} \tag{6.53}$$

from which the interpolation functions can be deduced.

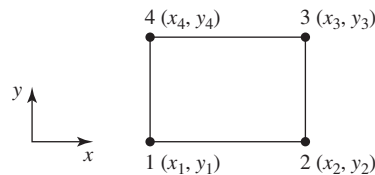


Figure 6.13 A four-node rectangular element defined in global coordinates.

The form of Equation 6.53 suggests that expression of the interpolation functions in terms of the nodal coordinates is algebraically complex. Fortunately, the complexity can be reduced by a more judicious choice of coordinates. For the rectangular element, we introduce the normalized coordinates (also known as *natural coordinates* or *serendipity coordinates*) r and s as

$$r = \frac{x - \bar{x}}{a} \quad s = \frac{y - \bar{y}}{b} \quad (6.54)$$

where $2a$ and $2b$ are the width and height of the rectangle, respectively, and the coordinates of the centroid are

$$\bar{x} = \frac{x_1 + x_2}{2} \quad \bar{y} = \frac{y_1 + y_4}{2} \quad (6.55)$$

as shown in Figure 6.14a. Therefore, r and s are such that the values range from -1 to $+1$, and the nodal coordinates are as in Figure 6.14b.

Applying the conditions that must be satisfied by each interpolation function at each node, we obtain (essentially by inspection)

$$\begin{aligned} N_1(r, s) &= \frac{1}{4}(1 - r)(1 - s) \\ N_2(r, s) &= \frac{1}{4}(1 + r)(1 - s) \\ N_3(r, s) &= \frac{1}{4}(1 + r)(1 + s) \\ N_4(r, s) &= \frac{1}{4}(1 - r)(1 + s) \end{aligned} \quad (6.56a)$$

hence

$$\phi(x, y) = \phi(r, s) = N_1(r, s)\phi_1 + N_2(r, s)\phi_2 + N_3(r, s)\phi_3 + N_4(r, s)\phi_4 \quad (6.56b)$$

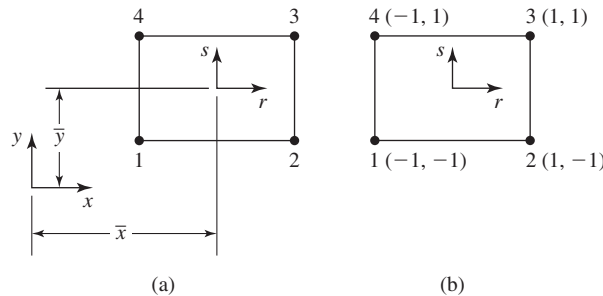


Figure 6.14 A four-node rectangular element showing (a) the translation to natural coordinates, (b) the natural coordinates of each node.

As in the case of triangular elements using area coordinates, the interpolation functions are much simpler algebraically when expressed in terms of the natural coordinates. Nevertheless, all required conditions are satisfied and the functional form is identical to that used to express the field variable in Equation 6.50. Also as with area coordinates, integrations involving the interpolation functions expressed in the natural coordinates are simplified, since the integrands are relatively simple polynomials (for rectangular elements) and the integration limits (when integrating over the area of the element) are -1 and $+1$. Further discussion of such integration requirements, particularly numerical integration techniques, is postponed until later in this chapter.

To develop a higher-order rectangular element, the logical progression is to place an additional node at the midpoint of each side of the element, as in Figure 6.15. This poses an immediate problem, however. Inspection of the Pascal triangle shows that we cannot construct a complete polynomial having eight terms, but we have a choice of two incomplete, symmetric cubic polynomials:

$$\phi(x, y) = a_0 + a_1x + a_2y + a_3x^2 + a_4xy + a_5y^2 + a_6x^3 + a_7y^3 \quad (6.57a)$$

$$\phi(x, y) = a_0 + a_1x + a_2y + a_3x^2 + a_4xy + a_5y^2 + a_6x^2y + a_7xy^2 \quad (6.57b)$$

Rather than grapple with choosing one or the other, we use the natural coordinates and the nodal conditions that must be satisfied by each interpolation function to obtain the functions serendipitously. For example, interpolation function N_1 must evaluate to zero at all nodes except node 1, where its value must be unity. At nodes 2, 3, and 6, $r = 1$, so including the term $r - 1$ satisfies the zero condition at those nodes. Similarly, at nodes 4 and 7, $s = 1$ so the term $s - 1$ ensures the zero condition at those two nodes. Finally, at node 5, $(r, s) = (0, -1)$, and at node 8, $(r, s) = (-1, 0)$. Hence, at nodes 5 and 8, the term $r + s + 1$ is identically zero. Using this reasoning, the interpolation function associated with node 1 is to be of the form

$$N_1(r, s) = (1 - r)(1 - s)(r + s + 1) \quad (6.58)$$

Evaluating at node 1 where $(r, s) = (-1, -1)$, we obtain $N_1 = -4$, so a correction is required to obtain the unity value. The final form is then

$$N_1(r, s) = \frac{1}{4}(r - 1)(1 - s)(r + s + 1) \quad (6.59a)$$

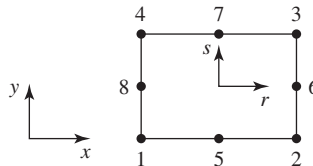


Figure 6.15 Eight-node rectangular element showing both global and natural coordinate axes.

A parallel procedure for the interpolation functions associated with the other three corner nodes leads to

$$N_2(r, s) = \frac{1}{4}(r+1)(1-s)(s-r+1) \quad (6.59b)$$

$$N_3(r, s) = \frac{1}{4}(1+r)(1+s)(r+s-1) \quad (6.59c)$$

$$N_4(r, s) = \frac{1}{4}(r-1)(1+s)(r-s+1) \quad (6.59d)$$

The form of the interpolation functions associated with the midside nodes is simpler to obtain than those for the corner nodes. For example, N_5 has a value of zero at nodes 2, 3, and 6 if it contains the term $r-1$ and is also zero at nodes 1, 4, and 8 if the term $1+r$ is included. Finally, if a zero value is at node 7, $(r, s) = (0, 1)$ is obtained by inclusion of $s-1$. The form for N_5 is

$$N_5 = \frac{1}{2}(1-r)(1+r)(1-s) = \frac{1}{2}(1-r^2)(1-s) \quad (6.59e)$$

where the leading coefficient ensures a unity value at node 5. For the other midside nodes,

$$N_6 = \frac{1}{2}(1+r)(1-s^2) \quad (6.59f)$$

$$N_7 = \frac{1}{2}(1-r^2)(1+s) \quad (6.59g)$$

$$N_8 = \frac{1}{2}(1-r)(1-s^2) \quad (6.59h)$$

are determined in the same manner.

Many other, successively higher-order, rectangular elements have been developed [1]. In general, these higher-order elements include internal nodes that, in modeling, are troublesome, as they cannot be connected to nodes of other elements. The internal nodes are eliminated mathematically. The elimination process is such that the mechanical effects of the internal nodes are assigned appropriately to the external nodes.

6.7 THREE-DIMENSIONAL ELEMENTS

As in the two-dimensional case, there are two main families of three-dimensional elements. One is based on extension of triangular elements to tetrahedrons and the other on extension of rectangular elements to rectangular parallelepipeds

(often simply called *brick* elements). The algebraically cumbersome techniques for deriving interpolation functions in global Cartesian coordinates has been illustrated for two-dimensional elements. Those developments are not repeated here for three-dimensional elements; the procedures are algebraically identical but even more complex. Instead, we utilize only the more amenable approach of using natural coordinates to develop the interpolation functions for the two basic elements of the tetrahedral and brick families.

6.7.1 Four-Node Tetrahedral Element

A four-node tetrahedral element is depicted in Figure 6.16 in relation to a global Cartesian coordinate system. The nodes are numbered 1–4 per the convention that node 1 can be selected arbitrarily and nodes 2–4 are then specified in a counterclockwise direction from node 1. (This convention is the same as used by most commercial finite element analysis software and is very important in assuring geometrically correct tetrahedrons. On the other hand, tetrahedral element definition for finite element models is so complex that it is almost always accomplished by automeshing capabilities of specific software packages.)

In a manner analogous to use of area coordinates, we now introduce the concept of *volume coordinates* using Figure 6.17. Point $P(x, y, z)$ is an arbitrary point in the tetrahedron defined by the four nodes. As indicated by the dashed lines, point P and the four nodes define four other tetrahedra having volumes

$$\begin{aligned} V_1 &= \text{vol}(P234) & V_2 &= \text{vol}(P134) \\ V_3 &= \text{vol}(P124) & V_4 &= \text{vol}(P123) \end{aligned} \quad (6.60)$$

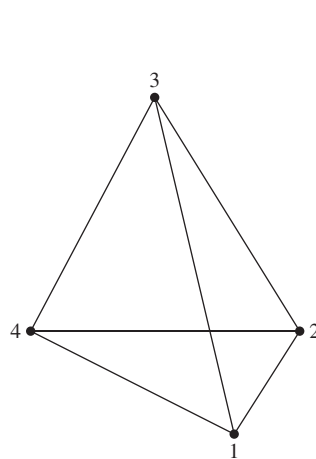


Figure 6.16 A four-node tetrahedral element.

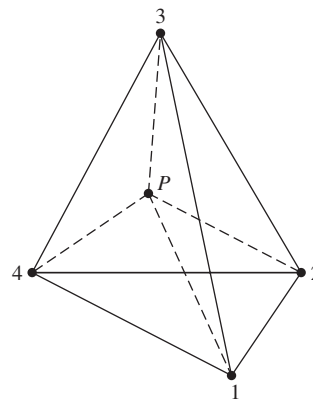


Figure 6.17 A four-node tetrahedral element, showing an arbitrary interest point defining four volumes.

The volume coordinates are defined as

$$\begin{aligned} L_1 &= \frac{V_1}{V} \\ L_2 &= \frac{V_2}{V} \\ L_3 &= \frac{V_3}{V} \\ L_4 &= \frac{V_4}{V} \end{aligned} \quad (6.61)$$

where V is the total volume of the element given by

$$V = \frac{1}{6} \begin{vmatrix} 1 & x_1 & y_1 & z_1 \\ 1 & x_2 & y_2 & z_2 \\ 1 & x_3 & y_3 & z_3 \\ 1 & x_4 & y_4 & z_4 \end{vmatrix} \quad (6.62)$$

As with area coordinates, the volume coordinates are not independent, since

$$V_1 + V_2 + V_3 + V_4 = V \quad (6.63)$$

Now let us examine the variation of the volume coordinates through the element. If, for example, point P corresponds to node 1, we find $V_1 = V$, $V_2 = V_3 = V_4 = 0$. Consequently $L_1 = 1$, $L_2 = L_3 = L_4 = 0$ at node 1. As P moves away from node 1, V_1 decreases linearly, since the volume of a tetrahedron is directly proportional to its height (the perpendicular distance from P to the plane defined by nodes 2, 3, and 4) and the area of its base (the triangle formed by nodes 2, 3, and 4). On any plane parallel to the base triangle of nodes 2, 3, 4, the value of L_1 is constant. Of particular importance is that, if P lies in the plane of nodes 2, 3, 4, the value of L_1 is zero. Identical observations apply to volume coordinates L_2 , L_3 , and L_4 . So the volume coordinates satisfy all required nodal conditions for interpolation functions, and we can express the field variable as

$$\phi(x, y, z) = L_1\phi_1 + L_2\phi_2 + L_3\phi_3 + L_4\phi_4 \quad (6.64)$$

Explicit representation of the interpolation functions (i.e., the volume coordinates) in terms of global coordinates is, as stated, algebraically complex but straightforward. Fortunately, such explicit representation is not generally required, as element formulation can be accomplished using volume coordinates only. As with area coordinates, integration of functions of volume coordinates (required in developing element characteristic matrices and load vectors) is relatively simple. Integrals of the form

$$\iiint_V L_1^a L_2^b L_3^c L_4^d dV \quad (6.65)$$

where a, b, c, d are positive integers and V is total element volume, appear in element formulation for various physical problems. As with area coordinates, integration in volume coordinates is straightforward [7], and we have the integration formula

$$\iiint_V L_1^a L_2^b L_3^c L_4^d dV = \frac{a!b!c!d!}{(a+b+c+d+3)!}(6V) \quad (6.66)$$

which is the three-dimensional analogy to Equation 6.49.

As another analogy with the two-dimensional triangular elements, the tetrahedral element is most useful in modeling irregular geometries. However, the tetrahedral element is not particularly amenable to use in conjunction with other element types, strictly as a result of the nodal configurations. This incompatibility is discussed in the following sections. As a final comment on the four-node tetrahedral element, we note that the field variable representation, as given by Equation 6.64, is a linear function of the Cartesian coordinates. Therefore, all the first partial derivatives of the field variable are constant. In structural applications, the tetrahedral element is a constant strain element; in general, the element exhibits constant gradients of the field variable in the coordinate directions.

Other elements of the tetrahedral family are depicted in Figure 6.18. The interpolation functions for the depicted elements are readily written in volume coordinates, as for higher-order two-dimensional triangular elements. Note particularly that the second element of the family has 10 nodes and a cubic form for the field variable and interpolation functions. A quadratic tetrahedral element cannot be constructed to exhibit geometric isotropy even if internal nodes are included.

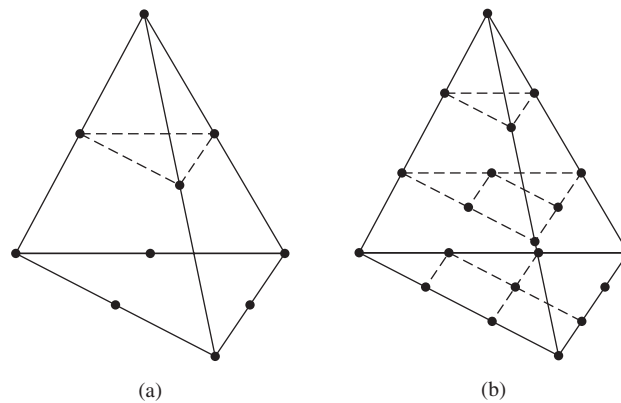


Figure 6.18 Higher-order tetrahedral elements:
(a) 10 node. (b) 20 node.

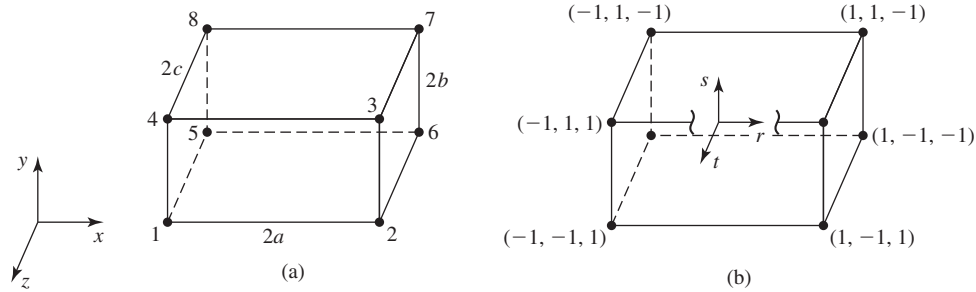


Figure 6.19 Eight-node brick element: (a) Global Cartesian coordinates. (b) Natural coordinates with an origin at the centroid.

6.7.2 Eight-Node Brick Element

The so-called eight node brick element (rectangular parallelepiped) is shown in Figure 6.19a in reference to a global Cartesian coordinate system. Here, we utilize the natural coordinates r, s, t of Figure 6.19b, defined as

$$\begin{aligned} r &= \frac{x - \bar{x}}{a} \\ s &= \frac{y - \bar{y}}{b} \\ t &= \frac{z - \bar{z}}{c} \end{aligned} \tag{6.67}$$

where $2a, 2b, 2c$ are the dimensions of the element in the x, y, z coordinates, respectively, and the coordinates of the element centroid are

$$\begin{aligned} \bar{x} &= \frac{x_2 - x_1}{2} \\ \bar{y} &= \frac{y_3 - y_2}{2} \\ \bar{z} &= \frac{z_5 - z_1}{2} \end{aligned} \tag{6.68}$$

The natural coordinates are defined such that the coordinate values vary between -1 and $+1$ over the domain of the element. As with the plane rectangular element, the natural coordinates provide for a straightforward development of the interpolation functions by using the appropriate monomial terms to satisfy nodal conditions. As we illustrated the procedure in several previous developments, we do not repeat the details here. Instead, we simply write the interpolation functions in terms of the natural coordinates and request that the reader

verify satisfaction of all nodal conditions. The interpolation functions are

$$\begin{aligned}
 N_1 &= \frac{1}{8}(1-r)(1-s)(1+t) \\
 N_2 &= \frac{1}{8}(1+r)(1-s)(1+t) \\
 N_3 &= \frac{1}{8}(1+r)(1+s)(1+t) \\
 N_4 &= \frac{1}{8}(1-r)(1+s)(1+t) \\
 N_5 &= \frac{1}{8}(1-r)(1-s)(1-t) \\
 N_6 &= \frac{1}{8}(1+r)(1-s)(1-t) \\
 N_7 &= \frac{1}{8}(1+r)(1+s)(1-t) \\
 N_8 &= \frac{1}{8}(1-r)(1+s)(1-t)
 \end{aligned} \tag{6.69}$$

and the field variable is described as

$$\phi(x, y, z) = \sum_{i=1}^8 N_i(r, s, t)\phi_i \tag{6.70}$$

If Equation 6.70 is expressed in terms of the global Cartesian coordinates, it is found to be of the form

$$\phi(x, y, z) = a_0 + a_1x + a_2y + a_3z + a_4xy + a_5xz + a_6yz + a_7xyz \tag{6.71}$$

showing that the field variable is expressed as an incomplete, symmetric polynomial. Geometric isotropy is therefore assured. The compatibility requirement is satisfied, as is the completeness condition. Recall that completeness requires that the first partial derivatives must be capable of assuming constant values (for C^0 problems). If, for example, we take the first partial derivative of Equation 6.71 with respect to x , we obtain

$$\frac{\partial \phi}{\partial x} = a_1 + a_4y + a_5z + a_7yz \tag{6.72}$$

which certainly does not appear to be constant at first glance. However, if we apply the derivative operation to Equation 6.70 while noting that

$$\frac{\partial \phi}{\partial x} = \frac{1}{a} \frac{\partial \phi}{\partial r} \tag{6.73}$$

the result is

$$\begin{aligned} \frac{\partial \phi}{\partial x} = & \frac{1}{8a}(1-s)(1+t)(\phi_2 - \phi_1) + \frac{1}{8a}(1+s)(1+t)(\phi_3 - \phi_4) \\ & + \frac{1}{8a}(1-s)(1-t)(\phi_6 - \phi_5) + \frac{1}{8a}(1+s)(1-t)(\phi_7 - \phi_8) \end{aligned} \quad (6.74)$$

Referring to Figure 6.19, observe that, if the gradient of the field variable in the x direction is constant, $\partial\phi/\partial x = C$, the nodal values are related by

$$\begin{aligned} \phi_2 &= \phi_1 + \frac{\partial \phi}{\partial x} dx = \phi_1 + C(2a) \\ \phi_3 &= \phi_4 + \frac{\partial \phi}{\partial x} dx = \phi_4 + C(2a) \\ \phi_6 &= \phi_5 + \frac{\partial \phi}{\partial x} dx = \phi_5 + C(2a) \\ \phi_7 &= \phi_8 + \frac{\partial \phi}{\partial x} dx = \phi_8 + C(2a) \end{aligned} \quad (6.75)$$

Substituting these relations into Equation 6.74, we find

$$\begin{aligned} \frac{\partial \phi}{\partial x} = & \frac{1}{8a}[(1-s)(1+t)(2aC) + (1+s)(1+t)(2aC) \\ & + (1-s)(1-t)(2aC) + (1+s)(1-t)(2aC)] \end{aligned} \quad (6.76a)$$

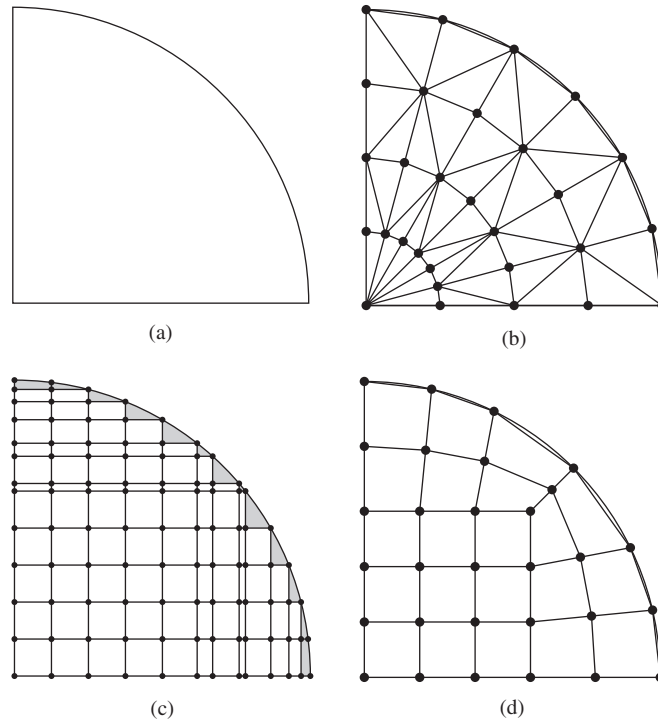
which, on expansion and simplification, results in

$$\frac{\partial \phi}{\partial x} \equiv C \quad (6.76b)$$

Observing that this result is valid at any point (r, s, t) within the element, it follows that the specified interpolation functions indeed allow for a constant gradient in the x direction. Following similar procedures shows that the other partial derivatives also satisfy the completeness condition.

6.8 ISOPARAMETRIC FORMULATION

The finite element method is a powerful technique for analyzing engineering problems involving complex, irregular geometries. However, the two- and three-dimensional elements discussed so far in this chapter (triangle, rectangle, tetrahedron, brick) cannot always be efficiently used for irregular geometries. Consider the plane area shown in Figure 6.20a, which is to be discretized via a mesh of finite elements. A possible mesh using triangular elements is shown in Figure 6.20b. Note that the outermost “row” of elements provides a chordal approximation to the circular boundary, and as the size of the elements is decreased (and the number of elements increased), the approximation becomes increasingly

**Figure 6.20**

(a) A domain to be modeled. (b) Triangular elements. (c) Rectangular elements. (d) Rectangular and quadrilateral elements.

closer to the actual geometry. However, also note that the elements in the inner “rows” become increasingly slender (i.e., the height to base ratio is large). In general, the ratio of the largest characteristic dimension of an element to the smallest characteristic dimension is known as the *aspect ratio*. Large aspect ratios increase the inaccuracy of the finite element representation and have a detrimental effect on convergence of finite element solutions [8]. An aspect ratio of 1 is ideal but cannot always be maintained. (Commercial finite element software packages provide warnings when an element’s aspect ratio exceeds some predetermined limit.) In Figure 6.20b, to maintain a reasonable aspect ratio for the inner elements, it would be necessary to reduce the height of each row of elements as the center of the sector is approached. This observation is also in keeping with the convergence requirements of the *h*-refinement method. Although the triangular element can be used to closely approximate a curved boundary, other considerations dictate a relatively large number of elements and associated computation time.

If we consider rectangular elements as in Figure 6.20c (an intentionally crude mesh for illustrative purposes), the problems are apparent. Unless the elements are very small, the area of the domain excluded from the model (the

shaded area in the figure) may be significant. For the case depicted, a large number of very small square elements best approximates the geometry.

At this point, the astute reader may think, Why not use triangular and rectangular elements in the same mesh to improve the model? Indeed, a combination of the element types can be used to improve the geometric accuracy of the model. The shaded areas of Figure 6.20c could be modeled by three-node triangular elements. Such combination of element types may not be the best in terms of solution accuracy since the rectangular element and the triangular element have, by necessity, different order polynomial representations of the field variable. The field variable is continuous across such element boundaries; this is guaranteed by the finite element formulation. However, conditions on derivatives of the field variable for the two element types are quite different. On a curved boundary such as that shown, the triangular element used to fill the “gaps” left by the rectangular elements may also have adverse aspect ratio characteristics.

Now examine Figure 6.20d, which shows the same area meshed with rectangular elements and a new element applied near the periphery of the domain. The new element has four nodes, straight sides, but is not rectangular. (Please note that the mesh shown is intentionally coarse for purposes of illustration.) The new element is known as a general two-dimensional *quadrilateral element* and is seen to mesh ideally with the rectangular element as well as approximate the curved boundary, just like the triangular element. The four-node quadrilateral element is derived from the four-node rectangular element (known as the *parent* element) element via a *mapping* process. Figure 6.21 shows the parent element and its natural (r, s) coordinates and the quadrilateral element in a global Cartesian coordinate system. The geometry of the quadrilateral element is described by

$$x = \sum_{i=1}^4 G_i(x, y)x_i \quad (6.77)$$

$$y = \sum_{i=1}^4 G_i(x, y)y_i \quad (6.78)$$

where the $G_i(x, y)$ can be considered as *geometric* interpolation functions, and each such function is associated with a particular node of the quadrilateral

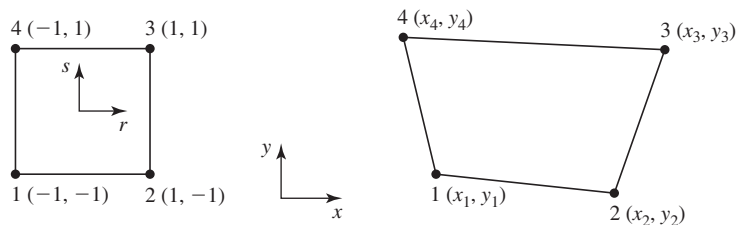


Figure 6.21 Mapping of a parent element into an isoparametric element. A rectangle is shown for example.

element. Given the geometry and the form of Equations 6.77 and 6.78, each function $G_i(x, y)$ must evaluate to unity at its associated node and to zero at each of the other three nodes.

These conditions are exactly the same as those imposed on the interpolation functions of the parent element. Consequently, the interpolation functions for the parent element can be used for the geometric functions, if we map the coordinates so that

$$\begin{aligned}(r, s) &= (-1, -1) \Rightarrow (x_1, y_1) \\(r, s) &= (1, -1) \Rightarrow (x_2, y_2) \\(r, s) &= (1, 1) \Rightarrow (x_3, y_3) \\(r, s) &= (-1, 1) \Rightarrow (x_4, y_4)\end{aligned}\tag{6.79}$$

where the symbol \Rightarrow is read as “maps to” or “corresponds to.” Note that the (r, s) coordinates used here are *not* the same as those defined by Equation 6.54. Instead, these are the actual rectangular coordinates of the 2 unit by 2 unit parent element.

Consequently, the geometric expressions become

$$\begin{aligned}x &= \sum_{i=1}^4 N_i(r, s)x_i \\y &= \sum_{i=1}^4 N_i(r, s)y_i\end{aligned}\tag{6.80}$$

Clearly, we can also express the field variable variation in the quadrilateral element as

$$\phi(x, y) = \phi(r, s) = \sum_{i=1}^4 N_i(r, s)\phi_i\tag{6.81}$$

if the mapping of Equation 6.79 is used, since all required nodal conditions are satisfied. Since the same interpolation functions are used for both the field variable and description of element geometry, the procedure is known as *isoparametric* (constant parameter) *mapping*. The element defined by such a procedure is known as an *isoparametric element*. The mapping of element boundaries is illustrated in the following example.

EXAMPLE 6.3

Figure 6.22 shows a quadrilateral element in global coordinates. Show that the mapping described by Equation 6.80 correctly describes the line connecting nodes 2 and 3 and determine the (x, y) coordinates corresponding to $(r, s) = (1, 0.5)$

■ Solution

First, we determine the equation of the line passing through nodes 2 and 3 strictly by geometry, using the equation of a two-dimensional straight line $y = mx + b$. Using the

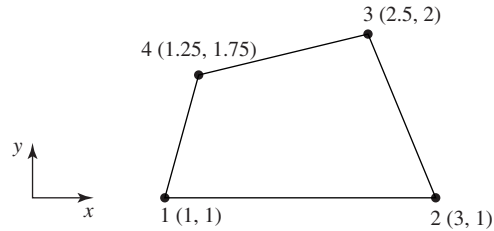


Figure 6.22 Quadrilateral element for Example 6.3.

known coordinates of nodes 2 and 3, we have

$$\text{Node 2: } 1 = 3m + b$$

$$\text{Node 3: } 2 = 2.5m + b$$

Solving simultaneously, the slope is

$$m = -2$$

and the y intercept is

$$b = 7$$

Therefore, element edge 2-3 is described by

$$y = -2x + 7$$

Using the interpolation functions given in Equation 6.56 and substituting nodal x and y coordinates, the geometric mapping of Equation 6.80 becomes

$$x = \frac{1}{4}(1-r)(1-s)(1) + \frac{1}{4}(1+r)(1-s)(3) + \frac{1}{4}(1+r)(1+s)(2.5) \\ + \frac{1}{4}(1-r)(1+s)(1.25)$$

$$y = \frac{1}{4}(1-r)(1-s)(1) + \frac{1}{4}(1+r)(1-s)(1) + \frac{1}{4}(1+r)(1+s)(2) \\ + \frac{1}{4}(1-r)(1+s)(1.75)$$

Noting that edge 2-3 corresponds to $r = 1$, the last two equations become

$$x = \frac{3}{2}(1-s) + \frac{2.5}{2}(1+s) = \frac{5.5}{2} - \frac{0.5}{2}s$$

$$y = \frac{1}{2}(1-s) + (1+s) = \frac{3}{2} + \frac{1}{2}s$$

Eliminating s gives

$$2x + y = \frac{14}{2}$$

which is the same as

$$y = -2x + 7$$

as desired.

For $(r, s) = (1, 0.5)$, we obtain

$$x = \frac{5.5}{2} - \frac{0.5}{2}(0.5) = 2.625$$

$$y = \frac{3}{2} + \frac{1}{2}(0.5) = 1.75$$

In formulating element characteristic matrices, various derivatives of the interpolation functions with respect to the global coordinates are required, as previously demonstrated. In isoparametric elements, both element geometry and variation of the interpolation functions are expressed in terms of the natural coordinates of the parent element, so some additional mathematical complication arises. Specifically, we must compute $\partial N_i / \partial x$ and $\partial N_i / \partial y$ (and, possibly, higher-order derivatives). Since the interpolation functions are expressed in (r, s) coordinates, we can formally write these derivatives as

$$\begin{aligned} \frac{\partial N_i}{\partial x} &= \frac{\partial N_i}{\partial r} \frac{\partial r}{\partial x} + \frac{\partial N_i}{\partial s} \frac{\partial s}{\partial x} \\ \frac{\partial N_i}{\partial y} &= \frac{\partial N_i}{\partial r} \frac{\partial r}{\partial y} + \frac{\partial N_i}{\partial s} \frac{\partial s}{\partial y} \end{aligned} \quad (6.82)$$

However, unless we invert the relations in Equation 6.80, the partial derivatives of the natural coordinates with respect to the global coordinates are not known. As it is virtually impossible to invert Equation 6.80 to explicit algebraic expressions, a different approach must be taken.

We take an indirect approach, by first examining the partial derivatives of the field variable with respect to the natural coordinates. From Equation 6.81, the partial derivatives of the field variable with respect to the natural coordinates can be expressed formally as

$$\begin{aligned} \frac{\partial \phi}{\partial r} &= \frac{\partial \phi}{\partial x} \frac{\partial x}{\partial r} + \frac{\partial \phi}{\partial y} \frac{\partial y}{\partial r} \\ \frac{\partial \phi}{\partial s} &= \frac{\partial \phi}{\partial x} \frac{\partial x}{\partial s} + \frac{\partial \phi}{\partial y} \frac{\partial y}{\partial s} \end{aligned} \quad (6.83)$$

In light of Equation 6.81, computation of the partial derivatives of the field variable requires the partial derivatives of each interpolation function as

$$\begin{aligned} \frac{\partial N_i}{\partial r} &= \frac{\partial N_i}{\partial x} \frac{\partial x}{\partial r} + \frac{\partial N_i}{\partial y} \frac{\partial y}{\partial r} \\ \frac{\partial N_i}{\partial s} &= \frac{\partial N_i}{\partial x} \frac{\partial x}{\partial s} + \frac{\partial N_i}{\partial y} \frac{\partial y}{\partial s} \end{aligned} \quad i = 1, 4 \quad (6.84)$$

Writing Equation 6.84 in matrix form,

$$\begin{Bmatrix} \frac{\partial N_i}{\partial r} \\ \frac{\partial N_i}{\partial s} \end{Bmatrix} = \begin{bmatrix} \frac{\partial x}{\partial r} & \frac{\partial y}{\partial r} \\ \frac{\partial x}{\partial s} & \frac{\partial y}{\partial s} \end{bmatrix} \begin{Bmatrix} \frac{\partial N_i}{\partial x} \\ \frac{\partial N_i}{\partial y} \end{Bmatrix} \quad i = 1, 4 \quad (6.85)$$

we observe that the 2×1 vector on the left-hand side is known, since the interpolation functions are expressed explicitly in the natural coordinates. Similarly, the terms in the 2×2 coefficient matrix on the right-hand side are known via Equation 6.80. The latter, known as the *Jacobian matrix*, denoted [J], is given by

$$[J] = \begin{bmatrix} \frac{\partial x}{\partial r} & \frac{\partial y}{\partial r} \\ \frac{\partial x}{\partial s} & \frac{\partial y}{\partial s} \end{bmatrix} = \begin{bmatrix} \sum_{i=1}^4 \frac{\partial N_i}{\partial r} x_i & \sum_{i=1}^4 \frac{\partial N_i}{\partial r} y_i \\ \sum_{i=1}^4 \frac{\partial N_i}{\partial s} x_i & \sum_{i=1}^4 \frac{\partial N_i}{\partial s} y_i \end{bmatrix} \quad (6.86)$$

If the inverse of the Jacobian matrix can be determined, Equation 6.85 can be solved for the partial derivatives of the interpolation functions with respect to the global coordinates to obtain

$$\begin{Bmatrix} \frac{\partial N_i}{\partial x} \\ \frac{\partial N_i}{\partial y} \end{Bmatrix} = [J]^{-1} \begin{Bmatrix} \frac{\partial N_i}{\partial r} \\ \frac{\partial N_i}{\partial s} \end{Bmatrix} = \begin{bmatrix} I_{11} & I_{12} \\ I_{21} & I_{22} \end{bmatrix} \begin{Bmatrix} \frac{\partial N_i}{\partial r} \\ \frac{\partial N_i}{\partial s} \end{Bmatrix} \quad i = 1, 4 \quad (6.87)$$

with the terms of the inverse of the Jacobian matrix denoted I_{ij} for convenience. Equation 6.87 can be used to obtain the partial derivatives of the field variable with respect to the global coordinates, as required in discretizing a governing differential equation by the finite element method. In addition, the derivatives are required in computing the “secondary” variables, including strain (then stress) in structural problems and heat flux in heat transfer. These and other problems are illustrated in subsequent chapters.

As we also know, various integrations are required to obtain element stiffness matrices and load vectors. For example, in computing the terms of the conductance matrix for two-dimensional heat transfer elements, integrals of the form

$$\iint_A \left(\frac{\partial N_i}{\partial x} \frac{\partial N_j}{\partial x} \right) dA$$

are encountered, and the integration is to be performed over the area of the element in global coordinates. However, for an isoparametric element such as the quadrilateral being discussed, the interpolation functions are in terms of the parent element coordinates. Hence, it is necessary to transform such integrals to

the natural coordinates. From Equation 6.87, we have

$$\frac{\partial N_i}{\partial x} \frac{\partial N_j}{\partial x} = \left(I_{11} \frac{\partial N_i}{\partial r} + I_{12} \frac{\partial N_i}{\partial s} \right) \left(I_{11} \frac{\partial N_j}{\partial r} + I_{12} \frac{\partial N_j}{\partial s} \right) \quad (6.88)$$

so the integrand is transformed using the terms of $[J]^{-1}$. As shown in advanced calculus [9], the differential area relationship is

$$dA = dx dy = |J| dr ds \quad (6.89)$$

so integrals of the form described previously become

$$\iint_A \left(\frac{\partial N_i}{\partial x} \frac{\partial N_j}{\partial x} \right) dA = \int_{-1}^1 \int_{-1}^1 \left(I_{11} \frac{\partial N_i}{\partial r} + I_{12} \frac{\partial N_i}{\partial s} \right) \left(I_{11} \frac{\partial N_j}{\partial r} + I_{12} \frac{\partial N_j}{\partial s} \right) |J| dr ds \quad (6.90)$$

Such integrals are discussed in greater detail in later chapters in problem-specific contexts. The intent of this discussion is to emphasize the importance of the Jacobian matrix in development of isoparametric elements.

Rather than work with individual interpolation functions, it is convenient to combine Equations 6.84 and 6.85 into matrix form as

$$\begin{Bmatrix} \frac{\partial [N]}{\partial r} \\ \frac{\partial [N]}{\partial s} \end{Bmatrix} = \begin{bmatrix} \frac{\partial x}{\partial r} & \frac{\partial y}{\partial r} \\ \frac{\partial x}{\partial s} & \frac{\partial y}{\partial s} \end{bmatrix} \begin{Bmatrix} \frac{\partial [N]}{\partial x} \\ \frac{\partial [N]}{\partial y} \end{Bmatrix} \quad (6.91)$$

where $[N]$ is the 1×4 row matrix

$$[N] = [N_1 \quad N_2 \quad N_3 \quad N_4] \quad (6.92)$$

and Equation 6.91 in matrix notation is the same as

$$\begin{Bmatrix} \frac{\partial}{\partial r} \\ \frac{\partial}{\partial s} \end{Bmatrix} [N] = \begin{bmatrix} \frac{\partial x}{\partial r} & \frac{\partial x}{\partial s} \\ \frac{\partial y}{\partial r} & \frac{\partial y}{\partial s} \end{bmatrix} \begin{Bmatrix} \frac{\partial}{\partial x} \\ \frac{\partial}{\partial y} \end{Bmatrix} [N] \quad (6.93)$$

We use this matrix notation to advantage in later chapters, when we examine specific applications.

While the isoparametric formulation just described is mathematically straightforward, the algebraic complexity is significant, as illustrated in the following example.

EXAMPLE 6.4

Determine the Jacobian matrix for a four-node, two-dimensional quadrilateral element having the parent element whose interpolation functions are given by Equation 6.56.

■ Solution

The partial derivatives of x and y with respect to r and s per Equations 6.56 and 6.80 are

$$\frac{\partial x}{\partial r} = \sum_{i=1}^4 \frac{\partial N_i}{\partial r} x_i = \frac{1}{4} [-(1-s)x_1 + (1-s)x_2 + (1+s)x_3 - (1+s)x_4]$$

$$\frac{\partial y}{\partial r} = \sum_{i=1}^4 \frac{\partial N_i}{\partial r} y_i = \frac{1}{4} [-(1-s)y_1 + (1-s)y_2 + (1+s)y_3 - (1+s)y_4]$$

$$\frac{\partial x}{\partial s} = \sum_{i=1}^4 \frac{\partial N_i}{\partial s} x_i = \frac{1}{4} [-(1-r)x_1 - (1+r)x_2 + (1+r)x_3 + (1-r)x_4]$$

$$\frac{\partial y}{\partial s} = \sum_{i=1}^4 \frac{\partial N_i}{\partial s} y_i = \frac{1}{4} [-(1-r)y_1 - (1+r)y_2 + (1+r)y_3 + (1-r)y_4]$$

The Jacobian matrix is then

$$[J] = \frac{1}{4} \begin{bmatrix} (1-s)(x_2 - x_1) + (1+s)(x_3 - x_4) & (1-s)(y_2 - y_1) + (1+s)(y_3 - y_4) \\ (1-r)(x_4 - x_1) + (1+r)(x_3 - x_2) & (1-r)(y_4 - y_1) + (1+r)(y_3 - y_2) \end{bmatrix}$$

Note that finding the inverse of this Jacobian matrix in explicit form is not an enviable task. The task is impossible except in certain special cases. For this reason, isoparametric element formulation is carried out using numerical integration, as discussed in Section 6.10.

The isoparametric formulation is by no means limited to linear parent elements. Many higher-order isoparametric elements have been formulated and used successfully [1]. Figure 6.23 depicts the isoparametric elements corresponding to the six-node triangle and the eight-node rectangle. Owing to the mapping being described by quadratic functions of the parent elements, the resulting elements have curved boundaries, which are also described by quadratic functions of the global coordinates. Such elements can be used to closely approximate irregular boundaries. However, note that curved elements do not, in general, exactly match a specified boundary curve.

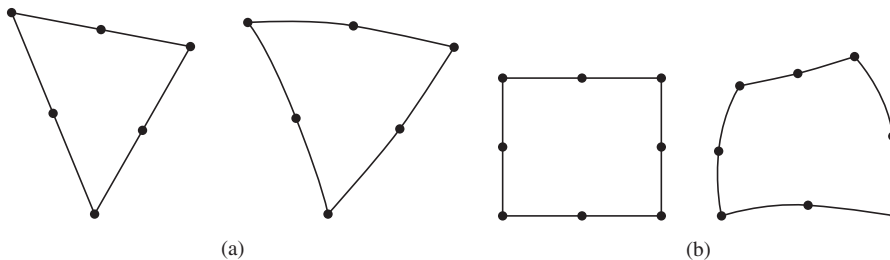


Figure 6.23 Isoparametric mapping of quadratic elements into curved elements: (a) Six-node triangle. (b) Eight-node rectangle.

6.9 AXISYMMETRIC ELEMENTS

Many three-dimensional field problems in engineering exhibit symmetry about an axis of rotation. Such problems, known as *axisymmetric problems*, can be solved using two-dimensional finite elements, which are most conveniently described in cylindrical (r, θ, z) coordinates. The required conditions for a problem to be axisymmetric are as follows:

1. The problem domain must possess an axis of symmetry, which is conventionally taken as the z axis; that is, the domain is geometrically a solid of revolution.
2. The boundary conditions are symmetric about the axis of revolution; thus, all boundary conditions are independent of the circumferential coordinate θ .
3. All loading conditions are symmetric about the axis of revolution; thus, they are also independent of the circumferential coordinate.

In addition, the material properties must be symmetric about the axis of revolution. This condition is, of course, automatically satisfied for isotropic materials.

If these conditions are met, the field variable ϕ is a function of radial and axial (r, z) coordinates only and described mathematically by two-dimensional governing equations.

Figure 6.24a depicts a cross section of an axisymmetric body assumed to be the domain of an axisymmetric problem. The cross section could represent the wall of a pressure vessel for stress or heat transfer analysis, an annular region of fluid flow, or blast furnace for steel production, to name a few examples. In

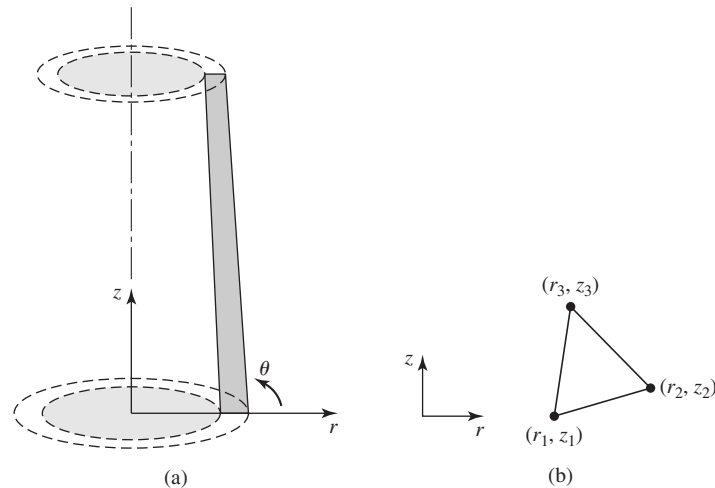


Figure 6.24

(a) An axisymmetric body and cylindrical coordinates. (b) A three-node triangle in cylindrical coordinates at an arbitrary value θ .

Figure 6.24b, a three-node triangular element is shown having nodal coordinates (r_i, z_i) . In the axisymmetric case, the field variable is discretized as

$$\phi(r, z) = \sum_{i=1}^3 N_i(r, z) \phi_i \quad (6.94)$$

where the interpolation functions $N_i(r, z)$ must satisfy the usual nodal conditions.

Noting that the nodal conditions are satisfied by the interpolation functions defined by Equation 6.37 if we simply substitute r for x and z for y , the interpolation functions for the axisymmetric triangular element are immediately obtained. Similarly, the interpolation functions in terms of area coordinates are also applicable.

Since, by definition of an axisymmetric problem, the problem, therefore its solution, is independent of the circumferential coordinate θ , so must be the interpolation functions. Consequently, any two-dimensional element and associated interpolation functions can be used for axisymmetric elements. What is the difference? The axisymmetric element is physically three dimensional. As depicted in Figure 6.25, the triangular axisymmetric element is actually a prism of revolution. The “nodes” are circles about the axis of revolution of the body, and the nodal conditions are satisfied at every point along the circumference defined by the node of a two-dimensional element. Although we use a triangular element for illustration, we reiterate that any two-dimensional element can be used to formulate an axisymmetric element.

As is shown in subsequent chapters in terms of specific axisymmetric problems, integration of various functions of the interpolation functions over the volume are required for element formulation. Symbolically, such integrals are represented as

$$F(r, \theta, z) = \iiint_V f(r, \theta, z) dV = \iiint f(r, \theta, z) r dr d\theta dz \quad (6.95)$$

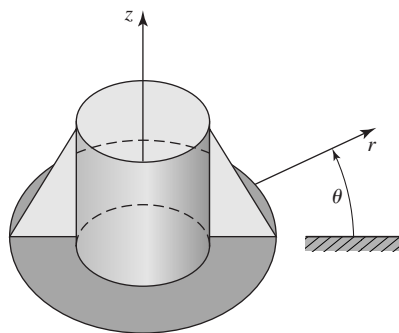


Figure 6.25 A three-dimensional representation of an axisymmetric element based on a three-node triangular element.

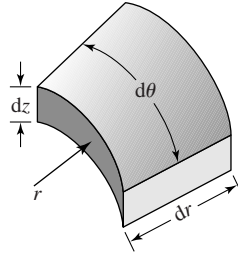


Figure 6.26 Differential volume in cylindrical coordinates.

where V is the volume of an element and $dV = r dr d\theta dz$ is the differential volume depicted in Figure 6.26. For axial symmetry, the integrand is independent of the circumferential coordinate θ , so the integration indicated in Equation 6.95 becomes

$$F(r, \theta, z) = F(r, z) = 2\pi \iint_A f(r, z)r dr dz \quad (6.96)$$

Equation 6.96 shows that the integration operations required for formulation of axisymmetric elements are distinctly different from those of two-dimensional elements, even though the interpolation functions are essentially identical. As stated, we show applications of axisymmetric elements in subsequent chapters. Also, *any* two-dimensional element can be readily converted to an axisymmetric element, provided the true three-dimensional nature of the element is taken into account when element characteristic matrices are formulated.

EXAMPLE 6.5

In following chapters, we show that integrals of the form

$$\int_V N_i N_j dV$$

where N_i, N_j are interpolation functions and V is element volume, must be evaluated in formulation of element matrices. Evaluate the integral with $i = 1, j = 2$ for an axisymmetric element based on the three-node triangle using the area coordinates as the interpolation functions.

■ Solution

For the axisymmetric element, we use Equation 6.96 to write

$$\int_V N_i N_j dV = 2\pi \int_A N_i N_j r dr dz = 2\pi \int_A L_i L_j r dr dz$$

where A is the element area. Owing to the presence of the variable r in the integrand, the integration formula, Equation 6.49, cannot be applied directly. However, we can express r in terms of the nodal coordinates r_1, r_2, r_3 and the area coordinates as

$$r = L_1 r_1 + L_2 r_2 + L_3 r_3$$

Then, noting that $dr dz = dA$, we have

$$2\pi \int_A L_i L_j r dr dz = 2\pi \int_A L_i L_j (L_1 r_1 + L_2 r_2 + L_3 r_3) dA$$

which is of the appropriate form for application of the integration formula. For $i = 1$, $j = 2$, the integral becomes

$$\begin{aligned} 2\pi \int_A L_1 L_2 r dr dz &= 2\pi \int_A L_1 L_2 (L_1 r_1 + L_2 r_2 + L_3 r_3) dA \\ &= 2\pi r_1 \int_A L_1^2 L_2 dA + 2\pi r_2 \int_A L_1 L_2^2 dA + 2\pi r_3 \int_A L_1 L_2 L_3 dA \end{aligned}$$

Applying the integration formula to each of the three integrals on the right,

$$\begin{aligned} 2\pi \int_A L_1 L_2 r dr dz &= 4\pi A \left[r_1 \frac{(2!)(1!)(0!)}{(2+1+0+2)!} + r_2 \frac{(1!)(2!)(0!)}{(1+2+0+2)!} + r_3 \frac{(1!)(1!)(1!)}{(1+1+1+2)!} \right] \\ &= 4\pi A \left(\frac{2r_1}{120} + \frac{2r_2}{120} + \frac{r_3}{120} \right) = \frac{\pi A}{30} (2r_1 + 2r_2 + r_3) \end{aligned}$$

The integration technique used in Example 6.5 is also applicable to higher-order, straight-sided triangular elements, as shown in the next example.

EXAMPLE 6.6

For an axisymmetric element based on the six-node, quadratic triangular element having interpolation functions given by Equation 6.47, evaluate the integral

$$I = \int_V N_2 N_4 dV$$

■ Solution

Using Equation 6.93,

$$I = \int_V N_2 N_4 dV = 2\pi \int_A N_2 N_4 r dr dz = 2\pi \int_A L_2 (2L_2 - 1) (4L_1 L_2) r dr dz$$

Now observe that, even though the interpolation functions vary quadratically over the element area, the area coordinates, by definition, vary linearly. Since the element sides are straight, the radial coordinate can still be expressed as

$$r = L_1 r_1 + L_2 r_2 + L_3 r_3$$

Therefore, we have

$$I = 2\pi \int_A L_2 (2L_2 - 1) (4L_1 L_2) (L_1 r_1 + L_2 r_2 + L_3 r_3) dA$$

or

$$I = 16\pi \int_A (L_1^2 L_2^3 r_1 + L_1 L_2^4 r_2 + L_1 L_2^3 L_3 r_3) dA \\ - 8\pi \int_A (L_1^2 L_2^2 r_1 + L_1 L_2^3 r_2 + L_1 L_2^2 L_3 r_3) dA$$

Application of the integration formula, Equation 6.49, to each of the six integrals represented here (left as an exercise), we find

$$I = \frac{\pi A}{315}(6r_2 - 4r_1 - 2r_3)$$

6.10 NUMERICAL INTEGRATION: GAUSSIAN QUADRATURE

Previous chapters show that integration of various functions of the field variable are required for formulation of finite element characteristic matrices. Chapter 5 reveals that the Galerkin method requires integration over the element domain (and, as seen, physical volume), once for each interpolation function (trial solution). In fact, an integration is required to obtain the value of every component of the stiffness matrix of a finite element. In addition, integrations are required to obtain nodal equivalents of nonnodal loadings.

In this chapter, we focus primarily on polynomial representations of the discretized representations of the field variable. In subsequent formulation of element characteristic matrices, we are faced with integrations of polynomial forms. A simple polynomial is relatively easy to integrate in closed form. In many cases, however, the integrands are rational functions, that is, ratios of polynomials; and these are quite tedious to integrate directly. In either case, in the finite element context, where large numbers of elements, hence huge numbers of integrations, are required, analytical methods are not efficient. Finite element software packages do not incorporate explicit integration of the element formulation equations. Instead, they use numerical techniques, the most popular of which is *Gaussian* (or *Gauss-Legendre*) quadrature [10].

The concept of Gaussian quadrature is first illustrated in one dimension in the context of an integral of the form

$$I = \int_{x_1}^{x_2} h(x) dx \quad (6.97)$$

Via the change of variable $r = ax + b$, Equation 6.97 can be converted to

$$I = \int_{-1}^1 f(r) dr \quad (6.98)$$

with $dr = a dx$. The coefficients a and b are determined so that the integration limits become minus and plus unity. This is conventional for the numerical integration procedure and also accords nicely with the range of the natural coordinates of many of the elements discussed in this chapter.

Per the Gaussian integration procedure, the integration represented by Equation 6.98 can be approximated by

$$I = \sum_{i=1}^m W_i f(r_i) \tag{6.99}$$

where W_i are Gaussian weighting factors and r_i are known as *sampling points* or *Gauss points*. The weighting factors and sampling points are determined [9] to minimize error, particularly in terms of polynomial functions. Of particular import in finite element analysis, a polynomial of order n can be *exactly* integrated. Referring to Equation 6.99, use of m sampling points and weighting factors results in an exact value of the integral for a polynomial of order $2m - 1$, if the sampling points and weighting factors are chosen in accordance with Table 6.1. This means, for example, that a cubic polynomial can be exactly integrated by Equation 6.99, using only two sampling points and evaluating the integrand at those points, multiplying by the weighting factors, and summing the results.

To illustrate how the sampling points and weighting factors are determined, we formally integrate a general polynomial in one dimension as

$$\int_{-1}^1 (a_0 + a_1 r + a_2 r^2 + a_3 r^3 + \dots + a_n r^n) dr = 2a_0 + \frac{2}{3}a_2 + \frac{2}{5}a_4 + \dots + \frac{2}{n+1}a_n \tag{6.100}$$

Table 6.1 Sampling points and weighting factors for Gaussian quadrature numerical integration of $\int_{-1}^1 f(r) dr \approx \sum_{i=1}^m W_i f(r_i)$. This is an abridged table, giving values sufficient for exact integration of a polynomial of order seven or less

m	r_i	W_i
1	0.0	2.0
2	0.577350269189626. . . -0.577350269189626. . .	1.0 1.0
3	0.0 0.774596669241483 -0.774596669241483	0.888888888888889 0.555555555555556 0.555555555555556
4	0.339981043583856 -0.339981043583856 0.861136311590453 -0.861136311590453	0.652145154862526 0.652145154862526 0.347854845137454 0.347854845137454

and we observe that, owing to the symmetry of the integration limits, all odd powers integrate to zero. Also note that we assume here that n is an even integer. The approximation to the integral per Equation 6.99 is

$$\begin{aligned}
 I \approx \sum_{i=1}^m W_i f(r_i) &= W_1(a_0 + a_1 r_1 + a_2 r_1^2 + a_3 r_1^3 + \cdots + a_n r_1^n) \\
 &+ W_2(a_0 + a_1 r_2 + a_2 r_2^2 + a_3 r_2^3 + \cdots + a_n r_2^n) \\
 &+ W_3(a_0 + a_1 r_3 + a_2 r_3^2 + a_3 r_3^3 + \cdots + a_n r_3^n) \\
 &\vdots \\
 &+ W_m(a_0 + a_1 r_m + a_2 r_m^2 + a_3 r_m^3 + \cdots + a_n r_m^n)
 \end{aligned} \tag{6.101}$$

Comparing Equations 6.100 and 6.101 in terms of the coefficients a_j of the polynomial, the approximation of Equation 6.101 becomes exact if

$$\begin{aligned}
 \sum_{i=1}^m W_i &= 2 \\
 \sum_{i=1}^m W_i r_i &= 0 \\
 \sum_{i=1}^m W_i r_i^2 &= \frac{2}{3} \\
 \sum_{i=1}^m W_i r_i^3 &= 0 \\
 \sum_{i=1}^m W_i r_i^4 &= \frac{2}{5} \\
 &\vdots \\
 \sum_{i=1}^m W_i r_i^{n-1} &= 0 \\
 \sum_{i=1}^m W_i r_i^n &= \frac{2}{n+1}
 \end{aligned} \tag{6.102}$$

where m is the number of sampling (Gauss) integration points.

Equation 6.102 represents n equations in $2m + 1$ unknowns. The unknowns are the weighting factors W_i , the sampling point values r_i , and most troublesome, the *number* of sampling points m . While we do not go into the complete theory of Gaussian quadrature, we illustrate by example how the sampling points and weights can be determined using both the equations and logic. First, note that the equations corresponding to odd powers of the polynomial indicate a zero summation. Second, note that the first equation is applicable regardless of the order of the polynomial; that is, the weighting factors must sum to the value of 2 if exactness is to be achieved.

If, for example, we have a linear polynomial $n = 1$, the first two of Equation 6.102 are applicable and lead to the conclusions that we need only one sampling point and that the appropriate values of the weighting factor and sample point to satisfy the two equations (in this case) are $W_1 = 2$ and $r_1 = 0$. Next, consider the case of a cubic polynomial, $n = 3$. In this case, we have

$$\begin{aligned}\sum_{i=1}^m W_i &= 2 \\ \sum_{i=1}^m W_i r_i &= 0 \\ \sum_{i=1}^m W_i r_i^2 &= \frac{2}{3}\end{aligned}$$

representing three equations in $2m + 1$ unknowns. If we let $m = 1$, the first two equations lead to $W_1 = 2$, $r_1 = 0$, but the third equation cannot be satisfied. On the other hand, if $m = 2$, we have

$$\begin{aligned}W_1 + W_2 &= 2 \\ W_1 r_1 + W_2 r_2 &= 0 \\ W_1 r_1^2 + W_2 r_2^2 &= \frac{2}{3}\end{aligned}$$

a system of three equations in four unknowns. We cannot directly solve these equations, but if we examine the case $W_1 = W_2 = 1$ and $r_1 = -r_2$, the first two equations are satisfied and the third equation becomes

$$r_1^2 + r_2^2 = 2r_1^2 = \frac{2}{3} \Rightarrow r_1 = \sqrt{\frac{1}{3}} = \frac{\sqrt{3}}{3} = 0.57735\dots$$

corresponding exactly to the second entry in Table 6.1. These weighting factors and Gauss points also integrate a quadratic polynomial exactly. The reader is urged to note that, because of the zero result from integrating the odd powers in the polynomial, exact results are obtained for *two* polynomial orders for each set of sampling points and weighting factors.

This discussion is by no means intended to be mathematically rigorous in terms of the theory underlying numerical integration. The intent is to give some insight as to the rationale behind the numerical values presented in Table 6.1.

EXAMPLE 6.7

Evaluate the integral

$$f(r) = \int_{-1}^1 (r^2 - 3r + 7) dr$$

using Gaussian quadrature so that the result is exact.

■ Solution

As the integrand is a polynomial of order 2, we have, for exact integration, $2m - 1 = 2$, which results in the required number of sampling points as $m = 3/2$. The calculated number of sampling points must be rounded up to the nearest integer value, so in this case, we must use two sampling points. Per Table 6.1, the sampling points are $r_i = \pm 0.5773503$ and the weighting factors are $W_i = 1.0$, $i = 1, 2$. Therefore,

$$\int_{-1}^1 (r^2 - 3r + 7) dr = (1)[(0.5773503)^2 - 3(0.5773503) + 7] \\ + (1)[(-0.5773503)^2 - 3(-0.5773503) + 7]$$

$$\int_{-1}^1 (r^2 - 3r + 7) dr = 14.666667$$

The result is readily verified as, indeed, being exact by direct integration.

The Gaussian quadrature numerical integration procedure is by no means limited to one dimension. In finite element analysis, integrals of the forms

$$I = \int_{-1}^1 \int_{-1}^1 f(r, s) dr ds \quad (6.103)$$

$$I = \int_{-1}^1 \int_{-1}^1 \int_{-1}^1 f(r, s, t) dr ds dt$$

are frequently encountered. Considering the first of Equation 6.103, we integrate first with respect to r (using the Gaussian technique) to obtain

$$I = \int_{-1}^1 \int_{-1}^1 f(r, s) dr ds = \int_{-1}^1 \sum_{i=1}^n [W_i f(r_i, s)] ds = \int_{-1}^1 g(s) ds \quad (6.104)$$

which, in turn, is integrated via quadrature to obtain

$$I = \sum_{j=1}^m W_j g(s_j) \quad (6.105)$$

combining Equations 6.98 and 6.99, we find

$$I = \int_{-1}^1 \int_{-1}^1 f(r, s) dr ds = \sum_{j=1}^m \sum_{i=1}^n W_j W_i f(r_i, s_j) \quad (6.106)$$

Equations 6.104–6.106 show that, for integration in two dimensions, we simply apply the Gaussian procedure sequentially, just as when we integrate formally. At each step, if we desire an exact result, the number of sampling points (hence, the weighting factors) is chosen by the order of the respective polynomial terms in r and s . The numerical result is exact. In practice, the number of sampling points is chosen to be the same for each integration step, with the higher-order prevailing, as illustrated in the following example.

EXAMPLE 6.8

Use Gaussian quadrature to obtain an exact value for the integral

$$I = \int_{-1}^1 \int_{-1}^1 (r^3 - 1)(s - 1)^2 dr ds$$

■ Solution

Considering first the integration with respect to r , we have a cubic order that requires two sampling points, which from Table 6.1 are given as $r_i = \pm 0.5773503$, and each of the corresponding weighting factors is unity. Similarly, for the integration with respect to s , the order is quadratic so the factors are the same. (In the following solution, we note, for simplicity of presentation, that the sampling points are numerically equal to $\sqrt{3}/3$.) Equation 6.106 is then, for this example,

$$\begin{aligned} I &= \sum_{j=1}^2 \sum_{i=1}^2 W_j W_i f(r_i, s_j) \\ &= \left[\left(\frac{\sqrt{3}}{3} \right)^3 - 1 \right] \left(\frac{\sqrt{3}}{3} - 1 \right)^2 + \left[\left(\frac{-\sqrt{3}}{3} \right)^3 - 1 \right] \left(\frac{\sqrt{3}}{3} - 1 \right)^2 \\ &\quad + \left[\left(\frac{\sqrt{3}}{3} \right)^3 - 1 \right] \left(\frac{-\sqrt{3}}{3} - 1 \right)^2 + \left[\left(\frac{-\sqrt{3}}{3} \right)^3 - 1 \right] \left(\frac{-\sqrt{3}}{3} - 1 \right)^2 = 5.33333333 \end{aligned}$$

And, as again may be verified by direct integration, the result is exact.

An analogous procedure shows that, for the three-dimensional case,

$$I = \int_{-1}^1 \int_{-1}^1 \int_{-1}^1 f(r, s, t) dr ds dt \approx \sum_{k=1}^l \sum_{j=1}^m \sum_{i=1}^n W_k W_j W_i f(r_i, s_j, t_k) \quad (6.107)$$

As in the case of one- and two-dimensional integration, the approximation described by Equation 6.107 can be made to give an exact value for a polynomial integrand if the sampling points are selected as previously described. The following example illustrates the procedure.

EXAMPLE 6.9

Use Gaussian quadrature to obtain an exact value of the integral

$$I = \int_{-1}^1 \int_{-1}^1 \int_{-1}^1 r^2(s^2 - 1)(t^4 - 2) dr ds dt$$

■ Solution

In this case, we have a quadratic polynomial in r , so two sampling points are required, with $r_i = \pm 0.5773503 = \pm\sqrt{3}/3$ and $W_i = 1$ per Table 6.1. The quadratic in s similarly requires two sampling points, $s_j = \pm 0.5773503 = \pm\sqrt{3}/3$, with weighting factors $W_j = 1.0$. For the quartic function in t , three sampling points are required for exactness and the values and weighting factors per Table 6.1 are

$$\begin{aligned} t_1 &= 0.0 & W_1 &= 0.8888889 \\ t_2 &= 0.7745967 & W_2 &= 0.5555556 \\ t_3 &= -0.7745967 & W_3 &= 0.5555556 \end{aligned}$$

For an exact solution, we then have

$$I = \sum_{k=1}^3 \sum_{j=1}^2 \sum_{i=1}^2 W_k W_j W_i f(r_i, s_j, t_k)$$

so a total of 12 terms is required. The required calculations are summarized in Table 6.2.

So we obtain

$$I = \int_{-1}^1 \int_{-1}^1 \int_{-1}^1 r^2(s^2 - 1)(t^4 - 2) dr ds dt = 3.2$$

and this result is exact.

Table 6.2 Sampling Points, Weighting Factors, and Calculations for Example 6.9

Point	r_i	s_j	t_k	W_i	W_j	W_k	$f(r_i, s_j, t_k)$	Cumulative Sum
1	0.57735	0.57735	0	1	1	0.8888889	0.395062	0.395062
2	0.57735	0.57735	0.774597	1	1	0.5555556	0.202469	0.597531
3	0.57735	0.57735	-0.774597	1	1	0.5555556	0.202469	0.8
4	0.57735	-0.57735	0	1	1	0.8888889	0.395062	1.195062
5	0.57735	-0.57735	0.774597	1	1	0.5555556	0.202469	1.397531
6	0.57735	-0.57735	-0.774597	1	1	0.5555556	0.202469	1.6
7	-0.57735	0.57735	0	1	1	0.8888889	0.395062	1.995062
8	-0.57735	0.57735	0.774597	1	1	0.5555556	0.202469	2.197531
9	-0.57735	0.57735	-0.774597	1	1	0.5555556	0.202469	2.4
10	-0.57735	-0.57735	0	1	1	0.8888889	0.395062	2.795062
11	-0.57735	-0.57735	0.774597	1	1	0.5555556	0.202469	2.997531
12	-0.57735	-0.57735	-0.774597	1	1	0.5555556	0.202469	3.2

Lest the reader be lulled into the false impression that numerical integration can always be made exact, we present the following example to illustrate that (1) numerical integration is not always exact but (2) numerical integration converges to exactness as the number of integration points is increased.

EXAMPLE 6.10

Evaluate the integral

$$I = \int_{-1}^1 \frac{r^2 - 1}{(r + 3)^2} dr$$

using Gaussian integration with one, two, and three integration points.

■ Solution

The integration procedure requires that we evaluate the integrand at discrete points and sum the results as follows (we do not present all the calculation details: the reader is urged to check our calculations)

One Integration Point

$$W_1 = 2 \quad r_1 = 0$$

$$I \approx 2 \left(\frac{-1}{3} \right) = -0.666667$$

Two Integration Points

$$W_1 = W_2 = 1 \quad r_1 = \frac{\sqrt{3}}{3} \quad r_2 = -r_1$$

$$I \approx -0.16568$$

Three Terms

$$W_1 = 0.8888888 \quad W_2 = 0.5555555 \dots \quad W_3 = -0.5555555 \dots$$

$$r_1 = 0 \quad r_{2,3} = \pm 0.7745966$$

$$I \approx -0.15923$$

Continuing with the four-point integration results in

$$I \approx -0.15891$$

Hence, we see a convergence to a value. If the exact result is obtained by formal integration, the result is $I = -0.15888$. As illustrated by this example, the Gaussian integration procedure is not always exact but does, indeed, converge to exact solutions as the number of sampling or Gauss points is increased.

6.11 CLOSING REMARKS

The developments presented in this chapter show how interpolation functions for one-, two-, and three-dimensional elements can be obtained via a systematic procedure. Also, the algebraically tedious procedure can often be bypassed using intuition and logic when natural coordinates are used. The interpolation functions discussed are standard polynomial forms but by no means exhaustive of the interpolation functions that have been developed for use in finite element analysis. For example, we make no mention of Legendre or Hermite polynomials for application to finite elements. These and other forms are well known and discussed in the finite element literature. As the objective of this text is to present the fundamentals of finite element analysis, the material of this chapter is intended to cover the basic concepts of interpolation functions without proposing to be comprehensive. The treatment here is intended to form a basis for formulation of finite element models of various physical problems in following chapters. In general, every element and the associated interpolation functions discussed here can be applied to specific problems, as is illustrated in the remainder of the text.

REFERENCES

1. Huebner, K. H., and E. A. Thornton. *The Finite Element Method for Engineers*, 2nd ed. New York: John Wiley and Sons, 1982.
2. Bathe, K. J. *Finite Element Procedures*. Englewood Cliffs, NJ: Prentice-Hall, 1996.
3. Burnett, D. S. *Finite Element Analysis*. Reading, MA: Addison-Wesley, 1987.
4. Zienkiewicz, O. C. *The Finite Element Method*, 3rd ed. London: McGraw-Hill, 1977.
5. Stasa, F. L. *Applied Finite Element Analysis for Engineers*. New York: Holt, Rinehart, and Winston, 1985.
6. *ANSYS Element Reference Manual*. Houston, PA: Swanson Analysis Systems, 1999.
7. Eisenberg, M. A., and L. E. Malvern. "On Finite Element Integration in Natural Coordinates." *International Journal for Numerical Methods in Engineering* 7 (1973).
8. Logan, D. L. *A First Course in the Finite Element Method Using ALGOR*. Boston: PWS Publishing Company, 1997.
9. Kreyszig, E. *Advanced Engineering Mathematics*, 8th ed. New York: John Wiley, 1999.
10. Stroud, A. H., and D. Secrest. *Gaussian Quadrature Formulas*. Englewood Cliffs, NJ: Prentice-Hall, 1966.

PROBLEMS

- 6.1 Verify that Equation 6.6, with the interpolation functions given by Equation 6.16, allows for rigid body translation of a two-dimensional beam element. (Hint: For the rigid body translation, $v_1 = v_2$, $\theta_1 = \theta_2 = 0$.)

- 6.2 Verify that Equation 6.6, with the interpolation functions given by Equation 6.16, allows for rigid body rotation of a two-dimensional beam element.
- 6.3 Consider the case of a two-dimensional beam element subjected to pure bending. Show that Equation 6.6 results in $d^2v/dx^2 = \text{constant}$, as required.
- 6.4 Show that shear force in a two-dimensional beam element is constant regardless of the values of the nodal displacements.
- 6.5 Show that interpolations function $N_1(s)$ in Example 6.1 is the same as

$$N_1(s) = \frac{(s - s_2)(s - s_3)(s - s_4)}{(s_1 - s_2)(s_1 - s_3)(s_1 - s_4)}$$

(Note: $N_1(s)$, as just given, is a particular case of the *Lagrange polynomial* of order n

$$L_j(s) = \prod_{i=1, i \neq j}^n \frac{s - s_i}{s_j - s_i}$$

where the symbol \prod indicates the product of all terms.)

- 6.6 Use the definition of the Lagrange polynomial given in Problem 6.5 to find the cubic polynomials corresponding to $j = 2$ and $j = 3$.
- 6.7 Use the Lagrange polynomial to determine the interpolation functions for the five-node line element shown in Figure P6.7.

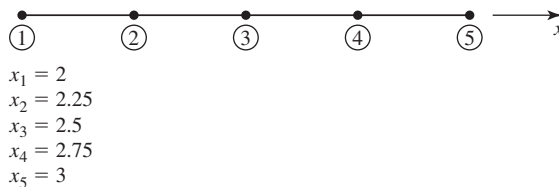


Figure P6.7

- 6.8 The quadratic polynomial

$$P(x, y) = a_0 + a_1x^2 + a_2xy + a_3y^2$$

is incomplete but symmetric. Is this function suitable for representing the field variable in a four-node rectangular element having 1 degree of freedom per node? Explain.

- 6.9 Determine all possible symmetric, incomplete fourth-order polynomials in two dimensions. Which of these might be useful for C^0 problems in finite element analysis?
- 6.10 Repeat Problem 6.9 for cubic polynomials in three dimensions.
- 6.11 Derive Equation 6.38.
- 6.12 Show that Equations 6.36 and 6.43 are identical.
- 6.13 Using area coordinates, develop interpolation functions for the 10-node triangular element shown in Figure P6.13. Note that the nodes are equally spaced on their edges.

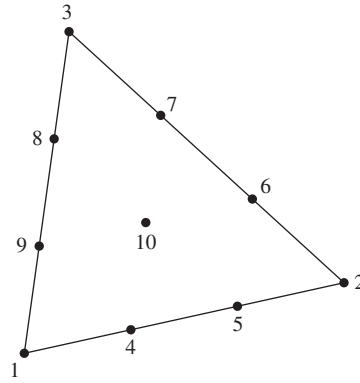


Figure P6.13

- 6.14 Show that node 10 in Figure P6.13 is located at the element centroid.
 6.15 Use the integration formula for area coordinates to evaluate the following integrals in terms of total area A :

a.
$$\iint_A L_2^2(2L_2 - 1)^2 dA$$

b.
$$\iint_A 4L_1L_2L_3(2L_1 - 1) dA$$

c.
$$\iint_A L_1^3L_2L_3 dA$$

d.
$$\iint_A L_1L_2^3L_3 dA$$

- 6.16 The interpolation functions for the four-node rectangular element as given by Equation 6.56 are such that

$$\sum_{i=1}^4 N_i(r, s) = 1$$

What is the significance of this observation?

- 6.17 Show that Equation 6.56 is such that constant values of the partial derivatives $\partial\phi/\partial r$, $\partial\phi/\partial s$ are possible in an element. Note that this ensures satisfaction of the completeness requirement for C^0 problems.
 6.18 Two three-node triangular elements share a common boundary, as shown in Figure P6.18. Show that the field variable ϕ is continuous across this interelement boundary.

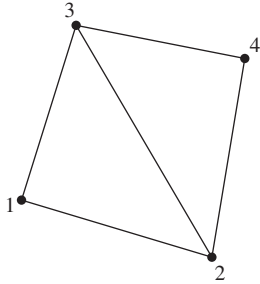


Figure P6.18

- 6.19 Repeat Problem 6.18 for the two four-node rectangular elements shown in Figure P6.19. The interpolation functions are as given by Equation 6.56.

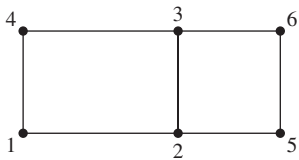


Figure P6.19

- 6.20 Examine the behavior of the partial derivatives $\partial\phi/\partial r$, $\partial\phi/\partial s$ across and along the interelement boundary defined by nodes 2 and 3 in Problem 6.19.
- 6.21 Determine the continuity conditions on ϕ and the partial derivatives $\partial\phi/\partial r$, $\partial\phi/\partial s$ on the boundary between the two eight-node rectangular elements shown in Figure P6.21. The interpolation functions are given by Equation 6.59.

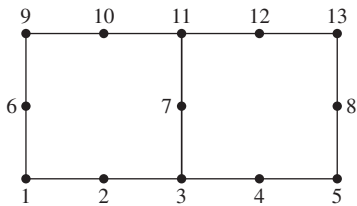


Figure P6.21

- 6.22 Verify that the interpolation functions given by Equations 6.59 satisfy the condition

$$\sum_{i=1}^8 N_i(r, s) = 1$$

- 6.23 Verify that Equation 6.62 correctly defines the volume of a tetrahedron.
- 6.24 In Example 6.5, the expression $r = L_1r_1 + L_2r_2 + L_3r_3$ is used to allow application of the integration formula in area coordinates. Prove that this expression is correct.

- 6.25 Use the integration formula of Equation 6.49 to confirm the result of Example 6.6.
- 6.26 Use the integration formula for area coordinates to show that

$$A = \int_A dA = \iint dx dy = \int_0^1 \int_0^{1-L_2} dL_1 dL_2$$

- 6.27 Consider the isoparametric quadrilateral element in Figure P6.27. Map the point $r = 0.5, s = 0$ in the parent element to the corresponding physical point in the quadrilateral element.

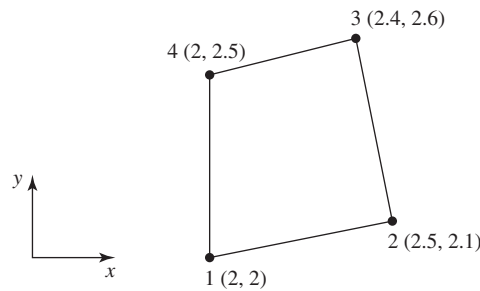


Figure P6.27

- 6.28 Again referring to the element in Figure P6.27, map the line $r = 0$ in the parent element to the physical element. Plot the mapping on a scaled drawing of the quadrilateral element.
- 6.29 Repeat Problem 6.28 for the line $s = 0$ in the parent element.
- 6.30 Consider the two-node line element in Figure P6.30 with interpolation functions

$$N_1(r) = 1 - r \quad N_2(r) = r$$

Using this as the parent element, examine the isoparametric mapping

$$x = N_1(r)x_1 + N_2(r)x_2$$

for arbitrary values x_1 and x_2 such that $x_1 < x_2$.

- a. What has been accomplished by the mapping?
- b. Determine the Jacobian matrix for the transformation.

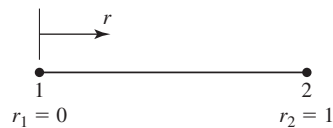


Figure P6.30

- 6.31 Consider the three-node line element in Figure P6.31 with interpolation functions

$$N_1(r) = (2r - 1)(r - 1)$$

$$N_2(r) = 4r(1 - r)$$

$$N_3(r) = r(2r - 1)$$

Use the element as the parent element in the isoparametric mapping

$$x = N_1(r)x_1 + N_2(r)x_2 + N_3(r)x_3$$

with $x_1 < x_2 < x_3$ but otherwise arbitrary nodal coordinates.

- How does the x coordinate vary between nodes of the isoparametric element?
- Has the basic element geometry changed from that of the parent element?
- Determine the Jacobian matrix for the transformation.
- Find the inverse of the Jacobian matrix.

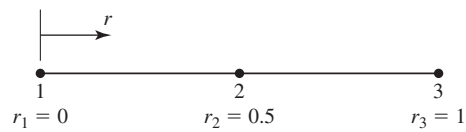


Figure P6.31

- 6.32** Consider again the three-node line element of Figure P6.31 as the parent element for the two-dimensional mapping defined by

$$x = N_1(r)x_1 + N_2(r)x_2 + N_2(r)x_3$$

$$y = N_1(r)y_1 + N_2(r)y_2 + N_2(r)y_3$$

where (x_i, y_i) are the coordinates of node i .

- Let $(x_1, y_1) = (1, 1)$, $(x_2, y_2) = (2, 3)$, $(x_3, y_3) = (4, 2)$ and plot the geometry of the isoparametric element to scale.
 - Could the resulting isoparametric element be used in a finite element analysis of heat conduction (refer to Chapter 5) through a curved solid with ideally insulated surfaces? Explain your answer.
- 6.33** Show by analytical integration that the result given in Example 6.9 is exact.
- 6.34** Use Gaussian quadrature to obtain exact values for the following integrals. Verify exactness by analytical integration.

a. $\int_0^3 (x^2 - 1) dx$

b. $\int_1^6 (y^3 + 2y) dy$

c. $\int_{-1}^1 (4r^3 + r) dr$

d. $\int_{-1}^1 (r^4 + 3r^2) dr$

e. $\int_{-1}^1 (r^4 + r^3 + r^2 + r + 1) dr$

6.35 Use Gaussian quadrature to obtain exact values for the following integrals in two dimensions. Verify exactness by analytical integration.

a.
$$\int_0^1 \int_0^2 xy \, dx \, dy$$

b.
$$\int_{-1}^1 \int_{-1}^1 (r^2 + 2rs + s^2) \, dr \, ds$$

c.
$$\int_{-1}^1 \int_{-1}^1 (r^3 - 1)(s^2 + s) \, dr \, ds$$

d.
$$\int_{-1}^1 \int_{-1}^1 (r^5 - 2r^3)(s^3 + s) \, dr \, ds$$

e.
$$\int_{-1}^1 \int_{-1}^1 (6r^4 - 1)(s^2 + s + 1) \, dr \, ds$$

6.36 Use Gaussian quadrature to obtain exact values for the following three-dimensional integrals. Verify exactness by analytical integration.

a.
$$\int_0^2 \int_0^2 \int_0^2 xyz \, dx \, dy \, dz$$

b.
$$\int_{-1}^1 \int_{-1}^1 \int_{-1}^1 t(r-1)(s^2-2) \, dr \, ds \, dt$$

c.
$$\int_{-1}^1 \int_{-1}^1 \int_{-1}^1 t^3 r^3 s^2 \, dr \, ds \, dt$$

d.
$$\int_{-1}^1 \int_{-1}^1 \int_{-1}^1 t^2 (r-2)^4 (s^2-1) \, dr \, ds \, dt$$

e.
$$\int_{-1}^1 \int_{-1}^1 \int_{-1}^1 (r^3 - r)(s+4)(t^2-1) \, dr \, ds \, dt$$

6.37 Evaluate each of the following integrals using two-point Gaussian quadrature. Compare each result with the corresponding analytical solution.

a.
$$\int_{-1}^1 \cos^2 \pi r \, dr$$

b.
$$\int_{-1}^1 \frac{r}{r^2 + 1} dr$$

c.
$$\int_{-1}^1 \sin \pi r \cos \pi r dr$$

d.
$$\int_{-1}^1 \int_{-1}^1 \frac{r^2 s}{(r^3 + s^2)} dr ds$$

6.38 Repeat Problem 6.37 using three-point Gaussian quadrature. Are the results converging to the exact solutions?

6.39 The integral

$$\int_{-1}^1 (r^3 + 2r^2 + 1) dr$$

can be evaluated exactly by using two-point Gaussian quadrature. Examine the effect on the result if three-point integration is applied.

7

CHAPTER

Applications in Heat Transfer

7.1 INTRODUCTION

In this chapter, the Galerkin method introduced in Chapter 5 and the interpolation function concepts of Chapter 6 are applied to several heat transfer situations. Conduction with convection is discussed for one-, two-, and three-dimensional problems. Boundary conditions and forcing functions include prescribed heat flux, insulated surfaces, prescribed temperatures, and convection. The one-dimensional case of heat transfer with mass transport is also developed. The three-dimensional case of axial symmetry is developed in detail using appropriately modified two-dimensional elements and interpolation functions. Heat transfer by radiation is not discussed, owing to the nonlinear nature of radiation effects. However, we examine transient heat transfer and include an introduction to finite difference techniques for solution of transient problems.

7.2 ONE-DIMENSIONAL CONDUCTION: QUADRATIC ELEMENT

Chapter 5 introduced the concept of one-dimensional heat conduction via the Galerkin finite element method. In the examples of Chapter 5, linear, two-node finite elements are used to illustrate the concepts involved. Given the development of the general interpolation concepts in Chapter 6, we now apply a higher-order (quadratic) element to a previous example to demonstrate that (1) the basic procedure of element formulation is unchanged, (2) the system assembly procedure is unchanged, and (3) the results are quite similar.

EXAMPLE 7.1

Solve Example 5.4 using two, three-node line elements with equally spaced nodes. The problem and numerical data are repeated here as Figure 7.1a.

■ Solution

Per Equation 5.62, the element equations are

$$k_x A N_i(x) \left. \frac{dT}{dx} \right|_{x_1}^{x_2} - k_x A \int_{x_1}^{x_2} \frac{dN_i}{dx} \frac{dT}{dx} dx + A \int_{x_1}^{x_2} Q N_i(x) dx = 0 \quad i = 1, 3$$

where now there are three interpolation functions per element.

The interpolation functions for a three-node line element are, per Equations 6.23–6.25

$$N_1(s) = 2 \left(s - \frac{1}{2} \right) (s - 1)$$

$$N_2(s) = -4s(s - 1)$$

$$N_3(s) = 2s \left(s - \frac{1}{2} \right)$$

The components of the conductance matrix are then calculated as

$$k_{ij} = k_x A \int_{x_1}^{x_2} \frac{dN_i}{dx} \frac{dN_j}{dx} dx \quad i, j = 1, 3$$

and the heat generation vector components are

$$f_{Qi} = A \int_{x_1}^{x_2} Q N_i dx \quad i = 1, 3$$

and all f_Q components are zero in this example, as there is no internal heat source.

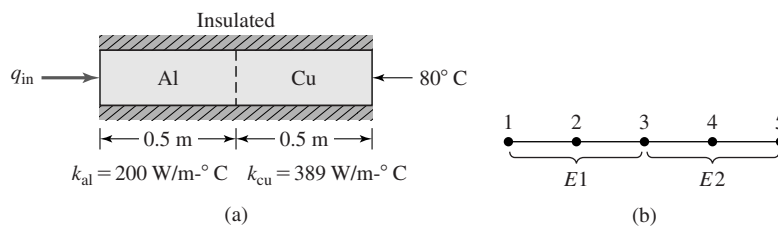


Figure 7.1

(a) Geometry and data for Example 7.1, outside diameter = 60 mm, $q_{in} = 4000 \text{ W/m}^2$. (b) Two-element model, using quadratic elements.

In terms of the dimensionless coordinate $s = x/L$, we have $dx = Lds$ and $d/dx = (1/L)d/ds$, so the terms of the conductance matrix are expressed as

$$k_{ij} = \frac{k_x A}{L} \int_0^1 \frac{dN_i}{ds} \frac{dN_j}{ds} ds \quad i, j = 1, 3$$

The derivatives of the interpolation functions are

$$\frac{dN_1}{ds} = 4s - 3$$

$$\frac{dN_2}{ds} = 4(1 - 2s)$$

$$\frac{dN_3}{ds} = 4s - 1$$

Therefore, on substitution for the derivatives,

$$\begin{aligned} k_{11} &= \frac{k_x A}{L} \int_0^1 (4s - 3)^2 ds = \frac{k_x A}{L} \int_0^1 (16s^2 - 24s + 9) ds \\ &= \frac{k_x A}{L} \left(\frac{16s^3}{3} - 12s^2 + 9s \right)_0^1 = \frac{7k_x A}{3L} \end{aligned}$$

Via mathematically identical procedures, the remaining terms of the conductance matrix are found to be

$$k_{12} = k_{21} = -\frac{8k_x A}{3L}$$

$$k_{13} = k_{31} = \frac{k_x A}{3L}$$

$$k_{22} = \frac{16k_x A}{3L}$$

$$k_{23} = k_{32} = -\frac{8k_x A}{3L}$$

$$k_{33} = \frac{7k_x A}{3L}$$

A two-element model with node numbers is shown in Figure 7.1b. Substituting numerical values, we obtain, for the aluminum half of the rod (element 1),

$$[k^{(1)}] = \frac{200(\pi/4)(0.006)^2}{3(0.5)} \begin{bmatrix} 7 & -8 & 1 \\ -8 & 16 & -8 \\ 1 & -8 & 7 \end{bmatrix} = \begin{bmatrix} 2.6389 & -3.0159 & 0.3770 \\ -3.0159 & 6.0319 & -3.0159 \\ 0.3770 & -3.0159 & 2.6389 \end{bmatrix}$$

7.2 One-Dimensional Conduction: Quadratic Element

225

and for the copper portion (element 2),

$$[k^{(2)}] = \frac{389(\pi/4)(0.006)^2}{3(0.5)} \begin{bmatrix} 7 & -8 & 1 \\ -8 & 16 & -8 \\ 1 & -8 & 7 \end{bmatrix} = \begin{bmatrix} 5.1327 & -5.8660 & 0.7332 \\ -5.8660 & 11.7320 & -5.8660 \\ 0.7332 & -5.8660 & 5.1327 \end{bmatrix}$$

At the internal nodes of each element, the flux terms are zero, owing to the nature of the interpolation functions [$N_2(x_1) = N_2(x_2) = 0$]. Similarly, at the junction between the two elements, the flux must be continuous and the equivalent “forcing” functions are zero. As no internal heat is generated, $Q = 0$, that portion of the force vector is zero for each element. Following the direct assembly procedure, the system conductance matrix is found to be

$$[K] = \begin{bmatrix} 2.6389 & -3.0159 & 0.3770 & 0 & 0 \\ -3.0159 & 6.0319 & -3.0159 & 0 & 0 \\ 0.3770 & -3.0159 & 7.7716 & -5.8660 & 0.7332 \\ 0 & 0 & -5.8660 & 11.7320 & -5.8660 \\ 0 & 0 & 0.7332 & -5.8660 & 5.1327 \end{bmatrix} \text{ W}^\circ\text{C}$$

and we note in particular that “overlap” exists only at the juncture between elements. The gradient term at node 1 is computed as

$$f_{g1} = -k_x A \left. \frac{dT}{dx} \right|_{x_1} = q_1 A = 4000 \left(\frac{\pi}{4} \right) (0.06)^2 = 11.3097 \text{ W}$$

while the heat flux at node 5 is an unknown to be calculated via the system equations.

The system equations are given by

$$\begin{bmatrix} 2.6389 & -3.0159 & 0.3770 & 0 & 0 \\ -3.0159 & 6.0319 & -3.0159 & 0 & 0 \\ 0.3770 & -3.0159 & 7.7716 & -5.8660 & 0.7332 \\ 0 & 0 & -5.8660 & 11.7320 & -5.8660 \\ 0 & 0 & 0.7332 & -5.8660 & 5.1327 \end{bmatrix} \begin{Bmatrix} T_1 \\ T_2 \\ T_3 \\ T_4 \\ 80 \end{Bmatrix} = \begin{Bmatrix} 11.3097 \\ 0 \\ 0 \\ 0 \\ -Aq_5 \end{Bmatrix}$$

Prior to solving for the unknown nodal temperatures T_1 – T_4 , the nonhomogeneous boundary condition $T_5 = 80^\circ\text{C}$ must be accounted for properly. In this case, we reduce the system of equations to 4×4 by transposing the last term of the third and fourth equations to the right-hand side to obtain

$$\begin{bmatrix} 2.3689 & -3.0159 & 0.3770 & 0 \\ -3.0159 & 6.0319 & -3.0159 & 0 \\ 0.3770 & -3.0159 & 7.7716 & -5.8660 \\ 0 & 0 & -5.8660 & 11.7320 \end{bmatrix} \begin{Bmatrix} T_1 \\ T_2 \\ T_3 \\ T_4 \end{Bmatrix} = \begin{Bmatrix} 11.3907 \\ 0 \\ -0.7332(80) \\ 5.8660(80) \end{Bmatrix}$$

$$= \begin{Bmatrix} 11.3097 \\ 0 \\ -58.6560 \\ 489.2800 \end{Bmatrix}$$

Solving the equations by Gaussian elimination (Appendix C), the nodal temperatures are

$$T_1 = 95.11^\circ\text{C}$$

$$T_2 = 90.14^\circ\text{C}$$

$$T_3 = 85.14^\circ\text{C}$$

$$T_4 = 82.57^\circ\text{C}$$

and the heat flux at node 5 is calculated using the fifth equation

$$-Aq_5 = 0.7332T_3 - 5.8660T_4 + 5.1327(80)$$

to obtain

$$q_5 = 4001.9 \text{ W/m}^2$$

which is observed to be in quite reasonable numerical agreement with the heat input at node 1.

The solution for the nodal temperatures in this example is identical for both the linear and quadratic interpolation functions. In fact, the solution we obtained is the exact solution (Problem 7.1) represented by a linear temperature distribution in each half of the bar. It can be shown [1] that, if an exact solution exists and the interpolation functions used in the finite element formulation include the terms appearing in the exact solution, then the finite element solution corresponds to the exact solution. In this example, the quadratic interpolation functions include the linear terms in addition to the quadratic terms and thus capture the exact, linear solution. The following example illustrates this feature in terms of the field variable representation.

EXAMPLE 7.2

For the quadratic field variable representation

$$\phi(x) = a_0 + a_1x + a_2x^2$$

determine the explicit form of the coefficients a_0, a_1, a_2 in terms of the nodal variables if the three nodes are equally spaced. Then use the results of Example 7.1 to show $a_2 = 0$ for that example.

■ Solution

Using the interpolation functions from Example 7.1, we can write the field variable representation in terms of the dimensionless variable s as

$$\phi(s) = (2s^2 - 3s + 1)\phi_1 + 4(s - s^2)\phi_2 + (2s^2 - s)\phi_3$$

Collecting coefficients of similar powers of s ,

$$\phi(s) = \phi_1 + (4\phi_2 - 3\phi_1 - \phi_3)s + (2\phi_1 - 4\phi_2 + 2\phi_3)s^2$$

Therefore,

$$\begin{aligned}a_0 &= \phi_1 \\a_1 &= 4\phi_2 - 3\phi_1 - \phi_3 \\a_2 &= 2\phi_1 - 4\phi_2 + 2\phi_3\end{aligned}$$

Using the temperature results of Example 7.1 for the aluminum element, we have

$$\begin{aligned}\phi_1 &= T_1 = 95.14 \\ \phi_2 &= T_2 = 90.14 \\ \phi_3 &= T_3 = 85.14 \\ a_2 &= 2(95.14) - 4(90.14) + 2(85.14) = 0\end{aligned}$$

For element 2, representing the copper portion of the bar, the same result is obtained.

7.3 ONE-DIMENSIONAL CONDUCTION WITH CONVECTION

One-dimensional heat conduction, in which no heat flows from the surface of the body under consideration (as in Figure 5.8), is not commonly encountered. A more practical situation exists when the body is surrounded by a fluid medium and heat flow occurs from the surface to the fluid via *convection*. Figure 7.2a shows a solid body, which we use to develop a one-dimensional model of heat transfer including both conduction and convection. Note that the representation is the same as in Figure 5.8 with the very important exception that the assumption of an insulated surface is removed. Instead, the body is assumed to be surrounded by a fluid medium to which heat is transferred by convection. If the fluid is in motion as a result of some external influence (a fan or pump, for example), the convective heat transfer is referred to as *forced convection*. On the other hand, if motion of the fluid exists only as a result of the heat transfer taking place, we have *natural convection*. Figure 7.2b depicts a control volume of differential length, which is assumed to have a constant cross-sectional area and uniform

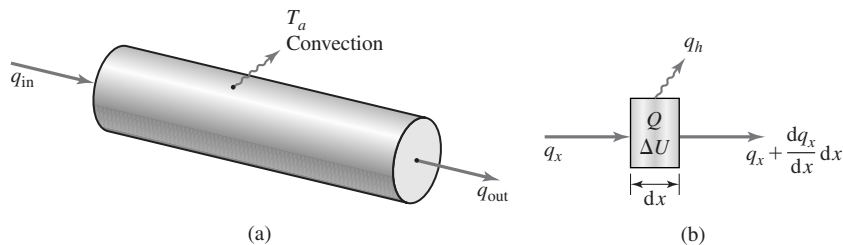


Figure 7.2 One-dimensional conduction with surface convection. (a) General model. (b) Differential element as a control volume.

material properties. The convective heat transfer across the surface, denoted q_h , represents the heat flow rate (heat flux) across the surface per unit *surface* area. To apply the principle of conservation of energy to the control volume, we need only add the convection term to Equation 5.54 to obtain

$$q_x A dt + Q A dx dt = \Delta U + \left(q_x + \frac{\partial q_x}{\partial x} dx \right) A dt + q_h P dx dt \quad (7.1)$$

where all terms are as previously defined except that P is the peripheral dimension of the differential element and q_h is the heat flux due to convection. The convective heat flux is given by [2]

$$q_h = h(T - T_a) \quad (7.2)$$

where

h = convection coefficient, $W/(m^2 \cdot ^\circ C)$, $Btu/(hr \cdot ft^2 \cdot ^\circ F)$

T = temperature of surface of the body

T_a = ambient fluid temperature

Substituting for q_h and assuming steady-state conditions such that $\Delta U = 0$, Equation 7.1 becomes

$$QA = A \frac{dq_x}{dx} + hP(T - T_a) \quad (7.3)$$

which, via Fourier's law Equation 5.55, becomes

$$k_x \frac{d^2 T}{dx^2} + Q = \frac{hP}{A}(T - T_a) \quad (7.4)$$

where we have assumed k_x to be constant.

While Equation 7.4 represents the one-dimensional formulation of conduction with convection, note that the temperature at any position x along the length of the body is not truly constant, owing to convection. Nevertheless, if the cross-sectional area is small relative to the length, the one-dimensional model can give useful results if we recognize that the computed temperatures represent average values over a cross section.

7.3.1 Finite Element Formulation

To develop the finite element equations, a two-node linear element for which

$$T(x) = N_1(x)T_1 + N_2(x)T_2 \quad (7.5)$$

is used in conjunction with Galerkin's method. For Equation 7.4, the residual equations (in analogy with Equation 5.61) are expressed as

$$\int_{x_1}^{x_2} \left[k_x \frac{d^2 T}{dx^2} + Q - \frac{hP}{A}(T - T_a) \right] N_i(x) A dx = 0 \quad i = 1, 2 \quad (7.6)$$

7.3 One-Dimensional Conduction with Convection

229

or

$$\begin{aligned}
 & A \int_{x_1}^{x_2} k_x \frac{d^2 T}{dx^2} N_i(x) dx - hP \int_{x_1}^{x_2} T(x) N_i(x) dx + A \int_{x_1}^{x_2} Q N_i(x) dx \\
 & + hPT_a \int_{x_1}^{x_2} N_i(x) dx = 0 \quad i = 1, 2
 \end{aligned} \quad (7.7)$$

Integrating the first term by parts and rearranging,

$$\begin{aligned}
 & k_x A \int_{x_1}^{x_2} \frac{dN_i}{dx} \frac{dT}{dx} dx + hP \int_{x_1}^{x_2} T(x) N_i(x) dx \\
 & = A \int_{x_1}^{x_2} Q N_i(x) dx + hPT_a \int_{x_1}^{x_2} N_i(x) dx + k_x A N_i(x) \left. \frac{dT}{dx} \right|_{x_1}^{x_2} \quad i = 1, 2
 \end{aligned} \quad (7.8)$$

Substituting for $T(x)$ from Equation 7.5 yields

$$\begin{aligned}
 & k_x A \int_{x_1}^{x_2} \frac{dN_i}{dx} \left(\frac{dN_1}{dx} T_1 + \frac{dN_2}{dx} T_2 \right) dx + hP \int_{x_1}^{x_2} N_i(x) [N_1(x) T_1 + N_2(x) T_2] dx \\
 & = A \int_{x_1}^{x_2} Q N_i(x) dx + hPT_a \int_{x_1}^{x_2} N_i(x) dx + k_x A N_i(x) \left. \frac{dT}{dx} \right|_{x_1}^{x_2} \quad i = 1, 2
 \end{aligned} \quad (7.9)$$

The two equations represented by Equation 7.9 are conveniently combined into a matrix form by rewriting Equation 7.5 as

$$T(x) = [N_1 \quad N_2] \begin{Bmatrix} T_1 \\ T_2 \end{Bmatrix} = [N]\{T\} \quad (7.10)$$

and substituting to obtain

$$\begin{aligned}
 & k_x A \int_{x_1}^{x_2} \left[\frac{dN}{dx} \right]^T \left[\frac{dN}{dx} \right] \{T\} dx + hP \int_{x_1}^{x_2} [N]^T [N] \{T\} dx \\
 & = A \int_{x_1}^{x_2} Q [N]^T dx + hPT_a \int_{x_1}^{x_2} [N]^T dx + k_x A [N]^T \left. \frac{dT}{dx} \right|_{x_1}^{x_2}
 \end{aligned} \quad (7.11)$$

Equation 7.11 is in the desired finite element form:

$$[k^{(e)}] \{T\} = \{f_Q^{(e)}\} + \{f_h^{(e)}\} + \{f_g^{(e)}\} \quad (7.12)$$

where $[k^{(e)}]$ is the conductance matrix defined as

$$[k^{(e)}] = k_x A \int_{x_1}^{x_2} \left[\frac{dN}{dx} \right]^T \left[\frac{dN}{dx} \right] dx + hP \int_{x_1}^{x_2} [N]^T [N] dx \quad (7.13)$$

The first integral is identical to that in Equation 5.66, representing the axial conduction effect, while the second integral accounts for convection.

Without loss of generality, we let $x_1 = 0$, $x_2 = L$ so that the interpolation functions are

$$\begin{aligned} N_1 &= 1 - \frac{x}{L} \\ N_2 &= \frac{x}{L} \end{aligned} \quad (7.14)$$

The results of the first integral are as given in Equation 5.68, so we need perform only the integrations indicated in the second term (Problem 7.2) to obtain

$$[k^{(e)}] = \frac{k_x A}{L} \begin{bmatrix} 1 & -1 \\ -1 & 1 \end{bmatrix} + \frac{hPL}{6} \begin{bmatrix} 2 & 1 \\ 1 & 2 \end{bmatrix} = [k_c^{(e)}] + [k_h^{(e)}] \quad (7.15)$$

where $[k_c^{(e)}]$ and $[k_h^{(e)}]$ represent the conductive and convective portions of the matrix, respectively. Note particularly that both portions are symmetric.

The forcing function vectors on the right-hand side of Equation 7.12 include the internal heat generation and boundary flux terms, as in Chapter 5. These are given by

$$\{f_Q^{(e)}\} = A \begin{Bmatrix} \int_0^L Q N_1 dx \\ 0 \\ \int_0^L Q N_2 dx \\ 0 \end{Bmatrix} \quad (7.16)$$

$$\{f_g^{(e)}\} = k_x A \begin{Bmatrix} -\frac{dT}{dx} \Big|_0 \\ \frac{dT}{dx} \Big|_L \end{Bmatrix} = A \begin{Bmatrix} q_{x=0} \\ -q_{x=L} \end{Bmatrix} = A \begin{Bmatrix} q_1 \\ -q_2 \end{Bmatrix} \quad (7.17)$$

where q_1 and q_2 are the boundary flux values at nodes 1 and 2, respectively. In addition, the forcing function arising from convection is

$$\{f_h^{(e)}\} = hPT_a \begin{Bmatrix} \int_0^L N_1 dx \\ 0 \\ \int_0^L N_2 dx \\ 0 \end{Bmatrix} = \frac{hPT_a L}{2} \begin{Bmatrix} 1 \\ 1 \end{Bmatrix} \quad (7.18)$$

where it is evident that the total element convection force is simply allocated equally to each node, like constant internal heat generation Q .

7.3 One-Dimensional Conduction with Convection

231

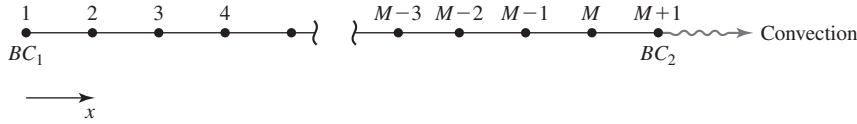


Figure 7.3 Convection boundary condition at node $M + 1$ of an M -element, one-dimensional heat transfer finite element model.

7.3.2 Boundary Conditions

In the one-dimensional case of heat transfer under consideration, two boundary conditions must be specified. Typically, this means that, if the finite element model of the problem is composed of M elements, one boundary condition is imposed at node 1 of element 1 and the second boundary condition is imposed at node 2 of element M . The boundary conditions are of three types:

1. *Imposed temperature.* The temperature at an end node is a known value; this condition occurs when an end of the body is subjected to a constant process temperature and heat is removed from the process by the body.
2. *Imposed heat flux.* The heat flow rate into, or out of, an end of the body is specified; while distinctly possible in a mathematical sense, this type of boundary condition is not often encountered in practice.
3. *Convection through an end node.* In this case, the end of the body is in contact with a fluid of known ambient temperature and the conduction flux at the boundary is removed via convection to the fluid media. Assuming that this condition applies at node 2 of element M of the finite element model, as in Figure 7.3, the convection boundary condition is expressed as

$$k_x \left. \frac{dT}{dx} \right|_{M+1} = -q_{M+1} = -h(T_{M+1} - T_a) \quad (7.19)$$

indicating that the conduction heat flux at the end node must be carried away by convection at that node. The area for convection in Equation 7.19 is the cross-sectional area of element M ; as this area is common to each of the three terms in the equation, the area has been omitted. An explanation of the algebraic signs in Equation 7.19 is appropriate here. If $T_{M+1} > T_a$, the temperature gradient is negative (given the positive direction of the x axis as shown); therefore, the flux and convection are positive terms.

The following example illustrates application of the one-dimensional conduction/convection problem.

EXAMPLE 7.3

Figure 7.4a depicts a cylindrical pin that is one of several in a small heat exchange device. The left end of the pin is subjected to a constant temperature of 180°F . The right end of the pin is in contact with a chilled water bath maintained at constant temperature of 40°F .

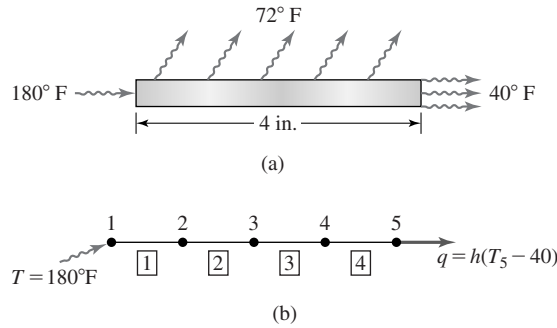


Figure 7.4 Example 7.3: (a) Cylindrical pin. (b) Finite element model.

The exterior surface of the pin is in contact with moving air at 72°F. The physical data are given as follows:

$$D = 0.5 \text{ in.}, \quad L = 4 \text{ in.}, \quad k_x = 120 \text{ Btu}/(\text{hr}\cdot\text{ft}\cdot^\circ\text{F}),$$

$$h_{\text{air}} = 50 \text{ Btu}/(\text{hr}\cdot\text{ft}^2\cdot^\circ\text{F}), \quad h_{\text{water}} = 100 \text{ Btu}/(\text{hr}\cdot\text{ft}^2\cdot^\circ\text{F})$$

Use four equal-length, two-node elements to obtain a finite element solution for the temperature distribution across the length of the pin and the heat flow rate through the pin.

■ Solution

Figure 7.4b shows the elements, node numbers, and boundary conditions. The boundary conditions are expressed as follows

At node 1: $T_1 = 180^\circ\text{F}$

At node 5: $k_x \left. \frac{dT}{dx} \right|_5 = -q_5 = -h(T_5 - 40)$

Element geometric data is then

$$L_e = 1 \text{ in.}, \quad P = \pi(0.5) = 1.5708 \text{ in.}, \quad A = (\pi/4)(0.5)^2 = 0.1963 \text{ in.}^2$$

The leading coefficients of the conductance matrix terms are

$$\frac{k_x A}{L_e} = \frac{120 \left(\frac{0.1963}{144} \right)}{\frac{1}{12}} = 1.9630 \text{ Btu}/(\text{hr}\cdot^\circ\text{F})$$

$$\frac{h_{\text{air}} P L_e}{6} = \frac{50 \left(\frac{1.5708}{12} \right) \left(\frac{1}{12} \right)}{6} = 0.0909 \text{ Btu}/(\text{hr}\cdot^\circ\text{F})$$

where conversion from inches to feet is to be noted.

7.3 One-Dimensional Conduction with Convection

233

Substituting into Equation 7.15, the element conductance matrix is

$$[k^{(e)}] = 1.9630 \begin{bmatrix} 1 & -1 \\ -1 & 1 \end{bmatrix} + 0.0909 \begin{bmatrix} 2 & 1 \\ 1 & 2 \end{bmatrix} = \begin{bmatrix} 2.1448 & -1.8721 \\ -1.8721 & 2.1448 \end{bmatrix}$$

Following the direct assembly procedure, the system conductance matrix is

$$[K] = \begin{bmatrix} 2.1448 & -1.8721 & 0 & 0 & 0 \\ -1.8721 & 4.2896 & -1.8721 & 0 & 0 \\ 0 & -1.8721 & 4.2896 & -1.8721 & 0 \\ 0 & 0 & -1.8721 & 4.2896 & -1.8721 \\ 0 & 0 & 0 & -1.8721 & 2.1448 \end{bmatrix}$$

As no internal heat is generated, $f_Q = 0$. The element convection force components per Equation 7.18 are

$$\{f_h^{(e)}\} = \frac{hPT_aL}{2} \begin{Bmatrix} 1 \\ 1 \end{Bmatrix} = \frac{50 \left(\frac{1.5708}{12} \right) (72) \left(\frac{1}{12} \right)}{2} = \begin{Bmatrix} 19.6375 \\ 19.6375 \end{Bmatrix} \text{ Btu/hr}$$

Assembling the contributions of each element at the nodes gives the system convection force vector as

$$\{F_h\} = \begin{Bmatrix} 19.6375 \\ 39.2750 \\ 39.2750 \\ 39.2750 \\ 19.6375 \end{Bmatrix} \text{ Btu/hr}$$

Noting the cancellation of terms at nodal connections, the system gradient vector becomes simply

$$\{F_g\} = \begin{Bmatrix} Aq_1 \\ 0 \\ 0 \\ 0 \\ -Aq_5 \end{Bmatrix} = \begin{Bmatrix} Aq_1 \\ 0 \\ 0 \\ 0 \\ -Ah_{\text{water}}(T_5 - 40) \end{Bmatrix} = \begin{Bmatrix} Aq_1 \\ 0 \\ 0 \\ 0 \\ -0.1364T_5 + 5.4542 \end{Bmatrix} \text{ Btu/hr}$$

and the boundary condition at the pin-water interface has been explicitly incorporated. Note that, as a result of the convection boundary condition, a term containing unknown nodal temperature T_5 appears in the gradient vector. This term is transposed in the final equations and results in an increase in value of the K_{55} term of the system matrix. The final assembled equations are

$$\begin{bmatrix} 2.1448 & -1.8721 & 0 & 0 & 0 \\ -1.8721 & 4.2896 & -1.8721 & 0 & 0 \\ 0 & -1.8721 & 4.2896 & -1.8721 & 0 \\ 0 & 0 & -1.8721 & 4.2896 & -1.8721 \\ 0 & 0 & 0 & -1.8721 & 2.2812 \end{bmatrix} \begin{Bmatrix} 180 \\ T_2 \\ T_3 \\ T_4 \\ T_5 \end{Bmatrix} = \begin{Bmatrix} 19.6375 + Aq_1 \\ 39.2750 \\ 39.2750 \\ 39.2750 \\ 25.0917 \end{Bmatrix}$$

Eliminating the first equation while taking care to include the effect of the specified temperature at node 1 on the remaining equations gives

$$\begin{bmatrix} 4.2896 & -1.8571 & 0 & 0 \\ -1.8721 & 4.2896 & -1.8721 & 0 \\ 0 & -1.8721 & 4.2896 & -1.8721 \\ 0 & 0 & -1.8721 & 2.2812 \end{bmatrix} \begin{Bmatrix} T_2 \\ T_3 \\ T_4 \\ T_5 \end{Bmatrix} = \begin{Bmatrix} 376.2530 \\ 39.2750 \\ 39.2750 \\ 25.0917 \end{Bmatrix}$$

Solving by Gaussian elimination, the nodal temperatures are obtained as

$$T_2 = 136.16^\circ\text{F}$$

$$T_3 = 111.02^\circ\text{F}$$

$$T_4 = 97.23^\circ\text{F}$$

$$T_5 = 90.79^\circ\text{F}$$

The heat flux at node 1 is computed by back substitution of T_2 into the first equation:

$$2.1448(180) - 1.8721(136.16) = 19.6375 + Aq_1$$

$$Aq_1 = 111.5156 \text{ Btu/hr}$$

$$q_1 = \frac{111.5156}{0.1963/144} \approx 81,805 \text{ Btu/hr-ft}^2$$

Although the pin length in this example is quite small, use of only four elements represents a coarse element mesh. To illustrate the effect, recall that, for the linear, two-node element the first derivative of the field variable, in this case, the temperature gradient, is constant; that is,

$$\frac{dT}{dx} = \frac{\Delta T}{\Delta x} = \frac{\Delta T}{L_e}$$

Using the computed nodal temperatures, the element gradients are

$$\text{Element 1: } \frac{dT}{dx} = \frac{136.16 - 180}{1} = -43.84 \frac{^\circ\text{F}}{\text{in.}}$$

$$\text{Element 2: } \frac{dT}{dx} = \frac{111.02 - 136.16}{1} = -25.14 \frac{^\circ\text{F}}{\text{in.}}$$

$$\text{Element 3: } \frac{dT}{dx} = \frac{97.23 - 111.02}{1} = -13.79 \frac{^\circ\text{F}}{\text{in.}}$$

$$\text{Element 4: } \frac{dT}{dx} = \frac{90.79 - 97.23}{1} = -6.44 \frac{^\circ\text{F}}{\text{in.}}$$

where the length is expressed in inches for numerical convenience. The computed gradient values show significant discontinuities at the nodal connections. As the number of elements is increased, the magnitude of such jump discontinuities in the gradient values decrease significantly as the finite element approximation approaches the true solution.

Table 7.1 Nodal Temperature Solutions

x (inches)	Four Elements, T (°F)	Eight Elements, T (°F)
0	180	180
0.5	158.08*	155.31
1.0	136.16	136.48
1.5	123.59*	122.19
2.0	111.02	111.41
2.5	104.13*	103.41
3.0	97.23	97.62
3.5	94.01*	93.63
4.0	90.79	91.16

To illustrate convergence as well as the effect on gradient values, an eight-element solution was obtained for this problem. Table 7.1 shows the nodal temperature solutions for both four- and eight-element models. Note that, in the table, values indicated by * are interpolated, nonnodal values.

7.4 HEAT TRANSFER IN TWO DIMENSIONS

A case in which heat transfer can be considered to be adequately described by a two-dimensional formulation is shown in Figure 7.5. The rectangular fin has dimensions $a \times b \times t$, and thickness t is assumed small in comparison to a and b . One edge of the fin is subjected to a known temperature while the other three edges and the faces of the fin are in contact with a fluid. Heat transfer then occurs from the core via conduction through the fin to its edges and faces, where convection takes place. The situation depicted could represent a cooling fin removing heat from some process or a heating fin moving heat from an energy source to a building space.

To develop the governing equations, we refer to a differential element of a solid body that has a small dimension in the z direction, as in Figure 7.6, and examine the principle of conservation of energy for the differential element. As we now deal with two dimensions, all derivatives are partial derivatives. Again, on the edges $x + dx$ and $y + dy$, the heat flux terms have been expanded in first-order Taylor series. We assume that the differential element depicted is in the interior of the body, so that convection occurs only at the surfaces of the element and not along the edges. Applying Equation 5.53 under the assumption of steady-state conditions (i.e., $\Delta U = 0$), we obtain

$$\begin{aligned}
 q_x t dy + q_y t dx + Q t dy dx = & \left(q_x + \frac{\partial q_x}{\partial x} dx \right) t dy + \left(q_y + \frac{\partial q_y}{\partial y} dy \right) t dx \\
 & + 2h(T - T_a) dy dx \qquad (7.20)
 \end{aligned}$$

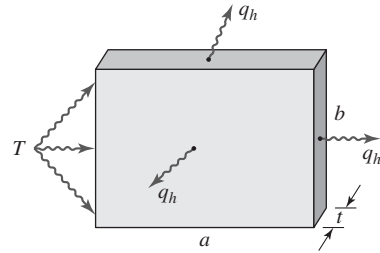


Figure 7.5 Two-dimensional conduction fin with face and edge convection.

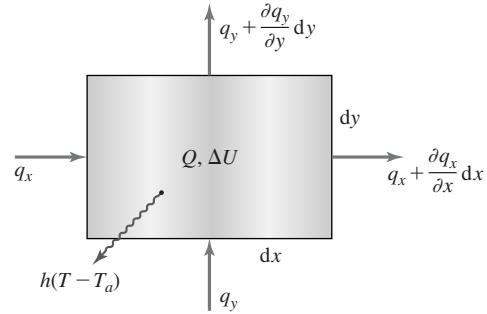


Figure 7.6 Differential element depicting two-dimensional conduction with surface convection.

where

t = thickness

h = the convection coefficient from the surfaces of the differential element

T_a = the ambient temperature of the surrounding fluid

Utilizing Fourier's law in the coordinate directions

$$\begin{aligned} q_x &= -k_x \frac{\partial T}{\partial x} \\ q_y &= -k_y \frac{\partial T}{\partial y} \end{aligned} \tag{7.21}$$

then substituting and simplifying yields

$$Q t \, dy \, dx = \frac{\partial}{\partial x} \left(-k_x \frac{\partial T}{\partial x} \right) t \, dy \, dx + \frac{\partial}{\partial y} \left(-k_y \frac{\partial T}{\partial y} \right) t \, dy \, dx + 2h(T - T_a) \, dy \, dx \tag{7.22}$$

where k_x and k_y are the thermal conductivities in the x and y directions, respectively. Equation 7.22 simplifies to

$$\frac{\partial}{\partial x} \left(t k_x \frac{\partial T}{\partial x} \right) + \frac{\partial}{\partial y} \left(t k_y \frac{\partial T}{\partial y} \right) + Q t = 2h(T - T_a) \tag{7.23}$$

Equation 7.23 is the governing equation for two-dimensional conduction with convection from the surfaces of the body. Convection from the edges is also possible, as is subsequently discussed in terms of the boundary conditions.

7.4.1 Finite Element Formulation

In developing a finite element approach to two-dimensional conduction with convection, we take a general approach initially; that is, a specific element geometry is not used. Instead, we assume a two-dimensional element having M nodes

such that the temperature distribution in the element is described by

$$T(x, y) = \sum_{i=1}^M N_i(x, y) T_i = [N]\{T\} \quad (7.24)$$

where $N_i(x, y)$ is the interpolation function associated with nodal temperature T_i , $[N]$ is the row matrix of interpolation functions, and $\{T\}$ is the column matrix (vector) of nodal temperatures.

Applying Galerkin's finite element method, the residual equations corresponding to Equation 7.23 are

$$\iint_A N_i(x, y) \left[\frac{\partial}{\partial x} \left(t k_x \frac{\partial T}{\partial x} \right) + \frac{\partial}{\partial y} \left(t k_y \frac{\partial T}{\partial y} \right) + Q t - 2h(T - T_a) \right] dA = 0 \quad i = 1, M \quad (7.25)$$

where thickness t is assumed constant and the integration is over the area of the element. (Strictly speaking, the integration is over the volume of the element, since the volume is the domain of interest.) To develop the finite element equations for the two-dimensional case, a bit of mathematical manipulation is required.

Consider the first two integrals in Equation 7.25 as

$$\begin{aligned} t \iint_A \left[\frac{\partial}{\partial x} \left(k_x \frac{\partial T}{\partial x} \right) N_i + \frac{\partial}{\partial y} \left(k_y \frac{\partial T}{\partial y} \right) N_i \right] dA \\ = -t \iint_A \left(\frac{\partial q_x}{\partial x} N_i + \frac{\partial q_y}{\partial y} N_i \right) dA \end{aligned} \quad (7.26)$$

and note that we have used Fourier's law per Equation 7.21. For illustration, we now assume a rectangular element, as shown in Figure 7.7a, and examine

$$t \iint_A \frac{\partial q_x}{\partial x} N_i dA = t \int_{y_1}^{y_2} \int_{x_1}^{x_2} \frac{\partial q_x}{\partial x} N_i dx dy \quad (7.27)$$

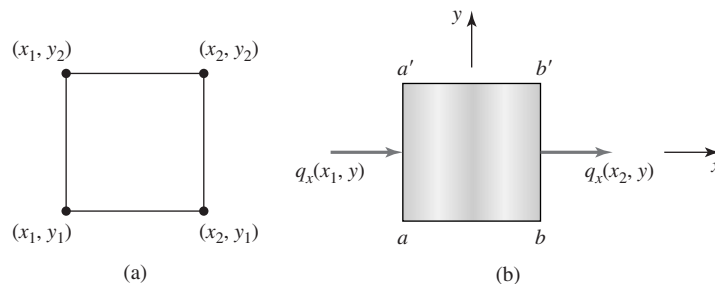


Figure 7.7 Illustration of boundary heat flux in x direction.

Integrating by parts on x with $u = N_i$ and $dv = \frac{\partial q_x}{\partial x} dx$, we obtain, formally,

$$\begin{aligned} t \iint_A \frac{\partial q_x}{\partial x} N_i dA &= t \int_{y_1}^{y_2} q_x N_i \Big|_{x_1}^{x_2} dy - t \int_{y_1}^{y_2} \int_{x_1}^{x_2} q_x \frac{\partial N_i}{\partial x} dx dy \\ &= t \int_{y_1}^{y_2} q_x N_i \Big|_{x_1}^{x_2} dy + t \int_A k_x \frac{\partial T}{\partial x} \frac{\partial N_i}{\partial x} dA \end{aligned} \quad (7.28)$$

Now let us examine the physical significance of the term

$$t \int_{y_1}^{y_2} q_x N_i \Big|_{x_1}^{x_2} dy = t \int_{y_1}^{y_2} [q_x(x_2, y) N_i(x_2, y) - q_x(x_1, y) N_i(x_1, y)] dy \quad (7.29)$$

The integrand is the weighted value (N_i is the scalar weighting function) of the heat flux in the x direction across edges $a-a'$ and $b-b'$ in Figure 7.7b. Hence, when we integrate on y , we obtain the *difference* in the weighted heat flow rate in the x direction across $b-b'$ and $a-a'$, respectively. Noting the obvious fact that the heat flow rate in the x direction across horizontal boundaries $a-b$ and $a'-b'$ is zero, the integral over the area of the element is equivalent to an integral around the periphery of the element, as given by

$$t \iint_A q_x N_i dA = t \oint_S q_x N_i n_x dS \quad (7.30)$$

In Equation 7.30, S is the periphery of the element and n_x is the x component of the *outward* unit vector normal (perpendicular) to the periphery. In our example, using a rectangular element, we have $n_x = 1$ along $b-b'$, $n_x = 0$ along $b'-a'$, $n_x = -1$ along $a'-a$, and $n_x = 0$ along $a-b$. Note that the use of the normal vector component ensures that the directional nature of the heat flow is accounted for properly. For theoretical reasons beyond the scope of this text, the integration around the periphery S is to be taken in the counterclockwise direction; that is, positively, per the right-hand rule.

An identical argument and development will show that, for the y -direction terms in equation Equation 7.26,

$$t \iint_A \frac{\partial}{\partial y} \left(k_y \frac{\partial T}{\partial y} \right) N_i dA = -t \oint_S q_y N_i n_y dS - \int_A k_y \frac{\partial T}{\partial y} \frac{\partial N_i}{\partial y} dA \quad (7.31)$$

These arguments, based on the specific case of a rectangular element, are intended to show an application of a general relation known as the *Green-Gauss theorem* (also known as *Green's theorem in the plane*) stated as follows: *Let $F(x, y)$ and $G(x, y)$ be continuous functions defined in a region of the x - y plane*

(for our purposes the region is the area of an element); then

$$\begin{aligned} \iint_A \left(\beta \frac{\partial F}{\partial x} + \beta \frac{\partial G}{\partial y} \right) &= \oint_S (\beta F n_x + \beta G n_y) dS \\ &\quad - \iint_A \left(\frac{\partial F}{\partial x} \frac{\partial \beta}{\partial x} + \frac{\partial G}{\partial y} \frac{\partial \beta}{\partial y} \right) dA \end{aligned} \quad (7.32)$$

Returning to Equation 7.26, we let $F = k_x \frac{\partial T}{\partial x}$, $G = k_y \frac{\partial T}{\partial y}$, and $\beta = N_i(x, y)$, and apply the Green-Gauss theorem to obtain

$$\begin{aligned} t \iint_A \left[\frac{\partial}{\partial x} \left(k_x \frac{\partial T}{\partial x} \right) N_i + \frac{\partial}{\partial y} \left(\frac{\partial T}{\partial y} \right) N_i \right] dA \\ = -t \oint_S (q_x n_x + q_y n_y) N_i dS - t \iint_A \left(k_x \frac{\partial T}{\partial x} \frac{\partial N_i}{\partial x} + k_y \frac{\partial T}{\partial y} \frac{\partial N_i}{\partial y} \right) dA \end{aligned} \quad (7.33)$$

Application of the Green-Gauss theorem, as in this development, is the two-dimensional counterpart of integration by parts in one dimension. The result is that we have introduced the boundary gradient terms as indicated by the first integral on the right-hand side of Equation 7.33 and ensured that the conductance matrix is symmetric, per the second integral, as will be seen in the remainder of the development.

Returning to the Galerkin residual equation represented by Equation 7.25 and substituting the relations developed via the Green-Gauss theorem (being careful to observe arithmetic signs), Equation 7.25 becomes

$$\begin{aligned} \iint_A \left(k_x \frac{\partial T}{\partial x} \frac{\partial N_i}{\partial x} + k_y \frac{\partial T}{\partial y} \frac{\partial N_i}{\partial y} \right) t dA + 2h \iint_A T N_i dA \\ = \iint_A Q N_i t dA + 2h T_a \iint_A N_i dA - t \oint_S (q_x n_x + q_y n_y) N_i dS \quad i = 1, M \end{aligned} \quad (7.34)$$

as the system of M equations for the two-dimensional finite element formulation via Galerkin's method. In analogy with the one-dimensional case of Equation 7.8, we observe that the left-hand side includes the unknown temperature distribution while the right-hand side is composed of forcing functions, representing internal heat generation, surface convection, and boundary heat flux.

At this point, we convert to matrix notation for ease of illustration by employing Equation 7.24 to convert Equation 7.34 to

$$\begin{aligned} \iint_A \left(k_x \left[\frac{\partial N}{\partial x} \right]^T \left[\frac{\partial N}{\partial x} \right] + k_y \left[\frac{\partial N}{\partial y} \right]^T \left[\frac{\partial N}{\partial y} \right] \right) \{T\} t dA + 2h \iint_A [N]^T [N] \{T\} dA \\ = \iint_A Q [N]^T t dA + 2h T_a \iint_A [N]^T dA - \oint_S q_s n_s [N]^T t dS \end{aligned} \quad (7.35)$$

which is of the form

$$[k^{(e)}] \{T\} = \{f_Q^{(e)}\} + \{f_h^{(e)}\} + \{f_g^{(e)}\} \quad (7.36)$$

as desired.

Comparison of Equations 7.35 and 7.36 shows that the conductance matrix is

$$\begin{aligned} [k^{(e)}] = & \iint_A \left(k_x \left[\frac{\partial N}{\partial x} \right]^T \left[\frac{\partial N}{\partial x} \right] + k_y \left[\frac{\partial N}{\partial y} \right]^T \left[\frac{\partial N}{\partial y} \right] \right) t \, dA \\ & + 2h \iint_A [N]^T [N] \, dA \end{aligned} \quad (7.37)$$

which for an element having M nodes is an $M \times M$ symmetric matrix. While we use the term *conductance matrix*, the first integral term on the right of Equation 7.37 represents the conduction “stiffness,” while the second integral represents convection from the lateral surfaces of the element to the surroundings. If the lateral surfaces do not exhibit convection (i.e., the surfaces are insulated), the convection terms are removed by setting $h = 0$. Note that, in many finite element software packages, the convection portion of the conductance matrix is not automatically included in element matrix formulation. Instead, lateral surface (as well as edge) convection effects are specified by applying convection “loads” to the surfaces as appropriate. The software then modifies the element matrices as required.

The element forcing functions are described in column matrix (vector) form as

$$\begin{aligned} \{f_Q^{(e)}\} &= \iint_A Q [N]^T t \, dA = \iint_A Q \{N\} t \, dA \\ \{f_h^{(e)}\} &= 2hT_a \iint_A [N]^T \, dA = 2hT_a \iint_A \{N\} \, dA \\ \{f_g^{(e)}\} &= - \oint_S q_s n_s [N]^T t \, dS = - \oint_S q_s n_s \{N\} t \, dS \end{aligned} \quad (7.38)$$

where $[N]^T = \{N\}$ is the $M \times 1$ column matrix of interpolation functions.

Equations 7.36–7.38 represent the general formulation of a finite element for two-dimensional heat conduction with convection from the surfaces. Note in particular that these equations are valid for an arbitrary element having M nodes and, therefore, any order of interpolation functions (linear, quadratic, cubic, etc.). In following examples, use of specific element geometries are illustrated.

7.4.2 Boundary Conditions

The boundary conditions for two-dimensional conduction with convection may be of three types, as illustrated by Figure 7.8 for a general two-dimensional domain. On portion S_1 of the boundary, the temperature is prescribed as a known

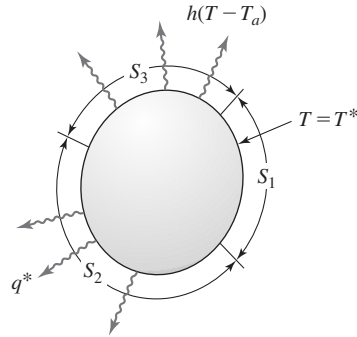


Figure 7.8 Types of boundary conditions for two-dimensional conduction with convection.

constant value $T_{S1} = T^*$. In a finite element model of such a domain, every element node located on S_1 has known temperature and the corresponding nodal equilibrium equations become “reaction” equations. The reaction “forces” are the heat fluxes at the nodes on S_1 . In using finite element software packages, such conditions are input data; the user of the software (“FE programmer”) enters such data as appropriate at the applicable nodes of the finite element model (in this case, specified temperatures).

The heat flux on portion S_2 of the boundary is prescribed as $q_{S2} = q^*$. This is analogous to specified nodal forces in a structural problem. Hence, for all elements having nodes on S_2 , the third of Equation 7.38 gives the corresponding nodal forcing functions as

$$\{f_g^{(e)}\} = - \oint_{S_2} q^* n_{S_2} \{N\} t \, dS \quad (7.39)$$

Finally, a portion S_3 of the boundary illustrates an edge convection condition. In this situation, the heat flux at the boundary must be equilibrated by the convection loss from S_3 . For all elements having edges on S_3 , the convection condition is expressed as

$$\{f_g^{(e)}\} = - \oint_{S_3} q_{S_3} n_{S_3} \{N\} t \, dS = - \oint_{S_3} h(T^{(e)} - T_a) \{N\} t \, dS \quad (7.40)$$

Noting that the right-hand side of Equation 7.40 involves the nodal temperatures, we rewrite the equation as

$$\{f_g^{(e)}\} = - \oint_{S_3} h[N]^T [N] \{T\} t \, dS_3 + \oint_{S_3} h T_a \{N\} t \, dS_3 \quad (7.41)$$

and observe that, when inserted into Equation 7.36, the first integral term on the right of Equation 7.41 adds stiffness to specific terms of the conductance matrix

associated with nodes on S_3 . To generalize, we rewrite Equation 7.41 as

$$\{f_g^{(e)}\} = -[k_{hS}^{(e)}]\{T\} + \{f_{hS}^{(e)}\} \quad (7.42)$$

where

$$[k_{hS}^{(e)}] = \oint_S h[N]^T [N] t \, dS \quad (7.43)$$

is the contribution to the element conductance matrix owing to convection on portion S of the element boundary and

$$\{f_{hS}^{(e)}\} = \oint_S h T_a \{N\} t \, dS \quad (7.44)$$

is the forcing function associated with convection on S .

Incorporating Equation 7.42 into Equation 7.36, we have

$$[k^{(e)}]\{T\} = \{f_Q^{(e)}\} + \{f_h^{(e)}\} + \{f_g^{(e)}\} + \{f_{hS}^{(e)}\} \quad (7.45)$$

where the element conductance matrix is now given by

$$\begin{aligned} [k^{(e)}] = & \iint_A \left(k_x \left[\frac{\partial N}{\partial x} \right]^T \left[\frac{\partial N}{\partial x} \right] + k_y \left[\frac{\partial N}{\partial y} \right]^T \left[\frac{\partial N}{\partial y} \right] \right) t \, dA \\ & + 2h \iint_A [N]^T [N] \, dA + h \oint_S [N]^T [N] t \, dS \end{aligned} \quad (7.46)$$

which now explicitly includes edge convection on portion(s) S of the element boundary subjected to convection.

EXAMPLE 7.4

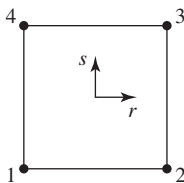


Figure 7.9 Element node numbering for Example 7.4; the length of each edge is 1 in.

Determine the conductance matrix (excluding edge convection) for a four-node, rectangular element having 0.5 in. thickness and equal sides of 1 in. The material has thermal properties $k_x = k_y = 20$ Btu/(hr-ft-°F) and $h = 50$ Btu/(hr-ft²-°F).

■ Solution

The element with node numbers is as shown in Figure 7.9 and the interpolation functions, Equation 6.56, are

$$N_1(r, s) = \frac{1}{4}(1-r)(1-s)$$

$$N_2(r, s) = \frac{1}{4}(1+r)(1-s)$$

7.4 Heat Transfer in Two Dimensions

243

$$N_3(r, s) = \frac{1}{4}(1+r)(1+s)$$

$$N_4(r, s) = \frac{1}{4}(1-r)(1+s)$$

in terms of the normalized coordinates r and s . For the 1-in. square element, we have $2a = 2b = 1$ and $dA = dx dy = ab dr ds$. The partial derivatives in terms of the normalized coordinates, via the chain rule, are

$$\frac{\partial N_i}{\partial x} = \frac{\partial N_i}{\partial r} \frac{\partial r}{\partial x} = \frac{1}{a} \frac{\partial N_i}{\partial r} \quad i = 1, 4$$

$$\frac{\partial N_i}{\partial y} = \frac{\partial N_i}{\partial s} \frac{\partial s}{\partial y} = \frac{1}{b} \frac{\partial N_i}{\partial s} \quad i = 1, 4$$

Therefore, Equation 7.37 becomes

$$\begin{aligned} [k^{(e)}] &= \int_{-1}^1 \int_{-1}^1 \left(k_x \left[\frac{\partial N}{\partial r} \right]^T \left[\frac{\partial N}{\partial r} \right] \frac{1}{a^2} + k_y \left[\frac{\partial N}{\partial s} \right]^T \left[\frac{\partial N}{\partial s} \right] \frac{1}{b^2} \right) tab dr ds \\ &\quad + 2h \int_{-1}^1 [N]^T [N] ab dr ds \end{aligned}$$

or, on a term by term basis,

$$\begin{aligned} k_{ij} &= \int_{-1}^1 \int_{-1}^1 \left(k_x \frac{\partial N_i}{\partial r} \frac{\partial N_j}{\partial r} \frac{1}{a^2} + k_y \frac{\partial N_i}{\partial s} \frac{\partial N_j}{\partial s} \frac{1}{b^2} \right) tab dr ds \\ &\quad + 2h \int_{-1}^1 \int_{-1}^1 N_i N_j ab dr ds \quad i, j = 1, 4 \end{aligned}$$

or

$$\begin{aligned} k_{ij} &= \int_{-1}^1 \int_{-1}^1 \left(k_x \frac{\partial N_i}{\partial r} \frac{\partial N_j}{\partial r} \frac{b}{a} + k_y \frac{\partial N_i}{\partial s} \frac{\partial N_j}{\partial s} \frac{a}{b} \right) t dr ds \\ &\quad + 2h \int_{-1}^1 \int_{-1}^1 N_i N_j ab dr ds \quad i, j = 1, 4 \end{aligned}$$

Assuming that k_x and k_y are constants, we have

$$\begin{aligned} k_{ij} &= k_x t \frac{b}{a} \int_{-1}^1 \int_{-1}^1 \frac{\partial N_i}{\partial r} \frac{\partial N_j}{\partial r} dr ds + k_y t \frac{a}{b} \int_{-1}^1 \int_{-1}^1 \frac{\partial N_i}{\partial s} \frac{\partial N_j}{\partial s} dr ds \\ &\quad + 2hab \int_{-1}^1 \int_{-1}^1 N_i N_j dr ds \quad i, j = 1, 4 \end{aligned}$$

The required partial derivatives are

$$\begin{aligned}\frac{\partial N_1}{\partial r} &= \frac{1}{4}(s-1) & \frac{\partial N_1}{\partial s} &= \frac{1}{4}(r-1) \\ \frac{\partial N_2}{\partial r} &= \frac{1}{4}(1-s) & \frac{\partial N_2}{\partial s} &= -\frac{1}{4}(1+r) \\ \frac{\partial N_3}{\partial r} &= \frac{1}{4}(1+s) & \frac{\partial N_3}{\partial s} &= \frac{1}{4}(1+r) \\ \frac{\partial N_4}{\partial r} &= -\frac{1}{4}(1+s) & \frac{\partial N_4}{\partial s} &= \frac{1}{4}(1-r)\end{aligned}$$

Substituting numerical values (noting that $a = b$), we obtain, for example,

$$\begin{aligned}k_{11} &= 20 \int_{-1}^1 \int_{-1}^1 \left[\frac{1}{16}(s-1)^2 + \frac{1}{16}(r-1)^2 \right] \left(\frac{0.5}{12} \right) dr ds \\ &\quad + 2(50) \int_{-1}^1 \int_{-1}^1 \frac{1}{16} (1-r)^2 (1-s)^2 \left(\frac{0.5}{12} \right)^2 dr ds\end{aligned}$$

Integrating first on r ,

$$\begin{aligned}k_{11} &= \frac{20(0.5)}{16(12)} \int_{-1}^1 (s-1)^2 r \Big|_{-1}^1 + \frac{(r-1)^3}{3} \Big|_{-1}^1 ds \\ &\quad - \frac{100}{16} \left(\frac{0.5}{12} \right)^2 \int_{-1}^1 (1-s)^2 \frac{(1-r)^3}{3} \Big|_{-1}^1 ds\end{aligned}$$

or

$$k_{11} = \frac{20(0.5)}{16(12)} \int_{-1}^1 \left[(s-1)^2(2) + \frac{8}{3} \right] ds + \frac{100}{16} \left(\frac{0.5}{12} \right)^2 \int_{-1}^1 (1-s)^2 \frac{8}{3} ds$$

Then, integrating on s , we obtain

$$k_{11} = \frac{20(0.5)}{16(12)} \left(\frac{2(s-1)^3}{3} + \frac{8}{3}s \right) \Big|_{-1}^1 - \frac{100}{16} \left(\frac{0.5}{12} \right)^2 \left(\frac{8}{3} \right) \left(\frac{(1-s)^3}{3} \right) \Big|_{-1}^1$$

or

$$k_{11} = \frac{20(0.5)}{16(12)} \left(\frac{16}{3} + \frac{16}{3} \right) + \frac{100}{16} \left(\frac{0.5}{12} \right)^2 \left(\frac{8}{3} \right) \left(\frac{8}{3} \right) = 0.6327 \text{ Btu}/(\text{hr} \cdot ^\circ\text{F})$$

The analytical integration procedure just used to determine k_{11} is *not* the method used by finite element software packages; instead, numerical methods are used, primarily the Gauss quadrature procedure discussed in Chapter 6. If we examine the terms in the integrands of the equation defining k_{ij} , we find that the integrands are quadratic functions

of r and s . Therefore, the integrals can be evaluated exactly by using two Gauss points in r and s . Per Table 6.1, the required Gauss points and weighting factors are $r_i, s_j = \pm 0.57735$ and $W_i, W_j = 1.0, i, j = 1, 2$. Using the numerical procedure for k_{11} , we write

$$\begin{aligned} k_{11} &= k_x t \frac{b}{a} \int_{-1}^1 \int_{-1}^1 \frac{1}{16} (s-1)^2 dr ds + k_y t \frac{b}{a} \int_{-1}^1 \int_{-1}^1 \frac{1}{16} (r-1)^2 dr ds \\ &\quad + 2hab \int_{-1}^1 \frac{1}{16} (r-1)^2 (s-1)^2 dr ds \\ &= k_x t \frac{b}{a} \sum_{i=1}^2 \sum_{j=1}^2 \frac{1}{16} W_i W_j (s_j - 1)^2 + k_y t \frac{a}{b} \sum_{i=1}^2 \sum_{j=1}^2 \frac{1}{16} W_i W_j (r_i - 1)^2 \\ &\quad + 2hab \sum_{i=1}^2 \sum_{j=1}^2 \frac{1}{16} W_i W_j (1 - r_i)^2 (1 - s_j)^2 \end{aligned}$$

and, using the specified integration points and weighting factors, this evaluates to

$$k_{11} = k_x t \frac{b}{a} \left(\frac{1}{3} \right) + k_y t \frac{a}{b} \left(\frac{1}{3} \right) + 2hab \left(\frac{4}{9} \right)$$

It is extremely important to note that the result expressed in the preceding equation is the correct value of k_{11} for *any* rectangular element used for the two-dimensional heat conduction analysis discussed in this section. The integrations need not be repeated for each element; only the geometric quantities and the conductance values need be substituted to obtain the value. Indeed, if we substitute the values for this example, we obtain

$$k_{11} = 0.6327 \text{ Btu}/(\text{hr}\cdot^\circ\text{F})$$

as per the analytical integration procedure.

Proceeding with the Gaussian integration procedure (calculation of some of these terms are to be evaluated as end-of-chapter problems), we find

$$k_{11} = k_{22} = k_{33} = k_{44} = 0.6327 \text{ Btu}/(\text{hr}\cdot^\circ\text{F})$$

Why are these values equal?

The off-diagonal terms (again using the numerical integration procedure) are calculated as

$$k_{12} = -0.1003$$

$$k_{13} = -0.2585$$

$$k_{14} = -0.1003$$

$$k_{23} = -0.1003$$

$$k_{24} = -0.2585$$

$$k_{34} = -0.1003$$

Btu/(hr-°F), and the complete element conductance matrix is

$$[k^{(e)}] = \begin{bmatrix} 0.6327 & -0.1003 & -0.2585 & -0.1003 \\ -0.1003 & 0.6327 & -0.1003 & -0.2585 \\ -0.2585 & -0.1003 & 0.6327 & -0.1003 \\ -0.1003 & -0.2585 & -0.1003 & 0.6327 \end{bmatrix} \text{ Btu}/(\text{hr}\cdot^\circ\text{F})$$

EXAMPLE 7.5

Figure 7.10a depicts a two-dimensional heating fin. The fin is attached to a pipe on its left edge, and the pipe conveys water at a constant temperature of 180°F. The fin is surrounded by air at temperature 68°F. The thermal properties of the fin are as given in Example 7.4. Use four equal-size four-node rectangular elements to obtain a finite element solution for the steady-state temperature distribution in the fin.

■ Solution

Figure 7.10b shows four elements with element and global node numbers. Given the numbering scheme selected, we have constant temperature conditions at global nodes 1, 2, and 3 such that

$$T_1 = T_2 = T_3 = 180^\circ\text{F}$$

while on the other edges, we have convection boundary conditions that require a bit of analysis to apply. For element 1 (Figure 7.10c), for instance, convection occurs along element edge 1-2 but not along the other three element edges. Noting that $s = -1$ and

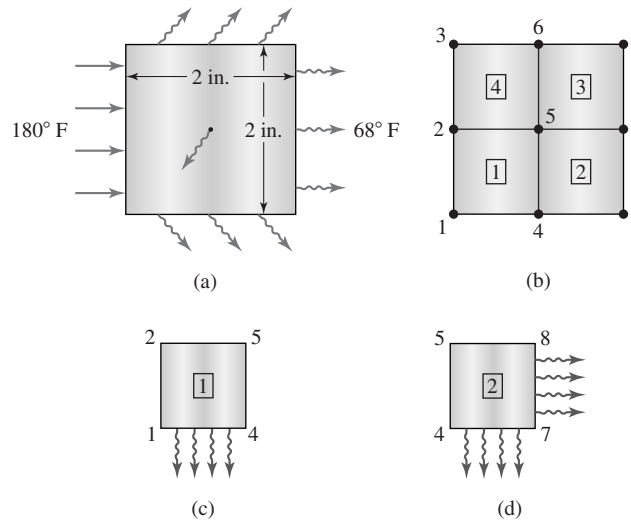


Figure 7.10 Example 7.5:
 (a) Two-dimensional fin. (b) Finite element model.
 (c) Element 1 edge convection. (d) Element 2 edge convection.

$N_3 = N_4 = 0$ on edge 1-2, Equation 7.43 becomes

$$\begin{aligned} [k_{hS}^{(1)}] &= \left(\frac{1}{4}\right) ht \int_{-1}^1 \begin{Bmatrix} 1-r \\ 1+r \\ 0 \\ 0 \end{Bmatrix} [1-r \quad 1+r \quad 0 \quad 0] a \, dr \\ &= \frac{hta}{4} \int_{-1}^1 \begin{bmatrix} (1-r)^2 & 1-r^2 & 0 & 0 \\ 1-r^2 & (1+r)^2 & 0 & 0 \\ 0 & 0 & 0 & 0 \\ 0 & 0 & 0 & 0 \end{bmatrix} dr \end{aligned}$$

Integrating as indicated gives

$$\begin{aligned} [k_{hS}^{(1)}] &= \frac{hta}{4(3)} \begin{bmatrix} 8 & 4 & 0 & 0 \\ 4 & 8 & 0 & 0 \\ 0 & 0 & 0 & 0 \\ 0 & 0 & 0 & 0 \end{bmatrix} = \frac{50(0.5)^2}{4(3)(12)^2} \begin{bmatrix} 8 & 4 & 0 & 0 \\ 4 & 8 & 0 & 0 \\ 0 & 0 & 0 & 0 \\ 0 & 0 & 0 & 0 \end{bmatrix} \\ &= \begin{bmatrix} 0.0579 & 0.0290 & 0 & 0 \\ 0.0290 & 0.0579 & 0 & 0 \\ 0 & 0 & 0 & 0 \\ 0 & 0 & 0 & 0 \end{bmatrix} \end{aligned}$$

where the units are Btu/(hr-°F).

The edge convection force vector for element 1 is, per Equation 7.44,

$$\begin{aligned} \{f_{hS}^{(1)}\} &= \frac{hT_a t}{2} \int_{-1}^1 \begin{Bmatrix} 1-r \\ 1+r \\ 0 \\ 0 \end{Bmatrix} a \, dr = \frac{hT_a t a}{2} \begin{Bmatrix} 2 \\ 2 \\ 0 \\ 0 \end{Bmatrix} = \frac{50(68)(0.5)^2}{2(12)^2} \begin{Bmatrix} 2 \\ 2 \\ 0 \\ 0 \end{Bmatrix} \\ &= \begin{Bmatrix} 5.9028 \\ 5.9028 \\ 0 \\ 0 \end{Bmatrix} \text{ Btu/hr} \end{aligned}$$

where we again utilize $s = -1$, $N_3 = N_4 = 0$ along the element edge bounded by nodes 1 and 2.

Next consider element 2. As depicted in Figure 7.10d, convection occurs along two element edges defined by element nodes 1-2 ($s = -1$) and element nodes 2-3 ($r = 1$). For element 2, Equation 7.43 is

$$\begin{aligned} [k_{hS}^{(2)}] &= \frac{ht}{4} \left(\int_{-1}^1 \begin{Bmatrix} 1-r \\ 1+r \\ 0 \\ 0 \end{Bmatrix} [1-r \quad 1+r \quad 0 \quad 0] a \, dr \right. \\ &\quad \left. + \int_{-1}^1 \begin{Bmatrix} 0 \\ 1-s \\ 1+s \\ 0 \end{Bmatrix} [0 \quad 1-s \quad 1+s \quad 0] b \, ds \right) \end{aligned}$$

or, after integrating,

$$[k_{hS}^{(2)}] = \frac{hta}{4(3)} \begin{bmatrix} 8 & 4 & 0 & 0 \\ 4 & 8 & 0 & 0 \\ 0 & 0 & 0 & 0 \\ 0 & 0 & 0 & 0 \end{bmatrix} + \frac{htb}{4(3)} \begin{bmatrix} 0 & 0 & 0 & 0 \\ 0 & 8 & 4 & 0 \\ 0 & 4 & 8 & 0 \\ 0 & 0 & 0 & 0 \end{bmatrix}$$

and, since $a = b$,

$$[k_{hS}^{(2)}] = \frac{50(0.5)^2}{4(3)(12)^2} \begin{bmatrix} 8 & 4 & 0 & 0 \\ 4 & 16 & 4 & 0 \\ 0 & 4 & 8 & 0 \\ 0 & 0 & 0 & 0 \end{bmatrix} = \begin{bmatrix} 0.0579 & 0.0290 & 0 & 0 \\ 0.0290 & 0.1157 & 0.0290 & 0 \\ 0 & 0.0290 & 0.0579 & 0 \\ 0 & 0 & 0 & 0 \end{bmatrix} \text{ Btu/(hr}\cdot\text{°F)}$$

Likewise, the element edge convection force vector is obtained by integration along the two edges as

$$\begin{aligned} \{f_{hS}^{(2)}\} &= \frac{hT_a t}{2} \left(\int_{-1}^1 \begin{Bmatrix} 1-r \\ 1+r \\ 0 \\ 0 \end{Bmatrix} a \, dr + \int_{-1}^1 \begin{Bmatrix} 0 \\ 1-s \\ 1+s \\ 0 \end{Bmatrix} b \, ds \right) \\ &= \frac{50(68)(0.5)^2}{2(12)^2} \begin{Bmatrix} 2 \\ 4 \\ 2 \\ 0 \end{Bmatrix} = \begin{Bmatrix} 5.9028 \\ 11.8056 \\ 5.9028 \\ 0 \end{Bmatrix} \text{ Btu/hr} \end{aligned}$$

Identical procedures applied to the appropriate edges of elements 3 and 4 result in

$$[k_{hS}^{(3)}] = \frac{50(0.5)^2}{4(3)(12)^2} \begin{bmatrix} 0 & 0 & 0 & 0 \\ 0 & 8 & 4 & 0 \\ 0 & 4 & 16 & 4 \\ 0 & 0 & 4 & 8 \end{bmatrix} = \begin{bmatrix} 0 & 0 & 0 & 0 \\ 0 & 0.0579 & 0.0290 & 0 \\ 0 & 0.0290 & 0.1157 & 0.0290 \\ 0 & 0 & 0.0290 & 0.0579 \end{bmatrix} \text{ Btu/(hr}\cdot\text{°F)}$$

$$[k_{hS}^{(4)}] = \frac{50(0.5)^2}{4(3)(12)^2} \begin{bmatrix} 0 & 0 & 0 & 0 \\ 0 & 0 & 0 & 0 \\ 0 & 0 & 8 & 4 \\ 0 & 0 & 4 & 8 \end{bmatrix} = \begin{bmatrix} 0 & 0 & 0 & 0 \\ 0 & 0 & 0 & 0 \\ 0 & 0 & 0.0579 & 0.0290 \\ 0 & 0 & 0.0290 & 0.0579 \end{bmatrix} \text{ Btu/(hr}\cdot\text{°F)}$$

$$\{f_{hS}^{(3)}\} = \begin{Bmatrix} 0 \\ 5.9028 \\ 11.8056 \\ 5.9028 \end{Bmatrix} \text{ Btu/hr}$$

$$\{f_{hS}^{(4)}\} = \begin{Bmatrix} 0 \\ 0 \\ 5.9028 \\ 5.9028 \end{Bmatrix} \text{ Btu/hr}$$

7.4 Heat Transfer in Two Dimensions

249

As no internal heat is generated, the corresponding $\{f_Q^{(e)}\}$ force vector for each element is zero; that is,

$$\{f_Q^{(e)}\} = \iint_A Q\{N\} dA = \{0\}$$

for each element.

On the other hand, each element exhibits convection from its surfaces, so the lateral convection force vector is

$$\{f_h^{(e)}\} = 2hT_a \iint_A \{N\} dA = 2hT_a \int_{-1}^1 \int_{-1}^1 \left(\frac{1}{4}\right) \begin{Bmatrix} (1-r)(1-s) \\ (1+r)(1-s) \\ (1+r)(1+s) \\ (1-r)(1+s) \end{Bmatrix} ab dr ds$$

which evaluates to

$$\{f_h^{(e)}\} = \frac{2hT_a ab}{4} \begin{Bmatrix} 4 \\ 4 \\ 4 \\ 4 \end{Bmatrix} = \frac{2(50)(68)(0.5)^2}{4(12)^2} \begin{Bmatrix} 4 \\ 4 \\ 4 \\ 4 \end{Bmatrix} = \begin{Bmatrix} 11.8056 \\ 11.8056 \\ 11.8056 \\ 11.8056 \end{Bmatrix}$$

and we note that, since the element is square, the surface convection forces are distributed equally to each of the four element nodes.

The global equations for the four-element model can now be assembled by writing the element-to-global nodal correspondence relations as

$$\begin{aligned} [L^{(1)}] &= [1 \quad 4 \quad 5 \quad 2] \\ [L^{(2)}] &= [4 \quad 7 \quad 8 \quad 5] \\ [L^{(3)}] &= [5 \quad 8 \quad 9 \quad 6] \\ [L^{(4)}] &= [2 \quad 5 \quad 6 \quad 3] \end{aligned}$$

and adding the edge convection terms to obtain the element stiffness matrices as

$$\begin{aligned} [k^{(1)}] &= \begin{bmatrix} 0.6906 & -0.0713 & -0.2585 & -0.1003 \\ -0.0713 & 0.6906 & -0.1003 & -0.2585 \\ -0.2585 & -0.1003 & 0.6327 & -0.1003 \\ -0.1003 & -0.2585 & -0.1003 & 0.6327 \end{bmatrix} \\ [k^{(2)}] &= \begin{bmatrix} 0.6906 & -0.0713 & -0.2585 & -0.1003 \\ -0.0713 & 0.7484 & -0.0713 & -0.2585 \\ -0.2585 & -0.0713 & 0.6906 & -0.1003 \\ -0.1003 & -0.2585 & -0.1003 & 0.6327 \end{bmatrix} \\ [k^{(3)}] &= \begin{bmatrix} 0.6327 & -0.1003 & -0.2585 & -0.1003 \\ -0.1003 & 0.6906 & -0.0713 & -0.2585 \\ -0.2585 & -0.0713 & 0.7484 & -0.0713 \\ -0.1003 & -0.2585 & -0.0713 & 0.6906 \end{bmatrix} \end{aligned}$$

$$[k^{(4)}] = \begin{bmatrix} 0.6327 & -0.1003 & -0.2585 & -0.1003 \\ -0.1003 & 0.6327 & -0.1003 & -0.2585 \\ -0.2585 & -0.1003 & 0.6906 & -0.0713 \\ -0.1003 & -0.2585 & -0.0713 & 0.6906 \end{bmatrix}$$

Utilizing the direct assembly-superposition method with the element-to-global node assignment relations, the global conductance matrix is

$$[K] = \begin{bmatrix} 0.6906 & -0.1003 & 0 & -0.0713 & -0.2585 & 0 & 0 & 0 & 0 \\ -0.1003 & 1.2654 & -0.1003 & -0.2585 & -0.2006 & -0.2585 & 0 & 0 & 0 \\ 0 & -0.1003 & 0.6906 & 0 & -0.2585 & -0.0713 & 0 & 0 & 0 \\ -0.0713 & -0.2585 & 0 & 1.3812 & -0.2006 & 0 & -0.0713 & -0.2585 & 0 \\ -0.2585 & -0.2006 & -0.2585 & -0.2006 & 2.5308 & -0.2006 & -0.2585 & -0.2006 & -0.2585 \\ 0 & -0.2585 & -0.0713 & 0 & -0.2006 & 1.3812 & 0 & -0.2585 & -0.0713 \\ 0 & 0 & 0 & -0.0713 & -0.2585 & 0 & 0.7484 & -0.2585 & 0 \\ 0 & 0 & 0 & -0.2585 & -0.2006 & -0.2585 & -0.2585 & 1.3812 & -0.0713 \\ 0 & 0 & 0 & 0 & -0.2585 & -0.0713 & 0 & -0.0713 & 0.7484 \end{bmatrix}$$

The nodal temperature vector is

$$\{T\} = \begin{Bmatrix} 180 \\ 180 \\ 180 \\ T_4 \\ T_5 \\ T_6 \\ T_7 \\ T_8 \\ T_9 \end{Bmatrix}$$

and we have explicitly incorporated the prescribed temperature boundary conditions.

Assembling the global force vector, noting that no internal heat is generated, we obtain

$$\{F\} = \begin{Bmatrix} 17.7084 + F_1 \\ 35.4168 + F_2 \\ 17.7084 + F_3 \\ 35.4168 \\ 47.2224 \\ 35.4168 \\ 23.6112 \\ 35.4168 \\ 23.6112 \end{Bmatrix} \text{ Btu/hr}$$

where we use F_1 , F_2 , and F_3 as general notation to indicate that these are unknown “reaction” forces. In fact, as will be shown, these terms are the heat flux components at nodes 1, 2, and 3.

7.4 Heat Transfer in Two Dimensions

251

The global equations for the four-element model are then expressed as

$$\begin{bmatrix} 0.6906 & -0.1003 & 0 & -0.0713 & -0.2585 & 0 & 0 & 0 & 0 \\ -0.1003 & 1.2654 & -0.1003 & -0.2585 & -0.2006 & -0.2585 & 0 & 0 & 0 \\ 0 & -0.1003 & 0.6906 & 0 & -0.2585 & -0.0713 & 0 & 0 & 0 \\ \hline -0.0713 & -0.2585 & 0 & 1.3812 & -0.2006 & 0 & -0.0713 & -0.2585 & 0 \\ -0.2585 & -0.2006 & -0.2585 & -0.2006 & 2.5308 & -0.2006 & -0.2585 & -0.2006 & -0.2585 \\ 0 & -0.2585 & -0.0713 & 0 & -0.2006 & 1.3812 & 0 & -0.2585 & -0.0713 \\ 0 & 0 & 0 & -0.0713 & -0.2585 & 0 & 0.7484 & -0.2585 & 0 \\ 0 & 0 & 0 & -0.2585 & -0.2006 & -0.2585 & -0.2585 & 1.3812 & -0.0713 \\ 0 & 0 & 0 & 0 & -0.2585 & -0.0713 & 0 & -0.0713 & 0.7484 \end{bmatrix} \begin{Bmatrix} 180 \\ 180 \\ 180 \\ T_4 \\ T_5 \\ T_6 \\ T_7 \\ T_8 \\ T_9 \end{Bmatrix} = \begin{Bmatrix} 17.7084 + F_1 \\ 35.4168 + F_2 \\ 17.7084 + F_3 \\ 35.4168 \\ 47.2224 \\ 35.4168 \\ 23.6112 \\ 35.4158 \\ 23.6112 \end{Bmatrix}$$

Taking into account the specified temperatures on nodes 1, 2, and 3, the global equations for the unknown temperatures become

$$\begin{bmatrix} 1.3812 & -0.2006 & 0 & -0.0713 & -0.2585 & 0 \\ -0.2006 & 2.5308 & -0.2006 & -0.2585 & -0.2006 & -0.2585 \\ 0 & -0.2006 & 1.3812 & 0 & -0.2585 & -0.0713 \\ -0.0713 & -0.2585 & 0 & 0.7484 & -0.2585 & 0 \\ -0.2585 & -0.2006 & -0.2585 & -0.2585 & 1.3812 & -0.0713 \\ 0 & -0.2585 & -0.0713 & 0 & -0.0713 & 0.7484 \end{bmatrix} \begin{Bmatrix} T_4 \\ T_5 \\ T_6 \\ T_7 \\ T_8 \\ T_9 \end{Bmatrix} = \begin{Bmatrix} 94.7808 \\ 176.3904 \\ 94.7808 \\ 23.6112 \\ 35.4168 \\ 23.6112 \end{Bmatrix}$$

The reader is urged to note that, in arriving at the last result, we partition the global matrix as shown by the dashed lines and apply Equation 3.46a to obtain the equations governing the “active” degrees of freedom. That is, the partitioned matrix is of the form

$$\begin{bmatrix} K_{cc} & K_{ca} \\ K_{ac} & K_{aa} \end{bmatrix} \begin{Bmatrix} T_c \\ T_a \end{Bmatrix} = \begin{Bmatrix} F_c \\ F_a \end{Bmatrix}$$

where the subscript c denotes terms associated with constrained (specified) temperatures and the subscript a denotes terms associated with active (unknown) temperatures. Hence, this 6×6 system represents

$$[K_{aa}]\{T_a\} = \{F_a\} - [K_{ac}]\{T_c\}$$

which now properly includes the effects of specified temperatures as forcing functions on the right-hand side.

Simultaneous solution of the global equations (in this case, we inverted the global stiffness matrix using a spreadsheet program) yields the nodal temperatures as

$$\begin{Bmatrix} T_4 \\ T_5 \\ T_6 \\ T_7 \\ T_8 \\ T_9 \end{Bmatrix} = \begin{Bmatrix} 106.507 \\ 111.982 \\ 106.507 \\ 89.041 \\ 90.966 \\ 89.041 \end{Bmatrix} \text{ } ^\circ\text{F}$$

If we now back substitute the computed nodal temperatures into the first three of the global equations, specifically,

$$\begin{aligned} 0.6906T_1 - 0.1003T_2 - 0.0713T_4 - 0.2585T_5 &= 17.7084 + F_1 \\ -0.1003T_1 + 1.2654T_2 - 0.1003T_3 - 0.2585T_4 - 0.2006T_5 - 0.2585T_6 &= 35.4168 + F_2 \\ -0.1003T_2 + 0.6906T_3 - 0.2585T_5 - 0.0713T_6 &= 17.7084 + F_3 \end{aligned}$$

we obtain the heat flow values at nodes 1, 2, and 3 as

$$\begin{Bmatrix} F_1 \\ F_2 \\ F_3 \end{Bmatrix} = \begin{Bmatrix} 52.008 \\ 78.720 \\ 52.008 \end{Bmatrix} \text{ Btu/hr}$$

Note that, in terms of the matrix partitioning, we are now solving

$$[K_{cc}]\{T_c\} + [K_{ca}]\{T_a\} = \{F_c\}$$

to obtain the unknown values in $\{F_c\}$.

Since there is no convection from the edges defined by nodes 1-2 and 1-3 and the temperature is specified on these edges, the reaction “forces” represent the heat input (flux) across these edges and should be in balance with the convection loss across the lateral surfaces of the body, and its edges, in a steady-state situation. This balance is a check that can and should be made on the accuracy of a finite element solution of a heat transfer problem and is analogous to checking equilibrium of a structural finite element solution.

Example 7.5 is illustrated in great detail to point out the systematic procedures for assembling the global matrices and force vectors. The astute reader ascertains, in following the solution, that symmetry conditions can be used to simplify the mathematics of the solution. As shown in Figure 7.11a, an axis (plane) of symmetry exists through the horizontal center of the plate. Therefore, the problem can be reduced to a two-element model, as shown in Figure 7.11b. Along the edge of symmetry, the y -direction heat flux components are in balance, and this edge can be treated as a perfectly insulated edge. One could then use only two elements, with the appropriately adjusted boundary conditions to obtain the same solution as in the example.

7.4 Heat Transfer in Two Dimensions

253

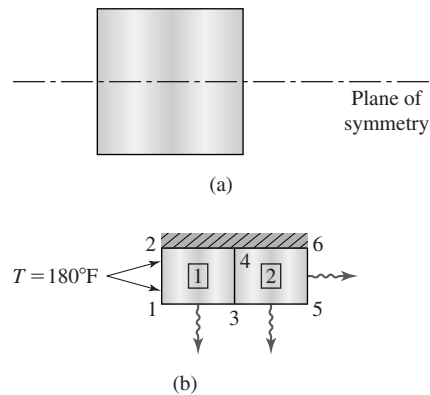


Figure 7.11 Model of Example 7.5, showing (a) the plane of symmetry and (b) a two-element model with adjusted boundary conditions.

7.4.3 Symmetry Conditions

As mentioned previously in connection with Example 7.5, symmetry conditions can be used to reduce the size of a finite element model (or any other computational model). Generally, the symmetry is observed geometrically; that is, the physical domain of interest is symmetric about an axis or plane. Geometric symmetry is not, however, sufficient to ensure that a problem is symmetric. In addition, the boundary conditions and applied loads must be symmetric about the axis or plane of geometric symmetry as well. To illustrate, consider Figure 7.12a, depicting a thin rectangular plate having a heat source located at the geometric center of the plate. The model is of a heat transfer fin removing heat from a central source (a pipe containing hot fluid, for example) via conduction and convection from the fin. Clearly, the situation depicted is symmetric geometrically. But, is the situation a symmetric problem? The loading is symmetric, since the heat source is centrally located in the domain. We also assume that $k_x = k_y$, so that the material properties are symmetric. Hence, we must examine the boundary conditions to determine if symmetry exists. If, for example, as shown in Figure 7.12b, the ambient temperatures external to the fin are uniform around the fin and the convection coefficients are the same on all surfaces, the problem is symmetric about both x and y axes and can be solved via the model in Figure 7.12c. For this situation, note that the heat from the source is conducted radially and, consequently, across the x axis, the heat flux q_y is zero and, across the y axis, the heat flux q_x must also be zero. These observations reveal the boundary conditions for the quarter-symmetry model shown in Figure 7.12d and the internal forcing function is taken as $Q/4$. On the other hand, let us assume that the upper edge of the plate is perfectly insulated, as in Figure 7.12e. In this case, we do not have

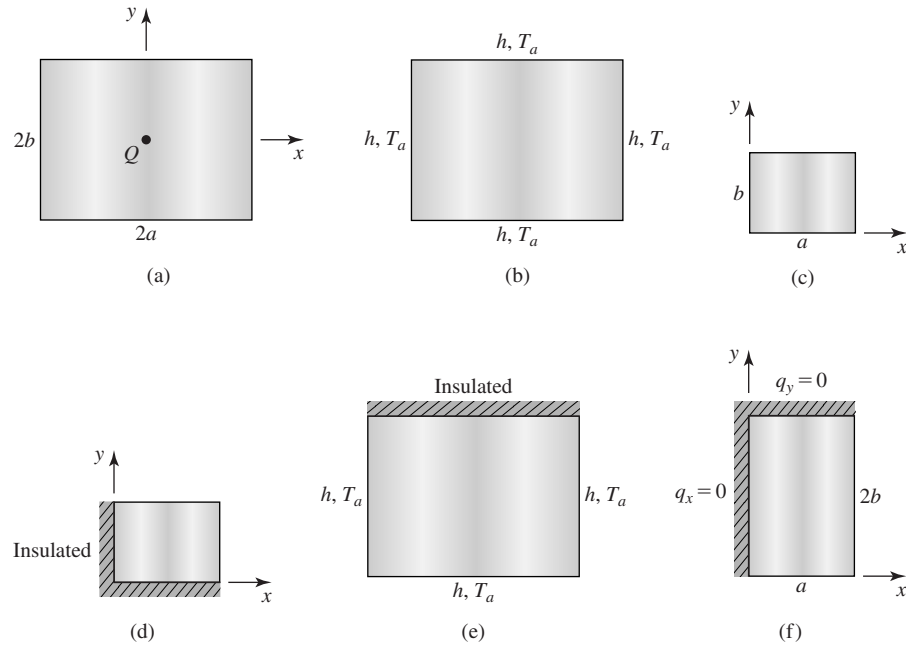


Figure 7.12 Illustrations of symmetry dictated by boundary conditions.

symmetric conditions about the x axis but symmetry about the y axis exists. For these conditions, we can use the “half-symmetry” model shown in Figure 7.12f, using the symmetry (boundary) condition $q_x = 0$ across $x = 0$ and apply the internal heat generation term $Q/2$.

Symmetry can be used to reduce the size of finite element models significantly. It must be remembered that symmetry is not simply a geometric occurrence. For symmetry, geometry, loading, material properties, and boundary conditions must all be symmetric (about an axis, axes, or plane) to reduce the model.

7.4.4 Element Resultants

In the approach just taken in heat transfer analysis, the primary nodal variable computed is temperature. Most often in such analyses, we are more interested in the amount of heat transferred than the nodal temperatures. (This is analogous to structural problems: We solve for nodal displacements but are more interested in stresses.) In finite element analyses of heat transfer problems, we must back substitute the nodal temperature solution into the “reaction” equations to obtain global heat transfer values. (As in Example 7.5, when we solved the partitioned matrices for the heat flux values at the constrained nodes.) Similarly, we can back

substitute the nodal temperatures to obtain estimates of heat transfer properties of individual elements as well.

The heat flux components for a two-dimensional element, per Fourier's law, are

$$\begin{aligned} q_x^{(e)} &= -k_x \frac{\partial T^{(e)}}{\partial x} = -k_x \sum_{i=1}^M \frac{\partial N_i}{\partial x} T_i^{(e)} \\ q_y^{(e)} &= -k_y \frac{\partial T^{(e)}}{\partial y} = -k_y \sum_{i=1}^M \frac{\partial N_i}{\partial y} T_i^{(e)} \end{aligned} \quad (7.47)$$

where we again denote the total number of element nodes as M . With the exception of the three-node triangular element, the flux components given by Equation 7.47 are not constant but vary with position in the element. As an example, the components for the four-node rectangular element are readily computed using the interpolation functions of Equation 6.56, repeated here as

$$\begin{aligned} N_1(r, s) &= \frac{1}{4}(1-r)(1-s) \\ N_2(r, s) &= \frac{1}{4}(1+r)(1-s) \\ N_3(r, s) &= \frac{1}{4}(1+r)(1+s) \\ N_4(r, s) &= \frac{1}{4}(1-r)(1+s) \end{aligned} \quad (7.48)$$

Recalling that

$$\frac{\partial}{\partial x} = \frac{1}{a} \frac{\partial}{\partial r} \quad \text{and} \quad \frac{\partial}{\partial y} = \frac{1}{b} \frac{\partial}{\partial s}$$

we have

$$\begin{aligned} q_x^{(e)} &= -\frac{k_x}{a} \sum_{i=1}^4 \frac{\partial N_i}{\partial r} T_i^{(e)} \\ &= -\frac{k_x}{4a} [(s-1)T_1^{(e)} + (1-s)T_2^{(e)} + (1+s)T_3^{(e)} - (1+s)T_4^{(e)}] \\ q_y^{(e)} &= -\frac{k_y}{b} \sum_{i=1}^4 \frac{\partial N_i}{\partial s} T_i^{(e)} \\ &= -\frac{k_y}{4b} [(r-1)T_1^{(e)} - (1+r)T_2^{(e)} + (1+r)T_3^{(e)} + (1-r)T_4^{(e)}] \end{aligned} \quad (7.49)$$

and these expressions simplify to

$$\begin{aligned} q_x^{(e)} &= -\frac{k_x}{4a}[(1-s)(T_2^{(e)} - T_1^{(e)}) + (1+s)(T_3^{(e)} - T_4^{(e)})] \\ q_y^{(e)} &= -\frac{k_y}{4b}[(1-r)(T_4^{(e)} - T_1^{(e)}) + (1+r)(T_3^{(e)} - T_2^{(e)})] \end{aligned} \quad (7.50)$$

The flux components, therefore the temperature gradients, vary linearly in a four-node rectangular element. However, recall that, for a C^0 formulation, the gradients are not, in general, continuous across element boundaries. Consequently, the element flux components associated with an individual element are customarily taken to be the values calculated at the centroid of the element. For the rectangular element, the centroid is located at $(r, s) = (0, 0)$, so the centroidal values are simply

$$\begin{aligned} q_x^{(e)} &= -\frac{k_x}{4a}(T_2^{(e)} + T_3^{(e)} - T_1^{(e)} - T_4^{(e)}) \\ q_y^{(e)} &= -\frac{k_y}{4b}(T_3^{(e)} + T_4^{(e)} - T_1^{(e)} - T_2^{(e)}) \end{aligned} \quad (7.51)$$

The centroidal values calculated per Equation 7.51, in general, are quite accurate for a fine mesh of elements. Some finite element software packages compute the values at the integration points (the Gauss points) and average those values for an element value to be applied at the element centroid. In either case, the computed values are needed to determine solution convergence and should be checked at every stage of a finite element analysis.

EXAMPLE 7.6

Calculate the centroidal heat flux components for elements 2 and 3 of Example 7.5.

■ Solution

From Example 7.4, we have $a = b = 0.5$ in., $k_x = k_y = 20$ Btu/(hr-ft-°F), and from Example 7.5, the nodal temperature vector is

$$\{T\} = \begin{Bmatrix} T_1 \\ T_2 \\ T_3 \\ T_4 \\ T_5 \\ T_6 \\ T_7 \\ T_8 \\ T_9 \end{Bmatrix} = \begin{Bmatrix} 180 \\ 180 \\ 180 \\ 106.507 \\ 111.982 \\ 106.507 \\ 89.041 \\ 90.966 \\ 89.041 \end{Bmatrix} \text{ } ^\circ\text{F}$$

For element 2, the element-global nodal correspondence relation can be written as

$$\begin{aligned} [T_1^{(2)} \quad T_2^{(2)} \quad T_3^{(2)} \quad T_4^{(2)}] &= [T_4 \quad T_7 \quad T_8 \quad T_5] \\ &= [106.507 \quad 89.041 \quad 90.966 \quad 111.982] \end{aligned}$$

Substituting numerical values into Equation 7.49,

$$q_x^{(2)} = -\frac{12(20)}{4(0.5)}(89.041 + 90.966 - 106.507 - 111.982) = 4617.84 \text{ Btu}/(\text{hr}\cdot\text{ft}^2)$$

$$q_y^{(2)} = -\frac{12(20)}{4(0.5)}(90.966 + 111.982 - 106.507 - 89.041) = -888.00 \text{ Btu}/(\text{hr}\cdot\text{ft}^2)$$

and, owing to the symmetry conditions, we have

$$q_x^{(3)} = 4617.84 \text{ Btu}/(\text{hr}\cdot\text{ft}^2)$$

$$q_y^{(3)} = 888.00 \text{ Btu}/(\text{hr}\cdot\text{ft}^2)$$

as may be verified by direct calculation. Recall that these values are calculated at the location of the element centroid.

The element resultants representing convection effects can also be readily computed once the nodal temperature solution is known. The convection resultants are of particular interest, since these represent the primary source of heat removal (or absorption) from a solid body. The convective heat flux, per Equation 7.2, is

$$q_x = h(T - T_a) \text{ Btu}/(\text{hr}\cdot\text{ft}^2) \text{ or } \text{W}/\text{m}^2 \quad (7.52)$$

where all terms are as previously defined. Hence, the total convective heat flow rate from a surface area A is

$$\dot{H}_h = \iint_A h(T - T_a) dA \quad (7.53)$$

For an individual element, the heat flow rate is

$$\dot{H}_h^{(e)} = \iint_A h(T^{(e)} - T_a) dA = \iint_A h([N]\{T\} - T_a) dA \quad (7.54)$$

The area of integration in Equation 7.54 includes all portions of the element surface subjected to convection conditions. In the case of a two-dimensional element, the area may include lateral surfaces (that is, convection perpendicular to the plane of the element) as well as the area of element edges located on a free boundary.

EXAMPLE 7.7

Determine the total heat flow rate of convection for element 3 of Example 7.5.

■ Solution

First we note that, for element 3, the element-to-global correspondence relation for nodal temperatures is

$$[T_1^{(3)} \quad T_2^{(3)} \quad T_3^{(3)} \quad T_4^{(3)}] = [T_5 \quad T_8 \quad T_9 \quad T_6]$$

Second, element 3 is subjected to convection on both lateral surfaces as well as the two edges defined by nodes 8-9 and 6-9. Consequently, three integrations are required as follows:

$$\begin{aligned}\dot{H}_h^{(e)} &= 2 \iint_{A^{(e)}} h([N]\{T\} - T_a) dA^{(e)} + \iint_{A_{8-9}} h([N]\{T\} - T_a) dA_{8-9} \\ &\quad + \iint_{A_{6-9}} h([N]\{T\} - T_a) dA_{6-9}\end{aligned}$$

where $A^{(e)}$ is element area in the xy plane and the multiplier in the first term (2) accounts for both lateral surfaces.

Transforming the first integral to normalized coordinates results in

$$\begin{aligned}I_1 &= 2hab \int_{-1}^1 \int_{-1}^1 ([N]\{T\} - T_a) dr ds = 2hab \int_{-1}^1 \int_{-1}^1 [N] dr ds \{T\} - 2habT_a \int_{-1}^1 dr ds \\ &= \frac{2hA}{4} \int_{-1}^1 \int_{-1}^1 [N] dr ds \{T\} - 2hAT_a\end{aligned}$$

Therefore, we need integrate the interpolation functions only over the area of the element, as all other terms are known constants. For example,

$$\int_{-1}^1 \int_{-1}^1 N_1 dr ds = \int_{-1}^1 \int_{-1}^1 \frac{1}{4}(1-r)(1-s) dr ds = \frac{1}{4} \left. \frac{(1-r)^2}{2} \right|_{-1}^1 \left. \frac{(1-s)^2}{2} \right|_{-1}^1 = 1$$

An identical result is obtained when the other three functions are integrated. The integral corresponding to convection from the element lateral surfaces is then

$$I_1 = 2hA \left(\frac{T_1^{(3)} + T_2^{(3)} + T_3^{(3)} + T_4^{(3)}}{4} - T_a \right)$$

The first term in the parentheses is the average of the nodal temperatures, and this is a general result for the rectangular element. Substituting numerical values

$$I_1 = \frac{2(50)(1)^2}{144} \left(\frac{111.982 + 90.966 + 89.041 + 106.507}{4} - 68 \right) = 21.96 \text{ Btu/hr}$$

Next, we consider the edge convection terms. Along edge 8-9,

$$I_2 = \iint_{A_{8-9}} h([N]\{T\} - T_a) dA_{8-9}$$

and, since $r = 1$ along that edge, $dA_{8-9} = tb ds$, and the integral becomes

$$\begin{aligned}I_2 &= htb \int_{-1}^1 ([N_{r=1}]\{T\} - T_a) ds \\ &= htb \int_{-1}^1 \frac{1}{4} [0 \quad 1-s \quad 1+s \quad 0] ds \{T\} - htbT_a \int_{-1}^1 ds\end{aligned}$$

$$\begin{aligned}
 &= h(2tb) \left[0 \quad \frac{1}{2} \quad \frac{1}{2} \quad 0 \right] \{T\} - h(2tb)T_a \\
 &= hA_{\text{edge}} \left(\frac{T_2^{(3)} + T_3^{(3)}}{2} - T_a \right)
 \end{aligned}$$

Again, we observe that the average temperature of the nodes associated with the area of the edge appears. Stated another way, the convection area is allocated equally to the two nodes, and this is another general result for the rectangular element. Inserting numerical values,

$$I_2 = \frac{50(0.5)(1)}{144} \left(\frac{90.966 + 89.041}{2} - 68 \right) = 3.82 \text{ Btu/hr}$$

By analogy, the edge convection along edge 6-9 is

$$\begin{aligned}
 I_3 &= hA_{\text{edge}} \left(\frac{T_3^{(3)} + T_4^{(3)}}{2} - T_a \right) = \frac{50(0.5)(1)}{144} \left(\frac{89.041 + 106.507}{2} - 68 \right) \\
 &= 5.17 \text{ Btu/hr}
 \end{aligned}$$

The total convective heat flow rate for element 3 is then

$$\dot{H}_h^{(3)} = I_1 + I_2 + I_3 = 30.95 \text{ Btu/hr}$$

7.4.5 Internal Heat Generation

To this point in the current discussion of heat transfer, only examples having no internal heat generation ($Q = 0$) have been considered. Also, for two-dimensional heat transfer, we considered only thin bodies such as fins. Certainly these are not the only cases of interest. Consider the situation of a body of constant cross section having length much larger than the cross-sectional dimensions, as shown in Figure 7.13a (we use a rectangular cross section for convenience). In addition, an internal heat source is imbedded in the body and runs parallel to the length. Practical examples include a floor slab containing a hot water or steam pipe for heating and a sidewalk or bridge deck having embedded heating cables to prevent ice accumulation. The internal heat generation source in this situation is known as a *line* source.

Except very near the ends of such a body, heat transfer effects in the z direction can be neglected and the situation treated as a two-dimensional problem, as depicted in Figure 7.13b. Assuming the pipe or heat cable to be small in comparison to the cross section of the body, the source is treated as acting at a single point in the cross section. If we model the problem via the finite element method, how do we account for the source in the formulation? Per the first of Equation 7.38, the nodal force vector corresponding to internal heat generation is

$$\{f_Q^{(e)}\} = \iint_A Q[N]^T t \, dA = \iint_A Q\{N\}t \, dA \quad (7.55)$$

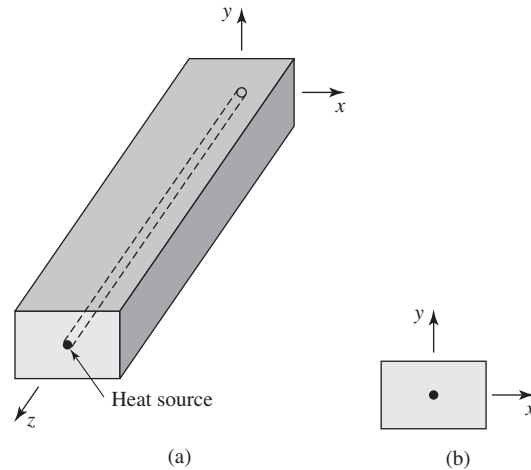


Figure 7.13
 (a) Long, slender body with internal heat source.
 (b) 2-D representation (unit thickness in z-direction).

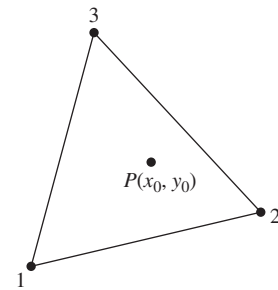


Figure 7.14
 Concentrated heat source Q^* located at point $P(x_0, y_0)$ in a triangular element.

where, as before, t is element thickness. In this type of problem, it is customary to take t as unity, so that all computations are *per unit length*. In accordance with this convention, the source strength is denoted Q^* , having units typically expressed as Btu/(hr-ft²) or W/m². Equation 7.55 then becomes

$$\{f_Q^{(e)}\} = \iint_A Q^* [N]^T dA = \iint_A Q^* \{N\} dA \quad (7.56)$$

The question is now mathematical: How do we integrate a function applicable at a single point in a two-dimensional domain? Mathematically, the operation is quite simple if the concept of the *Dirac delta* or *unit impulse* function is introduced. We choose not to take the strictly mathematical approach, however, in the interest of using an approach based on logic and all the foregoing information presented on interpolation functions.

For illustrative purposes, the heat source is assumed to be located at a known point $P = (x_0, y_0)$ in the interior of a three-node triangular element, as in Figure 7.14. If we know the temperature at each of the three nodes of the element, then the temperature at point P is a weighted combination of the nodal temperatures. By this point in the text, the reader is well aware that the weighting factors are the interpolation functions. If nodal values are interpolated to a specific point, a value at that point should properly be assigned to the nodes via the same interpolation functions evaluated at the point. Using this premise, the nodal forces for

the triangular element become (assuming Q^* to be constant)

$$\{f_Q^{(e)}\} = Q^* \iint_A \begin{Bmatrix} N_1(x_0, y_0) \\ N_2(x_0, y_0) \\ N_3(x_0, y_0) \end{Bmatrix} dA \quad (7.57)$$

For a three-node triangular element, the interpolation functions (from Chapter 6) are simply the area coordinates, so we now have

$$\{f_Q^{(e)}\} = Q^* \iint_A \begin{Bmatrix} L_1(x_0, y_0) \\ L_2(x_0, y_0) \\ L_3(x_0, y_0) \end{Bmatrix} dA = Q^* A \begin{Bmatrix} L_1(x_0, y_0) \\ L_2(x_0, y_0) \\ L_3(x_0, y_0) \end{Bmatrix} \quad (7.58)$$

Now consider the “behavior” of the area coordinates as the position of the interior point P varies in the element. As P approaches node 1, for example, area coordinate L_1 approaches unity value. Clearly, if the source is located at node 1, the entire source value should be allocated to that node. A similar argument can be made for each of the other nodes. Another very important point to observe here is that the total heat generation as allocated to the nodes by Equation 7.58 is equivalent to the source. If we sum the individual nodal contributions given in Equation 7.58, we obtain

$$\sum_{i=1}^3 Q_i^{*(e)} = \sum_{i=1}^3 (L_1^{(e)} + L_2^{(e)} + L_3^{(e)}) Q^* A = Q^* A \quad (7.59)$$

since $\sum_{i=1}^3 L_i = 1$ is known by the definition of area coordinates.

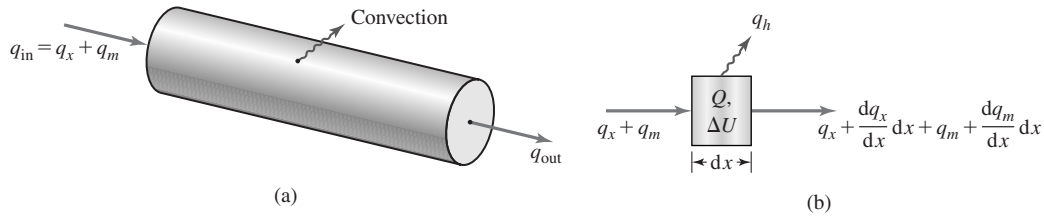
The foregoing approach using logic and our knowledge of interpolation functions is without mathematical rigor. If we approach the situation of a line source mathematically, the result is exactly the same as that given by Equation 7.58 for the triangular element. For any element chosen, the force vector corresponding to a line source (keep in mind that, in two-dimensions, this looks like a point source) the nodal force contributions are

$$\{f_Q^{(e)}\} = Q^* \iint_A \{N(x_0, y_0)\} dA \quad (7.60)$$

Thus, a source of internal heat generation is readily allocated to the nodes of a finite element via the interpolation functions of the specific element applied.

7.5 HEAT TRANSFER WITH MASS TRANSPORT

The finite element formulations and examples previously presented deal with solid media in which heat flows as a result of conduction and convection. An additional complication arises when the medium of interest is a flowing fluid. In such a case, heat flows by conduction, convection, and via motion of the media. The last effect, referred to as *mass transport*, is considered here for the

**Figure 7.15**

(a) One-dimensional conduction with convection and mass transport. (b) Control volume for energy balance.

one-dimensional case. Figure 7.15a is essentially Figure 7.2a with a major physical difference. The volume shown in Figure 7.15a represents a flowing fluid (as in a pipe, for example) and heat is transported as a result of the flow. The heat flux associated with mass transport is denoted q_m , as indicated in the figure. The additional flux term arising from mass transport is given by

$$q_m = \dot{m}cT \quad (\text{W or Btu/hr}) \quad (7.61)$$

where \dot{m} is mass flow rate (kg/hr or slug/hr), c is the specific heat of the fluid (W-hr/(kg-°C) or Btu/(slug-°F)), and $T(x)$ is the temperature of the fluid (°C or °F). A control volume of length dx of the flow is shown in Figure 7.15b, where the flux terms have been expressed as two-term Taylor series as in past derivations. Applying the principle of conservation of energy (in analogy with Equation 7.1),

$$\begin{aligned} q_x A dt + q_m dt + Q A dx dt = \Delta U + \left(q_x + \frac{dq_x}{dx} dx \right) A dt \\ + \left(q_m + \frac{dq_m}{dx} dx \right) dt + q_h P dx dt \end{aligned} \quad (7.62)$$

Considering steady-state conditions, $\Delta U = 0$, using Equations 5.51 and 7.2 and simplifying yields

$$\frac{d}{dx} \left(k_x \frac{dT}{dx} \right) + Q = \frac{dq_m}{dx} + \frac{hP}{A} (T - T_a) \quad (7.63)$$

where all terms are as previously defined. Substituting for q_m into Equation 7.63, we obtain

$$\frac{d}{dx} \left(k_x \frac{dT}{dx} \right) + Q = \frac{d}{dx} \left(\frac{\dot{m}c}{A} T \right) + \frac{hP}{A} (T - T_a) \quad (7.64)$$

which for constant material properties and constant mass flow rate (steady state) becomes

$$k_x \frac{d^2 T}{dx^2} + Q = \frac{\dot{m}c}{A} \frac{dT}{dx} + \frac{hP}{A} (T - T_a) \quad (7.65)$$

With the exception of the mass transport term, Equation 7.65 is identical to Equation 7.4. Consequently, if we apply Galerkin's finite element method, the procedure and results are identical to those of Section 7.3, except for additional stiffness matrix terms arising from mass transport. Rather than repeat the derivation of known terms, we develop only the additional terms. If Equation 7.65 is substituted into the residual equations for a two-node linear element (Equation 7.6), the additional terms are

$$\int_{x_1}^{x_2} \dot{m}c \frac{dT}{dx} N_i dx \quad i = 1, 2 \quad (7.66)$$

Substituting for T via Equation 7.5, this becomes

$$\int_{x_1}^{x_2} \dot{m}c \left[\frac{dN_1}{dx} T_1 + \frac{dN_2}{dx} T_2 \right] N_i dx \quad i = 1, 2 \quad (7.67)$$

Therefore, the additional stiffness matrix resulting from mass transport is

$$[k_{\dot{m}}] = \dot{m}c \int_{x_1}^{x_2} \begin{bmatrix} N_1 \frac{dN_1}{dx} & N_1 \frac{dN_2}{dx} \\ N_2 \frac{dN_1}{dx} & N_2 \frac{dN_2}{dx} \end{bmatrix} dx \quad (7.68)$$

EXAMPLE 7.8

Explicitly evaluate the stiffness matrix given by Equation 7.68 for the two-node element.

■ Solution

The interpolation functions are

$$N_1 = 1 - \frac{x}{L}$$

$$N_2 = \frac{x}{L}$$

and the required derivatives are

$$\frac{dN_1}{dx} = -\frac{1}{L}$$

$$\frac{dN_2}{dx} = \frac{1}{L}$$

Utilizing the change of variable $s = x/L$, Equation 7.68 becomes

$$[k_{\dot{m}}] = \frac{\dot{m}c}{L} \int_0^1 \begin{bmatrix} -(1-s) & (1-s) \\ -s & s \end{bmatrix} L ds = \dot{m}c \begin{bmatrix} -\frac{1}{2} & \frac{1}{2} \\ -\frac{1}{2} & \frac{1}{2} \end{bmatrix} = \frac{\dot{m}c}{2} \begin{bmatrix} -1 & 1 \\ -1 & 1 \end{bmatrix}$$

and note that the matrix is not symmetric.

Using the result of Example 7.8, the stiffness matrix for a one-dimensional heat transfer element with conduction, convection, and mass transport is given by

$$\begin{aligned} [k^{(e)}] &= \frac{k_x A}{L} \begin{bmatrix} 1 & -1 \\ -1 & 1 \end{bmatrix} + \frac{h P L}{6} \begin{bmatrix} 2 & 1 \\ 1 & 2 \end{bmatrix} + \frac{\dot{m} c}{2} \begin{bmatrix} -1 & 1 \\ -1 & 1 \end{bmatrix} \\ &= [k_c^{(e)}] + [k_h^{(e)}] + [k_m^{(e)}] \end{aligned} \quad (7.69)$$

where the conduction and convection terms are identical to those given in Equation 7.15. Note that the forcing functions and boundary conditions for the one-dimensional problem with mass transport are the same as given in Section 7.3, Equations 7.16 through 7.19.

EXAMPLE 7.9

Figure 7.16a shows a thin-walled tube that is part of an oil cooler. Engine oil enters the tube at the left end at temperature 50°C with a flow rate of 0.2 kg/min . The tube is surrounded by air flowing at a constant temperature of 15°C . The thermal properties of the oil are as follows:

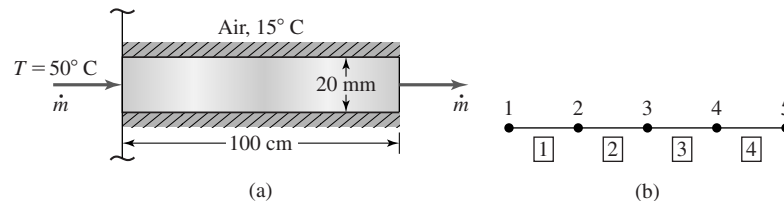
Thermal conductivity: $k_x = 0.156 \text{ W/(m}\cdot^\circ\text{C)}$

Specific heat: $c = 0.523 \text{ W}\cdot\text{hr}/(\text{kg}\cdot^\circ\text{C})$

The convection coefficient between the thin wall and the flowing air is $h = 300 \text{ W}/(\text{m}^2\cdot^\circ\text{C})$. The tube wall thickness is such that conduction effects in the wall are to be neglected; that is, the wall temperature is constant through its thickness and the same as the temperature of the oil in contact with the wall at any position along the length of the tube. Using four two-node finite elements, obtain an approximate solution for the temperature distribution along the length of the tube and determine the heat removal rate via convection.

■ Solution

The finite element model is shown schematically in Figure 7.16b, using equal length elements $L = 25 \text{ cm} = 0.025 \text{ m}$. The cross-sectional area is $A = (\pi/4)(20/1000)^2 =$

**Figure 7.16**

(a) Oil cooler tube of Example 7.9. (b) Element and node numbers for a four-element model.

7.5 Heat Transfer With Mass Transport

265

$3.14(10^{-4}) \text{ m}^2$. And the peripheral dimension (circumference) of each element is $P = \pi(20/1000) = 6.28(10^{-2}) \text{ m}$. The stiffness matrix for each element (note that all elements are identical) is computed via Equation 7.69 as follows:

$$\begin{aligned} [k_c^{(e)}] &= \frac{k_x A}{L} \begin{bmatrix} 1 & -1 \\ -1 & 1 \end{bmatrix} = \frac{0.156(3.14)(10^{-4})}{0.025} \begin{bmatrix} 1 & -1 \\ -1 & 1 \end{bmatrix} \\ &= \begin{bmatrix} 1.9594 & -1.9594 \\ -1.9594 & 1.9594 \end{bmatrix} (10^{-3}) \\ [k_h^{(e)}] &= \frac{hPL}{6} \begin{bmatrix} 2 & 1 \\ 1 & 2 \end{bmatrix} = \frac{300(6.28)(10^{-2})(0.025)}{6} \begin{bmatrix} 2 & 1 \\ 1 & 2 \end{bmatrix} = \begin{bmatrix} 0.157 & 0.0785 \\ 0.0785 & 0.157 \end{bmatrix} \\ [k_m^{(e)}] &= \frac{\dot{m}c}{2} \begin{bmatrix} -1 & 1 \\ -1 & 1 \end{bmatrix} = \frac{(0.2)(60)(0.523)}{2} \begin{bmatrix} -1 & 1 \\ -1 & 1 \end{bmatrix} = \begin{bmatrix} -3.138 & 3.138 \\ -3.138 & 3.138 \end{bmatrix} \\ [k^{(e)}] &= \begin{bmatrix} -2.9810 & 3.2165 \\ -3.0595 & 3.2950 \end{bmatrix} \end{aligned}$$

At this point, note that the mass transport effects dominate the stiffness matrix and we anticipate that very little heat is dissipated, as most of the heat is carried away with the flow. Also observe that, owing to the relative magnitudes, the conduction effects have been neglected.

Assembling the global stiffness matrix via the now familiar procedure, we obtain

$$[K] = \begin{bmatrix} -2.9810 & 3.2165 & 0 & 0 & 0 \\ -3.0595 & 0.314 & 3.2165 & 0 & 0 \\ 0 & -3.0595 & 0.314 & 3.2165 & 0 \\ 0 & 0 & -3.0595 & 0.314 & 3.2165 \\ 0 & 0 & 0 & -3.0595 & 3.2950 \end{bmatrix}$$

The convection-driven forcing function for each element per Equation 7.18 is

$$\{f_h^{(e)}\} = \frac{hPT_a L}{2} \begin{Bmatrix} 1 \\ 1 \end{Bmatrix} = \frac{300(6.28)(10^{-2})(15)(0.025)}{2} \begin{Bmatrix} 1 \\ 1 \end{Bmatrix} = \begin{Bmatrix} 3.5325 \\ 3.5325 \end{Bmatrix}$$

As there is no internal heat generation, the per-element contribution of Equation 7.16 is zero. Finally, we must examine the boundary conditions. At node 1, the temperature is specified but the heat flux $q_1 = F_1$ is unknown; at node 5 (the exit), the flux is also unknown. Unlike previous examples, where a convection boundary condition existed, here we assume that the heat removed at node 5 is strictly a result of mass transport. Physically, this means we define the problem such that heat transfer ends at node 5 and the heat remaining in the flow at this node (the exit) is carried away to some other process. Consequently, we do not consider either a conduction or convection boundary condition at node 5. Instead, we compute the temperature at node 5 then the heat removed at this node via the mass transport relation. In terms of the finite element model, this means

that we do not consider the heat flow through node 5 as an unknown (reaction force). With this in mind, we assemble the global force vector from the element force vectors to obtain

$$\{F\} = \begin{Bmatrix} 3.5325 + F_1 \\ 7.065 \\ 7.065 \\ 7.065 \\ 3.5325 \end{Bmatrix}$$

The assembled system (global) equations are then

$$[K]\{T\} = \begin{bmatrix} -2.9801 & 3.2165 & 0 & 0 & 0 \\ -3.0595 & 0.314 & 3.2165 & 0 & 0 \\ 0 & -3.0595 & 0.314 & 3.2165 & 0 \\ 0 & 0 & -3.0595 & 0.314 & 3.2165 \\ 0 & 0 & 0 & -3.0595 & 3.2950 \end{bmatrix} \begin{Bmatrix} T_1 \\ T_2 \\ T_3 \\ T_4 \\ T_5 \end{Bmatrix}$$

$$= \begin{Bmatrix} 3.5325 + F_1 \\ 7.065 \\ 7.065 \\ 7.065 \\ 3.5325 \end{Bmatrix}$$

Applying the known condition at node 1, $T = 50^\circ\text{C}$, the reduced system equations become

$$\begin{bmatrix} 0.314 & 3.2165 & 0 & 0 \\ -3.0595 & 0.314 & 3.2165 & 0 \\ 0 & -3.0595 & 0.314 & 3.2165 \\ 0 & 0 & -3.0595 & 3.2950 \end{bmatrix} \begin{Bmatrix} T_2 \\ T_3 \\ T_4 \\ T_5 \end{Bmatrix} = \begin{Bmatrix} 160.04 \\ 7.065 \\ 7.065 \\ 3.5325 \end{Bmatrix}$$

which yields the solution for the nodal temperatures as

$$\begin{Bmatrix} T_2 \\ T_3 \\ T_4 \\ T_5 \end{Bmatrix} = \begin{Bmatrix} 47.448 \\ 45.124 \\ 42.923 \\ 40.928 \end{Bmatrix} ^\circ\text{C}$$

As conduction effects have been seen to be negligible, the input rate is computed as

$$q_{in} = q_{m1} = \dot{m}cT_1 = 0.2(60)(0.523)(50) = 3138 \text{ W}$$

while, at node 5, the output rate is

$$q_{m5} = \dot{m}cT_5 = 0.2(60)(0.523)(40.928) = 2568.6 \text{ W}$$

The results show that only about 18 percent of input heat is removed, so the cooler is not very efficient.

7.6 HEAT TRANSFER IN THREE DIMENSIONS

As the procedure has been established, the governing equation for heat transfer in three dimensions is not derived in detail here. Instead, we simply present the equation as

$$\frac{\partial}{\partial x} \left(k_x \frac{\partial T}{\partial x} \right) + \frac{\partial}{\partial y} \left(k_y \frac{\partial T}{\partial y} \right) + \frac{\partial}{\partial z} \left(k_z \frac{\partial T}{\partial z} \right) + Q = 0 \quad (7.70)$$

and note that only conduction effects are included and steady-state conditions are assumed. In the three-dimensional case, convection effects are treated most efficiently as boundary conditions, as is discussed.

The domain to which Equation 7.70 applies is represented by a mesh of finite elements in which the temperature distribution is discretized as

$$T(x, y, z) = \sum_{i=1}^M N_i(x, y, z) T_i = [N]\{T\} \quad (7.71)$$

where M is the number of nodes per element. Application of the Galerkin method to Equation 7.70 results in M residual equations:

$$\iiint_V \left[\frac{\partial}{\partial x} \left(k_x \frac{\partial T}{\partial x} \right) + \frac{\partial}{\partial y} \left(k_y \frac{\partial T}{\partial y} \right) + \frac{\partial}{\partial z} \left(k_z \frac{\partial T}{\partial z} \right) + Q \right] N_i \, dV = 0 \quad (7.72)$$

$i = 1, \dots, M$

where, as usual, V is element volume.

In a manner analogous to Section 7.4 for the two-dimensional case, the derivative terms can be written as

$$\begin{aligned} \frac{\partial}{\partial x} \left(k_x \frac{\partial T}{\partial x} \right) N_i &= \frac{\partial}{\partial x} \left(k_x \frac{\partial T}{\partial x} N_i \right) - k_x \frac{\partial T}{\partial x} \frac{\partial N_i}{\partial x} \\ \frac{\partial}{\partial y} \left(k_y \frac{\partial T}{\partial y} \right) N_i &= \frac{\partial}{\partial y} \left(k_y \frac{\partial T}{\partial y} N_i \right) - k_y \frac{\partial T}{\partial y} \frac{\partial N_i}{\partial y} \\ \frac{\partial}{\partial z} \left(k_z \frac{\partial T}{\partial z} \right) N_i &= \frac{\partial}{\partial z} \left(k_z \frac{\partial T}{\partial z} N_i \right) - k_z \frac{\partial T}{\partial z} \frac{\partial N_i}{\partial z} \end{aligned} \quad (7.73)$$

and the residual equations become

$$\begin{aligned} &\iiint_V \left[\frac{\partial}{\partial x} \left(k_x \frac{\partial T}{\partial x} N_i \right) + \frac{\partial}{\partial y} \left(k_y \frac{\partial T}{\partial y} N_i \right) + \frac{\partial}{\partial z} \left(k_z \frac{\partial T}{\partial z} N_i \right) \right] dV + \iiint_V Q N_i \, dV \\ &= \iiint_V \left(k_x \frac{\partial T}{\partial x} \frac{\partial N_i}{\partial x} + k_y \frac{\partial T}{\partial y} \frac{\partial N_i}{\partial y} + k_z \frac{\partial T}{\partial z} \frac{\partial N_i}{\partial z} \right) dV \quad i = 1, \dots, M \end{aligned} \quad (7.74)$$

The integral on the left side of Equation 7.74 contains a perfect differential in three dimensions and can be replaced by an integral over the surface of the volume using Green's theorem in three dimensions: If $F(x, y, z)$, $G(x, y, z)$, and

$H(x, y, z)$ are functions defined in a region of xyz space (the element volume in our context), then

$$\iiint_V \left(\frac{\partial F}{\partial x} + \frac{\partial G}{\partial y} + \frac{\partial H}{\partial z} \right) dV = \iint_A (Fn_x + Gn_y + Hn_z) dA \quad (7.75)$$

where A is the surface area of the volume and n_x, n_y, n_z are the Cartesian components of the outward unit normal vector of the surface area. This theorem is the three-dimensional counterpart of integration by parts discussed earlier in this chapter.

Invoking Fourier's law and comparing Equation 7.75 to the first term of Equation 7.74, we have

$$\begin{aligned} & - \iint_A (q_x n_x + q_y n_y + q_z n_z) N_i dA + \iiint_V Q N_i dV \\ & = \iiint_V \left(k_x \frac{\partial T}{\partial x} \frac{\partial N_i}{\partial x} + k_y \frac{\partial T}{\partial y} \frac{\partial N_i}{\partial y} + k_z \frac{\partial T}{\partial z} \frac{\partial N_i}{\partial z} \right) dV \quad i = 1, \dots, M \end{aligned} \quad (7.76)$$

Inserting the matrix form of Equation 7.71 and rearranging, we have

$$\begin{aligned} & \iiint_V \left(k_x \frac{\partial [N]}{\partial x} \frac{\partial N_i}{\partial x} + k_y \frac{\partial [N]}{\partial y} \frac{\partial N_i}{\partial y} + k_z \frac{\partial [N]}{\partial z} \frac{\partial N_i}{\partial z} \right) \{T\} dV \\ & = \iiint_V Q N_i dV - \iint_A (q_x n_x + q_y n_y + q_z n_z) N_i dA \quad i = 1, \dots, M \end{aligned} \quad (7.77)$$

Equation 7.77 represents a system of M algebraic equations in the M unknown nodal temperatures $\{T\}$. With the exception that convection effects are not included here, Equation 7.77 is analogous to the two-dimensional case represented by Equation 7.34. In matrix notation, the system of equations for the three-dimensional element formulation is

$$\begin{aligned} & \iiint_V \left(k_x \frac{\partial [N]^T}{\partial x} \frac{\partial [N]}{\partial x} + k_y \frac{\partial [N]^T}{\partial y} \frac{\partial [N]}{\partial y} + k_z \frac{\partial [N]^T}{\partial z} \frac{\partial [N]}{\partial z} \right) dV \{T\} \\ & = \iiint_V Q [N]^T dV - \iint_A (q_x n_x + q_y n_y + q_z n_z) [N]^T dA \end{aligned} \quad (7.78)$$

and Equation 7.76 is in the desired form

$$[k^{(e)}] \{T^{(e)}\} = \{f_Q^{(e)}\} + \{f_q^{(e)}\} \quad (7.79)$$

Comparing the last two equations, the element conductance (stiffness) matrix is

$$[k^{(e)}] = \iiint_V \left(k_x \frac{\partial [N]^T}{\partial x} \frac{\partial [N]}{\partial x} + k_y \frac{\partial [N]^T}{\partial y} \frac{\partial [N]}{\partial y} + k_z \frac{\partial [N]^T}{\partial z} \frac{\partial [N]}{\partial z} \right) dV \quad (7.80)$$

the element force vector representing internal heat generation is

$$\{f_Q^{(e)}\} = \iiint_V Q[N]^T dV \quad (7.81)$$

and the element nodal force vector associated with heat flux across the element surface area is

$$\{f_q^{(e)}\} = - \iint_A (q_x n_x + q_y n_y + q_z n_z)[N]^T dA \quad (7.82)$$

7.6.1 System Assembly and Boundary Conditions

The procedure for assembling the global equations for a three-dimensional model for heat transfer analysis is identical to that of one- and two-dimensional problems. The element type is selected (tetrahedral, brick, quadrilateral solid, for example) based on geometric considerations, primarily. The volume is then divided into a mesh of elements by first defining nodes (in the global coordinate system) throughout the volume then each element by the sequence and number of nodes required for the element type. Element-to-global nodal correspondence relations are then determined for each element, and the global stiffness (conductance) matrix is assembled. Similarly, the global force vector is assembled by adding element contributions at nodes common to two or more elements. The latter procedure is straightforward in the case of internal generation, as given by Equation 7.81. However, in the case of the element gradient terms, Equation 7.82, the procedure is best described in terms of the global boundary conditions.

In the case of three-dimensional heat transfer, we have the same three types of boundary conditions as in two dimensions: (1) specified temperatures, (2) specified heat flux, and (3) convection conditions. The first case, specified temperatures, is taken into account in the usual manner, by reducing the system equations by simply substituting the known nodal temperatures into the system equations. The latter two cases involve only elements that have surfaces (element faces) on the outside surface of the global volume. To illustrate, Figure 7.17a shows two brick elements that share a common face in an assembled finite element model. For convenience, we take the common face to be perpendicular to the x axis. In Figure 7.17b, the two elements are shown separately with the associated normal vector components identified for the shared faces. For steady-state heat transfer, the heat flux across the face is the same for each element and, since the unit normal vectors are opposite, the gradient force terms cancel. The result is completely analogous to internal forces in a structural problem via Newton's third law of action and reaction. Therefore, on interelement boundaries (which are areas for three-dimensional elements), the element force terms defined by Equation 7.82 sum to zero in the global assembly process.

What of the element surface areas that are part of the surface area of the volume being modeled? Generally, these outside areas are subjected to convection

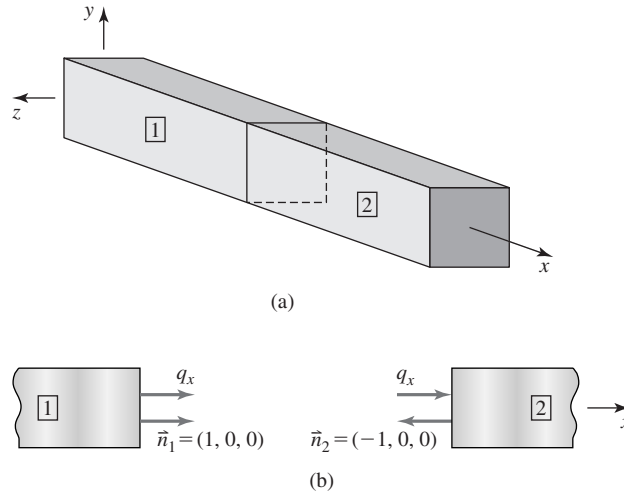


Figure 7.17
 (a) Common face in two 3-D elements. (b) Edge view of common face, illustrating cancellation of conduction gradient terms.

conditions. For such convection boundary conditions, the flux conditions of Equation 7.82 must be in balance with the convection from the area of concern. Mathematically, the condition is expressed as

$$\begin{aligned}
 \{f_q^{(e)}\} &= - \iint_A (q_x n_x + q_y n_y + q_z n_z) [N]^T dA = - \iint_A q_n n [N]^T dA \\
 &= - \iint_A h (T^{(e)} - T_a) [N]^T dA \qquad (7.83)
 \end{aligned}$$

where q_n is the flux normal to the surface area A of a specific element face on the global boundary and n is the unit outward normal vector to that face. As in two-dimensional analysis, the convection term in the rightmost integral of Equation 7.83 adds to the stiffness matrix when the expression for $T^{(e)}$ in terms of interpolation functions and nodal temperatures is substituted. Similarly, the ambient temperature terms add to the forcing function vector.

In most commercial finite element software packages, the three-dimensional heat transfer elements available do *not* explicitly consider the gradient force vector represented by Equation 7.82. Instead, such programs compute the system (global) stiffness matrix on the basis of conductance only and rely on the user to specify the flux or convection boundary conditions (and the specified temperature conditions, of course) as part of the loading (input) data.

Owing to the algebraic volume of calculation required, examples of general three-dimensional heat transfer are not presented here. A few three-dimensional problems are included in the end-of-chapter exercises and are intended to be solved by digital computer techniques.

7.7 AXISYMMETRIC HEAT TRANSFER

Chapter 6 illustrated the approach for utilizing two-dimensional elements and associated interpolation functions for axisymmetric problems. Here, we illustrate the formulation of finite elements to solve problems in axisymmetric heat transfer. Illustrated in Figure 7.18 is a body of revolution subjected to heat input at its base, and the heat input is assumed to be symmetric about the axis of revolution. Think of the situation as a cylindrical vessel heated by a source, such as a gas flame. This situation could, for example, represent a small crucible for melting metal prior to casting.

As an axisymmetric problem is three-dimensional, the basic governing equation is Equation 7.70, restated here under the assumption of homogeneity, so that $k_x = k_y = k_z = k$, as

$$k \left(\frac{\partial^2 T}{\partial x^2} + \frac{\partial^2 T}{\partial y^2} + \frac{\partial^2 T}{\partial z^2} \right) + Q = 0 \quad (7.84)$$

Equation 7.84 is applicable to steady-state conduction only and is expressed in rectangular coordinates. For axisymmetric problems, use of a cylindrical coordinate system (r, θ, z) is much more amenable to formulating the problem. To convert to cylindrical coordinates, the partial derivatives with respect to x and y in Equation 7.84 must be converted mathematically into the corresponding partial derivatives with respect to radial coordinate r and tangential (circumferential)

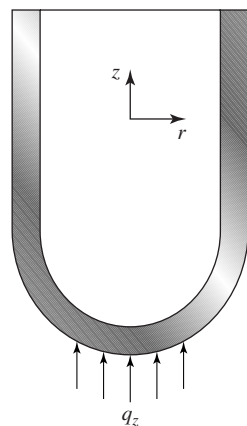


Figure 7.18 An axisymmetric heat transfer problem. All properties and inputs are symmetric about the z axis.

coordinate θ . In the following development, we present the general approach but leave the details as an end-of-chapter exercise.

The basic relations between the rectangular coordinates x , y and the cylindrical (polar) coordinates r , θ are

$$\begin{aligned}x &= r \cos \theta \\y &= r \sin \theta\end{aligned}\quad (7.85)$$

and inversely,

$$\begin{aligned}r^2 &= x^2 + y^2 \\ \tan \theta &= \frac{y}{x}\end{aligned}\quad (7.86)$$

Per the chain rule of differentiation, we have

$$\begin{aligned}\frac{\partial T}{\partial x} &= \frac{\partial T}{\partial r} \frac{\partial r}{\partial x} + \frac{\partial T}{\partial \theta} \frac{\partial \theta}{\partial x} \\ \frac{\partial T}{\partial y} &= \frac{\partial T}{\partial r} \frac{\partial r}{\partial y} + \frac{\partial T}{\partial \theta} \frac{\partial \theta}{\partial y}\end{aligned}\quad (7.87)$$

By implicit differentiation of Equation 7.86,

$$\begin{aligned}2r \frac{\partial r}{\partial x} &= 2x \Rightarrow \frac{\partial r}{\partial x} = \frac{x}{r} = \cos \theta \\ 2r \frac{\partial r}{\partial y} &= 2y \Rightarrow \frac{\partial r}{\partial y} = \frac{y}{r} = \sin \theta \\ \frac{1}{\sec^2 \theta} \frac{\partial \theta}{\partial x} &= -\frac{y}{x^2} \Rightarrow \frac{\partial \theta}{\partial x} = -\frac{\sin \theta}{r} \\ \frac{1}{\sec^2 \theta} \frac{\partial \theta}{\partial y} &= \frac{1}{x} \Rightarrow \frac{\partial \theta}{\partial y} = \frac{\cos \theta}{r}\end{aligned}\quad (7.88)$$

so that Equation 7.87 becomes

$$\begin{aligned}\frac{\partial T}{\partial x} &= \cos \theta \frac{\partial T}{\partial r} - \frac{\sin \theta}{r} \frac{\partial T}{\partial \theta} \\ \frac{\partial T}{\partial y} &= \sin \theta \frac{\partial T}{\partial r} + \frac{\cos \theta}{r} \frac{\partial T}{\partial \theta}\end{aligned}\quad (7.89)$$

For the second partial derivatives, we have

$$\begin{aligned}\frac{\partial^2 T}{\partial x^2} &= \frac{\partial}{\partial x} \left(\frac{\partial T}{\partial x} \right) = \cos \theta \frac{\partial}{\partial r} \left(\frac{\partial T}{\partial x} \right) - \frac{\sin \theta}{r} \frac{\partial}{\partial \theta} \left(\frac{\partial T}{\partial x} \right) \\ \frac{\partial^2 T}{\partial y^2} &= \frac{\partial}{\partial y} \left(\frac{\partial T}{\partial y} \right) = \sin \theta \frac{\partial}{\partial r} \left(\frac{\partial T}{\partial y} \right) + \frac{\cos \theta}{r} \frac{\partial}{\partial \theta} \left(\frac{\partial T}{\partial y} \right)\end{aligned}\quad (7.90)$$

Applying Equation 7.89 to the operations indicated in Equation 7.90 yields (with appropriate use of trigonometric identities)

$$\frac{\partial^2 T}{\partial x^2} + \frac{\partial^2 T}{\partial y^2} = \frac{\partial^2 T}{\partial r^2} + \frac{1}{r} \frac{\partial T}{\partial r} + \frac{1}{r^2} \frac{\partial^2 T}{\partial \theta^2} \quad (7.91)$$

where the derivation represents a general change of coordinates. To relate to an axisymmetric problem, recall that there is no dependence on the tangential coordinate θ . Consequently, when Equations 7.84 and 7.91 are combined, the governing equation for axisymmetric heat transfer is

$$k \left(\frac{\partial^2 T}{\partial r^2} + \frac{1}{r} \frac{\partial T}{\partial r} + \frac{\partial^2 T}{\partial z^2} \right) + Q = 0 \quad (7.92)$$

and, of course, note the absence of the tangential coordinate.

7.7.1 Finite Element Formulation

Per the general procedure, the total volume of the axisymmetric domain is discretized into finite elements. In each element, the temperature distribution is expressed in terms of the nodal temperatures and interpolation functions as

$$T^{(e)} = \sum_{i=1}^M N_i(r, z) T_i^{(e)} \quad (7.93)$$

where, as usual, M is the number of element nodes. Note particularly that the interpolation functions vary with radial coordinate r and axial coordinate z . Application of Galerkin's method using Equations 7.92 and 7.93 yields the residual equations

$$\iiint_V \left[k \left(\frac{\partial^2 T}{\partial r^2} + \frac{1}{r} \frac{\partial T}{\partial r} + \frac{\partial^2 T}{\partial z^2} \right) + Q \right] N_i r \, dr \, d\theta \, dz = 0 \quad i = 1, \dots, M \quad (7.94)$$

Observing that, for the axisymmetric case, the integrand is independent of the tangential coordinate θ , Equation 7.94 becomes

$$2\pi \iint_{A^{(e)}} \left[k \left(\frac{\partial^2 T}{\partial r^2} + \frac{1}{r} \frac{\partial T}{\partial r} + \frac{\partial^2 T}{\partial z^2} \right) + Q \right] N_i r \, dr \, dz = 0 \quad i = 1, \dots, M \quad (7.95)$$

where $A^{(e)}$ is the area of the element in the rz plane. The first two terms of the integrand can be combined to obtain

$$2\pi \iint_{A^{(e)}} \left[k \left(\frac{1}{r} \frac{\partial}{\partial r} \left(r \frac{\partial T}{\partial r} \right) + \frac{\partial^2 T}{\partial z^2} \right) + Q \right] N_i r \, dr \, dz = 0 \quad i = 1, \dots, M \quad (7.96)$$

Observing that r is independent of z , Equation 7.96 becomes

$$2\pi \iint_{A^{(e)}} \left[k \left[\frac{\partial}{\partial r} \left(r \frac{\partial T}{\partial r} \right) + \frac{\partial}{\partial z} \left(r \left(\frac{\partial T}{\partial z} \right) \right) \right] + Qr \right] N_i \, dr \, dz = 0 \quad i = 1, \dots, M \quad (7.97)$$

As in previous developments, we invoke the chain rule of differentiation as, for example,

$$\begin{aligned} \frac{\partial}{\partial r} \left(r N_i \frac{\partial T}{\partial r} \right) &= N_i \frac{\partial}{\partial r} \left(r \frac{\partial T}{\partial r} \right) + r \frac{\partial T}{\partial r} \frac{\partial N_i}{\partial r} \Rightarrow N_i \frac{\partial}{\partial r} \left(r \frac{\partial T}{\partial r} \right) \\ &= \frac{\partial}{\partial r} \left(r N_i \frac{\partial T}{\partial r} \right) - r \frac{\partial T}{\partial r} \frac{\partial N_i}{\partial r} \quad i = 1, \dots, M \end{aligned} \quad (7.98)$$

Noting that Equation 7.98 is also applicable to the z variable, the residual equations represented by Equation 7.97 can be written as

$$\begin{aligned} 2\pi \iint_{A^{(e)}} k \left[\frac{\partial}{\partial r} \left(r N_i \frac{\partial T}{\partial r} \right) + \frac{\partial}{\partial z} \left(r N_i \frac{\partial T}{\partial z} \right) \right] \, dr \, dz + 2\pi \iint_{A^{(E)}} Q N_i r \, dr \, dz \\ = 2\pi \iint_{A^{(e)}} k \left(\frac{\partial T}{\partial r} \frac{\partial N_i}{\partial r} + \frac{\partial T}{\partial z} \frac{\partial N_i}{\partial z} \right) r \, dr \, dz \quad i = 1, \dots, M \end{aligned} \quad (7.99)$$

The first integrand on the left side of Equation 7.99 is a perfect differential in two dimensions, and the Green-Gauss theorem can be applied to obtain

$$\begin{aligned} 2\pi \oint_{S^{(e)}} \left(k \frac{\partial T}{\partial r} n_r + k \frac{\partial T}{\partial z} n_z \right) r N_i \, dS + 2\pi \iint_{A^{(e)}} Q N_i r \, dr \, dz \\ = 2\pi \iint_{A^{(e)}} k \left(\frac{\partial T}{\partial r} \frac{\partial N_i}{\partial r} + \frac{\partial T}{\partial z} \frac{\partial N_i}{\partial z} \right) r \, dr \, dz \quad i = 1, \dots, M \end{aligned} \quad (7.100)$$

where S is the boundary (periphery) of the element and n_r and n_z are the radial and axial components of the outward unit vector normal to the boundary. Applying Fourier's law in cylindrical coordinates,

$$\begin{aligned} q_r &= -k \frac{\partial T}{\partial r} \\ q_z &= -k \frac{\partial T}{\partial z} \end{aligned} \quad (7.101)$$

and noting the analogy with Equation 7.33, we rewrite Equation 7.100 as

$$\begin{aligned} 2\pi k \iint_{A^{(e)}} \left(\frac{\partial T}{\partial r} \frac{\partial N_i}{\partial r} + \frac{\partial T}{\partial z} \frac{\partial N_i}{\partial z} \right) r \, dr \, dz \\ = 2\pi \iint_{A^{(e)}} Q N_i r \, dr \, dz - 2\pi \oint_{S^{(e)}} q_s n_s N_i r \, dS \quad i = 1, \dots, M \end{aligned} \quad (7.102)$$

The common term 2π could be omitted, but we leave it as a reminder of the three-dimensional nature of an axisymmetric problem. In particular, note that this term, in conjunction with r in the integrand of the last integral on the right-hand side of Equation 7.102, reinforces the fact that element boundaries are actually surfaces of revolution.

Noting that Equation 7.102 represents a system of M equations, the form of the system is that of

$$[k^{(e)}] \{T^{(e)}\} = \{f_Q^{(e)}\} + \{f_g^{(e)}\} \quad (7.103)$$

where $[k^{(e)}]$ is the element conductance matrix having individual terms defined by

$$k_{ij} = 2\pi k \iint_{A^{(e)}} \left(\frac{\partial N_i}{\partial r} \frac{\partial N_j}{\partial r} + \frac{\partial N_i}{\partial z} \frac{\partial N_j}{\partial z} \right) r \, dr \, dz \quad i, j = 1, \dots, M \quad (7.104)$$

and $\{T^{(e)}\}$ is the column matrix (vector) of element nodal temperatures per Equation 7.93. The element forcing functions include the internal heat generation terms given by

$$\{f_Q^{(e)}\} = 2\pi \iint_{A^{(e)}} Q \{N\} r \, dr \, dz \quad (7.105)$$

and the boundary gradient (flux) components

$$\{f_g^{(e)}\} = -2\pi \oint_{S^{(e)}} q_s n_s \{N\} r \, dS \quad (7.106)$$

As has been discussed for other cases, on boundaries common to two elements, the flux terms are self-canceling in the model assembly procedure. Therefore, Equation 7.106 is applicable to element boundaries on a free surface. For such surfaces, the boundary conditions are of one of the three types delineated in previous sections: specified temperature, specified heat flux, or convection conditions.

EXAMPLE 7.10

Calculate the terms of the conductance matrix for an axisymmetric element based on the three-node plane triangular element.

■ Solution

The element and nodal coordinates are as shown in Figure 7.19. From the discussions in Chapter 6, if we are to derive the interpolation functions from basic principles, we first express the temperature variation throughout the element as

$$T(r, z) = a_0 + a_1 r + a_2 z = N_1(r, z)T_1 + N_2(r, z)T_2 + N_3(r, z)T_3$$

apply the nodal conditions, and solve for the constants. Rearranging the results in terms of nodal temperatures then reveals the interpolation functions. However, the results are exactly the same as those of Chapter 6, if we simply replace x and y with r and z , so that

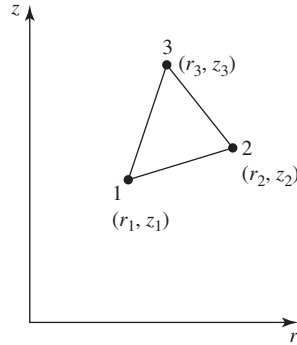


Figure 7.19 Cross section of a three-node axisymmetric element. Recall that the element is a body of revolution.

the interpolation functions are of the form

$$N_1(r, z) = \frac{1}{2A^{(e)}}(b_1 + c_1r + d_1z)$$

$$N_2(r, z) = \frac{1}{2A^{(e)}}(b_2 + c_2r + d_2z)$$

$$N_3(r, z) = \frac{1}{2A^{(e)}}(b_3 + c_3r + d_3z)$$

where

$$b_1 = r_2z_3 - r_3z_2 \quad b_2 = r_3z_1 - r_1z_3 \quad b_3 = r_1z_2 - r_2z_1$$

$$c_1 = z_2 - z_3 \quad c_2 = z_3 - z_1 \quad c_3 = z_1 - z_2$$

$$d_1 = r_3 - r_1 \quad d_2 = r_1 - r_3 \quad d_3 = r_2 - r_1$$

and $A^{(e)}$ is the area of the element in the rz plane.

Since the interpolation functions are linear, the partial derivatives are constants, so Equation 7.102 becomes

$$\begin{aligned} k_{ij} &= 2\pi k \left(\frac{\partial N_i}{\partial r} \frac{\partial N_j}{\partial r} + \frac{\partial N_i}{\partial z} \frac{\partial N_j}{\partial z} \right) \iint_{A^{(e)}} r \, dr \, dz \\ &= \frac{\pi k}{2(A^{(e)})^2} (c_i c_j + d_i d_j) \iint_{A^{(e)}} r \, dr \, dz \quad i, j = 1, 3 \end{aligned}$$

Recalling from elementary statics that the integral in the last equation represents the first moment of the area of the element about the z axis, we have

$$\iint_{A^{(e)}} r \, dr \, dz = \bar{r} A^{(e)}$$

where \bar{r} is the radial coordinate of the element centroid. The components of the conductance matrix are then

$$k_{ij} = \frac{\pi k \bar{r}}{2A^{(e)}} (c_i c_j + d_i d_j) \quad i, j = 1, 3$$

and the symmetry of the conductance matrix is evident.

7.8 TIME-DEPENDENT HEAT TRANSFER

The treatment of finite element analysis of heat transfer has, to this point, been limited to cases of steady-state conditions. No time dependence is included in such analyses, as we have assumed conditions such that a steady state is reached, and the transient conditions are not of interest. Certainly, transient, time-dependent effects are often quite important, and such effects determine whether a steady state is achieved and what that steady state will be. To illustrate time-dependent heat transfer in the context of finite element analysis, the one-dimensional case is discussed here.

The case of one-dimensional conduction without convection is detailed in Chapter 5. The governing equation, by consideration of energy balance in a control volume, Equation 5.54, is

$$q_x A dt + Q A dx dt = \Delta U + \left(q_x + \frac{\partial T}{\partial x} dx \right) A dt \quad (7.107)$$

where the temperature distribution $T(x, t)$ is now assumed to be dependent on both position and time. Further, the change in internal energy ΔU is not zero. Rather, the increase in internal energy during a small time interval is described by Equation 5.56, and the differential equation governing the temperature distribution, Equation 5.58, is

$$k_x \frac{\partial^2 T}{\partial x^2} + Q = c\rho \frac{\partial T}{\partial t} \quad (7.108)$$

where c and ρ denote material specific heat and density, respectively, and t is time. For time-dependent conduction, the governing equation is a second-order partial differential equation with constant coefficients.

Application of the finite element method for solution of Equation 7.108 proceeds by dividing the problem domain into finite-length, one-dimensional elements and discretizing the temperature distribution within each element as

$$T(x, t) = N_1(x)T_1(t) + N_2(x)T_2(t) = [N(x)]\{T(t)\} \quad (7.109)$$

which is the same as Equation 5.60 with the notable exception that *the nodal temperatures are functions of time*.

Let us now apply Galerkin's finite element method to Equation 7.108 to obtain the residual equations

$$\int_{x_1}^{x_2} \left(k_x \frac{\partial^2 T}{\partial x^2} + Q - c\rho \frac{\partial T}{\partial t} \right) N_i(x) A dx \quad i = 1, 2 \quad (7.110)$$

Noting that

$$N_i \frac{\partial^2 T}{\partial x^2} = \frac{\partial}{\partial x} \left(N_i \frac{\partial T}{\partial x} \right) - \frac{\partial N_i}{\partial x} \frac{\partial T}{\partial x} \quad (7.111)$$

the residual equations can be rearranged and expressed as

$$\begin{aligned} & \int_{x_1}^{x_2} k_x \frac{\partial N_i}{\partial x} \frac{\partial T}{\partial x} A \, dx + \int_{x_1}^{x_2} c \rho \frac{\partial T}{\partial t} N_i A \, dx \\ &= \int_{x_1}^{x_2} Q N_i A \, dx + \int_{x_1}^{x_2} k_x \frac{\partial}{\partial x} \left(N_i \frac{\partial T}{\partial x} \right) A \, dx \quad i = 1, 2 \end{aligned} \quad (7.112)$$

Comparing Equation 7.112 to Equations 5.63 and 5.64, we observe that the first integral on the left includes the conductance matrix, the first integral on the right is the forcing function associated with internal heat generation, and the second integral on the right represents the gradient boundary conditions. Utilizing Equation 7.109, Equation 7.112 can be written in detailed matrix form as

$$\begin{aligned} & c \rho A \int_{x_1}^{x_2} \begin{bmatrix} N_1 \\ N_2 \end{bmatrix} [N_1 \quad N_2] \, dx \begin{Bmatrix} \dot{T}_1 \\ \dot{T}_2 \end{Bmatrix} \\ &+ k_x A \int_{x_1}^{x_2} \begin{bmatrix} \frac{dN_1}{dx} \\ \frac{dN_2}{dx} \end{bmatrix} \begin{bmatrix} \frac{dN_1}{dx} & \frac{dN_2}{dx} \end{bmatrix} \, dx \begin{Bmatrix} T_1(t) \\ T_2(t) \end{Bmatrix} = \{f_Q\} + \{f_g\} \end{aligned} \quad (7.113)$$

where the dot denotes differentiation with respect to time. Note that the derivatives of the interpolation functions have now been expressed as ordinary derivatives, as appropriate. Equation 7.113 is most often expressed as

$$[C^{(e)}] \{\dot{T}^{(e)}\} + [k^{(e)}] \{T^{(e)}\} = \{f_Q^{(e)}\} + \{f_g^{(e)}\} \quad (7.114)$$

where $[C^{(e)}]$ is the element *capacitance matrix* defined by

$$[C^{(e)}] = c \rho A \int_{x_1}^{x_2} \begin{bmatrix} N_1 \\ N_2 \end{bmatrix} [N_1 \quad N_2] \, dx = c \rho A \int_{x_1}^{x_2} [N]^T [N] \, dx \quad (7.115)$$

and, as implied by the name, indicates the capacity of the element for heat storage. The capacitance matrix defined by Equation 7.115 is known as the *consistent* capacitance matrix. The consistent capacitance matrix is so called because it is formulated on the basis of the same interpolation functions used to describe the spatial distribution of temperature. In our approach, using Galerkin's method, the consistent matrix is a natural result of the mathematical procedure. An alternate approach produces a so-called lumped capacitance matrix. Whereas the consistent matrix distributes the capacitance throughout the element by virtue of the interpolation functions, the lumped capacitance matrix ascribes the storage capacity strictly to the nodes independently. The difference in the two approaches is discussed in terms of heat transfer and, in more detail, in Chapter 10 in the context of structural dynamics.

The model assembly procedure for a transient heat transfer problem is exactly the same as for a steady-state problem, with the notable exception that we must also assemble a global capacitance matrix. The rules are the same. Element nodes are assigned to global nodes and the element capacitance matrix terms are added to the appropriate global positions in the global capacitance matrix, as with the conductance matrix terms. Hence, on system assembly, we obtain the global equations

$$[C]\{\dot{T}\} + [K]\{T\} = \{F_Q\} + \{F_g\} \quad (7.116)$$

where we must recall that the gradient force vector $\{F_g\}$ is composed of either (1) unknown heat flux values to be determined (unknown reactions) or (2) convection terms to be equilibrated with the flux at a boundary node.

7.8.1 Finite Difference Methods for the Transient Response: Initial Conditions

The finite element discretization procedure has reduced the one-dimensional transient heat transfer problem to algebraic terms in the spatial variable via the interpolation functions. Yet Equation 7.116 represents a set of ordinary, coupled, first-order differential equations in time. Consequently, as opposed to the steady-state case, there is not a solution but multiple solutions as the system responds to time-dependent conditions. The boundary conditions for a transient problem are of the three types discussed for the steady-state case: specified nodal temperatures, specified heat flux, or convection conditions. However, note that the boundary conditions may also be time dependent. For example, a specified nodal temperature could increase linearly with time to some specified final value. In addition, an internal heat generation source Q may also vary with time.

A commonly used approach to obtaining solutions for ordinary differential equations of the form of Equation 7.116 is the *finite difference method*. As discussed briefly in Chapter 1, the finite difference method is based on approximating derivatives of a function as incremental changes in the value of the function corresponding to finite changes in the value of the independent variable. Recall that the first derivative of a function $f(t)$ is defined by

$$\dot{f} = \frac{df}{dt} = \lim_{\Delta t \rightarrow 0} \frac{f(t + \Delta t) - f(t)}{\Delta t} \quad (7.117)$$

Instead of requiring Δt to approach zero, we obtain an approximation to the value of the derivative by using a small, nonzero value of Δt to obtain

$$\dot{f} \cong \frac{f(t + \Delta t) - f(t)}{\Delta t} \quad (7.118)$$

and the selected value of Δt is known as the *time step*.

To apply the procedure to transient heat transfer, we approximate the time derivative of the nodal temperature matrix as

$$\{\dot{T}\} \cong \frac{\{T(t + \Delta t)\} - \{T(t)\}}{\Delta t} \quad (7.119)$$

Substituting, Equation 7.116 becomes

$$[C] \frac{\{T(t + \Delta t)\} - \{T(t)\}}{\Delta t} + [K]\{T(t)\} = \{F_Q(t)\} + \{F_g(t)\} \quad (7.120)$$

Note that, if the nodal temperatures are known at time t and the forcing functions are evaluated at time t , Equation 7.120 can be solved, algebraically, for the nodal temperatures at time $t + \Delta t$. Denoting the time at the i th time step as $t_i = i(\Delta t)$, $i = 0, 1, 2, \dots$, we obtain

$$[C]\{T(t_{i+1})\} = [C]\{T(t_i)\} - [K]\{T(t_i)\} \Delta t + \{F_Q(t_i)\} \Delta t + \{F_g(t_i)\} \Delta t \quad (7.121)$$

as the system of algebraic equations that can be solved for $\{T(t_{i+1})\}$. Formally, the solution is obtained by multiplying Equation 7.121 by the inverse of the capacitance matrix. For large matrices common to finite element models, inverting the matrix is very inefficient, so other techniques such as Gaussian elimination are more often used. Note, however, that the system of algebraic equations given by Equation 7.121 must be solved only once to obtain an *explicit* solution for the nodal temperatures at time t_{i+1} .

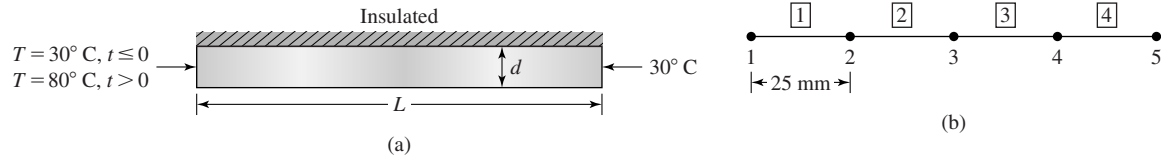
The method just described is known as a *forward difference scheme* (also known as *Euler's method*) and Equation 7.121 is a *two-point recurrence relation*. If the state of the system (nodal temperatures and forcing functions) is known at one point in time, Equation 7.121 gives the state at the next point in time. Solving the system sequentially at increasing values of the independent variable is often referred to as *marching* in time. To begin the solution procedure, the state of the system must be known at $t = 0$. Therefore, the *initial conditions* must be specified in addition to the applicable boundary conditions. Recall that the general solution to an ordinary, first-order differential equation contains one constant of integration. As we have one such equation corresponding to each nodal temperature, the value of each nodal temperature must be specified at time zero. If the initial conditions are so known, the recurrence relation can be used to compute succeeding nodal temperatures. Prior to discussing other schemes and the ramifications of time step selection, the following simple example is presented.

EXAMPLE 7.11

Figure 7.20a shows a cylindrical rod having diameter of 12 mm and length of 100 mm. The pin is of a material having thermal conductivity 230 W/(m·°C), specific heat 900 J/(kg·°C), and density 2700 kg/m³. The right-hand end of the rod is held in contact with a medium at a constant temperature of 30°C. At time zero, the entire rod is at a temperature of 30°C when a heat source is applied to the left end, bringing the temperature of the left end immediately to 80°C and maintaining that temperature indefinitely. Using the forward difference method and four two-node elements, determine both transient and steady-state temperature distributions in the rod. No internal heat is generated.

7.8 Time-Dependent Heat Transfer

281

**Figure 7.20**

(a) Cylindrical rod of Example 7.11. (b) Node and element numbers.

■ Solution

In the solution for this example, we set up the general procedure then present the results for one solution using one time step for the transient portion. The node numbers and element numbers are as shown in Figure 7.20b. Since the length and area of each element are the same, we compute the element capacitance matrix as

$$\begin{aligned} [C^{(e)}] &= \frac{cpAL}{6} \begin{bmatrix} 2 & 1 \\ 1 & 2 \end{bmatrix} = \frac{900(2700) \frac{\pi}{4} (0.012)^2 (0.025)}{6} \begin{bmatrix} 2 & 1 \\ 1 & 2 \end{bmatrix} \\ &= \begin{bmatrix} 2.2902 & 1.1451 \\ 1.1451 & 2.2902 \end{bmatrix} \text{ J}^\circ\text{C} \end{aligned}$$

where we have implicitly performed the integrations indicated in Equation 7.115 and leave the details as an end-of-chapter exercise. Similarly, the element conductance matrix is

$$\begin{aligned} [k^{(e)}] &= \frac{kA}{L} \begin{bmatrix} 1 & -1 \\ -1 & 1 \end{bmatrix} = \frac{200 \frac{\pi}{4} (0.012)^2}{0.025} \begin{bmatrix} 1 & -1 \\ -1 & 1 \end{bmatrix} \\ &= \begin{bmatrix} 0.9408 & -0.9408 \\ -0.9408 & 0.9408 \end{bmatrix} \text{ W}^\circ\text{C} \end{aligned}$$

For the one-dimensional case with uniform geometry and material properties, the system assembly is straightforward and results in the global matrices

$$[C] = \begin{bmatrix} 2.2902 & 1.1451 & 0 & 0 & 0 \\ 1.1451 & 4.5804 & 1.1451 & 0 & 0 \\ 0 & 1.1451 & 4.5804 & 1.1451 & 0 \\ 0 & 0 & 1.1451 & 4.5804 & 1.1451 \\ 0 & 0 & 0 & 1.1451 & 2.2902 \end{bmatrix}$$

$$[K] = \begin{bmatrix} 0.9408 & -0.9408 & 0 & 0 & 0 \\ -0.9408 & 1.8816 & -0.9408 & 0 & 0 \\ 0 & -0.9408 & 1.8816 & -0.9408 & 0 \\ 0 & 0 & -0.9408 & 1.8816 & -0.9408 \\ 0 & 0 & 0 & -0.9408 & 0.9408 \end{bmatrix}$$

As no internal heat is generated $\{F_Q\} = 0$ and, as we have specified boundary temperatures, the flux forcing term is an unknown. Note that, in the transient case, the flux terms

at the boundaries (the “reactions”) are time dependent and can be computed at each time step, as will be explained. Hence, the gradient “force vector” is

$$\{F_g\} = \begin{Bmatrix} q_1 A \\ 0 \\ 0 \\ 0 \\ -q_5 A \end{Bmatrix}$$

Having taken care of the boundary conditions, we now consider the initial conditions and examine the totality of the conditions on the solution procedure. It should be clear that, since we have the temperature of two nodes specified, the desired solution should provide the temperatures of the other three nodes and, therefore, should be a 3×3 system. The reduction to the 3×3 system is accomplished via the following observations:

1. If $T_1 = 80^\circ\text{C} = \text{constant}$, then $\dot{T}_1 = 0$.
2. If $T_5 = 30^\circ\text{C} = \text{constant}$, then $\dot{T}_5 = 0$.

The equations can be modified accordingly. In this example, the general equations become

$$[C] \begin{Bmatrix} 0 \\ \dot{T}_2 \\ \dot{T}_3 \\ \dot{T}_4 \\ 0 \end{Bmatrix} + [K] \begin{Bmatrix} 80 \\ T_2 \\ T_3 \\ T_4 \\ 30 \end{Bmatrix} = \begin{Bmatrix} q_1 A \\ 0 \\ 0 \\ 0 \\ -q_5 A \end{Bmatrix}$$

Consequently, the first and fifth equations become

$$1.1451 \dot{T}_2 + 0.9408(80) - 0.9408 T_2 = q_1 A$$

$$1.1451 \dot{T}_4 - 0.9408 T_4 + 0.9408(30) = -q_5 A$$

respectively. The three remaining equations are then written as

$$\begin{bmatrix} 4.5804 & 1.1451 & 0 \\ 1.1451 & 4.5804 & 1.1451 \\ 0 & 1.1451 & 4.5804 \end{bmatrix} \begin{Bmatrix} \dot{T}_2 \\ \dot{T}_3 \\ \dot{T}_4 \end{Bmatrix} + \begin{bmatrix} 1.8816 & -0.9408 & 0 \\ -0.9408 & 1.8816 & -0.9408 \\ 0 & -0.9408 & 1.8816 \end{bmatrix} \begin{Bmatrix} T_2 \\ T_3 \\ T_4 \end{Bmatrix} \\ = \begin{Bmatrix} 75.264 \\ 0 \\ 28.224 \end{Bmatrix}$$

For this example, the capacitance matrix is inverted (using a spreadsheet program) to obtain

$$[C]^{-1} = \begin{bmatrix} 0.2339 & -0.0624 & 0.0156 \\ -0.0624 & 0.2495 & -0.0624 \\ 0.0156 & -0.0624 & 0.2339 \end{bmatrix}$$

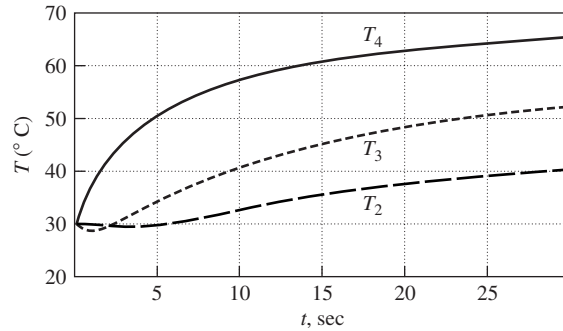


Figure 7.21 Time histories of the nodal temperatures.

where $[C]$ now represents the reduced 3×3 capacitance matrix. Utilizing Equation 7.121 and multiplying by $[C]^{-1}$ yields

$$\begin{Bmatrix} T_2 \\ T_3 \\ T_4 \end{Bmatrix}_{i+1} = \begin{Bmatrix} T_2 \\ T_3 \\ T_4 \end{Bmatrix}_i - \begin{bmatrix} 0.4988 & -0.3521 & 0.0880 \\ -0.3521 & 0.5869 & -0.3521 \\ 0.0880 & -0.3521 & 0.4988 \end{bmatrix} \begin{Bmatrix} T_2 \\ T_3 \\ T_4 \end{Bmatrix}_i \Delta t + \begin{Bmatrix} 18.0456 \\ -6.4558 \\ 7.7762 \end{Bmatrix} \Delta t$$

as the two-point recurrence relation.

Owing to the small matrix involved, the recurrence relation was programmed into a standard spreadsheet program using time step $\Delta t = 0.1$ sec. Calculations for nodal temperatures T_2 , T_3 , and T_4 are carried out until a steady state is reached. Time histories of each of the nodal temperature are shown in Figure 7.21. The figure shows that steady-state conditions $T_2 = 67.5^\circ\text{C}$, $T_3 = 55^\circ\text{C}$, and $T_4 = 42.5^\circ\text{C}$ are attained in about 30 sec. Interestingly, the results also show that the temperatures of nodes 3 and 4 initially decrease. Such phenomena are physically unacceptable and associated with use of a consistent capacitance matrix, as is discussed in Chapter 10.

7.8.2 Central Difference and Backward Difference Methods

The forward difference method discussed previously and used in Example 7.11 is but one of three commonly used finite difference methods. The others are the backward difference method and the central difference method. Each of these is discussed in turn and a single two-point recurrence relation is developed incorporating the three methods.

In the *backward difference method*, the finite approximation to the first derivative at time t is expressed as

$$\dot{T}(t) \cong \frac{T(t) - T(t - \Delta t)}{\Delta t} \quad (7.122)$$

so that we, in effect, look back in time to approximate the derivative during the previous time step. Substituting this relation into Equation 7.116 gives

$$[C] \frac{\{T(t)\} - \{T(t - \Delta t)\}}{\Delta t} + [K]\{T(t)\} = \{F_Q(t)\} + \{F_g(t)\} \quad (7.123)$$

In this method, we evaluate the nodal temperatures at time t based on the state of the system at time $t - \Delta t$, so we introduce the notation $t = t_i$, $t_{i-1} = t - \Delta t$, $i = 1, 2, 3, \dots$. Using the described notation and rearranging, Equation 7.123 becomes

$$([C] + [K]\Delta t)\{T(t_i)\} = [C]\{T(t_{i-1})\} + F_Q(t_i)\Delta t + F_g(t_i)\Delta t \quad i = 1, 2, 3, \dots \quad (7.124)$$

If the nodal temperatures are known at time t_{i-1} , Equation 7.124 can be solved for the nodal temperatures at the next time step (it is assumed that the forcing functions on the right-hand side are known and can be determined at t_i). Noting that the time index is relative, Equation 7.125 can also be expressed as

$$([C] + [K]\Delta t)\{T(t_{i+1})\} = [C]\{T(t_i)\} + F_Q(t_i)\Delta t + F_g(t_i)\Delta t \quad i = 0, 1, 2, \dots \quad (7.125)$$

If we compare Equation 7.125 with Equation 7.121, we find that the major difference lies in the treatment of the conductance matrix. In the latter case, the effects of conductance are, in effect, updated during the time step. In the case of the forward difference method, Equation 7.121, the conductance effects are held constant at the previous time step. We also observe that Equation 7.125 cannot be solved at each time step by “simply” inverting the capacitance matrix. The coefficient matrix on the left-hand side changes at each time step; therefore, more efficient methods are generally used to solve Equation 7.125.

Another approach to approximation of the first derivative is the central difference method. As the name implies, the method is a compromise of sorts between forward and backward difference methods. In a central difference scheme, the dependent variable and all forcing functions are evaluated at the center (midpoint) of the time step. In other words, average values are used. In the context of transient heat transfer, the time derivative of temperature is still as approximated by Equation 7.119 but the other terms in Equation 7.120 are evaluated at the midpoint of the time step. Using this approach, Equation 7.120 becomes

$$[C] \frac{\{T(t + \Delta t)\} - \{T(t)\}}{\Delta t} + [K] \left\{ \frac{T(t + \Delta t) + T(t)}{2} \right\} = \left\{ \frac{F_Q(t + \Delta t) + F_Q(t)}{2} \right\} + \left\{ \frac{F_g(t + \Delta t) + F_g(t)}{2} \right\} \quad (7.126)$$

The forcing functions on the right-hand side of Equation 7.126 are either known functions and can be evaluated or “reactions,” which are subsequently computed

via the constraint equations. The left-hand side of Equation 7.126 is now, however, quite different, in that the unknowns at each step $T_i(t + \Delta t)$ appear in both capacitance and conductance terms. Multiplying by Δt and rearranging Equation 7.126, we obtain

$$\begin{aligned} & \left([C] + [K] \frac{\Delta t}{2} \right) \{T(t + \Delta t)\} \\ & = \left([C] - [K] \frac{\Delta t}{2} \right) \{T(t)\} + \left\{ \frac{F_Q(t + \Delta t) + F_Q(t)}{2} \right\} + \left\{ \frac{F_g(t + \Delta t) + F_g(t)}{2} \right\} \end{aligned} \quad (7.127)$$

Equation 7.127 can be solved for the unknown nodal temperatures at time $t + \Delta t$ and the “marching” solution can progress in time until a steady state is reached. The central difference method is, in general, more accurate than the forward or backward difference method, in that it does not give preference to either temperatures at t or $t + \Delta t$ but, rather, gives equal credence to both.

In finite difference methods, the key parameter governing solution accuracy is the selected time step Δt . In a fashion similar to the finite element method, in which the smaller the elements are, physically, the better is the solution, the finite difference method converges more rapidly to the true solution as the time step is decreased. These ideas are amplified in Chapter 10, when we examine the dynamic behavior of structures.

7.9 CLOSING REMARKS

In Chapter 7, we expand the application of the finite element method into two- and three-dimensional, as well as axisymmetric, problems in heat transfer. While the majority of the chapter focuses on steady-state conditions, we also present the finite difference methods commonly used to examine transient effects. The basis of our approach is the Galerkin finite element method, and this text stays with that procedure, as it is so general in application. As we proceed into applications in fluid mechanics, solid mechanics, and structural dynamics in the following chapters, the Galerkin method is the basis for the development of many of the finite element models.

REFERENCES

1. Huebner, K. H., and E. A. Thornton. *The Finite Element Method for Engineers*, 2nd ed. New York: John Wiley and Sons, 1982.
2. Incropera, F. P., and D. P. DeWitt. *Introduction to Heat Transfer*, 3rd ed. New York: John Wiley and Sons, 1996.

PROBLEMS

- 7.1 For Example 7.1, determine the exact solution by integrating Equation 5.59 and applying the boundary conditions to evaluate the constants of integration.
- 7.2 Verify the convection-related terms in Equation 7.15 by direct integration.
- 7.3 For the data given in Example 7.4, use Gaussian quadrature with four integration points (two on r , two on s) to evaluate the terms of the stiffness matrix. Do your results agree with the values given in the example?
- 7.4 Using the computed nodal temperatures and heat flux values calculated in Example 7.5, perform a check calculation on the heat flow balance. That is, determine whether the heat input is in balance with the heat loss due to convection. How does this check indicate the accuracy of the finite element solution?
- 7.5 Consider the circular heat transfer pin shown in Figure P7.5. The base of the pin is held at constant temperature of 100°C (i.e., boiling water). The tip of the pin and its lateral surfaces undergo convection to a fluid at ambient temperature T_a . The convection coefficients for tip and lateral surfaces are equal. Given $k_x = 380 \text{ W/m}\cdot^\circ\text{C}$, $L = 8 \text{ cm}$, $h = 2500 \text{ W/m}^2\cdot^\circ\text{C}$, $d = 2 \text{ cm}$, $T_a = 30^\circ\text{C}$. Use a two-element finite element model with linear interpolation functions (i.e., a two-node element) to determine the nodal temperatures and the heat removal rate from the pin. Assume no internal heat generation.

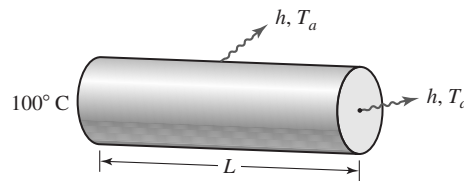


Figure P7.5

- 7.6 Repeat Problem 7.5 using four elements. Is convergence indicated?
- 7.7 The pin of Figure P7.5 represents a heating unit in a water heater. The base of the pin is held at fixed temperature 30°C . The pin is surrounded by flowing water at 55°C . Internal heat generation is to be taken as the constant value $Q = 25 \text{ W/cm}^3$. All other data are as given in Problem 7.5. Use a two-element model to determine the nodal temperatures and the net heat flow rate from the pin.
- 7.8 Solve Problem 7.5 under the assumption that the pin has a square cross section $1 \text{ cm} \times 1 \text{ cm}$. How do the results compare in terms of heat removal rate?
- 7.9 The efficiency of the pin shown in Figure P7.5 can be defined in several ways. One way is to assume that the maximum heat transfer occurs when the entire pin is at the same temperature as the base (in Problem 7.5, 100°C), so that convection is maximized. We then write

$$q_{\max} = \int_0^L h P (T_b - T_a) dx + h A (T_b - T_a)$$

where T_b represents the base temperature, P is the peripheral dimension, and A is cross-sectional area at the tip. The actual heat transfer is less than q_{\max} , so we

define efficiency as

$$\eta = \frac{q_{\text{act}}}{q_{\text{max}}}$$

Use this definition to determine the efficiency of the pin of Problem 7.5.

- 7.10** Figure P7.10 represents one tube of an automotive engine's radiator. The engine coolant is circulated through the tube at a constant rate determined by the water pump. Cooling is primarily via convection from flowing air around the tube as a result of vehicle motion. Coolant enters the tube at a temperature of 195°F and the flow rate is 0.3 gallons per minute (specific weight is 68.5 lb/ft³). The physical data are as follows: $L = 18$ in., $d = 0.3125$ in., $k_x = 225$ Btu/hr-ft-°F, $h = 37$ Btu/ft²-hr-°F. Determine the stiffness matrix and load vector for an element of arbitrary length to use in modeling this problem, assuming steady-state conditions. Is the assumption of steady-state conditions reasonable?

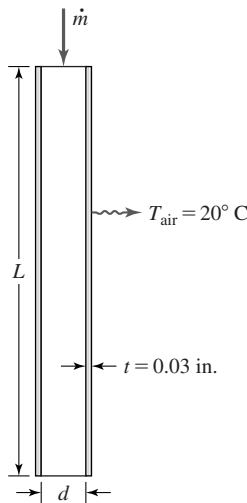


Figure P7.10

- 7.11** Use the results of Problem 7.10 to model the tube with four equal length elements and determine the nodal temperatures and the total heat flow from surface convection.
- 7.12** Consider the tapered heat transfer pin shown in Figure P7.12a. The base of the pin is held at constant temperature T_b , while the lateral surfaces and tip are surrounded by a fluid media held at constant temperature T_a . Conductance k_x and the convection coefficient h are known constants. Figure P7.12b shows the pin modeled as four tapered finite elements. Figure P7.12c shows the pin modeled as four constant cross-section elements with the area of each element equal to the average area of the actual pin. What are the pros and cons of the two modeling approaches? Keep in mind that use of four elements is only a starting

point, many more elements are required to obtain a convergent solution. How does the previous statement affect your answer?

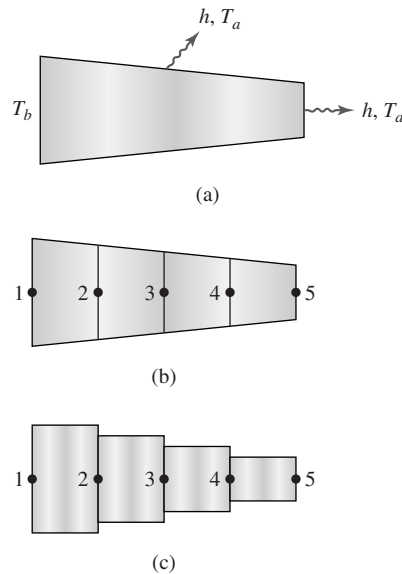


Figure P7.12

- 7.13 A cylindrical pin is constructed of a material for which the thermal conductivity decreases with temperature according to

$$k_x = k_0 - cT$$

and c is a positive constant. For this situation, show that the governing equation for steady-state, one-dimensional conduction with convection is

$$k_0 \frac{d^2 T}{dx^2} - \frac{d}{dx} \left(cT \frac{dT}{dx} \right) + Q = \frac{hP}{A} (T - T_a)$$

- 7.14 The governing equation for the situation described in Problem 7.13 is nonlinear. If the Galerkin finite element method is applied, an integral of the form

$$\int_{x_1}^{x_2} N_i \frac{d}{dx} \left(cT \frac{dT}{dx} \right) dx$$

appears in the conductance matrix formulation. Integrate this term by parts and discuss the results in terms of boundary flux conditions and the conductance matrix.

- 7.15 A vertical wall of “sandwich” construction shown in Figure P7.15a is held at constant temperature $T_1 = 68^\circ\text{F}$ on one surface and $T_2 = 28^\circ\text{F}$ on the other surface. Using only three elements (one for each material), as in Figure P7.15b, determine the nodal temperatures and heat flux through the wall per unit area. The dimensions of the wall in the y and z directions are very large in comparison to wall thickness.

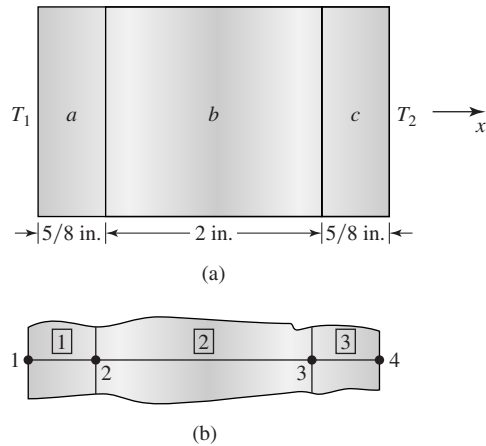


Figure P7.15

- 7.16** The wall of Problem 7.15 carries a centrally located electrical cable, which is to be treated as a line heat source of strength $Q^* = \text{constant}$, as shown in Figure P7.16. With this change, can the problem still be treated as one dimensional? If your answer is yes, solve the problem using three elements as in Problem 7.15. If your answer is no, explain.

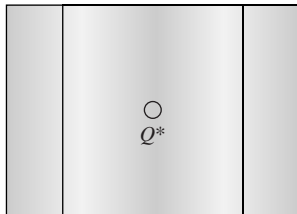


Figure P7.16

- 7.17** A common situation in polymer processing is depicted in Figure P7.17, which shows a “jacketed” pipe. The inner pipe is stainless steel having thermal conductivity k ; the outer pipe is carbon steel and assumed to be perfectly insulated. The annular region between the pipes contains a heat transfer medium at constant temperature T_1 . The inner pipe contains polymer material flowing

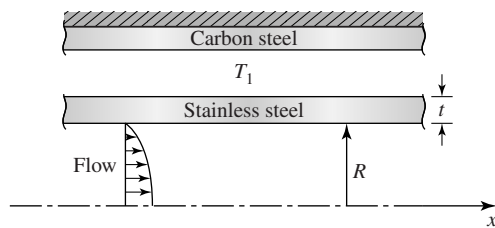


Figure P7.17

at constant mass flow rate \dot{m} . The convection coefficient between the stainless steel pipe wall and the polymer is h . Polymer specific heat c is also taken to be constant. Is this a one-dimensional problem? How would you solve this problem using the finite element method?

- 7.18 An office heater (often incorrectly called a *radiator*, since the heat transfer mode is convection) is composed of a central pipe containing heated water at constant temperature, as depicted in Figure P7.18. Several two-dimensional heat transfer fins are attached to the pipe as shown. The fins are equally spaced along the length of the pipe. Each fin has thickness of 0.125 in. and overall dimensions 4 in. \times 4 in. Convection from the edges of the fins can be neglected. Consider the pipe as a point source $Q^* = 600 \text{ Btu/hr-ft}^2$ and determine the net heat transfer to the ambient air at 20°C , if the convection coefficient is $h = 300 \text{ Btu}/(\text{hr-ft}^2\text{-}^\circ\text{F})$. Use four finite elements with linear interpolation functions (consider symmetry conditions here).

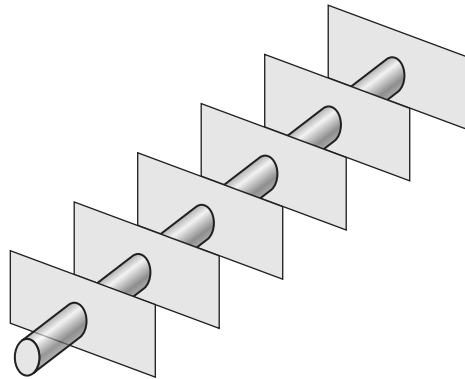


Figure P7.18

- 7.19 One who seriously considers the symmetry conditions of Problem 7.18 would realize that quarter symmetry exists and four elements represent 16 elements in the full problem domain. What are the boundary conditions for the symmetric model?
- 7.20 The rectangular fins shown in Figure P7.20 are mounted on a centrally located pipe carrying hot water. Temperature at the contact surface between fin and pipe is a constant T_1 . For each case depicted, determine the applicable symmetry conditions and the boundary conditions applicable to a finite element model.

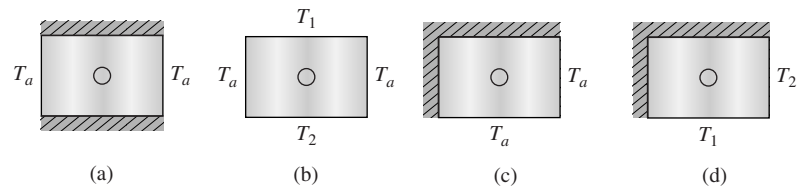


Figure P7.20

Note that the cross-hatched edges are perfectly insulated and it is assumed that the convection coefficients on all surfaces is the same constant.

- 7.21 Solve Example 7.5 using the two-element model in Figure 7.11b. How do the results compare to those of the four-element model?
- 7.22 The rectangular element shown in Figure P7.22 contains a line source of constant strength Q^* located at the element centroid. Determine $\{f_Q^{(e)}\}$.

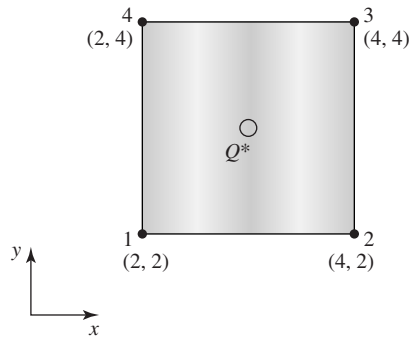


Figure P7.22

- 7.23 Determine the forcing function components of $\{f_Q^{(e)}\}$ for the axisymmetric element of Example 7.10 for the case of uniform internal heat generation Q .
- 7.24 A steel pipe (outside diameter of 60 mm and wall thickness of 5 mm) contains flowing water at constant temperature 80°C , as shown in Figure P7.24. The convection coefficient between the water and pipe is $2000 \text{ W/m}^2\text{-}^\circ\text{C}$. The pipe is surrounded by air at 20°C , and the convection at the outer pipe surface is $20 \text{ W/m}^2\text{-}^\circ\text{C}$. The thermal conductivity of the pipe material is $60 \text{ W/m}\text{-}^\circ\text{C}$. Determine the stiffness matrices and nodal forcing functions for the two axisymmetric elements shown.

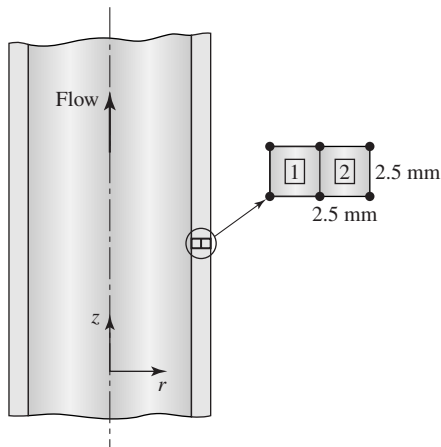


Figure P7.24

- 7.25 Assemble the global equations for the two elements of Problem 7.24. Use the global node numbers shown in Figure P7.25. Compute the nodal temperatures, and find the net heat flow (per unit surface area) into the surrounding air.

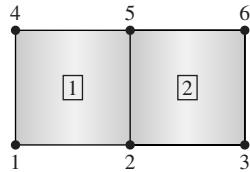


Figure P7.25

- 7.26 Solve the problem of Example 7.11 using a time step $\Delta t = 0.01$ sec. How do the results compare to those of the example solution?

CHAPTER

8

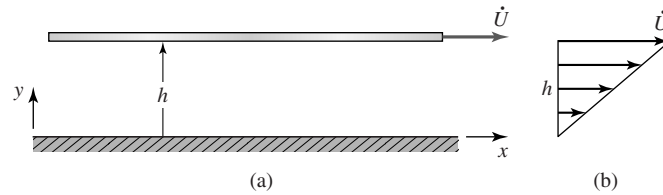
Applications in Fluid Mechanics

8.1 INTRODUCTION

The general topic of fluid mechanics encompasses a wide range of problems of interest in engineering applications. The most basic definition of a *fluid* is to state that a fluid is a material that conforms to the shape of its container. Thus, both liquids and gases are fluids. Alternately, it can be stated that a material which, in itself, cannot support shear stresses is a fluid. The reader familiar with the distortion energy theory of solids will recall that geometric distortion is the result of shear stress while normal stress results in volumetric change. Thus, a fluid readily distorts, since the resistance to shear is very low, and such distortion results in flow.

The physical behavior of fluids and gases is very different. The differences in behavior lead to various subfields in fluid mechanics. In general, liquids exhibit constant density and the study of fluid mechanics of liquids is generally referred to as *incompressible flow*. On the other hand, gases are highly compressible (recall Boyle's law from elementary physics [1]) and temperature dependent. Therefore, fluid mechanics problems involving gases are classified as cases of *compressible flow*.

In addition to considerations of compressibility, the relative degree to which a fluid can withstand some amount of shear leads to another classification of fluid mechanics problems. (Regardless of the definition, all fluids can support *some* shear.) The resistance of a fluid to shear is embodied in the material property known as viscosity. In a very practical sense, viscosity is a measure of the "thickness" of a fluid. Consider the differences encountered in stirring a container of water and a container of molasses. The act of stirring introduces shearing stresses in the fluid. The "thinner," less *viscous*, water is easy to stir; the "thicker," more viscous, molasses is harder to stir. The physical effect is represented by the shear stresses applied to the "stirrer" by the fluid. The concept of viscosity is

**Figure 8.1**

(a) Moving plate separated by a fluid layer from a fixed surface. (b) Velocity profile across the fluid thickness.

embodied in Newton's law of viscosity [2], which states that the shear stress in a fluid is proportional to the velocity gradient.

In a one-dimensional case, the velocity gradient and Newton's law of viscosity can be described in reference to Figure 8.1a. A long flat plate is moving with velocity \dot{U} in the x direction and separated from a fixed surface located at $y = 0$ by a thin fluid film of thickness h . Experiments show that the fluid adheres to both surfaces, so that the fluid velocity at the fixed surface is zero, and at the moving plate, the fluid velocity is \dot{U} (this phenomenon is known as the *no slip condition*). If pressure is constant throughout the fluid, the velocity distribution between the moving plate and the fixed surface is linear, as in Figure 8.1b, so the fluid velocity at any point is given by

$$\dot{u}(y) = \frac{y}{h}\dot{U} \quad (8.1)$$

To maintain the motion, a force in the direction of motion must be applied to the plate. The force is required to keep the plate in equilibrium, since the fluid exerts a friction force that opposes the motion. It is known from experiments that the force per unit area (frictional shearing stress) required to maintain motion is proportional to velocity \dot{U} of the moving plate and inversely proportional to distance h . In general, the frictional shearing stress is described in *Newton's law of viscosity* as

$$\tau = \mu \frac{d\dot{u}}{dy} \quad (8.2)$$

where the proportionality constant μ is called the *absolute viscosity* of the fluid. Absolute viscosity (hereafter simply *viscosity*) is a fundamental material property of fluid media since, as shown by Equation 8.2, the ability of a fluid to support shearing stress depends directly on viscosity.

The relative importance of viscosity effects leads to yet other subsets of fluid mechanics problems, as mentioned. Fluids that exhibit very little viscosity are termed *inviscid* and shearing stresses are ignored; on the other hand, fluids with significant viscosity must be considered to have associated significant shear effects. To place the discussion in perspective, water is considered to be an incompressible, viscous fluid, whereas air is a highly compressible yet inviscid

fluid. In general, liquids are most often treated as incompressible but the viscosity effects depend specifically on the fluid. Gases, on the other hand, are generally treated as compressible but inviscid.

In this chapter, we examine only incompressible fluid flow. The mathematics and previous study required for examination of compressible flow analysis is deemed beyond the scope of this text. We, however, introduce viscosity effects in the context of two-dimensional flow and present the basic finite element formulation for solving such problems. The extension to three-dimensional fluid flow is not necessarily as straightforward as in heat transfer and (as shown in Chapter 9) in solid mechanics. Our introduction to finite element analysis of fluid flow problems shows that the concepts developed thus far in the text can indeed be applied to fluid flow but, in the general case, the resulting equations, although algebraic as expected from the finite element method, are nonlinear and special solution procedures must be applied.

8.2 GOVERNING EQUATIONS FOR INCOMPRESSIBLE FLOW

One of the most important physical laws governing motion of any continuous medium is the principle of conservation of mass. The equation derived by application of this principle is known as the *continuity equation*. Figure 8.2 shows a differential volume (a control volume) located at an arbitrary, fixed position in a three-dimensional fluid flow. With respect to a fixed set of Cartesian axes, the velocity components parallel to the x , y , and z axes are denoted u , v , and w , respectively. (Note that here we take the standard convention of fluid mechanics by denoting velocities without the “dot” notation.) The principle of conservation of mass requires that the time rate of change of mass within the volume must

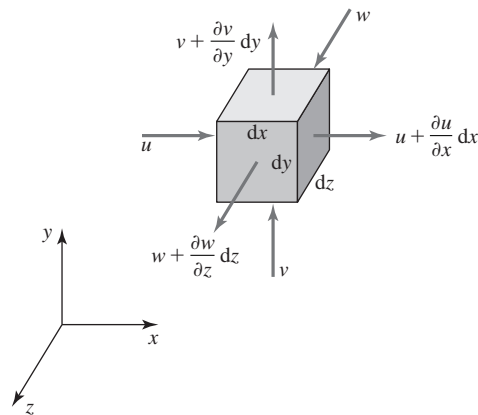


Figure 8.2 Differential volume element in three-dimensional flow.

be in balance with the net mass flow rate into the volume. Total mass inside the volume is ρdV , and since dV is constant, we must have

$$\frac{\partial \rho}{\partial t} dV = \sum (\text{mass flow in} - \text{mass flow out})$$

and the partial derivative is used because density may vary in space as well as time. Using the velocity components shown, the rate of change of mass in the control volume resulting from flow in the x direction is

$$\dot{m}_x = \rho u \, dy \, dz - \left[\rho u + \frac{\partial(\rho u)}{\partial x} dx \right] dy \, dz \quad (8.3a)$$

while the corresponding terms resulting from flow in the y and z directions are

$$\dot{m}_y = \rho v \, dx \, dz - \left[\rho v + \frac{\partial(\rho v)}{\partial y} dy \right] dx \, dz \quad (8.3b)$$

$$\dot{m}_z = \rho w \, dx \, dy - \left[\rho w + \frac{\partial(\rho w)}{\partial z} dz \right] dx \, dy \quad (8.3c)$$

The rate of change of mass then becomes

$$\frac{\partial \rho}{\partial t} dV = \dot{m}_x + \dot{m}_y + \dot{m}_z = - \left[\frac{\partial(\rho u)}{\partial x} + \frac{\partial(\rho v)}{\partial y} + \frac{\partial(\rho w)}{\partial z} \right] dx \, dy \, dz \quad (8.4)$$

Noting that $dV = dx \, dy \, dz$, Equation 8.4 can be written as

$$\frac{\partial \rho}{\partial t} + u \frac{\partial \rho}{\partial x} + v \frac{\partial \rho}{\partial y} + w \frac{\partial \rho}{\partial z} + \rho \left[\frac{\partial u}{\partial x} + \frac{\partial v}{\partial y} + \frac{\partial w}{\partial z} \right] = 0 \quad (8.5)$$

Equation 8.5 is the *continuity equation* for a general three-dimensional flow expressed in Cartesian coordinates.

Restricting the discussion to steady flow (with respect to time) of an incompressible fluid, density is independent of time and spatial coordinates so Equation 8.5 becomes

$$\frac{\partial u}{\partial x} + \frac{\partial v}{\partial y} + \frac{\partial w}{\partial z} = 0 \quad (8.6)$$

Equation 8.6 is the continuity equation for three-dimensional, incompressible, steady flow expressed in Cartesian coordinates. As this is one of the most fundamental equations in fluid flow, we use it extensively in developing the finite element approach to fluid mechanics.

8.2.1 Rotational and Irrotational Flow

Similar to rigid body dynamics, consideration must be given in fluid dynamics as to whether the flow motion represents translation, rotation, or a combination of the two types of motion. Generally, in fluid mechanics, *pure rotation* (i.e.,

8.2 Governing Equations for Incompressible Flow

297

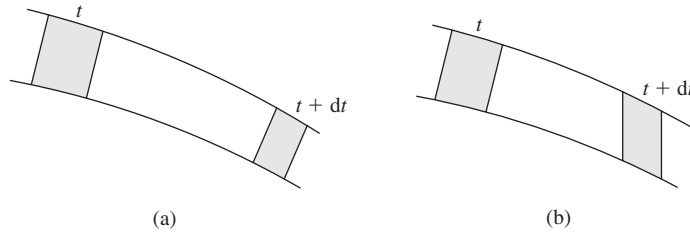


Figure 8.3 Fluid element in (a) rotational flow and (b) irrotational flow.

rotation about a fixed point) is not of as much concern as in rigid body dynamics. Instead, we classify fluid motion as *rotational* (translation and rotation combined) or *irrotational* (translation only). Owing to the inherent deformability of fluids, the definitions of *translation* and *rotation* are not quite the same as for rigid bodies. To understand the difference, we focus on the definition of *rotation* in regard to fluid flow.

A flow field is said to be *irrotational* if a typical element of the moving fluid undergoes no *net* rotation. A classic example often used to explain the concept is that of the passenger carriages on a Ferris wheel. As the wheel turns through one revolution, the carriages also move through a circular path but remain in fixed orientation relative to the gravitational field (assuming the passengers are well-behaved). As the carriage returns to the starting point, the angular orientation of the carriage is exactly the same as in the initial orientation, hence no *net* rotation occurred. To relate the concept to fluid flow, we consider Figure 8.3, depicting two-dimensional flow through a conduit. Figure 8.3a shows an element of fluid undergoing rotational flow. Note that, in this instance, we depict the fluid element as behaving essentially as a solid. The fluid has clearly undergone translation and rotation. Figure 8.3b depicts the same situation in the case of irrotational flow. The element has deformed (angularly), and we indicate that angular deformation via the two angles depicted. If the sum of these two angles is zero, the flow is defined to be irrotational. As is shown in most basic fluid mechanics textbooks [2], the conditions for irrotationality in three-dimensional flow are

$$\begin{aligned}\frac{\partial v}{\partial x} - \frac{\partial u}{\partial y} &= 0 \\ \frac{\partial w}{\partial x} - \frac{\partial u}{\partial z} &= 0 \\ \frac{\partial w}{\partial y} - \frac{\partial v}{\partial z} &= 0\end{aligned}\tag{8.7}$$

When the expressions given by Equations 8.7 are not satisfied, the flow is rotational and the rotational rates can be defined in terms of the partial derivatives of the same equation. In this text, we consider only irrotational flows and do not proceed beyond the relations of Equation 8.7.

8.3 THE STREAM FUNCTION IN TWO-DIMENSIONAL FLOW

We next consider the case of two-dimensional, steady, incompressible, irrotational flow. (Note that we implicitly assume that viscosity effects are negligible.) Applying these restrictions, the continuity equation is

$$\frac{\partial u}{\partial x} + \frac{\partial v}{\partial y} = 0 \quad (8.8)$$

and the irrotationality conditions reduce to

$$\frac{\partial u}{\partial y} - \frac{\partial v}{\partial x} = 0 \quad (8.9)$$

Equations 8.8 and 8.9 are satisfied if we introduce (define) the *stream function* $\psi(x, y)$ such that the velocity components are given by

$$\begin{aligned} u &= \frac{\partial \psi}{\partial y} \\ v &= -\frac{\partial \psi}{\partial x} \end{aligned} \quad (8.10)$$

These velocity components automatically satisfy the continuity equation. The irrotationality condition, Equation 8.10, becomes

$$\frac{\partial u}{\partial y} - \frac{\partial v}{\partial x} = \frac{\partial}{\partial y} \left(\frac{\partial \psi}{\partial y} \right) - \frac{\partial}{\partial x} \left(-\frac{\partial \psi}{\partial x} \right) = \frac{\partial^2 \psi}{\partial x^2} + \frac{\partial^2 \psi}{\partial y^2} = \nabla^2 \psi = 0 \quad (8.11)$$

Equation 8.11 is *Laplace's equation* and occurs in the governing equations for many physical phenomena. The symbol ∇ represents the *vector* derivative operator defined, in general, by

$$\nabla = \frac{\partial}{\partial x} \mathbf{i} + \frac{\partial}{\partial y} \mathbf{j} + \frac{\partial}{\partial z} \mathbf{k} \text{ in Cartesian coordinates} \quad \text{and} \quad \nabla^2 = \nabla \cdot \nabla$$

Let us now examine the physical significance of the stream function $\psi(x, y)$ in relation to the two-dimensional flow. In particular, we consider lines in the (x, y) plane (known as *streamlines*) along which the stream function is constant. If the stream function is constant, we can write

$$d\psi = \frac{\partial \psi}{\partial x} dx + \frac{\partial \psi}{\partial y} dy = 0 \quad (8.12)$$

or

$$d\psi = -v dx + u dy = 0 \quad (8.13)$$

The tangent vector at any point on a streamline can be expressed as $\mathbf{n}_t = dx\mathbf{i} + dy\mathbf{j}$ and the fluid velocity vector at the same point is $\mathbf{V} = u\mathbf{i} + v\mathbf{j}$. Hence, the vector product $\mathbf{V} \times \mathbf{n}_t = (-v dx + u dy)\mathbf{k}$ has zero magnitude, per

Equation 8.13. The vector product of two nonzero vectors is zero only if the vectors are parallel. Therefore, at any point on a streamline, the fluid velocity vector is tangent to the streamline.

8.3.1 Finite Element Formulation

Development of finite element characteristics for fluid flow based on the stream function is straightforward, since (1) the stream function $\psi(x, y)$ is a *scalar* function from which the velocity vector components are derived by differentiation and (2) the governing equation is essentially the same as that for two-dimensional heat conduction. To understand the significance of the latter point, reexamine Equation 7.23 and set $\psi = T$, $k_x = k_y = 1$, $Q = 0$, and $h = 0$. The result is the Laplace equation governing the stream function.

The stream function over the domain of interest is discretized into finite elements having M nodes:

$$\psi(x, y) = \sum_{i=1}^M N_i(x, y)\psi_i = [N]\{\psi\} \quad (8.14)$$

Using the Galerkin method, the element residual equations are

$$\int_{A^{(e)}} N_i(x, y) \left(\frac{\partial^2 \psi}{\partial x^2} + \frac{\partial^2 \psi}{\partial y^2} \right) dx dy = 0 \quad i = 1, M \quad (8.15)$$

or

$$\int_{A^{(e)}} [N]^T \left(\frac{\partial^2 \psi}{\partial x^2} + \frac{\partial^2 \psi}{\partial y^2} \right) dx dy = 0 \quad (8.16)$$

Application of the Green-Gauss theorem gives

$$\begin{aligned} \int_{S^{(e)}} [N]^T \frac{\partial \psi}{\partial x} n_x dS - \int_{A^{(e)}} \frac{\partial [N]^T}{\partial x} \frac{\partial \psi}{\partial x} dx dy + \int_{S^{(e)}} [N]^T \frac{\partial \psi}{\partial y} n_y dS \\ - \int_{A^{(e)}} \frac{\partial [N]^T}{\partial y} \frac{\partial \psi}{\partial y} dx dy = 0 \end{aligned} \quad (8.17)$$

where S represents the element boundary and (n_x, n_y) are the components of the outward unit vector normal to the boundary. Using Equations 8.10 and 8.14 results in

$$\int_{A^{(e)}} \left(\frac{\partial [N]^T}{\partial x} \frac{\partial [N]}{\partial x} + \frac{\partial [N]^T}{\partial y} \frac{\partial [N]}{\partial y} \right) dx dy \{\psi\} = \int_{S^{(e)}} [N]^T (un_y - vn_x) dS \quad (8.18)$$

and this equation is of the form

$$[k^{(e)}]\{\psi\} = \{f^{(e)}\} \quad (8.19)$$

The $M \times M$ element stiffness matrix is

$$[k^{(e)}] = \int_{A^{(e)}} \left(\frac{\partial [N]^T}{\partial x} \frac{\partial [N]}{\partial x} + \frac{\partial [N]^T}{\partial y} \frac{\partial [N]}{\partial y} \right) dx dy \quad (8.20)$$

and the nodal forces are represented by the $M \times 1$ column matrix

$$\{f^{(e)}\} = \int_{S^{(e)}} [N]^T (un_y - vn_x) dS \quad (8.21)$$

Since the nodal forces are obtained via integration along element boundaries and the unit normals for adjacent elements are equal and opposite, the forces on interelement boundaries cancel during the assembly process. Consequently, the forces defined by Equation 8.21 need be computed only for element boundaries that lie on global boundaries. This observation is in keeping with similar observations made previously in context of other problem types.

8.3.2 Boundary Conditions

As the governing equation for the stream function is a second-order, partial differential equation in two independent variables, four boundary conditions must be specified and satisfied to obtain the solution to a physical problem. The manner in which the boundary conditions are applied to a finite element model is discussed in relation to Figure 8.4a. The figure depicts a flow field between two parallel plates that form a smoothly converging channel. The plates are assumed sufficiently long in the z direction that the flow can be adequately modeled as two-dimensional. Owing to symmetry, we consider only the upper half of the flow field, as in Figure 8.4b. Section $a-b$ is assumed to be far enough from the convergent section that the fluid velocity has an x component only. Since we examine only steady flow, the velocity at $a-b$ is $U_{ab} = \text{constant}$. A similar argument applies at section $c-d$, far downstream, and we denote the x -velocity component at that section as $U_{cd} = \text{constant}$. How far upstream or downstream is enough to make these assumptions? The answer is a question of solution convergence. The distances involved should increase until there is no discernible difference in the flow solution. As a rule of thumb, the distances should be 10–15 times the width of the flow channel.

As a result of the symmetry and irrotationality of the flow, there can be no velocity component in the y direction along the line $y = 0$ (i.e., the x axis). The velocity along this line is tangent to the line at all values of x . Given these observations, the x axis is a streamline; hence, $\psi = \psi_1 = \text{constant}$ along the axis. Similarly, along the surface of the upper plate, there is no velocity component normal to the plate (impenetrability), so this too must be a streamline along which $\psi = \psi_2 = \text{constant}$. The values of ψ_1 and ψ_2 are two of the required boundary conditions. Recalling that the velocity components are defined as first partial derivatives of the stream function, the stream function must be known only within a constant. For example, a stream function of the form

8.3 The Stream Function in Two-Dimensional Flow

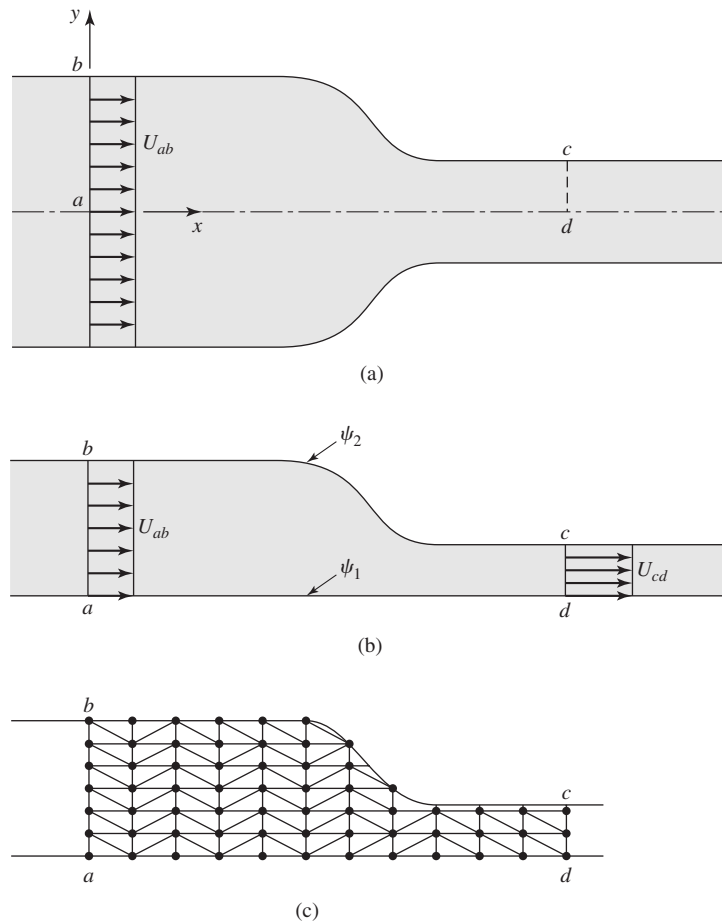


Figure 8.4
 (a) Uniform flow into a converging channel. (b) Half-symmetry model showing known velocities and boundary values of the stream function. (c) A relatively coarse finite element model of the flow domain, using three-node triangular elements. This model includes 65 degrees of freedom before applying boundary conditions.

$\psi(x, y) = C + f(x, y)$ contributes no velocity terms associated with the constant C . Hence, one (constant) value of the stream function can be arbitrarily specified. In this case, we choose to set $\psi_1 = 0$. To determine the value of ψ_2 , we note that, at section a - b (which we have arbitrarily chosen as $x = 0$, the velocity is

$$u = \frac{\partial \psi}{\partial y} = U_{ab} = \text{constant} = \frac{\psi_2 - \psi_1}{y_b - y_a} = \frac{\psi_2}{y_b} \quad (8.22)$$

so $\psi_2 = y_b U_{ab}$. At any point on $a-b$, we have $\psi = (\psi_2/y_b)y = U_{ab}y$, so the value of the stream function at any finite element node located on $a-b$ is known. Similarly, it can be shown that $\psi = (\psi_2/y_c)y = U_{ab}(y_b/y_c)y$ along $c-d$, so nodal values on that line are also known. If these arguments are carefully considered, we see that the boundary conditions on ψ at the “corners” of the domain are continuous and well-defined.

Next we consider the force conditions across sections $a-b$ and $c-d$. As noted, the y -velocity components along these sections are zero. In addition, the y components of the unit vectors normal to these sections are zero as well. Using these observations in conjunction with Equation 8.21, the nodal forces on any element nodes located on these sections are zero. The occurrence of zero forces is equivalent to stating that the streamlines are normal to the boundaries.

If we now utilize a mesh of triangular elements (for example), as in Figure 8.4c, and follow the general assembly procedure, we obtain a set of global equations of the form

$$[K]\{\psi\} = \{F\} \quad (8.23)$$

The forcing function on the right-hand side is zero at all interior nodes. At the boundary nodes on sections $a-b$ and $c-d$, we observe that the nodal forces are zero also. At all element nodes situated on the line $y = 0$, the nodal values of the stream function are $\psi = 0$, while at all element nodes on the upper plate profile the values are specified as $\psi = y_b U_{ab}$. The $\psi = 0$ conditions are analogous to the specification of zero displacements in a structural problem. With such conditions, the unknowns are the forces exerted at those nodes. Similarly, the specification of nonzero value of the stream function ψ along the upper plate profile is analogous to a specified displacement. The unknown is the force required to enforce that displacement.

The situation here is a bit complicated mathematically, as we have both zero and nonzero specified values of the nodal variable. In the following, we assume that the system equations have been assembled, and we rearrange the equations such that the column matrix of nodal values is

$$\{\psi\} = \begin{Bmatrix} \{\psi_0\} \\ \{\psi_s\} \\ \{\psi_u\} \end{Bmatrix} \quad (8.24)$$

where $\{\psi_0\}$ represents all nodes along the streamline for which $\psi = 0$, $\{\psi_s\}$ represents all nodes at which the value of ψ is specified, and $\{\psi_u\}$ corresponds to all nodes for which ψ is unknown. The corresponding global force matrix is

$$\{F\} = \begin{Bmatrix} \{F_0\} \\ \{F_s\} \\ \{0\} \end{Bmatrix} \quad (8.25)$$

and we note that all nodes at which ψ is unknown are internal nodes at which the nodal forces are known to be zero.

Using the notation just defined, the system equations can be rewritten (by partitioning the stiffness matrix) as

$$\begin{bmatrix} [K_{00}] & [K_{0s}] & [K_{0u}] \\ [K_{s0}] & [K_{ss}] & [K_{su}] \\ [K_{u0}] & [K_{us}] & [K_{uu}] \end{bmatrix} \begin{Bmatrix} \{\psi_0\} \\ \{\psi_s\} \\ \{\psi_u\} \end{Bmatrix} = \begin{Bmatrix} \{F_0\} \\ \{F_s\} \\ \{0\} \end{Bmatrix} \quad (8.26)$$

Since $\psi_0 = 0$, the first set of partitioned equations become

$$[K_{0s}]\{\psi_s\} + [K_{0u}]\{\psi_u\} = \{F_0\} \quad (8.27)$$

and the values of F_0 can be obtained only after solving for $\{\psi_u\}$ using the remaining equations. Hence, Equation 8.27 is analogous to the reaction force equations in structural problems and can be eliminated from the system temporarily. The remaining equations are

$$\begin{bmatrix} [K_{ss}] & [K_{su}] \\ [K_{us}] & [K_{uu}] \end{bmatrix} \begin{Bmatrix} \{\psi_s\} \\ \{\psi_u\} \end{Bmatrix} = \begin{Bmatrix} \{F_s\} \\ \{0\} \end{Bmatrix} \quad (8.28)$$

and it must be noted that, even though the stiffness matrix is symmetric, $[K_{su}]$ and $[K_{us}]$ are *not* the same. The first partition of Equation 8.28 is also a set of “reaction” equations given by

$$[K_{ss}]\{\psi_s\} + [K_{su}]\{\psi_u\} = \{F_s\} \quad (8.29)$$

and these are used to solve for $\{F_s\}$ but, again, *after* $\{\psi_u\}$ is determined. The second partition of Equation 8.28 is

$$[K_{us}]\{\psi_s\} + [K_{uu}]\{\psi_u\} = \{0\} \quad (8.30)$$

and these equations have the formal solution

$$\{\psi_u\} = -[K_{uu}]^{-1}[K_{us}]\{\psi_s\} \quad (8.31)$$

since the values in $\{\psi_s\}$ are known constants. Given the solution represented by Equation 8.31, the “reactions” in Equations 8.27 and 8.28 can be computed directly.

As the velocity components are of major importance in a fluid flow, we must next utilize the solution for the nodal values of the stream function to compute the velocity components. This computation is easily accomplished given Equation 8.14, in which the stream function is discretized in terms of the nodal values. Once we complete the already described solution procedure for the values of the stream function at the nodes, the velocity components at any point in a specified finite element are

$$\begin{aligned} u(x, y) &= \frac{\partial \psi}{\partial y} = \sum_{i=1}^M \frac{\partial N_i}{\partial y} \psi_i = \frac{\partial [N]^T}{\partial y} \{\psi\} \\ v(x, y) &= -\frac{\partial \psi}{\partial x} = -\sum_{i=1}^M \frac{\partial N_i}{\partial x} \psi_i = -\frac{\partial [N]^T}{\partial x} \{\psi\} \end{aligned} \quad (8.32)$$

Note that if, for example, a three-node triangular element is used, the velocity components as defined in Equation 8.32 have constant values everywhere in the element and are discontinuous across element boundaries. Therefore, a large number of small elements are required to obtain solution accuracy. Application of the stream function to a numerical example is delayed until we discuss an alternate approach, the velocity potential function, in the next section.

8.4 THE VELOCITY POTENTIAL FUNCTION IN TWO-DIMENSIONAL FLOW

Another approach to solving two-dimensional incompressible, inviscid flow problems is embodied in the velocity potential function. In this method, we hypothesize the existence of a *potential function* $\phi(x, y)$ such that

$$\begin{aligned}u(x, y) &= -\frac{\partial\phi}{\partial x} \\v(x, y) &= -\frac{\partial\phi}{\partial y}\end{aligned}\tag{8.33}$$

and we note that the velocity components defined by Equation 8.33 automatically satisfy the irrotationality condition. Substitution of the velocity definitions into the continuity equation for two-dimensional flow yields

$$\frac{\partial u}{\partial x} + \frac{\partial v}{\partial y} = \frac{\partial^2\phi}{\partial x^2} + \frac{\partial^2\phi}{\partial y^2} = 0\tag{8.34}$$

and, again, we obtain Laplace's equation as the governing equation for 2-D flow described by a potential function.

We examine the potential formulation in terms of the previous example of a converging flow between two parallel plates. Referring again to Figure 8.4a, we now observe that, along the lines on which the potential function is constant, we can write

$$d\phi = \frac{\partial\phi}{\partial x} dx + \frac{\partial\phi}{\partial y} dy = -(u dx + v dy) = 0\tag{8.35}$$

Observing that the quantity $u dx + v dy$ is the magnitude of the scalar product of the velocity vector and the tangent to the line of constant potential, we conclude that the velocity vector at any point on a line of constant potential is *perpendicular* to the line. Hence, the streamlines and lines of constant velocity potential (*equipotential lines*) form an orthogonal "net" (known as the *flow net*) as depicted in Figure 8.5.

The finite element formulation of an incompressible, inviscid, irrotational flow in terms of velocity potential is quite similar to that of the stream function approach, since the governing equation is Laplace's equation in both cases. By

8.4 The Velocity Potential Function in Two-Dimensional Flow

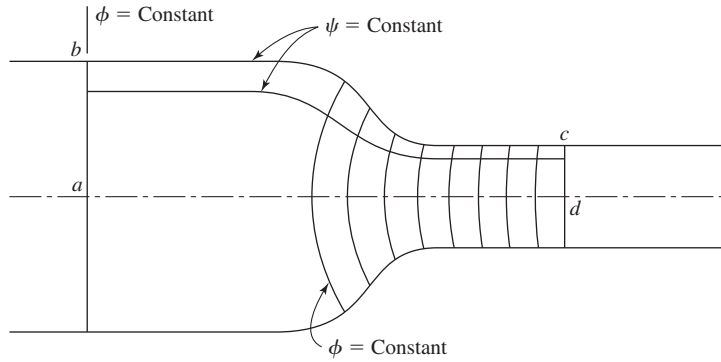


Figure 8.5 Flow net of lines of constant stream function ψ and constant velocity potential ϕ .

direct analogy with Equations 8.14–8.17, we write

$$\phi(x, y) = \sum_{i=1}^M N_i(x, y)\phi_i = [N] \{\phi\} \quad (8.36)$$

$$\int_{A^{(e)}} N_i(x, y) \left(\frac{\partial^2 \phi}{\partial x^2} + \frac{\partial^2 \phi}{\partial y^2} \right) dx dy = 0 \quad i = 1, M \quad (8.37)$$

$$\int_{A^{(e)}} [N^T] \left(\frac{\partial^2 \phi}{\partial x^2} + \frac{\partial^2 \phi}{\partial y^2} \right) dx dy = 0 \quad (8.38)$$

$$\begin{aligned} \int_{S^{(e)}} [N]^T \frac{\partial \phi}{\partial x} n_x dS - \int_{A^{(e)}} \frac{\partial [N]^T}{\partial x} \frac{\partial \phi}{\partial x} dx dy + \int_{S^{(e)}} [N]^T \frac{\partial \phi}{\partial y} n_y dS \\ - \int_{A^{(e)}} \frac{\partial [N]^T}{\partial y} \frac{\partial \phi}{\partial y} dx dy = 0 \end{aligned} \quad (8.39)$$

Utilizing Equation 8.36 in the area integrals of Equation 8.39 and substituting the velocity components into the boundary integrals, we obtain

$$\int_{A^{(e)}} \left(\frac{\partial [N]^T}{\partial x} \frac{\partial [N]}{\partial x} + \frac{\partial [N]^T}{\partial y} \frac{\partial [N]}{\partial y} \right) dx dy \{\phi\} = - \int_{S^{(e)}} [N]^T (un_x + vn_y) dS \quad (8.40)$$

or

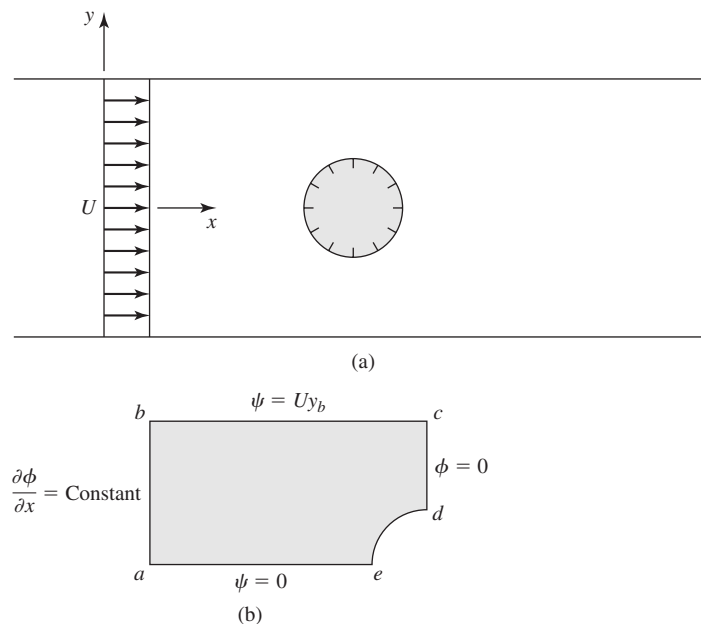
$$[k^{(e)}] \{\phi\} = \{f^{(e)}\} \quad (8.41)$$

The element stiffness matrix is observed to be identical to that of the stream function method. The nodal force vector is significantly different, however. Note that, in the right-hand integral in Equation 8.40, the term in parentheses is the scalar product of the velocity vector and the unit normal to an element boundary. Therefore, the nodal forces are allocations to the nodes of the flow across the element boundaries. (Recall that we assume unit dimension in the z direction, so the terms on the right-hand side of Equation 8.40 are volumetric flow rates.) As usual, on internal element boundaries, the contributions from adjacent elements are equal and opposite and cancel during the assembly step. Only elements on global boundaries have nonzero nodal force components.

EXAMPLE 8.1

To illustrate both the stream function and velocity potential methods, we now examine the case of a cylinder placed transversely to an otherwise uniform stream, as shown in Figure 8.6a. The underlying assumptions are

1. Far upstream from the cylinder, the flow field is uniform with $u = U = \text{constant}$ and $v = 0$.
2. Dimensions in the z direction are large, so that the flow can be considered two dimensional.
3. Far downstream from the cylinder, the flow is again uniform in accordance with assumption 1.

**Figure 8.6**

(a) Circular cylinder in a uniform, ideal flow. (b) Quarter-symmetry model of cylinder in a uniform stream.

■ Velocity Potential

Given the assumptions and geometry, we need consider only one-fourth of the flow field, as in Figure 8.6b, because of symmetry. The boundary conditions first are stated for the velocity potential formulation. Along $x = 0$ (a - b), we have $u = U = \text{constant}$ and $v = 0$. So,

$$u(0, y) = U = -\frac{\partial\phi}{\partial x}$$

$$v(0, y) = 0 = -\frac{\partial\phi}{\partial y}$$

and the unit (outward) normal vector to this surface is $(n_x, n_y) = (-1, 0)$. Hence, for every element having edges (therefore, nodes) on a - b , the nodal force vector is known as

$$\{f^{(e)}\} = - \int_{S^{(e)}} [N]^T (un_x + vn_y) dS = U \int_{S^{(e)}} [N]^T dS$$

and the integration path is simply $dS = dy$ between element nodes. Note the change in sign, owing to the orientation of the outward normal vector. Hence, the forces associated with flow into the region are positive and the forces associated with outflow are negative. (The sign associated with inflow and outflow forces depend on the choice of signs in Equation 8.33. If, in Equation 8.33, we choose positive signs, the formulation is essentially the same.)

The symmetry conditions are such that, on surface (edge) c - d , the y -velocity components are zero and $x = x_c$, so we can write

$$v = -\frac{\partial\phi}{\partial y} = -\frac{d\phi(x_c, y)}{dy} = 0$$

This relation can be satisfied if ϕ is independent of the y coordinate or $\phi(x_c, y)$ is constant. The first possibility is quite unlikely and requires that we assume the solution form. Hence, the conclusion is that the velocity potential function must take on a constant value on c - d . Note, most important, this conclusion *does not* imply that the x -velocity component is zero.

Along b - c , the fluid velocity has only an x component (impenetrability), so we can write this boundary condition as

$$\frac{\partial\phi}{\partial n} = \frac{\partial\phi}{\partial x}n_x + \frac{\partial\phi}{\partial y}n_y = -(un_x + vn_y) = 0$$

and since $v = 0$ and $n_x = 0$ on this edge, we find that all nodal forces are zero along b - c , but the values of the potential function are unknown.

The same argument holds for a - e - d . Using the symmetry conditions along this surface, there is no velocity perpendicular to the surface, and we arrive at the same conclusion: element nodes have zero nodal force values but unknown values of the potential function.

In summary, for the potential function formulation, the boundary conditions are

1. Boundary $a-b$: ϕ unknown, forces known.
2. Boundary $b-c$: ϕ unknown, forces = 0.
3. Boundary $c-d$: $\phi = \text{constant}$, forces unknown.
4. Boundary $a-e-d$: ϕ unknown, forces = 0.

Now let us consider assembling the global equations. Per the usual assembly procedure, the equations are of the matrix form

$$[K]\{\phi\} = \{F\}$$

and the force vector on the right-hand side contains both known and unknown values. The vector of nodal potential values $\{\phi\}$ is unknown—we have no specified values. We do know that, along $c-d$, the nodal values of the potential function are constant, but we do not know the value of the constant. However, in light of Equation 8.33, the velocity components are defined in terms of first partial derivatives, so an arbitrary constant in the potential function is of no consequence, as with the stream function formulation. Therefore, we need specify only an arbitrary value of ϕ at nodes on $c-d$ in the model, and the system of equations becomes solvable.

■ Stream Function Formulation

Developing the finite element model for this particular problem in terms of the stream function is a bit simpler than for the velocity potential. For reasons that become clear when we write the boundary conditions, we also need consider only one-quarter of the flow field in the stream function approach. The model is also as shown in Figure 8.6b. Along $a-e$, the symmetry conditions are such that the y -velocity components are zero. On $e-d$, the velocity components normal to the cylinder must be zero, as the cylinder is impenetrable. Hence, $a-e-d$ is a streamline and we arbitrarily set $\psi = 0$ on that streamline. Clearly, the upper surface $b-c$ is also a streamline and, using previous arguments from the convergent flow example, we have $\psi = U y_b$ along this edge. (Note that, if we had chosen the value of the stream function along $a-e-d$ to be a nonzero value C , the value along $b-c$ would be $\psi = U y_b + C$.) On $a-b$ and $c-d$, the nodal forces are zero, also per the previous discussion, and the nodal values of the stream function are unknown. Except for the geometrical differences, the solution procedure is the same as that for the converging flow.

A relatively coarse mesh of four-node quadrilateral elements used for solving this problem using the stream function is shown in Figure 8.7a. For computation, the values $U = 40$, distance $a-b = y_b = 5$, and cylinder radius = 1 are used. The resulting streamlines (lines of constant ψ) are shown in Figure 8.7b. Recalling that the streamlines are lines to which fluid velocity is tangent at all points, the results appear to be correct intuitively. Note that, on the left boundary, the streamlines appear to be very nearly perpendicular to the boundary, as required if the uniform velocity condition on that boundary is satisfied.

For the problem at hand, we have the luxury of comparing the finite element results with an “approximately exact” solution, which gives the stream function as

$$\psi = U \frac{x^2 + y^2 - R^2}{x^2 + y^2} y$$

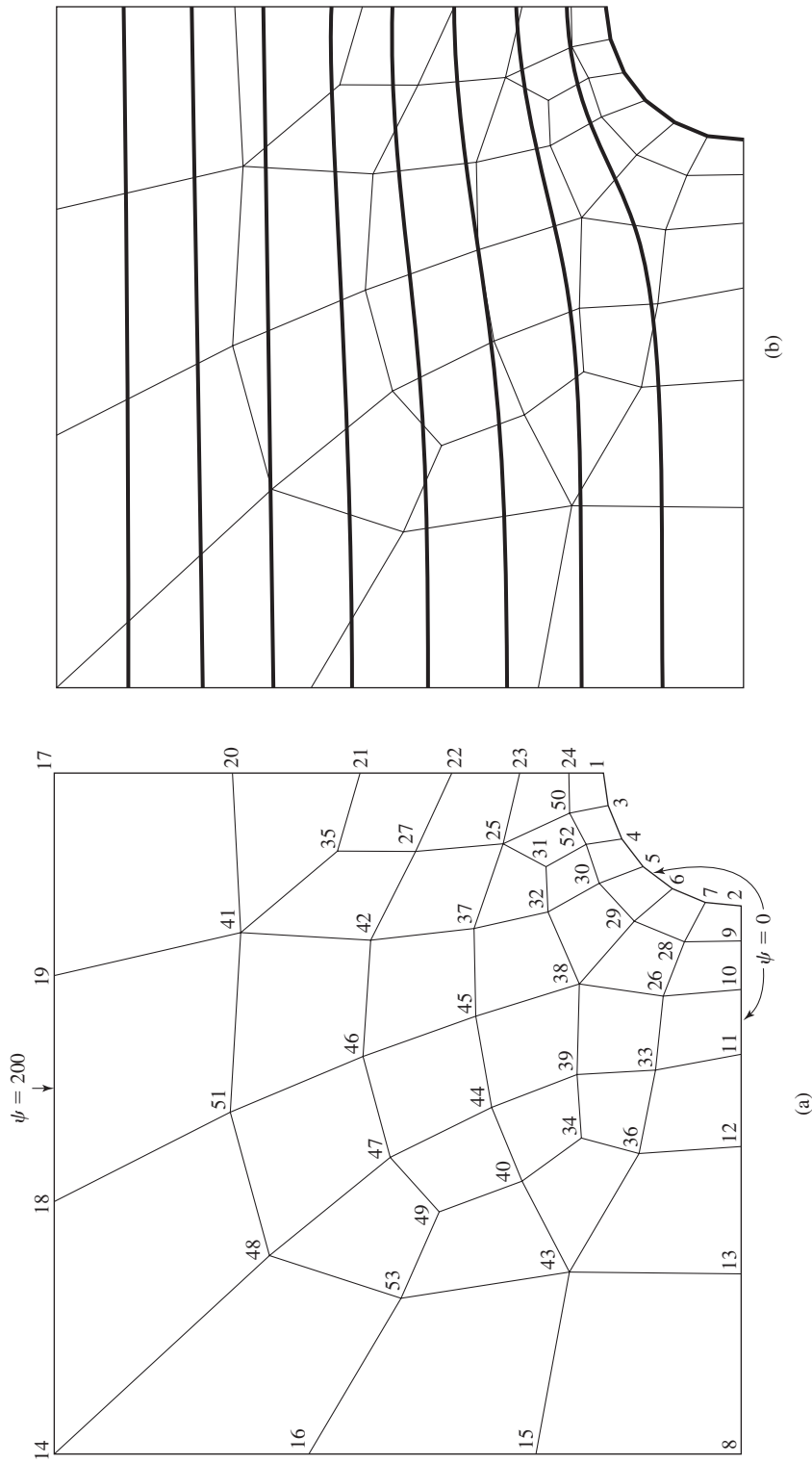


Figure 8.7 (a) Coarse, finite element mesh for stream function solution; 40 elements. (b) Streamlines ($\psi = \text{constant}$) for finite element solution of Example 8.1.

Table 8.1 Selected Nodal Stream Function and Velocity Values for Solution of Example 8.1

Node	ψ_{FE}	ψ_{Exact}	V_{FE}	V_{Exact}
1	0	0	75.184	80
2	0	0	1.963	0
8	0	0	38.735	38.4
16	123.63	122.17	40.533	40.510
20	142.48	137.40	44.903	42.914
21	100.03	99.37	47.109	45.215
22	67.10	64.67	51.535	49.121
23	40.55	39.36	57.836	55.499
24	18.98	18.28	68.142	65.425
45	67.88	65.89	41.706	40.799
46	103.87	100.74	42.359	41.018

This solution is actually for a cylinder in a uniform stream of indefinite extent in both the x and y directions (hence, the use of the oxymoron, approximately exact) but is sufficient for comparison purposes. Table 8.1 lists values of ψ obtained by the finite element solution and the preceding analytical solution at several selected nodes in the model. The computed magnitude of the fluid velocity at those points is also given. The nominal errors in the finite element solution versus the analytical solution are about 4 percent for the value of the stream function and 6 percent for the velocity magnitude. While not shown here, a refined element mesh consisting of 218 elements was used in a second solution and the errors decreased to less than 1 percent for both the stream function value and the velocity magnitude.

Earlier in the chapter, the analogy between the heat conduction problem and the stream function formulation is mentioned. It may be of interest to the reader to note that the stream function solution presented in Example 8.1 is generated using a commercial software package and a two-dimensional heat transfer element. The particular software does not contain a fluid element of the type required for the problem. However, by setting the thermal conductivities to unity and specifying zero internal heat generation, the problem, mathematically, is the same. That is, nodal temperatures become nodal values of the stream function. Similarly, spatial derivatives of temperature (flux values) become velocity components if the appropriate sign changes are taken into account. The mathematical similarity of the two problems is further illustrated by the finite element solution of the previous example using the velocity potential function.

EXAMPLE 8.2

Obtain a finite element solution for the problem of Example 8.1 via the velocity potential approach, using, specifically, the heat conduction formulation modified as required.

8.4 The Velocity Potential Function in Two-Dimensional Flow

■ Solution

First let us note the analogies

$$u = -\frac{\partial \phi}{\partial x} \Rightarrow q_x = -k_x \frac{\partial T}{\partial x}$$

$$v = -\frac{\partial \phi}{\partial y} \Rightarrow q_y = -k_y \frac{\partial T}{\partial y}$$

so that, if $k_x = k_y = 1$, then the velocity potential is directly analogous to temperature and the velocity components are analogous to the respective flux terms. Hence, the boundary conditions, in terms of thermal variables become

$$q_x = U \quad q_y = 0 \quad \text{on } a-b$$

$$q_x = q_y = 0 \quad \text{on } b-c \text{ and } a-e-d$$

$$T = \text{constant} = 0 \quad \text{on } c-d \text{ (the value is arbitrary)}$$

Figure 8.8 shows a coarse mesh finite element solution that plots the lines of constant velocity potential ϕ (in the thermal solution, these lines are lines of constant temperature,

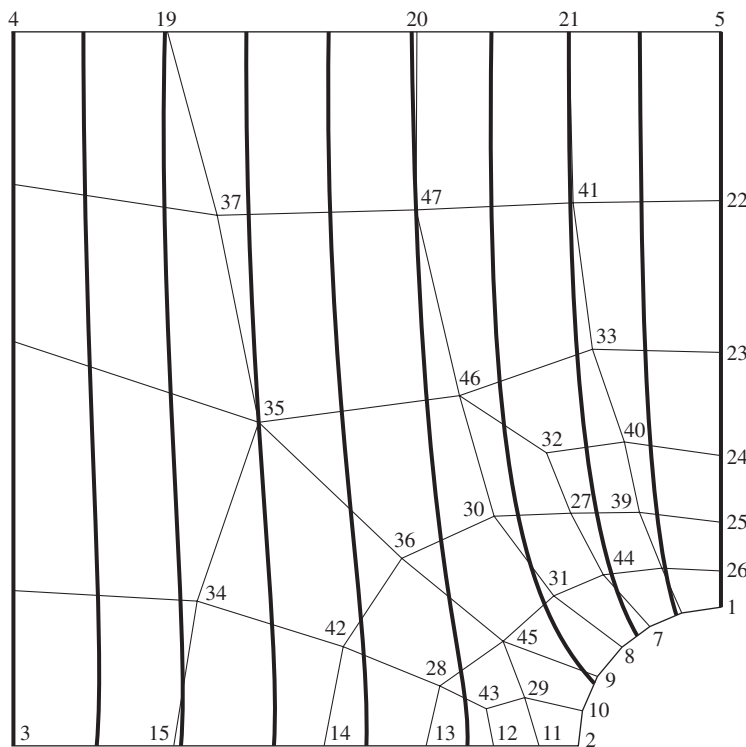


Figure 8.8 Lines of constant velocity potential ϕ for the finite element solution of Example 8.2.

Table 8.2 Velocity Components at Selected Nodes in Example 8.2

Node	u	v
4	40.423	0.480
19	41.019	0.527
20	42.309	0.594
21	43.339	0.516
5	43.676	0.002

or *isotherms*). A direct comparison between this finite element solution and that described for the stream function approach is not possible, since the element meshes are different. However, we can assess accuracy of the velocity potential solution by examination of the results in terms of the boundary conditions. For example, along the upper horizontal boundary, the y -velocity component must be zero, from which it follows that lines of constant ϕ must be perpendicular to the boundary. Visually, this condition appears to be reasonably well-satisfied in Figure 8.8. An examination of the actual data presents a slightly different picture. Table 8.2 lists the computed velocity components at each node along the upper surface. Clearly, the values of the y -velocity component v are not zero, so additional solutions using refined element meshes are in order.

Observing that the stream function and velocity potential methods are amenable to solving the same types of problems, the question arises as to which should be selected in a given instance. In each approach, the stiffness matrix is the same, whereas the nodal forces differ in formulation but require the same basic information. Hence, there is no significant difference in the two procedures. However, if one uses the stream function approach, the flow is readily visualized, since velocity is tangent to streamlines. It can also be shown [2] that the difference in value of two adjacent streamlines is equal to the flow rate (per unit depth) between those streamlines.

8.4.1 Flow around Multiple Bodies

For an ideal (inviscid, incompressible) flow around multiple bodies, the stream function approach is rather straightforward to apply, especially in finite element analysis, if the appropriate boundary conditions can be determined. To begin the illustration, let us reconsider flow around a cylinder as in Example 8.1. Observing that Equation 8.11 governing the stream function is linear, the principle of superposition is applicable; that is, the sum of any two solutions to the equation is also a solution. In particular, we consider the stream function to be given by

$$\psi(x, y) = \psi_1(x, y) + a\psi_2(x, y) \quad (8.42)$$

where a is a constant to be determined. The boundary conditions at the horizontal surfaces (S_1) are satisfied by ψ_1 , while the boundary conditions on the surface

8.4 The Velocity Potential Function in Two-Dimensional Flow

313

of the cylinder (S_2) are satisfied by ψ_2 . The constant a must be determined so that the combination of the two stream functions satisfies a known condition at some point in the flow. Hence, the conditions on the two solutions (stream functions) are

$$\frac{\partial^2 \psi_1}{\partial x^2} + \frac{\partial^2 \psi_1}{\partial y^2} = 0 \quad (\text{everywhere in the domain}) \quad (8.43)$$

$$\frac{\partial^2 \psi_2}{\partial x^2} + \frac{\partial^2 \psi_2}{\partial y^2} = 0 \quad (\text{everywhere in the domain})$$

$$\psi_1 = U y_b \quad \text{on } S_1 \quad (8.44)$$

$$\psi_1 = 0 \quad \text{on } S_2 \quad (8.45)$$

$$\psi_2 = 0 \quad \text{on } S_1 \quad (8.46)$$

$$\psi_2 = 1 \quad \text{on } S_2 \quad (8.47)$$

Note that the value of ψ_2 is (temporarily) set equal to unity on the surface of the cylinder. The procedure is then to obtain two finite element solutions, one for each stream function, and associated boundary conditions. Given the two solutions, the constant a can be determined and the complete solution known. The constant a , for example, is found by computing the velocity at a far upstream position (where the velocity is known) and calculating a to meet the known condition.

In the case of uniform flow past a cylinder, the solutions give the trivial result that $a = \text{arbitrary constant}$, since we have only one surface in the flow, hence one arbitrary constant. The situation is different if we have multiple bodies, however, as discussed next.

Consider Figure 8.9, depicting two arbitrarily shaped bodies located in an ideal fluid flow, which has a uniform velocity profile at a distance upstream from the two obstacles. In this case, we consider *three* solutions to the governing

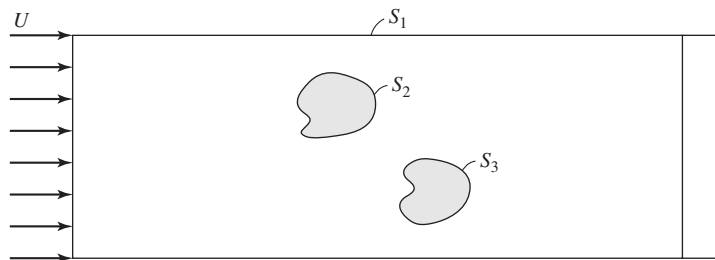


Figure 8.9 Two arbitrary bodies in a uniform stream. The boundary conditions must be specified on S_1 , S_2 , and S_3 within a constant.

equation, so that the stream function can be represented by [3]

$$\psi(x, y) = \psi_1(x, y) + a\psi_2(x, y) + b\psi_3(x, y) \quad (8.48)$$

where a and b are constants to be determined. Again, we know that each independent solution in Equation 8.48 must satisfy Equation 8.11 and, recalling that the stream function must take on constant value on an impenetrable surface, we can express the boundary conditions on each solution as

$$\begin{aligned} \psi_1 &= U y_b && \text{on } S_1 \\ \psi_1 &= 0 && \text{on } S_2 \text{ and } S_3 \\ \psi_2 &= 0 && \text{on } S_1 \text{ and } S_3 \\ \psi_2 &= 1 && \text{on } S_2 \\ \psi_3 &= 0 && \text{on } S_1 \text{ and } S_2 \\ \psi_3 &= 1 && \text{on } S_3 \end{aligned} \quad (8.49)$$

To obtain a solution for the flow problem depicted in Figure 8.9, we must

1. Obtain a solution for ψ_1 satisfying the governing equation and the boundary conditions stated for ψ_1 .
2. Obtain a solution for ψ_2 satisfying the governing equation and the boundary conditions stated for ψ_2 .
3. Obtain a solution for ψ_3 satisfying the governing equation and the boundary conditions stated for ψ_3 .
4. Combine the results at (in this case) two points, where the velocity or stream function is known in value, to determine the constants a and b in Equation 8.48. For this example, any two points on section a - b are appropriate, as we know the velocity is uniform in that section.

As a practical note, this procedure is *not* generally included in finite element software packages. One must, in fact, obtain the three solutions and hand calculate the constants a and b , then adjust the boundary conditions (the constant values of the stream function) for entry into the next run of the software. In this case, not only the computed results (stream function values, velocities) but the values of the computed constants a and b are considerations for convergence of the finite element solutions. The procedure described may seem tedious, and it is to a certain extent, but the alternatives (other than finite element analysis) are much more cumbersome.

8.5 INCOMPRESSIBLE VISCOUS FLOW

The idealized inviscid flows analyzed via the stream function or velocity potential function can reveal valuable information in many cases. Since no fluid is truly inviscid, the accuracy of these analyses decreases with increasing viscosity

of a real fluid. To illustrate viscosity effects (and the arising complications) we now examine application of the finite element method to a restricted class of incompressible viscous flows.

The assumptions and restrictions applicable to the following developments are

1. The flow can be considered two dimensional.
2. No heat transfer is involved.
3. Density and viscosity are constant.
4. The flow is steady with respect to time.

Under these conditions, the famed Navier-Stokes equations [4, 5], representing conservation of momentum, can be reduced to [6]

$$\begin{aligned} \rho u \frac{\partial u}{\partial x} + \rho v \frac{\partial u}{\partial y} - \mu \frac{\partial^2 u}{\partial x^2} - \mu \frac{\partial^2 u}{\partial y^2} + \frac{\partial p}{\partial x} &= F_{Bx} \\ \rho u \frac{\partial v}{\partial x} + \rho v \frac{\partial v}{\partial y} - \mu \frac{\partial^2 v}{\partial x^2} - \mu \frac{\partial^2 v}{\partial y^2} + \frac{\partial p}{\partial y} &= F_{By} \end{aligned} \quad (8.50)$$

where

u and $v = x$ -, and y -velocity components, respectively

ρ = density of the fluid

p = pressure

μ = absolute fluid viscosity

F_{Bx}, F_{By} = body force per unit volume in the x and y directions, respectively

Note carefully that Equation 8.50 is nonlinear, owing to the presence of the *convective inertia* terms of the form $\rho u(\partial u/\partial x)$. Rather than treat the nonlinear terms directly at this point, we first consider the following special case.

8.5.1 Stokes Flow

For fluid flow in which the velocities are very small, the inertia terms (i.e., the preceding nonlinear terms) can be shown to be negligible in comparison to the viscous effects. Such flow, known as *Stokes flow* (or *creeping flow*), is commonly encountered in the processing of high-viscosity fluids, such as molten polymers. Neglecting the inertia terms, the momentum equations become

$$\begin{aligned} -\mu \frac{\partial^2 u}{\partial x^2} - \mu \frac{\partial^2 u}{\partial y^2} + \frac{\partial p}{\partial x} &= F_{Bx} \\ -\mu \frac{\partial^2 v}{\partial x^2} - \mu \frac{\partial^2 v}{\partial y^2} + \frac{\partial p}{\partial y} &= F_{By} \end{aligned} \quad (8.51)$$

Equation 8.51 and the continuity condition, Equation 8.8, form a system of three equations in the three unknowns $u(x, y)$, $v(x, y)$, and $p(x, y)$. Hence, a finite element formulation includes three nodal variables, and these are discretized as

$$\begin{aligned} u(x, y) &= \sum_{i=1}^M N_i(x, y)u_i = [N]^T \{u\} \\ v(x, y) &= \sum_{i=1}^M N_i(x, y)v_i = [N]^T \{v\} \\ p(x, y) &= \sum_{i=1}^M N_i(x, y)p_i = [N]^T \{p\} \end{aligned} \quad (8.52)$$

Application of Galerkin's method to a two-dimensional finite element (assumed to have uniform unit thickness in the z direction) yields the residual equations

$$\begin{aligned} \int_{A^{(e)}} N_i \left(-\mu \frac{\partial^2 u}{\partial x^2} - \mu \frac{\partial^2 u}{\partial y^2} + \frac{\partial p}{\partial x} - F_{Bx} \right) dA &= 0 \\ \int_{A^{(e)}} N_i \left(-\mu \frac{\partial^2 v}{\partial x^2} - \mu \frac{\partial^2 v}{\partial y^2} + \frac{\partial p}{\partial y} - F_{By} \right) dA &= 0 \quad i = 1, M \\ \int_{A^{(e)}} N_i \left(\frac{\partial u}{\partial x} + \frac{\partial v}{\partial y} \right) dA &= 0 \end{aligned} \quad (8.53)$$

As the procedures required to obtain the various element matrices are covered in detail in previous developments, we do not examine Equation 8.53 in its entirety. Instead, only a few representative terms are developed and the remaining results stated by inference.

First, consider the viscous terms containing second spatial derivatives of velocity components such as

$$-\int_{A^{(e)}} \mu N_i \left(\frac{\partial^2 u}{\partial x^2} + \frac{\partial^2 u}{\partial y^2} \right) dA \quad i = 1, M \quad (8.54)$$

which can be expressed as

$$-\int_{A^{(e)}} \mu \left[\frac{\partial}{\partial x} \left(N_i \frac{\partial u}{\partial x} \right) + \frac{\partial}{\partial y} \left(N_i \frac{\partial u}{\partial y} \right) \right] dA + \int_{A^{(e)}} \mu \left(\frac{\partial N_i}{\partial x} \frac{\partial u}{\partial x} + \frac{\partial N_i}{\partial y} \frac{\partial u}{\partial y} \right) dA \quad i = 1, M \quad (8.55)$$

Application of the Green-Gauss theorem to the first integral in expression (8.55) yields

$$-\int_{A^{(e)}} \mu \left[\frac{\partial}{\partial x} \left(N_i \frac{\partial u}{\partial x} \right) + \frac{\partial}{\partial y} \left(N_i \frac{\partial u}{\partial y} \right) \right] dA = -\int_{S^{(e)}} \mu N_i \left(\frac{\partial u}{\partial x} n_x + \frac{\partial u}{\partial y} n_y \right) dS \quad i = 1, M \quad (8.56)$$

where $S^{(e)}$ is the element boundary and (n_x, n_y) are the components of the unit outward normal vector to the boundary. Hence, the integral in expression (8.54) becomes

$$\begin{aligned} -\int_{A^{(e)}} \mu N_i \left(\frac{\partial^2 u}{\partial x^2} + \frac{\partial^2 u}{\partial y^2} \right) dA &= -\int_{S^{(e)}} \mu N_i \left(\frac{\partial u}{\partial x} n_x + \frac{\partial u}{\partial y} n_y \right) dS \\ &+ \int_{A^{(e)}} \mu \left(\frac{\partial N_i}{\partial x} \frac{\partial u}{\partial x} + \frac{\partial N_i}{\partial y} \frac{\partial u}{\partial y} \right) dA \quad (8.57) \end{aligned}$$

Note that the first term on the right-hand side of Equation 8.57 represents a nodal boundary force term for the element. Such terms arise from shearing stress. As we observed many times, these terms cancel on interelement boundaries and must be considered only on the global boundaries of a finite element model. Hence, these terms are considered only in the assembly step. The second integral in Equation 8.57 is a portion of the “stiffness” matrix for the fluid problem, and as this term is related to the x velocity and the viscosity, we denote this portion of the matrix $[k_{u\mu}]$. Recalling that Equation 8.57 represents M equations, the integral is converted to matrix form using the first of Equation 8.52 to obtain

$$\int_{A^{(e)}} \mu \left(\frac{\partial [N]^T}{\partial x} \frac{\partial [N]}{\partial x} + \frac{\partial [N]^T}{\partial y} \frac{\partial [N]}{\partial y} \right) dA \{u\} = [k_{u\mu}] \{u\} \quad (8.58)$$

Using the same approach with the second of Equation 8.53, the results are similar. We obtain the analogous result

$$\begin{aligned} -\int_{A^{(e)}} \mu N_i \left(\frac{\partial^2 v}{\partial x^2} + \frac{\partial^2 v}{\partial y^2} \right) dA &= -\int_{S^{(e)}} \mu N_i \left(\frac{\partial v}{\partial x} n_x + \frac{\partial v}{\partial y} n_y \right) dS \\ &+ \int_{A^{(e)}} \mu \left(\frac{\partial N_i}{\partial x} \frac{\partial v}{\partial x} + \frac{\partial N_i}{\partial y} \frac{\partial v}{\partial y} \right) dA \quad (8.59) \end{aligned}$$

Proceeding as before, we can write the area integrals on the right as

$$\int_{A^{(e)}} \mu \left(\frac{\partial [N]^T}{\partial x} \frac{\partial [N]}{\partial x} + \frac{\partial [N]^T}{\partial y} \frac{\partial [N]}{\partial y} \right) dA \{v\} = [k_{v\mu}] \{v\} \quad (8.60)$$

Considering next the pressure terms and converting to matrix notation, the first of Equation 8.53 leads to

$$\int_{A^{(e)}} [N]^T \frac{\partial [N]}{\partial x} dA \{p\} = [k_{px}] \{p\} \quad (8.61)$$

and similarly the second momentum equation contains

$$\int_{A^{(e)}} [N]^T \frac{\partial [N]}{\partial y} dA \{p\} = [k_{py}] \{p\} \quad (8.62)$$

The nodal force components corresponding to the body forces are readily shown to be given by

$$\begin{aligned} \{f_{Bx}\} &= \int_{A^{(e)}} [N]^T F_{Bx} dA \\ \{f_{By}\} &= \int_{A^{(e)}} [N]^T F_{By} dA \end{aligned} \quad (8.63)$$

Combining the notation developed in Equations 8.58–8.63, the momentum equations for the finite element are

$$\begin{aligned} [k_{u\mu}] \{u\} + [k_{px}] \{p\} &= \{f_{Bx}\} + \{f_{x\tau}\} \\ [k_{v\mu}] \{v\} + [k_{py}] \{p\} &= \{f_{By}\} + \{f_{y\tau}\} \end{aligned} \quad (8.64)$$

where, for completeness, the nodal forces corresponding to the integrals over element boundaries $S^{(e)}$ in Equations 8.57 and 8.59 have been included.

Finally, the continuity equation is expressed in terms of the nodal velocities in matrix form as

$$\int_{A^{(e)}} [N]^T \frac{\partial [N]}{\partial x} dA \{u\} + \int_{A^{(e)}} [N]^T \frac{\partial [N]}{\partial y} dA \{v\} = [k_u] \{u\} + [k_v] \{v\} = 0 \quad (8.65)$$

where

$$\begin{aligned} [k_u] &= [k_{px}] = \int_{A^{(e)}} [N]^T \frac{\partial [N]}{\partial x} dA \\ [k_v] &= [k_{py}] = \int_{A^{(e)}} [N]^T \frac{\partial [N]}{\partial y} dA \end{aligned} \quad (8.66)$$

As formulated here, Equations 8.64 and 8.65 are a system of $3M$ algebraic equations governing the $3M$ unknown nodal values $\{u\}$, $\{v\}$, $\{p\}$ and can be expressed

formally as the system

$$\begin{bmatrix} [k_{u\mu}] & [0] & [k_{p_x}] \\ [0] & [k_{v\mu}] & [k_{p_y}] \\ [k_u] & [k_v] & [0] \end{bmatrix} \begin{Bmatrix} \{u\} \\ \{v\} \\ \{p\} \end{Bmatrix} = \begin{Bmatrix} \{f_{B_x}\} \\ \{f_{B_y}\} \\ \{0\} \end{Bmatrix} \Rightarrow [k^{(e)}] \{\delta^{(e)}\} = \{f^{(e)}\} \quad (8.67)$$

where $[k^{(e)}]$ represents the complete element stiffness matrix. Note that the element stiffness matrix is composed of nine $M \times M$ submatrices, and although the individual submatrices are symmetric, the stiffness matrix is *not* symmetric.

The development leading to Equation 8.67 is based on evaluation of both the velocity components and pressure at the same number of nodes. This is not necessarily the case for a fluid element. Computational research [7] shows that better accuracy is obtained if the velocity components are evaluated at a larger number of nodes than pressures. In other words, the velocity components are discretized using higher-order interpolation functions than the pressure variable. For example, a six-node quadratic triangular element could be used for velocities, while the pressure variable is interpolated only at the corner nodes, using linear interpolation functions. In such a case, Equation 8.66 does not hold.

The arrangement of the equations and associated definition of the element stiffness matrix in Equation 8.67 is based on ordering the nodal variables as

$$\{\delta\}^T = [u_1 \quad u_2 \quad u_3 \quad v_1 \quad v_2 \quad v_3 \quad p_1 \quad p_2 \quad p_3]$$

(using a three-node element, for example). Such ordering is well-suited to illustrate development of the element equations. However, if the global equations for a multielement model are assembled and the global nodal variables are similarly ordered, that is,

$$\{\Delta\}^T = [U_1 \quad U_2 \cdots V_1 \quad V_2 \cdots P_1 \quad P_2 \cdots P_N]$$

the computational requirements are prohibitively inefficient, because the global stiffness has a large *bandwidth*. On the other hand, if the nodal variables are ordered as

$$\{\Delta\}^T = [U_1 \quad V_1 \quad P_1 \quad U_2 \quad V_2 \quad P_2 \cdots U_N \quad V_N \quad P_N]$$

computational efficiency is greatly improved, as the matrix bandwidth is significantly reduced. For a more detailed discussion of banded matrices and associated computational techniques, see [8].

EXAMPLE 8.3

Consider the flow between the plates of Figure 8.4 to be a viscous, creeping flow and determine the boundary conditions for a finite element model. Assume that the flow is fully developed at sections *a-b* and *c-d* and the constant volume flow rate per unit thickness is Q .

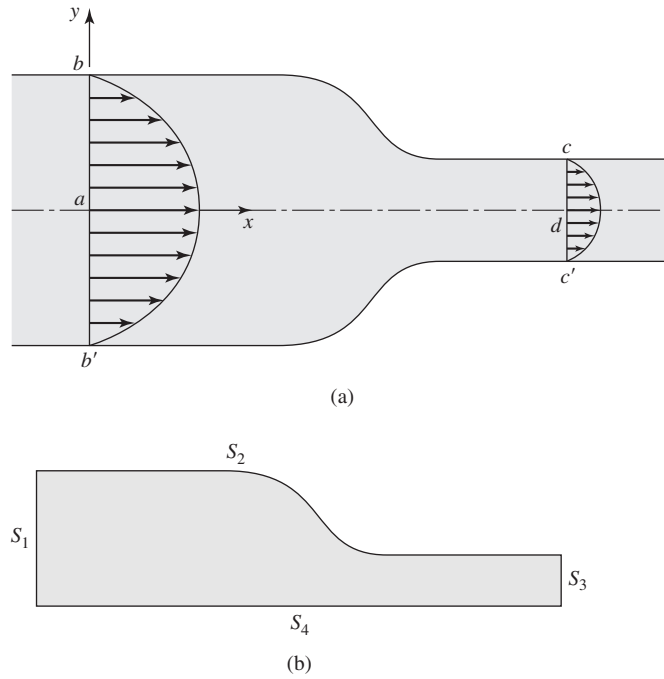


Figure 8.10
(a) Velocity of fully developed flow. (b) Boundary conditions.

■ **Solution**

For fully developed flow, the velocity profiles at $a-b$ and $c-d$ are parabolic, as shown in Figure 8.10a. Denoting the maximum velocities at these sections as U_{ab} and U_{cd} , we have

$$u(x_a, y) = U_{ab} \left(1 - \frac{y^2}{y_b^2} \right)$$

$$v(x_a, y) = 0$$

$$u(x_c, y) = U_{cd} \left(1 - \frac{y^2}{y_b^2} \right)$$

$$v(x_c, y) = 0$$

The volume flow rate is obtained by integrating the velocity profiles as

$$Q = 2 \int_0^{y_b} u(x_a, y) dy = 2 \int_0^{y_d} u(x_c, y) dy$$

Substituting the velocity expressions and integrating yields

$$U_{ab} = \frac{3Q}{4y_b} \quad U_{cd} = \frac{3Q}{4y_d}$$

and thus the velocity components at all element nodes on $a-b$ and $c-d$ are known.

Next consider the contact between fluid and plate along $b-c$. As in cases of inviscid flow discussed earlier, we invoke the condition of impenetrability to observe that velocity components normal to this boundary are zero. In addition, since the flow is viscous, we invoke the no-slip condition, which requires that tangential velocity components also be zero at the fluid-solid interface. Hence, for all element nodes on $b-c$, both velocity components u_i and v_i are zero.

The final required boundary conditions are obtained by observing the condition of symmetry along $a-d$, where $v = v(x, 0) = 0$. The boundary conditions are summarized next in reference to Figure 8.10b:

$$\begin{aligned} U_I &= U_{ab} \left(1 - \frac{y_I^2}{y_b^2} \right) & V_I &= 0 & \text{on } S_1 (a-b) \\ U_I &= U_{cd} \left(1 - \frac{y_I^2}{y_d^2} \right) & V_I &= 0 & \text{on } S_2 (b-c) \\ U_I &= V_I = 0 & & & \text{on } S_3 (c-d) \\ V_I &= 0 & & & \text{on } S_4 (a-d) \end{aligned}$$

where I is an element node on one of the global boundary segments.

The system equations corresponding to each of the specified nodal velocities just summarized become constraint equations and are eliminated via the usual procedures prior to solving for the unknown nodal variables. Associated with each specified velocity is an unknown “reaction” force represented by the shear stress-related forces in Equations 8.56, and these forces can be computed using the constraint equations after the global solution is obtained. This is the case for all equations associated with element nodes on segments S_1 , S_2 , and S_3 . On S_4 , the situation is a little different and additional comment is warranted. As the velocity components in the x direction along S_4 are not specified, a question arises as to the disposition of the shear-related forces in the x direction. These forces are given by

$$f_{x\tau} = \int_{S^{(e)}} \mu N_i \left(\frac{\partial u}{\partial x} n_x + \frac{\partial u}{\partial y} n_y \right) dS$$

as embodied in Equation 8.57. On the boundary in question, the unit outward normal vector is defined by $(n_x, n_y) = (0, -1)$, so the first term in this integral is zero. In view of the symmetry conditions about $a-c$, we also have $\partial u / \partial y = 0$, so the shear forces in the x direction along S_4 are also zero. With this observation and the boundary conditions, the global matrix equations become a tractable system of algebraic equations that can be solved for the unknown values of the nodal variables.

8.5.2 Viscous Flow with Inertia

Having discussed slow flows, in which the inertia terms were negligible, we now consider the more general, nonlinear case. All the developments of the previous

section on Stokes flow are applicable here; we now add the nonlinear terms arising from the convective inertia terms. From the first of Equation 8.50, we add a term of the form

$$\int_{A^{(e)}} \rho \left(u \frac{\partial u}{\partial x} + v \frac{\partial u}{\partial y} \right) dA \Rightarrow \rho \int_{A^{(e)}} \left([N]\{u\} \frac{\partial [N]}{\partial x} \{u\} + [N]\{v\} \frac{\partial [N]}{\partial y} \{u\} \right) dA \quad (8.68)$$

and from the second equation of 8.50,

$$\int_{A^{(e)}} \rho \left(u \frac{\partial v}{\partial x} + v \frac{\partial v}{\partial y} \right) dA \Rightarrow \rho \int_{A^{(e)}} \left([N]\{u\} \frac{\partial [N]}{\partial x} \{v\} + [N]\{v\} \frac{\partial [N]}{\partial y} \{v\} \right) dA \quad (8.69)$$

As expressed, Equation 8.68 is not conformable to matrix multiplication, as in being able to write the expression in the form $[k]\{u\}$, and this is a direct result of the nonlinearity of the equations. While a complete treatment of the nonlinear equations governing viscous fluid flow is well beyond the scope of this text, we discuss an iterative approximation for the problem.

Let us assume that for a particular two-dimensional geometry, we have solved the Stokes (creeping) flow problem and have all the nodal velocities of the Stokes flow finite element model available. For each element in the finite element model, we denote the Stokes flow solution for the average velocity components (evaluated at the centroid of each element) as (\bar{u}, \bar{v}) ; then, we express the approximation for the inertia terms (as exemplified by Equation 8.69) as

$$\int_{A^{(e)}} \rho \left(u \frac{\partial u}{\partial x} + v \frac{\partial u}{\partial y} \right) dA = \int_{A^{(e)}} \rho \left(\bar{u} \frac{\partial [N]}{\partial x} + \bar{v} \frac{\partial [N]}{\partial y} \right) dA \{u\} = [k_{uv}]\{u\} \quad (8.70)$$

Similarly, we find the y-momentum equation contribution to be

$$\int_{A^{(e)}} \rho \left(u \frac{\partial v}{\partial x} + v \frac{\partial v}{\partial y} \right) dA = \int_{A^{(e)}} \rho \left(\bar{u} \frac{\partial [N]}{\partial x} + \bar{v} \frac{\partial [N]}{\partial y} \right) dA \{v\} = [k_{vu}]\{v\} \quad (8.71)$$

Equations 8.70 and 8.71 refer to an individual element. The assembly procedures are the same as discussed before; now we add additional terms to the stiffness matrix as a result of inertia. These terms are readily identifiable in Equations 8.70 and 8.71. In the viscous inertia flow, the solution requires iteration to achieve satisfactory results. The use of the Stokes flow velocities and pressures represent only the first iteration (approximation). At each iteration, the newly computed velocity components are used for the next iteration.

For both creeping flow and flow with inertia, the governing equations can also be developed in terms of a stream function [3]. However, the resulting (single) governing equation in each case is found to be fourth order. Consequently, elements exhibiting continuity greater than C^0 are required.

8.6 SUMMARY

Application of the finite element method to fluid flow problems is, in one sense, quite straightforward and, in another sense, very complex. In the idealized cases of inviscid flow, the finite element problem is easily formulated in terms of a single variable. Such problems are neither routine nor realistic, as no fluid is truly without viscosity. As shown, introduction of the very real property of fluid viscosity and the historically known, nonlinear governing equations of fluid flow make the finite element method for fluid mechanics analysis difficult and cumbersome, to say the least.

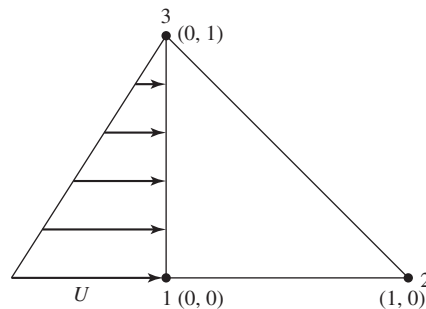
The literature of fluid mechanics is rife with research results on the application of finite element methods to fluid mechanics problems. The literature is so voluminous, in fact, that we do not cite references, but the reader will find that many finite element software packages include fluid elements of various types. These include “pipe elements,” “acoustic fluid elements,” and “combination elements.” The reader is warned to be aware of the restrictions and assumptions underlying the “various sorts” of fluid elements available in a given software package and use care in application.

REFERENCES

1. Halliday, D., R. Resnick, and J. Walker. *Fundamentals of Physics*, 6th ed. New York: John Wiley and Sons, 1997.
2. Crowe, C. T., J. A. Roberson, and D. F. Elger. *Engineering Fluid Mechanics*, 7th ed. New York: John Wiley and Sons, 1998.
3. Huebner, K. H., and E. A. Thornton. *The Finite Element Method for Engineers*. New York: John Wiley and Sons, 1982.
4. Navier, M. “Memoire sur les Lois dur Mouvement des Fluides.” *Mem. De l’Acad d. Sci.* (1827).
5. Stokes, G. G. “On the Theories of Internal Friction of Fluids in Motion.” *Transactions of the Cambridge Philosophical Society* (1845).
6. Schlichting, H. *Boundary Layer Theory*, 7th ed. New York: McGraw-Hill, 1979.
7. Baker, A. J. *Finite Element Computational Fluid Mechanics*. New York: McGraw-Hill, 1983.
8. Stasa, F. L. *Applied Finite Element Analysis for Engineers*. New York: Holt, Rinehart and Winston, 1985.

PROBLEMS

- 8.1 Per the standard definition of viscosity described in Section 8.1, how would you describe the property of viscosity, physically, in terms of an everyday example (do not use water and molasses—I already used that example)?
- 8.2 How would you design an experiment to determine the *relative* viscosity between two fluids? What fluids might you use in this test?
- 8.3 Look into a fluid mechanics text or reference book. What is the definition of a *Newtonian fluid*?
- 8.4 Equation 8.5 is a rather complicated partial differential equation, what does it really mean? Explain how that equation takes the very simple form of Equation 8.6.
- 8.5 If you visually examine a fluid flow, could you determine whether it was rotational or irrotational? Why? Why not?
- 8.6 Why do we use the Green-Gauss theorem in going from Equation 8.16 to Equation 8.17? Refer to Chapter 5.
- 8.7 Recalling that Equation 8.21 is based on unit depth in a two-dimensional flow, what do the nodal forces represent physically?
- 8.8 Given the three-node triangular element shown in Figure P8.8, compute the nodal forces corresponding to the flow conditions shown, assuming unit depth into the plane.

**Figure P8.8**

- 8.9 Per Equation 8.32, how do the fluid *velocity* components vary within
- A linear, three-node triangular element.
 - A four-node rectangular element.
 - A six-node triangular element.
 - An eight-node rectangular element.
 - Given questions *a–d*, how would you decide which element to use in a finite element analysis?
- 8.10 We show, in this chapter, that both stream function and velocity potential methods are governed by Laplace's equation. Many other physical problems are governed by this equation. Consult mathematical references and find other applications of Laplace's equation. While you are at it (and learning

the history of our profession is part of becoming an engineer), find out about Laplace.

- 8.11** Consider the uniform (ideal) flow shown in Figure P8.11. Use the four triangular elements shown to compute the stream function and derive the velocity components. Note that, in this case, if you do not obtain a uniform flow field, you have made errors in either your formulation or your calculations. The horizontal boundaries are to be taken as fixed surfaces. The coordinates of node 3 are (1.5, 1).

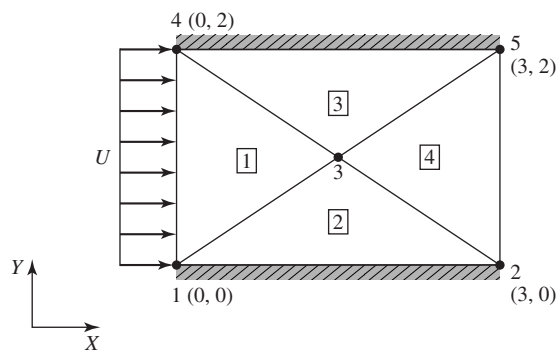


Figure P8.11

- 8.12** Now repeat Problem 8.11 with the inlet flow shown in Figure P8.12. Does the basic finite element formulation change? Do you have to redefine geometry or elements? Your answer to this question will give you insight as to how to use finite element software. Once the geometry and elements have been defined, various problems can be solved by simply changing boundary conditions or forcing functions.

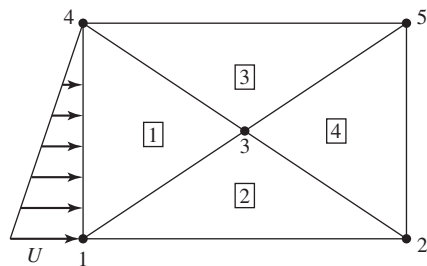
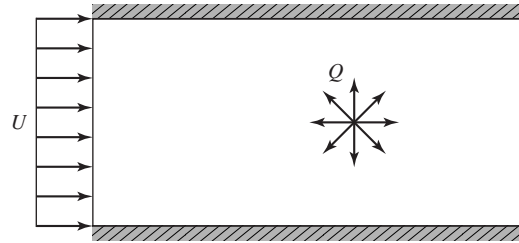


Figure P8.12

- 8.13** Consider the flow situation depicted in Figure P8.13. Upstream, the flow is uniform. At a known point between the two solid walls, a source of constant strength Q (volume per unit time) exists (via the action of a pump for example). How would the source be accounted for in a finite element formulation? (Examine the heat transfer analogy.)

**Figure P8.13**

- 8.14** Reconsider Example 8.1 and assume the cylinder is a heating rod held at constant surface temperature T_0 . The uniform inlet stream is at known temperature $T_i < T_0$. The horizontal boundaries are perfectly insulated and steady-state conditions are assumed. In the context of finite element analysis, can the flow problem and the heat transfer problem be solved independently?

CHAPTER

9

Applications in Solid Mechanics

9.1 INTRODUCTION

The bar and beam elements discussed in Chapters 2–4 are line elements, as only a single coordinate axis is required to define the element reference frame, hence, the stiffness matrices. As shown, these elements can be successfully used to model truss and frame structures in two and three dimensions. For application of the finite element method to more general solid structures, the line elements are of little use, however. Instead, elements are needed that can be used to model complex geometries subjected to various types of loading and constraint conditions.

In this chapter, we develop the finite element equations for both two- and three-dimensional elements for use in stress analysis of linearly elastic solids. The principle of minimum potential energy is used for the developments, as that principle is somewhat easier to apply to solid mechanics problems than Galerkin's method. It must be emphasized, however, that Galerkin's method is the more general procedure and applicable to a wider range of problems.

The constant strain triangle for plane stress is considered first, as the CST is the simplest element to develop mathematically. The procedure is shown to be common to other elements as well; a rectangular element formulated for plane strain is used to illustrate this commonality. Plane quadrilateral, axisymmetric, and general three-dimensional elements are also examined. An approach for application of the finite element method to solving torsion problems of noncircular sections is also presented.

9.2 PLANE STRESS

A commonly occurring situation in solid mechanics, known as *plane stress*, is defined by the following assumptions in conjunction with Figure 9.1:

1. The body is small in one coordinate direction (the z direction by convention) in comparison to the other dimensions; the dimension in the z direction (hereafter, the thickness) is either uniform or symmetric about the xy plane; thickness t , if in general, is less than one-tenth of the smallest dimension in the xy plane, would qualify for “small.”
2. The body is subjected to loading only in the xy plane.
3. The material of the body is linearly elastic, isotropic, and homogeneous.

The last assumption is not required for plane stress but is utilized in this text as we consider only elastic deformations.

Given a situation that satisfies the plane stress assumptions, the only nonzero stress components are σ_x , σ_y , and τ_{xy} . Note that the nominal stresses perpendicular to the xy plane (σ_z , τ_{xz} , τ_{yz}) are zero as a result of the plane stress assumptions. Therefore, the equilibrium equations (Appendix B) for plane stress are

$$\begin{aligned}\frac{\partial \sigma_x}{\partial x} + \frac{\partial \tau_{xy}}{\partial x} &= 0 \\ \frac{\partial \sigma_y}{\partial y} + \frac{\partial \tau_{xy}}{\partial y} &= 0\end{aligned}\tag{9.1}$$

where we implicitly assume that $\tau_{xy} = \tau_{yx}$. Utilizing the elastic stress-strain relations from Appendix B, Equation B.12 with $\sigma_z = \tau_{xz} = \tau_{yz} = 0$, the nonzero stress components can be expressed as (Problem 9.1)

$$\begin{aligned}\sigma_x &= \frac{E}{1 - \nu^2}(\epsilon_x + \nu\epsilon_y) \\ \sigma_y &= \frac{E}{1 - \nu^2}(\epsilon_y + \nu\epsilon_x) \\ \tau_{xy} &= \frac{E}{2(1 + \nu)}\gamma_{xy} = G\gamma_{xy}\end{aligned}\tag{9.2}$$

where E is the modulus of elasticity and ν is Poisson’s ratio for the material. In the shear stress-strain relation, the shear modulus $G = E/2(1 + \nu)$ has been introduced.

The stress-strain relations given by Equation 9.2 can be conveniently written in matrix form:

$$\begin{Bmatrix} \sigma_x \\ \sigma_y \\ \tau_{xy} \end{Bmatrix} = \frac{E}{1 - \nu^2} \begin{bmatrix} 1 & \nu & 0 \\ \nu & 1 & 0 \\ 0 & 0 & \frac{1 - \nu}{2} \end{bmatrix} \begin{Bmatrix} \epsilon_x \\ \epsilon_y \\ \gamma_{xy} \end{Bmatrix}\tag{9.3}$$

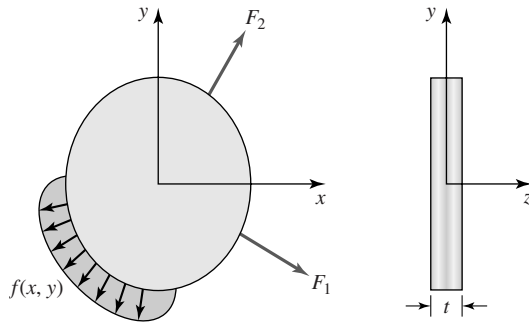


Figure 9.1 An illustration of plane stress conditions.

or

$$\{\sigma\} = [D]\{\varepsilon\} \quad (9.4)$$

where

$$\{\sigma\} = \begin{Bmatrix} \sigma_x \\ \sigma_y \\ \tau_{xy} \end{Bmatrix} \quad (9.5)$$

is the column matrix of stress components,

$$[D] = \frac{E}{1 - \nu^2} \begin{bmatrix} 1 & \nu & 0 \\ \nu & 1 & 0 \\ 0 & 0 & \frac{1 - \nu}{2} \end{bmatrix} \quad (9.6)$$

is the elastic material property matrix for plane stress, and

$$\{\varepsilon\} = \begin{Bmatrix} \varepsilon_x \\ \varepsilon_y \\ \gamma_{xy} \end{Bmatrix} \quad (9.7)$$

is the column matrix of strain components.

For a state of plane stress, the strain energy per unit volume, Equation 2.43, becomes

$$u_e = \frac{1}{2}(\sigma_x \varepsilon_x + \sigma_y \varepsilon_y + \tau_{xy} \gamma_{xy}) \quad (9.8)$$

or, using the matrix notation,

$$u_e = \frac{1}{2}\{\varepsilon\}^T \{\sigma\} = \frac{1}{2}\{\varepsilon\}^T [D] \{\varepsilon\} \quad (9.9)$$

Use of $\{\varepsilon\}^T$ allows the matrix operation to reproduce the quadratic form of the strain energy. Note that a quadratic relation in any variable z can be expressed

as $\{z\}^T [A] \{z\}$, where $[A]$ is a coefficient matrix. This is the subject of an end-of-chapter problem.

The total strain energy of a body subjected to plane stress is then

$$U_e = \frac{1}{2} \iiint_V \{\epsilon\}^T [D] \{\epsilon\} dV \quad (9.10)$$

where V is total volume of the body and $dV = t dx dy$. The form of Equation 9.10 will in fact be found to apply in general and is not restricted to the case of plane stress. In other situations, the strain components and material property matrix may be defined differently, but the form of the strain energy expression does not change. We use this result extensively in applying the principle of minimum potential energy in following developments.

9.2.1 Finite Element Formulation: Constant Strain Triangle

Figure 9.2a depicts a three-node triangular element assumed to represent a sub-domain of a body subjected to plane stress. Element nodes are numbered as shown, and nodal displacements in the x -coordinate direction are $u_1, u_2,$ and u_3 , while displacements in the y direction are $v_1, v_2,$ and v_3 . (For plane stress, displacement in the z direction is neglected). As noted in the introduction, the displacement field in structural problems is a vector field and must be discretized accordingly. For the triangular element in plane stress, we write the discretized displacement field as

$$\begin{aligned} u(x, y) &= N_1(x, y)u_1 + N_2(x, y)u_2 + N_3(x, y)u_3 = [N]\{u\} \\ v(x, y) &= N_1(x, y)v_1 + N_2(x, y)v_2 + N_3(x, y)v_3 = [N]\{v\} \end{aligned} \quad (9.11)$$

where $N_1, N_2,$ and N_3 are the interpolation functions as defined in Equation 6.37. Using the discretized representation of the displacement field, the element strain

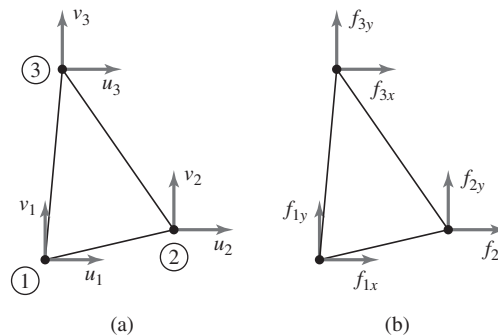


Figure 9.2

(a) Nodal displacement notation for a plane stress element. (b) Nodal forces.

components are then

$$\begin{aligned}\epsilon_x &= \frac{\partial u}{\partial x} = \frac{\partial N_1}{\partial x}u_1 + \frac{\partial N_2}{\partial x}u_2 + \frac{\partial N_3}{\partial x}u_3 \\ \epsilon_y &= \frac{\partial v}{\partial y} = \frac{\partial N_1}{\partial y}v_1 + \frac{\partial N_2}{\partial y}v_2 + \frac{\partial N_3}{\partial y}v_3 \\ \gamma_{xy} &= \frac{\partial u}{\partial y} + \frac{\partial v}{\partial x} = \frac{\partial N_1}{\partial y}u_1 + \frac{\partial N_2}{\partial y}u_2 + \frac{\partial N_3}{\partial y}u_3 + \frac{\partial N_1}{\partial x}v_1 + \frac{\partial N_2}{\partial x}v_2 + \frac{\partial N_3}{\partial x}v_3\end{aligned}\quad (9.12)$$

Defining the element displacement column matrix (vector) as

$$\{\delta^{(e)}\} = \begin{Bmatrix} u_1 \\ u_2 \\ u_3 \\ v_1 \\ v_2 \\ v_3 \end{Bmatrix} \quad (9.13)$$

the element strain matrix can be expressed as

$$\{\epsilon\} = \begin{bmatrix} \frac{\partial N_1}{\partial x} & \frac{\partial N_2}{\partial x} & \frac{\partial N_3}{\partial x} & 0 & 0 & 0 \\ 0 & 0 & 0 & \frac{\partial N_1}{\partial y} & \frac{\partial N_2}{\partial y} & \frac{\partial N_3}{\partial y} \\ \frac{\partial N_1}{\partial y} & \frac{\partial N_2}{\partial y} & \frac{\partial N_3}{\partial y} & \frac{\partial N_1}{\partial x} & \frac{\partial N_2}{\partial x} & \frac{\partial N_3}{\partial x} \end{bmatrix} \begin{Bmatrix} u_1 \\ u_2 \\ u_3 \\ v_1 \\ v_2 \\ v_3 \end{Bmatrix} = [B]\{\delta^{(e)}\} \quad (9.14)$$

where $[B]$ is the 3×6 matrix of partial derivatives of the interpolation functions as indicated, also known as the strain-displacement matrix. Referring to Equation 6.37, we observe that the partial derivatives appearing in Equation 9.14 are constants, since the interpolation functions are linear in the spatial variables. Hence, the strain components are constant throughout the volume of the element. Consequently, the three-node, triangular element for plane stress is known as a *constant strain triangle*.

By direct analogy with Equation 9.10, the elastic strain energy of the element is

$$U_e^{(e)} = \frac{1}{2} \iiint_{V^{(e)}} \{\epsilon\}^T [D] \{\epsilon\} dV^{(e)} = \frac{1}{2} \iiint_{V^{(e)}} \{\delta^{(e)}\}^T [B]^T [D] [B] \{\delta^{(e)}\} dV^{(e)} \quad (9.15)$$

As shall be seen in subsequent examples, Equation 9.15 is a generally applicable relation for the elastic strain energy of structural elements. For the constant strain triangle, we already observed that the strains are constant over the element volume. Assuming that the elastic properties similarly do not vary, Equation 9.15

becomes simply

$$\begin{aligned} U_e^{(e)} &= \frac{1}{2} \{\delta^{(e)}\}^T [B]^T [D] [B] \{\delta^{(e)}\} \iiint_{V^{(e)}} dV^{(e)} \\ &= \frac{1}{2} \{\delta^{(e)}\}^T (V^{(e)} [B]^T [D] [B]) \{\delta^{(e)}\} \end{aligned} \quad (9.16)$$

where $V^{(e)}$ is the total volume of the element.

Considering the element forces to be as in Figure 9.2b (for this element formulation, we require that forces be applied only at nodes; distributed loads are considered subsequently), the work done by the applied forces can be expressed as

$$W = f_{1x}u_1 + f_{2x}u_2 + f_{3x}u_3 + f_{1y}v_1 + f_{2y}v_2 + f_{3y}v_3 \quad (9.17)$$

and we note that the subscript notation becomes unwieldy rather quickly in the case of 2-D stress analysis. To simplify the notation, we use the force notation

$$\{f\} = \begin{Bmatrix} f_{1x} \\ f_{2x} \\ f_{3x} \\ f_{1y} \\ f_{2y} \\ f_{3y} \end{Bmatrix} \quad (9.18)$$

so that we can express the work of the external forces (using Equation 9.13) as

$$W = \{\delta\}^T \{f\} \quad (9.19)$$

Per Equation 2.53, the total potential energy for an element is then

$$\Pi = U_e - W = \frac{V^e}{2} \{\delta\}^T [B]^T [D] [B] \{\delta\} - \{\delta\}^T \{f\} \quad (9.20)$$

If the element is a portion of a larger structure that is in equilibrium, then the element must be in equilibrium. Consequently, the total potential energy of the element must be minimum (we consider only stable equilibrium), and for this minimum, we must have mathematically

$$\frac{\partial \Pi}{\partial \delta_i} = 0 \quad i = 1, 6 \quad (9.21)$$

If the indicated mathematical operations of Equation 9.21 are carried out on Equation 9.20, the result is the matrix relation

$$V^e [B]^T [D] [B] \{\delta\} = \{f\} \quad (9.22)$$

and this matrix equation is of the form

$$[k] \{\delta\} = \{f\} \quad (9.23)$$

where $[k]$ is the element stiffness matrix defined by

$$[k] = V^e [B]^T [D] [B] \quad (9.24)$$

and we must keep in mind that we are dealing with only a constant strain triangle at this point.

This theoretical development may not be obvious to the reader. To make the process more clear, especially the application of Equation 9.21, we examine the element stiffness matrix in more detail. First, we represent Equation 9.20 as

$$\Pi = \frac{1}{2} \{\delta\}^T [k] \{\delta\} - \{\delta\}^T \{f\} \quad (9.25)$$

and expand the relation formally to obtain the *quadratic* function

$$\begin{aligned} \Pi = & \frac{1}{2} (k_{11}\delta_1^2 + 2k_{12}\delta_1\delta_2 + 2k_{13}\delta_1\delta_3 + 2k_{14}\delta_1\delta_4 + \cdots + 2k_{56}\delta_5\delta_6 + k_{66}\delta_6^2) \\ & - f_{1x}\delta_1 - f_{2x}\delta_2 - f_{3x}\delta_3 - f_{1y}\delta_4 - f_{2y}\delta_5 - f_{3y}\delta_6 \end{aligned} \quad (9.26)$$

The quadratic function representation of total potential energy is characteristic of linearly elastic systems. (Recall the energy expressions for the strain energy of spring and bar elements of Chapter 2.)

The partial derivatives of Equation 9.21 are then in the form

$$\begin{aligned} \frac{\partial \Pi}{\partial \delta_1} &= k_{11}\delta_1 + k_{12}\delta_2 + k_{13}\delta_3 + k_{14}\delta_4 + k_{15}\delta_5 + k_{16}\delta_6 - f_{1x} = 0 \\ \frac{\partial \Pi}{\partial \delta_2} &= k_{21}\delta_1 + k_{22}\delta_2 + k_{23}\delta_3 + k_{24}\delta_4 + k_{25}\delta_5 + k_{26}\delta_6 - f_{2x} = 0 \end{aligned} \quad (9.27)$$

for example. Equations 9.27 are the scalar equations representing equilibrium of nodes 1 and 2 in the x -coordinate direction. The remaining four equations similarly represent nodal equilibrium conditions in the respective coordinate directions.

As we are dealing with an elastic element, the stiffness matrix should be symmetric. Examining Equation 9.27, we should have $k_{12} = k_{21}$, for example. Whether this is the case may not be obvious in consideration of Equation 9.24, since $[D]$ is a symmetric matrix but $[B]$ is not symmetric. A fundamental property of matrix multiplication (Appendix A) is as follows: If $[G]$ is a real, symmetric $N \times N$ matrix and $[F]$ is a real $N \times M$ matrix, the matrix triple product $[F]^T [G] [F]$ is a real, symmetric $M \times M$ matrix. Thus, the stiffness matrix as given by Equation 9.24 is a symmetric 6×6 matrix, since $[D]$ is 3×3 and symmetric and $[B]$ is a 6×3 real matrix.

9.2.2 Stiffness Matrix Evaluation

The stiffness matrix for the constant strain triangle element given by Equation 9.24 is now evaluated in detail. The interpolation functions per

Equation 6.37 are

$$\begin{aligned}
 N_1(x, y) &= \frac{1}{2A}[(x_2y_3 - x_3y_2) + (y_2 - y_3)x + (x_3 - x_2)y] \\
 &= \frac{1}{2A}(\alpha_1 + \beta_1x + \gamma_1y) \\
 N_2(x, y) &= \frac{1}{2A}[(x_3y_1 - x_1y_3) + (y_3 - y_1)x + (x_1 - x_3)y] \\
 &= \frac{1}{2A}(\alpha_2 + \beta_2x + \gamma_2y) \\
 N_3(x, y) &= \frac{1}{2A}[(x_1y_2 - x_2y_1) + (y_1 - y_2)x + (x_2 - x_1)y] \\
 &= \frac{1}{2A}(\alpha_3 + \beta_3x + \gamma_3y)
 \end{aligned} \tag{9.28}$$

so the required partial derivatives are

$$\begin{aligned}
 \frac{\partial N_1}{\partial x} &= \frac{1}{2A}(y_2 - y_3) = \frac{\beta_1}{2A} \\
 \frac{\partial N_2}{\partial x} &= \frac{1}{2A}(y_3 - y_1) = \frac{\beta_2}{2A} & \frac{\partial N_3}{\partial x} &= \frac{1}{2A}(y_1 - y_2) = \frac{\beta_3}{2A} \\
 \frac{\partial N_1}{\partial y} &= \frac{1}{2A}(x_3 - x_2) = \frac{\gamma_1}{2A} \\
 \frac{\partial N_2}{\partial y} &= \frac{1}{2A}(x_1 - x_3) = \frac{\gamma_2}{2A} & \frac{\partial N_3}{\partial y} &= \frac{1}{2A}(x_2 - x_1) = \frac{\gamma_3}{2A}
 \end{aligned} \tag{9.29}$$

The $[B]$ (strain-displacement) matrix is then

$$\begin{aligned}
 [B] &= \frac{1}{2A} \begin{bmatrix} y_2 - y_3 & y_3 - y_1 & y_1 - y_2 & 0 & 0 & 0 \\ 0 & 0 & 0 & x_3 - x_2 & x_1 - x_3 & x_2 - x_1 \\ x_3 - x_2 & x_1 - x_3 & x_2 - x_1 & y_2 - y_3 & y_3 - y_1 & y_1 - y_2 \end{bmatrix} \\
 &= \frac{1}{2A} \begin{bmatrix} \beta_1 & \beta_2 & \beta_3 & 0 & 0 & 0 \\ 0 & 0 & 0 & \gamma_1 & \gamma_2 & \gamma_3 \\ \gamma_1 & \gamma_2 & \gamma_3 & \beta_1 & \beta_2 & \beta_3 \end{bmatrix}
 \end{aligned} \tag{9.30}$$

Noting that, for constant thickness, element volume is tA , substitution into Equation 9.24 results in

$$[k] = \frac{Et}{4A(1 - \nu^2)} \begin{bmatrix} \beta_1 & 0 & \gamma_1 \\ \beta_2 & 0 & \gamma_2 \\ \beta_3 & 0 & \gamma_3 \\ 0 & \gamma_1 & \beta_1 \\ 0 & \gamma_2 & \beta_2 \\ 0 & \gamma_3 & \beta_3 \end{bmatrix} \begin{bmatrix} 1 & \nu & 0 \\ \nu & 1 & 0 \\ 0 & 0 & \frac{1 - \nu}{2} \end{bmatrix} \begin{bmatrix} \beta_1 & \beta_2 & \beta_3 & 0 & 0 & 0 \\ 0 & 0 & 0 & \gamma_1 & \gamma_2 & \gamma_3 \\ \gamma_1 & \gamma_2 & \gamma_3 & \beta_1 & \beta_2 & \beta_3 \end{bmatrix} \tag{9.31}$$

Performing the matrix multiplications of Equation 9.31 gives the element stiffness matrix as

$$[k] = \frac{Et}{4A(1-\nu^2)} \begin{bmatrix} \beta_1^2 + C\gamma_1^2 & \beta_1\beta_2 + C\gamma_1\gamma_2 & \beta_1\beta_3 + C\gamma_1\gamma_3 & \frac{1+\nu}{2}\beta_1\gamma_1 & \nu\beta_1\gamma_2 + C\beta_2\gamma_1 & \nu\beta_1\gamma_3 + C\beta_3\gamma_1 \\ & \beta_2^2 + C\gamma_2^2 & \beta_2\beta_3 + C\gamma_2\gamma_3 & \nu\beta_2\gamma_1 + C\beta_1\gamma_2 & \frac{1+\nu}{2}\beta_2\gamma_2 & \nu\beta_2\gamma_3 + C\beta_3\gamma_2 \\ & & \beta_3^2 + C\gamma_3^2 & \nu\beta_3\gamma_1 + C\beta_1\gamma_3 & \nu\beta_3\gamma_2 + C\beta_2\gamma_3 & \frac{1+\nu}{2}\beta_3\gamma_3 \\ & SYM & & \gamma_1^2 + C\beta_1^2 & \gamma_1\gamma_2 + C\beta_1\beta_2 & \gamma_1\gamma_3 + C\beta_1\beta_3 \\ & & & & \gamma_2^2 + C\beta_2^2 & \gamma_2\gamma_3 + C\beta_2\beta_3 \\ & & & & & \gamma_3^2 + C\beta_3^2 \end{bmatrix} \quad (9.32)$$

where $C = (1 - \nu)/2$. Equation 9.32 is the explicit representation of the stiffness matrix for a constant strain triangular element in plane stress, presented for illustrative purposes. In finite element software, such explicit representation is not often used; instead, the matrix triple product of Equation 9.24 is applied directly to obtain the stiffness matrix.

9.2.3 Distributed Loads and Body Force

Frequently, the boundary conditions for structural problems involve distributed loading on some portion of the geometric boundary. Such loadings may arise from applied pressure (normal stress) or shearing loads. In plane stress, these distributed loads act on element edges that lie on the global boundary. As a general example, Figure 9.3a depicts a CST element having normal and tangential loads p_n and p_t acting along the edge defined by element nodes 2 and 3. Element thickness is denoted t , and the loads are assumed to be expressed in terms of force per unit area. We seek to replace the distributed loads with equivalent forces acting at nodes 2 and 3. In keeping with the minimum potential energy approach, the concentrated nodal loads are determined such that the mechanical work is the same as that of the distributed loads.

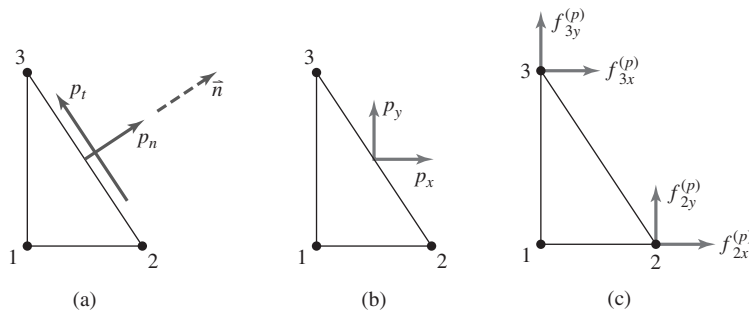


Figure 9.3 Conversion of distributed loading to work-equivalent nodal forces.

First, the distributed loads are converted to equivalent loadings in the global coordinate directions, as in Figure 9.3b, via

$$\begin{aligned} p_x &= p_n n_x - p_t n_y \\ p_y &= p_n n_y + p_t n_x \end{aligned} \quad (9.33)$$

with n_x and n_y corresponding to the components of the unit outward normal vector to edge 2-3. Here, we use the notation p for such loadings, as the units are those of pressure. The mechanical work done by the distributed loads is

$$W_p = t \int_2^3 p_x u(x, y) \, dS + t \int_2^3 p_y v(x, y) \, dS \quad (9.34)$$

where the integrations are performed along the edge defined by nodes 2 and 3. Recalling that interpolation function $N_1(x, y)$ is zero along edge 2-3, the finite element representations of the displacements along the edge are

$$\begin{aligned} u(x, y) &= N_2(x, y)u_2 + N_3(x, y)u_3 \\ v(x, y) &= N_2(x, y)v_2 + N_3(x, y)v_3 \end{aligned} \quad (9.35)$$

The work expression becomes

$$\begin{aligned} W_p &= t \int_2^3 p_x [N_2(x, y)u_2 + N_3(x, y)u_3] \, dS \\ &\quad + t \int_2^3 p_y [N_2(x, y)v_2 + N_3(x, y)v_3] \, dS \end{aligned} \quad (9.36)$$

and is of the form

$$W_p = f_{2x}^{(p)} u_2 + f_{3x}^{(p)} u_3 + f_{2y}^{(p)} v_2 + f_{3y}^{(p)} v_3 \quad (9.37)$$

Comparison of the last two equations yields the equivalent nodal forces as

$$\begin{aligned} f_{2x}^{(p)} &= t \int_2^3 p_x N_2(x, y) \, dS \\ f_{3x}^{(p)} &= t \int_2^3 p_x N_3(x, y) \, dS \\ f_{2y}^{(p)} &= t \int_2^3 p_y N_2(x, y) \, dS \\ f_{3y}^{(p)} &= t \int_2^3 p_y N_3(x, y) \, dS \end{aligned} \quad (9.38)$$

as depicted in Figure 9.3c. Recalling again for emphasis that $N_1(x, y)$ is zero along the integration path, Equation 9.38 can be expressed in the compact form

$$\{f^{(p)}\} = \int_S [N]^T \begin{Bmatrix} p_x \\ p_y \end{Bmatrix} t \, dS \quad (9.39)$$

with

$$[N]^T = \begin{bmatrix} N_1 & 0 \\ N_2 & 0 \\ N_3 & 0 \\ 0 & N_1 \\ 0 & N_2 \\ 0 & N_3 \end{bmatrix} \quad (9.40)$$

$$\{f^{(p)}\} = \begin{Bmatrix} f_{1x}^{(p)} \\ f_{2x}^{(p)} \\ f_{3x}^{(p)} \\ f_{1y}^{(p)} \\ f_{2y}^{(p)} \\ f_{3y}^{(p)} \end{Bmatrix} \quad (9.41)$$

The reader is urged to write out in detail the matrix multiplication indicated in Equation 9.39 to ensure that the result is correct. Although developed in the context of the three-node triangular element, Equation 9.39 will prove generally applicable for two-dimensional elements and require only minor modification for application to three-dimensional problems.

EXAMPLE 9.1

Given the triangular plane stress element shown in Figure 9.4a, determine the nodal forces equivalent to the distributed loads shown via the method of work equivalence discussed previously. Element thickness is 0.2 in. and uniform.

■ Solution

Using the nodal coordinates specified, the interpolation functions (with element area $A = 1$) are

$$N_1(x, y) = \frac{1}{2}[2 - 2x] = 1 - x$$

$$N_2(x, y) = \frac{1}{2}[2x - y]$$

$$N_3(x, y) = \frac{1}{2}y$$

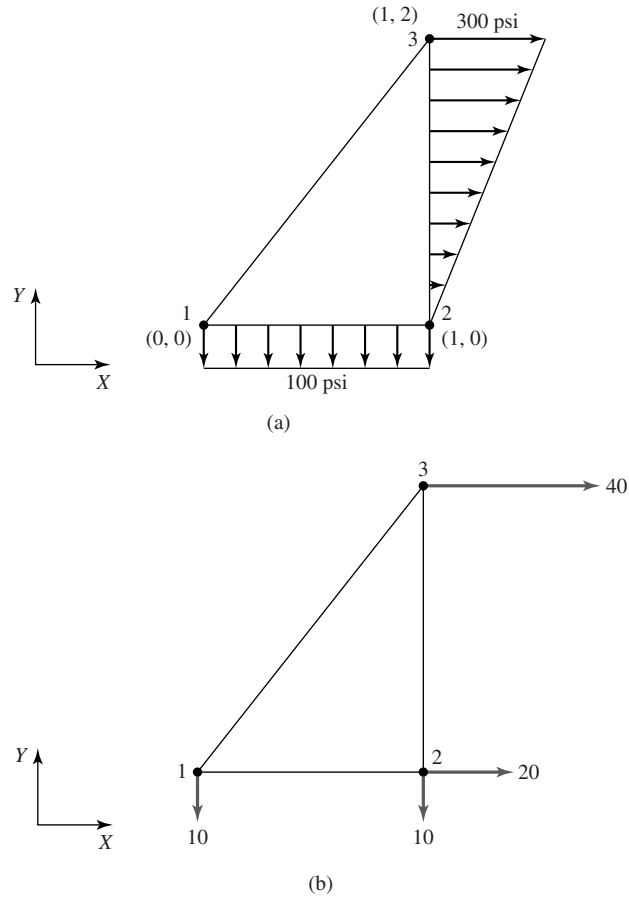


Figure 9.4
(a) Distributed loads on a triangular element.
(b) Work-equivalent nodal forces.

Along edge 1-2, $y = 0$, $p_x = 0$, $p_y = -100$ psi; hence, Equation 9.39 becomes

$$\begin{aligned} \{f^{(p)}\} &= \int_S \begin{bmatrix} 1-x & 0 \\ x & 0 \\ 0 & 0 \\ 0 & 1-x \\ 0 & x \\ 0 & 0 \end{bmatrix} \begin{Bmatrix} 0 \\ -100 \end{Bmatrix} t \, dS \\ &= 0.2 \int_0^1 \begin{bmatrix} 1-x & 0 \\ x & 0 \\ 0 & 0 \\ 0 & 1-x \\ 0 & x \\ 0 & 0 \end{bmatrix} \begin{Bmatrix} 0 \\ -100 \end{Bmatrix} dx = \begin{Bmatrix} 0 \\ 0 \\ 0 \\ -10 \\ -10 \\ 0 \end{Bmatrix} \text{ lb} \end{aligned}$$

For edge 2-3, we have $x = 1$, $p_x = 150y$, $p_y = 0$, so that

$$\begin{aligned} \{f^{(p)}\} &= \int_S \begin{bmatrix} 0 & 0 \\ \frac{1}{2}(2-y) & 0 \\ \frac{y}{2} & 0 \\ 0 & \frac{1}{2}(2-y) \\ 0 & \frac{y}{2} \\ 0 & 0 \end{bmatrix} \begin{Bmatrix} 150y \\ 0 \end{Bmatrix} t \, dS \\ &= 0.2 \int_0^2 \begin{bmatrix} 0 & 0 \\ \frac{1}{2}(2-y) & 0 \\ \frac{y}{2} & 0 \\ 0 & \frac{1}{2}(2-y) \\ 0 & \frac{y}{2} \\ 0 & 0 \end{bmatrix} \begin{Bmatrix} 150y \\ 0 \end{Bmatrix} dy = \begin{Bmatrix} 0 \\ 20 \\ 40 \\ 0 \\ 0 \\ 0 \end{Bmatrix} \text{ lb} \end{aligned}$$

Combining the results, the nodal force vector arising from the distributed loads for the element shown is then

$$\{f^{(p)}\} = \begin{Bmatrix} f_{1x} \\ f_{2x} \\ f_{3x} \\ f_{1y} \\ f_{2y} \\ f_{3y} \end{Bmatrix} = \begin{Bmatrix} 0 \\ 20 \\ 40 \\ -10 \\ -10 \\ 0 \end{Bmatrix} \text{ lb}$$

as shown in Figure 9.4b.

In addition to distributed edge loads on element boundaries, so-called body forces may also arise. In general, a body force is a noncontact force acting on a body on a per unit mass basis. The most commonly encountered body forces are gravitational attraction (weight), centrifugal force arising from rotational motion, and magnetic force. Currently, we consider only the two-dimensional case in which the body force is described by the vector $\begin{Bmatrix} F_{BX} \\ F_{BY} \end{Bmatrix}$ in which F_{BX} and F_{BY} are forces per unit mass acting on the body in the respective coordinate directions. As with distributed loads, the body forces are to be replaced by equivalent nodal forces. Considering a differential mass $\rho t \, dx \, dy$ undergoing displacements (u, v) in the coordinate directions, mechanical work done by the

body forces is

$$dW_b = \rho F_{BX} u t \, dx \, dy + \rho F_{BY} v t \, dx \, dy \quad (9.42)$$

Considering the volume of interest to be a CST element in which the displacements are expressed in terms of interpolation functions and nodal displacements as

$$\begin{Bmatrix} u(x, y) \\ v(x, y) \end{Bmatrix} = \begin{bmatrix} N_1 & N_2 & N_3 & 0 & 0 & 0 \\ 0 & 0 & 0 & N_1 & N_2 & N_3 \end{bmatrix} \begin{Bmatrix} u_1 \\ u_2 \\ u_3 \\ v_1 \\ v_2 \\ v_3 \end{Bmatrix} = [N] \begin{Bmatrix} u \\ v \end{Bmatrix} \quad (9.43)$$

the total work done by the body forces acting on the element is expressed in terms of nodal displacement as

$$\begin{aligned} W_b &= \rho t \iint_A F_{BX} (N_1 u_1 + N_2 u_2 + N_3 u_3) \, dx \, dy \\ &\quad + \rho t \iint_A F_{BY} (N_1 v_1 + N_2 v_2 + N_3 v_3) \, dx \, dy \end{aligned} \quad (9.44)$$

As desired, Equation 9.44 is in the form

$$W_b = f_{1x}^{(b)} u_1 + f_{2x}^{(b)} u_2 + f_{3x}^{(b)} u_3 + f_{1y}^{(b)} v_1 + f_{2y}^{(b)} v_2 + f_{3y}^{(b)} v_3 \quad (9.45)$$

in terms of equivalent concentrated nodal forces. The superscript (b) is used to indicate nodal-equivalent body force. Comparison of the last two equations yields the nodal force components as

$$\begin{aligned} f_{ix}^{(b)} &= \rho t \int_A N_i F_{BX} \, dx \, dy \quad i = 1, 3 \\ f_{iy}^{(b)} &= \rho t \int_A N_i F_{BY} \, dx \, dy \quad i = 1, 3 \end{aligned} \quad (9.46)$$

The nodal force components equivalent to the applied body forces can also be written in the compact matrix form

$$\{f^{(b)}\} = \rho t \int_A [N]^T \begin{Bmatrix} F_{BX} \\ F_{BY} \end{Bmatrix} \, dx \, dy \quad (9.47)$$

While developed in the specific context of a constant strain triangular element in plane stress, Equation 9.47 proves to be a general result for two-dimensional elements. A quite similar expression holds for three-dimensional elements.

EXAMPLE 9.2

Determine the nodal force components representing the body force for the element of Example 9.1, if the body force is gravitational attraction in the y direction, so that

$$\begin{Bmatrix} F_{BX} \\ F_{BY} \end{Bmatrix} = \begin{Bmatrix} 0 \\ -386.4 \end{Bmatrix} \text{ in./sec}^2$$

given the density of the element material is $\rho = 7.3 \times 10^{-4}$ slug/in.³.

■ Solution

As the x component of the body force is zero, the x components of the nodal force vector will be, too, so we need not consider those components. The y components are computed using the second of Equation 9.46:

$$f_{iy}^{(b)} = \rho t \int_A N_i F_{BY} dx dy \quad i = 1, 3$$

From the previous example, the interpolation functions are

$$N_1(x, y) = \frac{1}{2}[2 - 2x] = 1 - x$$

$$N_2(x, y) = \frac{1}{2}[2x - y]$$

$$N_3(x, y) = \frac{1}{2}y$$

We have, in this instance,

$$f_{1y}^{(b)} = \rho t \iint_A F_{BY} N_1 dx dy = \rho t \iint_A F_{BY}(1 - x) dx dy$$

$$f_{2y}^{(b)} = \rho t \iint_A F_{BY} N_2 dx dy = \rho t \iint_A \frac{F_{BY}}{2}(2x - y) dx dy$$

$$f_{3y}^{(b)} = \rho t \iint_A F_{BY} N_3 dx dy = \rho t \iint_A \frac{F_{BY}}{2}y dx dy$$

The limits of integration must be determined on the basis of the geometry of the area. In this example, we utilize x as the basic integration variable and compute the y -integration limits in terms of x . For the element under consideration, as x varies between zero and one, y is the linear function $y = 2x$ so the integrations become

$$\begin{aligned} f_{1y}^{(b)} &= \rho t F_{BY} \int_0^1 \int_0^{2x} (1 - x) dy dx = \rho t F_{BY} \int_0^1 2x(1 - x) dx = \rho t F_{BY} \left(x^2 - \frac{2x^3}{3} \right) \Big|_0^1 \\ &= \frac{\rho t F_{BY}}{3} = -0.0189 \text{ lb} \end{aligned}$$

$$\begin{aligned}
 f_{2y}^{(b)} &= \rho t F_{BY} \int_0^1 \int_0^{2x} \frac{1}{2}(2x - y) \, dy \, dx = \frac{\rho t F_{BY}}{2} \int_0^1 2x^2 \, dx \\
 &= \frac{\rho t F_{BY}}{2} \left(\frac{2}{3} \right) = \frac{\rho t F_{BY}}{3} = -0.0189 \text{ lb} \\
 f_{3y}^{(b)} &= \frac{\rho t F_{BY}}{2} \int_0^1 \int_0^{2x} y \, dx \, dy = \frac{\rho t F_{BY}}{2} \int_0^1 2x^2 \, dx = \frac{\rho t F_{BY}}{3} = -0.0189 \text{ lb}
 \end{aligned}$$

showing that the body force is equally distributed to the element nodes.

If we now combine the concepts just developed for the CST element in plane stress, we have a general element equation that includes directly applied nodal forces, nodal force equivalents for distributed edge loadings, and nodal equivalents for body forces as

$$[k]\{\delta\} = \{f\} + \{f^{(p)}\} + \{f^{(b)}\} \quad (9.48)$$

where the stiffness matrix is given by Equation 9.24 and the load vectors are as just described. Equation 9.48 is generally applicable to finite elements used in elastic analysis. As will be learned in studying advanced finite element analysis, Equation 9.48 can be supplemented by addition of force vectors arising from plastic deformation, thermal gradients or temperature-dependent material properties, thermal swelling from radiation effects, and the dynamic effects of acceleration.

9.3 PLANE STRAIN: RECTANGULAR ELEMENT

A solid body is said to be in a state of *plane strain* if it satisfies all the assumptions of plane stress theory *except* that the body's thickness (length in the z direction) is *large* in comparison to the dimension in the xy plane. Mathematically, *plane strain* is defined as a state of loading and geometry such that

$$\epsilon_z = \frac{\partial w}{\partial z} = 0 \quad \gamma_{xz} = \frac{\partial u}{\partial z} + \frac{\partial w}{\partial x} = 0 \quad \gamma_{yz} = \frac{\partial v}{\partial z} + \frac{\partial w}{\partial y} = 0 \quad (9.49)$$

(See Appendix B for a discussion of the general stress-strain relations.)

Physically, the interpretation is that the body is so long in the z direction that the normal strain, induced by only the Poisson effect, is so small as to be negligible and, as we assume only xy -plane loadings are applied, shearing strains are also small and neglected. (One might think of plane strain as in the example of a hydroelectric dam—a large, long structure subjected to transverse loading only, not unlike a beam.) Under the prescribed conditions for plane strain, the

constitutive equations for the nonzero stress components become

$$\begin{aligned}\sigma_x &= \frac{E}{(1+\nu)(1-2\nu)}[(1-\nu)\epsilon_x + \nu\epsilon_y] \\ \sigma_y &= \frac{E}{(1+\nu)(1-2\nu)}[(1-\nu)\epsilon_y + \nu\epsilon_x] \\ \tau_{xy} &= \frac{E}{2(1+\nu)}\gamma_{xy} = G\gamma_{xy}\end{aligned}\quad (9.50)$$

and, while not zero, the normal stress in the z direction is considered negligible in comparison to the other stress components.

The elastic strain energy for a body of volume V in plane strain is

$$U_e = \frac{1}{2} \iiint_V (\sigma_x \epsilon_x + \sigma_y \epsilon_y + \tau_{xy} \gamma_{xy}) dV \quad (9.51)$$

which can be expressed in matrix notation as

$$U_e = \frac{1}{2} \iiint_V [\sigma_x \quad \sigma_y \quad \tau_{xy}] \begin{Bmatrix} \epsilon_x \\ \epsilon_y \\ \gamma_{xy} \end{Bmatrix} dV \quad (9.52)$$

Combining Equations 9.50 and 9.52 with considerable algebraic manipulation, the elastic strain energy is found to be

$$\begin{aligned}U_e &= \frac{1}{2} \iiint_V [\epsilon_x \quad \epsilon_y \quad \gamma_{xy}] \frac{E}{(1+\nu)(1-2\nu)} \\ &\quad \times \begin{bmatrix} 1-\nu & \nu & 0 \\ \nu & 1-\nu & 0 \\ 0 & 0 & \frac{1-2\nu}{2} \end{bmatrix} \begin{Bmatrix} \epsilon_x \\ \epsilon_y \\ \gamma_{xy} \end{Bmatrix} dV\end{aligned}\quad (9.53)$$

and is similar to the case of plane stress, in that we can express the energy as

$$U_e = \frac{1}{2} \iiint_V \{\epsilon\}^T [D] \{\epsilon\} dV$$

with the exception that the elastic property matrix for plane strain is defined as

$$[D] = \frac{E}{(1+\nu)(1-2\nu)} \begin{bmatrix} 1-\nu & \nu & 0 \\ \nu & 1-\nu & 0 \\ 0 & 0 & \frac{1-2\nu}{2} \end{bmatrix} \quad (9.54)$$

The nonzero strain components in terms of displacements are

$$\begin{aligned}\epsilon_x &= \frac{\partial u}{\partial x} \\ \epsilon_y &= \frac{\partial v}{\partial y} \\ \gamma_{xy} &= \frac{\partial u}{\partial y} + \frac{\partial v}{\partial x}\end{aligned}\quad (9.55)$$

For a four-node rectangular element (for example only), the column matrix of strain components is expressed as

$$\{\epsilon\} = \begin{Bmatrix} \epsilon_x \\ \epsilon_y \\ \gamma_{xy} \end{Bmatrix} = \begin{bmatrix} \frac{\partial N_1}{\partial x} & \frac{\partial N_2}{\partial x} & \frac{\partial N_3}{\partial x} & \frac{\partial N_4}{\partial x} & 0 & 0 & 0 & 0 \\ 0 & 0 & 0 & 0 & \frac{\partial N_1}{\partial y} & \frac{\partial N_2}{\partial y} & \frac{\partial N_3}{\partial y} & \frac{\partial N_4}{\partial y} \\ \frac{\partial N_1}{\partial y} & \frac{\partial N_2}{\partial x} & \frac{\partial N_3}{\partial y} & \frac{\partial N_4}{\partial x} & \frac{\partial N_1}{\partial x} & \frac{\partial N_2}{\partial x} & \frac{\partial N_3}{\partial x} & \frac{\partial N_4}{\partial x} \end{bmatrix} \begin{Bmatrix} u_1 \\ u_2 \\ u_3 \\ u_4 \\ v_1 \\ v_2 \\ v_3 \\ v_4 \end{Bmatrix}\quad (9.56)$$

in terms of the interpolation functions and the nodal displacements. As is customary, Equation 9.56 is written as

$$\{\epsilon\} = [B]\{\delta\}\quad (9.57)$$

with $[B]$ representing the matrix of derivatives of interpolation functions and $\{\delta\}$ is the column matrix of nodal displacements. Hence, total strain energy of an element is

$$U_e = \frac{1}{2}\{\delta\}^T \iiint_V [B]^T [D][B] dV \{\delta\} = \frac{1}{2}\{\delta\}^T [k]\{\delta\}\quad (9.58)$$

and the element stiffness matrix is again given by

$$[k^{(e)}] = \iiint_{V^{(e)}} [B]^T [D][B] dV^{(e)}\quad (9.59)$$

The interpolation functions for the four-node rectangular element per Equation 6.56 are

$$\begin{aligned}N_1(r, s) &= \frac{1}{4}(1-r)(1-s) \\ N_2(r, s) &= \frac{1}{4}(1+r)(1-s) \\ N_3(r, s) &= \frac{1}{4}(1+r)(1+s) \\ N_4(r, s) &= \frac{1}{4}(1-r)(1+s)\end{aligned}\quad (9.60)$$

9.3 Plane Strain: Rectangular Element

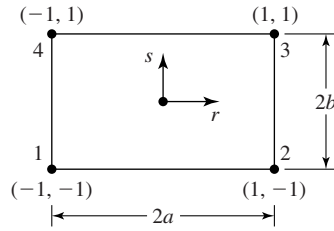


Figure 9.5 A rectangular element of width 2a and height 2b.

with the natural coordinates defined as in Figure 9.5. To compute the strain components in terms of the natural coordinates, the chain rule is applied to obtain

$$\begin{aligned} \frac{\partial}{\partial x} &= \frac{\partial}{\partial r} \frac{\partial r}{\partial x} = \frac{1}{a} \frac{\partial}{\partial r} \\ \frac{\partial}{\partial y} &= \frac{\partial}{\partial s} \frac{\partial s}{\partial y} = \frac{1}{b} \frac{\partial}{\partial s} \end{aligned} \tag{9.61}$$

Performing the indicated differentiations, the strain components are found to be

$$\begin{aligned} \{\varepsilon\} &= \begin{Bmatrix} \varepsilon_x \\ \varepsilon_y \\ \gamma_{xy} \end{Bmatrix} \\ &= \begin{bmatrix} \frac{s-1}{4a} & \frac{1-s}{4a} & \frac{1+s}{4a} & -\frac{1+s}{4a} & 0 & 0 & 0 & 0 \\ 0 & 0 & 0 & 0 & \frac{r-1}{4b} & -\frac{1+r}{4b} & \frac{1+r}{4b} & \frac{1-r}{4b} \\ \frac{r-1}{4b} & -\frac{1+r}{4b} & \frac{1+r}{4b} & \frac{1-r}{4b} & \frac{s-1}{4a} & \frac{1-s}{4a} & \frac{1+s}{4a} & -\frac{1+s}{4a} \end{bmatrix} \begin{Bmatrix} u_1 \\ u_2 \\ u_3 \\ u_4 \\ v_1 \\ v_2 \\ v_3 \\ v_4 \end{Bmatrix} \end{aligned} \tag{9.62}$$

showing that the normal strain ε_x varies linearly in the y direction, normal strain ε_y varies linearly in the x direction, and shear strain γ_{xy} varies linearly in both coordinate directions (realizing that the natural coordinate r corresponds to the x axis and natural coordinate s corresponds to the y axis).

From Equation 9.62, the [B] matrix is readily identified as

$$[B] = \begin{bmatrix} \frac{s-1}{4a} & \frac{1-s}{4a} & \frac{1+s}{4a} & -\frac{1+s}{4a} & 0 & 0 & 0 & 0 \\ 0 & 0 & 0 & 0 & \frac{r-1}{4b} & -\frac{1+r}{4b} & \frac{1+r}{4b} & \frac{1-r}{4b} \\ \frac{r-1}{4b} & -\frac{1+r}{4b} & \frac{1+r}{4b} & \frac{1-r}{4b} & \frac{s-1}{4a} & \frac{1-s}{4a} & \frac{1+s}{4a} & -\frac{1+s}{4a} \end{bmatrix} \tag{9.63}$$

hence, the element stiffness matrix is given, formally, by

$$\begin{aligned}
 [k^{(e)}] &= \iiint_{V^{(e)}} [B^T][D][B] dV^{(e)} \\
 &= \frac{Etab}{(1+\nu)(1-2\nu)} \int_{-1}^1 \int_{-1}^1 \begin{bmatrix} \frac{s-1}{4a} & 0 & \frac{r-1}{4b} \\ \frac{1-s}{4a} & 0 & -\frac{1+r}{4b} \\ \frac{1+s}{4a} & 0 & \frac{1+r}{4b} \\ -\frac{1+s}{4a} & 0 & \frac{1-r}{4b} \\ 0 & \frac{r-1}{4b} & \frac{s-1}{4a} \\ 0 & -\frac{1+r}{4b} & \frac{1-s}{4a} \\ 0 & \frac{1+r}{4b} & \frac{1+s}{4a} \\ 0 & \frac{1-r}{4b} & -\frac{1+s}{4a} \end{bmatrix} \begin{bmatrix} 1-\nu & \nu & 0 \\ \nu & 1-\nu & 0 \\ 0 & 0 & \frac{(1+\nu)(1-2\nu)}{2(1+\nu)} \end{bmatrix} \\
 &\times \begin{bmatrix} \frac{s-1}{4a} & \frac{1-s}{4a} & \frac{1+s}{4a} & -\frac{1+s}{4a} & 0 & 0 & 0 & 0 \\ 0 & 0 & 0 & 0 & \frac{r-1}{4b} & -\frac{1+r}{4b} & \frac{1+r}{4b} & \frac{1-r}{4b} \\ \frac{r-1}{4b} & -\frac{1+r}{4b} & \frac{1+r}{4b} & \frac{1-r}{4b} & \frac{s-1}{4a} & \frac{1-s}{4a} & \frac{1+s}{4a} & -\frac{1+s}{4a} \end{bmatrix} dr ds \quad (9.64)
 \end{aligned}$$

The element stiffness matrix as defined by Equation 9.64 is an 8×8 symmetric matrix, which therefore, contains 36 independent terms. Hence, 36 integrations are required to obtain the complete stiffness matrix. The integrations are straightforward but algebraic tedious. Here, we develop only a single term of the stiffness matrix in detail, then discuss the more-efficient numerical methods used in finite element software packages.

If we carry out the matrix multiplications just indicated, the first diagonal term of the stiffness matrix is found (after a bit of algebra) to be

$$k_{11}^{(e)} = \frac{Etb}{16a(1+2\nu)} \int_{-1}^1 \int_{-1}^1 (s-1)^2 dr ds + \frac{Eta}{32b(1+\nu)} \int_{-1}^1 \int_{-1}^1 (r-1)^2 dr ds \quad (9.65)$$

and this term evaluates to

$$\begin{aligned}
 k_{11}^{(e)} &= \frac{Etb}{16a(1+2\nu)} \left. \frac{2(s-1)^3}{3} \right|_{-1}^1 + \frac{Eta}{32b(1+\nu)} \left. \frac{2(r-1)^3}{3} \right|_{-1}^1 \\
 &= \frac{Etb}{16a(1+2\nu)} \left(\frac{16}{3} \right) + \frac{Eta}{32b(1+\nu)} \left(\frac{16}{3} \right) \quad (9.66)
 \end{aligned}$$

Note that the integrands are quadratic functions of the natural coordinates. In fact, analysis of Equation 9.64 reveals that every term of the element stiffness matrix requires integration of quadratic functions of the natural coordinates. From the earlier discussion of Gaussian integration (Chapter 6), we know that a quadratic polynomial can be integrated exactly using only two integration (or evaluation) points. As here we deal with integration in two dimensions, we must evaluate the integrand at the Gauss points

$$r_i = \pm \frac{\sqrt{3}}{3} \quad s_j = \pm \frac{\sqrt{3}}{3}$$

with weighting factors $W_i = W_j = 1$. If we apply the numerical integration technique to evaluation of $k_{11}^{(e)}$, we obtain, as expected, the result identical to that given by Equation 9.66. More important, the Gauss integration procedure can be applied directly to Equation 9.64 to obtain the *entire* element stiffness matrix as

$$[k^{(e)}] = tab \sum_{i=1}^2 \sum_{j=1}^2 W_i W_j [B(r_i, s_j)]^T [D] [B(r_i, s_j)] \quad (9.67)$$

where the matrix triple product is evaluated four times, in accordance with the number of integration points required. The summations and matrix multiplications required in Equation 9.67 are easily programmed and ideally suited to digital computer implementation.

While written specifically for the four-node rectangular element, Equation 9.67 is applicable to higher-order elements as well. Recall that, as the polynomial order increases, exact integration via Gaussian quadrature requires increase in both number and change in value of the integration points and weighting factors. By providing a “look-up” table of values fashioned after Table 6.1, computer implementation of Equation 9.67 can be readily adapted to higher-order elements.

We use the triangular element to illustrate plane stress and the rectangular element to illustrate plane strain. If the developments are followed clearly, it is apparent that either element can be used for either state of stress. The only difference is in the stress-strain relations exhibited by the $[D]$ matrix. This situation is true of *any* element shape and order (in terms of number of nodes and order of polynomial interpolation functions). Our use of the examples of triangular and rectangular elements are not meant to be restrictive in any way.

9.4 ISOPARAMETRIC FORMULATION OF THE PLANE QUADRILATERAL ELEMENT

While useful for analysis of plane problems in solid mechanics, the triangular and rectangular elements just discussed exhibit shortcomings. Geometrically, the triangular element is quite useful in modeling irregular shapes having curved boundaries. However, since element strains are constant, a large number of small elements are required to obtain reasonable accuracy, particular in areas of high

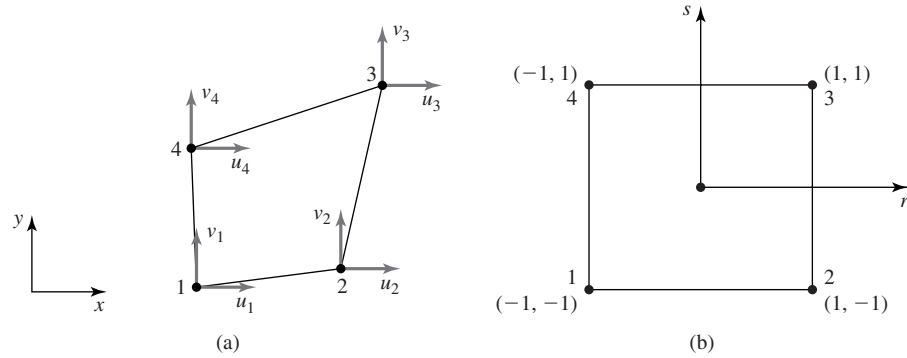


Figure 9.6

(a) A four-node, two-dimensional isoparametric element. (b) The parent element in natural coordinates.

stress gradients, such as near geometric discontinuities. In comparison, the rectangular element provides the more-reasonable linear variation of strain components but is not amenable to irregular shapes. An element having the desirable characteristic of strain variation in the element as well as the ability to closely approximate curves is the four-node quadrilateral element. We now develop the quadrilateral element using an isoparametric formulation adaptable to either plane stress or plane strain.

A general quadrilateral element is shown in Figure 9.6a, having element node numbers and nodal displacements as indicated. The coordinates of node i are (x_i, y_i) and refer to a global coordinate system. The element is formed by mapping the parent element shown in Figure 9.6b, using the procedures developed in Section 6.8. Recalling that, in the isoparametric approach, the geometric mapping functions are identical to the interpolation functions used to discretize the displacements, the geometric mapping is defined by

$$\begin{aligned}
 x &= \sum_{i=1}^4 N_i(r, s)x_i \\
 y &= \sum_{i=1}^4 N_i(r, s)y_i
 \end{aligned}
 \tag{9.68}$$

and the interpolation functions are as given in Equation 9.60, so that the displacements are described as

$$\begin{aligned}
 u(x, y) &= \sum_{i=1}^4 N_i(r, s)u_i \\
 v(x, y) &= \sum_{i=1}^4 N_i(r, s)v_i
 \end{aligned}
 \tag{9.69}$$

9.4 Isoparametric Formulation of the Plane Quadrilateral Element

349

Now, the mathematical complications arise in computing the strain components as given by Equation 9.55 and rewritten here as

$$\{\varepsilon\} = \begin{Bmatrix} \varepsilon_x \\ \varepsilon_y \\ \gamma_{xy} \end{Bmatrix} = \begin{Bmatrix} \frac{\partial u}{\partial x} \\ \frac{\partial v}{\partial y} \\ \frac{\partial u}{\partial y} + \frac{\partial v}{\partial x} \end{Bmatrix} = \begin{bmatrix} \frac{\partial}{\partial x} & 0 \\ 0 & \frac{\partial}{\partial y} \\ \frac{\partial}{\partial y} & \frac{\partial}{\partial x} \end{bmatrix} \begin{Bmatrix} u \\ v \end{Bmatrix} \quad (9.70)$$

Using Equation 6.83 with $\phi = u$, we have

$$\begin{aligned} \frac{\partial u}{\partial r} &= \frac{\partial u}{\partial x} \frac{\partial x}{\partial r} + \frac{\partial u}{\partial y} \frac{\partial y}{\partial r} \\ \frac{\partial u}{\partial s} &= \frac{\partial u}{\partial x} \frac{\partial x}{\partial s} + \frac{\partial u}{\partial y} \frac{\partial y}{\partial s} \end{aligned} \quad (9.71)$$

with similar expressions for the partial derivative of the v displacement. Writing Equation 9.71 in matrix form

$$\begin{Bmatrix} \frac{\partial u}{\partial r} \\ \frac{\partial u}{\partial s} \end{Bmatrix} = \begin{bmatrix} \frac{\partial x}{\partial r} & \frac{\partial y}{\partial r} \\ \frac{\partial x}{\partial s} & \frac{\partial y}{\partial s} \end{bmatrix} \begin{Bmatrix} \frac{\partial u}{\partial x} \\ \frac{\partial u}{\partial y} \end{Bmatrix} = [J] \begin{Bmatrix} \frac{\partial u}{\partial x} \\ \frac{\partial u}{\partial y} \end{Bmatrix} \quad (9.72)$$

and the Jacobian matrix is identified as

$$[J] = \begin{bmatrix} J_{11} & J_{12} \\ J_{21} & J_{22} \end{bmatrix} = \begin{bmatrix} \frac{\partial x}{\partial r} & \frac{\partial y}{\partial r} \\ \frac{\partial x}{\partial s} & \frac{\partial y}{\partial s} \end{bmatrix} \quad (9.73)$$

as in Equation 6.83. Note that, per the geometric mapping of Equation 9.68, the components of $[J]$ are known as functions of the partial derivatives of the interpolation functions and the nodal coordinates in the xy plane. For example,

$$J_{11} = \frac{\partial x}{\partial r} = \sum_{i=1}^4 \frac{\partial N_i}{\partial r} x_i = \frac{1}{4}[(s-1)x_1 + (1-s)x_2 + (1+s)x_3 - (1+s)x_4] \quad (9.74)$$

a first-order polynomial in the natural (mapping) coordinate s . The other terms are similarly first-order polynomials.

Formally, Equation 9.72 can be solved for the partial derivatives of displacement component u with respect to x and y by multiplying by the inverse of the Jacobian matrix. As noted in Chapter 6, finding the inverse of the Jacobian matrix in algebraic form is not an enviable task. Instead, numerical methods are used, again based on Gaussian quadrature, and the remainder of the derivation here is toward that end. Rather than invert the Jacobian matrix, Equation 9.72

can be solved via Cramer's rule. Application of Cramer's rule results in

$$\frac{\partial u}{\partial x} = \frac{\begin{vmatrix} \frac{\partial u}{\partial r} & J_{12} \\ \frac{\partial u}{\partial s} & J_{22} \end{vmatrix}}{|J|} = \frac{1}{|J|} [J_{22} \quad -J_{12}] \begin{Bmatrix} \frac{\partial u}{\partial r} \\ \frac{\partial u}{\partial s} \end{Bmatrix} \quad (9.75)$$

$$\frac{\partial u}{\partial y} = \frac{\begin{vmatrix} J_{11} & \frac{\partial u}{\partial r} \\ J_{21} & \frac{\partial u}{\partial s} \end{vmatrix}}{|J|} = \frac{1}{|J|} [-J_{21} \quad +J_{11}] \begin{Bmatrix} \frac{\partial u}{\partial r} \\ \frac{\partial u}{\partial s} \end{Bmatrix}$$

or, in a more compact form,

$$\begin{Bmatrix} \frac{\partial u}{\partial x} \\ \frac{\partial u}{\partial y} \end{Bmatrix} = \frac{1}{|J|} \begin{bmatrix} J_{22} & -J_{12} \\ -J_{21} & J_{11} \end{bmatrix} \begin{Bmatrix} \frac{\partial u}{\partial r} \\ \frac{\partial u}{\partial s} \end{Bmatrix} \quad (9.76)$$

The determinant of the Jacobian matrix $|J|$ is commonly called simply the *Jacobian*.

Since the interpolation functions are the same for both displacement components, an identical procedure results in

$$\begin{Bmatrix} \frac{\partial v}{\partial x} \\ \frac{\partial v}{\partial y} \end{Bmatrix} = \frac{1}{|J|} \begin{bmatrix} J_{22} & -J_{12} \\ -J_{21} & J_{11} \end{bmatrix} \begin{Bmatrix} \frac{\partial v}{\partial r} \\ \frac{\partial v}{\partial s} \end{Bmatrix} \quad (9.77)$$

for the partial derivatives of the v displacement component with respect to global coordinates.

Let us return to the problem of computing the strain components per Equation 9.70. Utilizing Equations 9.76 and 9.77, the strain components are expressed as

$$\{\varepsilon\} = \begin{Bmatrix} \varepsilon_x \\ \varepsilon_y \\ \gamma_{xy} \end{Bmatrix} = \begin{Bmatrix} \frac{\partial u}{\partial x} \\ \frac{\partial v}{\partial y} \\ \frac{\partial u}{\partial y} + \frac{\partial v}{\partial x} \end{Bmatrix} = \frac{1}{|J|} \begin{bmatrix} J_{22} & -J_{12} & 0 & 0 \\ 0 & 0 & -J_{21} & J_{11} \\ -J_{21} & J_{11} & J_{22} & -J_{12} \end{bmatrix} \begin{Bmatrix} \frac{\partial u}{\partial r} \\ \frac{\partial u}{\partial s} \\ \frac{\partial v}{\partial r} \\ \frac{\partial v}{\partial s} \end{Bmatrix} = [G] \begin{Bmatrix} \frac{\partial u}{\partial r} \\ \frac{\partial u}{\partial s} \\ \frac{\partial v}{\partial r} \\ \frac{\partial v}{\partial s} \end{Bmatrix} \quad (9.78)$$

9.4 Isoparametric Formulation of the Plane Quadrilateral Element

351

with what we will call the *geometric mapping matrix*, defined as

$$[G] = \frac{1}{|J|} \begin{bmatrix} J_{22} & -J_{12} & 0 & 0 \\ 0 & 0 & -J_{21} & J_{11} \\ -J_{21} & J_{11} & J_{22} & -J_{12} \end{bmatrix} \quad (9.79)$$

We must expand the column matrix on the extreme right-hand side of Equation 9.78 in terms of the discretized approximation to the displacements. Via Equation 9.69, we have

$$\begin{Bmatrix} \frac{\partial u}{\partial r} \\ \frac{\partial u}{\partial s} \\ \frac{\partial v}{\partial r} \\ \frac{\partial v}{\partial s} \end{Bmatrix} = \begin{bmatrix} \frac{\partial N_1}{\partial r} & \frac{\partial N_2}{\partial r} & \frac{\partial N_3}{\partial r} & \frac{\partial N_4}{\partial r} & 0 & 0 & 0 & 0 \\ \frac{\partial N_1}{\partial s} & \frac{\partial N_2}{\partial s} & \frac{\partial N_3}{\partial s} & \frac{\partial N_4}{\partial s} & 0 & 0 & 0 & 0 \\ 0 & 0 & 0 & 0 & \frac{\partial N_1}{\partial r} & \frac{\partial N_2}{\partial r} & \frac{\partial N_3}{\partial r} & \frac{\partial N_4}{\partial r} \\ 0 & 0 & 0 & 0 & \frac{\partial N_1}{\partial s} & \frac{\partial N_2}{\partial s} & \frac{\partial N_3}{\partial s} & \frac{\partial N_4}{\partial s} \end{bmatrix} \begin{Bmatrix} u_1 \\ u_2 \\ u_3 \\ u_4 \\ v_1 \\ v_2 \\ v_3 \\ v_4 \end{Bmatrix} \quad (9.80)$$

where we reemphasize that the indicated partial derivatives are known functions of the natural coordinates of the parent element. For shorthand notation, Equation 9.80 is rewritten as

$$\begin{Bmatrix} \frac{\partial u}{\partial r} \\ \frac{\partial u}{\partial s} \\ \frac{\partial v}{\partial r} \\ \frac{\partial v}{\partial s} \end{Bmatrix} = [P] \{\delta\} \quad (9.81)$$

in which $[P]$ is the matrix of partial derivatives and $\{\delta\}$ is the column matrix of nodal displacement components.

Combining Equations 9.78 and 9.81, we obtain the sought-after relation for the strain components in terms of nodal displacement components as

$$\{\epsilon\} = [G][P]\{\delta\} \quad (9.82)$$

and, by analogy with previous developments, matrix $[B] = [G][P]$ has been determined such that

$$\{\epsilon\} = [B]\{\delta\} \quad (9.83)$$

and the element stiffness matrix is defined by

$$[k^{(e)}] = t \int_A [B]^T [D] [B] dA \quad (9.84)$$

with t representing the constant element thickness, and the integration is performed over the area of the element (in the physical xy plane). In Equation 9.84, the stiffness may represent a plane stress element or a plane strain element, depending on whether the material property matrix $[D]$ is defined by Equation 9.6 or 9.54, respectively. (Also note that, for plane strain, it is customary to take the element thickness as unity.)

The integration indicated by Equation 9.84 are in the x - y global space, but the $[B]$ matrix is defined in terms of the natural coordinates in the parent element space. Therefore, a bit more analysis is required to obtain a final form. In the physical space, we have $dA = dx dy$, but we wish to integrate using the natural coordinates over their respective ranges of -1 to $+1$. In the case of the four-node rectangular element, the conversion is straightforward, as x is related only to r and y is related only to s , as indicated in Equation 9.61. In the isoparametric case at hand, the situation is not quite so simple. The derivation is not repeated here, but it is shown in many calculus texts [1] that

$$dA = dx dy = |J| dr ds \quad (9.85)$$

hence, Equation 9.84 becomes

$$[k^{(e)}] = t \int_A [B]^T [D] [B] |J| dr ds = t \int_{-1}^1 \int_{-1}^1 [B]^T [D] [B] |J| dr ds \quad (9.86)$$

As noted, the terms of the $[B]$ matrix are known functions of the natural coordinates, as is the Jacobian $|J|$. The terms in the stiffness matrix represented by Equation 9.86, in fact, are integrals of ratios of polynomials and the integrations are very difficult, usually impossible, to perform exactly. Instead, Gaussian quadrature is used and the integrations are replaced with sums of the integrand evaluated at specified Gauss points as defined in Chapter 6. For p integration points in the variable r and q integration points in the variable s , the stiffness matrix is approximated by

$$[k^{(e)}] = t \sum_{i=1}^p \sum_{j=1}^q W_i W_j [B(r_i, s_j)]^T [D] [B(r_i, s_j)] |J(r_i, s_j)| dr ds \quad (9.87)$$

Since $[B]$ includes the determinant of the Jacobian matrix in the denominator, the numerical integration does not necessarily result in an exact solution, since the ratio of polynomials is not necessarily a polynomial. Nevertheless, the Gaussian procedure is used for this element, as if the integrand is a quadratic in both r and s , with good results. In such case, we use two Gauss points for each variable, as is illustrated in the following example.

EXAMPLE 9.3

Evaluate the stiffness matrix for the isoparametric quadrilateral element shown in Figure 9.7 for plane stress with $E = 30(10)^6$ psi, $\nu = 0.3$, $t = 1$ in. Note that the properties are those of steel.

9.4 Isoparametric Formulation of the Plane Quadrilateral Element

353

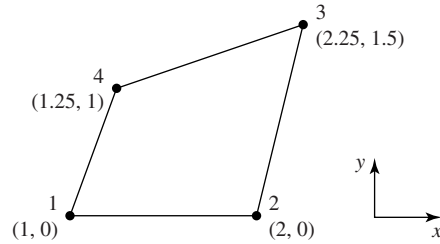


Figure 9.7 Dimensions are in inches.
Axes are shown for orientation only.

■ Solution

The mapping functions are

$$x(r, s) = \frac{1}{4}[(1-r)(1-s)(1) + (1+r)(1-s)(2) + (1+r)(1+s)(2.25) + (1-r)(1+s)(1.25)]$$

$$y(r, s) = \frac{1}{4}[(1-r)(1-s)(0) + (1+r)(1-s)(0) + (1+r)(1+s)(1.5) + (1-r)(1+s)(1)]$$

and the terms of the Jacobian matrix are

$$J_{11} = \frac{\partial x}{\partial r} = \frac{1}{2}$$

$$J_{12} = \frac{\partial y}{\partial r} = \frac{1}{4}(0.5 - 0.5s)$$

$$J_{21} = \frac{\partial x}{\partial s} = \frac{1}{2}$$

$$J_{22} = \frac{\partial y}{\partial s} = \frac{1}{4}(2.5 - 0.5r)$$

and the determinant is

$$|J| = J_{11}J_{22} - J_{12}J_{21} = \frac{1}{16}(4 - r + s)$$

Therefore, the geometric matrix $[G]$ of Equation 9.79 is known in terms of ratios of monomials in r and s as

$$[G] = \frac{4}{4-r+s} \begin{bmatrix} 2.5 - 0.5r & -(0.5 - 0.5s) & 0 & 0 \\ 0 & 0 & -2 & 2 \\ -2 & 2 & 2.5 - 0.5r & -(0.5 - 0.5s) \end{bmatrix}$$

For plane stress with the values given, the material property matrix is

$$[D] = 32.97(10)^6 \begin{bmatrix} 1 & 0.3 & 0 \\ 0.3 & 1 & 0 \\ 0 & 0 & 0.35 \end{bmatrix} \text{ psi}$$

Next, we note that, since the matrix of partial derivatives $[P]$ as defined in Equation 9.81 is also composed of monomials in r and s ,

$$[P] = \frac{1}{4} \begin{bmatrix} s-1 & 1-s & 1+s & -(1+s) & 0 & 0 & 0 & 0 \\ r-1 & -(1+r) & 1+r & 1-r & 0 & 0 & 0 & 0 \\ 0 & 0 & 0 & 0 & s-1 & 1-s & 1+s & -(1+s) \\ 0 & 0 & 0 & 0 & r-1 & -(1+r) & 1+r & 1-r \end{bmatrix}$$

the stiffness matrix of Equation 9.86 is no more than quadratic in the natural coordinates. Hence, we select four integration points given by

$$r_i = s_j = \pm \frac{\sqrt{3}}{3}$$

and weighting factors

$$W_i = W_j = 1.0$$

per Table 6.1.

The element stiffness matrix is then given by

$$[k^{(e)}] = t \sum_{i=1}^2 \sum_{j=1}^2 W_i W_j [B(r_i, s_j)]^T [D][B(r_i, s_j)] |J(r_i, s_j)|$$

The numerical results for this example are obtained via a computer program written in MATLAB using the built-in matrix functions of that software package. The stiffness matrix is calculated to be

$$[k^{(e)}] = \begin{bmatrix} 2305 & -1759 & -617 & 72 & 798 & -152 & -214 & -432 \\ -1759 & 1957 & 471 & -669 & -52 & -522 & 14 & 560 \\ -617 & 471 & 166 & -19 & -214 & 41 & 57 & 116 \\ 72 & -669 & -19 & 616 & -533 & 633 & 143 & -244 \\ 798 & -52 & -214 & -533 & 1453 & -169 & -389 & -895 \\ -152 & -522 & -41 & 633 & -169 & 993 & 45 & -869 \\ -214 & 14 & 57 & 143 & -389 & 45 & 104 & 240 \\ -432 & 560 & 116 & -244 & -895 & -869 & 240 & 1524 \end{bmatrix} 10^3 \text{ lb/in.}$$

EXAMPLE 9.4

A classic example of plane stress analysis is shown in Figure 9.8a. A uniform thin plate with a central hole of radius a is subjected to uniaxial stress σ_0 . Use the finite element method to determine the stress concentration factor given the physical data $\sigma_0 = 1000$ psi, $a = 0.5$ in., $h = 3$ in., $w = 6$ in., $E = 10(10)^6$ psi, and Poisson's ratio = 0.3.

■ Solution

The solution for this example is obtained using commercial finite element software with plane quadrilateral elements. The initial (coarse) element mesh, shown in Figure 9.8b, is composed of 33 elements. Note that the symmetry conditions have been used to reduce the model to quarter-size and the corresponding boundary conditions are as shown on the figure. For this model, the maximum stress (as expected) is calculated to occur at node 1 (at the top of the hole) and has a magnitude of 3101 psi.

9.4 Isoparametric Formulation of the Plane Quadrilateral Element

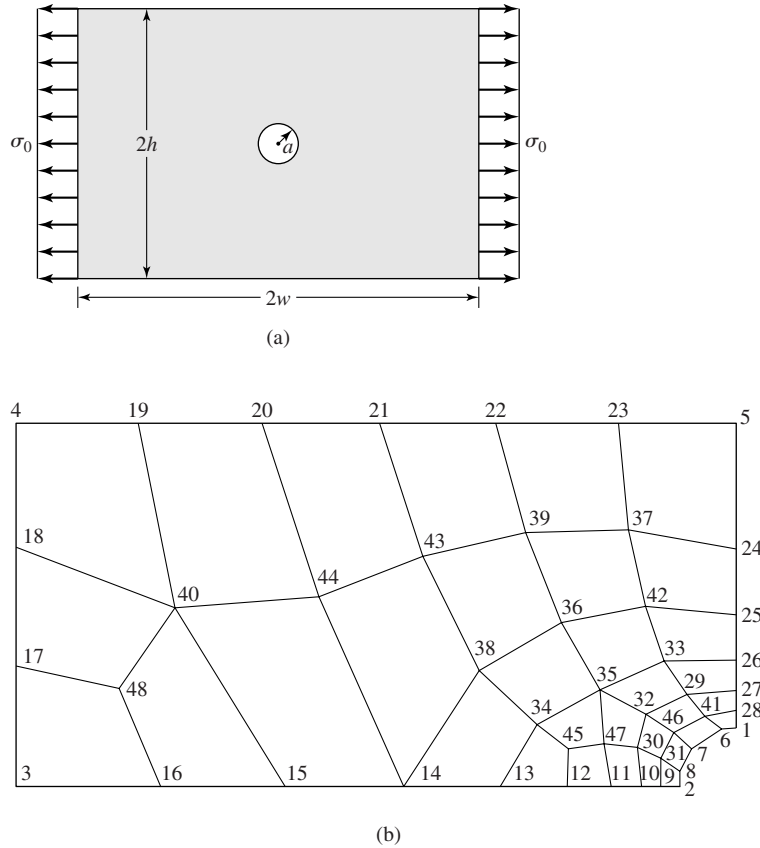
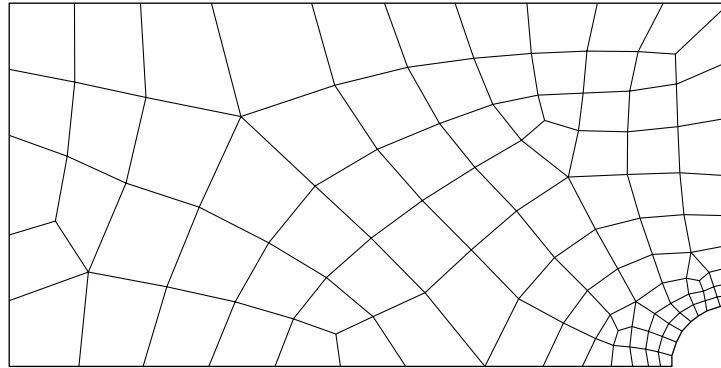


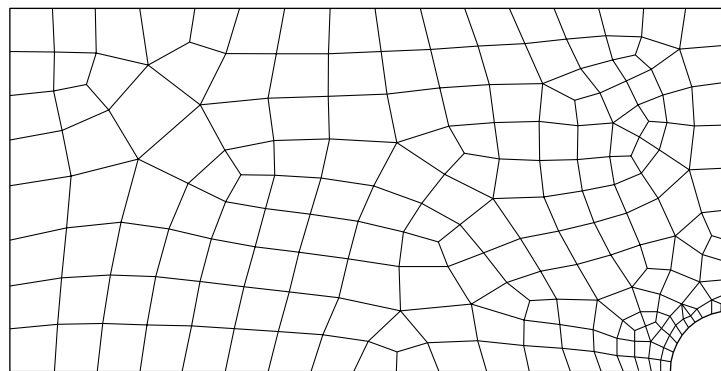
Figure 9.8
 (a) A uniformly loaded plate in plane stress with a central hole of radius a . (b) A coarse finite element mesh using quadrilateral elements. Node numbers are as shown (31 elements).

To examine the solution convergence, a refined model is shown in Figure 9.8c, using 101 elements. For this model, the maximum stress also occurs at node 1 and has a calculated magnitude of 3032 psi. Hence, between the two models, the maximum stress values changed on the order of 2.3 percent. It is interesting to note that the maximum displacement given by the two models is essentially the same. This observation reinforces the need to examine the derived variables for convergence, not simply the directly computed variables.

As a final step in examining the convergence, the model shown in Figure 9.8d containing 192 elements is also solved. (The node numbers are eliminated for clarity.) The maximum computed stress, again at node 1, is 3024 psi, a miniscule change relative to the previous model, so we conclude that convergence has been attained. (The change in maximum displacement is essentially nil.) Hence, we conclude that the stress concentration factor $K_t = \sigma_{\max} / \sigma_0 = 3024 / 1000 = 3.024$ is applicable to the geometry and loading of this example. It is interesting to note that the theoretical (hence, the subscript t)



(c)



(d)

Figure 9.8 (Continued)

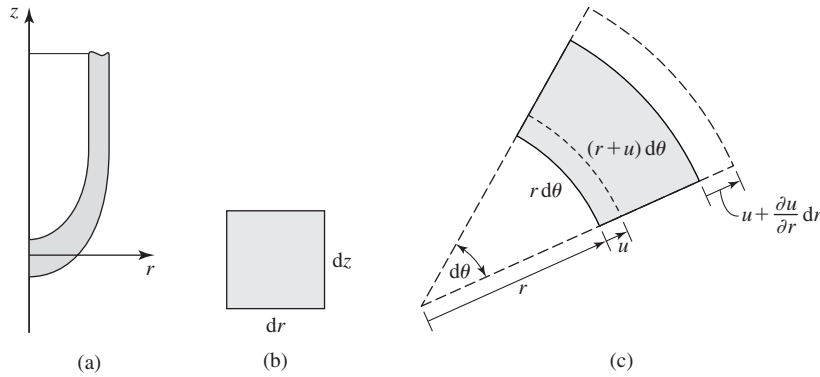
(c) Refined mesh of 101 elements. Node numbers are removed for clarity. (d) An additional refined mesh with 192 elements.

stress concentration factor for this problem as computed by the mathematical theory of elasticity is exactly 3. The same result is shown in many texts on machine design and stress analysis [2].

9.5 AXISYMMETRIC STRESS ANALYSIS

The concept of axisymmetry is discussed in Chapter 6 in terms of general interpolation functions. Here, we specialize the axisymmetric concept to problems of elastic stress analysis. To satisfy the conditions for axisymmetric stress, the problem must be such that

1. The solid body under stress must be a solid of revolution; by convention, the axis of revolution is the z axis in a cylindrical coordinate system (r, θ, z) .
2. The loading of the body is symmetric about the z axis.

**Figure 9.9**

(a) Cross section of an axisymmetric body. (b) Differential element in an rz plane. (c) Differential element in an r - θ plane illustrating tangential deformation. Dashed lines represent deformed positions.

3. All boundary (constraint) conditions are symmetric about the z axis.
4. Materials properties are also symmetric (automatically satisfied by a linearly elastic, homogeneous, isotropic material).

If these conditions are satisfied, the displacement field is independent of the tangential coordinate θ , and hence the stress analysis is mathematically two-dimensional, even though the physical problem is three-dimensional. To develop the axisymmetric equations, we examine Figure 9.9a, representing a solid of revolution that satisfies the preceding requirements. Figure 9.9b is a differential element of the body in the rz plane; that is, any section through the body for which θ is constant. We cannot ignore the tangential coordinate completely, however, since as depicted in Figure 9.9c, there is strain in the tangential direction (recall the basic definition of hoop stress in thin-walled pressure vessels from mechanics of materials). Note that, in the radial direction, the element undergoes displacement, which introduces increase in circumference and associated circumferential strain.

We denote the radial displacement as u , the tangential (circumferential) displacement as v , and the axial displacement as w . From Figure 9.9c, the radial strain is

$$\epsilon_r = \frac{1}{dr} \left(u + \frac{\partial u}{\partial r} dr - u \right) = \frac{\partial u}{\partial r} \quad (9.88)$$

The axial strain is

$$\epsilon_z = \frac{1}{dz} \left(w + \frac{\partial w}{\partial z} dz - w \right) = \frac{\partial w}{\partial z} \quad (9.89)$$

and these relations are as expected, since the rz plane is effectively the same as a rectangular coordinate system. In the circumferential direction, the differential element undergoes an expansion defined by considering the original arc length

versus the deformed arc length. Prior to deformation, the arc length is $ds = r d\theta$, while after deformation, arc length is $ds = (r + u) d\theta$. The tangential strain is

$$\varepsilon_{\theta} = \frac{(r + u)(d\theta) - r d\theta}{r d\theta} = \frac{u}{r} \quad (9.90)$$

and we observe that, even though the problem is independent of the tangential coordinate, the tangential strain must be considered in the problem formulation. Note that, if $r = 0$, the preceding expression for the tangential strain is troublesome mathematically, since division by zero is indicated. The situation occurs, for example, if we examine stresses in a rotating solid body, in which case the stresses are induced by centrifugal force (normal acceleration). Additional discussion of this problem is included later when we discuss element formulation.

Additionally, the shear strain components are

$$\begin{aligned} \gamma_{rz} &= \frac{\partial u}{\partial z} + \frac{\partial w}{\partial r} \\ \gamma_{r\theta} &= 0 \\ \gamma_{\theta z} &= 0 \end{aligned} \quad (9.91)$$

If we substitute the strain components into the generalized stress-strain relations of Appendix B (and, in this case, we utilize $\theta = y$), we obtain

$$\begin{aligned} \sigma_r &= \frac{E}{(1 + \nu)(1 - 2\nu)} [(1 - \nu)\varepsilon_r + \nu(\varepsilon_{\theta} + \varepsilon_z)] \\ \sigma_{\theta} &= \frac{E}{(1 + \nu)(1 - 2\nu)} [(1 - \nu)\varepsilon_{\theta} + \nu(\varepsilon_r + \varepsilon_z)] \\ \sigma_z &= \frac{E}{(1 + \nu)(1 - 2\nu)} [(1 - \nu)\varepsilon_z + \nu(\varepsilon_r + \varepsilon_{\theta})] \\ \tau_{rz} &= \frac{E}{2(1 + \nu)} \gamma_{rz} = G\gamma_{rz} \end{aligned} \quad (9.92)$$

For convenience in finite element development, Equation 9.92 is expressed in matrix form as

$$\begin{Bmatrix} \sigma_r \\ \sigma_{\theta} \\ \sigma_z \\ \tau_{rz} \end{Bmatrix} = \frac{E}{(1 + \nu)(1 - 2\nu)} \begin{bmatrix} 1 - \nu & \nu & \nu & 0 \\ \nu & 1 - \nu & \nu & 0 \\ \nu & \nu & 1 - \nu & 0 \\ 0 & 0 & 0 & \frac{1 - 2\nu}{2} \end{bmatrix} \begin{Bmatrix} \varepsilon_r \\ \varepsilon_{\theta} \\ \varepsilon_z \\ \gamma_{rz} \end{Bmatrix} \quad (9.93)$$

in which we identify the material property matrix for axisymmetric elasticity as

$$[D] = \frac{E}{(1 + \nu)(1 - 2\nu)} \begin{bmatrix} 1 - \nu & \nu & \nu & 0 \\ \nu & 1 - \nu & \nu & 0 \\ \nu & \nu & 1 - \nu & 0 \\ 0 & 0 & 0 & \frac{1 - 2\nu}{2} \end{bmatrix} \quad (9.94)$$

9.5.1 Finite Element Formulation

Recall from the general discussion of interpolation functions in Chapter 6 that essentially any two-dimensional element can be used to generate an axisymmetric element. As there is, by definition, no dependence on the θ coordinate and no circumferential displacement, the displacement field for the axisymmetric stress problem can be expressed as

$$u(r, z) = \sum_{i=1}^M N_i(r, z) u_i$$

$$w(r, z) = \sum_{i=1}^M N_i(r, z) w_i$$
(9.95)

with u_i and w_i representing the nodal radial and axial displacements, respectively. For illustrative purposes, we now assume the case of a three-node triangular element.

The strain components become

$$\varepsilon_r = \frac{\partial u}{\partial r} = \sum_{i=1}^3 \frac{\partial N_i}{\partial r} u_i$$

$$\varepsilon_\theta = \frac{u}{r} = \sum_{i=1}^3 \frac{N_i}{r} u_i$$

$$\varepsilon_z = \frac{\partial w}{\partial z} = \sum_{i=1}^3 \frac{\partial N_i}{\partial z} w_i$$

$$\gamma_{rz} = \frac{\partial u}{\partial z} + \frac{\partial w}{\partial r} = \sum_{i=1}^3 \frac{\partial N_i}{\partial z} u_i + \sum_{i=1}^3 \frac{\partial N_i}{\partial r} w_i$$
(9.96)

and these are conveniently expressed in the matrix form

$$\begin{Bmatrix} \varepsilon_r \\ \varepsilon_\theta \\ \varepsilon_z \\ \gamma_{rz} \end{Bmatrix} = \begin{bmatrix} \frac{\partial N_1}{\partial r} & \frac{\partial N_2}{\partial r} & \frac{\partial N_3}{\partial r} & 0 & 0 & 0 \\ \frac{N_1}{r} & \frac{N_2}{r} & \frac{N_3}{r} & 0 & 0 & 0 \\ 0 & 0 & 0 & \frac{\partial N_1}{\partial z} & \frac{\partial N_2}{\partial z} & \frac{\partial N_3}{\partial z} \\ \frac{\partial N_1}{\partial z} & \frac{\partial N_2}{\partial z} & \frac{\partial N_3}{\partial z} & \frac{\partial N_1}{\partial r} & \frac{\partial N_2}{\partial r} & \frac{\partial N_3}{\partial r} \end{bmatrix} \begin{Bmatrix} u_1 \\ u_2 \\ u_3 \\ w_1 \\ w_2 \\ w_3 \end{Bmatrix}$$
(9.97)

In keeping with previous developments, Equation 9.97 is denoted $\{\varepsilon\} = [B]\{\delta\}$ with $[B]$ representing the 4×6 matrix involving the interpolation functions. Thus total strain energy of the elements, as described by Equation 9.15 or 9.58

and the stiffness matrix, is

$$[k^{(e)}] = \iiint_{V^{(e)}} [B]^T [D] [B] dV^{(e)} \quad (9.98)$$

While Equation 9.98 is becoming rather familiar, a word or two of caution is appropriate. Recall in particular that, although the interpolation functions used here are two dimensional, the axisymmetric element is truly three dimensional (toroidal). Second, the element is not a constant strain element, owing to the inverse variation of ϵ_θ with radial position, so the integrand in Equation 9.98 is not constant. Finally, note that $[D]$ is significantly different in comparison to the counterpart material property matrices for plane stress and plane strain. Taking the first observation into account and recalling Equation 6.93, the stiffness matrix is defined by

$$[k^{(e)}] = 2\pi \iint_{A^{(e)}} [B]^T [D] [B] r dr dz \quad (9.99)$$

and is a 6×6 symmetric matrix requiring, in theory, evaluation of 21 integrals. Explicit term-by-term integration is not recommended, owing to the algebraic complexity. When high accuracy is required, Gauss-type numerical integration using integration points specifically determined for triangular regions [3] is used. Another approach is to evaluate matrix $[B]$ at the centroid of the element in an rz plane. In this case, the matrices in the integrand become constant and the stiffness matrix is approximated by

$$[k^{(e)}] \approx 2\pi \bar{r} A [\bar{B}]^T [D] [\bar{B}] \quad (9.100)$$

Of course, the accuracy of the approximation improves as element size is decreased.

Referring to a previous observation, formulation of the $[B]$ matrix is troublesome if $r = 0$ is included in the domain. In this occurrence, three terms of Equation 9.97 “blow up,” owing to division by zero. If the stiffness matrix is evaluated using the centroidal approximation of Equation 9.100, the problem is avoided, since the radial coordinate of the centroid of any element cannot be zero in an axisymmetric finite element model. Nevertheless, radial and tangential strain and stress components cannot be evaluated at nodes for which $r = 0$. Physically, we know that the radial and tangential displacements at $r = 0$ in an axisymmetric problem must be zero. Mathematically, the observation is not accounted for in the general finite element formulation, which is for an arbitrary domain. One technique for avoiding the problem is to include a hole, coinciding with the z axis and having a small, but finite radius [4].

9.5.2 Element Loads

Axisymmetric problems often involve surface forces in the form of internal or external pressure and body forces arising from rotation of the body (centrifugal

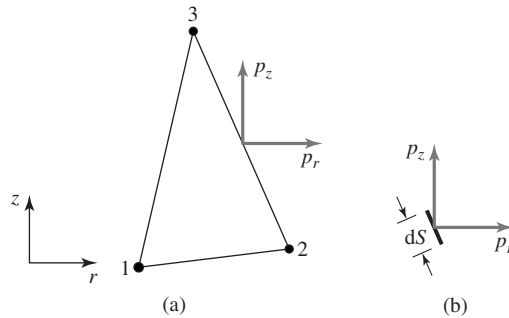


Figure 9.10
(a) Axisymmetric element. (b) Differential length
of the element edge.

force) and gravity. In each case, the external influences are reduced to nodal forces using the work equivalence concept previously introduced.

The triangular axisymmetric element shown in Figure 9.10a is subjected to pressures p_r and p_z in the radial and axial directions, respectively. The equivalent nodal forces are determined by analogy with Equation 9.39, with the notable exception depicted in Figure 9.10b, showing a differential length dS of the element edge in question. As dS is located a radial distance r from the axis of symmetry, the area on which the pressure components act is $2\pi r dS$. The nodal forces are given by

$$\{f^{(p)}\} = \begin{Bmatrix} f_r^{(p)} \\ f_z^{(p)} \end{Bmatrix} = 2\pi \int_S [N]^T \begin{Bmatrix} p_r \\ p_z \end{Bmatrix} r dS \quad (9.101)$$

and the path of integration S is the element edge. In this expression, $[N]^T$ is as defined by Equation 9.40.

EXAMPLE 9.5

Calculate the nodal forces corresponding to a uniform radial pressure $p_r = 10$ psi acting as shown on the axisymmetric element in Figure 9.11.

■ Solution

As we have pressure on one face only and no axial pressure, we immediately observe that

$$f_{r2} = f_{z1} = f_{z2} = f_{z3} = 0$$

The nonzero terms are

$$f_{r1} = 2\pi \int_S N_1 p_r r dS$$

$$f_{r3} = 2\pi \int_S N_3 p_r r dS$$

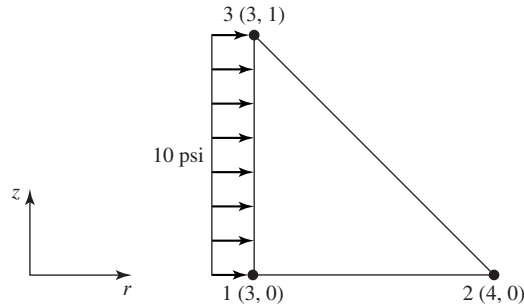


Figure 9.11 Uniform radial pressure.
Dimensions are in inches.

Using Equation 9.28 with r, z in place of x, y , the interpolation functions are

$$N_1 = 4 - r - z$$

$$N_2 = r - 3$$

$$N_3 = z$$

and along the integration path ($r = 3$), we have

$$N_1 = 1 - z$$

$$N_2 = 0$$

$$N_3 = z$$

If the integration path is *from* node 1 *to* node 3, then $dS = dz$ and

$$f_{r1} = 2\pi(10)(3) \int_0^1 z \, dz = 30\pi \text{ lb}$$

$$f_{r3} = 2\pi(10)(3) \int_0^1 (1 - z) \, dz = 30\pi \text{ lb}$$

Note that, if the integration path is taken in the opposite sense (i.e., *from* node 3 *to* node 2), then $dS = -dz$ and the same results are obtained.

Body forces acting on axisymmetric elements are accounted for in a manner similar to that discussed for the plane stress element, while taking into consideration the geometric differences. If body forces (force per unit mass) R_B and Z_B act in the radial and axial directions, respectively, the equivalent nodal forces are calculated as

$$\{f^{(B)}\} = 2\pi\rho \int_{A^{(e)}} [N]^T \begin{Bmatrix} R_B \\ Z_B \end{Bmatrix} r \, dr \, dz \quad (9.102)$$

For the three-node triangular element, $[N]^T$ would again be as given in Equation 9.40. Extension to other element types is similar.

Generally, radial body force arises from rotation of an axisymmetric body about the z axis. For constant angular velocity ω , the radial body force component R_B is equal to the magnitude of the normal acceleration component $r\omega^2$ and directed in the positive radial direction.

EXAMPLE 9.6

The axisymmetric element of Figure 9.11 is part of a body rotating with angular velocity 10 rad/s about the z axis and subjected to gravity in the negative z direction. Compute the equivalent nodal forces. Density is $7.3(10)^{-4}$ lb-s²/in.⁴

■ Solution

For the stated conditions, we have

$$R_B = r\omega^2 = 100r \text{ in./s}^2$$

$$Z_B = -g = -386.4 \text{ in./s}^2$$

Using the interpolation functions as given in Example 9.5,

$$f_{r1} = 2\pi\rho \int_A N_1 R_B r \, dr \, dz = 2\pi\rho(100) \int_3^4 \int_0^{4-r} (4-r-z)r^2 \, dz \, dr = 0.84 \text{ lb}$$

$$f_{r2} = 2\pi\rho \int_A N_2 R_B r \, dr \, dz = 2\pi\rho(100) \int_3^4 \int_0^{4-r} (r-3)r^2 \, dz \, dr = 0.98 \text{ lb}$$

$$f_{r3} = 2\pi\rho \int_A N_3 R_B r \, dr \, dz = 2\pi\rho(100) \int_3^4 \int_0^{4-r} zr^2 \, dz \, dr = 0.84 \text{ lb}$$

$$f_{z1} = 2\pi\rho \int_A N_1 Z_B r \, dr \, dz = -2\pi\rho(386.4) \int_3^4 \int_0^{4-r} (4-r-z)r \, dz \, dr = -1.00 \text{ lb}$$

$$f_{z2} = 2\pi\rho \int_A N_2 Z_B r \, dr \, dz = -2\pi\rho(386.4) \int_3^4 \int_0^{4-r} (r-3)r \, dz \, dr = -1.08 \text{ lb}$$

$$f_{z3} = 2\pi\rho \int_A N_3 Z_B r \, dr \, dz = -2\pi\rho(386.4) \int_3^4 \int_0^{4-r} zr \, dz \, dr = -1.00 \text{ lb}$$

The integrations required to obtain the given results are straightforward but algebraically tedious. Another approach that can be used and is increasingly accurate for decreasing element size is to evaluate the body forces and the integrand at the centroid of the cross section of the element area as an approximation. Using this approximation, it can be shown that

$$\int_A N_i(\bar{r}, \bar{z}) \bar{r} \, dz \, dr = \frac{\bar{r}A}{3} \quad i = 1, 3$$

so the body forces are allocated equally to each node. For the present example, the result is

$$\begin{aligned} f_{r1} = f_{r2} = f_{r3} &= 0.88 \text{ lb} \\ f_{z1} = f_{z2} = f_{z3} &= -1.03 \text{ lb} \end{aligned}$$

Note that, within the numerical accuracy used here, the total radial force and the total axial force are the same for the two methods.

9.6 GENERAL THREE-DIMENSIONAL STRESS ELEMENTS

While the conditions of plane stress, plane strain, and axisymmetry are frequently encountered, more often than not the geometry of a structure and the applied loads are such that a general three-dimensional state of stress exists. In the general case, there are three displacement components u , v , and w in the directions of the x , y , and z axes, respectively, and six strain components given by (Appendix B)

$$\{\epsilon\} = \begin{Bmatrix} \epsilon_x \\ \epsilon_y \\ \epsilon_z \\ \gamma_{xy} \\ \gamma_{xz} \\ \gamma_{yz} \end{Bmatrix} = \begin{Bmatrix} \frac{\partial u}{\partial x} \\ \frac{\partial v}{\partial y} \\ \frac{\partial w}{\partial z} \\ \frac{\partial u}{\partial y} + \frac{\partial v}{\partial x} \\ \frac{\partial u}{\partial z} + \frac{\partial w}{\partial x} \\ \frac{\partial v}{\partial z} + \frac{\partial w}{\partial y} \end{Bmatrix} \quad (9.103)$$

For convenience of presentation, the strain-displacement relations of Equation 9.103 can be expressed as

$$\{\epsilon\} = \begin{bmatrix} \frac{\partial}{\partial x} & 0 & 0 \\ 0 & \frac{\partial}{\partial y} & 0 \\ 0 & 0 & \frac{\partial}{\partial z} \\ \frac{\partial}{\partial y} & \frac{\partial}{\partial x} & 0 \\ \frac{\partial}{\partial z} & 0 & \frac{\partial}{\partial x} \\ 0 & \frac{\partial}{\partial z} & \frac{\partial}{\partial y} \end{bmatrix} \begin{Bmatrix} u \\ v \\ w \end{Bmatrix} = [L] \begin{Bmatrix} u \\ v \\ w \end{Bmatrix} \quad (9.104)$$

and matrix $[L]$ is the 6×3 matrix of derivative operators.

The stress-strain relations, Equation B.12, are expressed in matrix form as

$$\begin{aligned} \{\sigma\} &= \begin{Bmatrix} \sigma_x \\ \sigma_y \\ \sigma_z \\ \tau_{xy} \\ \tau_{xz} \\ \tau_{yz} \end{Bmatrix} \\ &= \frac{E}{(1+\nu)(1-2\nu)} \begin{bmatrix} 1-\nu & \nu & \nu & 0 & 0 & 0 \\ \nu & 1-\nu & \nu & 0 & 0 & 0 \\ \nu & \nu & 1-\nu & 0 & 0 & 0 \\ 0 & 0 & 0 & \frac{1-2\nu}{2} & 0 & 0 \\ 0 & 0 & 0 & 0 & \frac{1-2\nu}{2} & 0 \\ 0 & 0 & 0 & 0 & 0 & \frac{1-2\nu}{2} \end{bmatrix} \{\epsilon\} = [D]\{\epsilon\} \end{aligned} \quad (9.105)$$

Note that, for the general case, the material property matrix $[D]$ is a 6×6 matrix involving only the elastic modulus and Poisson's ratio (we continue to restrict the presentation to linear elasticity). Also note that the displacement components are continuous functions of the Cartesian coordinates.

9.6.1 Finite Element Formulation

Following the general procedure established in the context of two-dimensional elements, a three-dimensional elastic stress element having M nodes is formulated by first discretizing the displacement components as

$$\begin{aligned} u(x, y, z) &= \sum_{i=1}^M N_i(x, y, z) u_i \\ v(x, y, z) &= \sum_{i=1}^M N_i(x, y, z) v_i \\ w(x, y, z) &= \sum_{i=1}^M N_i(x, y, z) w_i \end{aligned} \quad (9.106)$$

As usual, the Cartesian nodal displacements are u_i , v_i , and w_i and $N_i(x, y, z)$ is the interpolation function associated with node i . At this point, we make no assumption regarding the element shape or number of nodes. Instead, we simply note that the interpolation functions may be any of those discussed in Chapter 6 for three-dimensional elements.

Introducing the vector (column matrix) of nodal displacements,

$$\{\delta\} = [u_1 \quad u_2 \quad \cdots \quad u_M \quad v_1 \quad v_2 \quad \cdots \quad v_M \quad w_1 \quad w_2 \quad \cdots \quad w_M]^T \quad (9.107)$$

the discretized representation of the displacement field can be written in matrix form as

$$\begin{Bmatrix} u \\ v \\ w \end{Bmatrix} = \begin{bmatrix} [N] & [0] & [0] \\ [0] & [N] & [0] \\ [0] & [0] & [N] \end{bmatrix} \{\delta\} = [N_3]\{\delta\} \quad (9.108)$$

In the last equation, each submatrix $[N]$ is the $1 \times M$ row matrix of interpolation functions

$$[N] = [N_1 \quad N_2 \quad \cdots \quad N_M] \quad (9.109)$$

so the matrix we have chosen to denote as $[N_3]$ is a $3 \times 3M$ matrix composed of the interpolation functions and many zero values. (Before proceeding, we emphasize that the order of nodal displacements in Equation 9.107 is convenient for purposes of development but *not* efficient for computational purposes. Much higher computational efficiency is obtained in the model solution phase if the displacement vector is defined as $\{\delta\} = [u_1 \ v_1 \ w_1 \ u_2 \ v_2 \ w_2 \ \cdots \ u_M \ v_M \ w_M]^T$.)

Recalling Equations 9.10 and 9.19, total potential energy of an element can be expressed as

$$\Pi = U_e - W = \frac{1}{2} \iiint_V \{\epsilon\}^T [D] \{\epsilon\} dV - \{\delta\}^T \{f\} \quad (9.110)$$

The element nodal force vector is defined in the column matrix

$$\{f\} = [f_{1x} \ f_{2x} \ \cdots \ f_{Mx} \ f_{1y} \ f_{2y} \ \cdots \ f_{My} \ f_{1z} \ f_{2z} \ \cdots \ f_{Mz}]^T \quad (9.111)$$

and may include the effects of concentrated forces applied at the nodes, nodal equivalents to body forces, and nodal equivalents to applied pressure loadings.

Considering the foregoing developments, Equation 9.110 can be expressed (using Equations 9.104, 9.105, and 9.108), as

$$\Pi = U_e - W = \frac{1}{2} \iiint_V \delta^T [L]^T [N_3]^T [D] [L] [N_3] \{\delta\} dV - \{\delta\}^T \{f\} \quad (9.112)$$

As the nodal displacement components are independent of the integration over the volume, Equation 9.112 can be written as

$$\Pi = U_e - W = \frac{1}{2} \{\delta\}^T \iiint_V [L]^T [N_3]^T [D] [L] [N_3] dV \{\delta\} - \{\delta\}^T \{f\} \quad (9.113)$$

which is in the form

$$\Pi = U_e - W = \frac{1}{2} \{\delta\}^T \iiint_V [B]^T [D] [B] dV \{\delta\} - \{\delta\}^T \{f\} \quad (9.114)$$

In Equation 9.114, the strain-displacement matrix is given by

$$[B] = [L][N_3] = \begin{bmatrix} \frac{\partial}{\partial x} & 0 & 0 \\ 0 & \frac{\partial}{\partial y} & 0 \\ 0 & 0 & \frac{\partial}{\partial z} \\ \frac{\partial}{\partial y} & \frac{\partial}{\partial x} & 0 \\ \frac{\partial}{\partial z} & 0 & \frac{\partial}{\partial z} \\ 0 & \frac{\partial}{\partial z} & \frac{\partial}{\partial y} \end{bmatrix} \begin{bmatrix} [N] & [0] & [0] \\ [0] & [N] & [0] \\ [0] & [0] & [N] \end{bmatrix} \quad (9.115)$$

and is observed to be a $6 \times 3M$ matrix composed of the first partial derivatives of the interpolation functions.

Application of the principle of minimum potential energy to Equation 9.114 yields, in analogy with Equation 9.22,

$$\iiint_V [B]^T [D] [B] dV \{\delta\} = \{f\} \quad (9.116)$$

as the system of nodal equilibrium equation for a general three-dimensional stress element. From Equation 9.116, we identify the element stiffness matrix as

$$[k] = \iiint_V [B]^T [D] [B] dV \quad (9.117)$$

and the element stiffness matrix so defined is a $3M \times 3M$ symmetric matrix, as expected for a linear elastic element. The integrations indicated in Equation 9.117 depend on the specific element type in question. For a four-node, linear tetrahedral element (Section 6.7), all the partial derivatives of the volume coordinates are constants, so the strains are constant—this is the 3-D analogy to a constant strain triangle in two dimensions. In the linear tetrahedral element, the terms of the $[B]$ matrix are constant and the integrations reduce to a constant multiple of element volume.

If the element to be developed is an eight-node brick element, the interpolation functions, Equation 6.69, are such that strains vary linearly and the integrands in Equation 9.117 are not constant. The integrands are polynomials in the spatial variables, however, and therefore amenable to exact integration by Gaussian quadrature in three dimensions. Similarly, for higher-order elements, the integrations required to formulate the stiffness matrix are performed numerically.

The eight-node brick element can be transformed into a generally shaped parallelepiped element using the isoparametric procedure discussed in Section 6.8. If the eight-node element is used as the parent element, the resulting

isoparametric element has planar faces and is analogous to the two-dimensional quadrilateral element. If the parent element is of higher-order interpolation functions, an element with general (curved) surfaces results.

Regardless of the specific element type or types used in a three-dimensional finite element analysis, the procedure for assembling the global equilibrium equations is the same as discussed several times, so we do not belabor the point here. As in previous developments, the assembled global equations are of the form

$$[K]\{\Delta\} = \{F\} \quad (9.118)$$

with $[K]$ representing the assembled global stiffness matrix, $\{\Delta\}$ representing the column matrix of global displacements, and $\{F\}$ representing the column matrix of applied nodal forces. The nodal forces may include directly applied external forces at nodes, the work-equivalent nodal forces corresponding to body forces and forces arising from applied pressure on element faces.

9.7 STRAIN AND STRESS COMPUTATION

Using the stiffness method espoused in this text, the solution phase of a finite element analysis results in the computation of unknown nodal displacements as well as reaction forces at constrained nodes. Computation of strain components, then stress components, is a secondary (postprocessing) phase of the analysis. Once the displacements are known, the strain components (at each node in the model) are readily computed using Equation 9.104, which, given the discretization in the finite element context, becomes

$$\{\varepsilon\} = [L] \begin{Bmatrix} u \\ v \\ w \end{Bmatrix} = [L][N_3]\{\delta\} = [B]\{\delta\} \quad (9.119)$$

It must be emphasized that Equation 9.119 represents the calculation of strain components for an *individual element* and must be carried out for *every* element in the finite element model. However, the computation is straightforward, since the $[B]$ matrix has been computed for each element to determine the element stiffness matrix, hence the element contributions to the global stiffness matrix.

Similarly, element stress components are computed as

$$\{\sigma\} = [D][B]\{\delta\} \quad (9.120)$$

and the material property matrix $[D]$ depends on the state of stress, as previously discussed. Equations 9.119 and 9.120 are general in the sense that the equations are valid for any state of stress if the strain-displacement matrix $[B]$ and the material property matrix $[D]$ are properly defined for a particular state of stress. (In this context, recall that we consider only linearly elastic deformation in this text.)

The element strain and stress components, as computed, are expressed in the element coordinate system. In general, for the elements commonly used in

stress analysis, the coordinate system for each element is the same as the global coordinate system. It is a fact of human nature, especially of engineers, that we select the simplest frame in which to describe a particular occurrence or event. This is a way of saying that we tend to choose a coordinate system for convenience and that convenience is most often related to the geometry of the problem at hand. The selected coordinate system seldom, if ever, corresponds to maximum loading conditions. Specifically, if we consider the element stress calculation represented by Equation 9.120, the stress components are referred, and calculated with reference, to a specified Cartesian coordinate system. To determine the critical loading on any model, we must apply one of the so-called failure theories. As we limit the discussion to linearly elastic behavior, the “failure” in our context is yielding of the material. There are several commonly accepted failure theories for yielding in a general state of stress. The two most commonly applied are the *maximum shear stress theory* and the *distortion energy theory*. We discuss each of these briefly. In a general, three-dimensional state of stress, the *principal stresses* σ_1 , σ_2 , and σ_3 are given by the roots of the cubic equation represented by the determinant [2]

$$\begin{vmatrix} \sigma_x - \sigma & \tau_{xy} & \tau_{xz} \\ \tau_{xy} & \sigma_y - \sigma & \tau_{yz} \\ \tau_{xz} & \tau_{yz} & \sigma_z - \sigma \end{vmatrix} = 0 \quad (9.121)$$

Customarily, the principal stresses are ordered so that $\sigma_1 > \sigma_2 > \sigma_3$. Via the usual convention, a positive normal stress corresponds to tension, while a negative normal stress is compressive. So, while σ_3 is algebraically the smallest of the three principal stresses, it may represent a compressive stress having significantly large magnitude. Also recall that the principal stresses occur on mutually orthogonal planes (the *principal planes*) and the shear stress components on those planes are zero.

Having computed the principal stress components, the maximum shear stress is

$$\tau_{\max} = \text{largest of} \left(\frac{|\sigma_1 - \sigma_2|}{2}, \frac{|\sigma_1 - \sigma_3|}{2}, \frac{|\sigma_2 - \sigma_3|}{2} \right) \quad (9.122)$$

The three shear stress components in Equation 9.122 are known to occur on planes oriented 45° from the principal planes.

The maximum shear stress theory (MSST) holds that failure (yielding) in a general state of stress occurs when the maximum shear stress as given by Equation 9.122 equals or exceeds the maximum shear stress occurring in a uniaxial tension test at yielding. It is quite easy to show that the maximum shear stress in a tensile test at yielding has value equal to one-half the tensile yield strength of the material. Hence, the failure value in the MSST is $\tau_{\max} = S_y/2 = S_{ys}$. In this notation, S_y is tensile yield strength and S_{ys} represents yield strength in shear.

The distortion energy theory (DET) is based on the strain energy stored in a material under a given state of stress. The theory holds that a uniform tensile or

compressive state of stress (also known as *hydrostatic* stress) does not cause distortion and, hence, does not contribute to yielding. If the principal stresses have been computed, total elastic strain energy is given by

$$\begin{aligned} U_e &= \frac{1}{2} \iiint_V (\sigma_1 \varepsilon_1 + \sigma_2 \varepsilon_2 + \sigma_3 \varepsilon_3) dV \\ &= \frac{1}{2E} [\sigma_1^2 + \sigma_2^2 + \sigma_3^2 - 2\nu(\sigma_1 \sigma_2 + \sigma_1 \sigma_3 + \sigma_2 \sigma_3)] V \end{aligned} \quad (9.123)$$

To arrive at distortion energy, the average (hydrostatic) stress is defined as

$$\sigma_{av} = \frac{\sigma_1 + \sigma_2 + \sigma_3}{3} \quad (9.124)$$

and the corresponding strain energy is

$$U_{hyd} = \frac{3\sigma_{av}^2}{2E} (1 - 2\nu) V \quad (9.125)$$

The distortion energy is then defined as

$$U_d = U_e - U_{hyd} \quad (9.126)$$

After a considerable amount of algebraic manipulation, the distortion energy in terms of the principal stress components is found to be given by

$$U_d = \frac{1 + \nu}{3E} \left[\frac{(\sigma_1 - \sigma_2)^2 + (\sigma_1 - \sigma_3)^2 + (\sigma_2 - \sigma_3)^2}{2} \right]^{1/2} V \quad (9.127)$$

The DET states that failure (yielding) occurs in a general state of stress when the distortion energy per unit volume equals or exceeds the distortion energy per unit volume occurring in a uniaxial tension test at yielding. It is relatively easy to show (see Problem 9.20) that, at yielding in a tensile test, the distortion energy is given by

$$U_d = \frac{1 + \nu}{3E} S_y^2 V \quad (9.128)$$

and, as before, we use S_y to denote the tensile yield strength. Hence, Equations 9.127 and 9.128 give the failure (yielding) criterion for the DET as

$$\left[\frac{(\sigma_1 - \sigma_2)^2 + (\sigma_1 - \sigma_3)^2 + (\sigma_2 - \sigma_3)^2}{2} \right]^{1/2} \geq S_y \quad (9.129)$$

The DET as described in Equation 9.129 leads to the concept of an *equivalent stress* (known historically as the *Von Mises stress*) defined as

$$\sigma_e = \left[\frac{(\sigma_1 - \sigma_2)^2 + (\sigma_1 - \sigma_3)^2 + (\sigma_2 - \sigma_3)^2}{2} \right]^{1/2} \quad (9.130)$$

and failure (yielding) can then be equivalently defined as

$$\sigma_e \geq S_y \quad (9.131)$$

Even though we do not present the algebraic details here, the DET can be shown to be equivalent to another elastic failure theory, known as the *octahedral shear stress theory* (OSST). For all practical purposes, the OSST holds that yielding occurs when the maximum shear stress exceeds $0.577S_y$. In comparison to the MSST, the OSST gives the material more “credit” for strength in shear.

Why do we go into detail on these failure theories in the context of finite element analysis? As noted previously, strain and stress components are calculated in the specified coordinate system. The coordinate system seldom is such that maximum stress conditions are automatically obtained. Here is the point: Essentially every finite element software package not only computes strain and stress components in the global and element coordinate systems but also principal stresses and the equivalent (Von Mises) stress for every element. In deciding whether a design is acceptable (and this is why we use FEA, isn't it?), we must examine the propensity to failure. The examination of stress data is the responsibility of the user of FEA software. The software does *not* produce results that indicate failure unless the analyst carefully considers the data in terms of specific failure criteria.

Among the stress- and strain-related items generally available as a result of solution are the computed stresses (in the specified coordinate system), the principal stresses, the equivalent stress, the principal strains, and strain energy. With the exception of strain energy, the stress data are available on either a nodal or element basis. The distinction is significant, and the analyst must be acutely aware of the distinction. Since strain components (therefore, stress components) are not in general continuous across element boundaries, nodal stresses are computed as average values based on all elements connected to a specific node. On the other hand, element stresses represent values computed at the element centroid. Hence, element stress data are more accurate and should be used in making engineering judgments. To illustrate, we present some of the stress data obtained in the solution of Example 9.4 based on two-dimensional, four-node quadrilateral elements. In the model, node 107 (selected randomly) is common to four elements. Table 9.1 lists the stresses computed at this node in terms of the four connected elements. The values are obtained by computing the nodal stresses for each of the four elements independently, then extracting the values

Table 9.1 Stress Values (psi) Computed at Node 107 of Example 9.4

	σ_x	σ_y	τ_{xy}
Element 1	2049.3	187.36	118.4
Element 2	2149.4	315.59	91.89
Element 12	1987.3	322.72	204.13
Element 99	1853.8	186.88	378.36
Average	2009.8	253.14	198.19

Table 9.2 Element Stress Components (psi) for Four Elements Sharing a Common Node in Example 9.4

	σ_x	σ_y	τ_{xy}	σ_e
Element 1	2553.5	209.71	179.87	2475.8
Element 2	1922.7	351.69	43.55	1774.8
Element 12	1827.5	264.42	154.44	1731.5
Element 99	2189.0	249.14	480.57	2236.4

for the common node. The last row of the table lists the average values of the three stress components at the common node. Clearly, the nodal stresses are not continuous from element to element at the common node. As previously discussed, the magnitudes of the discontinuities should decrease as the element mesh is refined.

In contrast, the *element* stress components for the same four elements are shown in Table 9.2. The values listed in the table are computed at the element centroid and include the equivalent (Von Mises) stress as defined previously. While not included in the table, the principal stress components are also available from the solution. In general, the element stresses should be used in results evaluation, especially in terms of application of failure theories.

9.8 PRACTICAL CONSIDERATIONS

Probably the most critical step in application of the finite element method is the choice of element type for a given problem. The solid elements discussed in this chapter are among the simplest elements available for use in stress analysis. Many more element types are available to the finite element analyst. (One commercial software system has no fewer than 141 element types.) The differences in elements for stress analysis fall into three categories: (1) number of nodes, hence, polynomial order of interpolation functions; (2) type of material behavior (elastic, plastic, thermal stress, for example); and (3) loading and geometry of the structure to be modeled (plane stress, plane strain, axisymmetric, general three dimensional, bending, torsion).

As an example, consider Figure 9.12, which shows a flat plate supported at the corners and loaded by a pressure distribution $p(x, y)$ acting in the negative z direction. The primary mode of deformation of the plate is bending in the z direction. To adequately describe the behavior, a finite element used to model the plate must be such that continuity of slope in both xz and yz planes is ensured. Therefore, a three-dimensional solid element as described in Section 9.8 would not be appropriate as only the displacement components are included as nodal variables. Instead, an element that includes partial derivatives representing the slopes must be included as nodal variables. Plate elements have been developed on the basis of the theory of thin plates (usually only covered in graduate programs) in which

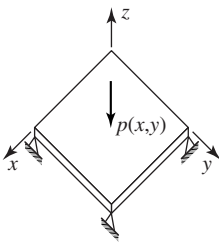


Figure 9.12
Example of a thin
plate subjected to
bending.

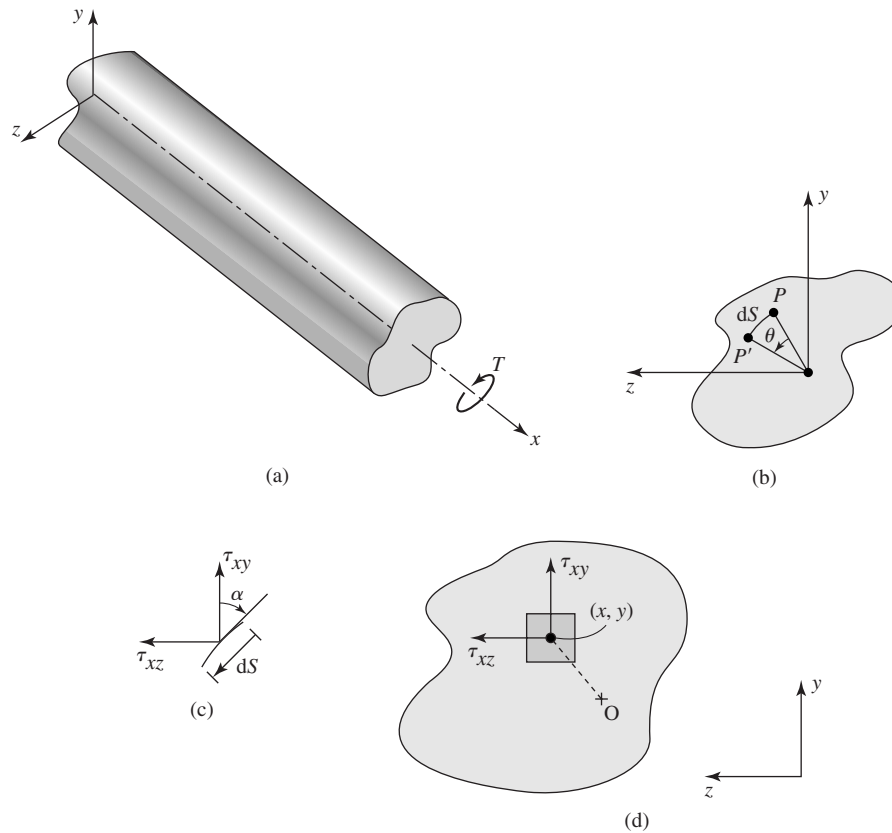


Figure 9.13

(a) A general, noncircular section in torsion. (b) Motion of a point from P to P' as a result of cross-section rotation. (c) A differential element at the surface of a torsion member. (d) A differential element showing the contribution of shear stress to torque.

the bending deflection is governed by a fourth-order partial differential equation. The simplest such element is a four-node element using cubic interpolation functions and having 4 degrees of freedom (displacement, two slopes, and a mixed second derivative) at each node [4]. A similar situation exists with shell (thin curved plate) structures. Specialized elements are required (and available) for structural analysis of shell structures. The major point here is that a breadth of knowledge and experience is required for a finite element analyst to become truly proficient at selecting the correct element type(s) for a finite element model and, subsequently interpreting the results of the analysis.

Once the element type has been selected, the task becomes that of defining the model geometry as a mesh of finite elements. In its most rudimentary form, this task involves defining the coordinate location of every node in the model

(note that, by default, the nodes define the geometry) followed by definition of all elements in terms of nodes. Many years ago, in the early development of the finite element method, the tasks of node and element definition were labor intensive, as the definitions required use of the specific language statements of a particular finite element software system. The tasks were laborious, to say the least, and prone to error. With currently technology, especially graphical user interfaces and portability of computer-aided design (CAD) databases, these tasks have been greatly simplified. It is now possible, with many FEA programs, to “import” the geometry of a component, structure, or assembly directly from a CAD system, so that geometry does not need to be defined. The finite element software can then automatically create a mesh (*automeshing*) of finite elements to represent the geometry. The advantages of this capability include (1) the finite element analyst need not redefine the geometry; consequently, (2) the designer’s intent is not changed inadvertently; and (3) the finite element analyst is relieved of the burden of specifying the details of the node and element definitions. The major disadvantage is that the analyst is not in *direct* control of the meshing operation.

The word direct is emphasized. In automeshing, the software user has some control over the meshing process. There are two general types of automeshing software, generally referred to as *free meshing* and *mapped meshing*. In free meshing, the user specifies a general, qualitative mesh description, ranging from coarse to fine, with 10 or more gradations between the extremes. The software then generates the mesh accordingly. In mapped meshing, the user specifies quantitative information regarding node spacing, hence, element size, and the software uses the prescribed information to generate nodes and elements. In either method, the software user has some degree of control over the element mesh.

A very important aspect of meshing a model with elements is to ensure that, in regions of geometric discontinuity, a finer mesh (smaller elements) is defined in the region. This is true in all finite element analyses (structural, thermal, and fluid), because it is known that gradients are higher in such areas and finer meshes are required to adequately describe the physical behavior. In mapped meshing, this is defined by the software user. Fortunately, in free meshing, this aspect is accounted for in the software. As an example, refer back to Example 9.4, in which we examined the stress concentration factor for a hole in a thin plate subjected to tension. The solution was modeled using the free mesh feature of a finite element software system. Figure 9.8b is a coarse mesh as generated by the software. Geometry is defined by four lines and a quarter-circular arc; these, in turn, define a single area of interest. Having specified the element type (in this case a plane stress, elastic, quadrilateral), the area meshing feature is used to generate the elements as shown. It is important to note the relatively fine mesh in the vicinity of the arc representing the hole. This is generated by the software automatically in recognition of the geometry. The mesh-refined models of Figure 9.8c and 9.8d are also generated by the free meshing routine. From each of these cases, we see that, not only does the number of elements increase, but the

relative size of the elements in the vicinity of the hole is maintained relative to elements far removed from the discontinuity.

The automeshing capabilities of finite software as briefly described here are extremely important in reducing the burden of defining a finite element model of any geometric situation and should be used to the maximum extent. However, recall that the results of a finite element analysis must be judged by human knowledge of engineering principles. Automated model definition is a nicety of modern finite element software; automated analysis of results is not.

Analysis of results is the postprocessing phase of finite element analysis. Practical models contain hundreds, if not thousands, of elements, and the computed displacements, strains, stresses, and so forth are available for every element. Poring through the data can be a seemingly endless task. Fortunately, finite element software has, as part of the postprocessing phase, routines for sorting the results data in many ways. Of particular importance in stress analysis, the data can be sorted in ascending or descending order of essentially any stress component chosen by the user. Hence, one can readily determine the maximum equivalent stress, for example, and determine the location of that stress by the associated element location. In addition, with modern computer technology, it is possible to produce color-coded stress contour plots of an entire model, to visually observe the stress distribution, the deformed shape, the strain energy distribution, and many other criteria.

9.9 TORSION

Torsion (twisting) of structural members having circular cross sections is a common problem studied in elementary mechanics of materials. (Recall that earlier we developed a finite element for such cases.) A major assumption (and the assumption is quite valid for elastic deformation) in torsion of circular members is that plane sections remain plane after twisting. In the case of torsion of a non-circular cross section, this assumption is not valid and the problem is hence more complicated. A general structural member subjected to torsion is shown in Figure 9.13a. The member is subjected to torque T acting about the x axis, and it is assumed that the cross section is uniform along the length. An arbitrary point located on a cross section at position x is shown in Figure 9.13b. If the cross section twists through angle θ , the point moves through arc ds and the displacement components in the y and z directions are

$$\begin{aligned}v &= -z\theta \\w &= y\theta\end{aligned}\tag{9.132}$$

respectively. Since the angle of twist varies along the length of the member, we conclude that the displacement components of Equation 9.132 are described by

$$v = v(x, z) \quad w = w(x, y)\tag{9.133}$$

Owing to the noncircular cross section, plane sections do not remain plane; instead, there is warping, hence displacement, in the x direction described by

$$u = u(y, z) \quad (9.134)$$

Applying the definitions of the normal strain components to Equation 9.133 and 9.134, we find

$$\begin{aligned} \epsilon_x &= \frac{\partial u}{\partial x} = 0 \\ \epsilon_y &= \frac{\partial v}{\partial y} = 0 \\ \epsilon_z &= \frac{\partial w}{\partial z} = 0 \end{aligned} \quad (9.135)$$

and it follows that the normal stress components are $\sigma_x = \sigma_y = \sigma_z = 0$. To compute the shear strain components, we introduce the angle of twist *per unit length* ϕ such that the rotation of any cross section can be expressed as $\theta = \phi x$. The displacement components are then expressed as

$$u = u(y, z) \quad v = -\phi x z \quad w = \phi x y \quad (9.136)$$

and the shear strain components are

$$\begin{aligned} \gamma_{xy} &= \frac{\partial u}{\partial y} + \frac{\partial v}{\partial x} = \frac{\partial u}{\partial y} - \phi z \\ \gamma_{xz} &= \frac{\partial u}{\partial z} + \frac{\partial w}{\partial x} = \frac{\partial u}{\partial z} + \phi y \\ \gamma_{yz} &= \frac{\partial v}{\partial z} + \frac{\partial w}{\partial y} = 0 \end{aligned} \quad (9.137)$$

It follows from the stress-strain relations that the only nonzero stress components are τ_{xy} and τ_{xz} and the only equilibrium equation (Appendix B) not identically satisfied becomes

$$\frac{\partial \tau_{xy}}{\partial y} + \frac{\partial \tau_{xz}}{\partial z} = 0 \quad (9.138)$$

We now hypothesize the existence of a scalar function $\psi(y, z)$ such that

$$\tau_{xy} = \frac{\partial \psi}{\partial z} \quad \tau_{xz} = -\frac{\partial \psi}{\partial y} \quad (9.139)$$

In the context of the torsion problem, scalar function ψ is known as *Prandtl's stress function* and is generally analogous to the stream function and potential function introduced in Chapter 8 for ideal fluid flow. If the relations of Equation 9.139 are substituted into Equation 9.138, we find that the equilibrium condition is automatically satisfied. To discover the governing equation for the stress

function, we compute the stress components as

$$\begin{aligned}\tau_{xy} &= G\gamma_{xy} = G\left(\frac{\partial u}{\partial y} - \phi z\right) \\ \tau_{xz} &= G\gamma_{yz} = G\left(\frac{\partial u}{\partial z} + \phi y\right)\end{aligned}\quad (9.140)$$

and note that

$$\begin{aligned}\frac{\partial \tau_{xy}}{\partial z} &= G\left(\frac{\partial^2 u}{\partial y \partial z} - \phi\right) \\ \frac{\partial \tau_{xz}}{\partial y} &= G\left(\frac{\partial^2 u}{\partial y \partial z} + \phi\right)\end{aligned}\quad (9.141)$$

Combining the last two equations results in

$$\frac{\partial \tau_{xy}}{\partial z} - \frac{\partial \tau_{xz}}{\partial y} = \frac{\partial^2 \psi}{\partial y^2} + \frac{\partial^2 \psi}{\partial z^2} = -2G\phi \quad (9.142)$$

as the governing equation for Prandtl's stress function. As with the fluid formulations of Chapter 8, note the analogy of Equation 9.142 with the case of heat conduction. Here the term $2G\phi$ is analogous to internal heat generation Q .

9.9.1 Boundary Condition

At the outside surface of the torsion member, no stress acts normal to the surface, so the resultant of the shear stress components must be tangent to the surface. This is illustrated in Figure 9.13c showing a differential element dS of the surface (with the positive sense defined by the right-hand rule). For the normal stress to be zero, we must have

$$\tau_{xy} \sin \alpha - \tau_{xz} \cos \alpha = 0 \quad (9.143)$$

or

$$\tau_{xy} \frac{dz}{ds} - \tau_{xz} \frac{dy}{ds} = 0 \quad (9.144)$$

Substituting the stress function relations, we obtain

$$\frac{\partial \psi}{\partial z} \frac{dz}{ds} + \frac{d\psi}{dy} \frac{dy}{ds} = \frac{d\psi}{ds} = 0 \quad (9.145)$$

which shows that the value of the stress function is constant on the surface. The value is arbitrary and most often taken to be zero.

9.9.2 Torque

The stress function formulation of the torsion problem as given previously does not explicitly include the applied torque. To obtain an expression relating the

applied torque and the stress function, we must consider the moment equilibrium condition. Referring to the differential element of a cross section shown in Figure 9.13d, the differential torque corresponding to the shear stresses acting on the element is

$$dT = (y\tau_{xz} - z\tau_{xy}) dA \quad (9.146)$$

and the total torque is computed as

$$T = \iint_A (y\tau_{xz} - z\tau_{xy}) dA = - \iint_A \left(y \frac{\partial \psi}{\partial y} + z \frac{\partial \psi}{\partial z} \right) dy dz = 2 \iint_A \psi dA \quad (9.147)$$

The final result in the last equation is obtained by integrating by parts and noting the condition $\psi = 0$ on the surface.

9.9.3 Finite Element Formulation

Since the governing equation for the stress function is analogous to the heat conduction equation, it is not necessary to repeat the details of element formulation. Instead, we reiterate the analogies and point out one very distinct difference in how a finite element analysis of the torsion problem is conducted when the stress function is used. First, note that the stress function is discretized as

$$\psi\{y, z\} = \sum_i^M N_i(y, z)\psi_i \quad (9.148)$$

so that the finite element computations result in nodal values analogous to nodal temperatures (with the conductivity values set to unity). Second, the torsion term $2G\phi$ is analogous to internal heat generation Q . However, the angle of twist per unit length ϕ is actually the unknown we wish to compute in the first place. Preferably, in such a problem, we specify the geometry, material properties, and applied torque, then compute the angle of twist per unit length as well as stress values. However, the formulation here is such that we must specify a value for angle of twist per unit length, compute the nodal values of the stress function, then obtain the torque by summing the contributions of all elements to Equation 9.147. Since the governing equation is linear, the angle of twist per unit length and the computed torque can be scaled in ratio as required. The procedure is illustrated in the following example.

EXAMPLE 9.7

Figure 9.14a shows a shaft having a square cross section with 50-mm sides. The material has shear modulus 80 Gpa. Shaft length is 1 m. The shaft is fixed at one end and subjected to torque T at the other end. Determine the total angle of twist if the applied torque is 100 N-m.

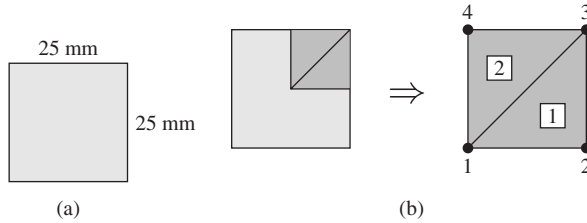


Figure 9.14 Finite element model of Example 9.7.

■ **Solution**

Observing the symmetry conditions, we model one-fourth of the cross section using three-node linear triangular elements, as in Figure 9.14b. For simplicity of illustration, we use only two elements and note that, at nodes 2, 3, and 4, the value of the stress function is specified as zero, since these nodes are on the surface. Also note that the planes of symmetry are such that the partial derivatives of the stress function across those planes are zero. These conditions correspond to zero normal heat flux (perfect insulation) in a conduction problem.

The element stiffness matrices are given by

$$[k^{(e)}] = \iint_A \left(\left[\frac{\partial N}{\partial y} \right]^T \left[\frac{\partial N}{\partial y} \right] + \left[\frac{\partial N}{\partial z} \right]^T \left[\frac{\partial N}{\partial z} \right] \right) dA$$

and element nodal forces are

$$\{f^{(e)}\} = \iint_A 2G\phi [N]^T dA$$

(Note the use of y, z coordinates in accord with the coordinate system used in the preceding developments.)

These relations are obtained by analogy with Equation 7.35 for heat conduction. The interpolation functions are as defined in Equation 9.28.

Element 1

$$\begin{aligned} N_1 &= \frac{1}{2A}(625 - 25y) & \frac{\partial N_1}{\partial y} &= -\frac{25}{2A} & \frac{\partial N_1}{\partial z} &= 0 \\ N_2 &= \frac{1}{2A}(25y - 25z) & \frac{\partial N_2}{\partial y} &= \frac{25}{2A} & \frac{\partial N_2}{\partial z} &= -\frac{25}{2A} \\ N_3 &= \frac{1}{2A}(25z) & \frac{\partial N_3}{\partial y} &= 0 & \frac{\partial N_3}{\partial z} &= \frac{25}{2A} \end{aligned}$$

Since the partial derivatives are all constant, the stiffness matrix is

$$[k^{(1)}] = \frac{1}{4A} \begin{Bmatrix} -25 \\ 25 \\ 0 \end{Bmatrix} [-25 \quad 25 \quad 0] + \frac{1}{4A} \begin{Bmatrix} 0 \\ -25 \\ 25 \end{Bmatrix} [0 \quad -25 \quad 25]$$

or

$$[k^{(1)}] = \frac{1}{1250} \begin{bmatrix} 625 & -625 & 0 \\ -625 & 625 & 0 \\ 0 & 0 & 0 \end{bmatrix} + \frac{1}{1250} \begin{bmatrix} 0 & 0 & 0 \\ 0 & 625 & -625 \\ 0 & -625 & 625 \end{bmatrix}$$

$$= \begin{bmatrix} 0.5 & -0.5 & 0 \\ -0.5 & 1 & -0.5 \\ 0 & -0.5 & 0.5 \end{bmatrix}$$

The element nodal forces are readily shown to be given by

$$\{f^{(1)}\} = \frac{2G\phi A}{3} \begin{Bmatrix} 1 \\ 1 \\ 1 \end{Bmatrix}$$

which we leave in this general form for the time being.

Element 2

$$N_1 = \frac{1}{2A}(625 - 25z) \quad \frac{\partial N_1}{\partial y} = 0 \quad \frac{\partial N_1}{\partial z} = -\frac{25}{2A}$$

$$N_2 = \frac{1}{2A}(25y) \quad \frac{\partial N_2}{\partial y} = \frac{25}{2A} \quad \frac{\partial N_2}{\partial z} = 0$$

$$N_3 = \frac{1}{2A}(25z - 25y) \quad \frac{\partial N_3}{\partial y} = -\frac{25}{2A} \quad \frac{\partial N_3}{\partial z} = \frac{25}{2A}$$

$$[k^{(2)}] = \frac{1}{4A} \begin{Bmatrix} 0 \\ 25 \\ -25 \end{Bmatrix} [0 \quad 25 \quad -25] + \frac{1}{4A} \begin{Bmatrix} -25 \\ 0 \\ 25 \end{Bmatrix} [-25 \quad 0 \quad 25]$$

$$[k^{(2)}] = \frac{1}{1250} \begin{bmatrix} 0 & 0 & 0 \\ 0 & 625 & -625 \\ 0 & -625 & 625 \end{bmatrix} + \frac{1}{1250} \begin{bmatrix} 625 & 0 & -625 \\ 0 & 0 & 0 \\ -625 & 0 & 625 \end{bmatrix}$$

$$= \begin{bmatrix} 0.5 & 0 & -0.5 \\ 0 & 0.5 & -0.5 \\ -0.5 & -0.5 & 1.0 \end{bmatrix}$$

For element 2, the nodal forces are also given by

$$\{f^{(2)}\} = \frac{2G\phi A}{3} \begin{Bmatrix} 1 \\ 1 \\ 1 \end{Bmatrix}$$

Noting the element to global nodal correspondences, the assembled system equations are

$$\begin{bmatrix} 1 & -0.5 & 0 & -0.5 \\ -0.5 & 1 & -0.5 & 0 \\ 0 & -0.5 & 1 & -0.5 \\ -0.5 & 0 & -0.5 & 1 \end{bmatrix} \begin{Bmatrix} \psi_1 \\ \psi_2 \\ \psi_3 \\ \psi_4 \end{Bmatrix} = \frac{2G\phi A}{3} \begin{Bmatrix} 2 \\ 1 \\ 2 \\ 1 \end{Bmatrix}$$

Since nodes 2, 3, and 4 are on the outside surface, we set $\psi_2 = \psi_3 = \psi_4 = 0$ to obtain the solution

$$\psi_1 = \frac{4G\phi A}{3}$$

We still have not addressed the problem that the angle of twist per unit length is unknown and continue to ignore that problem temporarily, since for this very simple two-element model, we can continue with the hand solution. The torque is given by Equation 9.149 as

$$T = 2 \iint_A \psi \, dA$$

but the integration is over the entire cross section. Hence, we must sum the contribution from each element and, in this case, since we applied the symmetry conditions to reduce the model to one-fourth size, multiply the result by 4. For each element, the torque contribution is

$$T^{(e)} = 2 \iint_A [N^{(e)}] \, dA \{ \psi^{(e)} \}$$

and for the linear triangular element this simply becomes

$$T^{(e)} = \frac{2A}{3} (\psi_1^{(e)} + \psi_2^{(e)} + \psi_3^{(e)})$$

Accounting for the use of symmetry, the total torque indicated by our two-element solution is

$$T = 4 \frac{2A}{3} (\psi_1^{(1)} + \psi_2^{(2)}) = \frac{64}{9} G \phi A^2$$

or

$$\frac{T}{\phi} = \frac{64}{9} G A^2$$

Now we address the problem of unknown angle of twist per unit length. Noting, in the last equation, the ratio is constant for specified shear modulus and cross-sectional area, we could simply specify an arbitrary value of ϕ , follow the solution procedure to compute the corresponding torque, compute the ratio, and scale the result as needed. If, for example, we had assumed $\phi = 10^{-6}$ rad/mm, our result would be

$$T = \frac{64}{9} (80)(10^3)(10^{-6})(312.5)^2 = 55555.6 \text{ N}\cdot\text{mm} \Rightarrow 55.6 \text{ N}\cdot\text{m}$$

Thus, to answer the original question, we compute the angle of twist per unit length corresponding to the specified torque as

$$\phi = \frac{100}{55.6} (10^{-6}) \approx 1.8(10^{-6}) \text{ rad/mm}$$

and the total angle of twist would be

$$\theta = \phi L = 1.8(10^{-6})(1000) = 1.8(10^{-3}) \text{ rad}$$

or about 0.1 degree. The exact solution [5] for this problem shows the angle of twist per unit length to be $\phi = 1.42(10^{-6})$ rad/mm. Hence, our very simple model is in error by about 27 percent.

9.10 SUMMARY

In this chapter, we present the development of the most basic finite elements used in stress analysis in solid mechanics. As the finite element method was originally developed for stress analysis, the range of element and problem types that can be analyzed by the method are very large. Our description of the basic concepts is intended to give the reader insight on the general procedures used to develop element equations and understand the ramifications on element, hence, model, formulation for various states of stress. As mentioned in the context of plate bending in Section 9.8, finite element analysis involves many advanced topics in engineering not generally covered in an undergraduate program. The interested reader is referred to the many advanced-level texts on the finite element method for further study. The intent here is to introduce the basic concepts and generate interest in learning more of the subject.

REFERENCES

1. Kreyszig, E. *Advanced Engineering Mathematics*, 5th ed. New York: John Wiley and Sons, 1983.
2. Shigley, J. E. *Mechanical Engineering Design*, 6th ed. New York: McGraw-Hill, 1998.
3. Cowper, G. R. "Gaussian Quadrature Formulas for Triangles." *International Journal for Numerical Methods in Engineering* 7 (1973).
4. Huebner, K. H., and E. A. Thornton. *The Finite Element Method for Engineers*, 2nd ed. New York: John Wiley and Sons, 1982.
5. Timoshenko, S. P., and J. N. Goodier. *Theory of Elasticity*, New York: McGraw-Hill, 1970.

PROBLEMS

- 9.1 Use the general stress-strain relations from Appendix B and the assumptions of plane stress to derive Equations 9.2.
- 9.2 Let $\{z\}$ be the $N \times 1$ column matrix $[z_1 \ z_2 \ z_3 \ \cdots \ z_N]^T$ and let $[A]$ be an $N \times N$ real-valued matrix. Show that the matrix product $\{z\}^T [A] \{z\}$ always results in a scalar, quadratic function of the components z_i .

- 9.3 Beginning with the general elastic stress-strain relations, derive Equation 9.50 for the conditions of plane strain.
- 9.4 Determine the strain-displacement matrix $[B]$ for a three-node triangular element in plane strain.
- 9.5 Determine the strain-displacement matrix $[B]$ for a four-node rectangular element in plane stress.
- 9.6 Using the interpolation functions given in Equation 9.28, determine the explicit expression for the strain energy in a three-node triangular element in plane stress.
- 9.7 The constant strain triangular element shown in Figure P9.7 is subjected to a uniformly distributed pressure as shown. Determine the equivalent nodal forces.

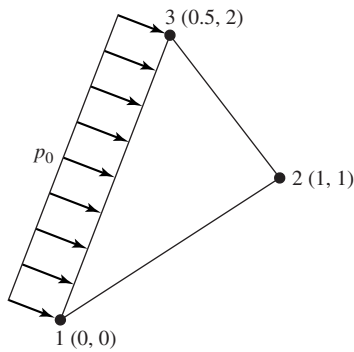


Figure P9.7

- 9.8 The constant strain triangular element shown in Figure P9.8 is subjected to the linearly varying pressure as shown and a body force from gravity ($g = 386.4 \text{ in./s}^2$) in the negative y direction. Determine the equivalent nodal forces.

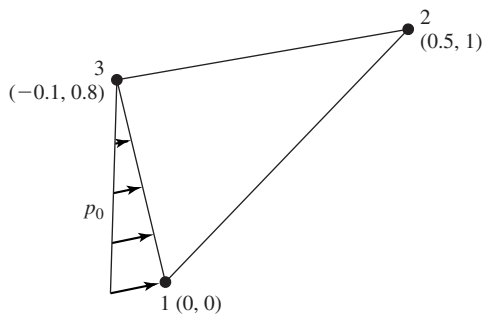


Figure P9.8

- 9.9 The element of Figure P9.7 is of a material for which the modulus of elasticity is $E = 15 \times 10^6 \text{ psi}$ and Poisson's ratio is $\nu = 0.3$. Determine the element stiffness matrix if the element is subjected to plane stress.

- 9.10 Repeat Problem 9.9 for plane strain.
- 9.11 Repeat Problem 9.9 for an axisymmetric element.
- 9.12 The overall loading of the element in Problem 9.7 is such that the nodal displacements are $u_1 = 0.003$ in., $v_1 = 0$, $u_2 = 0.001$ in., $v_2 = 0.0005$ in., $u_3 = 0.0015$ in., $v_3 = 0$. Calculate the element strain, stress, and strain energy assuming plane stress conditions.
- 9.13 Repeat Problem 9.13 for plane strain conditions.
- 9.14 A thin plate of unit thickness is supported and loaded as shown in Figure P9.14. The material is steel, for which $E = 30 \times 10^6$ and $\nu = 0.3$. Using the four constant strain triangular elements shown by the dashed lines, compute the deflection of point A. Compare the total strain energy with the work of the external force system.

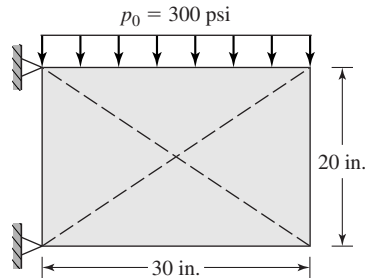


Figure P9.14

- 9.15 Integrate Equation 9.65 by the Gaussian numerical procedure to verify Equation 9.66.
- 9.16 A three-node triangular element having nodal coordinates, shown in Figure P9.16, is to be used as an axisymmetric element. The material properties are $E = 82$ GPa and $\nu = 0.3$. The dimensions are in millimeters. Calculate the element stiffness matrix using both the exact definition of Equation 9.99 and the centroidal approximation of Equation 9.100. Are the results significantly different?

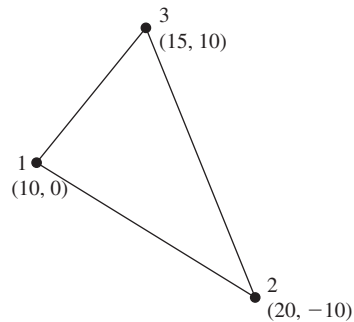


Figure P9.16

- 9.17 The axisymmetric element in Figure P9.16 is subjected to a uniform, normal pressure p_0 acting on the surface defined by nodes 1 and 3. Compute the equivalent nodal forces.
- 9.18 The axisymmetric element in Figure P9.16 is part of a body rotating about the z axis at a constant rate of 3600 revolutions per minute. Determine the corresponding nodal forces.
- 9.19 Consider the higher-order three-dimensional element shown in Figure P9.19, which is assumed to be subjected to a general state of stress. The element has 20 nodes, but all nodes are not shown for clarity.
- What is the order of the polynomial used for interpolation functions?
 - How will the strains (therefore, stresses) vary with position in the element?
 - What is the size of the stiffness matrix?
 - What advantages and disadvantages are apparent in using this element in comparison to an eight-node brick element?

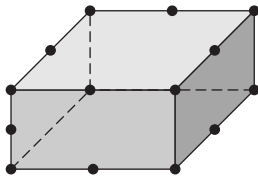
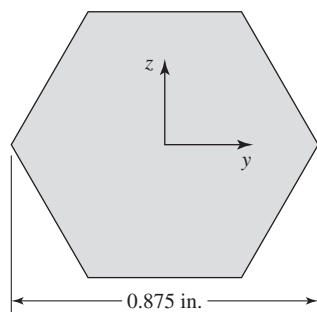


Figure P9.19

- 9.20 Show that in a uniaxial tension test the distortion energy at yielding is given by Equation 9.128.
- 9.21 A finite element analysis of a certain component yields the maximum principal stresses $\sigma_1 = 200$ MPa, $\sigma_2 = 0$, $\sigma_3 = -90$ MPa. If the tensile strength of the material is 270 MPa, is yielding indicated according to the distortion energy theory? If not, what is the “safety factor” (ratio of yield strength to equivalent stress)?
- 9.22 Repeat Problem 9.21 if the applicable failure theory is the maximum shear stress theory.
- 9.23 The torsion problem as developed in Section 9.9 has a governing equation analogous to that of two-dimensional heat conduction. The stress function is analogous to temperature, and the angle of twist per unit length term ($2G\phi$) is analogous to internal heat generation.
- What heat transfer quantities are analogous to the shear stress components in the torsion problem?
 - If one solved a torsion problem using finite element software for two-dimensional heat transfer, how would the torque be computed?
- 9.24 The torsion problem as developed in Section 9.9 is two-dimensional when posed in terms of the Prandtl stress function. Could three-dimensional elastic solid elements (such as the eight-node brick element) be used to model the torsion problem? If yes, how would a pure torsional loading be applied?
- 9.25 Figure P9.25 shows the cross section of a hexagonal shaft used in a quick-change power transmission coupling. The shear modulus of the material is 12×10^6 psi

**Figure P9.25**

and the shaft length is 12 in. Determine the total angle of twist when the shaft is subjected to a net torque of 250 ft-lb. Use linear triangular elements and take advantage of all appropriate symmetry conditions.

CHAPTER 10

Structural Dynamics

10.1 INTRODUCTION

In addition to static analyses, the finite element method is a powerful tool for analyzing the dynamic response of structures. As illustrated in Chapter 7, the finite element method in combination with the finite difference method can be used to examine the transient response of heat transfer situations. A similar approach can be used to analyze the transient dynamic response of mechanical structures. However, in the analysis of structures, an additional tool is available. The tool, known as *modal analysis*, has its basis in the fact that every mechanical structure exhibits natural modes of vibration (dynamic response) and these modes can be readily computed given the elastic and inertia characteristics of the structure.

In this chapter, we introduce the concept of natural modes of vibration via the simple harmonic oscillator system. Using the finite element concepts developed in earlier chapters, the simple harmonic oscillator is represented as a finite element system and the basic ideas of natural frequency and natural mode are introduced. The single degree of freedom simple harmonic oscillator is then extended to multiple degrees of freedom, to illustrate the existence of multiple natural frequencies and vibration modes. From this basis, we proceed to more general dynamic analyses using the finite element method.

10.2 THE SIMPLE HARMONIC OSCILLATOR

The so-called simple harmonic oscillator is a combination of a linear elastic spring having free length L and a concentrated mass as shown in Figure 10.1a. The mass of the spring is considered negligible. The system is assumed to be subjected to gravity in the vertical direction, and the upper end of the spring is attached to a rigid support. With the system in equilibrium as in Figure 10.1b, the

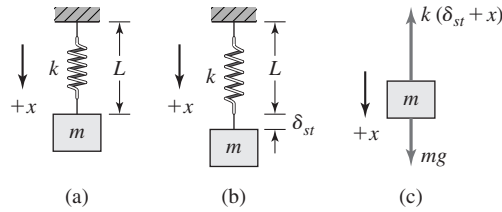


Figure 10.1

(a) Simple harmonic oscillator. (b) Static equilibrium position. (c) Free-body diagram for arbitrary position x .

gravitational force is in equilibrium with the spring force so

$$\sum F_x = 0 = mg - k\delta_{st} \tag{10.1}$$

where δ_{st} is the equilibrium elongation of the spring and x is measured positive downward from the equilibrium position; that is, when $x = 0$, the system is at its equilibrium position.

If, by some action, the mass is displaced from its equilibrium position, the force system becomes unbalanced, as shown by the free-body diagram of Figure 10.1c. We must apply Newton's second law to obtain

$$\sum F_x = ma_x = m \frac{d^2x}{dt^2} = mg - k(\delta_{st} + x) \tag{10.2}$$

Incorporating the equilibrium condition expressed by Equation 10.1, Equation 10.2 becomes

$$m \frac{d^2x}{dt^2} + kx = 0 \tag{10.3}$$

Equation 10.3 is a second-order, linear, ordinary differential equation with constant coefficients. (And physically, we assume that the coefficients m and k are positive.) Equation 10.3 is most-often expressed in the form

$$\frac{d^2x}{dt^2} + \frac{k}{m}x = \frac{d^2x}{dt^2} + \omega^2x = 0 \tag{10.4}$$

The general solution for Equation 10.4 is

$$x(t) = A \sin \omega t + B \cos \omega t \tag{10.5}$$

where A and B are the constants of integration. Recall that the solution of a second-order differential equation requires the specification of two constants to determine the solution to a specific problem. When the differential equation describes the time response of a mechanical system, the constants of integration are most-often called the *initial conditions*.

10.2 The Simple Harmonic Oscillator

Equation 10.5 shows that the variation of displacement of the mass as a function of time is periodic. Using basic trigonometric identities, Equation 10.5 can be equivalently expressed as

$$x(t) = C \sin(\omega t + \phi) \tag{10.6}$$

where the constants A and B have been replaced by constants of integration C and ϕ . Per Equation 10.6, the mass oscillates sinusoidally at *circular frequency* ω and with constant *amplitude* C . Phase angle ϕ is indicative of position at time 0 since $x(0) = C \sin \phi$. Also, note that, since $x(t)$ is measured about the equilibrium position, the oscillation occurs about that position. The circular frequency is

$$\omega = \sqrt{\frac{k}{m}} \text{ rad/sec} \tag{10.7}$$

and is a constant value determined by the physical characteristics of the system. In this simple case, the *natural circular frequency*, as it is often called, depends on the spring constant and mass only. Therefore, if the mass is displaced from the equilibrium position and released, the oscillatory motion occurs at a constant frequency determined by the physical parameters of the system. In the case described, the oscillatory motion is described as *free vibration*, since the system is free of all external forces excepting gravitational attraction.

Next, we consider the simple harmonic oscillator in the finite element context. From Chapter 2, the stiffness matrix of the spring is

$$[k^{(e)}] = k \begin{bmatrix} 1 & -1 \\ -1 & 1 \end{bmatrix} \tag{10.8}$$

and the equilibrium equations for the element are

$$k \begin{bmatrix} 1 & -1 \\ -1 & 1 \end{bmatrix} \begin{Bmatrix} u_1 \\ u_2 \end{Bmatrix} = \begin{Bmatrix} f_1 \\ f_2 \end{Bmatrix} \tag{10.9}$$

which is identical to Equation 2.4. However, the spring element is not in static equilibrium, so we must examine the nodal forces in detail.

Figure 10.2 shows free-body diagrams of the spring element and mass, respectively. The free-body diagrams depict snapshots in time when the system is in motion and, hence, are dynamic free-body diagrams. As the mass of the spring is considered negligible, Equation 10.9 is valid for the spring element. For the mass, we have

$$\sum F_x = ma_x = m \frac{d^2u_2}{dt^2} = mg - f_2 \tag{10.10}$$

from which the force on node 2 is

$$f_2 = mg - m \frac{d^2u_2}{dt^2} \tag{10.11}$$

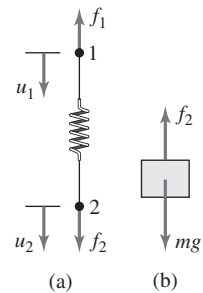


Figure 10.2 Free-body diagrams of (a) a spring and (b) a mass, when treated as parts of a finite element system.

Substituting for f_2 in Equation 10.9 gives

$$k \begin{bmatrix} 1 & -1 \\ -1 & 1 \end{bmatrix} \begin{Bmatrix} u_1 \\ u_2 \end{Bmatrix} = \begin{Bmatrix} f_1 \\ mg - m\ddot{u}_2 \end{Bmatrix} \quad (10.12)$$

where $\ddot{u}_2 = d^2u_2/dt^2$. The dynamic effect of the inertia of the attached mass is shown in the second of the two equations represented by Equation 10.12. Equation 10.12 can also be expressed as

$$\begin{bmatrix} 0 & 0 \\ 0 & m \end{bmatrix} \begin{Bmatrix} \ddot{u}_1 \\ \ddot{u}_2 \end{Bmatrix} + k \begin{bmatrix} 1 & -1 \\ -1 & 1 \end{bmatrix} \begin{Bmatrix} u_1 \\ u_2 \end{Bmatrix} = \begin{Bmatrix} f_1 \\ mg \end{Bmatrix} \quad (10.13)$$

where we have introduced the mass matrix

$$[m] = \begin{bmatrix} 0 & 0 \\ 0 & m \end{bmatrix} \quad (10.14)$$

and the nodal acceleration matrix

$$\{\ddot{u}\} = \begin{Bmatrix} \ddot{u}_1 \\ \ddot{u}_2 \end{Bmatrix} \quad (10.15)$$

For the simple harmonic oscillator of Figure 10.1, we have the constraint (boundary) condition $u_1 = 0$, so the first of Equation 10.13 becomes simply $-ku_2 = f_1$, while the second equation is

$$m\ddot{u}_2 + ku_2 = mg \quad (10.16)$$

Note that Equation 10.16 is *not* the same as Equation 10.3. Do the two equations represent the same physical phenomenon? To show that the answer is yes, we solve Equation 10.16 and compare the results with the solution given in Equation 10.6.

Recalling that the solution of any differential equation is the sum of a homogeneous (complementary) solution and a particular solution, both solutions must be obtained for Equation 10.16, since the equation is not homogeneous (i.e., the right-hand side is nonzero). Setting the right-hand side to zero, the form of the homogeneous equation is the same as that of Equation 10.3, so by analogy, the homogeneous solution is

$$u_{2h}(t) = C \sin(\omega t + \phi) \quad (10.17)$$

where ω , C , and ϕ are as previously defined. The particular solution must satisfy Equation 10.16 exactly for all values of time. As the right-hand side is constant, the particular solution must also be constant; hence,

$$u_{2p}(t) = \frac{mg}{k} = \delta_{st} \quad (10.18)$$

which represents the static equilibrium solution per Equation 10.1. The complete solution is then

$$u_2(t) = u_{2h}(t) + u_{2p}(t) = \delta_{st} + C \sin(\omega t + \phi) \quad (10.19)$$

Equation 10.19 represents a sinusoidal oscillation around the equilibrium position and is, therefore, the same as the solution given in Equation 10.6. Given the displacement of node 2, the reaction force at node 1 is obtained via the constraint equation as

$$f_1 = -ku_2(t) = -k(\delta_{st} + C \sin(\omega t + \phi)) \quad (10.20)$$

Amplitude C and phase angle ϕ are determined by application of the initial conditions, as illustrated in the following example.

EXAMPLE 10.1

A simple harmonic oscillator has $k = 25$ lb/in. and $mg = 20$ lb. The mass is displaced downward a distance of 1.5 in. from the equilibrium position. The mass is released from that position with zero initial velocity at $t = 0$. Determine (a) the natural circular frequency, (b) the amplitude of the oscillatory motion, and (c) the phase angle of the oscillatory motion.

■ Solution

The natural circular frequency is

$$\omega = \sqrt{\frac{k}{m}} = \sqrt{\frac{25}{20/386.4}} = 21.98 \text{ rad/sec}$$

where, for consistency of units, the mass is obtained from the weight using $g = 386.4$ in./s².

The given initial conditions are

$$u_2(t = 0) = \delta_{st} + 1.5 \text{ in.} \quad \dot{u}_2(t = 0) = 0 \text{ in./sec}$$

and the static deflection is $\delta_{st} = W/k = 20/25 = 0.8$ in. Therefore, we have $u_2(0) = 2.3$ in. The motion of node 2 (hence, the mass) is then given by Equation 10.19 as

$$u_2(t) = 0.8 + C \sin(21.98t + \phi) \text{ in.}$$

and the velocity is

$$\dot{u}_2(t) = \frac{du_2}{dt} = 21.98C \cos(21.98t + \phi) \text{ in./sec}$$

Applying the initial conditions results in the equations

$$u_2(t = 0) = 2.3 = 0.8 + C \sin \phi$$

$$\dot{u}_2(t) = 0 = 21.98C \cos \phi$$

The initial velocity equation is satisfied by $C = 0$ or $\phi = \pi/2$. If the former is true, the initial displacement equation cannot be satisfied, so we conclude that $\phi = \pi/2$. Substituting into the displacement equation then gives the amplitude C as 1.5 in. The complete motion solution is

$$u_2(t) = 0.8 + 1.5 \sin\left(21.98t + \frac{\pi}{2}\right) = 0.8 + 1.5 \cos(21.98t) \text{ in.}$$

indicating that the mass oscillates 1.5 in. above and below the static equilibrium position continuously in time and completes one cycle every $2\pi/21.98$ sec. Therefore, the cyclic frequency is

$$f = \frac{\omega}{2\pi} = \frac{21.98}{2\pi} = 3.5 \text{ cycles/sec (Hz)}$$

The cyclic frequency is often simply referred to as the *natural frequency*. The time required to complete one cycle of motion is known as the *period* of oscillation, given by

$$\tau = \frac{1}{f} = \frac{1}{3.5} = 0.286 \text{ sec}$$

10.2.1 Forced Vibration

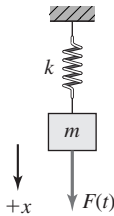


Figure 10.3 Simple harmonic oscillator subjected to external force $F(t)$.

Figure 10.3 shows a simple harmonic oscillator in which the mass is acted on by a time-varying external force $F(t)$. The resulting motion is known as *forced vibration*, owing to the presence of the external forcing function. As the only difference in the applicable free-body diagrams is the external force acting on the mass, the finite element form of the system equations can be written directly from Equation 10.13 as

$$\begin{bmatrix} 0 & 0 \\ 0 & m \end{bmatrix} \begin{Bmatrix} \ddot{u}_1 \\ \ddot{u}_2 \end{Bmatrix} + k \begin{bmatrix} 1 & -1 \\ -1 & 1 \end{bmatrix} \begin{Bmatrix} u_1 \\ u_2 \end{Bmatrix} = \begin{Bmatrix} f_1 \\ mg + F(t) \end{Bmatrix} \quad (10.21)$$

While the constraint equation for the reaction force at node 1 is unchanged, the differential equation for the motion of node 2 is now

$$m\ddot{u}_2 + ku_2 = mg + F(t) \quad (10.22)$$

The complete solution for Equation 10.22 is the sum of the homogeneous solution and two particular solutions, since two nonzero terms are on the right-hand side. As we already obtained the homogeneous solution and the particular solution for the mg term, we focus on the particular solution for the external force. The particular solution of interest must satisfy

$$m\ddot{u}_2 + ku_2 = F(t) \quad (10.23)$$

exactly for all values of time. Dividing by the mass, we obtain

$$\ddot{u}_2 + \omega^2 u_2 = \frac{F(t)}{m} \quad (10.24)$$

where $\omega^2 = k/m$ is the square of the natural circular frequency. Of particular importance in structural dynamic analysis is the case when external forcing functions exhibit sinusoidal variation in time, since such forces are quite common. Therefore, we consider the case in which

$$F(t) = F_0 \sin \omega_f t \quad (10.25)$$

where F_0 is the amplitude or maximum value of the force and ω_f is the circular frequency of the forcing function, or *forcing frequency* for short. Equation 10.24 becomes

$$\ddot{u}_2 + \omega^2 u_2 = \frac{F_0}{m} \sin \omega_f t \quad (10.26)$$

To satisfy Equation 10.24 exactly for all values of time, the terms on the left must contain a sine function identical to the sine term on the right-hand side. Since the second derivative of the sine function is another sine function, we assume a solution in the form $u_2(t) = U \sin \omega_f t$, where U is a constant to be determined. Differentiating twice and substituting, Equation 10.26 becomes

$$-U \omega_f^2 \sin \omega_f t + U \omega^2 \sin \omega_f t = \frac{F_0}{m} \sin \omega_f t \quad (10.27)$$

from which

$$U = \frac{F_0/m}{\omega^2 - \omega_f^2} \quad (10.28)$$

The particular solution representing response of the simple harmonic oscillator to a sinusoidally varying force is then

$$u_2(t) = \frac{F_0/m}{\omega^2 - \omega_f^2} \sin \omega_f t \quad (10.29)$$

The motion represented by Equation 10.29 is most often simply called the *forced response* and exhibits two important characteristics: (1) the frequency of the forced response is the same as the frequency of the forcing function, and (2) if the circular frequency of the forcing function is very near the natural circular frequency of the system, the denominator in Equation 10.29 becomes very small. The latter is an extremely important observation, as the result is large amplitude of motion. In the case $\omega_f = \omega$, Equation 10.29 indicates an infinite amplitude. This condition is known as *resonance*, and for this reason, the natural circular frequency of the system is often called the *resonant frequency*. Mathematically, Equation 10.29 is not a valid solution for the resonant condition (Problem 10.5); however, the correct solution for the resonant condition nevertheless exhibits unbounded amplitude growth with time.

The simple harmonic oscillator just modeled contains no device for energy dissipation (*damping*). Consequently, the free vibration solution, Equation 10.20, represents motion that continues without end. Physically, such motion is not possible, since all systems contain some type of dissipation mechanism, such as internal or external friction, air resistance, or devices specifically designed for the purpose. Similarly, the infinite amplitude indicated for the resonant condition cannot be attained by a real system because of the presence of damping. However, relatively large, yet bounded, amplitudes occur at or near the resonant frequency. Hence, the resonant condition is to be avoided if at all possible. As is subsequently shown, physical systems actually exhibit multiple natural frequencies, so multiple resonant conditions exist.

10.3 MULTIPLE DEGREES-OF-FREEDOM SYSTEMS

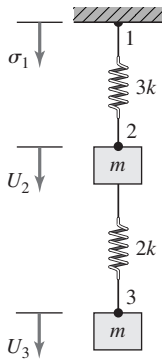


Figure 10.4 A spring-mass system exhibiting 2 degrees of freedom.

Figure 10.4 shows a system of two spring elements having concentrated masses attached at nodes 2 and 3 in the global coordinate system. As in previous examples, the system is subjected to gravity and the upper spring is attached to a rigid support at node 1. Of interest here is the dynamic response of the system of two springs and two masses when the equilibrium condition is disturbed by some external influence and then free to oscillate without external force. We could take the Newtonian mechanics approach by drawing the appropriate free-body diagrams and applying Newton’s second law of motion to obtain the governing equations. Instead, we take the finite element approach. By now, the procedure of assembling the system stiffness matrix should be routine. Following the procedure, we obtain

$$[K] = \begin{bmatrix} 3k & -3k & 0 \\ -3k & 5k & -2k \\ 0 & -2k & 2k \end{bmatrix} \quad (10.30)$$

as the system stiffness matrix. But what of the mass/inertia matrix? As the masses are concentrated at element nodes, we define the system mass matrix as

$$[M] = \begin{bmatrix} 0 & 0 & 0 \\ 0 & m & 0 \\ 0 & 0 & m \end{bmatrix} \quad (10.31)$$

The equations of motion can be expressed as

$$[M] \begin{Bmatrix} \ddot{U}_1 \\ \ddot{U}_2 \\ \ddot{U}_3 \end{Bmatrix} + [K] \begin{Bmatrix} U_1 \\ U_2 \\ U_3 \end{Bmatrix} = \begin{Bmatrix} R_1 \\ mg \\ mg \end{Bmatrix} \quad (10.32)$$

where R_1 is the dynamic reaction force at node 1.

Invoking the constraint condition $U_1 = 0$, Equation 10.32 become

$$\begin{bmatrix} m & 0 \\ 0 & m \end{bmatrix} \begin{Bmatrix} \ddot{U}_2 \\ \ddot{U}_3 \end{Bmatrix} + \begin{bmatrix} 5k & -2k \\ -2k & 2k \end{bmatrix} \begin{Bmatrix} U_2 \\ U_3 \end{Bmatrix} = \begin{Bmatrix} mg \\ mg \end{Bmatrix} \quad (10.33)$$

which is a system of two second-order, linear, ordinary differential equations in the two unknown system displacements U_2 and U_3 . As the gravitational forces indicated by the forcing function represent the static equilibrium condition, these are neglected and the system of equations rewritten as

$$\begin{bmatrix} m & 0 \\ 0 & m \end{bmatrix} \begin{Bmatrix} \ddot{U}_2 \\ \ddot{U}_3 \end{Bmatrix} + \begin{bmatrix} 5k & -2k \\ -2k & 2k \end{bmatrix} \begin{Bmatrix} U_2 \\ U_3 \end{Bmatrix} = \begin{Bmatrix} 0 \\ 0 \end{Bmatrix} \quad (10.34)$$

As a practical matter, most finite element software packages do *not* include the structural weight in an analysis problem. Instead, inclusion of the structural

10.3 Multiple Degrees-of-Freedom Systems

395

weight is an option that must be selected by the user of the software. Whether to include gravitational effects is a judgment made by the analyst based on the specifics of a given structural geometry and loading.

The system of second-order, linear, ordinary, homogeneous differential equations given by Equation 10.34 represents the free-vibration response of the 2 degrees-of-freedom system of Figure 10.4. As a freely oscillating system, we seek solutions in the form of harmonic motion as

$$\begin{aligned}U_2(t) &= A_2 \sin(\omega t + \phi) \\U_3(t) &= A_3 \sin(\omega t + \phi)\end{aligned}\quad (10.35)$$

where A_2 and A_3 are the vibration amplitudes of nodes 2 and 3 (the masses attached to nodes 2 and 3); ω is an unknown, assumed harmonic circular frequency of motion; and ϕ is the phase angle of such motion. Taking the second derivatives with respect to time of the assumed solutions and substituting into Equation 10.34 results in

$$-\omega^2 \begin{bmatrix} m & 0 \\ 0 & m \end{bmatrix} \begin{Bmatrix} A_2 \\ A_3 \end{Bmatrix} \sin(\omega t + \phi) + \begin{bmatrix} 5k & -2k \\ -2k & 2k \end{bmatrix} \begin{Bmatrix} A_2 \\ A_3 \end{Bmatrix} \sin(\omega t + \phi) = \begin{Bmatrix} 0 \\ 0 \end{Bmatrix}\quad (10.36)$$

or

$$\begin{bmatrix} 5k - m\omega^2 & -2k \\ -2k & 2k - m\omega^2 \end{bmatrix} \begin{Bmatrix} A_2 \\ A_3 \end{Bmatrix} \sin(\omega t + \phi) = \begin{Bmatrix} 0 \\ 0 \end{Bmatrix}\quad (10.37)$$

Equation 10.37 is a system of two, homogeneous algebraic equations, which must be solved for the vibration amplitudes A_2 and A_3 . From linear algebra, a system of homogeneous algebraic equations has nontrivial solutions if and only if the determinant of the coefficient matrix is zero. Therefore, for nontrivial solutions,

$$\begin{vmatrix} 5k - m\omega^2 & -2k \\ -2k & 2k - m\omega^2 \end{vmatrix} = 0\quad (10.38)$$

which gives

$$(5k - m\omega^2)(2k - m\omega^2) - 4k^2 = 0\quad (10.39)$$

Equation 10.39 is known as the *characteristic equation* or *frequency equation* of the physical system. As k and m are known positive constants, Equation 10.39 is treated as a quadratic equation in the unknown ω^2 and solved by the quadratic formula to obtain *two* roots

$$\begin{aligned}\omega_1^2 &= \frac{k}{m} \\ \omega_2^2 &= 6\frac{k}{m}\end{aligned}\quad (10.40)$$

or

$$\begin{aligned}\omega_1 &= \sqrt{\frac{k}{m}} \\ \omega_2 &= \sqrt{6\frac{k}{m}}\end{aligned}\tag{10.41}$$

In mathematical rigor, there are four roots, since the negative values corresponding to Equation 10.41 also satisfy the frequency equation. The negative values are rejected because a negative frequency has no physical meaning and use of the negative values in the assumed solution (Equation 10.35) introduces only a phase shift and represents the same motion as that corresponding to the positive root.

The 2 degrees-of-freedom system of Figure 10.4 is found to have two natural circular frequencies of oscillation. As is customary, the numerically smaller of the two is designated as ω_1 and known as the *fundamental* frequency. The task remains to determine the amplitudes A_2 and A_3 in the assumed solution. For this purpose, Equation 10.37 is

$$\begin{bmatrix} 5k - m\omega^2 & -2k \\ -2k & 2k - m\omega^2 \end{bmatrix} \begin{Bmatrix} A_2 \\ A_3 \end{Bmatrix} = \begin{Bmatrix} 0 \\ 0 \end{Bmatrix}\tag{10.42}$$

As Equation 10.42 is a set of homogeneous equations, we can find no absolute values of the amplitudes. We can, however, obtain information regarding the numerical relations among the amplitudes as follows. If we substitute $\omega^2 = \omega_1^2 = k/m$ into *either* algebraic equation, we obtain $A_3 = 2A_2$, which defines the *amplitude ratio* $A_3/A_2 = 2$ for the first, or fundamental, mode of vibration. That is, if the system oscillates at its fundamental frequency ω_1 , the amplitude of oscillation of m_2 is twice that of m_1 . (Note that we are unable to calculate the absolute value of either amplitude; only the ratio can be determined. The absolute values depend on the initial conditions of motion, as is subsequently illustrated.) The displacement equations for the fundamental mode are then

$$\begin{aligned}U_2(t) &= A_2^{(1)} \sin(\omega_1 t + \phi_1) \\ U_3(t) &= A_3^{(1)} \sin(\omega_1 + \phi_1) = 2A_2^{(1)} \sin(\omega_1 t + \phi_1)\end{aligned}\tag{10.43}$$

where the superscript on the amplitudes is used to indicate that the displacements correspond to vibration at the fundamental frequency.

Next we substitute the second natural circular frequency $\omega^2 = \omega_2^2 = 6k/m$ into either equation and obtain the relation $A_3 = -0.5A_2$, which defines the second amplitude ratio as $A_3/A_2 = -0.5$. So, in the second natural mode of vibration, the masses move in opposite directions. The displacements corresponding to the second frequency are then

$$\begin{aligned}U_2(t) &= A_2^{(2)} \sin(\omega_2 t + \phi_2) \\ U_3(t) &= A_3^{(2)} \sin(\omega_2 + \phi_2) = -0.5A_2^{(2)} \sin(\omega_2 t + \phi_2)\end{aligned}\tag{10.44}$$

where again the superscript refers to the frequency.

10.3 Multiple Degrees-of-Freedom Systems

397

Therefore, the free-vibration response of the 2 degree-of-freedom system is given by

$$\begin{aligned} U_2(t) &= A_2^{(1)} \sin(\omega_1 t + \phi_1) + A_2^{(2)} \sin(\omega_2 t + \phi_2) \\ U_3(t) &= 2A_2^{(1)} \sin(\omega_1 t + \phi_1) - 0.5A_2^{(2)} \sin(\omega_2 t + \phi_2) \end{aligned} \quad (10.45)$$

and we note the four unknown constants in the solution; specifically, these are the amplitudes $A_2^{(1)}$, $A_2^{(2)}$ and the phase angles ϕ_1 and ϕ_2 . Evaluation of the constants is illustrated in a subsequent example.

Depending on the reader's mathematical background, the analysis of the 2 degree-of-freedom vibration problem may be recognized as an *eigenvalue problem* [1]. The computed natural circular frequencies are the eigenvalues of the problem and the amplitude ratios represent the eigenvectors of the problem. Equation 10.45 represents the response of the system in terms of the natural modes of vibration. Such a solution is often referred to as being obtained by *modal superposition* or simply *modal analysis*. To represent the complete solution for the system, we use the matrix notation

$$\begin{Bmatrix} U_2(t) \\ U_3(t) \end{Bmatrix} = \begin{Bmatrix} A_2^{(1)} \\ 2A_2^{(1)} \end{Bmatrix} \sin(\omega_1 t + \phi_1) + \begin{Bmatrix} A_2^{(2)} \\ -0.5A_2^{(2)} \end{Bmatrix} \sin(\omega_2 t + \phi_2) \quad (10.46)$$

which shows that the modes interact to produce the overall motion of the system.

EXAMPLE 10.2

Given the system of Figure 10.4 with $k = 40$ lb/in. and $mg = W = 20$ lb, determine

- The natural frequencies of the system.
- The free response, if the initial conditions are

$$U_2(t=0) = 1 \text{ in.} \quad U_3(t=0) = 0.5 \text{ in.} \quad \dot{U}_2(t=0) = \dot{U}_3(t=0) = 0$$

These initial conditions are specified in reference to the equilibrium position of the system, so the computed displacement functions do not include the effect of gravity.

■ Solution

Per Equation 10.41, the natural circular frequencies are

$$\begin{aligned} \omega_1 &= \sqrt{\frac{k}{m}} = \sqrt{\frac{40}{20/g}} = \sqrt{\frac{40(386.4)}{20}} = 27.8 \text{ rad/sec} \\ \omega_2 &= \sqrt{\frac{6k}{m}} = \sqrt{\frac{6(40)}{20/g}} = \sqrt{\frac{6(40)(386.4)}{20}} = 68.1 \text{ rad/sec} \end{aligned}$$

The free-vibration response is given by Equation 10.35 as

$$\begin{aligned} U_2(t) &= A_2^{(1)} \sin(27.8t + \phi_1) + A_2^{(2)} \sin(68.1t + \phi_2) \\ U_3(t) &= 2A_2^{(1)} \sin(27.8t + \phi_1) - 0.5A_2^{(2)} \sin(68.1t + \phi_2) \end{aligned}$$

The amplitudes and phase angles are determined by applying the initial conditions, which are

$$\begin{aligned}U_2(0) &= 1 = A_2^{(1)} \sin \phi_1 + A_2^{(2)} \sin \phi_2 \\U_3(0) &= 0.5 = 2A_2^{(1)} \sin \phi_1 - 0.5A_2^{(2)} \sin \phi_2 \\\dot{U}_2(0) &= 0 = 27.8A_2^{(1)} \cos \phi_1 + 68.1A_2^{(2)} \cos \phi_2 \\\dot{U}_3(0) &= 0 = 2(27.8)A_2^{(1)} \cos \phi_1 - 0.5(68.1)A_2^{(2)} \cos \phi_2\end{aligned}$$

The initial conditions produce a system of four algebraic equations in the four unknowns $A_2^{(1)}$, $A_2^{(2)}$, ϕ_1 , ϕ_2 . Solution of the equations is not trivial, owing to the presence of the trigonometric functions. Letting $P = A_2^{(1)} \sin \phi_1$ and $Q = A_2^{(2)} \sin \phi_2$, the displacement initial condition equations become

$$\begin{aligned}P + Q &= 1 \\2P - 0.5Q &= 0.5\end{aligned}$$

which are readily solved to obtain

$$P = A_2^{(1)} \sin \phi_1 = 0.4 \quad \text{and} \quad Q = A_2^{(2)} \sin \phi_2 = 0.6$$

Similarly, setting $R = A_2^{(1)} \cos \phi_1$ and $S = A_2^{(2)} \sin \phi_2$, the initial velocity equations are

$$\begin{aligned}27.8R + 68.1S &= 0 \\2(27.8)R - 0.5(68.1)S &= 0\end{aligned}$$

representing a homogeneous system in the variables R and S . Nontrivial solutions exist only if the determinant of the coefficient matrix is zero. In this case, the determinant is not zero, as may easily be verified by direct computation. There are no nontrivial solutions; hence, $R = S = 0$. Based on physical argument, the amplitudes cannot be zero, so we must conclude that $\cos \phi_1 = \cos \phi_2 = 0 \Rightarrow \phi_1 = \phi_2 = \pi/2$. It follows that the sine function of the phase angles have unity value; hence, $A_2^{(1)} = 0.4$ and $A_2^{(2)} = 0.6$. Substituting the amplitudes into the general solution form while noting that $\sin(\omega t + \pi/2) = \cos \omega t$, the free-vibration response of each mass is

$$\begin{aligned}U_2(t) &= 0.4 \cos 27.8t + 0.6 \cos 68.1t \\U_3(t) &= 0.8 \cos 27.8t - 0.3 \cos 68.1t\end{aligned}$$

The displacement response of each mass is seen to be a combination of motions corresponding to the natural circular frequencies of the system. Such a phenomenon is characteristic of vibrating structural systems. All the natural modes of vibration participate in the general motion of a structure.

10.3.1 Many-Degrees-of-Freedom Systems

As illustrated by the system of two springs and masses, there are two natural frequencies and two natural modes of vibration. If we extend the analysis to

10.3 Multiple Degrees-of-Freedom Systems

399

a system of springs and masses having N degrees of freedom, as depicted in Figure 10.5, and apply the assembly procedure for a finite element analysis, the finite element equations are of the form

$$[M]\{\ddot{U}\} + [K]\{U\} = \{0\} \quad (10.47)$$

where $[M]$ is the system mass matrix and $[K]$ is the system stiffness matrix. To determine the natural frequencies and mode shapes of the system's vibration modes, we assume, as in the 1 and 2 degrees-of-freedom cases, that

$$U_i(t) = A_i \sin(\omega t + \phi) \quad (10.48)$$

Substitution of the assumed solution into the system equations leads to the frequency equation

$$|[K] - \omega^2[M]| = 0 \quad (10.49)$$

which is a polynomial of order N in the variable ω^2 . The solution of Equation 10.49 results in N natural frequencies ω_j , which, for structural systems, can be shown to be real but not necessarily distinct; that is, repeated roots can occur. As discussed many times, the finite element equations cannot be solved unless boundary conditions are applied so that the equations become inhomogeneous. A similar phenomenon exists when determining the system natural frequencies and mode shapes. If the system is not constrained, rigid body motion is possible and one or more of the computed natural frequencies has a value of zero. A three-dimensional system has six zero-valued natural frequencies, corresponding to rigid body translation in the three coordinate axes and rigid body rotations about the three coordinate axes. Therefore, if improperly constrained, a structural system exhibits repeated zero roots of the frequency equation.

Assuming that constraints are properly applied, the frequencies resulting from the solution of Equation 10.49 are substituted, one at a time, into Equation 10.47 and the amplitude ratios (eigenvectors) computed for each natural mode of vibration. The general solution for each degree of freedom is then expressed as

$$U_i(t) = \sum_{j=1}^N A_i^{(j)} \sin(\omega_j t + \phi_j) \quad i = 1, N \quad (10.50)$$

illustrating that the displacement of each mass is the sum of contributions from each of the N natural modes. Displacement solutions expressed by Equation 10.50 are said to be obtained by *modal superposition*. We add the independent solutions of the linear differential equations of motion.

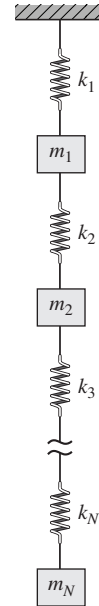


Figure 10.5 A spring-mass system exhibiting arbitrarily many degrees of freedom.

EXAMPLE 10.3

Determine the natural frequencies and modal amplitude vectors for the 3 degrees-of-freedom system depicted in Figure 10.6a.

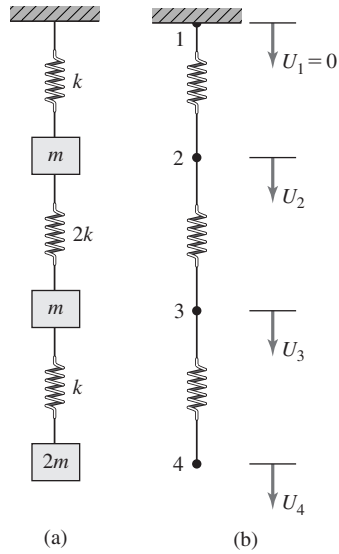


Figure 10.6 System with 3 degrees of freedom for Example 10.3.

■ **Solution**

The finite element model is shown in Figure 10.6b, with node and element numbers as indicated. Assembly of the global stiffness matrix results in

$$[K] = \begin{bmatrix} k & -k & 0 & 0 \\ -k & 3k & -2k & 0 \\ 0 & -2k & 3k & -k \\ 0 & 0 & -k & k \end{bmatrix}$$

Similarly, the assembled global mass matrix is

$$[M] = \begin{bmatrix} 0 & 0 & 0 & 0 \\ 0 & m & 0 & 0 \\ 0 & 0 & m & 0 \\ 0 & 0 & 0 & 2m \end{bmatrix}$$

Owing to the constraint $U_1 = 0$, we need consider only the last three equations of motion, given by

$$\begin{bmatrix} m & 0 & 0 \\ 0 & m & 0 \\ 0 & 0 & 2m \end{bmatrix} \begin{Bmatrix} \ddot{U}_2 \\ \ddot{U}_3 \\ \ddot{U}_4 \end{Bmatrix} + \begin{bmatrix} 3k & -2k & 0 \\ -2k & 3k & -k \\ 0 & -k & k \end{bmatrix} \begin{Bmatrix} U_2 \\ U_3 \\ U_4 \end{Bmatrix} = \begin{Bmatrix} 0 \\ 0 \\ 0 \end{Bmatrix}$$

Assuming sinusoidal response as $U_i = A_i \sin(\omega t + \phi)$, $i = 2, 4$ and substituting into the equations of motion leads to the frequency equation

$$\begin{vmatrix} 3k - \omega^2 m & -2k & 0 \\ -2k & 3k - \omega^2 m & -k \\ 0 & -k & k - 2\omega^2 m \end{vmatrix} = 0$$

10.3 Multiple Degrees-of-Freedom Systems

401

Expanding the determinant and simplifying gives

$$\omega^6 - 6.5\frac{k}{m}\omega^4 + 7.5\left(\frac{k}{m}\right)^2\omega^2 - \left(\frac{k}{m}\right)^3 = 0$$

which will be treated as a cubic equation in the unknown ω^2 . Setting $\omega^2 = C(k/m)$, the frequency equation becomes

$$(C^3 - 6.5C^2 + 7.5C - 1)\left(\frac{k}{m}\right)^3 = 0$$

which has the roots

$$C_1 = 0.1532 \quad C_2 = 1.2912 \quad C_3 = 5.0556$$

The corresponding natural circular frequencies are

$$\omega_1 = 0.3914\sqrt{\frac{k}{m}}$$

$$\omega_2 = 1.1363\sqrt{\frac{k}{m}}$$

$$\omega_3 = 2.2485\sqrt{\frac{k}{m}}$$

To obtain the amplitude ratios, we substitute the natural circular frequencies into the amplitude equations one at a time while setting (arbitrarily) $A_2^{(i)} = 1$, $i = 1, 2, 3$ and solve for the amplitudes $A_3^{(i)}$ and $A_4^{(i)}$. Using ω_1 results in

$$\begin{aligned}(3k - \omega_1^2 m)A_2^{(1)} - 2kA_3^{(1)} &= 0 \\ -2kA_2^{(1)} + (3k - \omega_1^2 m)A_3^{(1)} - kA_4^{(1)} &= 0 \\ -kA_3^{(1)} + (k - 2\omega_1^2 m)A_4^{(1)} &= 0\end{aligned}$$

Substituting $\omega_1 = 0.3914\sqrt{k/m}$, we obtain

$$\begin{aligned}2.847A_2^{(1)} - 2A_3^{(1)} &= 0 \\ -2A_2^{(1)} + 2.847A_3^{(1)} - A_4^{(1)} &= 0 \\ -A_3^{(1)} + 0.694A_4^{(1)} &= 0\end{aligned}$$

As discussed, the amplitude equations are homogeneous; explicit solutions cannot be obtained. We can, however, determine the amplitude ratios by setting $A_2^{(1)} = 1$ to obtain

$$\begin{aligned}A_3^{(1)} &= 1.4235 \\ A_4^{(1)} &= 2.0511\end{aligned}$$

The amplitude vector corresponding to the fundamental mode ω_1 is then represented as

$$\{A^{(1)}\} = A_2^{(1)} \begin{Bmatrix} 1 \\ 1.4325 \\ 2.0511 \end{Bmatrix}$$

and this is the *eigenvector* corresponding to the *eigenvalue* ω_1 . Proceeding identically with the values for the other two frequencies, ω_2 and ω_3 , the resulting amplitude vectors are

$$\{A^{(2)}\} = A_2^{(2)} \begin{Bmatrix} 1 \\ 0.8544 \\ -0.5399 \end{Bmatrix}$$

$$\{A^{(3)}\} = A_2^{(3)} \begin{Bmatrix} 1 \\ -1.0279 \\ 0.1128 \end{Bmatrix}$$

This example illustrates that an N degree-of-freedom system exhibits N natural modes of vibration defined by N natural circular frequencies and the corresponding N amplitude vectors (mode shapes). While the examples deal with discrete spring-mass systems, where the motions of the masses are easily visualized as recognizable events, structural systems modeled via finite elements exhibit N natural frequencies and N mode shapes, where N is the number of degrees of freedom (displacements in structural systems) represented by the finite element model. Accuracy of the computed frequencies as well as use of the natural modes of vibration to examine response to external forces is delineated in following sections.

10.4 BAR ELEMENTS: CONSISTENT MASS MATRIX

In the preceding discussions of spring-mass systems, the mass (inertia) matrix in each case is a lumped (diagonal) matrix, since each mass is directly attached to an element node. In these simple cases, we neglect the mass of the spring elements in comparison to the concentrated masses. In the general case of solid structures, the mass is distributed geometrically throughout the structure and the inertia properties of the structure depend directly on the mass distribution. To illustrate the effects of distributed mass, we first consider longitudinal (axial) vibration of the bar element of Chapter 2.

The bar element shown in Figure 10.7a is the same as the bar element introduced in Chapter 2 with the very important difference that displacements and applied forces are now assumed to be time dependent, as indicated. The free-body diagram of a differential element of length dx is shown in Figure 10.7b, where cross-sectional area A is assumed constant. Applying Newton's second law to the differential element gives

$$\left(\sigma + \frac{\partial \sigma}{\partial x} dx \right) A - \sigma A = (\rho A dx) \frac{\partial^2 u}{\partial t^2} \quad (10.51)$$

10.4 Bar Elements: Consistent Mass Matrix

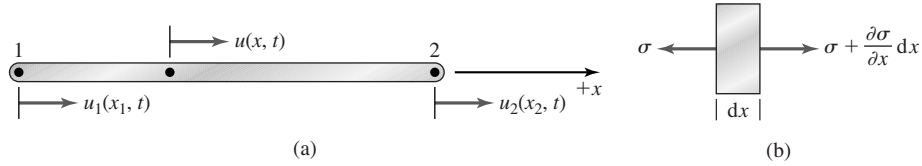


Figure 10.7

(a) Bar element exhibiting time-dependent displacement. (b) Free-body diagram of a differential element.

where ρ is density of the bar material. Note the use of partial derivative operators, since displacement is now considered to depend on both position and time. Substituting the stress-strain relation $\sigma = E\varepsilon = E(\partial u/\partial x)$, Equation 10.51 becomes

$$E \frac{\partial^2 u}{\partial x^2} = \rho \frac{\partial^2 u}{\partial t^2} \quad (10.52)$$

Equation 10.52 is the *one-dimensional wave equation*, the governing equation for propagation of elastic displacement waves in the axial bar.

In the dynamic case, the axial displacement is discretized as

$$u(x, t) = N_1(x)u_1(t) + N_2(x)u_2(t) \quad (10.53)$$

where the nodal displacements are now expressed explicitly as time dependent, but the interpolation functions remain dependent only on the spatial variable. Consequently, the interpolation functions are identical to those used previously for equilibrium situations involving the bar element: $N_1(x) = 1 - (x/L)$ and $N_2(x) = x/L$. Application of Galerkin's method to Equation 10.52 in analogy to Equation 5.29 yields the residual equations as

$$\int_0^L N_i(x) \left(E \frac{\partial^2 u}{\partial x^2} - \rho \frac{\partial^2 u}{\partial t^2} \right) A dx = 0 \quad i = 1, 2 \quad (10.54)$$

Assuming constant material properties, Equation 10.54 can be written as

$$\rho A \int_0^L N_i(x) \frac{\partial^2 u}{\partial t^2} dx = AE \int_0^L N_i(x) \frac{\partial^2 u}{\partial x^2} dx \quad i = 1, 2 \quad (10.55)$$

Mathematical treatment of the right-hand side of Equation 10.55 is identical to that presented in Chapter 5 and is not repeated here, other than to recall that the result of the integration and combination of the two residual equations in matrix form is

$$\frac{AE}{L} \begin{bmatrix} 1 & -1 \\ -1 & 1 \end{bmatrix} \begin{Bmatrix} u_1 \\ u_2 \end{Bmatrix} = \begin{Bmatrix} f_1 \\ f_2 \end{Bmatrix} \Rightarrow [k]\{u\} = \{f\} \quad (10.56)$$

Substituting the discretized approximation for $u(x, t)$, the integral on the left becomes

$$\rho A \int_0^L N_i(x) \frac{\partial^2 u}{\partial t^2} dx = \rho A \int_0^L N_i(N_1 \ddot{u}_1 + N_2 \ddot{u}_2) dx \quad i = 1, 2 \quad (10.57)$$

where the double-dot notation indicates differentiation with respect to time. The two equations represented by Equation 10.57 are written in matrix form as

$$\rho A \int_0^L \begin{bmatrix} N_1^2 & N_1 N_2 \\ N_1 N_2 & N_2^2 \end{bmatrix} dx \begin{Bmatrix} \ddot{u}_1 \\ \ddot{u}_2 \end{Bmatrix} = \frac{\rho AL}{6} \begin{bmatrix} 2 & 1 \\ 1 & 2 \end{bmatrix} \begin{Bmatrix} \ddot{u}_1 \\ \ddot{u}_2 \end{Bmatrix} = [m]\{\ddot{u}\} \quad (10.58)$$

and the reader is urged to confirm the result by performing the indicated integrations. Also note that the mass matrix is symmetric but not singular. Equation 10.58 defines the *consistent* mass matrix for the bar element. The term *consistent* is used because the interpolation functions used in formulating the mass matrix are the same as (consistent with) those used to describe the spatial variation of displacement. Combining Equations 10.56 and 10.58 per Equation 10.55, we obtain the dynamic finite element equations for a bar element as

$$\frac{\rho AL}{6} \begin{bmatrix} 2 & 1 \\ 1 & 2 \end{bmatrix} \begin{Bmatrix} \ddot{u}_1 \\ \ddot{u}_2 \end{Bmatrix} + \frac{AE}{L} \begin{bmatrix} 1 & -1 \\ -1 & 1 \end{bmatrix} \begin{Bmatrix} u_1 \\ u_2 \end{Bmatrix} = \begin{Bmatrix} f_1 \\ f_2 \end{Bmatrix} \quad (10.59)$$

or

$$[m]\{\ddot{u}\} + [k]\{u\} = \{f\} \quad (10.60)$$

and we note that $\rho AL = m$ is the total mass of the element. (Why is the sign of the second term positive?)

Given the governing equations, let us now determine the natural frequencies of a bar element in axial vibration. Per the foregoing discussion of free vibration, we set the nodal force vector to zero and write the frequency equation as

$$|[k] - \omega^2[m]| = 0 \quad (10.61)$$

to obtain

$$\begin{vmatrix} k - \omega^2 \frac{m}{3} & -\left(k + \omega^2 \frac{m}{6}\right) \\ -\left(k + \omega^2 \frac{m}{6}\right) & k - \omega^2 \frac{m}{3} \end{vmatrix} = 0 \quad (10.62)$$

Expanding Equation 10.62 results in a quadratic equation in ω^2

$$\left(k - \omega^2 \frac{m}{3}\right)^2 - \left(k + \omega^2 \frac{m}{6}\right)^2 = 0 \quad (10.63)$$

or

$$\omega^2 \left(\omega^2 - 12 \frac{k}{m} \right) = 0 \quad (10.64)$$

Equation 10.64 has roots $\omega^2 = 0$ and $\omega^2 = 12k/m$. The zero root arises because we specify no constraint on the element; hence, rigid body motion is possible and represented by the zero-valued natural circular frequency. The nonzero natural circular frequency corresponds to axial displacement waves in the bar, which could occur, for example, if the free bar were subjected to an axial impulse at one end. In such a case, rigid body motion would occur but axial vibration would simultaneously occur with circular frequency $\omega_1 = \sqrt{12k/m} = (3.46/L)\sqrt{E/\rho}$. The following example illustrates determination of natural circular frequencies for a constrained bar.

EXAMPLE 10.4

Using two equal-length finite elements, determine the natural circular frequencies of the solid circular shaft fixed at one end shown in Figure 10.8a.

■ Solution

The elements and node numbers are shown in Figure 10.8b. The characteristic stiffness of each element is

$$k = \frac{AE}{L/2} = \frac{2AE}{L}$$

so that the element stiffness matrices are

$$[k^{(1)}] = [k^{(2)}] = \frac{2AE}{L} \begin{bmatrix} 1 & -1 \\ -1 & 1 \end{bmatrix}$$

The mass of each element is

$$m = \frac{\rho AL}{2}$$

and the element consistent mass matrices are

$$[m^{(1)}] = [m^{(2)}] = \frac{\rho AL}{12} \begin{bmatrix} 2 & 1 \\ 1 & 2 \end{bmatrix}$$

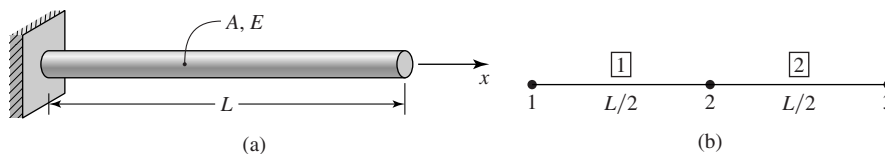


Figure 10.8

(a) Circular shaft of Example 10.4. (b) Model using two bar elements.

Following the direct assembly procedure, the global stiffness matrix is

$$[K] = \frac{2AE}{L} \begin{bmatrix} 1 & -1 & 0 \\ -1 & 2 & -1 \\ 0 & -1 & 1 \end{bmatrix}$$

and the global consistent mass matrix is

$$[M] = \frac{\rho AL}{12} \begin{bmatrix} 2 & 1 & 0 \\ 1 & 4 & 1 \\ 0 & 1 & 2 \end{bmatrix}$$

The global equations of motion are then

$$\frac{\rho AL}{12} \begin{bmatrix} 2 & 1 & 0 \\ 1 & 4 & 1 \\ 0 & 1 & 2 \end{bmatrix} \begin{Bmatrix} \ddot{U}_1 \\ \ddot{U}_2 \\ \ddot{U}_3 \end{Bmatrix} + \frac{2AE}{L} \begin{bmatrix} 1 & -1 & 0 \\ -1 & 2 & -1 \\ 0 & -1 & 1 \end{bmatrix} \begin{Bmatrix} U_1 \\ U_2 \\ U_3 \end{Bmatrix} = \begin{Bmatrix} 0 \\ 0 \\ 0 \end{Bmatrix}$$

Applying the constraint condition $U_1 = 0$, we have

$$\frac{\rho AL}{12} \begin{bmatrix} 4 & 1 \\ 1 & 2 \end{bmatrix} \begin{Bmatrix} \ddot{U}_2 \\ \ddot{U}_3 \end{Bmatrix} + \frac{2AE}{L} \begin{bmatrix} 2 & -1 \\ -1 & 1 \end{bmatrix} \begin{Bmatrix} U_2 \\ U_3 \end{Bmatrix} = \begin{Bmatrix} 0 \\ 0 \end{Bmatrix}$$

as the homogeneous equations governing free vibration. For convenience, the last equation is rewritten as

$$\begin{bmatrix} 4 & 1 \\ 1 & 2 \end{bmatrix} \begin{Bmatrix} \ddot{U}_2 \\ \ddot{U}_3 \end{Bmatrix} + \frac{24E}{\rho L^2} \begin{bmatrix} 2 & -1 \\ -1 & 1 \end{bmatrix} \begin{Bmatrix} U_2 \\ U_3 \end{Bmatrix} = \begin{Bmatrix} 0 \\ 0 \end{Bmatrix}$$

Assuming sinusoidal responses

$$U_2 = A_2 \sin(\omega t + \phi) \quad U_3 = A_3 \sin(\omega t + \phi)$$

differentiating twice and substituting results in

$$-\omega^2 \begin{bmatrix} 4 & 1 \\ 1 & 2 \end{bmatrix} \begin{Bmatrix} A_2 \\ A_3 \end{Bmatrix} \sin(\omega t + \phi) + \frac{24E}{\rho L^2} \begin{bmatrix} 2 & -1 \\ -1 & 1 \end{bmatrix} \begin{Bmatrix} A_2 \\ A_3 \end{Bmatrix} \sin(\omega t + \phi) = \begin{Bmatrix} 0 \\ 0 \end{Bmatrix}$$

Again, we obtain a set of homogeneous algebraic equations that have nontrivial solutions only if the determinant of the coefficient matrix is zero. Letting $\lambda = 24E/\rho L^2$, the frequency equation is given by the determinant

$$\begin{vmatrix} 2\lambda - 4\omega^2 & -\lambda - \omega^2 \\ -\lambda - \omega^2 & \lambda - 2\omega^2 \end{vmatrix} = 0$$

which, when expanded and simplified, is

$$7\omega^4 - 10\lambda\omega^2 + \lambda^2 = 0$$

Treating the frequency equation as a quadratic in ω^2 , the roots are obtained as

$$\omega_1^2 = 0.1082\lambda \quad \omega_2^2 = 1.3204\lambda$$

Substituting for λ , the natural circular frequencies are

$$\omega_1 = \frac{1.611}{L} \sqrt{\frac{E}{\rho}} \quad \omega_2 = \frac{5.629}{L} \sqrt{\frac{E}{\rho}} \text{ rad/sec}$$

For comparison purposes, we note that the exact solution [2] for the natural circular frequencies of a bar in axial vibration yields the fundamental natural circular frequency as $1.571/L\sqrt{E/\rho}$ and the second frequency as $4.712/L\sqrt{E/\rho}$. Therefore, the error for the first computed frequency is about 2.5 percent, while the error in the second frequency is about 19 percent.

It is also informative to note (see Problem 10.12) that, if the lumped mass matrix approach is used for this example, we obtain

$$\omega_1 = \frac{1.531}{L} \sqrt{\frac{E}{\rho}} \quad \omega_2 = \frac{3.696}{L} \sqrt{\frac{E}{\rho}} \text{ rad/sec}$$

The solution for Example 10.4 yielded two natural circular frequencies for free axial vibration of a bar fixed at one end. Such a bar has an infinite number of natural frequencies, like any element or structure having continuously distributed mass. In finite element modeling, the partial differential equations governing motion of continuous systems are discretized into a finite number of algebraic equations for approximate solutions. Hence, the number of frequencies obtainable via a finite element approach is limited by the discretization inherent to the finite element model.

The inertia characteristics of a bar element can also be represented by a lumped mass matrix, similar to the approach used in the spring-mass examples earlier in this chapter. In the lumped matrix approach, half the total mass of the element is assumed to be concentrated at each node and the connecting material is treated as a massless spring with axial stiffness. The lumped mass matrix for a bar element is then

$$[m] = \frac{\rho AL}{2} \begin{bmatrix} 1 & 0 \\ 0 & 1 \end{bmatrix} \quad (10.65)$$

Use of lumped mass matrices offers computational advantages. Since the element mass matrix is diagonal, assembled global mass matrices also are diagonal. On the other hand, although more computationally difficult in use, consistent mass matrices can be proven to provide upper bounds for the natural circular frequencies [3]. No such proof exists for lumped matrices. Nevertheless, lumped mass matrices are often used, particularly with bar and beam elements, to obtain reasonably accurate predictions of dynamic response.

10.5 BEAM ELEMENTS

We now develop the mass matrix for a beam element in flexural vibration. First, the consistent mass matrix is obtained using an approach analogous to that for the bar element in the previous section. Figure 10.9 depicts a differential element of a beam in flexure under the assumption that the applied loads are time dependent. As the situation is otherwise the same as that of Figure 5.3 except for the use of

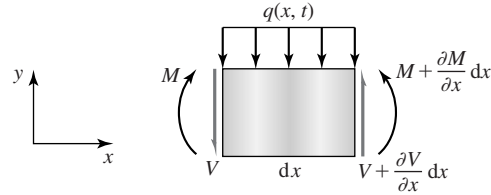


Figure 10.9 Differential element of a beam subjected to time-dependent loading.

partial derivatives, we apply Newton's second law of motion to the differential element in the y direction to obtain

$$\sum F_y = ma_y \Rightarrow V + \frac{\partial V}{\partial x} dx - V - q(x, t) dx = (\rho A dx) \frac{\partial^2 v}{\partial t^2} \quad (10.66)$$

where ρ is the material density and A is the cross-sectional area of the element. The quantity ρA represents mass per unit length in the x direction. Equation 10.66 simplifies to

$$\frac{\partial V}{\partial x} - q(x, t) = \rho A \frac{\partial^2 v}{\partial t^2} \quad (10.67)$$

As we are dealing with the small deflection theory of beam flexure, beam slopes, therefore rotations, are small. Therefore, we neglect the rotational inertia of the differential beam element and apply the moment equilibrium equation. The result is identical to that of Equation 5.37, repeated here as

$$\frac{\partial M}{\partial x} = -V \quad (10.68)$$

Substituting the moment-shear relation into Equation 10.67 gives

$$-\frac{\partial^2 M}{\partial x^2} - q(x, t) = \rho A \frac{\partial^2 v}{\partial t^2} \quad (10.69)$$

Finally, the flexure formula

$$M = EI_z \frac{\partial^2 v}{\partial x^2} \quad (10.70)$$

is substituted into Equation 10.69 to obtain the governing equation for dynamic beam deflection as

$$-\frac{\partial^2}{\partial x^2} \left(EI_z \frac{\partial^2 v}{\partial x^2} \right) - q(x, t) = \rho A \frac{\partial^2 v}{\partial t^2} \quad (10.71)$$

Under the assumptions of constant elastic modulus E and moment of inertia I_z , the governing equation becomes

$$\rho A \frac{\partial^2 v}{\partial t^2} + EI_z \frac{\partial^4 v}{\partial x^4} = -q(x, t) \quad (10.72)$$

As in the case of the bar element, transverse beam deflection is discretized using the same interpolation functions previously developed for the beam function. Now, however, the nodal displacements are assumed to be time dependent. Hence,

$$v(x, t) = N_1(x)v_1(t) + N_2(x)\theta_1(t) + N_3(x)v_2(t) + N_4(x)\theta_2(t) \quad (10.73)$$

and the interpolation functions are as given in Equation 4.26 or 4.29. Application of Galerkin's method to Equation 10.72 for a finite element of length L results in the residual equations

$$\int_0^L N_i(x) \left(\rho A \frac{\partial^2 v}{\partial t^2} + EI_z \frac{\partial^4 v}{\partial x^4} + q \right) dx = 0 \quad i = 1, 4 \quad (10.74)$$

As the last two terms of the integrand are the same as treated in Equation 5.42, development of the stiffness matrix and nodal force vector are not repeated here. Instead, we focus on the first term of the integrand, which represents the terms of the mass matrix.

For each of the four equations represented by Equation 10.74, the first integral term becomes

$$\rho A \int_0^L N_i(N_1\ddot{v}_1 + N_2\ddot{\theta}_1 + N_3\ddot{v}_2 + N_4\ddot{\theta}_2) dx = \rho A \int_0^L N_i[N] dx \begin{Bmatrix} \ddot{v}_1 \\ \ddot{\theta}_1 \\ \ddot{v}_2 \\ \ddot{\theta}_2 \end{Bmatrix} \quad i = 1, 4 \quad (10.75)$$

and, when all four equations are expressed in matrix form, the inertia terms become

$$\rho A \int_0^L [N]^T [N] dx \begin{Bmatrix} \ddot{v}_1 \\ \ddot{\theta}_1 \\ \ddot{v}_2 \\ \ddot{\theta}_2 \end{Bmatrix} = [m^{(e)}] \begin{Bmatrix} \ddot{v}_1 \\ \ddot{\theta}_1 \\ \ddot{v}_2 \\ \ddot{\theta}_2 \end{Bmatrix} \quad (10.76)$$

The consistent mass matrix for a two-dimensional beam element is given by

$$[m^{(e)}] = \rho A \int_0^L [N]^T [N] dx \quad (10.77)$$

Substitution for the interpolation functions and performing the required integrations gives the mass matrix as

$$[m^{(e)}] = \frac{\rho AL}{420} \begin{bmatrix} 156 & 22L & 54 & -13L \\ 22L & 4L^2 & 13L & -3L^2 \\ 54 & 13L & 156 & -22L \\ -13L & -3L^2 & -22L & 4L^2 \end{bmatrix} \quad (10.78)$$

and it is to be noted that we have assumed constant cross-sectional area in this development.

Combining the mass matrix with previously obtained results for the stiffness matrix and force vector, the finite element equations of motion for a beam element are

$$[m^{(e)}] \begin{Bmatrix} \ddot{v}_1 \\ \ddot{\theta}_1 \\ \ddot{v}_2 \\ \ddot{\theta}_2 \end{Bmatrix} + [k^{(e)}] \begin{Bmatrix} v_1 \\ \theta_1 \\ v_2 \\ \theta_2 \end{Bmatrix} = - \int_0^L [N]^T q(x, t) dx + \begin{Bmatrix} -V_1(t) \\ -M_1(t) \\ V_2(t) \\ M_2(t) \end{Bmatrix} \quad (10.79)$$

and all quantities are as previously defined. In the dynamic case, the nodal shear forces and bending moments may be time dependent, as indicated.

Assembly procedures for the beam element including the mass matrix are identical to those for the static equilibrium case. The global mass matrix is directly assembled, using the individual element mass matrices in conjunction with the element-to-global displacement relations. While system assembly is procedurally straightforward, the process is tedious when carried out by hand. Consequently, a complex example is not attempted. Instead, a relatively simple example of natural frequency determination is examined.

EXAMPLE 10.5

Using a single finite element, determine the natural circular frequencies of vibration of a cantilevered beam of length L , assuming constant values of ρ , E , and A .

■ Solution

The beam is depicted in Figure 10.10, with node 1 at the fixed support such that the boundary (constraint) conditions are $v_1 = \theta_1 = 0$. For free vibration, applied force and bending moment at the free end (node 2) are $V_2 = M_2 = 0$ and there is no applied distributed load. Under these conditions, the first two equations represented by Equation 10.79 are constraint equations and not of interest. Using the constraint conditions and the known applied forces, the last two equations are

$$\frac{\rho AL}{420} \begin{bmatrix} 156 & -22L \\ -22L & 4L^2 \end{bmatrix} \begin{Bmatrix} \ddot{v}_2 \\ \ddot{\theta}_2 \end{Bmatrix} + \frac{EI_z}{L^3} \begin{bmatrix} 12 & -6L \\ -6L & 4L^2 \end{bmatrix} \begin{Bmatrix} v_2 \\ \theta_2 \end{Bmatrix} = \begin{Bmatrix} 0 \\ 0 \end{Bmatrix}$$

For computational convenience, the equations are rewritten as

$$\begin{bmatrix} 156 & -22L \\ -22L & 4L^2 \end{bmatrix} \begin{Bmatrix} \ddot{v}_2 \\ \ddot{\theta}_2 \end{Bmatrix} + \frac{420EI_z}{mL^3} \begin{bmatrix} 12 & -6L \\ -6L & 4L^2 \end{bmatrix} \begin{Bmatrix} v_2 \\ \theta_2 \end{Bmatrix} = \begin{Bmatrix} 0 \\ 0 \end{Bmatrix}$$

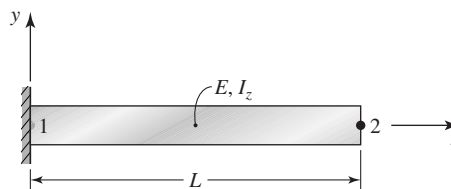


Figure 10.10 The cantilevered beam of Example 10.5 modeled as one element.

with $m = \rho AL$ representing the total mass of the beam. Assuming a sinusoidal displacement response, the frequency equation becomes

$$\begin{vmatrix} 12\lambda - 156\omega^2 & -6\lambda L + 22\omega^2 L \\ -6\lambda L + 22\omega^2 L & 4L^2(\lambda - \omega^2) \end{vmatrix} = 0$$

with $\lambda = 420EI_z/mL^3$. After expanding the determinant and performing considerable algebraic manipulation, the frequency equation becomes

$$5\omega^4 - 102\lambda\omega^2 + 3\lambda^2 = 0$$

Solving as a quadratic in ω^2 , the roots are

$$\omega_1^2 = 0.02945\lambda \quad \omega_2^2 = 20.37\lambda$$

Substituting for λ in terms of the beam physical parameters, we obtain

$$\omega_1 = 3.517\sqrt{\frac{EI_z}{mL^3}} \quad \omega_2 = 92.50\sqrt{\frac{EI_z}{mL^3}} \text{ rad/sec}$$

as the finite element approximations to the first two natural circular frequencies. For comparison, the exact solution gives

$$\omega_1^{\text{exact}} = 3.516\sqrt{\frac{EI_z}{mL^3}} \quad \omega_2^{\text{exact}} = 22.03\sqrt{\frac{EI_z}{mL^3}} \text{ rad/sec}$$

The fundamental frequency computed via a single element is essentially the same as the exact solution, whereas the second computed frequency is considerably larger than the corresponding exact value. As noted previously, a continuous system exhibits an infinite number of natural modes; we obtained only two modes in this example. If the number of elements is increased, the number of frequencies (natural modes) that can be computed increases as the number of degrees of freedom increases. In concert, the accuracy of the computed frequencies improves.

If the current example is refined by using two elements having length $L/2$ and the solution procedure repeated, we can compute four natural frequencies, the lowest two given by

$$\omega_1 = 3.516\sqrt{\frac{EI_z}{mL^3}} \quad \omega_2 = 24.5\sqrt{\frac{EI_z}{mL^3}}$$

and we observe that the second natural circular frequency has improved (in terms of the exact solution) significantly. The third and fourth frequencies from this solution are found to be quite high in relation to the known exact values.

As indicated by the foregoing example, the number of natural frequencies and mode shapes that can be computed depend directly on the number of degrees of freedom of the finite element model. Also, as would be expected for convergence, as the number of degrees of freedom increases, the computed frequencies become closer to the exact values. As a general rule, the lower values (numerically) converge more rapidly to exact solution values. While this is discussed

in more detail in conjunction with specific examples to follow, a general rule of thumb for frequency analysis is as follows: If the finite element analyst is interested in the first P modes of vibration of a structure, at least $2P$ modes should be calculated. Note that this implies the capability of calculating a subset of frequencies rather than all frequencies of a model. Indeed, this is possible and extremely important, since a practical finite element model may have thousands of degrees of freedom, hence thousands of natural frequencies. The computational burden of calculating all the frequencies is overwhelming and unnecessary, as is discussed further in the following section.

10.6 MASS MATRIX FOR A GENERAL ELEMENT: EQUATIONS OF MOTION

The previous examples dealt with relatively simple systems composed of linear springs and the bar and beam elements. In these cases, direct application of Newton's second law and Galerkin's finite element method led directly to the formulation of the matrix equations of motion; hence, the element mass matrices. For more general structural elements, an energy-based approach is preferred, as for static analyses. The approach to be taken here is based on *Lagrangian mechanics* and uses an energy method based loosely on *Lagrange's equations of motion* [4].

Prior to examining a general case, we consider the simple harmonic oscillator of Figure 10.1. At an arbitrary position x with the system assumed to be in motion, kinetic energy of the mass is

$$T = \frac{1}{2}m\dot{x}^2 \quad (10.80)$$

and the total potential energy is

$$U_e = \frac{1}{2}k(\delta_{st} + x)^2 - mg(\delta_{st} + x) \quad (10.81)$$

therefore, the total mechanical energy is

$$E_m = T + U_e = \frac{1}{2}m\dot{x}^2 + \frac{1}{2}k(\delta_{st} + x)^2 - mg(\delta_{st} + x) \quad (10.82)$$

As the simple harmonic oscillator model contains no mechanism for energy removal, the principle of conservation of mechanical energy applies; hence,

$$\frac{dE_m}{dt} = 0 = m\dot{x}\ddot{x} + k(\delta_{st} + x)\dot{x} - mg\dot{x} \quad (10.83)$$

or

$$m\ddot{x} + k(\delta_{st} + x) = mg \quad (10.84)$$

and the result is exactly the same as obtained via Newton's second law in Equation 10.2.

10.6 Mass Matrix for a General Element: Equations of Motion

413

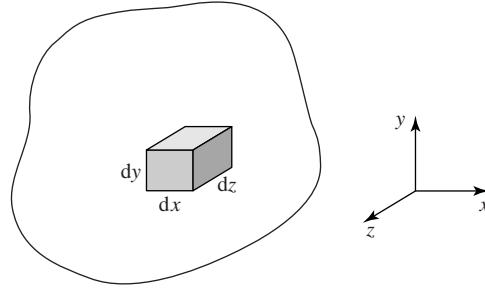


Figure 10.11 Differential element of a general three-dimensional body.

For the general case, we consider the three-dimensional body depicted in Figure 10.11 and examine a differential mass $dm = \rho \, dx \, dy \, dz$ located at arbitrary position (x, y, z) . Displacement of the differential mass in the coordinate directions are (u, v, w) and the velocity components are $(\dot{u}, \dot{v}, \dot{w})$, respectively. As we previously examined the potential energy, we now focus on kinetic energy of the differential mass given by

$$dT = \frac{1}{2}(\dot{u}^2 + \dot{v}^2 + \dot{w}^2) \, dm = \frac{1}{2}(\dot{u}^2 + \dot{v}^2 + \dot{w}^2)\rho \, dx \, dy \, dz \quad (10.85)$$

Total kinetic energy of the body is then

$$T = \frac{1}{2} \iiint (\dot{u}^2 + \dot{v}^2 + \dot{w}^2) \, dm = \frac{1}{2} \iiint (\dot{u}^2 + \dot{v}^2 + \dot{w}^2)\rho \, dx \, dy \, dz \quad (10.86)$$

and the integration is performed over the entire mass (volume) of the body.

Considering the body to be a finite element with the displacement field discretized as

$$\begin{aligned} u(x, y, z, t) &= \sum_{i=1}^M N_i(x, y, z) u_i(t) = [N]\{u\} \\ v(x, y, z, t) &= \sum_{i=1}^M N_i(x, y, z) v_i(t) = [N]\{v\} \\ w(x, y, z, t) &= \sum_{i=1}^M N_i(x, y, z) w_i(t) = [N]\{w\} \end{aligned} \quad (10.87)$$

(where M is the number of element nodes), the velocity components can be expressed as

$$\begin{aligned} \dot{u} &= \frac{\partial u}{\partial t} = [N]\{\dot{u}\} \\ \dot{v} &= \frac{\partial v}{\partial t} = [N]\{\dot{v}\} \\ \dot{w} &= \frac{\partial w}{\partial t} = [N]\{\dot{w}\} \end{aligned} \quad (10.88)$$

The element kinetic energy expressed in terms of nodal velocities and interpolation functions is then written as

$$T^{(e)} = \frac{1}{2} \iiint_{V^{(e)}} (\{\dot{u}\}^T [N]^T [N] \{\dot{u}\} + \{\dot{v}\}^T [N]^T [N] \{\dot{v}\} + \{\dot{w}\}^T [N]^T [N] \{\dot{w}\}) \rho \, dV^{(e)} \quad (10.89)$$

Denoting the nodal velocities as

$$\{\hat{\delta}\} = \begin{Bmatrix} \{\dot{u}\} \\ \{\dot{v}\} \\ \{\dot{w}\} \end{Bmatrix} \quad (10.90)$$

a $3M \times 1$ column matrix, the kinetic energy is expressed as

$$T^{(e)} = \frac{1}{2} \{\hat{\delta}\}^T \iiint_{V^{(e)}} \begin{bmatrix} [N]^T [N] & 0 & 0 \\ 0 & [N]^T [N] & 0 \\ 0 & 0 & [N]^T [N] \end{bmatrix} \rho \, dV^{(e)} \{\hat{\delta}\} \\ = \frac{1}{2} \{\hat{\delta}\}^T [m^{(e)}] \{\hat{\delta}\} \quad (10.91)$$

and the element mass matrix is thus identified as

$$[m^{(e)}] = \iiint_{V^{(e)}} \begin{bmatrix} [N]^T [N] & 0 & 0 \\ 0 & [N]^T [N] & 0 \\ 0 & 0 & [N]^T [N] \end{bmatrix} \rho \, dV^{(e)} \quad (10.92)$$

Note that, in Equation 10.92, the zero terms actually represent $M \times M$ null matrices. Therefore, the mass matrix as derived is a $3M \times 3M$ matrix, which is also readily shown to be symmetric. Also note that the mass matrix of Equation 10.92 is a *consistent* mass matrix. The following example illustrates the computations for a two-dimensional element.

EXAMPLE 10.6

Formulate the mass matrix for the two-dimensional rectangular element depicted in Figure 10.12. The element has uniform thickness 5 mm and density $\rho = 7.83 \times 10^{-6} \text{ kg/mm}^3$.

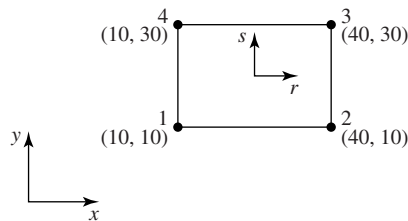


Figure 10.12 The rectangular element of Example 10.6.

10.6 Mass Matrix for a General Element: Equations of Motion

415

■ Solution

Per Equation 6.56, the interpolation functions in terms of serendipity or natural coordinates are

$$N_1(r, s) = \frac{1}{4}(1-r)(1-s)$$

$$N_2(r, s) = \frac{1}{4}(1+r)(1-s)$$

$$N_3(r, s) = \frac{1}{4}(1+r)(1+s)$$

$$N_4(r, s) = \frac{1}{4}(1-r)(1+s)$$

with $r = (x - 25)/15$ and $s = (y - 20)/10$. For integration in the natural coordinates, $dx = 15 dr$ and $dy = 10 ds$. The mass matrix is 8×8 and the nonzero terms are defined by

$$\begin{aligned} \iiint_{V^{(e)}} [N]^T [N] \rho \, dV^{(e)} &= \rho t \int_{-1}^1 \int_{-1}^1 [N]^T [N] (15 \, dr)(10 \, ds) \\ &= 150(5)\rho \int_{-1}^1 \int_{-1}^1 [N]^T [N] \, dr \, ds \end{aligned}$$

In this solution, we compute a few terms for illustration, then present the overall results. For example,

$$\begin{aligned} m_{11} &= 150(5)\rho \int_{-1}^1 \int_{-1}^1 N_1^2 \, dr \, ds = \frac{150(5)}{16} \rho \int_{-1}^1 \int_{-1}^1 (1-r)^2 (1-s)^2 \, dr \, ds \\ &= \frac{150(5)}{16} \rho \left[\frac{(1-r)^3}{3} \frac{(1-s)^3}{3} \right]_{-1}^1 = \frac{750}{16} \rho \left(\frac{64}{9} \right) = \frac{4(750)}{9} (7.830)(10)^{-6} \\ &= 2.6(10)^{-3} \text{ kg} \end{aligned}$$

Similarly,

$$\begin{aligned} m_{12} &= 150(5)\rho \int_{-1}^1 \int_{-1}^1 N_1 N_2 \, dr \, ds = \frac{150(5)}{16} \rho \int_{-1}^1 \int_{-1}^1 (1-r^2)(1-s)^2 \, dr \, ds \\ &= \frac{150(5)}{16} \rho \left[\left(r - \frac{r^3}{3} \right) \left(\frac{(1-s)^3}{3} \right) (-1) \right]_{-1}^1 \\ &= \frac{150(5)}{16} (7.83)(10)^{-6} \left(\frac{32}{9} \right) = 1.3(10)^{-3} \text{ kg} \end{aligned}$$

If we carry out all the integrations indicated to form the mass matrix, the final result for the rectangular element is

$$[m^{(e)}] = \begin{bmatrix} 2.6 & 1.3 & 0.7 & 1.3 & 0 & 0 & 0 & 0 \\ 1.3 & 2.6 & 1.3 & 0.7 & 0 & 0 & 0 & 0 \\ 0.7 & 1.3 & 2.6 & 1.3 & 0 & 0 & 0 & 0 \\ 1.3 & 0.7 & 1.3 & 2.6 & 0 & 0 & 0 & 0 \\ 0 & 0 & 0 & 0 & 2.6 & 1.3 & 0.7 & 1.3 \\ 0 & 0 & 0 & 0 & 1.3 & 2.6 & 1.3 & 0.7 \\ 0 & 0 & 0 & 0 & 0.7 & 1.3 & 2.6 & 1.3 \\ 0 & 0 & 0 & 0 & 1.3 & 0.7 & 1.3 & 2.6 \end{bmatrix} (10)^{-3} \text{ kg}$$

We observe that the element mass matrix is symmetric, as expected. Also note that storing the entire matrix as shown would be quite inefficient, since only the 4×4 submatrix of nonzero terms is needed.

Having developed a general formulation for the mass matrix of a finite element, we return to the determination of the equations of motion of a structure modeled via the finite element method and subjected to dynamic (that is, time-dependent) loading. If we have in hand, as we do, the mass and stiffness matrices of a finite element, we can assemble the global equations for a finite element model of a structure and obtain an expression for the total energy in the form

$$\frac{1}{2}\{\dot{q}\}^T[M]\{\dot{q}\} + \frac{1}{2}\{q\}^T[K]\{q\} - \{q\}^T\{f\} = E \quad (10.93)$$

where $\{q\}$ is the column matrix of displacements described in the global coordinate system and all other terms are as previously defined. (At this point, we reemphasize that Equation 10.93 models the response of an ideal elastic system, which contains no mechanism for energy dissipation.) For a system as described, total mechanical energy is constant, so that $dE/dt = 0$. As the mechanical energy is expressed as a function of both velocity and displacement, the minimization procedure requires that

$$\frac{dE}{dt} = \frac{\partial E}{\partial \dot{q}_i} \frac{\partial \dot{q}_i}{\partial t} + \frac{\partial E}{\partial q_i} \frac{\partial q_i}{\partial t} = 0 \quad i = 1, P \quad (10.94)$$

where we now represent the total number of degrees of freedom of the model as P to avoid confusion with the mass matrix notation $[M]$. Application of Equation 10.94 to the energy represented by Equation 10.93 yields a system of ordinary differential equations

$$[M]\{\ddot{q}\} + [K]\{q\} = \{F\} \quad (10.95)$$

Equation 10.94 is not necessarily mathematically rigorous in every case. However, for the systems under consideration, in which there is no energy removal mechanism and the total potential energy includes the effect of external forces, the

10.6 Mass Matrix for a General Element: Equations of Motion

417

resulting equations of motion are the same as those given by both the *Lagrangian* approach and *variational principles* [5].

Examination of Equation 10.95 in light of known facts about the stiffness and mass matrices reveals that the differential equations are coupled, at least through the stiffness matrix, which is known to be symmetric but not diagonal. The phenomena embodied here is referred to as *elastic coupling*, as the coupling terms arise from the elastic stiffness matrix. In consistent mass matrices, the equations are also coupled by the nondiagonal nature of the mass matrix; therefore, the term *inertia coupling* is applied when the mass matrix is not diagonal. Obtaining solutions for coupled differential equations is not generally a straightforward procedure. We show, however, that the modal characteristics embodied in the equations of motion can be used to advantage in examining system response to harmonic (sinusoidal) forcing functions. The so-called *harmonic response* is a capability of essentially any finite element software package, and the general techniques are discussed in the following section, after a brief discussion of natural modes.

In the absence of externally applied nodal forces, Equation 10.95 is a system of P homogeneous, linear second-order differential equations in the independent variable time. Hence, we have an eigenvalue problem in which the eigenvalues are the natural circular frequencies of oscillation of the structural system, and the eigenvectors are the amplitude vectors (mode shapes) corresponding to the natural frequencies. The frequency equation is represented by the determinant

$$|-\omega^2[M] + [K]| = 0 \quad (10.96)$$

If formally expanded, this determinant yields a polynomial of order P in the variable ω^2 . Solution of the frequency polynomial results in computation of P natural circular frequencies and P modal amplitude vectors. The free-vibration response of such a system is then described by the sum (superposition) of the natural vibration modes as

$$\delta_i(t) = \sum_{j=1}^P A_i^{(j)} \sin(\omega_j t + \phi_j) \quad i = 1, P \quad (10.97)$$

Note that the superposition indicated by Equation 10.97 is valid only for linear differential equations.

In Equation 10.97, the $A_i^{(j)}$ and ϕ_j are to be determined to satisfy given initial conditions. In accord with previous examples for simpler systems, we know that the amplitude vectors for a given modal frequency can be determined within a single unknown constant, so we can write the modal amplitude vectors as

$$\{A^{(i)}\} = A_1^{(i)} \begin{Bmatrix} 1 \\ \beta_2^{(i)} \\ \beta_3^{(i)} \\ \vdots \\ \beta_P^{(i)} \end{Bmatrix} \quad i = 1, P \quad (10.98)$$

where the β terms are known constants resulting from substitution of the natural circular frequencies into the governing equations for the amplitudes. For a system having P degrees of freedom, we have $2P$ unknown constants $A_1^{(i)}$ and ϕ_i , $i = 1, P$ in the motion solution. The constants are determined by application of $2P$ initial conditions, which are generally specified as the displacements and velocities of the nodes at time $t = 0$. While the natural modes of free vibration are important in and of themselves, application of modal analysis to the harmonically forced response of structural systems is a very important concept. Prior to examination of the forced response, we derive a very important property of the principal vibration modes.

10.7 ORTHOGONALITY OF THE PRINCIPAL MODES

The principal modes of vibration of systems with multiple degrees of freedom share a fundamental mathematical property known as *orthogonality*. The free-vibration response of a multiple degrees-of-freedom system is described by Equation 10.95 with $\{F\} = 0$ as

$$[M]\{\ddot{q}\} + [K]\{q\} = \{0\} \quad (10.99)$$

Assuming that we have solved for the natural circular frequencies and the modal amplitude vectors via the assumed solution form $q_i(t) = A_i \sin(\omega t + \phi)$, substitution of a particular frequency ω_i into Equation 10.99 gives

$$-\omega_i^2 [M]\{A^{(i)}\} + [K]\{A^{(i)}\} = 0 \quad (10.100)$$

and for any other frequency ω_j

$$-\omega_j^2 [M]\{A^{(j)}\} + [K]\{A^{(j)}\} = 0 \quad (10.101)$$

Multiplying Equation 10.100 by $\{A^{(j)}\}^T$ and Equation 10.101 by $\{A^{(i)}\}^T$ gives

$$-\omega_i^2 \{A^{(j)}\}^T [M]\{A^{(i)}\} + \{A^{(j)}\}^T [K]\{A^{(i)}\} = 0 \quad (10.102)$$

$$-\omega_j^2 \{A^{(i)}\}^T [M]\{A^{(j)}\} + \{A^{(i)}\}^T [K]\{A^{(j)}\} = 0 \quad (10.103)$$

Subtracting Equation 10.102 from Equation 10.103, we have

$$\{A^{(j)}\}^T [M]\{A^{(i)}\} (\omega_i^2 - \omega_j^2) = 0 \quad i \neq j \quad (10.104)$$

In arriving at the result represented by Equation 10.104, we utilize the fact from matrix algebra that $[A]^T [B] [C] = [C]^T [B] [A]$, where $[A]$, $[B]$, $[C]$ are any three matrices for which the triple product is defined. As the two circular frequencies in Equation 10.104 are distinct, we conclude that

$$\{A^{(j)}\}^T [M]\{A^{(i)}\} = 0 \quad i \neq j \quad (10.105)$$

Equation 10.105 is the mathematical statement of *orthogonality of the principal modes of vibration*. The orthogonality property provides a very powerful mathematical technique for decoupling the equations of motion of a multiple degrees-of-freedom system.

For a system exhibiting P degrees of freedom, we define the *modal matrix* as a $P \times P$ matrix in which the columns are the amplitude vectors for each natural mode of vibration; that is,

$$[A] = [\{A^{(1)}\} \{A^{(2)}\} \dots \{A^{(P)}\}] \quad (10.106)$$

and consider the matrix triple product $[S] = [A]^T [M] [A]$. Per the orthogonality condition, Equation 10.105, each off-diagonal term of the matrix represented by the triple product is zero; hence, the matrix $[S] = [A]^T [M] [A]$ is a *diagonal* matrix. The diagonal (nonzero) terms of the matrix have magnitude

$$S_{ii} = \{A^{(i)}\}^T [M] \{A^{(i)}\} \quad i = 1, P \quad (10.107)$$

As each modal amplitude vector is known only within a constant multiple (recall in earlier examples that we set $A_1^{(i)} = 1$ arbitrarily), the modal amplitude vectors can be manipulated such that the diagonal terms described by Equation 10.107 can be made to assume any desired numerical value. In particular, if the value is selected as unity, so that

$$S_{ii} = \{A^{(i)}\}^T [M] \{A^{(i)}\} = 1 \quad i = 1, P \quad (10.108)$$

then the modal amplitude vectors are said to be *orthonormal* and the matrix triple product becomes

$$[S] = [A]^T [M] [A] = [I] \quad (10.109)$$

where $[I]$ is the $P \times P$ identity matrix.

Normalizing the modal amplitude vectors per Equation 10.108 is a straightforward procedure, as follows. Let a specific modal amplitude be represented by Equation 10.98 in which the first term is arbitrarily assigned value of unity. The corresponding diagonal term of the modal matrix is then

$$\sum_{j=1}^P \sum_{k=1}^P m_{jk} A_j^{(i)} A_k^{(i)} = S_{ii} = \text{constant} \quad (10.110)$$

If we redefine the terms of the modal amplitude vector so that

$$A_j^{(i)} = \frac{A_j^{(i)}}{\sqrt{S_{ii}}} = \frac{A_j^{(i)}}{\sqrt{\sum_{j=1}^P \sum_{k=1}^P m_{jk} A_j^{(i)} A_k^{(i)}}} \quad i = 1, P \quad (10.111)$$

the matrix described by Equation 10.109 is indeed the identity matrix.

Having established the orthogonality concept and normalized the modal matrix, we return to the general problem described by Equation 10.95, in which the force vector is no longer assumed to be zero. For reasons that will become

apparent, we introduce the change of variables

$$\{q\} = [A]\{p\} \quad (10.112)$$

where $\{p\}$ is the column matrix of *generalized displacements*, which are linear combinations of the actual nodal displacements $\{q\}$, and $[A]$ is the normalized modal matrix. Equation 10.95 then becomes

$$[M][A]\{\ddot{p}\} + [K][A]\{p\} = \{F\} \quad (10.113)$$

Premultiplying by $[A]^T$, we obtain

$$[A]^T[M][A]\{\ddot{p}\} + [A]^T[K][A]\{p\} = [A]^T\{F\} \quad (10.114)$$

Utilizing the orthogonality principle, Equation 10.114 is

$$[I]\{\ddot{p}\} + [A]^T[k][A]\{p\} = [A]^T\{F\} \quad (10.115)$$

Now we must examine the stiffness effects as represented by $[A]^T[K][A]$. Given that $[K]$ is a symmetric matrix, the triple product $[A]^T[K][A]$ is also a symmetric matrix. Following the previous development of orthogonality of the principal modes, the triple product $[A]^T[K][A]$ is also easily shown to be a diagonal matrix. The values of the diagonal terms are found by multiplying Equation 10.100 by $\{A^{(i)}\}^T$ to obtain

$$-\omega_i^2 \{A^{(i)}\}^T [M] \{A^{(i)}\} + \{A^{(i)}\}^T [K] \{A^{(i)}\} = 0 \quad i = 1, P \quad (10.116)$$

If the modal amplitude vectors have been normalized as described previously, Equation 10.116 is

$$\{A^{(i)}\}^T [K] \{A^{(i)}\} = \omega_i^2 \quad i = 1, P \quad (10.117)$$

hence, the matrix triple product $[A]^T[K][A]$ produces a diagonal matrix having diagonal terms equal to the squares of the natural circular frequencies of the principal modes of vibration; that is,

$$[A]^T[K][A] = \begin{bmatrix} \omega_1^2 & 0 & \cdot & \cdot & \cdot & 0 \\ 0 & \omega_2^2 & & & & \cdot \\ \cdot & & \cdot & & & \cdot \\ \cdot & & & \cdot & & \cdot \\ \cdot & & & & \cdot & \cdot \\ 0 & \cdot & \cdot & \cdot & \cdot & \omega_P^2 \end{bmatrix} \quad (10.118)$$

Finally, Equation 10.115 becomes

$$[I]\{\ddot{p}\} + [\omega^2]\{p\} = [A]^T\{F\} \quad (10.119)$$

with matrix $[\omega^2]$ representing the diagonal matrix defined in Equation 10.118.

EXAMPLE 10.7

Using the data of Example 10.3, normalize the modal matrix and verify that $[A]^T[M][A] = [I]$ and $[A]^T[K][A] = [\omega^2]$.

10.7 Orthogonality of the Principal Modes

421

■ Solution

For the first mode, we have

$$\begin{aligned} S_{11} &= \{A^{(1)}\}^T [M] \{A^{(1)}\} = [1 \quad 1.4325 \quad 2.0511] \begin{bmatrix} m & 0 & 0 \\ 0 & m & 0 \\ 0 & 0 & 2m \end{bmatrix} \begin{Bmatrix} 1 \\ 1.4325 \\ 2.0511 \end{Bmatrix} \\ &= 11.4404m \end{aligned}$$

so the first modal amplitude vector is normalized by dividing each term by $\sqrt{S_{11}} = 3.3824\sqrt{m}$, which gives the normalized vector as

$$\{A^{(1)}\} = \frac{1}{\sqrt{m}} \begin{Bmatrix} 0.2956 \\ 0.4289 \\ 0.6064 \end{Bmatrix}$$

Applying the same procedure to the modal amplitude vectors for the second and third modes gives

$$\{A^{(2)}\} = \frac{1}{\sqrt{m}} \begin{Bmatrix} 0.6575 \\ 0.5618 \\ -0.3550 \end{Bmatrix} \quad \{A^{(3)}\} = \frac{1}{\sqrt{m}} \begin{Bmatrix} 0.6930 \\ -0.7124 \\ 0.0782 \end{Bmatrix}$$

and the normalized modal matrix is

$$[A] = \frac{1}{\sqrt{m}} \begin{bmatrix} 0.2956 & 0.6575 & 0.6930 \\ 0.4289 & 0.5618 & -0.7124 \\ 0.6064 & -0.3550 & 0.0782 \end{bmatrix}$$

To verify Equation 10.109, we form the triple product

$$\begin{aligned} [A]^T [M] [A] &= \frac{1}{m} \begin{bmatrix} 0.2956 & 0.4289 & 0.6064 \\ 0.6575 & 0.5618 & -0.3550 \\ 0.6930 & -0.7124 & 0.0782 \end{bmatrix} \begin{bmatrix} m & 0 & 0 \\ 0 & m & 0 \\ 0 & 0 & 2m \end{bmatrix} \\ &\times \begin{bmatrix} 0.2956 & 0.6575 & 0.6930 \\ 0.4289 & 0.5618 & -0.7124 \\ 0.6064 & -0.3550 & 0.0782 \end{bmatrix} = \begin{bmatrix} 1 & 0 & 0 \\ 0 & 1 & 0 \\ 0 & 0 & 1 \end{bmatrix} \end{aligned}$$

as expected.

The triple product with respect to the stiffness matrix is

$$\begin{aligned} [A]^T [K] [A] &= \frac{k}{m} \begin{bmatrix} 0.2956 & 0.4289 & 0.6064 \\ 0.6575 & 0.5618 & -0.3550 \\ 0.6990 & -0.7124 & 0.0782 \end{bmatrix} \begin{bmatrix} 3 & -2 & 0 \\ -2 & 3 & -1 \\ 0 & -1 & 1 \end{bmatrix} \\ &\times \begin{bmatrix} 0.2956 & 0.6575 & 0.6990 \\ 0.4289 & 0.5618 & -0.7124 \\ 0.6064 & -0.3550 & 0.0782 \end{bmatrix} \end{aligned}$$

which evaluates to

$$[A]^T [K] [A] = \frac{k}{m} \begin{bmatrix} 0.1532 & 0 & 0 \\ 0 & 1.2912 & 0 \\ 0 & 0 & 5.0557 \end{bmatrix} = \begin{bmatrix} \omega_1^2 & 0 & 0 \\ 0 & \omega_2^2 & 0 \\ 0 & 0 & \omega_3^2 \end{bmatrix}$$

10.8 HARMONIC RESPONSE USING MODE SUPERPOSITION

The orthogonality condition of the principal modes is especially useful in analyzing the steady-state response of finite element models to harmonic forcing functions. In this context, a harmonic forcing function is described as $F(t) = F_0 \sin \omega_f t$, where F_0 is a constant force magnitude and ω_f is a constant circular frequency of the forcing function. Prior to applying the mode superposition method, a complete modal analysis must be performed to obtain the natural circular frequencies and normalized modal amplitude vectors (hence, the normalized modal matrix). Using the techniques of the previous section, the equations of motion for the forced case become

$$[I]\{\ddot{p}\} + [\omega^2]\{p\} = [A]^T\{F\} \quad (10.120)$$

Assuming that the structural model under consideration exhibits P total degrees of freedom, Equation 10.120 represents a set of P uncoupled, ordinary differential equations of the form

$$\ddot{p}_i + \omega_i^2 p_i = \sum_{j=1}^P A_j^{(i)} F_j(t) \quad i = 1, P \quad (10.121)$$

Observing that the right-hand side is a known linear combination of harmonic forces (these are the so-called generalized forces), the solution to each of the equations is a summation of particular solutions corresponding to each of the harmonic force terms. By analogy with the procedure used for forced vibration of a single degree-of-freedom system in Section 10.2, the solutions of Equation 10.121 are given by

$$p_i(t) = \sum_{j=1}^P \frac{A_j^{(i)} F_{j0}}{\omega_i^2 - \omega_{jf}^2} \sin \omega_{jf} t \quad i = 1, P \quad (10.122)$$

Hence, the generalized displacements $p_i(t)$ are represented by a combination of independent harmonic motions having frequencies corresponding to the forcing frequencies. Note that, if a forcing frequency is close in value to one of the natural frequencies, the denominator term becomes small and the forced response amplitude is large; hence, there are many possibilities for a resonant condition.

The mode superposition method provides mathematical convenience in obtaining the forced response, because the equations of motion become uncoupled and solution is straightforward. However, Equation 10.122 gives the displacement response of generalized displacements rather than actual nodal displacements, owing to the transformation described by Equation 10.112. As the modal matrix is known, conversion of the generalized displacements to actual displacements requires only multiplication by the normalized modal matrix.

EXAMPLE 10.8

Again consider the 3 degrees-of-freedom system of Example 10.3 and determine the steady state response when a downward force $F = F_0 \sin \omega_f t$ is applied to mass 2.

■ Solution

For the given conditions, the applied nodal force vector is

$$\{F(t)\} = \begin{Bmatrix} 0 \\ F_0 \sin \omega_f t \\ 0 \end{Bmatrix}$$

and the generalized forces are

$$[A]^T \{F\} = \frac{1}{\sqrt{m}} \begin{bmatrix} 0.2956 & 0.4209 & 0.6064 \\ 0.6575 & 0.5618 & -0.3550 \\ 0.6930 & -0.7124 & 0.0782 \end{bmatrix} \begin{Bmatrix} 0 \\ F_0 \sin \omega_f t \\ 0 \end{Bmatrix} = \begin{Bmatrix} 0.4209 \\ 0.5618 \\ -0.7124 \end{Bmatrix} \frac{F_0 \sin \omega_f t}{\sqrt{m}}$$

The equations of motion for the generalized coordinates are then

$$\begin{aligned} \ddot{p}_1 + \omega_1^2 p_1 &= \frac{0.4209 F_0 \sin \omega_f t}{\sqrt{m}} \\ \ddot{p}_2 + \omega_2^2 p_2 &= \frac{0.5618 F_0 \sin \omega_f t}{\sqrt{m}} \\ \ddot{p}_3 + \omega_3^2 p_3 &= \frac{-0.7124 F_0 \sin \omega_f t}{\sqrt{m}} \end{aligned}$$

for which the solutions are

$$\begin{aligned} p_1(t) &= \frac{0.4209 F_0 \sin \omega_f t}{(\omega_1^2 - \omega_f^2) \sqrt{m}} \\ p_2(t) &= \frac{0.5618 F_0 \sin \omega_f t}{(\omega_2^2 - \omega_f^2) \sqrt{m}} \\ p_3(t) &= \frac{-0.7124 F_0 \sin \omega_f t}{(\omega_3^2 - \omega_f^2) \sqrt{m}} \end{aligned}$$

The actual displacements, $x(t) = q(t)$ in this case, are obtained by application of Equation 10.112:

$$\{x\} = [A]\{p\} = \frac{1}{\sqrt{m}} \begin{bmatrix} 0.2956 & 0.6575 & 0.6930 \\ 0.4209 & 0.5618 & -0.7124 \\ 0.6064 & -0.3550 & 0.0782 \end{bmatrix} \begin{Bmatrix} \frac{0.4209}{\omega_1^2 - \omega_f^2} \\ \frac{0.5618}{\omega_2^2 - \omega_f^2} \\ \frac{-0.7124}{\omega_3^2 - \omega_f^2} \end{Bmatrix} \frac{F_0 \sin \omega_f t}{\sqrt{m}}$$

Expanding, the steady-state displacements are given by

$$x_1(t) = \left(\frac{0.1244}{\omega_1^2 - \omega_f^2} + \frac{0.3694}{\omega_2^2 - \omega_f^2} + \frac{-0.4937}{\omega_3^2 - \omega_f^2} \right) \frac{F_0 \sin \omega_f t}{m}$$

$$x_2(t) = \left(\frac{0.1772}{\omega_1^2 - \omega_f^2} + \frac{0.3156}{\omega_2^2 - \omega_f^2} + \frac{0.5075}{\omega_3^2 - \omega_f^2} \right) \frac{F_0 \sin \omega_f t}{m}$$

$$x_3(t) = \left(\frac{0.2552}{\omega_1^2 - \omega_f^2} + \frac{-0.1994}{\omega_2^2 - \omega_f^2} + \frac{-0.0557}{\omega_3^2 - \omega_f^2} \right) \frac{F_0 \sin \omega_f t}{m}$$

A few observations need to be made regarding the displacements calculated in this example:

1. The displacement of each mass is a sinusoidal oscillation about the equilibrium position, and the circular frequency of the oscillation is the same as the frequency of the forcing function.
2. The characteristics of the principal modes of vibration are reflected in the solutions, owing to the effects of the natural circular frequencies and modal amplitude vectors in determining the forced oscillation amplitudes.
3. The displacement solutions represent only the forced motion of each mass; in addition, free vibration may also exist in superposition with the forced response.
4. Energy dissipation mechanisms are not incorporated into the model.

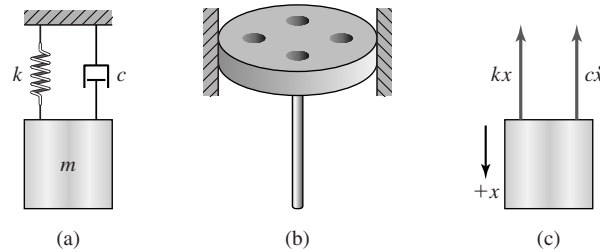
The mode superposition method may seem quite complicated and, when attempting to obtain solutions by hand, the method is indeed tedious. However, the required computations are readily amenable to digital computer techniques and quite easily programmed. Additional ramifications of computer techniques for the method will be discussed in a following article.

10.9 ENERGY DISSIPATION: STRUCTURAL DAMPING

To this point, the dynamic analysis techniques dealt only with structural systems in which there is no mechanism for energy dissipation. As stated earlier, all real systems exhibit such dissipation and, unlike the simple models presented, do not oscillate forever, as predicted by the ideal model solutions. In structural systems, the phenomenon of energy dissipation is referred to as *damping*. Damping may take on many physical forms, including devices specifically designed for the purpose (passive and active damping devices), sliding friction, and the internal dissipation characteristics of materials subjected to cyclic loading. In this section, we begin with an idealized model of damping for the simple harmonic oscillator and extend the damping concept to full-scale structural models.

10.9 Energy Dissipation: Structural Damping

425

**Figure 10.13**

(a) A spring-mass system with damping. (b) The schematic representation of a dashpot piston. (c) A free-body diagram of a mass with the damping force included.

Figure 10.13a depicts a simple harmonic oscillator to which has been added a *dashpot*. A *dashpot* is a damping device that utilizes a piston moving through a viscous fluid to remove energy via shear stress in the fluid and associated heat generation. The piston typically has small holes to allow the fluid to pass through but is otherwise sealed on its periphery, as schematically depicted in Figure 10.13b. The force exerted by such a device is known to be directly proportional to the velocity of the piston as

$$f_d = -c\dot{x} \quad (10.123)$$

where f_d is the damping force, c is the damping coefficient of the device, and \dot{x} is velocity of the mass assumed to be directly and rigidly connected to the piston of the damper. The dynamic free-body diagram of Figure 10.13c represents a situation at an arbitrary time with the system in motion. As in the undamped case considered earlier, we assume that displacement is measured from the equilibrium position. Under the conditions stated, the equation of motion of the mass is

$$m\ddot{x} + c\dot{x} + kx = 0 \quad (10.124)$$

Owing to the form of Equation 10.124, the solution is assumed in exponential form as

$$x(t) = C e^{st} \quad (10.125)$$

where C and s are constants to be determined. Substitution of the assumed solution yields

$$(ms^2 + cs + k)C e^{st} = 0 \quad (10.126)$$

As we seek nontrivial solutions valid for all values of time, we conclude that

$$ms^2 + cs + k = 0 \quad (10.127)$$

must hold if we are to obtain a general solution. Equation 10.127 is the characteristic equation (also the frequency equation) for the damped single degree-of-freedom system. From analyses of undamped vibration, we know that the natural

frequency given by $\omega^2 = k/m$ is an important property of the system, so we modify the characteristic equation to

$$s^2 + \frac{c}{m}s + \omega^2 = 0 \quad (10.128)$$

Solving Equation 10.128 by the quadratic formula yields two roots, as expected, given by

$$s_1 = \frac{1}{2} \left[\left(\frac{c}{m} \right)^2 - \sqrt{\left(\frac{c}{m} \right)^2 - 4\omega^2} \right] \quad (10.129a)$$

$$s_2 = \frac{1}{2} \left[\left(\frac{c}{m} \right)^2 + \sqrt{\left(\frac{c}{m} \right)^2 - 4\omega^2} \right] \quad (10.129b)$$

The most important characteristic of the roots is the value of $(c/m)^2 - 4\omega^2$, and there are three cases of importance:

1. If $(c/m)^2 - 4\omega^2 > 0$, the roots are real, distinct, and negative; and the displacement response is the sum of decaying exponentials.
2. If $(c/m)^2 - 4\omega^2 = 0$, we have a case of repeated roots; for this situation, the displacement is also shown to be a decaying exponential. It is convenient to define this as a critical case and let the value of the damping coefficient c correspond to the so-called *critical damping coefficient*. Hence, $c_c^2 = 4\omega^2 m^2$ or $c_c = 2m\omega$.
3. If $(c/m)^2 - 4\omega^2 < 0$, the roots of the characteristic equation are imaginary; this case can be shown [2] to represent decaying sinusoidal oscillations.

Regardless of the amount of damping present, the free-vibration response, as shown by the preceding analysis, is an exponentially decaying function in time. This gives more credence to our previous discussion of harmonic response, in which we ignored the free vibrations. In general, a system response is defined primarily by the applied forcing functions, as the natural (free, principal) vibrations die out with damping. The response of a damped spring-mass system corresponding to each of the three cases of damping is depicted in Figure 10.14.

We now define the *damping ratio* as $\zeta = c/2m\omega$ and note that, if $\zeta > 1$, we have what is known as *overdamped* motion; if $\zeta = 1$, the motion is said to be *critically damped*; and if $\zeta < 1$, the motion is *underdamped*. As most structural systems are underdamped, we focus on the case of $\zeta < 1$. For this situation, it is readily shown [2] that the response of a damped harmonic oscillator is described by

$$x(t) = e^{-\zeta\omega t} (A \sin \omega_d t + B \cos \omega_d t) \quad (10.130)$$

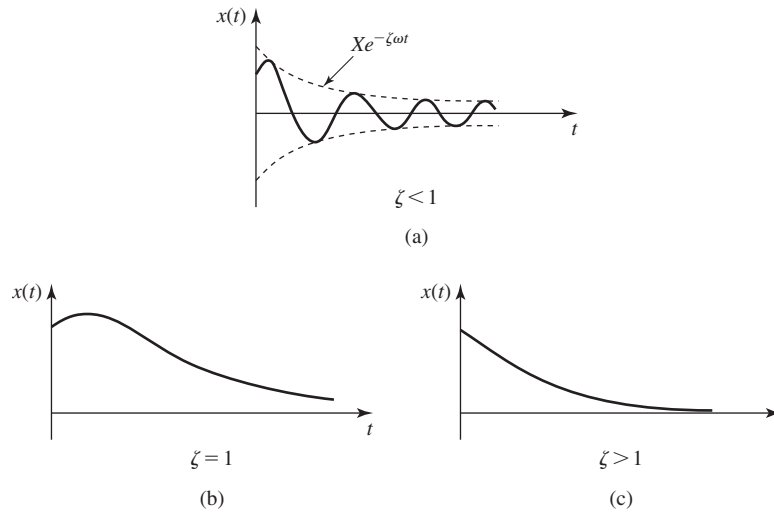


Figure 10.14 Characteristic damped motions: (a) Underdamped. (b) Critically damped. (c) Overdamped.

where ω_d is the *damped natural circular frequency*, given by

$$\omega_d^2 = (1 - \zeta^2) \frac{k}{m} \quad (10.131)$$

and the coefficients are determined by the initial conditions.

While we demonstrate the effect of damping via the simple harmonic oscillator, several points can be made that are applicable to any structural system:

1. The natural frequencies of vibration of a system are reduced by the effect of damping, per Equation 10.131.
2. The free vibrations decay exponentially to zero because of the effects of damping.
3. In light of point 2, in the case of forced vibration, the steady-state solution is driven only by the forcing functions.
4. Damping is assumed to be linearly proportional to nodal velocities.

10.9.1 General Structural Damping

An elastic structure subjected to dynamic loading does not, in general, have specific damping elements attached. Instead, the energy dissipation characteristics of the structure are inherent to its mechanical properties. How does, for example, a cantilevered beam, when “tweaked” at one end, finally stop vibrating? (If the reader has a flexible ruler at hand, many experiments can be performed to exhibit the change in fundamental frequency as a function of beam length as well as the

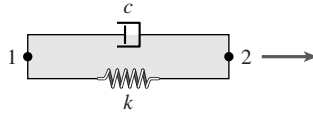


Figure 10.15 A model of a bar element with damping.

decay of the motion.) The answer to the damping question is complex. For example, structures are subjected to the atmosphere, so that air resistance is a factor. Air resistance is, in general, proportional to velocity squared, so this effect is nonlinear. Fortunately, air resistance in most cases is negligible. On the other hand, the internal friction of a material is not negligible and must be considered.

If we incorporate the concepts of damping as applied to the simple harmonic oscillator, the equations of motion of a finite element model of a structure become

$$[M]\{\ddot{q}\} + [C]\{\dot{q}\} + [K]\{q\} = \{F(t)\} \quad (10.132)$$

where $[C]$ is the system viscous damping matrix assembled by the usual rules. For example, a bar element with damping is mathematically modeled as a linear spring and a dashpot connected in parallel to the element nodes as in Figure 10.15. The element damping matrix is

$$[c^{(e)}] = \begin{bmatrix} c & -c \\ -c & c \end{bmatrix} \quad (10.133)$$

and the element equations of motion are

$$[m^{(e)}]\{\ddot{u}\} + [c^{(e)}]\{\dot{u}\} + [k^{(e)}]\{u\} = \{f^{(e)}\} \quad (10.134)$$

The element damping matrix is symmetric and singular, and the individual terms are assigned to the global damping matrix in the same manner as the mass and stiffness matrices. Assembly of the global equations of motion for a finite element model of a damped structure is simple. Determination of the effective viscous damping coefficients for structural elements is not so simple.

Damping due to internal friction is known as *structural damping*, and experiments on many different elastic materials have shown that the energy loss per motion cycle in structural damping is proportional to the material stiffness and the square of displacement amplitude [2]. That is,

$$\Delta U_{\text{cycle}} = \lambda k X^2 \quad (10.135)$$

where λ is a dimensionless structural damping coefficient, k is the material stiffness, and X is the displacement amplitude. By equating the energy loss per cycle to the energy loss per cycle in viscous damping, an equivalent viscous damping coefficient is obtained:

$$c_{\text{eq}} = \frac{\lambda k}{\omega} \quad (10.136)$$

where ω is circular frequency of oscillation. That the equivalent damping coefficient depends on frequency is somewhat troublesome, since the implication is that different coefficients are required for different frequencies. If we consider a single degree-of-freedom system for which $\omega = \sqrt{k/m}$, the equivalent damping coefficient given by Equation 10.136 becomes

$$c_{\text{eq}} = \frac{\lambda k}{\omega} = \lambda \frac{k}{\sqrt{k/m}} = \lambda \sqrt{km} \quad (10.137)$$

indicating that the damping coefficient is proportional, at least in a general sense, to both stiffness and mass. We return to this observation shortly.

Next we consider the application of the transformation using the normalized matrix as described in Section 10.7. Applying the transformation to Equation 10.132 results in

$$\{\ddot{p}\} + [A]^T [C] [A] \{\dot{p}\} + [\omega^2] \{p\} = [A]^T \{F(t)\} \quad (10.138)$$

The transformed damping matrix

$$[C'] = [A]^T [C] [A] \quad (10.139)$$

is easily shown to be a symmetric matrix, but the matrix is *not necessarily diagonal*. The transformation does not necessarily result in decoupling the equations of motion, and the simplification of the mode superposition method is not necessarily available. If, however, the damping matrix is such that

$$[C] = \alpha [M] + \beta [K] \quad (10.140)$$

where α and β are constants, then

$$[C'] = \alpha [A]^T [M] [A] + \beta [A]^T [K] [A] = \alpha [I] + \beta [\omega^2] \quad (10.141)$$

is a diagonal matrix and the differential equations of motion are decoupled. Note that the assertion of Equation 10.140 leads directly to the diagonalization of the damping matrix as given by Equation 10.141. Hence, Equation 10.138 becomes

$$\{\ddot{p}\} + (\alpha + \beta[\omega^2])\{\dot{p}\} + [\omega^2]\{p\} = [A]^T \{F(t)\} \quad (10.142)$$

As the differential equations represented by Equation 10.142 are decoupled, let us now examine the solution of one such equation

$$\ddot{p}_i + (\alpha + \beta\omega_i^2)\dot{p}_i + \omega_i^2 p_i = \sum_{j=1}^P A_j^{(i)} F_j(t) \quad (10.143)$$

where P is the total number of degrees of freedom. Without loss of generality and for convenience of illustration, we consider Equation 10.143 for only one of the terms on the right-hand side, assumed to be a harmonic force such that

$$\ddot{p}_i + (\alpha + \beta\omega_i^2)\dot{p}_i + \omega_i^2 p_i = F_0 \sin \omega_f t \quad (10.144)$$

and assume that the solution is

$$p_i(t) = X_i \sin \omega_f t + Y_i \cos \omega_f t \quad (10.145)$$

Substitution of the assumed solution into the governing equation yields

$$-X_i \omega_f^2 \sin \omega_f t - Y_i \omega_f^2 \cos \omega_f t + (\alpha + \beta \omega_i^2) \omega_f (X_i \cos \omega_f t - Y_i \sin \omega_f t) + \omega_i^2 X_i \sin \omega_f t + \omega_i^2 Y_i \cos \omega_f t = F_0 \sin \omega_f t \quad (10.146)$$

Equating coefficients of sine and cosine terms yields the algebraic equations

$$\begin{bmatrix} \omega_i^2 - \omega_f^2 & -\omega_f(\alpha + \beta \omega_i^2) \\ \omega_f(\alpha + \beta \omega_i^2) & \omega_i^2 - \omega_f^2 \end{bmatrix} \begin{Bmatrix} X_i \\ Y_i \end{Bmatrix} = \begin{Bmatrix} F_0 \\ 0 \end{Bmatrix} \quad (10.147)$$

for determination of the forced amplitudes X_i and Y_i . The solutions are

$$X_i = \frac{F_0(\omega_i^2 - \omega_f^2)}{(\omega_i^2 - \omega_f^2)^2 + \omega_f^2(\alpha + \beta \omega_i^2)^2} \quad (10.148)$$

$$Y_i = \frac{-F_0 \omega_f(\alpha + \beta \omega_i^2)}{(\omega_i^2 - \omega_f^2)^2 + \omega_f^2(\alpha + \beta \omega_i^2)^2}$$

To examine the character of the solution represented by Equation 10.145, we convert the solution to the form

$$p_i(t) = Z_i \sin(\omega_f t + \phi_i) \quad (10.149)$$

with

$$Z_i = \sqrt{X_i^2 + Y_i^2} \quad \text{and} \quad \phi_i = \tan^{-1} \frac{Y_i}{X_i}$$

to obtain

$$p_i(t) = \frac{F_0}{\sqrt{(\omega_i^2 - \omega_f^2)^2 + \omega_f^2(\alpha + \beta \omega_i^2)^2}} \sin(\omega_f t + \phi_i) \quad (10.150)$$

$$\phi_i = \tan^{-1} \left(\frac{-\omega_f^2(\alpha + \beta \omega_i^2)}{\omega_i^2 - \omega_f^2} \right) \quad (10.151)$$

Again, the mathematics required to obtain these solutions are algebraically tedious; however, Equations 10.150 and 10.151 are perfectly general, in that the equations give the solution for every equation in 10.142, provided the applied nodal forces are harmonic. Such solutions are easily generated via digital computer software. The actual displacements are then obtained by application of Equation 10.112, as in the case of undamped systems.

The equivalent viscous damping described in Equation 10.140 is known as *Rayleigh damping* [6] and used very often in structural analysis. It can be shown, by comparison to a damped single degree-of-freedom system that

$$\alpha + \beta \omega_i^2 = 2\omega_i \zeta_i \quad (10.152)$$

10.9 Energy Dissipation: Structural Damping

431

where ζ_i is the damping ratio corresponding to the i th mode of vibration, that is,

$$\zeta_i = \frac{\alpha}{2\omega_i} + \frac{\beta\omega_i}{2} \quad (10.153)$$

represents the degree of damping for the i th mode. Equation 10.153 provides a means of estimating α and β if realistic estimates of the degree of damping for two modes are known. The realistic estimates are most generally obtained experimentally or may be applied by rule of thumb. The following example illustrates the computations and the effect on other modes.

EXAMPLE 10.9

Experiments on a prototype structure indicate that the effective viscous damping ratio is $\zeta = 0.03$ (3 percent) when the oscillation frequency is $\omega = 5$ rad/sec and $\zeta = 0.1$ (10 percent) for frequency $\omega = 15$ rad/sec. Determine the Rayleigh damping factors α and β for these known conditions.

■ Solution

Applying Equation 10.153 to each of the known conditions yields

$$\begin{aligned} 0.03 &= \frac{\alpha}{2(5)} + \frac{5\beta}{2} \\ 0.1 &= \frac{\alpha}{2(15)} + \frac{15\beta}{2} \end{aligned}$$

Simultaneous solution provides the Rayleigh coefficients as

$$\begin{aligned} \alpha &= -0.0375 \\ \beta &= 0.0135 \end{aligned}$$

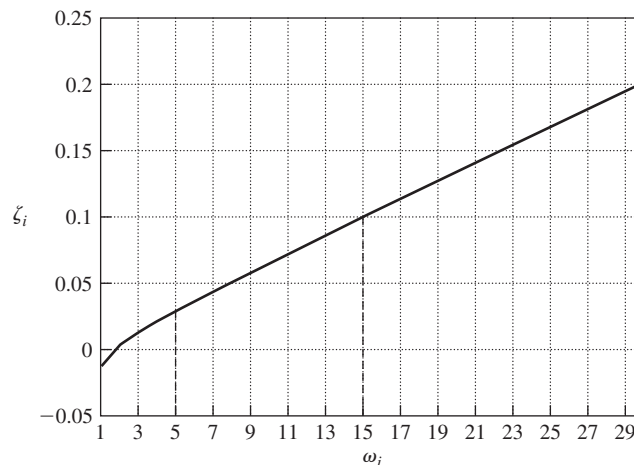


Figure 10.16 Equivalent damping factor versus frequency for Example 10.9.

If we were to apply the equivalent damping given by these values to the entire frequency spectrum of a structure, the effective damping ratio for any mode would be given by

$$\zeta_i = \frac{-0.0375 + 0.0135 \omega_i^2}{2\omega_i}$$

If the values of α and β are applied to a multiple degrees-of-freedom system, the damping ratio for each frequency is different. To illustrate the variation, Figure 10.16 depicts the modal damping ratio as a function of frequency. The plot shows that, of course, the ratios for the specified frequencies are exact and the damping ratios vary significantly for other frequencies.

Rayleigh damping as just described is not the only approach to structural damping used in finite element analysis. Finite element software packages also include options for specifying damping as a material-dependent property, as opposed to a property of the structure, as well as defining specific damping elements (finite elements) that may be added at any geometric location in the structure. The last capability allows the finite element analyst to examine the effects of energy dissipation elements as applied to specific locations.

10.10 TRANSIENT DYNAMIC RESPONSE

In Chapter 7, finite difference methods for direct numerical integration of finite element models of heat transfer problems are introduced. In those applications, we deal with a scalar field variable, temperature, and first-order governing equations. Therefore, we need only to develop finite difference approximations to first derivatives. For structural dynamic systems, we have a set of second-order differential equations

$$[M]\{\ddot{\delta}\} + [C]\{\dot{\delta}\} + [K]\{\delta\} = \{F(t)\} \quad (10.154)$$

representing the assembled finite element model of a structure subjected to general (nonharmonic) forcing functions. In applying finite difference methods to Equation 10.154, we assume that the state of the system is known at time t and we wish to compute the displacements at time $t + \Delta t$; that is, we wish to solve

$$[M]\{\ddot{\delta}(t + \Delta t)\} + [C]\{\dot{\delta}(t + \Delta t)\} + [K]\{\delta(t + \Delta t)\} = \{F(t + \Delta t)\} \quad (10.155)$$

for $\{\delta(t + \Delta t)\}$.

Many finite difference techniques exist for solving the system of equations represented by Equation 10.155. Here, we describe Newmark's method [7] also referred to as the *constant acceleration method*. In the Newmark method, it is assumed that the acceleration during an integration time step Δt is constant and an average value. For constant acceleration, we can write the kinematic relations

$$\delta(t + \Delta t) = \delta(t) + \dot{\delta}(t)\Delta t + \ddot{\delta}_{av} \frac{\Delta t^2}{2} \quad (10.156)$$

$$\dot{\delta}(t + \Delta t) = \dot{\delta}(t) + \ddot{\delta}_{av}\Delta t \quad (10.157)$$

The constant, average acceleration is

$$\ddot{\delta}_{av} = \frac{\ddot{\delta}(t + \Delta t) + \ddot{\delta}(t)}{2} \quad (10.158)$$

Combining Equations 10.156 and 10.158 yields

$$\delta(t + \Delta t) = \delta(t) + \dot{\delta}(t)\Delta t + [\ddot{\delta}(t + \Delta t) + \ddot{\delta}(t)]\frac{\Delta t^2}{4} \quad (10.159)$$

which is solved for the acceleration at $t + \Delta t$ to obtain

$$\ddot{\delta}(t + \Delta t) = \frac{4}{\Delta t^2}[\delta(t + \Delta t) - \delta(t)] - \frac{4}{\Delta t}\dot{\delta}(t) - \ddot{\delta}(t) \quad (10.160)$$

If we also substitute Equations 10.158 and 10.160 into Equation 10.157, we find the velocity at time $t + \Delta t$ to be given by

$$\dot{\delta}(t + \Delta t) = \frac{2}{\Delta t}[\delta(t + \Delta t) - \delta(t)] - \dot{\delta}(t) \quad (10.161)$$

Equations 10.160 and 10.161 express acceleration and velocity at $t + \Delta t$ in terms of known conditions at the previous time step and the displacement at $t + \Delta t$. If these relations are substituted into Equation 10.155, we obtain, after a bit of algebraic manipulation,

$$\begin{aligned} & \frac{4}{\Delta t^2}[M]\{\delta(t + \Delta t)\} + \frac{2}{\Delta t}[C]\{\delta(t + \Delta t)\} + [K]\{\delta(t + \Delta t)\} \\ & = \{F(t + \Delta t)\} + [M]\left(\{\dot{\delta}(t)\} + \frac{4}{\Delta t}\{\dot{\delta}(t)\} + \frac{4}{\Delta t^2}\{\delta(t)\}\right) \\ & \quad + [C]\left(\{\dot{\delta}(t)\} + \frac{2}{\Delta t}\{\delta(t)\}\right) \end{aligned} \quad (10.162)$$

Equation 10.162 is the recurrence relation for the Newmark method. While the relation may look complicated, it must be realized that the mass, damping, and stiffness matrices are known, so the equations are just an algebraic system in the unknown displacements at time $t + \Delta t$. The right-hand side of the system is known in terms of the solution at the previous time step and the applied forces. Equation 10.162 is often written symbolically as

$$[\bar{K}]\{\delta(t + \Delta t)\} = \{F_{\text{eff}}(t + \Delta t)\} \quad (10.163)$$

with

$$[\bar{K}] = \frac{4}{\Delta t^2}[M] + \frac{2}{\Delta t}[C] + [K] \quad (10.164)$$

$$\begin{aligned} \{F_{\text{eff}}(t + \Delta t)\} & = \{F(t + \Delta t)\} \\ & \quad + [M]\left(\{\dot{\delta}(t)\} + \frac{4}{\Delta t}\{\dot{\delta}(t)\} + \frac{4}{\Delta t^2}\{\delta(t)\}\right) \\ & \quad + [C]\left(\{\dot{\delta}(t)\} + \frac{2}{\Delta t}\{\delta(t)\}\right) \end{aligned} \quad (10.165)$$

The system of algebraic equations represented by Equation 10.163 can be solved at each time step for the unknown displacements. For a constant time step Δt , matrix $[\bar{K}]$ is constant and need be computed only once. The right-hand side $\{F_{\text{eff}}(t + \Delta t)\}$ must, of course, be updated at each time step. At each time step, the system of algebraic equations must be solved to obtain displacements. For this reason, the procedure is known as an implicit method. By back substitution through the appropriate relations, velocities and accelerations can also be obtained.

The Newmark method is known to be *unconditionally stable* [8]. While the details are beyond the scope of this text, stability (more to the point, instability) of a finite difference technique means that, under certain conditions, the computed displacements may grow without bound as the solution procedure “marches” in time. Several finite difference methods are known to be *conditionally stable*, meaning that accurate results are obtained only if the time step Δt is less than a prescribed critical value. This is not the case with the Newmark method. This does not mean, however, that the results are independent of the selected time step. Accuracy of any finite difference technique improves as the time step is reduced, and this phenomenon is a convergence concern similar to mesh refinement in a finite element model. For dynamic response of a finite element model, we must be concerned with not only the convergence related to the finite element mesh but also the time step convergence of the finite difference method selected. As discussed in a following section, finite element software for the transient dynamic response requires the user to specify “load steps,” which represent the change in loading as a function of time. The software then solves the finite element equations as if the problem is one of static equilibrium at the specified loading condition. It is very important to note that the system equations represented by Equation 10.163 are based on the finite element model, even though the solution procedure is that of the finite difference technique in time.

10.11 BAR ELEMENT MASS MATRIX IN TWO-DIMENSIONAL TRUSS STRUCTURES

The bar-element-consistent mass matrix defined in Equation 10.58 is valid only for axial vibrations. When bar elements are used in modeling two- and three-dimensional truss structures, additional considerations are required, and the mass matrix modified accordingly. When a truss undergoes deflection, either statically or dynamically, individual elements experience both axial and transverse displacement resulting from overall structural displacement and element interconnections at nodes. In Chapter 3, transverse displacement of elements was ignored in development of the element stiffness matrix as there is no transverse stiffness owing to the assumption of pin connections, hence free rotation. However, in the dynamic case, transverse motion introduces additional kinetic energy, which must be taken into account.

10.11 Bar Element Mass Matrix in Two-Dimensional Truss Structures

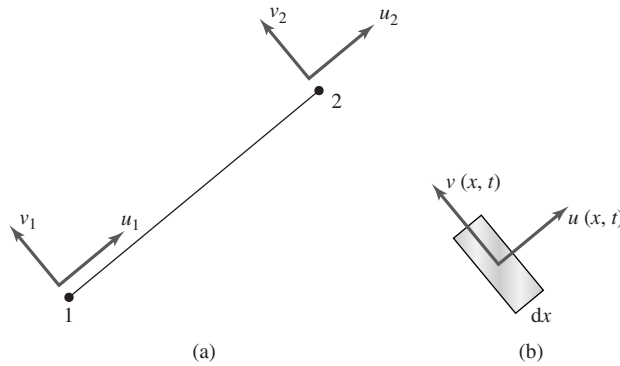


Figure 10.17 A bar element in two-dimensional motion:
(a) Nodal displacements. (b) Differential element.

Consider the differential volume of a bar element undergoing both axial and transverse displacement, as shown in Figure 10.17. We assume a dynamic situation such that both displacement components vary with position and time. The kinetic energy of the differential volume is

$$dT = \frac{1}{2} \rho A dx \left[\left(\frac{\partial u}{\partial t} \right)^2 + \left(\frac{\partial v}{\partial t} \right)^2 \right] = \frac{1}{2} \rho A dx (\dot{u}^2 + \dot{v}^2) \quad (10.166)$$

and the total kinetic energy of the bar becomes

$$T = \frac{1}{2} \rho A \int_0^L \dot{u}^2 dx + \frac{1}{2} \rho A \int_0^L \dot{v}^2 dx \quad (10.167)$$

Observing that the transverse displacement can be expressed in terms of the transverse displacements of the element nodes, using the same interpolation functions as for axial displacement, we have

$$\begin{aligned} u(x, t) &= N_1(x)u_1(t) + N_2(x)u_2(t) \\ v(x, t) &= N_1(x)v_1(t) + N_2(x)v_2(t) \end{aligned} \quad (10.168)$$

Using matrix notation, the velocities are written as

$$\begin{aligned} \dot{u}(x, t) &= [N_1 \quad N_2] \begin{Bmatrix} \dot{u}_1 \\ \dot{u}_2 \end{Bmatrix} \\ \dot{v}(x, t) &= [N_1 \quad N_2] \begin{Bmatrix} \dot{v}_1 \\ \dot{v}_2 \end{Bmatrix} \end{aligned} \quad (10.169)$$

and element kinetic energy becomes

$$T = \frac{1}{2} \rho A \{\dot{u}\}^T \int_0^L [N]^T [N] dx \{\dot{u}\} + \frac{1}{2} \rho A \{\dot{v}\}^T \int_0^L [N]^T [N] dx \{\dot{v}\} \quad (10.170)$$

Expressing the nodal velocities as

$$\{\dot{\delta}\} = \begin{Bmatrix} \dot{u}_1 \\ \dot{v}_1 \\ \dot{u}_2 \\ \dot{v}_2 \end{Bmatrix} \quad (10.171)$$

the kinetic energy expression can be rewritten in the form

$$\begin{aligned} T &= \frac{1}{2} \{\dot{\delta}\}^T [m_2^{(e)}] \{\dot{\delta}\} \\ &= \frac{1}{2} \{\dot{\delta}\}^T \rho A \int_0^L \begin{bmatrix} N_1^2 & 0 & N_1 N_2 & 0 \\ 0 & N_1^2 & 0 & N_1 N_2 \\ N_1 N_2 & 0 & N_2^2 & 0 \\ 0 & N_1 N_2 & 0 & N_2^2 \end{bmatrix} dx \{\dot{\delta}\} \end{aligned} \quad (10.172)$$

From Equation 10.172, the mass matrix of the bar element in two dimensions is identified as

$$[m_2^{(e)}] = \rho A \int_0^L \begin{bmatrix} N_1^2 & 0 & N_1 N_2 & 0 \\ 0 & N_1^2 & 0 & N_1 N_2 \\ N_1 N_2 & 0 & N_2^2 & 0 \\ 0 & N_1 N_2 & 0 & N_2^2 \end{bmatrix} dx = \frac{\rho AL}{6} \begin{bmatrix} 2 & 0 & 1 & 0 \\ 0 & 2 & 0 & 1 \\ 1 & 0 & 2 & 0 \\ 0 & 1 & 0 & 2 \end{bmatrix} \quad (10.173)$$

The mass matrix defined by Equation 10.173 is described in the element (local) coordinate system, since the axial and transverse directions are defined in terms of the axis of the element. How, then, is this mass matrix transformed to the global coordinate system of a structure? Recall that, in Chapter 3, the element axial displacements are expressed in terms of global displacements via a rotation transformation of the element x axis. To reiterate, the transverse displacements were not considered, as no stiffness is associated with the transverse motion. Now, however, the transverse displacements must be included in the transformation to global coordinates because of the associated mass and kinetic energy.

Figure 10.18 depicts a single node of a bar element oriented at angle θ relative to the X axis of a global coordinate system. Nodal displacements in the element frame are u_2, v_2 and corresponding global displacements are U_3, U_4 , respectively. As the displacement in the two coordinate systems must be the same, we have

$$\begin{aligned} u_2 &= U_3 \cos \theta + U_4 \sin \theta \\ v_2 &= -U_3 \sin \theta + U_4 \cos \theta \end{aligned} \quad (10.174)$$

or

$$\begin{Bmatrix} u_2 \\ v_2 \end{Bmatrix} = \begin{bmatrix} \cos \theta & \sin \theta \\ -\sin \theta & \cos \theta \end{bmatrix} \begin{Bmatrix} U_3 \\ U_4 \end{Bmatrix} \quad (10.175)$$

10.11 Bar Element Mass Matrix in Two-Dimensional Truss Structures

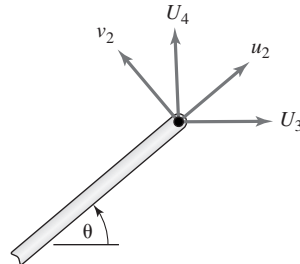


Figure 10.18 The relation of element and global displacements at a single node.

As the same relation holds at the other element node, the complete transformation is

$$\begin{Bmatrix} u_1 \\ v_1 \\ u_2 \\ v_2 \end{Bmatrix} = \begin{bmatrix} \cos \theta & \sin \theta & 0 & 0 \\ -\sin \theta & \cos \theta & 0 & 0 \\ 0 & 0 & \cos \theta & \sin \theta \\ 0 & 0 & -\sin \theta & \cos \theta \end{bmatrix} \begin{Bmatrix} U_1 \\ U_2 \\ U_3 \\ U_4 \end{Bmatrix} = [R] \{U\} \quad (10.176)$$

Since the nodal velocities are related by the same transformation, substitution into the kinetic energy expression shows that the mass matrix in the global coordinate system is

$$[M_2^{(e)}] = [R]^T [m_2^{(e)}] [R] \quad (10.177)$$

where we again use the subscript to indicate that the mass matrix is applicable to two-dimensional structures.

If the matrix multiplications indicated in Equation 10.177 are performed for an arbitrary angle, the resulting global mass matrix for a bar element is found to be

$$[M_2^{(e)}] = \frac{\rho AL}{6} \begin{bmatrix} 2 & 0 & 1 & 0 \\ 0 & 2 & 0 & 1 \\ 1 & 0 & 2 & 0 \\ 0 & 1 & 0 & 2 \end{bmatrix} \quad (10.178)$$

and the result is exactly the same as the mass matrix in the element coordinate system regardless of element orientation in the global system. This phenomenon should come as no surprise. Mass is an absolute scalar property and therefore independent of coordinate system. A similar development leads to the same conclusion when a bar element is used in modeling three-dimensional truss structures.

The complication described for including the additional transverse inertia effects of the bar element are also applicable to the one-dimensional beam (flexure) element. The mass matrix for the beam element given by Equation 10.78 is applicable only in a one-dimensional model. If the flexure element is used in modeling two- or three-dimensional frame structures, additional consideration must be given to formulation of the element mass matrix owing to axial inertia

effects. For beam elements, most finite software packages include axial effects (i.e., the beam element is a combination of the bar element and the two-dimensional flexure element) and all appropriate inertia effects are included in formulation of the consistent mass matrix.

EXAMPLE 10.10

As a complete example of modal analysis, we return to the truss structure of Section 3.7, repeated here as Figure 10.19. Note that, for the current example, the static loads applied in the earlier example have been removed. As we are interested here in the free-vibration response of the structure, the static loads are of no consequence in the dynamic analysis. With the additional specification that material density is $\rho = 2.6(10)^{-4}$ lb-s²/in.⁴, we solve the eigenvalue problem to determine the natural circular frequencies and modal amplitude vectors for free vibration of the structure.

As the global stiffness matrix has already been assembled, the procedure is not repeated here. We must, however, assemble the global mass matrix using the element numbers and global node numbers as shown. The element and global mass matrices for the bar element in two dimensions are given by Equation 10.178 as

$$[m^{(e)}] = \frac{\rho AL}{6} \begin{bmatrix} 2 & 0 & 1 & 0 \\ 0 & 2 & 0 & 1 \\ 1 & 0 & 2 & 0 \\ 0 & 1 & 0 & 2 \end{bmatrix}$$

As elements 1, 3, 4, 5, 7, and 8 have the same length, area, and density, we have

$$\begin{aligned} [M^{(1)}] &= [M^{(3)}] = [M^{(4)}] = [M^{(5)}] = [M^{(7)}] = [M^{(8)}] \\ &= \frac{(2.6)(10)^{-4}(1.5)(40)}{6} \begin{bmatrix} 2 & 0 & 1 & 0 \\ 0 & 2 & 0 & 1 \\ 1 & 0 & 2 & 0 \\ 0 & 1 & 0 & 2 \end{bmatrix} \\ &= \begin{bmatrix} 5.2 & 0 & 2.6 & 0 \\ 0 & 5.2 & 0 & 2.6 \\ 2.6 & 0 & 5.2 & 0 \\ 0 & 2.6 & 0 & 5.2 \end{bmatrix} (10)^{-3} \text{ lb-s}^2/\text{in.} \end{aligned}$$

while for elements 2 and 6

$$\begin{aligned} [M^{(2)}] &= [M^{(6)}] = \frac{2.6(10)^{-4}(1.5)(40\sqrt{2})}{6} \begin{bmatrix} 2 & 0 & 1 & 0 \\ 0 & 2 & 0 & 1 \\ 1 & 0 & 2 & 0 \\ 0 & 1 & 0 & 2 \end{bmatrix} \\ &= \begin{bmatrix} 7.36 & 0 & 3.68 & 0 \\ 0 & 7.36 & 0 & 3.68 \\ 3.68 & 0 & 7.36 & 0 \\ 0 & 3.68 & 0 & 7.36 \end{bmatrix} (10)^{-3} \text{ lb-s}^2/\text{in.} \end{aligned}$$

10.11 Bar Element Mass Matrix in Two-Dimensional Truss Structures

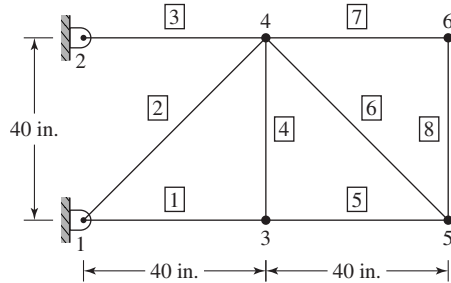


Figure 10.19 Eight-element truss of Example 10.10.

The element-to-global displacement relations are as given in Chapter 3. Using the direct assembly procedure, the global mass matrix is

$$[M] = \begin{bmatrix} 12.56 & 0 & 0 & 0 & 2.6 & 0 & 3.68 & 0 & 0 & 0 & 0 & 0 \\ 0 & 12.56 & 0 & 0 & 0 & 2.6 & 0 & 3.68 & 0 & 0 & 0 & 0 \\ 0 & 0 & 5.2 & 0 & 0 & 0 & 2.6 & 0 & 0 & 0 & 0 & 0 \\ 0 & 0 & 0 & 5.2 & 0 & 0 & 0 & 2.6 & 0 & 0 & 0 & 0 \\ 2.6 & 0 & 0 & 0 & 7.8 & 0 & 2.6 & 0 & 2.6 & 0 & 0 & 0 \\ 0 & 2.6 & 0 & 0 & 0 & 7.8 & 0 & 2.6 & 0 & 2.6 & 0 & 0 \\ 3.68 & 0 & 2.6 & 0 & 2.6 & 0 & 22.52 & 0 & 3.68 & 0 & 2.6 & 0 \\ 0 & 3.68 & 0 & 2.6 & 0 & 2.6 & 0 & 22.52 & 0 & 3.68 & 0 & 2.6 \\ 0 & 0 & 0 & 0 & 2.6 & 0 & 3.68 & 0 & 17.76 & 0 & 2.6 & 0 \\ 0 & 0 & 0 & 0 & 0 & 2.6 & 0 & 3.68 & 0 & 17.76 & 0 & 2.6 \\ 0 & 0 & 0 & 0 & 0 & 0 & 2.6 & 0 & 2.6 & 0 & 10.4 & 0 \\ 0 & 0 & 0 & 0 & 0 & 0 & 0 & 2.6 & 0 & 2.6 & 0 & 10.4 \end{bmatrix} (10)^{-3}$$

Applying the constraint conditions $U_1 = U_2 = U_3 = U_4 = 0$, the mass matrix for the active degrees of freedom becomes

$$[M_a] = \begin{bmatrix} 7.8 & 0 & 2.6 & 0 & 2.6 & 0 & 0 & 0 \\ 0 & 7.8 & 0 & 2.6 & 0 & 2.6 & 0 & 0 \\ 2.6 & 0 & 22.52 & 0 & 3.68 & 0 & 2.6 & 0 \\ 0 & 2.6 & 0 & 22.52 & 0 & 3.68 & 0 & 2.6 \\ 2.6 & 0 & 3.68 & 0 & 17.76 & 0 & 2.6 & 0 \\ 0 & 2.6 & 0 & 3.68 & 0 & 17.76 & 0 & 2.6 \\ 0 & 0 & 2.6 & 0 & 2.6 & 0 & 10.4 & 0 \\ 0 & 0 & 0 & 2.6 & 0 & 2.6 & 0 & 10.4 \end{bmatrix} (10)^{-3} \text{ lb-s}^2/\text{in.}$$

Extracting the data from Section 3.7, the stiffness matrix for the active degrees of freedom is

$$[K_a] = \begin{bmatrix} 7.5 & 0 & 0 & 0 & -3.75 & 0 & 0 & 0 \\ 0 & 3.75 & 0 & -3.75 & 0 & 0 & 0 & 0 \\ 0 & 0 & 10.15 & 0 & -1.325 & 1.325 & -3.75 & 0 \\ 0 & -3.75 & 0 & 6.4 & 1.325 & -1.325 & 0 & 0 \\ -3.75 & 0 & -1.325 & 1.325 & 5.075 & -1.325 & 0 & 0 \\ 0 & 0 & 1.325 & -1.325 & -1.325 & 5.075 & 0 & -3.75 \\ 0 & 0 & -3.75 & 0 & 0 & 0 & 3.75 & 0 \\ 0 & 0 & 0 & 0 & 0 & -3.75 & 0 & 3.75 \end{bmatrix} 10^5 \text{ lb/in.}$$

The finite element model for the truss exhibits 8 degrees of freedom; hence, the characteristic determinant

$$|-\omega^2[M] + [K]| = 0$$

yields, theoretically, eight natural frequencies of oscillation and eight corresponding modal shapes (modal amplitude vectors). For this example, the natural modes were computed using the student edition of the ANSYS program [9], with the results shown in Table 10.1. The corresponding modal amplitude vectors (normalized to the mass matrix as discussed relative to orthogonality) are shown in Table 10.2.

The frequencies are observed to be quite large in magnitude. The fundamental frequency, about 122 cycles/sec is beyond the general comprehension of the human eye-brain interface (30 Hz is the accepted cutoff based on computer graphics research [10]). The high frequencies are not uncommon in such structures. The data used in this example correspond approximately to the material properties of aluminum; a light material with good stiffness relative to weight. Recalling the basic relation $\omega = \sqrt{k/m}$, high natural frequencies should be expected.

The mode shapes provide an indication of the geometric nature of the natural modes. As such, the numbers in Table 10.2 are not at all indicative of amplitude values; instead,

Table 10.1 Natural Modes

Mode	Frequency	
	Rad/sec	Hz
1	767.1	122.1
2	2082.3	331.4
3	2958.7	470.9
4	4504.8	716.9
5	6790.9	1080.8
6	7975.9	1269.4
7	8664.5	1379.0
8	8977.4	1428.8

10.11 Bar Element Mass Matrix in Two-Dimensional Truss Structures

Table 10.2 Modal Amplitude Vectors

Displacement	Mode							
	1	2	3	4	5	6	7	8
U_5	0.2605	2.194	1.213	-3.594	-1.445	-1.802	4.772	-4.368
U_6	2.207	-3.282	3.125	-2.1412	5.826	-0.934	1.058	0.727
U_7	-0.7754	0.7169	2.888	2.370	-0.142	-3.830	-2.174	-0.464
U_8	2.128	-2.686	1.957	-0.4322	-4.274	0.569	-0.341	0.483
U_9	0.5156	3.855	1.706	-3.934	-0.055	1.981	-2.781	3.956
U_{10}	4.118	2.556	-1.459	1.133	0.908	1.629	-3.319	-4.407
U_{11}	-0.7894	0.9712	4.183	4.917	0.737	6.077	4.392	-1.205
U_{12}	4.213	2.901	-1.888	2.818	0.604	-3.400	4.828	5.344

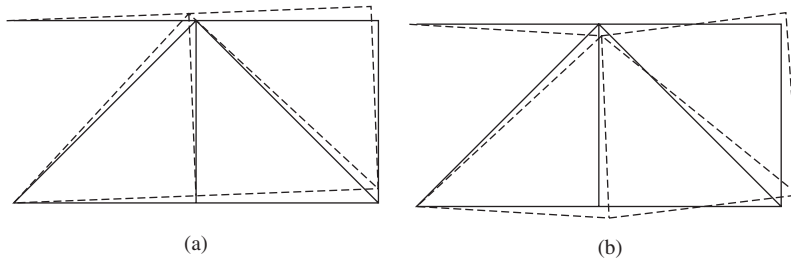


Figure 10.20

- (a) Fundamental mode shape of the truss in Example 10.10.
- (b) Second mode shape of the truss.

these are *relative* values of the motion of each node. It is more insightful to examine plots of the *mode shapes*; that is, plots of the structure depicting the shape of the structure if it did indeed oscillate in one of its natural modes. To this end, we present the mode shape corresponding to mode 1 in Figure 10.20a. Note that, in this fundamental mode, the truss vibrates much as a cantilevered beam about the constrained nodes. On the other hand, Figure 10.20b illustrates the mode shape for mode 2 oscillation. In mode 2, the structure exhibits an antisymmetric motion, in which the “halves” of the structure move in opposition to one another. Examination of the other modes reveals additional differences in the mode shapes.

Noting that Table 10.2 is, in fact, the modal matrix, it is a relatively simple matter to check the orthogonality conditions by forming the matrix triple products

$$[A]^T [M] [A] = [I]$$

$$[A]^T [K] [A] = \omega^2 [I]$$

Within reasonable numerical accuracy, the relations are indeed true for this example. We leave the detailed check as an exercise.

10.12 PRACTICAL CONSIDERATIONS

The major problem inherent to dynamic structural analysis is the time-consuming and costly amount of computation required. In a finite difference technique, such as that represented by Equation 10.163, the system of equations must be solved at every time step over the time interval of interest. For convergence, the time step is generally quite small, so the amount of computation required is huge. In modal analysis, the burden is in computing natural frequencies and mode shapes. As practical finite element models can contain tens of thousands of degrees of freedom, the time and expense of computing all of the frequencies and mode shapes is prohibitive. Fortunately, to obtain reasonable approximations of dynamic response, it is seldom necessary to solve the full eigenvalue problem. Two practical arguments underlie the preceding statement. First, the lower-valued frequencies and corresponding mode shapes are more important in describing structural behavior. This is because the higher-valued frequencies most often represent vibration of individual elements and do not contribute significantly to overall structural response. Second, when structures are subjected to time-dependent forcing functions, the range of forcing frequencies to be experienced is reasonably predictable. Therefore, only system natural frequencies around that range are of concern in examining resonance possibilities.

Based on these arguments, many techniques have been developed that allow the computation (approximately) of a subset of natural frequencies and mode shapes of a structural system modeled by finite elements. While a complete discussion of the details is beyond the scope of this text, the following discussion explains the basic premises. (See Bathe [6] for a very good, rigorous description of the various techniques.) Using our notation, the eigenvalue problem that must be solved to obtain natural frequencies and mode shapes is written as

$$[K]\{A\} = \omega^2[M]\{A\} \quad (10.179)$$

The problem represented by Equation 10.179 is reduced in complexity by *static condensation* (or, more often, *Guyan reduction* [11]) using the assumption that all the structural mass can be lumped (concentrated) at some specific degrees of freedom without significantly affecting the frequencies and mode shapes of interest. Using the subscript *a* (active) to represent degrees of freedom of interest and subscript *c* (constrained) to denote all other degrees of freedom Equation 10.179 can be partitioned into

$$\begin{bmatrix} [K_{aa}] & [K_{ac}] \\ [K_{ca}] & [K_{cc}] \end{bmatrix} \begin{Bmatrix} \{A_a\} \\ \{A_c\} \end{Bmatrix} = \omega^2 \begin{bmatrix} [M_{aa}] & [0] \\ [0] & [0] \end{bmatrix} \begin{Bmatrix} \{A_a\} \\ \{A_c\} \end{Bmatrix} \quad (10.180)$$

In Equation 10.180, $[M_{aa}]$ is a diagonal matrix, so the mass has been lumped at the degrees of freedom of interest. The “constrained” degrees of freedom are constrained only in the sense that we assign zero mass to those degrees. The lower partition of Equation 10.180 is

$$[K_{ca}]\{A_a\} + [K_{cc}]\{A_c\} = \{0\} \quad (10.181)$$

and this equation can be solved as

$$\{A_c\} = -[K_{cc}]^{-1}[K_{ca}]\{A_a\} \quad (10.182)$$

to eliminate $\{A_c\}$. Substituting Equation 10.182 into the upper partition of Equation 10.180, we obtain

$$([K_{aa}] - [K_{ac}][K_{cc}]^{-1}[K_{ca}])\{A_a\} = \omega^2[M_{aa}]\{A_a\} \quad (10.183)$$

as the *reduced eigenvalue problem*. Note that all terms of the original stiffness matrix are retained but not those of the mass matrix. Another way of saying this is that the stiffness matrix is exact but the mass matrix is approximate.

The difficult part of this reduction procedure lies in selecting the degrees of freedom to be retained and associated with the lumped mass terms. Fortunately, finite element software systems have such selection built into the software. The user generally need specify only the number of degrees of freedom to be retained, and the software selects those degrees of freedom based on the smallest ratios of diagonal terms of the stiffness and mass matrices. Other algorithms are used if the user is interested in obtaining the dynamic modes within a specified frequency. In any case, the retained degrees of freedom are most often called *dynamic degrees of freedom* or *master degrees of freedom*.

This discussion is meant to be for general information and does not represent a hard and fast method for reducing and solving eigenvalue problems. Indeed, reference to Equation 10.182 shows that the procedure requires finding the inverse of a huge matrix to accomplish the reduction. Nevertheless, several powerful techniques have been developed around the general reduction idea. These include subspace iteration [12] and the Lanczos method [13]. The user of a particular finite element analysis software system must become familiar with the various options presented for dynamic analysis, as multiple computational schemes are available, depending on model size and user needs.

10.13 SUMMARY

The application of the finite element method to structural dynamics is introduced in the general context of linear systems. The basic ideas of natural frequency and mode shapes are introduced using both discrete spring-mass systems and general structural elements. Use of the natural modes of vibration to solve more-general problems of forced vibration is emphasized. In addition, the Newmark finite difference method for solving transient response to general forcing functions is developed. The chapter is intended only as a general introduction to structural dynamics. Indeed, many fine texts are devoted completely to the topic.

REFERENCES

1. Inman, D. J. *Engineering Vibration*, 2nd ed. Upper Saddle River, NJ: Prentice-Hall, 2001.
2. Hutton, D. V. *Applied Mechanical Vibrations*. New York: McGraw-Hill, 1980.
3. Huebner, K. H., and E. A. Thornton. *The Finite Element Method for Engineers*, 2nd ed. New York: John Wiley and Sons, 1982.

4. Ginsberg, J. H. *Advanced Engineering Dynamics*, 2nd ed. New York: Cambridge University Press, 1985.
5. Goldstein, H. *Classical Mechanics*, 2nd ed. Reading, MA: Addison-Wesley, 1980.
6. Bathe, K.-J. *Finite Element Procedures*. Englewood Cliffs, NJ: Prentice-Hall, 1996.
7. Newmark, N. M. "A Method of Computation for Structural Dynamics." *ASCE Journal of Engineering, Mechanics Division* 85 (1959).
8. Zienkiewicz, O. C. *The Finite Method*, 3rd ed. New York: McGraw-Hill, 1977.
9. *ANSYS User's Reference Manual*. Houghton, PA: Swanson Analysis Systems Inc., 2001.
10. Zeid, I. *CAD/CAM Theory and Practice*. New York: McGraw-Hill, 1991.
11. Guyan, R. J. "Reduction of Stiffness and Mass Matrices." *AIAA Journal* 3, no. 2 (1965).
12. Bathe, K.-J. "Convergence of Subspace Iteration." In *Formulations and Numerical Algorithms in Finite Element Analysis*. Cambridge, MA: MIT Press, 1977.
13. Lanczos, C. "An Iteration Method for the Solution of the Eigenvalue Problem of Linear Differential and Integral Operators." *Journal of the Research of the National Bureau of Standards* 45 (1950).

PROBLEMS

- 10.1 Verify by direct substitution that Equation 10.5 is the general solution of Equation 10.4.
- 10.2 A simple harmonic oscillator has $m = 3$ kg, $k = 5$ N/mm. The mass receives an impact such that the initial velocity is 5 mm/sec and the initial displacement is zero. Calculate the ensuing free vibration.
- 10.3 The equilibrium deflection of a spring-mass system as in Figure 10.1 is measured to be 1.4 in. Calculate the natural circular frequency, the cyclic frequency, and period of free vibrations.
- 10.4 Show that the forced amplitude given by Equation 10.28 can be expressed as

$$U = \frac{X_0}{1 - r^2} \quad r \neq 1$$

with $X_0 = F_0/k$ equivalent static deflection and $r = \omega_f/\omega \equiv$ frequency ratio.

- 10.5 Determine the solution to Equation 10.26 for the case $\omega_f = \omega$. Note that, for this condition, Equation 10.29 is *not* the correct solution.
- 10.6 Combine Equations 10.5 and 10.29 to obtain the complete response of a simple harmonic oscillator, including both free and forced vibration terms. Show that, for initial conditions given by $x(t = 0) = x_0$ and $\dot{x}(t = 0) = v_0$, the complete response becomes

$$x(t) = \frac{v_0}{\omega} \sin \omega t + x_0 \cos \omega t + \frac{X_0}{1 - r^2} (\sin \omega_f t - r \sin \omega t)$$

with X_0 and r as defined in Problem 10.4.

- 10.7 Use the result of Problem 10.6 with $x_0 = v_0 = 0$, $r = 0.95$, $X_0 = 2$, $\omega_f = 10$ rad/sec and plot the complete response $x(t)$ for several motion cycles.

- 10.8** For the problem in Example 10.2, what initial conditions would be required so that the system moved (a) in the fundamental mode only or (b) in the second mode only?
- 10.9** Using the data and solution of Example 10.2, normalize the modal matrix per the procedure of Section 10.7 and verify that the differential equations are uncoupled by the procedure.
- 10.10** Using the two-element solution given in Example 10.4, determine the modal amplitude vectors. Normalize the modal amplitude vectors and show that matrix product $[A]^T[M][A]$ is the identity matrix.
- 10.11** The 2 degrees-of-freedom system in Figure 10.4 is subjected to an external force $F_2 = 10 \sin 8t$ lb applied to node 2 and external force $F_3 = 6 \sin 4t$ lb applied to node 3. Use the normalized modal matrix to uncouple the differential equations and solve for the forced response of the nodal displacements. Use the numerical data of Example 10.2.
- 10.12** Solve the problem of Example 10.4 using two equal-length bar elements except that the mass matrices are *lumped*; that is, take the element mass matrices as

$$[m^{(1)}] = [m^{(2)}] = \frac{\rho AL}{4} \begin{bmatrix} 1 & 0 \\ 0 & 1 \end{bmatrix}$$

How do the computed natural frequencies compare with those obtained using consistent mass matrices?

- 10.13** Obtain a refined solution for Example 10.4 using three equal-length elements and lumped mass matrices. How do the frequencies compare to the two-element solution?
- 10.14** Considering the rotational degrees of freedom involved in a beam element, how would one define a lumped mass matrix for a beam element?
- 10.15** Verify the consistent mass matrix for the beam element given by Equation 10.78 by direct integration.
- 10.16** Verify the mass matrix result of Example 10.6 using Gaussian quadrature numerical integration.
- 10.17** Show that, within the accuracy of the calculations as given, the sum of all terms in the rectangular element mass matrix in Example 10.6 is twice the total mass of the element. Why?
- 10.18** What are the values of the terms of a lumped mass matrix for the element in Example 10.6?
- 10.19** Assume that the dynamic response equations for a finite element have been uncoupled and are given by Equation 10.120 but the external forces are not sinusoidal. How would you solve the differential equations for a general forcing function or functions?
- 10.20** Given the solution data of Example 10.7, assume that the system is changed to include damping such that the system damping matrix (after setting $u_1 = 0$) is given by

$$[C] = \begin{bmatrix} 2c & -c & 0 \\ -c & 2c & -c \\ 0 & -c & c \end{bmatrix}$$

Show that the matrix product $[A]^T[C][A]$ does not result in a diagonal matrix.

- 10.21 Perform the matrix multiplications indicated in Equation 10.177 to verify the result given in Equation 10.178.
- 10.22 For the truss in Example 10.10, reformulate the system mass matrix using lumped element mass matrices. Resolve for the frequencies and mode shapes using the finite element software available to you, if it has the lumped matrix available as an option (most finite element software includes this option).
- 10.23 If you formally apply a reduction procedure such as outlined in Section 10.12, which degrees of freedom would be important to retain if, say, we wish to compute only four of the eight frequencies?

APPENDIX

A

Matrix Mathematics

A.1 DEFINITIONS

The mathematical description of many physical problems is often simplified by the use of rectangular arrays of scalar quantities of the form

$$[A] = \begin{bmatrix} a_{11} & a_{12} & \cdots & a_{1n} \\ a_{21} & a_{22} & \cdots & a_{2n} \\ \vdots & \vdots & \vdots & \vdots \\ a_{m1} & a_{m2} & \cdots & a_{mn} \end{bmatrix} \quad (\text{A.1})$$

Such an array is known as a *matrix*, and the scalar values that compose the array are the *elements* of the matrix. The position of each element a_{ij} is identified by the *row* subscript i and the *column* subscript j .

The number of rows and columns determine the *order* of a matrix. A matrix having m rows and n columns is said to be of order “ m by n ” (usually denoted as $m \times n$). If the number of rows and columns in a matrix are the same, the matrix is a *square matrix* and said to be of order n . A matrix having only one row is called a *row matrix* or *row vector*. Similarly, a matrix with a single column is a *column matrix* or *column vector*.

If the rows and columns of a matrix $[A]$ are interchanged, the resulting matrix is known as the *transpose* of $[A]$, denoted by $[A]^T$. For the matrix defined in Equation A.1, the transpose is

$$[A]^T = \begin{bmatrix} a_{11} & a_{12} & \cdots & a_{1n} \\ a_{21} & a_{22} & \cdots & a_{2n} \\ \vdots & \vdots & \vdots & \vdots \\ a_{m1} & a_{m2} & \cdots & a_{mn} \end{bmatrix} \quad (\text{A.2})$$

and we observe that, if $[A]$ is of order m by n , then $[A]^T$ is of order n by m . For

example, if $[A]$ is given by

$$[A] = \begin{bmatrix} 2 & -1 & 3 \\ 4 & 0 & 2 \end{bmatrix}$$

the transpose of $[A]$ is

$$[A]^T = \begin{bmatrix} 2 & 4 \\ -1 & 0 \\ 3 & 2 \end{bmatrix}$$

Several important special types of matrices are defined next. A *diagonal* matrix is a square matrix composed of elements such that $a_{ij} = 0$ and $i \neq j$. Therefore, the only nonzero terms are those on the main diagonal (upper left to lower right). For example,

$$[A] = \begin{bmatrix} 2 & 0 & 0 \\ 0 & 1 & 0 \\ 0 & 0 & 3 \end{bmatrix}$$

is a diagonal matrix.

An *identity* matrix (denoted $[I]$) is a diagonal matrix in which the value of the nonzero terms is unity. Hence,

$$[A] = [I] = \begin{bmatrix} 1 & 0 & 0 \\ 0 & 1 & 0 \\ 0 & 0 & 1 \end{bmatrix}$$

is an identity matrix.

A *null* matrix (also known as a zero matrix $[0]$) is a matrix of any order in which the value of all elements is 0.

A *symmetric* matrix is a square matrix composed of elements such that the nondiagonal values are symmetric about the main diagonal. Mathematically, symmetry is expressed as $a_{ij} = a_{ji}$ and $i \neq j$. For example, the matrix

$$[A] = \begin{bmatrix} 2 & -2 & 0 \\ -2 & 4 & -3 \\ 0 & -3 & 1 \end{bmatrix}$$

is a symmetric matrix. Note that the transpose of a symmetric matrix is the same as the original matrix.

A *skew symmetric* matrix is a square matrix in which the diagonal terms a_{ii} have a value of 0 and the off-diagonal terms have values such that $a_{ij} = -a_{ji}$. An example of a skew symmetric matrix is

$$[A] = \begin{bmatrix} 0 & -2 & 0 \\ 2 & 0 & 3 \\ 0 & -3 & 0 \end{bmatrix}$$

For a skew symmetric matrix, we observe that the transpose is obtained by changing the algebraic sign of each element of the matrix.

A.2 ALGEBRAIC OPERATIONS

Addition and *subtraction* of matrices can be defined only for matrices of the same order. If $[A]$ and $[B]$ are both $m \times n$ matrices, the two are said to be *conformable* for addition or subtraction. The sum of two $m \times n$ matrices is another $m \times n$ matrix having elements obtained by summing the corresponding elements of the original matrices. Symbolically, matrix addition is expressed as

$$[C] = [A] + [B] \quad (\text{A.3})$$

where

$$c_{ij} = a_{ij} + b_{ij} \quad i = 1, m \quad j = 1, n \quad (\text{A.4})$$

The operation of matrix subtraction is similarly defined. Matrix addition and subtraction are *commutative* and *associative*; that is,

$$[A] + [B] = [B] + [A] \quad (\text{A.5})$$

$$[A] + ([B] + [C]) = ([A] + [B]) + [C] \quad (\text{A.6})$$

The product of a scalar and a matrix is a matrix in which every element of the original matrix is multiplied by the scalar. If a scalar u multiplies matrix $[A]$, then

$$[B] = u[A] \quad (\text{A.7})$$

where the elements of $[B]$ are given by

$$b_{ij} = ua_{ij} \quad i = 1, m \quad j = 1, n \quad (\text{A.8})$$

Matrix multiplication is defined in such a way as to facilitate the solution of simultaneous linear equations. The *product* of two matrices $[A]$ and $[B]$ denoted

$$[C] = [A][B] \quad (\text{A.9})$$

exists only if the number of columns in $[A]$ is equal to the number of rows in $[B]$. If this condition is satisfied, the matrices are said to be *conformable for multiplication*. If $[A]$ is of order $m \times p$ and $[B]$ is of order $p \times n$, the matrix product $[C] = [A][B]$ is an $m \times n$ matrix having elements defined by

$$c_{ij} = \sum_{k=1}^p a_{ik}b_{kj} \quad (\text{A.10})$$

Thus, each element c_{ij} is the sum of products of the elements in the i th row of $[A]$ and the corresponding elements in the j th column of $[B]$. When referring to the matrix product $[A][B]$, matrix $[A]$ is called the *premultiplier* and matrix $[B]$ is the *postmultiplier*.

In general, matrix multiplication is *not* commutative; that is,

$$[A][B] \neq [B][A] \quad (\text{A.11})$$

Matrix multiplication does satisfy the *associative* and *distributive* laws, and we can therefore write

$$\begin{aligned}([A][B])[C] &= [A]([B][C]) \\ [A]([B] + [C]) &= [A][B] + [A][C] \\ ([A] + [B])[C] &= [A][C] + [B][C]\end{aligned}\tag{A.12}$$

In addition to being noncommutative, matrix algebra differs from scalar algebra in other ways. For example, the equality $[A][B] = [A][C]$ does not necessarily imply $[B] = [C]$, since algebraic summing is involved in forming the matrix products. As another example, if the product of two matrices is a null matrix, that is, $[A][B] = [0]$, the result does not necessarily imply that either $[A]$ or $[B]$ is a null matrix.

A.3 DETERMINANTS

The *determinant* of a square matrix is a *scalar* value that is unique for a given matrix. The determinant of an $n \times n$ matrix is represented symbolically as

$$\det[A] = |A| = \begin{vmatrix} a_{11} & a_{12} & \cdots & a_{1n} \\ a_{21} & a_{22} & \cdots & a_{2n} \\ \vdots & \vdots & \ddots & \vdots \\ a_{n1} & a_{n2} & \cdots & a_{nn} \end{vmatrix}\tag{A.13}$$

and is evaluated according to a very specific procedure. First, consider the 2×2 matrix

$$[A] = \begin{bmatrix} a_{11} & a_{12} \\ a_{21} & a_{22} \end{bmatrix}\tag{A.14}$$

for which the determinant is defined as

$$|A| = \begin{vmatrix} a_{11} & a_{12} \\ a_{21} & a_{22} \end{vmatrix} \equiv a_{11}a_{22} - a_{12}a_{21}\tag{A.15}$$

Given the definition of Equation A.15, the determinant of a square matrix of any order can be determined.

Next, consider the determinant of a 3×3 matrix

$$|A| = \begin{vmatrix} a_{11} & a_{12} & a_{13} \\ a_{21} & a_{22} & a_{23} \\ a_{31} & a_{32} & a_{33} \end{vmatrix}\tag{A.16}$$

defined as

$$|A| = a_{11}(a_{22}a_{33} - a_{23}a_{32}) - a_{12}(a_{21}a_{33} - a_{23}a_{31}) + a_{13}(a_{21}a_{32} - a_{22}a_{31})\tag{A.17}$$

Note that the expressions in parentheses are the determinants of the second-order matrices obtained by striking out the first row and the first, second, and third columns, respectively. These are known as *minors*. A minor of a determinant is

another determinant formed by removing an equal number of rows and columns from the original determinant. The minor obtained by removing row i and column j is denoted $|M_{ij}|$. Using this notation, Equation A.17 becomes

$$|A| = a_{11}|M_{11}| - a_{12}|M_{12}| + a_{13}|M_{13}| \quad (\text{A.18})$$

and the determinant is said to be expanded in terms of the *cofactors* of the first row. The cofactors of an element a_{ij} are obtained by applying the appropriate algebraic sign to the minor $|M_{ij}|$ as follows. If the sum of row number i and column number j is even, the sign of the cofactor is positive; if $i + j$ is odd, the sign of the cofactor is negative. Denoting the cofactor as C_{ij} we can write

$$C_{ij} = (-1)^{i+j}|M_{ij}| \quad (\text{A.19})$$

The determinant given in Equation A.18 can then be expressed in terms of cofactors as

$$|A| = a_{11}C_{11} + a_{12}C_{12} + a_{13}C_{13} \quad (\text{A.20})$$

The determinant of a square matrix of *any* order can be obtained by expanding the determinant in terms of the cofactors of any row i as

$$|A| = \sum_{j=1}^n a_{ij}C_{ij} \quad (\text{A.21})$$

or any column j as

$$|A| = \sum_{i=1}^n a_{ij}C_{ij} \quad (\text{A.22})$$

Application of Equation A.21 or A.22 requires that the cofactors C_{ij} be further expanded to the point that all minors are of order 2 and can be evaluated by Equation A.15.

A.4 MATRIX INVERSION

The *inverse* of a square matrix $[A]$ is a square matrix denoted by $[A]^{-1}$ and satisfies

$$[A]^{-1}[A] = [A][A]^{-1} = [I] \quad (\text{A.23})$$

that is, the product of a square matrix and its inverse is the identity matrix of order n . The concept of the inverse of a matrix is of prime importance in solving simultaneous linear equations by matrix methods. Consider the algebraic system

$$\begin{aligned} a_{11}x_1 + a_{12}x_2 + a_{13}x_3 &= y_1 \\ a_{21}x_1 + a_{22}x_2 + a_{23}x_3 &= y_2 \\ a_{31}x_1 + a_{32}x_2 + a_{33}x_3 &= y_3 \end{aligned} \quad (\text{A.24})$$

which can be written in matrix form as

$$[A]\{x\} = \{y\} \quad (\text{A.25})$$

where

$$[A] = \begin{bmatrix} a_{11} & a_{12} & a_{13} \\ a_{21} & a_{22} & a_{23} \\ a_{31} & a_{32} & a_{33} \end{bmatrix} \quad (\text{A.26})$$

is the 3×3 coefficient matrix,

$$\{x\} = \begin{Bmatrix} x_1 \\ x_2 \\ x_3 \end{Bmatrix} \quad (\text{A.27})$$

is the 3×1 column matrix (vector) of unknowns, and

$$\{y\} = \begin{Bmatrix} y_1 \\ y_2 \\ y_3 \end{Bmatrix} \quad (\text{A.28})$$

is the 3×1 column matrix (vector) representing the right-hand sides of the equations (the “forcing functions”).

If the inverse of matrix $[A]$ can be determined, we can multiply both sides of Equation A.25 by the inverse to obtain

$$[A]^{-1}[A]\{x\} = [A]^{-1}\{y\} \quad (\text{A.29})$$

Noting that

$$[A]^{-1}[A]\{x\} = ([A]^{-1}[A])\{x\} = [I]\{x\} = \{x\} \quad (\text{A.30})$$

the solution for the simultaneous equations is given by Equation A.29 directly as

$$\{x\} = [A]^{-1}\{y\} \quad (\text{A.31})$$

While presented in the context of a system of three equations, the result represented by Equation A.31 is applicable to any number of simultaneous algebraic equations and gives the unique solution for the system of equations.

The inverse of matrix $[A]$ can be determined in terms of its cofactors and determinant as follows. Let the *cofactor matrix* $[C]$ be the square matrix having as elements the cofactors defined in Equation A.19. The *adjoint* of $[A]$ is defined as

$$\text{adj}[A] = [C]^T \quad (\text{A.32})$$

The inverse of $[A]$ is then formally given by

$$[A]^{-1} = \frac{\text{adj}[A]}{|A|} \quad (\text{A.33})$$

If the determinant of $[A]$ is 0, Equation A.33 shows that the inverse does not exist. In this case, the matrix is said to be *singular* and Equation A.31 provides no solution for the system of equations. Singularity of the coefficient matrix indicates one of two possibilities: (1) no solution exists or (2) multiple (non-unique) solutions exist. In the latter case, the algebraic equations are not linearly independent.

Calculation of the inverse of a matrix per Equation A.33 is cumbersome and not very practical. Fortunately, many more efficient techniques exist. One such technique is the *Gauss-Jordan reduction* method, which is illustrated using a 2×2 matrix:

$$[A] = \begin{bmatrix} a_{11} & a_{12} \\ a_{21} & a_{22} \end{bmatrix} \quad (\text{A.34})$$

The gist of the Gauss-Jordan method is to perform simple row and column operations such that the matrix is reduced to an identity matrix. The sequence of operations required to accomplish this reduction produces the inverse. If we divide the first row by a_{11} , the operation is the same as the multiplication

$$[B_1][A] = \begin{bmatrix} \frac{1}{a_{11}} & 0 \\ 0 & 1 \end{bmatrix} \begin{bmatrix} a_{11} & a_{12} \\ a_{21} & a_{22} \end{bmatrix} = \begin{bmatrix} 1 & \frac{a_{12}}{a_{11}} \\ a_{21} & a_{22} \end{bmatrix} \quad (\text{A.35})$$

Next, multiply the first row by a_{21} and subtract from the second row, which is equivalent to the matrix multiplication

$$[B_2][B_1][A] = \begin{bmatrix} 1 & 0 \\ -a_{21} & 1 \end{bmatrix} \begin{bmatrix} 1 & \frac{a_{12}}{a_{11}} \\ a_{21} & a_{22} \end{bmatrix} = \begin{bmatrix} 1 & \frac{a_{12}}{a_{11}} \\ 0 & a_{22} - \frac{a_{12}}{a_{11}}a_{21} \end{bmatrix} = \begin{bmatrix} 1 & \frac{a_{12}}{a_{11}} \\ 0 & |A| \end{bmatrix} \quad (\text{A.36})$$

Multiply the second row by $a_{11}/|A|$:

$$[B_3][B_2][B_1][A] = \begin{bmatrix} 1 & 0 \\ 0 & \frac{a_{11}}{|A|} \end{bmatrix} \begin{bmatrix} 1 & \frac{a_{12}}{a_{11}} \\ 0 & \frac{|A|}{a_{11}} \end{bmatrix} = \begin{bmatrix} 1 & \frac{a_{12}}{a_{11}} \\ 0 & 1 \end{bmatrix} \quad (\text{A.37})$$

Finally, multiply the second row by a_{12}/a_{11} and subtract from the first row:

$$[B_4][B_3][B_2][B_1][A] = \begin{bmatrix} 1 & -\frac{a_{12}}{a_{11}} \\ 0 & 1 \end{bmatrix} \begin{bmatrix} 1 & \frac{a_{12}}{a_{11}} \\ 0 & 1 \end{bmatrix} = \begin{bmatrix} 1 & 0 \\ 0 & 1 \end{bmatrix} = [I] \quad (\text{A.38})$$

Considering Equation A.23, we see that

$$[A]^{-1} = [B_4][B_3][B_2][B_1] \quad (\text{A.39})$$

and carrying out the multiplications in Equation A.39 results in

$$[A]^{-1} = \frac{1}{|A|} \begin{bmatrix} a_{22} & -a_{12} \\ -a_{21} & a_{11} \end{bmatrix} \quad (\text{A.40})$$

This application of the Gauss-Jordan procedure may appear cumbersome, but the procedure is quite amenable to computer implementation.

A.5 MATRIX PARTITIONING

Any matrix can be subdivided or *partitioned* into a number of submatrices of lower order. The concept of matrix partitioning is most useful in reducing the size of a system of equations and accounting for specified values of a subset of the dependent variables. Consider a system of n linear algebraic equations governing n unknowns x_i expressed in matrix form as

$$[A]\{x\} = \{f\} \quad (\text{A.41})$$

in which we want to eliminate the first p unknowns. The matrix equation can be written in partitioned form as

$$\begin{bmatrix} [A_{11}] & [A_{12}] \\ [A_{21}] & [A_{22}] \end{bmatrix} \begin{Bmatrix} \{X_1\} \\ \{X_2\} \end{Bmatrix} = \begin{Bmatrix} \{F_1\} \\ \{F_2\} \end{Bmatrix} \quad (\text{A.42})$$

where the orders of the submatrices are as follows

$$\begin{aligned} [A_{11}] &\Rightarrow p \times p \\ [A_{12}] &\Rightarrow p \times (n - p) \\ [A_{21}] &\Rightarrow (n - p) \times p \\ [A_{22}] &\Rightarrow (n - p) \times (n - p) \\ \{X_1\}, \{F_1\} &\Rightarrow p \times 1 \\ \{X_2\}, \{F_2\} &\Rightarrow (n - p) \times 1 \end{aligned} \quad (\text{A.43})$$

The complete set of equations can now be written in terms of the matrix partitions as

$$\begin{aligned} [A_{11}]\{X_1\} + [A_{12}]\{X_2\} &= \{F_1\} \\ [A_{21}]\{X_1\} + [A_{22}]\{X_2\} &= \{F_2\} \end{aligned} \quad (\text{A.44})$$

The first p equations (the upper partition) are solved as

$$\{X_1\} = [A_{11}]^{-1}(\{F_1\} - [A_{12}]\{X_2\}) \quad (\text{A.45})$$

(implicitly assuming that the inverse of A_{11} exists). Substitution of Equation A.45 into the remaining $n - p$ equations (the lower partition) yields

$$([A_{22}] - [A_{21}][A_{11}]^{-1}[A_{12}])\{X_2\} = \{F_2\} - [A_{21}][A_{11}]^{-1}\{F_1\} \quad (\text{A.46})$$

Equation A.46 is the reduced set of $n - p$ algebraic equations representing the original system and containing all the effects of the first p equations. In the context of finite element analysis, this procedure is referred to as *static condensation*.

As another application (commonly encountered in finite element analysis), we consider the case in which the partitioned values $\{X_1\}$ are known but the corresponding right-hand side partition $\{F_1\}$ is unknown. In this occurrence, the lower partitioned equations are solved directly for $\{X_2\}$ to obtain

$$\{X_2\} = [A_{22}]^{-1}(\{F_2\} - [A_{21}]\{X_1\}) \quad (\text{A.47})$$

The unknown values of $\{F_1\}$ can then be calculated directly using the equations of the upper partition.

APPENDIX B

Equations of Elasticity

B.1 STRAIN-DISPLACEMENT RELATIONS

In general, the concept of *normal strain* is introduced and defined in the context of a uniaxial tension test. The elongated length L of a portion of the test specimen having original length L_0 (the gauge length) is measured and the corresponding normal strain defined as

$$\varepsilon = \frac{L - L_0}{L_0} = \frac{\Delta L}{L_0} \quad (\text{B.1})$$

which is simply interpreted as “change in length per unit original length” and is observed to be a dimensionless quantity. Similarly, the idea of shear strain is often introduced in terms of a simple torsion test of a bar having a circular cross section. In each case, the test geometry and applied loads are designed to produce a simple, uniform state of strain dominated by one major component.

In real structures subjected to routine operating loads, strain is not generally uniform nor limited to a single component. Instead, strain varies throughout the geometry and can be composed of up to six independent components, including both normal and shearing strains. Therefore, we are led to examine the appropriate definitions of strain at a point. For the general case, we denote $u = u(x, y, z)$, $v = v(x, y, z)$, and $w = w(x, y, z)$ as the displacements in the x , y , and z coordinate directions, respectively. (The displacements may also vary with time; for now, we consider only the static case.) Figure B.1(a) depicts an infinitesimal element having undeformed edge lengths dx , dy , dz located at an arbitrary point (x, y, z) in a solid body. For simplicity, we first assume that this element is loaded in tension in the x direction only and examine the resulting deformation as shown (greatly exaggerated) in Figure B.1(b). Displacement of point P is u while that of point Q is $u + (\partial u / \partial x) dx$ such that the deformed length in the x direction is given by

$$dx' = dx + u_Q - u_P = dx + u + \frac{\partial u}{\partial x} dx - u = dx + \frac{\partial u}{\partial x} dx \quad (\text{B.2})$$

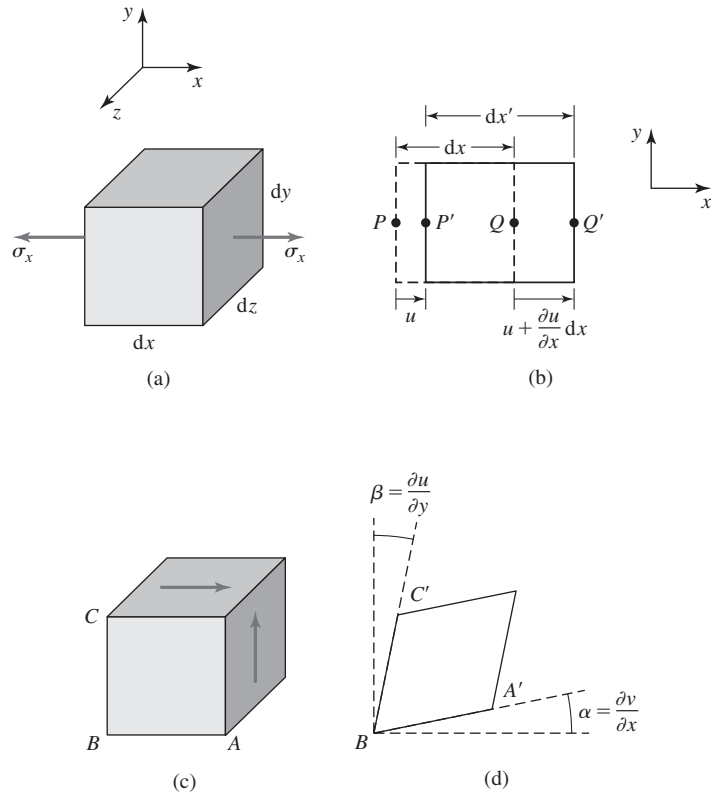


Figure B.1
 (a) A differential element in uniaxial stress; (b) resulting axial deformation; (c) differential element subjected to shear; (d) angular changes used to define shear strain.

The normal strain in the x direction at the point depicted is then

$$\epsilon_x = \frac{dx' - dx}{dx} = \frac{\partial u}{\partial x} \tag{B.3}$$

Similar consideration of changes of length in the y and z directions yields the general definitions of the associated normal strain components as

$$\epsilon_y = \frac{\partial v}{\partial y} \quad \text{and} \quad \epsilon_z = \frac{\partial w}{\partial z} \tag{B.4}$$

To examine shearing of the infinitesimal solid, we next consider the situation shown in Figure B.1(c), in which applied surface tractions result in shear of the

element, as depicted in Figure B.1(d). Unlike normal strain, the effects of shearing are seen to be distortions of the original rectangular shape of the solid. Such distortion is quantified by angular changes, and we consequently define *shear strain* as a “change in the angle of an angle that was originally a right angle.” On first reading, this may sound redundant but it is not. Consider the definition in the context of Figure B.1(c) and B.1(d); angle ABC was a right angle in the undeformed state but has been distorted to $A'BC'$ by shearing. The change of the angle is composed of two parts, denoted α and β , given by the slopes of BA' and BC' , respectively as $\partial v/\partial x$ and $\partial u/\partial y$. Thus, the shear strain is

$$\gamma_{xy} = \frac{\partial u}{\partial y} + \frac{\partial v}{\partial x} \quad (\text{B.5})$$

where the double subscript is used to indicate the plane in which the angular change occurs. Similar consideration of distortion in xz and yz planes results in

$$\gamma_{xz} = \frac{\partial u}{\partial z} + \frac{\partial w}{\partial x} \quad \text{and} \quad \gamma_{yz} = \frac{\partial v}{\partial z} + \frac{\partial w}{\partial y} \quad (\text{B.6})$$

as the shear strain components, respectively.

Equations B.3–B.6 provide the basic definitions of the six possible independent strain components in three-dimensional deformation. It must be emphasized that these strain-displacement relations are valid only for small deformations. Additional terms must be included if large deformations occur as a result of geometry or material characteristics. As continually is the case as we proceed, it is convenient to express the strain-displacement relations in matrix form. To accomplish this task, we define the displacement vector as

$$\{\delta\} = \begin{Bmatrix} u(x, y, z) \\ v(x, y, z) \\ w(x, y, z) \end{Bmatrix} \quad (\text{B.7})$$

(noting that this vector describes a continuous displacement field) and the strain vector as

$$\{\varepsilon\} = \begin{Bmatrix} \varepsilon_x \\ \varepsilon_y \\ \varepsilon_z \\ \gamma_{xy} \\ \gamma_{xz} \\ \gamma_{yz} \end{Bmatrix} \quad (\text{B.8})$$

The strain-displacement relations are then expressed in the compact form

$$\{\varepsilon\} = [L]\{\delta\} \quad (\text{B.9})$$

where $[L]$ is the derivative operator matrix given by

$$[L] = \begin{bmatrix} \frac{\partial}{\partial x} & 0 & 0 \\ 0 & \frac{\partial}{\partial y} & 0 \\ 0 & 0 & \frac{\partial}{\partial z} \\ \frac{\partial}{\partial y} & \frac{\partial}{\partial x} & 0 \\ \frac{\partial}{\partial z} & 0 & \frac{\partial}{\partial x} \\ 0 & \frac{\partial}{\partial z} & \frac{\partial}{\partial y} \end{bmatrix} \quad (\text{B.10})$$

B.2 STRESS-STRAIN RELATIONS

The equations between stress and strain applicable to a particular material are known as the *constitutive equations* for that material. In the most general type of material possible, it is shown in advanced work in continuum mechanics that the constitutive equations can contain up to 81 independent material constants. However, for a homogeneous, isotropic, linearly elastic material, it is readily shown that only two independent material constants are required to completely specify the relations. These two constants should be quite familiar from elementary strength of materials theory as the modulus of elasticity (Young's modulus) and Poisson's ratio. Again referring to the simple uniaxial tension test, the *modulus of elasticity* is defined as the slope of the stress-strain curve in the elastic region or

$$E = \frac{\sigma_x}{\epsilon_x} \quad (\text{B.10})$$

where it is assumed that the axis of loading corresponds to the x axis. As strain is dimensionless, the modulus of elasticity has the units of stress usually expressed in lb/in.² or megapascal (MPa).

Poisson's ratio is a measure of the well-known phenomenon that an elastic body strained in one direction also experiences strain in mutually perpendicular directions. In the uniaxial tension test, elongation of the test specimen in the loading direction is accompanied by contraction in the plane perpendicular to the loading direction. If the loading axis is x , this means that the specimen changes dimensions and thus experiences strain in the y and z directions as well, even though no external loading exists in those directions. Formally, Poisson's ratio is defined as

$$\nu = - \frac{\text{unit lateral contraction}}{\text{unit axial elongation}} \quad (\text{B.11})$$

and we note that Poisson's ratio is algebraically positive and the negative sign assures this, since numerator and denominator always have opposite signs. Thus, in

the tension test, if ϵ_x represents the strain resulting from applied load, the induced strain components are given by $\epsilon_y = \epsilon_z = -\nu\epsilon_x$.

The general stress-strain relations for a homogeneous, isotropic, linearly elastic material subjected to a general three-dimensional deformation are as follows:

$$\sigma_x = \frac{E}{(1+\nu)(1-2\nu)}[(1-\nu)\epsilon_x + \nu(\epsilon_y + \epsilon_z)] \quad (\text{B.12a})$$

$$\sigma_y = \frac{E}{(1+\nu)(1-2\nu)}[(1-\nu)\epsilon_y + \nu(\epsilon_x + \epsilon_z)] \quad (\text{B.12b})$$

$$\sigma_z = \frac{E}{(1+\nu)(1-2\nu)}[(1-\nu)\epsilon_z + \nu(\epsilon_x + \epsilon_y)] \quad (\text{B.12c})$$

$$\tau_{xy} = \frac{E}{2(1+\nu)}\gamma_{xy} = G\gamma_{xy} \quad (\text{B.12d})$$

$$\tau_{xz} = \frac{E}{2(1+\nu)}\gamma_{xz} = G\gamma_{xz} \quad (\text{B.12e})$$

$$\tau_{yz} = \frac{E}{2(1+\nu)}\gamma_{yz} = G\gamma_{yz} \quad (\text{B.12f})$$

where we introduce the *shear modulus* or *modulus of rigidity*, defined by

$$G = \frac{E}{2(1+\nu)} \quad (\text{B.13})$$

We may observe from the general relations that the normal components of stress and strain are interrelated in a rather complicated fashion through the Poisson effect but are independent of shear strains. Similarly, the shear stress components* are unaffected by normal strains.

The stress-strain relations can easily be expressed in matrix form by defining the *material property matrix* $[D]$ as

$$[D] = \frac{E}{(1+\nu)(1-2\nu)} \begin{bmatrix} 1-\nu & \nu & \nu & 0 & 0 & 0 \\ \nu & 1-\nu & \nu & 0 & 0 & 0 \\ \nu & \nu & 1-\nu & 0 & 0 & 0 \\ 0 & 0 & 0 & \frac{1-2\nu}{2} & 0 & 0 \\ 0 & 0 & 0 & 0 & \frac{1-2\nu}{2} & 0 \\ 0 & 0 & 0 & 0 & 0 & \frac{1-2\nu}{2} \end{bmatrix} \quad (\text{B.14})$$

*The double subscript notation used for shearing stresses is explained as follows: The first subscript defines the axial direction perpendicular to the surface on which the shearing stress acts, while the second subscript denotes the axis parallel to the shearing stress. Thus, τ_{xy} denotes a shearing stress acting in the direction of the x axis on a surface perpendicular to the y axis. Via moment equilibrium, it is readily shown that $\tau_{xy} = \tau_{yx}$, $\tau_{xz} = \tau_{zx}$, and $\tau_{yz} = \tau_{zy}$.

and writing

$$\{\sigma\} = \begin{Bmatrix} \sigma_x \\ \sigma_y \\ \sigma_z \\ \tau_{xy} \\ \tau_{xz} \\ \tau_{yz} \end{Bmatrix} = [D]\{\epsilon\} = [D][L]\{\delta\} \tag{B.15}$$

Here $\{\sigma\}$ denotes the 6×1 matrix of stress components. We do not use the term *stress vector*, since, as we subsequently observe, that term has a generally accepted meaning quite different from the matrix defined here.

B.3 EQUILIBRIUM EQUATIONS

To obtain the equations of equilibrium for a deformed solid body, we examine the general state of stress at an arbitrary point in the body via an infinitesimal differential element, as shown in Figure B.2. All stress components are assumed to

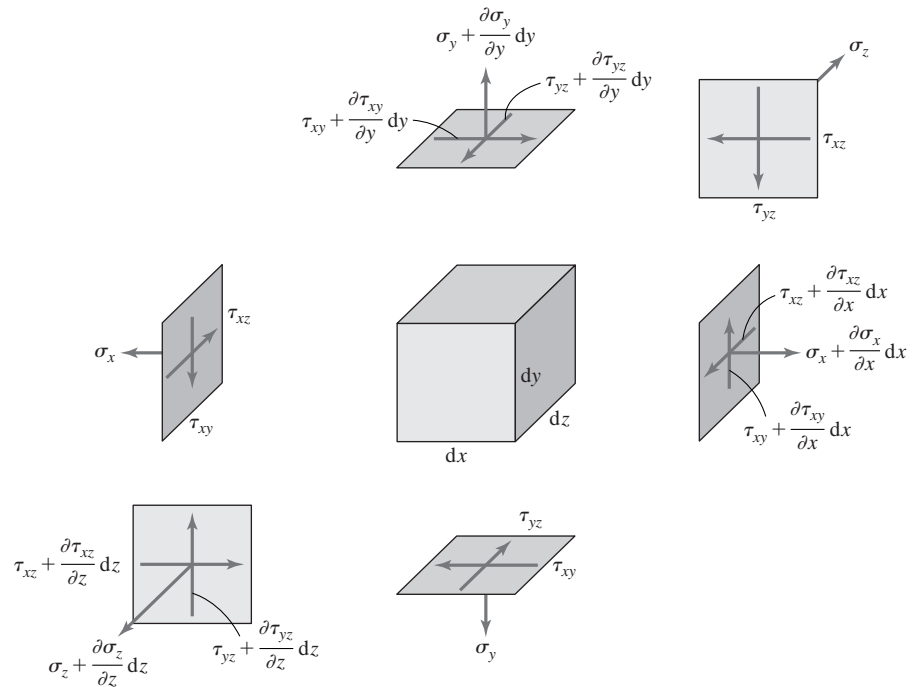


Figure B.2 A three-dimensional element in a general state of stress.

vary spatially, and these variations are expressed in terms of first-order Taylor series expansions, as indicated. In addition to the stress components shown, it is assumed that the element is subjected to a *body force* having axial components B_x , B_y , B_z . The body force is expressed as force per unit volume and represents the action of an external influence that affects the body as a whole. The most common body force is that of gravitational attraction while magnetic and centrifugal forces are also examples.

Applying the condition of force equilibrium in the direction of the x axis for the element of Figure B.2 results in

$$\begin{aligned} & \left(\sigma_x + \frac{\partial \sigma_x}{\partial x} dx \right) dy dz - \sigma_x dy dz + \left(\tau_{xy} + \frac{\partial \tau_{xy}}{\partial y} dy \right) dx dz - \tau_{xy} dx dz \\ & + \left(\tau_{xz} + \frac{\partial \tau_{xz}}{\partial z} dz \right) dx dy - \tau_{xz} dx dy + B_x dx dy dz = 0 \end{aligned} \quad (\text{B.16})$$

Expanding and simplifying Equation B.16 yields

$$\frac{\partial \sigma_x}{\partial x} + \frac{\partial \tau_{xy}}{\partial y} + \frac{\partial \tau_{xz}}{\partial z} + B_x = 0 \quad (\text{B.17})$$

Similarly, applying the force equilibrium conditions in the y and z coordinate directions yields

$$\frac{\partial \tau_{xy}}{\partial x} + \frac{\partial \sigma_y}{\partial y} + \frac{\partial \tau_{yz}}{\partial z} + B_y = 0 \quad (\text{B.18})$$

$$\frac{\partial \tau_{xz}}{\partial x} + \frac{\partial \tau_{yz}}{\partial y} + \frac{\partial \sigma_z}{\partial z} + B_z = 0 \quad (\text{B.19})$$

respectively.

B.4 COMPATIBILITY EQUATIONS

Equations B.3–B.6 define six strain components in terms of three displacement components. A fundamental premise of the theory of continuum mechanics is that a continuous body remains continuous during and after deformation. Therefore, the displacement and strain functions must be continuous and single valued. Given a continuous displacement field u , v , w , it is straightforward to compute continuous, single-valued strain components via the strain-displacement relations. However, the inverse case is a bit more complicated. That is, given a field of six continuous, single-valued strain components, we have six partial differential equations to solve to obtain the displacement components. In this case, there is no assurance that the resulting displacements will meet the requirements of continuity and single-valuedness. To ensure that displacements are continuous when computed in this manner, additional relations among the strain components

have been derived, and these are known as the *compatibility equations*. There are six independent compatibility equations, one of which is

$$\frac{\partial^2 \epsilon_x}{\partial y^2} + \frac{\partial^2 \epsilon_y}{\partial x^2} = \frac{\partial^2 \gamma_{xy}}{\partial x \partial y} \quad (\text{B.20})$$

The other five equations are similarly second-order relations. While not used explicitly in this text, the compatibility equations are absolutely essential in advanced methods in continuum mechanics and the theory of elasticity.

APPENDIX

C

Solution Techniques for Linear Algebraic Equations

C.1 CRAMER'S METHOD

Cramer's method, also known as *Cramer's rule*, provides a systematic means of solving linear equations. In practicality, the method is best applied to systems of no more than two or three equations. Nevertheless, the method provides insight into certain conditions regarding the existence of solutions and is included here for that reason.

Consider the system of equations

$$\begin{aligned}a_{11}x_1 + a_{12}x_2 &= f_1 \\ a_{21}x_1 + a_{22}x_2 &= f_2\end{aligned}\tag{C.1}$$

or in matrix form

$$[A]\{x\} = \{f\}\tag{C.2}$$

Multiplying the first equation by a_{22} , the second by a_{12} , and subtracting the second from the first gives

$$(a_{11}a_{22} - a_{12}a_{21})x_1 = f_1a_{22} - f_2a_{12}\tag{C.3}$$

Therefore, if $(a_{11}a_{22} - a_{12}a_{21}) \neq 0$, we solve for x_1 as

$$x_1 = \frac{f_1a_{22} - f_2a_{12}}{a_{11}a_{22} - a_{12}a_{21}}\tag{C.4}$$

Via a similar procedure,

$$x_2 = \frac{f_2a_{11} - f_1a_{21}}{a_{11}a_{22} - a_{12}a_{21}}\tag{C.5}$$

Note that the denominator of each solution is the same and equal to the determinant of the coefficient matrix

$$|A| = \begin{vmatrix} a_{11} & a_{12} \\ a_{21} & a_{22} \end{vmatrix} = a_{11}a_{22} - a_{12}a_{21} \quad (\text{C.6})$$

and again, it is assumed that the determinant is nonzero.

Now, consider the numerator of Equation C.4, as follows. Replace the first column of the coefficient matrix $[A]$ with the right-hand side column matrix $\{f\}$ and calculate the determinant of the resulting matrix (denoted $[A_1]$) to obtain

$$|A_1| = \begin{vmatrix} f_1 & a_{12} \\ f_2 & a_{22} \end{vmatrix} = f_1a_{22} - f_2a_{12} \quad (\text{C.7})$$

The determinant so obtained is exactly the numerator of Equation C.4. If we similarly replace the second column of $[A]$ with the right-hand side column matrix and calculate the determinant, we have

$$|A_2| = \begin{vmatrix} a_{11} & f_1 \\ a_{21} & f_2 \end{vmatrix} = f_2a_{11} - f_1a_{21} \quad (\text{C.8})$$

and the result of Equation C.8 is identical to the numerator of Equation C.5. Although presented for a system of only two equations, the results are applicable to any number of linear algebraic equations as follows:

Cramer's rule: Given a system of n linear algebraic equations in n unknowns x_i , $i = 1, n$, expressed in matrix form as

$$[A]\{x\} = \{f\} \quad (\text{C.9})$$

where $\{f\}$ is known, solutions are given by the ratio of determinants

$$x_i = \frac{|A_i|}{|A|} \quad i = 1, n \quad (\text{C.10})$$

provided $|A| \neq 0$.

Matrices $[A_i]$ are formed by replacing the i th column of the coefficient matrix $[A]$ with the right-hand side column matrix.

Note that, if the right-hand side $\{f\} = \{0\}$, Cramer's rule gives the trivial result $\{x\} = \{0\}$.

Now consider the case in which the determinant of the coefficient matrix is 0. In this event, the solutions for the system represented by Equation C.1 are, formally,

$$\begin{aligned} 0x_1 &= f_1a_{22} - f_2a_{12} \\ 0x_2 &= f_2a_{11} - f_1a_{21} \end{aligned} \quad (\text{C.11})$$

Equations (C.11) must be considered under two cases:

1. If the right-hand sides are nonzero, no solutions exist, since we cannot multiply any number by 0 and obtain a nonzero result.

2. If the right-hand sides are 0, the equations indicate that *any* values of x_1 and x_2 are solutions; this case corresponds to the *homogeneous* equations that occur if $\{f\} = \{0\}$. Thus, a system of linear homogeneous algebraic equations can have nontrivial solutions if and only if the determinant of the coefficient matrix is 0. The fact is, however, that the solutions are not just *any* values of x_1 and x_2 , and we see this by examining the determinant

$$|A| = a_{11}a_{22} - a_{12}a_{21} = 0 \quad (\text{C.12})$$

or

$$\frac{a_{11}}{a_{21}} = \frac{a_{12}}{a_{22}} \quad (\text{C.13})$$

Equation C.13 states that the coefficients of x_1 and x_2 in the two equations are in constant ratio. Thus, the equations are not independent and, in fact, represent a straight line in the x_1x_2 plane. There do, then, exist an infinite number of solutions (x_1, x_2) , but there also exists a relation between the coordinates x_1 and x_2 . The argument just presented for two equations is also general for any number of equations. If the system is homogeneous, nontrivial solutions exist only if the determinant of the coefficient matrix is 0.

C.2 GAUSS ELIMINATION

In Appendix A, dealing with matrix mathematics, the concept of inverting the coefficient matrix to obtain the solution for a system of linear algebraic equations is discussed. For large systems of equations, calculation of the inverse of the coefficient matrix is time consuming and expensive. Fortunately, the operation of inverting the matrix is not necessary to obtain solutions. Many other methods are more computationally efficient. The method of Gauss elimination is one such technique. Gauss elimination utilizes simple algebraic operations (multiplication, division, addition, and subtraction) to successively eliminate unknowns from a system of equations generally described by

$$[A]\{x\} = \{f\} \Rightarrow \begin{bmatrix} a_{11} & a_{12} & \cdots & a_{1n} \\ a_{21} & a_{22} & \cdots & a_{2n} \\ \vdots & \vdots & \ddots & \vdots \\ a_{n1} & a_{n2} & \cdots & a_{nn} \end{bmatrix} \begin{Bmatrix} x_1 \\ x_2 \\ \vdots \\ x_n \end{Bmatrix} = \begin{Bmatrix} f_1 \\ f_2 \\ \vdots \\ f_n \end{Bmatrix} \quad (\text{C.14a})$$

so that the system of equations is transformed to the form

$$[B]\{x\} = \{g\} \Rightarrow \begin{bmatrix} b_{11} & b_{12} & \cdots & b_{1n} \\ 0 & b_{22} & \cdots & b_{2n} \\ 0 & 0 & \ddots & \vdots \\ 0 & 0 & 0 & b_{nn} \end{bmatrix} \begin{Bmatrix} x_1 \\ x_2 \\ \vdots \\ x_n \end{Bmatrix} = \begin{Bmatrix} g_1 \\ g_2 \\ \vdots \\ g_n \end{Bmatrix} \quad (\text{C.14b})$$

In Equation C.14b, the original coefficient matrix has been transformed to *upper triangular form* as all elements below the main diagonal are 0. In this form, the solution for x_n is simply g_n/b_{nn} and the remaining values x_i are obtained by successive back substitution into the remaining equations.

The Gauss method is readily amenable to computer implementation, as described by the following algorithm. For the general form of Equation C.13, we first wish to eliminate x_1 from the second through n th equations. To accomplish this task, we must perform row operations such that the coefficient matrix element $a_{i1} = 0$, $i = 2, n$. Selecting a_{11} as the *pivot* element, we can multiply the first row by a_{21}/a_{11} and subtract the result from the second row to obtain

$$\begin{aligned} a_{21}^{(1)} &= a_{21} - a_{11} \frac{a_{21}}{a_{11}} = 0 \\ a_{22}^{(1)} &= a_{22} - a_{12} \frac{a_{21}}{a_{11}} \\ &\vdots \\ a_{2n}^{(1)} &= a_{2n} - a_{1n} \frac{a_{21}}{a_{11}} \\ f_2^{(1)} &= f_2 - f_1 \frac{a_{21}}{a_{11}} \end{aligned} \quad (\text{C.15})$$

In these relations, the superscript is used to indicate that the results are from operation on the first column. The same procedure is used to eliminate x_1 from the remaining equations; that is, multiply the first equation by a_{i1}/a_{11} and subtract the result from the i th equation. (Note that, if a_{i1} is 0, no operation is required.) The procedure results in

$$\begin{aligned} a_{i1}^{(1)} &= 0 \quad i = 2, n \\ a_{ij}^{(1)} &= a_{ij} - a_{1j} \frac{a_{i1}}{a_{11}} \quad i = 2, n \quad j = 2, n \\ f_i^{(1)} &= f_i - f_1 \frac{a_{i1}}{a_{11}} \quad i = 2, n \end{aligned} \quad (\text{C.16})$$

The result of the operations using a_{11} as the pivot element are represented symbolically as

$$\begin{bmatrix} a_{11} & a_{12} & \cdots & a_{1n} \\ 0 & a_{22}^{(1)} & \cdots & a_{2n}^{(1)} \\ 0 & \vdots & \ddots & \vdots \\ 0 & a_{n2}^{(1)} & \cdots & a_{nn}^{(1)} \end{bmatrix} \begin{Bmatrix} x_1 \\ x_2 \\ \vdots \\ x_n \end{Bmatrix} = \begin{Bmatrix} f_1 \\ f_2^{(1)} \\ \vdots \\ f_n^{(1)} \end{Bmatrix} \quad (\text{C.17})$$

and variable x_1 has been eliminated from all but the first equation. The procedure next takes (newly calculated) element $a_{22}^{(1)}$ as the pivot element and the operations

are repeated so that all elements in the second column below $a_{22}^{(1)}$ become 0. Carrying out the computations, using each successive diagonal element as the pivot element, transforms the system of equations to the form of Equation C.14. The solution is then obtained, as noted, by back substitution

$$\begin{aligned}x_n &= \frac{g_n}{b_{nn}} \\x_{n-1} &= \frac{1}{b_{n-1,n-1}}(g_{n-1} - b_{n-1,n}x_n) \\&\vdots \\x_i &= \frac{1}{b_{ii}}\left(g_i - \sum_{j=i+1}^n b_{ij}x_j\right)\end{aligned}\tag{C.18}$$

The Gauss elimination procedure is easily programmed using array storage and looping functions (DO loops), and it is much more efficient than inverting the coefficient matrix. If the coefficient matrix is symmetric (common to many finite element formulations), storage requirements for the matrix can be reduced considerably, and the Gauss elimination algorithm is also simplified.

C.3 LU DECOMPOSITION

Another efficient method for solving systems of linear equations is the so-called *LU* decomposition method. In this method, a system of linear algebraic equations, as in Equation C.14, are to be solved. The procedure is to decompose the coefficient matrix $[A]$ into two components $[L]$ and $[U]$ so that

$$[A] = [L][U] = \begin{bmatrix} L_{11} & 0 & \cdots & 0 \\ L_{21} & L_{22} & \cdots & 0 \\ \vdots & \vdots & \ddots & \vdots \\ L_{n1} & L_{n2} & \cdots & L_{nn} \end{bmatrix} \begin{bmatrix} U_{11} & U_{12} & \cdots & U_{1n} \\ 0 & U_{22} & \cdots & U_{2n} \\ \vdots & \vdots & \ddots & \vdots \\ 0 & \cdots & \cdots & U_{nn} \end{bmatrix}\tag{C.19}$$

Hence, $[L]$ is a *lower triangular matrix* and $[U]$ is an *upper triangular matrix*. Here, we assume that $[A]$ is a known $n \times n$ square matrix. Expansion of Equation C.19 shows that we have a system of equations with a greater number of unknowns than the number of equations, so the decomposition into the *LU* representation is not well defined. In the *LU* method, the diagonal elements of $[L]$ must have unity value, so that

$$[L] = \begin{bmatrix} 1 & 0 & \cdots & 0 \\ L_{21} & 1 & \cdots & 0 \\ \vdots & \vdots & \ddots & \vdots \\ L_{n1} & L_{n2} & \cdots & 1 \end{bmatrix}\tag{C.20}$$

For illustration, we assume a 3×3 system and write

$$\begin{bmatrix} a_{11} & a_{12} & a_{13} \\ a_{21} & a_{22} & a_{23} \\ a_{31} & a_{32} & a_{33} \end{bmatrix} = \begin{bmatrix} 1 & 0 & 0 \\ L_{21} & 1 & 0 \\ L_{31} & L_{32} & 1 \end{bmatrix} \begin{bmatrix} U_{11} & U_{12} & U_{13} \\ 0 & U_{22} & U_{23} \\ 0 & 0 & U_{33} \end{bmatrix} \quad (\text{C.21})$$

Matrix Equation C.21 represents these nine equations:

$$\begin{aligned} a_{11} &= U_{11} \\ a_{12} &= U_{12} \\ a_{21} &= L_{21}U_{11} \\ a_{22} &= L_{21}U_{12} + U_{22} \\ a_{13} &= U_{13} \\ a_{31} &= L_{31}U_{11} \\ a_{32} &= L_{31}U_{12} + L_{32}U_{22} \\ a_{23} &= L_{21}U_{13} + U_{23} \\ a_{33} &= L_{31}U_{13} + L_{32}U_{23} + U_{33} \end{aligned} \quad (\text{C.22})$$

Equation C.22 is written in a sequence such that, at each step, only a single unknown appears in the equation. We rewrite the coefficient matrix $[A]$ and divide the matrix into “zones” as

$$[A] = \begin{bmatrix} \textcircled{1} & \textcircled{2} & \textcircled{3} \\ a_{11} & a_{12} & a_{13} \\ a_{21} & a_{22} & a_{23} \\ a_{31} & a_{32} & a_{33} \end{bmatrix} \quad (\text{C.23})$$

With reference to Equation C.22, we observe that the first equation corresponds to zone 1, the next three equations represent zone 2, and the last five equations represent zone 3. In each zone, the equations include only the elements of $[A]$ that are in the zone and only elements of $[L]$ and $[U]$ from previous zones and the current zone. Hence, the LU decomposition procedure described here is also known as an *active zone* method.

For a system of n equations, the procedure is readily generalized to obtain the following results

$$U_{ii} = a_{ii} \quad i = 1, n \quad (\text{C.24})$$

$$L_{ii} = 1$$

$$L_{i1} = \frac{a_{i1}}{U_{11}} \quad i = 2, n \quad (\text{C.25})$$

The remaining terms obtained from active zone i , with i ranging from 2 to n , are

$$L_{ij} = \frac{a_{ij} - \sum_{m=1}^{j-1} L_{im}U_{mj}}{U_{jj}} \quad i = 2, n \quad j = 2, 3, 4, \dots, i-1 \quad i \neq j \quad (\text{C.26})$$

$$U_{ji} = a_{ji} - \sum_{m=1}^{j-1} L_{jm}U_{mi}$$

$$U_{ii} = a_{ii} - \sum_{m=1}^{i-1} L_{im}U_{mi} \quad i = 2, n \quad (\text{C.27})$$

Thus, the decomposition procedure is straightforward and readily amenable to computer implementation.

Now that the decomposition procedure has been developed, we return to the task of solving the equations. As we now have the equations expressed in the form of the triangular matrices $[L]$ and $[U]$ as

$$[L][U]\{x\} = \{f\} \quad (\text{C.28})$$

we see that the product

$$[U]\{x\} = \{z\} \quad (\text{C.29})$$

is an $n \times 1$ column matrix, so Equation C.28 can be expressed as

$$[L]\{z\} = \{f\} \quad (\text{C.30})$$

and owing to the triangular structure of $[L]$, the solution for Equation C.30 is obtained easily as (in order)

$$z_1 = f_1$$

$$z_i = f_i - \sum_{j=1}^{i-1} L_{ij}z_j \quad i = 2, n \quad (\text{C.31})$$

Formation of the intermediate solutions, represented by Equation C.31, is generally referred to as the *forward sweep*.

With the z_i value known from Equation C.31, the solutions for the original unknowns are obtained via Equation C.29 as

$$x_n = \frac{z_n}{U_{nn}}$$

$$x_i = \frac{1}{U_{ii}} \left(z_i - \sum_{j=i+1}^n U_{ij}x_j \right) \quad (\text{C.32})$$

The process of solution represented by Equation C.32 is known as the *backward sweep* or *back substitution*.

In the LU method, the major computational time is expended in decomposing the coefficient matrix into the triangular forms. However, this step need be accomplished only once, after which the forward sweep and back substitution processes can be applied to any number of different right-hand forcing functions $\{f\}$. Further, if the coefficient matrix is symmetric and banded (as is most often the case in finite element analysis), the method can be quite efficient.

C.4 FRONTAL SOLUTION

The frontal solution method (also known as the *wave front solution*) is an especially efficient method for solving finite element equations, since the coefficient matrix (the stiffness matrix) is generally symmetric and banded. In the frontal method, assembly of the system stiffness matrix is combined with the solution phase. The method results in a considerable reduction in computer memory requirements, especially for large models.

The technique is described with reference to Figure C.1, which shows an assemblage of one-dimensional bar elements. For this simple example, we know that the system equations are of the form

$$\begin{bmatrix} K_{11} & K_{12} & 0 & 0 & 0 & 0 \\ K_{12} & K_{22} & K_{23} & 0 & 0 & 0 \\ 0 & K_{23} & K_{33} & K_{34} & 0 & 0 \\ 0 & 0 & K_{34} & K_{44} & K_{45} & 0 \\ 0 & 0 & 0 & K_{45} & K_{55} & K_{56} \\ 0 & 0 & 0 & 0 & K_{56} & K_{66} \end{bmatrix} \begin{Bmatrix} U_1 \\ U_2 \\ U_3 \\ U_4 \\ U_5 \\ U_6 \end{Bmatrix} = \begin{Bmatrix} F_1 \\ F_2 \\ F_3 \\ F_4 \\ F_5 \\ F_6 \end{Bmatrix} \quad (\text{C.33})$$

Clearly, the stiffness matrix is banded and *sparse* (many zero-valued terms). In the frontal solution technique, the entire system stiffness matrix is not assembled as such. Instead, the method utilizes the fact that a degree of freedom (an unknown) can be eliminated when the rows and columns of the stiffness matrix corresponding to that degree of freedom are complete. In this context, eliminating a degree of freedom means that we can write an equation for that degree of freedom in terms of other degrees of freedom and forcing functions. When such an equation is obtained, it is written to a file and removed from memory. As is shown, the net result is triangularization of the system stiffness matrix and the solutions are obtained by simple back substitution.

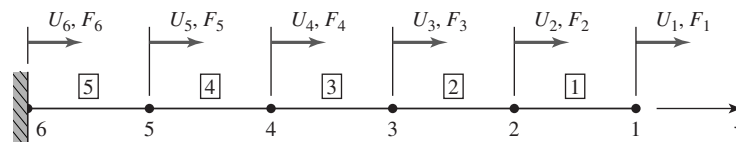


Figure C.1 A system of bar elements used to illustrate the frontal solution method.

For simplicity of illustration, let each element in Figure C.1 have characteristic stiffness k . We begin by defining a 6×6 null matrix $[K]$ and proceed with the assembly step, taking the elements in numerical order. Adding the element stiffness matrix for element 1 to the system matrix, we obtain

$$\begin{bmatrix} k & -k & 0 & 0 & 0 & 0 \\ -k & k & 0 & 0 & 0 & 0 \\ 0 & 0 & 0 & 0 & 0 & 0 \\ 0 & 0 & 0 & 0 & 0 & 0 \\ 0 & 0 & 0 & 0 & 0 & 0 \\ 0 & 0 & 0 & 0 & 0 & 0 \end{bmatrix} \begin{Bmatrix} U_1 \\ U_2 \\ U_3 \\ U_4 \\ U_5 \\ U_6 \end{Bmatrix} = \begin{Bmatrix} F_1 \\ F_2 \\ F_3 \\ F_4 \\ F_5 \\ F_6 \end{Bmatrix} \quad (\text{C.34})$$

Since U_1 is associated only with element 1, displacement U_1 appears in none of the other equations and can be eliminated now. (To illustrate the effect on the matrix, we do not actually eliminate the degree of freedom from the equations.) The first row of Equation C.34 is

$$kU_1 - kU_2 = F_1 \quad (\text{C.35})$$

and can be solved for U_1 once U_2 is known. Mathematically eliminating U_1 from the second row, we have

$$\begin{bmatrix} k & -k & 0 & 0 & 0 & 0 \\ 0 & 0 & 0 & 0 & 0 & 0 \\ 0 & 0 & 0 & 0 & 0 & 0 \\ 0 & 0 & 0 & 0 & 0 & 0 \\ 0 & 0 & 0 & 0 & 0 & 0 \\ 0 & 0 & 0 & 0 & 0 & 0 \end{bmatrix} \begin{Bmatrix} U_1 \\ U_2 \\ U_3 \\ U_4 \\ U_5 \\ U_6 \end{Bmatrix} = \begin{Bmatrix} F_1 \\ F_1 + F_2 \\ F_3 \\ F_4 \\ F_5 \\ F_6 \end{Bmatrix} \quad (\text{C.36})$$

Next, we “process” element 2 and add the element stiffness matrix terms to the appropriate locations in the coefficient matrix to obtain

$$\begin{bmatrix} k & -k & 0 & 0 & 0 & 0 \\ 0 & k & -k & 0 & 0 & 0 \\ 0 & -k & k & 0 & 0 & 0 \\ 0 & 0 & 0 & 0 & 0 & 0 \\ 0 & 0 & 0 & 0 & 0 & 0 \\ 0 & 0 & 0 & 0 & 0 & 0 \end{bmatrix} \begin{Bmatrix} U_1 \\ U_2 \\ U_3 \\ U_4 \\ U_5 \\ U_6 \end{Bmatrix} = \begin{Bmatrix} F_1 \\ F_1 + F_2 \\ F_3 \\ F_4 \\ F_5 \\ F_6 \end{Bmatrix} \quad (\text{C.37})$$

Displacement U_2 does not appear in any remaining equations and is now eliminated to obtain

$$\begin{bmatrix} k & -k & 0 & 0 & 0 & 0 \\ 0 & k & -k & 0 & 0 & 0 \\ 0 & 0 & 0 & 0 & 0 & 0 \\ 0 & 0 & 0 & 0 & 0 & 0 \\ 0 & 0 & 0 & 0 & 0 & 0 \\ 0 & 0 & 0 & 0 & 0 & 0 \end{bmatrix} \begin{Bmatrix} U_1 \\ U_2 \\ U_3 \\ U_4 \\ U_5 \\ U_6 \end{Bmatrix} = \begin{Bmatrix} F_1 \\ F_1 + F_2 \\ F_1 + F_2 + F_3 \\ F_4 \\ F_5 \\ F_6 \end{Bmatrix} \quad (\text{C.38})$$

In sequence, processing the remaining elements and following the elimination procedure results in

$$\begin{bmatrix} k & -k & 0 & 0 & 0 & 0 \\ 0 & k & -k & 0 & 0 & 0 \\ 0 & 0 & k & -k & 0 & 0 \\ 0 & 0 & 0 & k & -k & 0 \\ 0 & 0 & 0 & 0 & k & -k \\ 0 & 0 & 0 & 0 & -k & k \end{bmatrix} \begin{Bmatrix} U_1 \\ U_2 \\ U_3 \\ U_4 \\ U_5 \\ U_6 \end{Bmatrix} = \begin{Bmatrix} F_1 \\ F_1 + F_2 \\ F_1 + F_2 + F_3 \\ F_1 + F_2 + F_3 + F_4 \\ F_1 + F_2 + F_3 + F_4 + F_5 \\ F_6 \end{Bmatrix} \quad (\text{C.39})$$

Noting that the last equation in the system of Equation C.39 is a constraint equation (and could have been ignored at the beginning), we observe that the procedure has triangularized the system stiffness matrix without formally assembling that matrix. If we take out the constraint equation, the remaining equations are easily solved by back substitution. Also note that the forces are assumed to be known.

The frontal solution method has been described in terms of one-dimensional elements for simplicity. In fact, the speed and efficiency of the procedure are of most advantage in large two- and three-dimensional models. The method is discussed briefly here so that the reader using a finite element software package that uses a wave-type solution has some information about the procedure.

APPENDIX D

The Finite Element Personal Computer Program

With permission of the estate of Dr. Charles E. Knight, the Finite Element Personal Computer (FEPC) program is available to users of this text via the website www.mhhe.com/hutton<www.mhhe.com/hutton>. FEPC is a finite element software package supporting bar, beam, plane solid, and axisymmetric solid elements and hence is limited to two-dimensional structural applications. Dr. Knight's *A Finite Element Method Primer for Mechanical Design* is available via the website and includes basic concepts as well as an appendix delineating FEPC capabilities and limitations. The following material presents a general description of the programs' capabilities and limitations. A complete users guide is available on the website.

FEPC is actually a set of three programs that perform the operations of pre-processing (model development), model solution, and postprocessing (results analysis). FEPCIP is the input processor used to input and check a model and prepare data files for the solution program FEPC. The output processor is FEPCOP and this program reads solution output files and produces graphic displays.

All the programs are menu driven, with automatic branching to submenus when appropriate. The Files menu of the input processor is used to recall a previously stored model or store a new model. Models are stored as *filename.MOD* where filename is user specified and can contain a maximum of 20 characters. The analysis file, which becomes the actual input to the FEPC solution phase, is *filename.ANA*.

D.1 PREPROCESSING

Model definition is activated by the Model Data menu. Selection of Model Data leads to a submenu used to define element type, material properties, nodes,

elements, restraints (displacement constraints), and loads. Element type is limited to bar (truss), beam, plane stress, plane strain, or axisymmetric. Only a single element type can be used in a model. Up to 10 material property sets can be used in a model and should be defined in numerical order. Nodes can be defined by direct input of node number and the X , Y coordinates of the node. Nodes for truss and beam elements are always defined in this manner. Nodes for plane and axisymmetric elements can also be defined by direct input but an automeshing capability for two-dimensional (2-D) areas is included and discussed subsequently. Similarly, elements are defined by specification of the nodes and material property number. For truss and beam elements, the order of node specification is of no consequence. However, for plane or axisymmetric elements, the nodes must be specified in a counterclockwise order around the element area. Displacement constraints are applied by setting the values and selecting the node to which the values apply. Loads are applied as nodal forces or element edge pressures for 2-D solid elements.

The 2-D Automesh Generation section of the program is used for area mesh generation of two-dimensional plane stress, plane strain, or axisymmetric models. The approach used is a coordinate transformation mapping of a grid of square elements in an integer area into a grid of elements in the geometric area. The geometric area is defined using points that are subsequently used to define lines and arcs that enclose the area. The integer grid is bounded by lines that correspond to the lines and arcs of the geometric area. Grid points bound the square elements in the integer area map to element nodes in the geometric area. The mapping process is iterative and consists of distorting the integer area grid to fit into the geometric area. Thus the user has some control over element size and shape via the size of the integer grid.

D.2 SOLUTION

When a model has been defined and saved as *filename.ANA*, the solution is generated by the FEPC.EXE program. During execution, several other files are generated and stored. Also, screen messages are issued to report on progress of the solution phase. A listing of all printed output is stored in *filename.LST*. This file contains the input data, all numerical output, and any error messages issued during execution. Two additional files are created for use by the output processor. The node and element data is placed in *filename.MSH* and nodal displacement and element stress data is stored in *filename.NVL*.

D.3 POSTPROCESSING

The output processor FEPCOP.EXE is used to display the solution results in graphic form. (The printed form of the numerical output data is in the .LST file.) Displacement results can be displayed as a plot of the deformed element mesh

superimposed over a plot of the undeformed model. Displacements are scaled such that the deformed shape is exaggerated for clarity.

For two-dimensional solid models, stress components can be displayed as contour plots. The stress components available from the solution are the normal, shear, and von Mises stress components for plane stress and plane strain, and the radial, axial, shear, and hoop stress components for axisymmetric models. For models using truss or beam elements, stress components are plotted as bar charts.

E APPENDIX

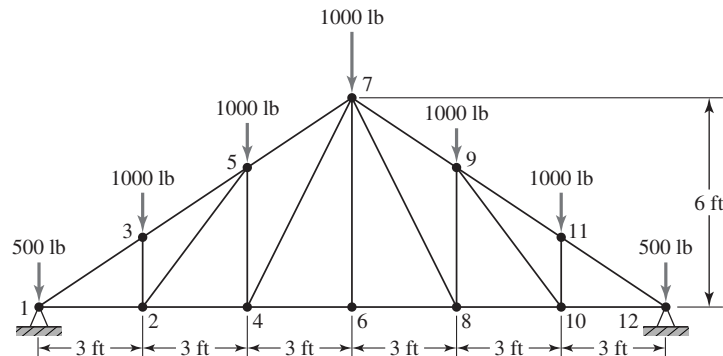
Problems for Computer Solution

The following problems are intended for solution using finite element analysis software. In general, the problems associated with Chapters 3, 4, and 9 can be solved using the FEPC software (Appendix D) if another software package is not available. The instructor may choose to change loading, material properties, or geometry for any of these problems at his or her discretion.

E.1 CHAPTER 3

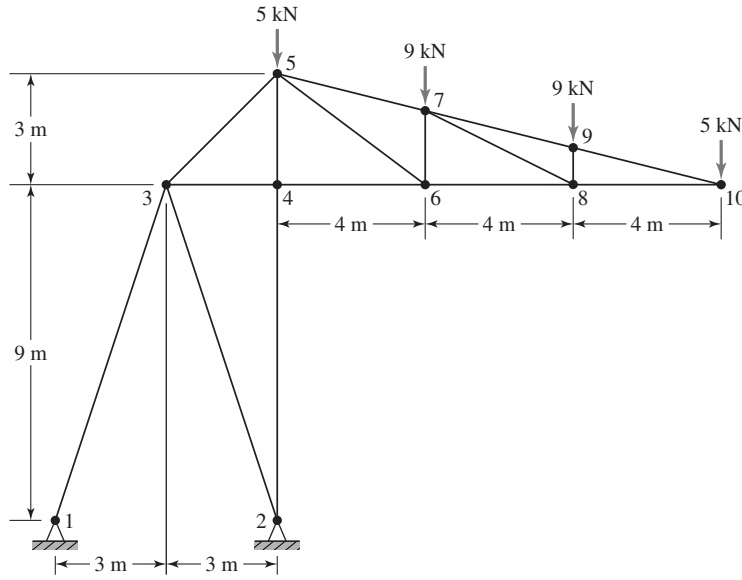
Problems E3.1–E3.7 involve two-dimensional trusses to be modeled using the bar element (in some analysis software this may be called a *bar*, *link*, *spar*, or *truss element*). In each problem, determine the magnitude and location of the maximum deflection, the stress in each member, and the reaction forces. Use the computed reaction forces to check the equilibrium. Node numbers, where included, are for reference only and can be changed at the analyst's discretion.

E3.1 Each member is steel having $E = 30(10^6)$ psi and the cross-sectional area is 1.2 in.^2



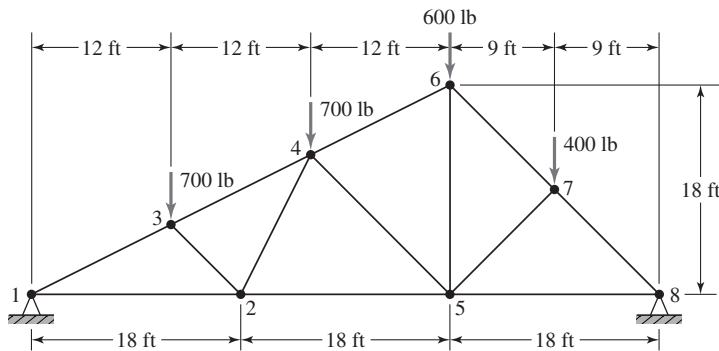
Problem E3.1

E3.2 All members are hollow circular tubing having outside diameter 100 mm and wall thickness 10 mm. The modulus of elasticity is 207 GPa.



Problem E3.2

E3.3 All truss members are 2" × 4" lumber having $E = 3(10^6)$ psi.

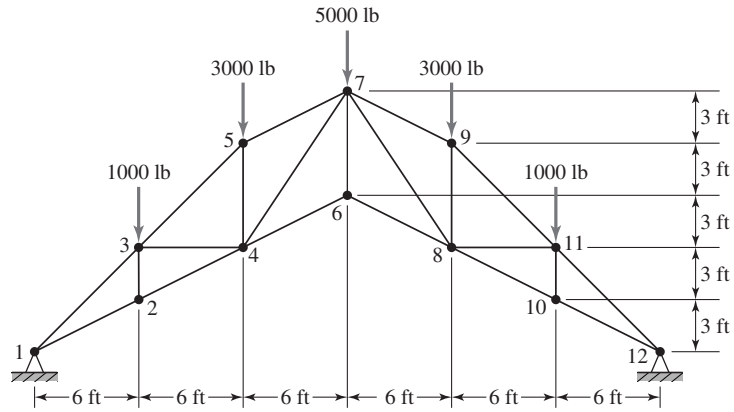


Problem E3.3

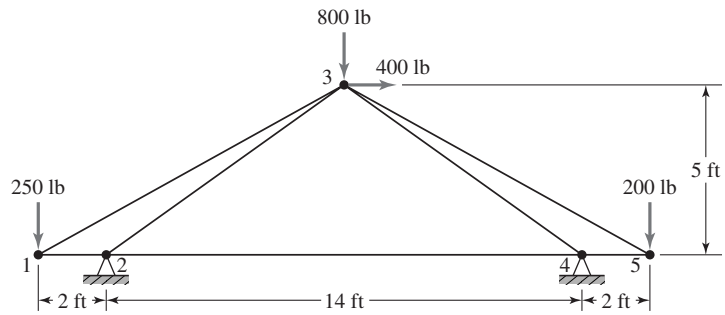
E3.4 The truss members are square tubular aluminum members having 2.5" outside dimension and 0.25" wall thickness. The modulus of elasticity is 10^7 psi.

E3.5 All members are identical with cross-sectional area of 1.6 in.² and modulus of elasticity $15(10^6)$ psi.

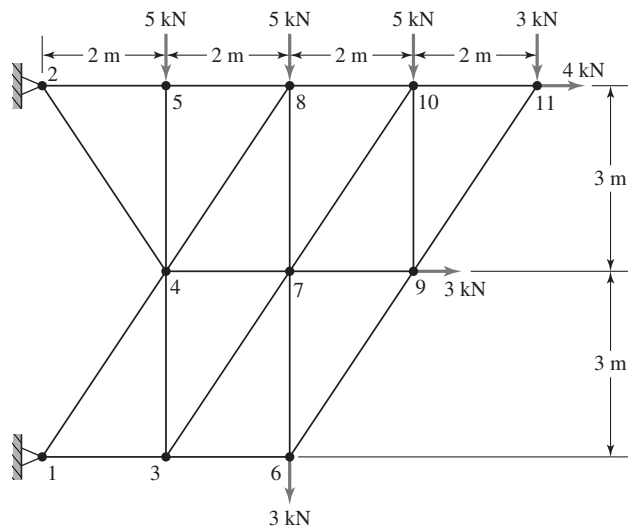
E3.6 The horizontal members are solid, square steel bars having basic dimension 30 mm; all other members are flat steel sheet stock 6 mm thick by 50 mm wide. Use $E = 207$ GPa. Are the computed stresses reasonable for structural steel?



Problem E3.4

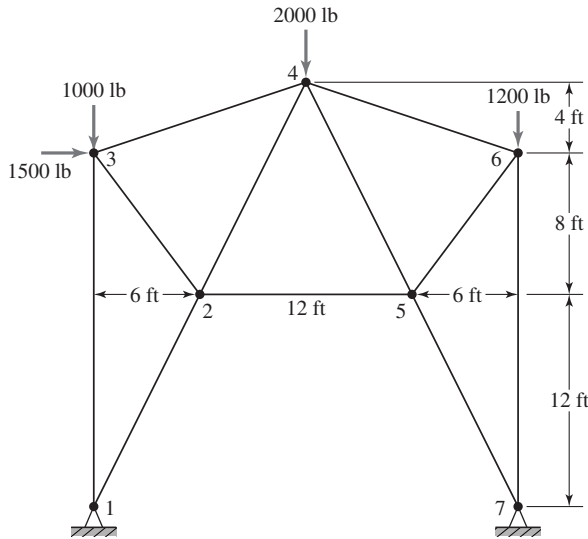


Problem E3.5



Problem E3.6

E3.7 The truss is composed of solid circular steel members 2" in diameter. The modulus of elasticity is $30(10^6)$ psi. Other than deflection and stress, what concerns should be considered with this truss? Does your answer relate to the relatively low computed stress values?



Problem E3.7

E.2 CHAPTER 4

The problems in this section deal with frame structures (that is, structures in which the joints are fixed and transmit bending moment, unlike the pin joint assumption of trusses).

E4.1–E4.7 Solve problems E3.1–E3.7, respectively, assuming that the joints are fixed as in welded or riveted joints. Additional required information is as follows.

For E3.1,

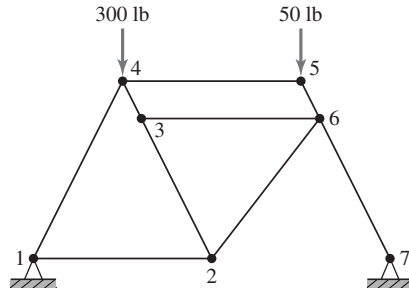
$$I_z = 0.4 \text{ in.}^4$$

For E3.5,

$$I_z = 0.53 \text{ in.}^4$$

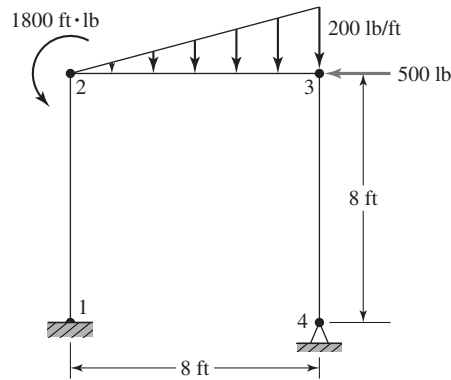
E4.8 The figure shows a basic model of a bicycle frame. All members are 1" diameter circular tubing having wall thickness 0.1" and are made of titanium, which has a modulus of elasticity of $15(10^6)$ psi. Determine the maximum deflection and the stress in each member. The nodal coordinates (in inches) are as follows:

	<i>x</i>	<i>y</i>
1	0	0
2	18	0
3	11	14
4	9	18
5	27	18
6	29	14
7	36	0



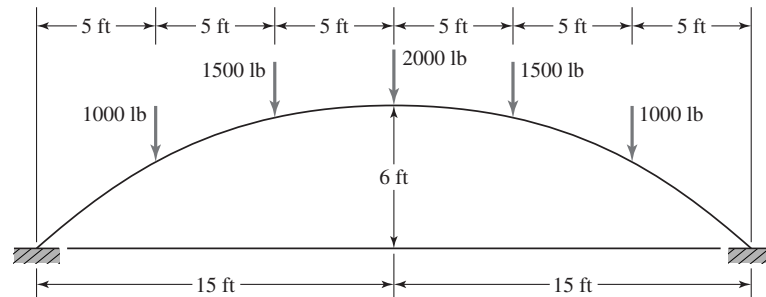
Problem E4.8

E4.9 Determine the maximum deflection and maximum stress in the frame structure shown if the structural members are 1" diameter, solid aluminum tubes for which $E = 10(10^6)$ psi.



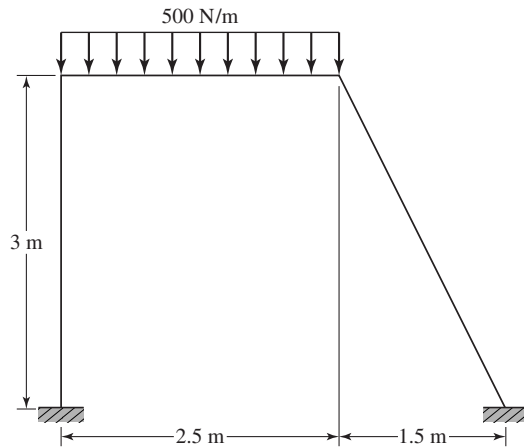
Problem E4.9

E4.10 The figure shows an arch that is the main support structure for a footbridge. The arch is constructed of standard AISC 6I17.5 I-beams (height = 6 in.; $A = 5.02$ in.²; $I_z = 26.0$ in.⁴). Use straight beam elements to model this bridge and examine convergence of solution as the number of elements is increased from 6 to 12 to 18. In examining convergence, look at both deflection and stress. Also note that, owing to the direction of loading, axial effects must be included. $E = 30(10^6)$ psi.

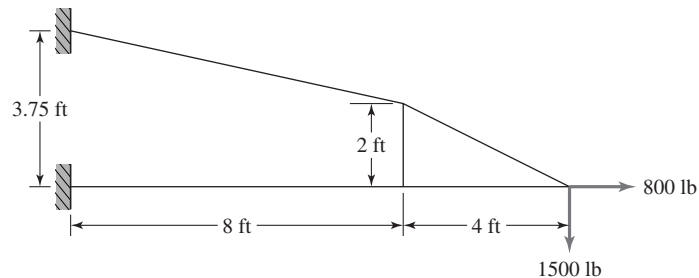


Problem E4.10

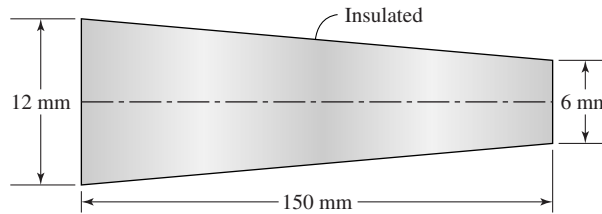
- E4.11** The frame structure shown is composed of 10 mm × 10 mm solid square members having $E = 100$ GPa. Determine the maximum deflection, maximum slope, and maximum stress.

**Problem E4.11**

- E4.12** The structure shown is a model of the support for a freeway light post. For uniformity in wind loading, the structural members are circular. The outside diameter of each member is 3.0" and wall thickness is 0.25". Compute the deflection at each structural joint and determine maximum stresses. Examine the effects on your solution of using more elements (i.e., refine the mesh). $E = 10^7$ psi.

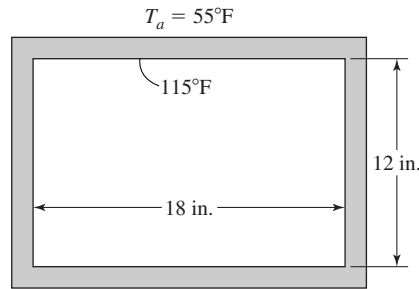
**Problem E4.12****E.3 CHAPTER 7**

- E7.1** A tapered circular heat transfer pin (known as a *pin fin*) is insulated all around its circumference, as shown. The large end ($D = 12$ mm) is maintained at a constant temperature of 90°C , while the smaller end ($D = 6$ mm) is at 30°C . Determine the steady-state heat flow through the pin using a mesh of straight elements. Thermal conductivity of the material is $k = 200$ W/m $^\circ\text{C}$.
- E7.2** A rectangular duct in a home heating system has dimensions $12'' \times 18''$ as shown. The duct is insulated with a uniform layer of fiberglass $1''$ thick. The



Problem E7.1

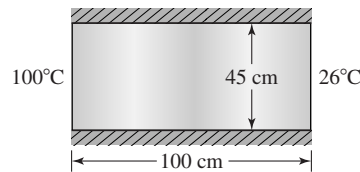
duct (steel sheet metal) is maintained at a constant temperature of 115°F. The ambient air temperature around the duct is 55°F.



Problem E7.2

- (a) Calculate the temperature distribution in the insulation and the heat loss per unit length to the surrounding air. Thermal conductivity of the insulation is uniform in all directions and has value $k = 0.025 \text{ Btu/hr-ft}^\circ\text{F}$; the convection coefficient to the ambient air is $h = 5 \text{ Btu/hr-ft}^2\text{-}^\circ\text{F}$.
- (b) Repeat the calculations for an insulation thickness of 2 in.

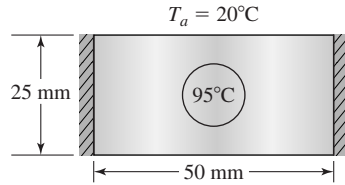
E7.3 The figure represents a cross section of a long bar insulated on the upper and lower surfaces; hence, the problem is to be treated as two dimensional on a per unit length basis. The left edge is maintained at constant temperature of 100°C and the right edge is maintained at 26°C. The material has uniform conductivity $k = 35 \text{ W/m}^\circ\text{C}$. Determine the temperature distribution and the steady-state heat flow rate. What element should you use? (Triangular, square? Perform the analysis with different elements to observe differences in the solutions.) Refine the mesh and examine convergence.



Problem E7.3

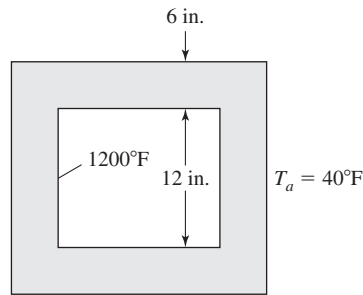
E7.4 A thin copper tube (12 mm diameter) containing water at an average temperature of 95°C is imbedded in a long slender solid slab, as shown. The vertical edges

are insulated. The horizontal edges are exposed to an ambient temperature of 20°C and the associated convection coefficient is $h = 20 \text{ W/m}^2\text{-}^\circ\text{C}$. The material has uniform conductivity $k = 200 \text{ W/m}\text{-}^\circ\text{C}$. Compute the net steady-state heat transfer rate and the temperature distribution in the cross section.



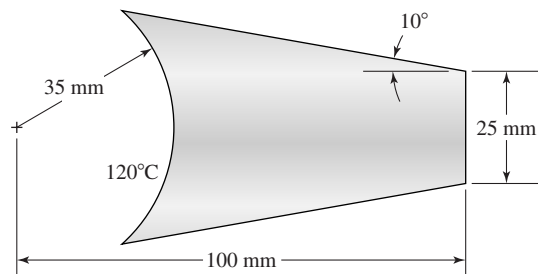
Problem E7.4

E7.5 The figure shows a horizontal cross section of a chimney exhausting the gases generated by a wood stove. The flue is insulated with firebrick 6" thick and having uniform conductivity $k = 2.5 \text{ Btu/hr}\text{-ft}\text{-}^\circ\text{F}$. The chimney is surrounded by air at ambient temperature 40°F and the convection coefficient is $5 \text{ Btu/hr}\text{-ft}^2\text{-}^\circ\text{F}$. Determine the temperature distribution in the firebrick and the heat loss per unit length.



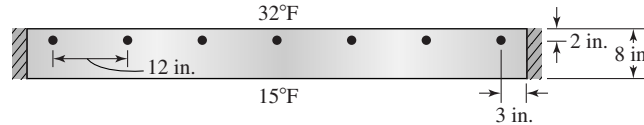
Problem E7.5

E7.6 The heat transfer fin shown is attached to a pipe conveying a fluid at average temperature 120°C . The thickness of the fin is 3 mm. The fin is surrounded by air at temperature 30°C and subject to convection on all surfaces with $h = 20 \text{ W/m}^2\text{-}^\circ\text{C}$. The fin material has uniform conductivity $k = 50 \text{ W/m}\text{-}^\circ\text{C}$. Determine the heat transfer rate from the fin and the temperature distribution in the fin.

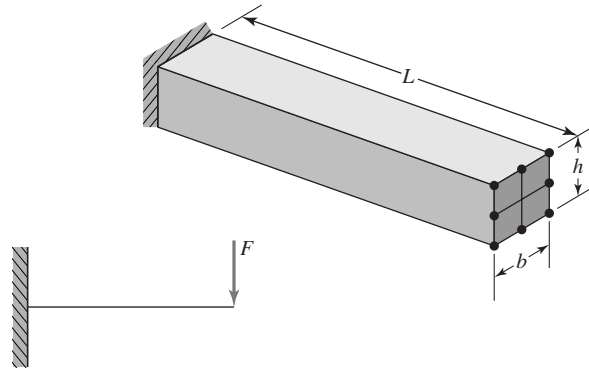


Problem E7.6

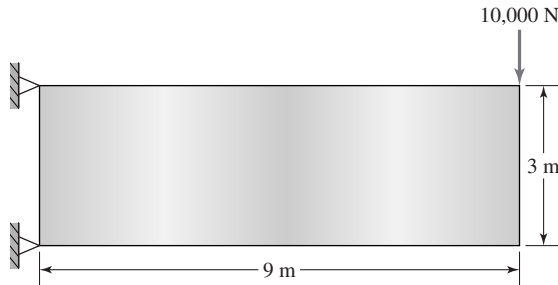
- E7.7** The cross section shown is of a campus footbridge, having embedded heat cables to prevent ice accumulation. The vertical edges are insulated and the horizontal surfaces are at the steady temperatures shown. The material has uniform conductivity $k = 0.6$ Btu/hr-ft- $^{\circ}$ F and the cables have source strength 200 Btu/hr-in. Compute the net heat transfer rate and the temperature distribution.

**Problem E7.7****E.4 CHAPTER 9**

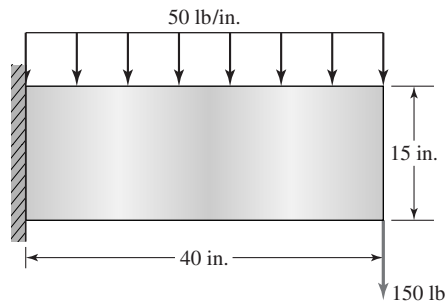
- E9.1** The cantilever beam shown is subjected to a concentrated load F applied at the end. Model this beam using three-dimensional brick elements and compare the finite element solution to elementary beam theory. How do you apply the concentrated load in the FE model?

**Problem E9.1**

- E9.2** Refer to a standard mechanical design text and obtain the geometric parameters of a standard involute gear tooth profile. Assuming a tooth to be fixed at the root diameter, determine the stress distribution in a gear tooth when the load acts at (a) at the tip of the tooth and (b) the pitch diameter. (c) Are your results in accord with classic gear tooth theory?
- E9.3** A flat plate of thickness 25 mm is loaded as shown; the material has modulus of elasticity $E = 150$ GPa and Poisson's ratio 0.3. Determine the maximum deflection, maximum stress, and the reaction forces assuming a state of plane stress.
- E9.4** Repeat Problem E9.3 if the thickness varies from 25 mm at the left end to 15 mm at the right.
- E9.5** A thin, 0.5" thickness, steel plate is subjected to the loading shown. Determine the maximum displacement and the stress distribution in the plate. Use $E = 30(10^6)$ and Poisson's ratio 0.3.

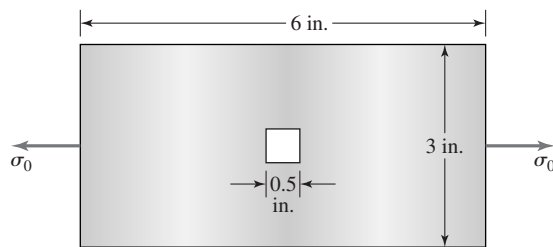


Problem E9.3



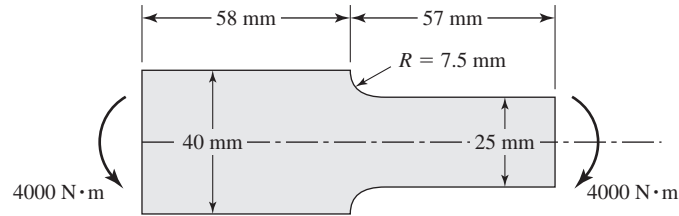
Problem E9.5

- E9.6** A uniform thin plate subjected to a uniform tensile stress as shown has a central rectangular opening. Use the finite element method to determine the stress concentration factor arising from the cutout. Use the material properties of steel. Would your results change if you use the material properties of aluminum? Why? Why not?



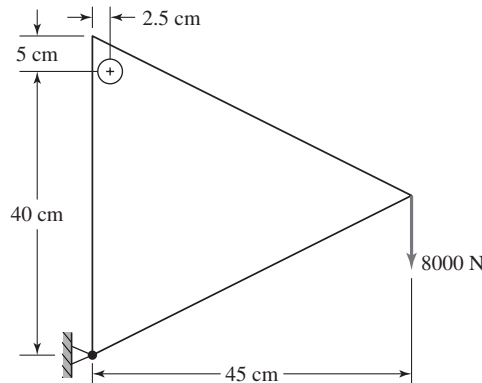
Problem E9.6

- E9.7** The figure shows a common situation in mechanical design. A fillet radius is used to smooth the transition between sections having different dimensions. Use the finite element method to determine the stress concentration factor arising from the fillet radius at the section change. Material thickness is 0.25" and $E = 15(10^6)$ psi. How do you model the moment loading?



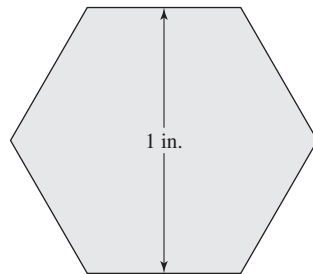
Problem E9.7

E9.8 The gusset plate shown is attached at the upper left via a 1.5 cm diameter rivet and held free at the lower left (model as a pin connection). The plate is loaded as shown. Assuming that the rivet is rigid, compute the stress distribution around the circumference of the rivet. Also determine the maximum deflection. The gusset has thickness 14 mm, modulus of elasticity 207 GPa, and Poisson's ratio 0.28.



Problem E9.8

E9.9 Noncircular shaft sections are often used for quick-change couplings. The figure shows a hexagonal cross section used for such a purpose. The shaft length is 6" and subjected to a net torque of 2800 in.-lb. If the material is steel, compute the total angle of twist. (Note: It is highly likely that your *FE* software will have no element directly applicable to this problem. Analogy may be required.)

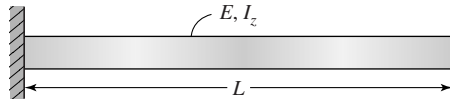


Problem E9.9

E.5 CHAPTER 10

E10.1–10.7 For each truss of Problems E3.1–E3.7 and E4.1–4.7, determine the lowest five natural frequencies and mode shapes. How do these vary with pin joint versus rigid frame assumptions? (Note that, where a material is not specified, the instructor will provide the density value.)

E10.8 Use the modal analysis capability of your finite element software to determine the natural frequencies and mode shapes of the cantilevered beam shown. Use mesh refinement to observe convergence of the frequencies. Compare with published values in many standard vibration texts. What do the higher frequencies represent? How many frequencies can you calculate?

**Problem E10.8**

INDEX

A

Absolute viscosity, 294
Active zone, 468
Adjoint, 452
Admissible functions, 132
Air, 294
ALGOR, 12
Amplitude, 389, 391
Amplitude ratio, 396
ANSYS, 12
Applications
 fluid mechanics, 293–326.
 See also Fluid mechanics
 Galerkin's method (beam element), 149–152
 Galerkin's method (spar element), 148–149
 heat transfer, 222–292.
 See also Heat transfer
 solid mechanics, 327–386.
 See also Solid mechanics
Area coordinates, 179–181
Aspect ratio, 194
Assembly of global stiffness matrix, 61–67
Associative, 449
Automeshing, 374–375
Automeshing software, 374
Axial strain, 357
Axial stress, 113, 120
Axisymmetric elements, 202–206
Axisymmetric heat transfer, 271–276
Axisymmetric problems, 202
Axisymmetric stress analysis, 356–364

B

Back substitution, 469
Backward difference method, 283–284
Backward sweep, 469
Bandwidth, 319
Bar element, 19, 31–38
Bar element consistent mass matrix, 402–407
Bar element mass matrix (two-dimensional truss structures), 434–441

Beam cross sections, 92
Beam elements, 407–412
Beam theory. *See* Flexure elements
Bending stress, 113, 120
Blending functions. *See* Interpolation functions
Body force
 axisymmetric stress analysis, 362–363
 equilibrium equations, 461
 plane stress, 379
Book, overview, 16–17
Boundary conditions
 axisymmetric heat transfer, 275
 defined, 1
 one-dimensional conduction with convection, 213
 stream function, 300–304
 torsion, 377
 truss structures, 67–68
 two-dimensional conduction with convection, 240–253
Boundary value problems, 1
Boyle's law, 293
Brick element, 191–193

C

C^0 -continuity, 163
 C^1 -continuity, 163
 C^n -continuity, 163
Calculus of variations, 45
Capacitance matrix, 278, 279
Castigliano's first theorem, 40–44
Central difference method, 284–285
Chain rule of differentiation, 272, 274
Characteristic equation, 395
Circular frequency, 389
Coefficient matrix, 452
Cofactor matrix, 452
Cofactors, 451
Column matrix, 447
Column vector, 447
Commutative, 449
Compatibility, 165
Compatibility conditions, 24
Complete polynomial, 174
Complete structure, 21
Completeness, 166
Compressible flow, 293
Compressible flow analysis, 295
Computer software
 ALGOR, 12
 ANSYS, 12
 aspect ratio, 194
 automeshing software, 374
 conductance matrix, 240
 COSMOS/M, 12
 damping, 432
 FEPC software, 473–475
 fluid elements, 323
 indication of failure, 371
 pressure on transverse face of beam, 152
 problems for computer solution, 476–487
 reaction equations, 241
 structural weight, 394–395
 three-dimensional heat transfer, 270
 transient dynamic response, 434
Conditionally stable, 434
Conductance matrix, 240–242
Conformable for multiplication, 449
Conservative force, 45
Consistent capacitance matrix, 278
Consistent mass matrix, 404, 414
Constant acceleration method, 432
Constant parameter mapping, 196
Constant strain triangle (CST), 179, 330–333
Constitutive equations, 458
Constraint equation, 25
Continuity equation, 295, 296
Convection, 227
Convective inertia, 315
Convergence
 compatibility, 165
 displacement of tapered cylinder, 4–6
 isoparametric quadrilateral element, 355
 mesh refinement, 164–165
 MWR solution, 137–138
 structural dynamics, 442

- COSMOS/M, 12
Coupling, 417
Cramer's rule, 350, 463–465
Creeping flow, 315
Critical damping coefficient, 426
Critically damped, 426, 427
CST, 179, 330–333
Curved-boundary domain, 4
Cyclic frequency, 392
- D**
- Damped natural circular frequency, 427
Damping, 424–432
 critical damping coefficient, 426
 matrix, 428
 over/underdamped, 426, 427
 physical forms, 424
 ratio, 426
 Rayleigh, 430, 432
 software packages, 432
 structural, 428
Damping matrix, 428
Damping ratio, 426
Dashpot, 425
Deflected beam element, 92
Degrees of freedom
 calculating, 3
 dynamics, 443
 many degrees-of-freedom
 system, 398–402
 master, 443
 N degrees-of-freedom system, 402
 two degrees-of-freedom system, 395
DET, 369–371
Determinant, 450–451
Diagonal matrix, 419, 420, 448
Differential equation, 388, 390
Differential equation theory, 8
Dirac delta, 260
Direct assembly of global stiffness
 matrix, 61–67
Direct stiffness method, 53, 63
Direction cosines, 61
Displacement, 6, 12
Displacement method, 12
Distortion energy theory
 (DET), 369–371
Distributed loads, work
 equivalence, 106–114
Dot notation, 295
Double subscript notation
 (shearing stresses), 459n
Double-dot notation, 404
- Dynamic analysis. *See* Structural
 dynamics
Dynamic degrees of freedom, 443
- E**
- Eigenvalue problem, 397
Eigenvector, 402
Eight-node brick
 element, 191–193, 367
Eight-node rectangular element, 186
Elastic bar element, 31–38
Elastic coupling, 417
Elastic failure theory, 369–371
Element capacitance matrix, 278
Element conductance matrix, 242
Element coordinate system, 20
Element damping matrix, 428
Element displacement location
 vector, 66
Element free-body diagrams, 55
Element load vector, 102–106
Element stiffness matrix, 21–22
Element transformation, 58–61
Elementary beam theory, 91–94
Elementary strength of materials
 theory, 150
Element-node connectivity table, 66
Elements (matrix), 447
Element-to-system displacement
 correspondence, 104
Energy dissipation, 424.
 See also Damping
- Equation
 characteristics, 395
 compatibility, 461–462
 constitutive, 458
 constraint, 26
 continuity, 295, 296
 equilibrium, 460–461
 frequency, 395, 417
 Laplace's, 298
 Navier-Stokes, 315
 nodal equilibrium, 53–58
 one-dimensional wave, 403
Equations of elasticity, 455–462
 compatibility equations, 461–462
 equilibrium equations, 460–461
 strain-displacement
 relations, 455–458
 stress-strain relations, 458–460
Equations of motion, 412–418
Equipotential lines, 304
Equivalent stress, 370
- Equivalent viscous damping
 coefficient, 428
Euler's method, 280
Exterior nodes, 2
- F**
- Failure theories, 369–371
FEA. *See* Finite element
 method (FEM)
FEA software. *See* Computer
 software
FEM. *See* Finite element
 method (FEM)
FEPICIP, 473
FEPICOP, 473
Ferris wheel, 297
Field, 1
Field problems, 1
Field variables, 1
Fillet radius, 485
Finite difference method
 backward difference
 method, 283–284
 central difference method, 284–285
 finite element method,
 compared, 7–10
 forward difference method, 280
 key parameter, 285
 time step, 279, 285
 what is it, 279
Finite element, 2, 12
Finite element analysis (FEA).
 See Finite element method (FEM)
Finite element formulation
 axisymmetric heat transfer, 273–276
 axisymmetric stress
 analysis, 359–360
 general three-dimensional stress
 analysis, 365–368
 one-dimensional conduction with
 convection, 227–230
 plane stress, 330–333
 stream function, 299–300
 torsion, 378
 two-dimensional conduction with
 convection, 236–240
Finite element method (FEM)
 basic premise, 19
 defined, 1
 exact solutions, compared, 4–7
 examples, 12–15
 finite difference method,
 compared, 7–10

- Finite element method—*Cont.*
historical overview, 11–12
how does it work, 1–4
objective, 164
postprocessing, 11
preprocessing step, 10
solution phase, 10–11
Finite Element Method Primer for Mechanical Design, A (Knight), 473
Finite element method software.
See Computer software
Finite Element Personal Computer (FEPC) program, 473
First derivative, 279
First theorem of Castigliano, 40–44
Flexibility method, 12, 52
Flexure element stiffness matrix, 98–101
Flexure element with axial loading, 114–120
Flexure elements, 91–130
element load vector, 102–106
elementary beam theory, 91–94
flexure element stiffness matrix, 98–101
flexure element with axial loading, 114–120
general three-dimensional beam element, 120–124
stress stiffening, 114
2-D beam (flexure element), 94–98
work equivalence (distributed loads), 106–114
Flexure formula, 150
Flow net, 304
Flow with inertia, 321–323
Fluid, 293
Fluid mechanics, 293–326
continuity equation, 295, 296
incompressible viscous flow, 314–323
incompressible/compressible flow, 293
Laplace's equation, 298
literature, 323
rotational/irrotational flow, 296–297
software packages, 323
Stokes flow, 315–321
stream function, 298–304
velocity potential function, 304–314
viscosity, 293–295
viscous flow with inertia, 321–323
Fluid viscosity, 293–295
Forced convection, 227
Forced response, 393
Forced vibration, 392–393
Forcing frequency, 393
Forcing functions, 452
Formal equilibrium approach, 53
Forward difference scheme, 280
Forward sweep, 469
Fourier's law
axisymmetric heat transfer, 274
one-dimensional conduction with convection, 228
three-dimensional conduction with convection, 267
two-dimensional conduction with convection, 237–240
Fourier's law of heat conduction, 153
Four-node quadrilateral element, 195
Four-node rectangular element, 184–185
Four-node tetrahedral element, 188–190
Free meshing, 374
Free vibration, 389
Frequency equation, 395, 417
Friction force, 45
Frontal solution method, 470–472
Function
admissible, 132
forcing, 452
potential, 304
Prandtl's stress, 376, 377
stream, 298–304
Fundamental frequency, 396
- G**
- Galerkin finite element method, 140–148, 285
Galerkin's weighted residual method, 133–139
Garbage in, garbage out, 10
Gases, 295
Gauss elimination, 465–467
Gauss points, 207
Gaussian quadrature, 206–213
Gauss-Jordan reduction, 453
Gauss-Legendre quadrature, 206
General structural damping, 427–432
General three-dimensional beam element, 120–124
Generalized displacements, 420
Generalized forces, 422
Geometric interpolation functions, 195
Geometric isotropy
brick element, 192
complete polynomial, 174
h-refinement, 176
incomplete polynomial, 174
mathematical function, 174
rectangular element, 184
triangular element, 178
two-dimensional conduction with convection, 240
Geometric mapping matrix, 351
Global capacitance matrix, 279
Global coordinate system, 21
Global damping matrix, 428
Global displacement notation, 54
Global stiffness matrix, 58, 61–67
Green-Gauss theorem, 238
Green's theorem in the plane, 238
Guyan reduction, 442
- H**
- Half-symmetry model, 254
Harmonic oscillator, 387–393, 412
Harmonic response, 417
Harmonic response using mode superposition, 422–424
Heat transfer, 222–292
axisymmetric, 271–276
mass transport, with, 261–266
one dimensional conduction with convection, 227–235
one-dimensional conduction (quadratic element), 222–227
three-dimensional, 267–271
time-dependent, 277–285. *See also* Time-dependent heat transfer
two-dimensional conduction with convection, 235–261.
See also Two-dimensional conduction with convection
Hermite polynomials, 214
Higher-order isoparametric elements, 201
Higher-order one-dimensional elements, 170–173
Higher-order rectangular element, 186–187
Higher-order tetrahedral elements, 190
Higher-order triangular elements, 182
Historical overview, 11–12
Hooke's law, 34
h-refinement, 164
Hydrostatic stress, 370

- I**
- Identity matrix, 448
 - Incomplete polynomial, 174–175
 - Incompressible flow, 293
 - Incompressible flow analysis.
 See Fluid mechanics
 - Incompressible viscous
 flow, 314–323
 - Inertia coupling, 417
 - Initial conditions, 280, 388, 391
 - Integration step, 8
 - Interelement boundaries, 145
 - Interior nodes, 2
 - Internal heat generation
 (two-dimensional heat
 transfer), 259–261
 - Interpolation, 3
 - Interpolation functions, 3, 163–221
 - axisymmetric elements, 202–206
 - brick element, 191–193
 - C^0 -continuity, 163
 - compatibility, 165
 - completeness, 166
 - geometric isotropy.
 See Geometric isotropy
 - higher-order one-dimensional
 elements, 170–173
 - isoparametric formulation, 193–201
 - mesh refinement, 164–165
 - numerical integration (Gaussian
 quadrature), 206–213
 - polynomial forms (geometric
 isotropy), 174–176
 - polynomial forms (one-dimensional
 elements), 166–173
 - rectangular elements, 184–187
 - tetrahedral element, 188–190
 - three-dimensional
 elements, 187–193
 - triangular elements, 176–183
 - Inverse of a matrix, 177, 451–454
 - Inverse of the Jacobian matrix, 199
 - Inviscid, 294
 - Irrotational flow, 297
 - Isoparametric element, 196
 - Isoparametric formulation, 193–201
 - Isoparametric formulation of plane
 quadrilateral element, 347–356
 - Isoparametric mapping, 196
- J**
- Jacobian, 350
 - Jacobian matrix, 199, 200, 349
- K**
- Knight, Charles E., 473
- L**
- Lagrangian approach, 417
 - Lagrangian mechanics, 412
 - Lagrange's equations of motion, 412
 - Lanczos method, 443
 - Laplace's equation, 298, 304
 - Least squares, 132
 - Legendre polynomials, 214
 - Line elements, 131
 - Line source, 259
 - Linear elastic spring, 20
 - Linear spring as finite
 element, 20–31
 - Link element, 19
 - Liquids, 295
 - Load-deflection curve, 20
 - Local coordinate system, 20
 - Lower triangular matrix, 467
 - LU decomposition, 467–470
 - Lumped capacitance matrix, 278
 - Lumped mass matrix, 407
- M**
- Magnitude of gradient discontinuities
 at nodes, 145
 - Many degree-of-freedom
 system, 398–402
 - Mapped meshing, 374
 - Mapping, 195
 - Marching, 280, 285
 - Mass, 437
 - Mass matrix, 390
 - Mass matrix for general element
 (equations of motion), 412–418
 - Mass transport, 261–266
 - Master degrees of freedom, 443
 - Material property matrix, 459
 - Matrix. *See also* Matrix mathematics
 - capacitance, 278, 279
 - coefficient, 452
 - cofactor, 452
 - column, 447
 - conductance, 240–242
 - consistent mass, 404
 - damping, 428
 - defined, 447
 - diagonal, 419, 420, 448
 - geometric mapping, 351
 - identity, 448
 - inverse of, 177, 451–453
 - Jacobian, 199, 200, 349
 - lower triangular, 467
 - lumped mass, 407
 - mass, 390
 - material property, 459
 - modal, 419
 - nodal acceleration, 390
 - null, 448
 - order, 447
 - row, 447
 - skew symmetric, 448
 - square, 447
 - stiffness. *See* Stiffness matrix
 - symmetric, 448
 - system mass, 394
 - upper triangular, 467
 - zero, 448
 - Matrix addition, 449
 - Matrix inversion, 177, 451–453
 - Matrix mathematics, 447–454
 - addition/subtraction, 449
 - algebraic operations, 449–450
 - definitions, 447–448
 - determinants, 450–451
 - matrix partitioning, 454
 - multiplication, 449–450
 - scalar algebra, contrasted, 450
 - Matrix multiplication, 449–450
 - Matrix partitioning, 454
 - Matrix subtraction, 449
 - Maximum shear stress theory
 (MSST), 369
 - Megapascal (MPa), 458
 - Mesh, 4
 - Mesh refinement, 164–165
 - Meshing, 4, 374
 - Mesh-refined models, 374
 - Method of weighted residuals
 (MWR), 131–162
 - application of Galerkin's method to
 beam element, 149–152
 - application of Galerkin's method to
 spar element, 148–149
 - convergence, 137–138
 - defined, 131–132
 - Galerkin finite element
 method, 140–148
 - Galerkin's weighted residual
 method, 133–139
 - general concept, 132
 - one-dimensional heat
 conduction, 152–158
 - trial functions, 131, 138, 140
 - variations, 132–133

- Minimum potential energy, 44–47, 158
Minor, 450
Modal analysis, 387, 397
Modal matrix, 419
Modal superposition, 397, 399
Mode superposition, 422–424
Model definition step, 10
Modulus of elasticity, 458
Modulus of rigidity, 459
Molten polymers, 315
MPa, 458
MSC/NASTRAN, 12, 18
MSST, 369
MWR. *See* Method of weighted residuals (MWR)
- N**
- N* degree-of-freedom system, 402
NASTRAN, 12
Natural circular frequency, 389
Natural convection, 227
Natural coordinates, 185, 186
Natural frequency, 392
Natural modes of vibration, 387, 443
Navier-Stokes equations, 315
Net force, 21
Neutral surface, 92
Newmark method, 432–434
Newton's law of viscosity, 294
Newton's second law
 bar elements, 402
 linear spring, 22
 multiple degrees-of-freedom systems, 394
 simple harmonic oscillator, 388
No slip condition, 294
Nodal acceleration matrix, 390
Nodal displacement correspondence table, 62
Nodal displacements, 21
Nodal equilibrium equations, 53–58
Nodal free-body diagrams, 55
Nodal load positive convention, 102
Node, 2
Noncircular shaft sections, 486
Nonconservative force, 45
Nonhomogeneous boundary condition, 29
Normal strain, 455–456
Normalized coordinates, 185
Null matrix, 448
Numerical integration (Gaussian quadrature), 206–213
- O**
- Octahedral shear stress theory (OSST), 371
One dimensional conduction with convection, 227–235
One-dimensional conduction (quadratic element), 222–227
One-dimensional heat conduction, 152–158
One-dimensional wave equation, 403
Order (matrix), 447
Orthogonality, 418
Orthogonality of principal modes, 418–421
Orthonormal, 419
OSST, 371
Overdamped, 426, 427
Overview of book, 16–17
- P**
- Parent element, 195
Partitioning (matrix), 454
Pascal pyramid, 175
Pascal triangle, 174, 175
Period of oscillation, 392
Phase angle, 389, 391
Plane quadrilateral element, 347–356
Plane strain (rectangular element), 342–347
Plane stress, 328–342
 assumptions, 328
 distributed loads/body face, 335–342
 finite element formulation (CST), 330–333
 stiffness matrix evaluation, 333–335
Plate bending, 372–373
Point collocation, 132
Poisson's ratio, 458
Polynomial forms
 geometric isotropy, 174–176
 one-dimensional elements, 166–173
Polynomial trial functions, 138
Postmultiplier, 449
Postprocessing, 11
Potential function, 304
Practical considerations
 solid mechanics, 372–375
 structural dynamics, 424–443
Prandtl's stress function, 376, 377
p-refinement, 164
Premultiplier, 449
Preprocessing, 10
Principal planes, 369
Principal stresses, 369
Principle of conservation of energy, 153
Principle of conservation of mass, 295
Principle of minimum potential energy, 44–47, 158
Product (matrices), 448
Pure rotation, 296
- Q**
- $Q/2$, 254
 $Q/4$, 253
Quadrilateral element, 194–196
Quarter-symmetry model, 253
Quick-change coupling, 486
- R**
- Radial strain, 357
Ratio
 amplitude, 396
 aspect, 194
 damping, 426
 Poisson's, 458
Rayleigh damping, 430, 432
Reaction equations
 stream function, 303
 two-dimensional conduction with convection, 241, 254
Rectangular elements, 184–187
Rectangular parallelepiped (brick element), 191–193
Recurrence relation, 8
Reduced eigenvalue problem, 443
Refined finite element mesh, 4
Residual error, 132
Resonance, 393
Resonant frequency, 393
Right-hand rule, 238
Rotational flow, 297
Row matrix, 447
Row vector, 447
- S**
- Sampling points, 207
Second-order differential equation, 388
Serendipity coordinates, 185
Shape functions. *See* Interpolation functions
Shear modulus, 459
Shear strain, 455–456
Simple cantilever truss, 51–52
Simple harmonic oscillator, 387–393, 412

- Singular, 22, 452
Six-node quadratic triangular element, 319
Six-node triangular element, 181–182
Skew symmetric matrix, 448
Software packages. *See* Computer software
Solid mechanics, 327–386.
 See also Stress
 automeshing, 374–375
 axisymmetric stress analysis, 356–364
 DET, 369–371
 failure theories, 369–371
 general three-dimensional stress elements, 364–368
 isoparametric formulation of plane quadrilateral element, 347–356
 MSST, 369
 OSST, 371
 plane strain (rectangular element), 342–347
 plane stress, 328–342
 practical considerations, 372–375
 strain/stress computation, 368–372
 torsion, 375–382
Solution, 476–487
Solution convergence. *See* Convergence
Solution phase, 10–11
Solution techniques for linear algebraic equations, 463–472
 Cramer's method, 463–465
 frontal solution, 470–472
 Gauss elimination, 465–467
 LU decomposition, 467–470
Spar element, 19
spar element stiffness matrix, 121
Sparse, 470
Spring constant, 20
Spring rate, 20
Spring stiffness, 20
Spring-mass system, 394–402
Square matrix, 447
Static condensation, 442, 454
Stiffness matrix
 element, 21–22
 flexure element, 98–101
 global, 58, 61–67
 spar element, 121
 system, 25
 xy plane flexure, 121
 xz plane bending, 121
Stiffness method, 52
Stokes flow, 315–321
Strain, 4
Strain energy, 38–39
Strain energy density, 39
Strain energy per unit volume, 39
Strain/stress computation, 368–372
Stream function, 298–304
Streamlines, 298
Stress
 equivalent, 370
 hydrostatic, 370
 plane, 338–342
 principal, 369
 von Mises, 370
Stress analysis. *See* Solid mechanics
Stress stiffening, 114
Stress vector, 460
Structural damping, 428
Structural dynamics, 387–446
 bar element mass matrix (two-dimensional truss structures), 434–441
 bar-element-consistent mass matrix, 402–407
 beam elements, 407–412
 energy dissipation (structural damping), 424–432.
 See also Damping
 harmonic response using mode superposition, 422–424
 mass matrix for general element (equations of motion), 412–418
 multiple degrees-of-freedom systems, 394–402
 Newmark method, 432–434
 orthogonality of principal modes, 418–421
 practical considerations, 442–443
 simple harmonic oscillator, 387–393
 transient dynamic response, 432–434
Subspace iteration, 443
Superposition procedure, 25
Symmetric matrix, 22, 448
Symmetry
 incomplete polynomial, 174–175
 matrix, 448
 simplification of mathematics of solution, 252
 stiffness matrix, 22
 two-dimensional conduction with convection, 253–254
System mass matrix, 394
System stiffness matrix, 25
System viscous damping matrix, 428
- T**
- Tapered cylinder, 4–6
Ten-node tetrahedral element, 188
Tensile stress, 113
Tetrahedral element, 188–190
Theory of continuum mechanics, 461
Theory of thin plates, 372–373
Thin curved plate structures, 373
Three-dimensional elements, 187–193
Three-dimensional heat transfer, 267–271
Three-dimensional stress elements, 364–368
Three-dimensional trusses, 79–83
Three-node triangular element, 178–179
Time step, 279, 285
Time-dependent heat transfer, 277–285
 capacitance matrix, 278, 279
 finite difference method, 279–285
Torque, 377–378
Torsion, 375–382
Torsional finite element notation, 122
Total potential energy, 45
Transient dynamic response, 432–434
Transient effects. *See* Time-dependent heat transfer
Translation, 297
Transpose, 447–448
Trial functions, 131, 138, 140
Triangular axisymmetric element, 203
Triangular elements
 area coordinates, 179–181
 constant strain triangle (CST), 179
 integration in area coordinates, 182–183
 interpolation functions, 176–183
 six-node triangular element, 181–182
Truss element, 19
Truss structures, 51–90
 boundary conditions, constraint forces, 67–68
 comprehensive example, 72–78
 defined, 51
 direct assembly of global stiffness matrix, 61–67
 direction cosines, 61
 element strain and stress, 68–72
 element transformation, 58–61
 nodal equilibrium equations, 53–58
 3-D trusses, 79–83
Twenty-node tetrahedral element, 188
Two degree-of-freedom system, 395

Two-dimensional beam (flexure element), 94–98
 Two-dimensional conduction with convection, 235–261
 boundary conditions, 240–253
 conductance matrix, 240–242
 element resultants, 254–259
 finite element formulation, 236–240
 internal heat generation, 259–261
 reaction equations, 241, 254
 symmetry conditions, 253–254
 Two-dimensional quadrilateral element, 195
 Two-point recurrence relation, 280

U

Unconditionally stable, 434
 Underdamped, 426, 427

Unit impulse, 260
 Upper triangular form, 466
 Upper triangular matrix, 467

V

Variational principles, 417
 Velocity potential function, 304–314
 Viscosity, 293–295
 Viscous flow with inertia, 321–323
 Volume coordinates, 188–189
 Von Mises stress, 370

W

Water, 294
 Wave front solution, 470
 Work equivalence (distributed loads), 106–114

X

xy plane flexure stiffness matrix, 121
xz plane bending stiffness matrix, 121

Y

Young's modulus, 458

Z

Zero matrix, 448
 Zones, 468